Cranfield Multi-Strand Conference: Creating Wealth Through Research and Innovation (CMC 2008)

Foreword from Professor Sir John O'Reilly
DSc PhD CEng FREng FIET CPhys CSci FInstP FBCS

Vice-Chancellor, Cranfield University

Developments in science, engineering and technology are constantly opening up new business opportunities. Rolls-Royce and Boeing, for example, deploy sensing technologies to monitor the health of their products in use, enabling these firms to offer new and innovative services to their customers. In the health arena, sensing technologies are being used to monitor and diagnose patients' health and wellbeing remotely. When appropriately deployed these technologies not only have commercial benefits, but also environmental benefits, reducing material consumption and waste.

To create wealth from innovation in today's world, we need to explore how different disciplines link and create new opportunities to provide solutions for society at large.

The 2008 Cranfield Multi-Strand Conference provided a forum for talented researchers to come together and explore these issues in an open and collaborative environment. During the conference, we heard keynote speeches from senior people in industry, government and academia, who shared their experience of how new products and services can be delivered through innovation.

A particular aim was to provide a welcoming and supportive forum for early-stage researchers to present and discuss their work with more established figures in their various fields. The format of the conference was designed to embrace the interdisciplinary character of research today, encouraging contributors who have a science, engineering or technology focus to explore associated management and policy considerations.

Cranfield University is delighted to publish the Proceedings of CMC 2008 and to make available the best of the papers presented over the two days.

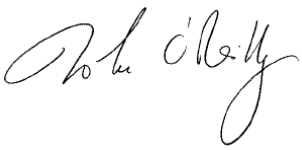

 Published by Cranfield University Press ISBN: 978-0-9557436-7-2 http://hdl.handle.net/1826/3832

Organisers

Conference Co-Chairs

- Professor David Stephenson FREng
- Professor Joe Nellis AcSS

Organising Committee

- Professor Tim Baines
- Professor Peter Hill
- Dr David Mba
- Professor Andy Neely
- Dr Colin Pilbeam
- Professor Rajkumar Roy
- Dr Claire Turner

Advisory Board

- Dr Fariba Alamdari Boeing USA
- Dr J.C. Attard EITL, Dubai
- Martin Baxter, Deputy Chief Executive, Institute of Environmental Management & Assessment
- Sir David Brown Motorola UK
- Dr N F Chin PowerNets Hong Kong
- Professor I Darwazeh UCL
- Andrew Furlong IChemE
- Tony Hey Microsoft USA
- Paul Jackson IET
- Dr Robert Kirby-Harris IoP
- John Loughhead UKERC
- Patrick McDonald HSE UK
- Keith Mans RAeS
- Professor Jose Moura CMU USA
- Dr John Murphy BAe Systems
- Dr Mike Rodd BCS
- Dr Malcolm Skingle GSK
- Justin Taberham , Director of Policy, CIWEM
- Professor John McCanny ECTI Ireland
- Professor Ron Pethig Wales
- Dr Randal Richards RCUK
- Professor Jose da Rocha Portugal
- Professor Anthony Woodman ICRI India

Conference Secretariat

- Cranfield University Business Development Office

Sponsors

 Published by Cranfield University Press ISBN: 978-0-9557436-7-2 http://hdl.handle.net/1826/3832

Table of Contents

 Published by Cranfield University Press ISBN: 978-0-9557436-7-2 http://hdl.handle.net/1826/3832

 Published by Cranfield University Press ISBN: 978-0-9557436-7-2 http://hdl.handle.net/1826/3832

Acoustic Emission (AE) Technology for Spur Gear Monitoring

R.I.Raja Hamzah*, D.Mba.
School of Engineering, Cranfield University, Cranfield, Bedfordshire MK43 0SX.
*E-mail: r.i.raja-hamzah.2003@cranfield.ac.uk

Abstract

Effective plant or machine maintenance strategies have become important aspect in enhancing company or organizations profitability. Condition Based Maintenance (CBM) philosophy has become widely accepted by most industries today as a key element in reducing operating cost, increasing safety and life cycle costs within an environmental friendly umbrella. One of the important keys to a successful CBM is condition monitoring. The investigation reported in this paper was centered on the application of the Acoustic Emissions (AE) technology for operational spur gear monitoring. The aim of this research program is to investigate the influence of specific film thickness ( ) on the generation of AE activity. It is concluded from the experimental results that AE may offer potential for monitoring operational gear conditions.

Introduction

The application of AE for gear condition monitoring is still at its infancy. AE is defined as the range of phenomena that results in structure borne propagating waves being generated by the rapid release of energy from localised sources within and/or on the surface of the material [1]. Typical frequency content of AE is between 100kHz to 1Mhz. The main source of AE during gear mesh is postulated to come from asperity interactions between meshing surfaces[2].

Life of the gears are very much dependent on the specific film thickness (λ) of its lubricant, which is the ratio of oil film thickness over the composite gear surface roughness. Studies in elastohydrodynamic lubrication (EHL) have shown that this ratio is influenced by load, speed and temperature of the gears [3]. Whilst the ratio in excess of 2 is usually recommended in practice, the actual ratio during the operation is very difficult to ascertain.

This paper looks into the feasibility of AE to monitor the specific film thickness (λ) of the operational spur gear. This investigation builds on the investigation of Raja Hamzah et al. [4] by exploring further the relationship between AE r.m.s and specific film thickness (λ).

 Published by Cranfield University Press ISBN: 978-0-9557436-7-2 http://hdl.handle.net/1826/3832

Experimental Setup and Procedure

The test rig employed during this research was a standard back-to-back oil bath lubricated gear box, see figure 1(left). Gears and lubricant data used for the test were summarized in table 1.

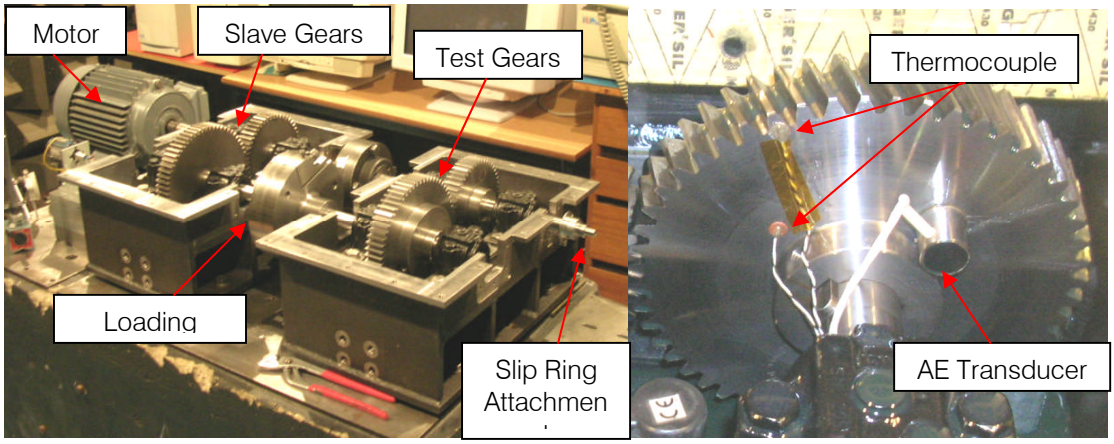

Figure 1 Back-to-back test gearbox arrangement and location where AE transducer and thermocouples were mounted on the pinion test gear.

Table 1 Gear and Lubricant Data

Gear Data	*Spur*	*Lubricant Properties*	*Mobilgear 636*
No. of teeth, pinion: gear	*49 : 65*	*Viscosity @ 40 °C (cSt)*	*680.0*
Contact Ratio	*1.33*	*@100 °C (cSt)*	*39.2*
Module (mm)	*3.00*	*Density @ 15.6 °C (kg/l)*	*0.91*
Surface roughness, Ra (□m)	*2.00*	*Viscosity Index*	*90.0*
Face width (mm)	*30.00*	*Pour point (°C)*	*-9.0*
Pressure angle (°)	*20.00*	*Flash point (°C)*	*285.0*
Helix angle (°)	*0.00*	*Pressure viscosity*	
Modulus of Elasticity (GPa)	*228.00*	*coefficient, □ (mm^2/N)*	*$2.2X10^{-8}$*

Wide band type of transducer (Physical Acoustic Corporation, type WD) having a relative flat response between 100kHz and 1MHz together with two 'J-type' thermocouples were mounted on the test pinion for acquiring AE signals and gear temperature during the test, see figure 1(right). Signals from AE transducer and thermocouples were transmitted to commercial data acquisition system via silver contact slip ring. Prior to data acquisition system, AE signals were amplified at 40dB. Continuous AE r.m.s was recorded in real time at time constant and time driven rate of 80 milliseconds. Gear temperatures were recorded at the sampling rate of 1Hz.

 Published by Cranfield University Press ISBN: 978-0-9557436-7-2 http://hdl.handle.net/1826/3832

Series of tests were undertaken in an attempt to understand the λ on the generation of AE activity by varying load, speed and temperature of the gear. Four different loads (60, 120, 250, 370Nm) and three different speeds (700, 1450 and 2850 rpm) were used during the load and speed variation tests whilst only three loads (60, 120 and 250Nm) and two speed (700 and 1450 rpm) were used during the temperature variation tests. Prior to every tests, the gearbox was run until steady temperature was reached ($\pm$1°C for the period of 30 minutes). During the temperature variation tests, gear temperature was reduced by spraying liquid nitrogen onto the test wheel, whilst the gear still in operation, until it reached approximately 0°C.

Results and Discussions

The estimation of oil film thickness (*h*) used in this paper was based on the pinion temperature acquired during the test. Viscosity and oil film thickness (*h*) were calculated using eq. (1)[5] and eq. (2) [3]. Specific film thickness (λ) is the ratio of oil film thickness (*h*) over the composite surface roughness (σ_{rms}) of the meshing surfaces, see eq. (3).

$$ln\ ln\ (v+0.7) = A+B\ ln\ (T) \quad (1)$$

$$h = \frac{k(\eta_0 \mu)^{0.7} R^{0.43}}{w^{0.13}} \mu m \quad (2)$$

where, $k = 1.6\alpha^{0.6} E^{0.03}$

$$\lambda = h / \sigma_{rms} \quad (3)$$

Gears in operation experience three of the lubrication regimes which are boundary ($\lambda < 1$), mixed or partial EHL ($1 \leq \lambda \leq 5$) and full EHL ($\lambda > 5$). Under boundary lubrication, the friction is mainly due to the interaction of asperities whilst under mixed or partial EHL friction is affected by both the interaction of asperities and the elastohydrodynamic and hydrodynamic effects. However, under full EHL and hydrodynamic lubrication there is no interaction between asperities taking place [6].

Figure 2 illustrates the changes in AE r.m.s at different load and speed conditions for the test range undertaken. AE r.m.s data points plotted in this figure were the average of 2000 AE r.m.s. data points acquired during the test. The maximum temperature variation during the tests was approximately 3.2°C. It is important to keep the temperature consistent during the entire tests as the temperature has influence on λ as well. The plot shows that the increase in loads increased the AE r.m.s, a direct consequence of the reduction in λ, refer eq. (2) and (3). The reduction in λ results in the increased in asperity interactions between meshing surfaces which directly increased AE r.m.s. It is important to note that the variations in AE r.m.s with load were small at 700 and 1450rpm as compared to 2850rpm. Tan et al [7] ran similar test at the λ region

 Published by Cranfield University Press ISBN: 978-0-9557436-7-2 http://hdl.handle.net/1826/3832

highlighted in the figure and concluded that load has minimum influence on the generation of AE activity. At 2850rpm, the oil film thickness is thick enough to cause significant change in the level of asperities between meshing surfaces. This results in the change of AE r.m.s levels as the level of asperities between meshing surfaces changes with load.

Figure 2 also shows that the increase in speed results in the increase of AE r.m.s levels for all load conditions. The result contradicts EHL theory whereby the increase in speed should result in the increase of λ thereby reducing asperity interactions between meshing surfaces, refer eq. (2) and (3). The increase in AE r.m.s with the increase in speed is attributed to the high strain rate experience by the asperities which generate larger amplitude AE response at higher speed and the contribution of lubricant friction between gears in mesh [7].

Figure 3 illustrates normalised AE r.m.s values for temperature variation tests. AE r.m.s. for each test was normalised by considering the minimum and maximum values as '0' and '1' respectively. The AE r.m.s between minimum and maximum values was calculated as the ratio between '0' and '1'. The plot shows that the increase in λ, a direct consequence of reduction in gear temperature during the test, results in the reduction of normalised AE r.m.s level at all speed and load conditions. It is interesting to note that the significant reduction in the normalised AE r.m.s occur at the mixed or partial EHL region ($1 \leq \lambda \leq 5$) whereby the level of asperities between meshing surfaces change significantly. This strengthens the postulate that the source of AE during gear mesh is asperity contact.

Fi

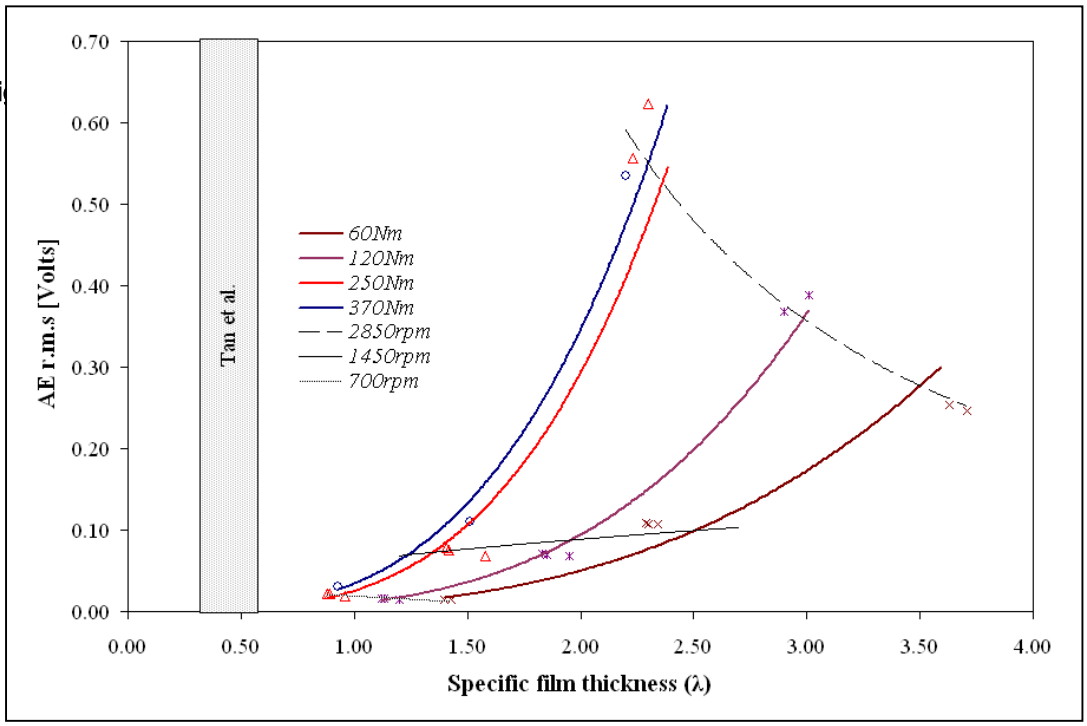

 Published by Cranfield University Press ISBN: 978-0-9557436-7-2 http://hdl.handle.net/1826/3832

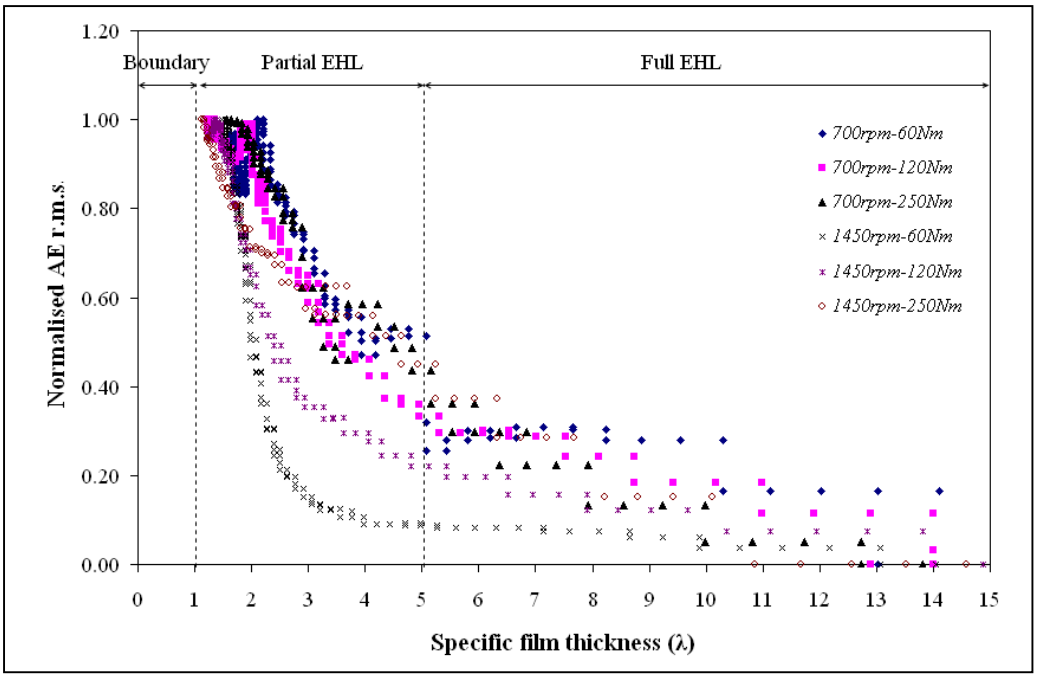

Figure 3 Normalised AE r.m.s at different specific film thickness (λ)

Conclusion

An increase in specific λ under the same load and speed conditions results in the reduction of AE r.m.s level, a direct consequence of the reduction in asperity interactions between meshing surfaces. The correlation between λ and AE r.m.s observed from this research program will form the foundation for significant advancement in applying AE technology to monitor operational gear conditions.

Nomenclature

α = pressure exponent of viscosity (mm^2/N)
η_o = dynamic viscosity (Pa s)
R = equivalent radius (m)
v = kinematic viscosity of the oil (mm^2/s)
A = constant for specific oil
E = modulus of elasticity (Pa)
u = entraining velocity (m/s)
w = load per unit length of cylinder (N/m)
T = absolute temperature of the oil (K)
B = constant for specific oil

References

1. Condition Monitoring and Diagnostic of Machines. Acoustic emission – general guidelines. ISO/DIS 22096, 2006.

 Published by Cranfield University Press ISBN: 978-0-9557436-7-2 http://hdl.handle.net/1826/3832

2. Tan, C.K., Mba, D., Identification of Acoustic Emission Source During a Comparative Study on Diagnosis of a Spur Gearbox, Tribol. Int., Vol. 38, pp. 469-480, 2005.
3. Dowson, D., Higginson, G.R., Elastohydrodynamic Lubrication, 1st ed., Pergamon Press, Oxford, UK, 1977.
4. Raja Hamzah, R.I., Mba, D., Acoustic Emission and Specific Film Thickness for Operating Spur Gears, ASME Journal of Tribology, Vol. 129(4), pp. 860-867, 2007.
5. Alexander, D.L., Viscosity of Lubricants, Lubrication, Vol. 78(3), pp. 1-16, 1992.
6. Martin, K.F., A Review of Friction Prediction in Gear Teeth, Wear, Vol. 49, pp. 201-238, 1978.
7. Tan, C.K., Mba, D., Experimentally Established Correlation between Acoustic Emission Activity, Load, Speed and Asperity Contact of Spur Gear under Partial Elastohydrodynamic Lubrication, Journal of Engineering Tribology, ImechE, Part J, Vol. 219, pp. 401-409, 2005.

 Published by Cranfield University Press ISBN: 978-0-9557436-7-2 http://hdl.handle.net/1826/3832

Solving Real-Life Multi-Objective Optimisation Problems: A Mathematical Approach

S. S. Askar*, [a], A. Tiwari [a], J. Mehnen[a], J. J. Ramsden[b]

[a] Manufacturing Department, Decision Engineering Centre, School of applied Science, Cranfield University, Cranfield MK 43 0AL, UK

[b] Microsystems and Nanotechnology Centre, School of Applied Science, Cranfield University, Cranfield MK43 0AL, UK.

Abstract

This paper presents a mathematical approach based on Karush-Kuhn-Tucker theorem for solving multi-objective optimisation problems. This method is used to formulate the exact equation of two-objective Pareto front problems which are continuous, differentiable, and convex. The approach was tested using a benchmark problem and a mechanical engineering problem. Due to its analytical character the suggested technique yields – in contrast to the typical numerical approaches – precise descriptions of the Pareto front.

Keywords Karush-Kuhn-Tucker, Pareto front, optimisation

Introduction

Problems that have more than one objective functions are of great importance in engineering and many other disciplines. These kinds of problems are known with multi-objective optimisation problems (MOOP). The solutions of such problems are difficult because objectives may be contradicting each other. Because of this conflict one generally cannot find a single ideal solution which concurrently satisfies all the objectives at the same time. Consequently, a solution that is extreme with respect to one objective function requires a compromise in other objective functions [1]. However, finding these solutions plays an important role in MOOP and mathematically the problem is considered to be solved when the Pareto optimal set, i.e. the set of best compromise solutions is found. The general consensus of the engineers and mathematicians is that the Pareto set may contain information which can help the designer make a decision and thus arrive at better trade off solutions. In addition, this information might show the designer an issue ignored such as ease of manufacture or assembly. The main purpose of this paper is to present the proposed approach that can be used to solve a certain class of multi-objective problems. This class covers the huge set of continuous, differentiable and convex functions. The core of the method depends on Karush-Kuhn-Tucker (KKT) theorem. This paper focuses on formulating the equation of the Pareto front using an analytical form. This will be achieved by implementing the steps of the proposed method. The remainder of the paper is devoted as follows. Some preliminaries are presented in section 2. In section 3 some theoretical results around KKT approach have been shown. The steps of the proposed approach are

* Corresponding author: Tel. +44(0)1234750111 5656
E-mail: s.e.a.askar@cranfield.ac.uk

 Published by Cranfield University Press ISBN: 978-0-9557436-7-2 http://hdl.handle.net/1826/3832

illustrated in section 4. In section 5 we describe the selected test problems. In section 6 we show the results obtained in the experiments performed and compare with existing results. Finally, in section 7 conclusions are established.

Preliminaries

General formulation of constrained MOOP

A standard constrained multi-objective optimisation problem can be stated as follows [1]:

$$\text{Maximise/Minimise} \quad \begin{aligned} &\vec{f}(\vec{x}) = \left(f_1(\vec{x}), f_2(\vec{x}),..., f_M(\vec{x})\right)^T \\ &\vec{g}(\vec{x}) = \left(g_1(\vec{x}), g_2(\vec{x}),..., g_J(\vec{x})\right)^T \le 0 \\ &\vec{h}(\vec{x}) = \left(h_1(\vec{x}), h_2(\vec{x}),..., h_K(\vec{x})\right)^T = 0 \\ &x_i^{(L)} \le x_i \le x_i^{(U)} \end{aligned} \tag{1}$$

where M is the number of the functions which are associated with J inequality and K equality constraints. $\vec{x} = (x_1, x_2,..., x_n)$ is the vector of decision variables. Each decision value x_i and $i = 1,2,...,n$ is restricted to take a value within a lower value $x_i^{(L)}$ and an upper value $x_i^{(U)}$. Note that any maximisation objective function can be converted into a minimisation objective by changing its sign.

Convexity

A function $f : R^n \to R$ is a convex function if for any two pairs of solutions $\vec{x}_1, \vec{x}_2 \in R^n$ the following condition is true:

$$f(\lambda \vec{x}_1 + (1-\lambda)\vec{x}_2) \le \lambda f(\vec{x}_1) + (1-\lambda) f(\vec{x}_2), \quad \text{for all } 0 \le \lambda \le 1. \tag{2}$$

Theorem

Suppose $f(\vec{x})$ has continuous second partial derivatives on some open convex set C in R^n. If the Hessian H $f(\vec{x})$ of $f(\vec{x})$ is positive semi-definite (resp. positive definite) on C, then $f(\vec{x})$ is convex (resp. strictly convex) on C. [12]

Karush-Kuhn-Tucker (KKT) sufficient condition for Pareto-optimality

Let the objective functions be convex and the constraint functions of the problem shown in equation (1) are non-convex. Let the objective and constraint functions be continuously differentiable at a feasible solution $\vec{x}^*$. A sufficient condition for $\vec{x}^*$ to be Pareto-optimal is that there exist vectors $\vec{\lambda} > 0$ and $\vec{\mu} \ge 0$ (where $\vec{\lambda} \in R^M$ and $\vec{\mu} \in R^J$) such that the following conditions hold [2]:

 Published by Cranfield University Press ISBN: 978-0-9557436-7-2 http://hdl.handle.net/1826/3832

$$\sum_{m=1}^{M} \bar{\lambda}_m \nabla f_m(\bar{x}^*) - \sum_{j=1}^{J} \bar{\mu}_j \nabla g_j(\bar{x}^*) = 0,$$
$$\bar{\mu}_j g_j(\bar{x}^*) = 0 \quad for\ all \quad j = 1,2,..,J \tag{3}$$

Theoretical results on KKT approach

Since the paper by Kuhn and Tucker [3] has been published in 1950, several studies dealing with multi-objective optimisation have been reported. Many valuable results have been found over the past several years. For instance, Benson [4] examined the existence of efficient and properly efficient solutions for the vector maximisation problem. A generalisation of Kuhn-Tucker sufficiency conditions has been presented by Hanson [5]. Craven [6] presented a modified kind of Kuhn-Tucker condition applicable to the minimum but not necessarily assuming convexity. Three optimality concepts, weak, proper, and Pareto optimality have been presented by Miettinen et al. [7] using cones. Svanbery [8] presented and investigated a class of globally convergent optimisation methods based on the concept of conservative convex separable approximations. A survey of state-of-the-art techniques that construct Pareto front analytically has been reported by Askar et al. [11].

Mathematical Approach

The steps of the proposed method are the following:

Step 1: Check the convexity of the objectives using the Hessian Matrix H.

$$H = \begin{bmatrix} \frac{\partial^2 f}{\partial x_1^2} & \frac{\partial^2 f}{\partial x_1 \partial x_2} & \cdots & \frac{\partial^2 f}{\partial x_1 \partial x_n} \\ \frac{\partial^2 f}{\partial x_2 \partial x_1} & \frac{\partial^2 f}{\partial x_2^2} & \cdots & \frac{\partial^2 f}{\partial x_2 \partial x_n} \\ \vdots & \vdots & \ddots & \vdots \\ \frac{\partial^2 f}{\partial x_n \partial x_1} & \frac{\partial^2 f}{\partial x_n \partial x_2} & \cdots & \frac{\partial^2 f}{\partial x_n^2} \end{bmatrix} \tag{4}$$

If $H \geq 0$ or $H > 0$ then the objective function is convex otherwise it is concave (Theorem 2.3).

Step 2: Check the continuity and differentiability of the objective functions.

Step 3: Solve the KKT equations so as to find the Pareto optimal solution as a function of the vector parameter $\bar{\lambda}$.

Step 4: Substituting with the Pareto optimal solutions obtained by step 3 on f_1 and f_2 to get the equation of the true Pareto front.

 Published by Cranfield University Press ISBN: 978-0-9557436-7-2 http://hdl.handle.net/1826/3832

Test Problems

To test the suggested method, two problems have been selected to validate the proposed approach.

Problem 1: (Fonseca and Fleming) [9]

Design variables: x_i, $i = 1,...,n$. Here without restricting generality the special case $n = 2$ is assumed.

Cost functions: Minimise the following two objective functions:

$$f_1 = 1 - \exp\left(- \sum_{i=1}^{n} (x_i - \frac{1}{\sqrt{n}})^2 \right)$$
$$f_2 = 1 - \exp\left(- \sum_{i=1}^{n} (x_i + \frac{1}{\sqrt{n}})^2 \right) \quad (5)$$

Constraints: $-4 \le x_i \le 4 \quad i = 1,...,n$

Problem 2: (Four-bars plane truss problem) [10]

Design variables: x_1, x_2, x_3 and x_4

Objective functions: The problem is formulated as two conflicting objective functions of minimising both the volume V of the truss (f_1) and the displacement Δ of the joint (f_2), subject to given physical restriction regarding the feasible cross-sectional areas x_1, x_2, x_3, x_4 of the four bars. The stress on the truss is caused by three forces of magnitude F and $2F$ as depicted in Figure 1 below:

$$f_1(x) = L\left(2x_1 + \sqrt{2}x_2 + \sqrt{2}x_3 + x_4\right)$$
$$f_2(x) = \frac{F\,L}{E}\left(\frac{2}{x_1} + \frac{2\sqrt{2}}{x_2} + \frac{2\sqrt{2}}{x_3} + \frac{1}{x_4}\right)$$

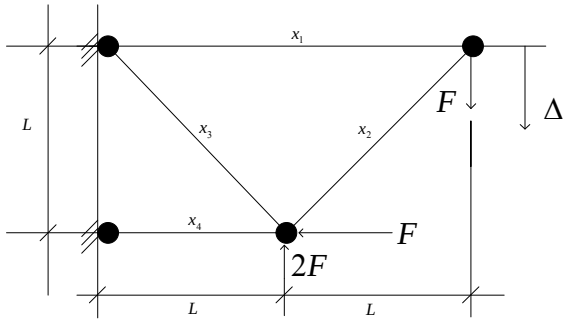

Figure 1: Four-bars plane truss

Constraints: $F/\sigma \le x_1, x_4 \le 3(F/\sigma), \quad \sqrt{2}\,(F/\sigma) \le x_2, x_3 \le 3(F/\sigma),$

Constant parameters: $F = 10\ kN,\ E = 2 \times 10^5\ kn/cm^2,\ L = 200\ cm$ and $\sigma = 10\ kN/cm^2$

 Published by Cranfield University Press ISBN: 978-0-9557436-7-2 http://hdl.handle.net/1826/3832

Obtained Results versus Existing Results

The results obtained using the suggested approach have been compared with the results generated by NSGA-II [1] which is a standard evolutionary algorithm. The results generated by NSGA-II have been produced using population size = 100 with total number of generations equals 100.

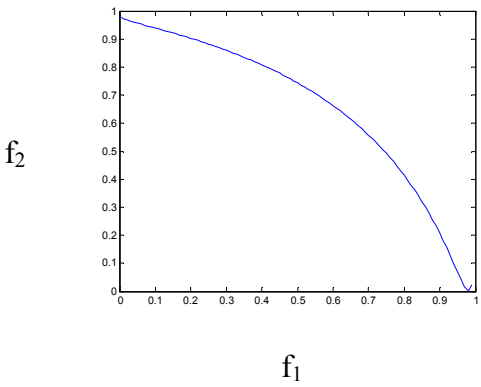

Figure 2a: Solution of problem 1 using proposed method

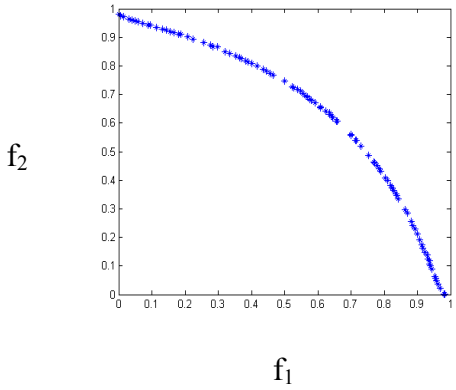

Figure 2b: Approximation of problem 1 using NSGA-II

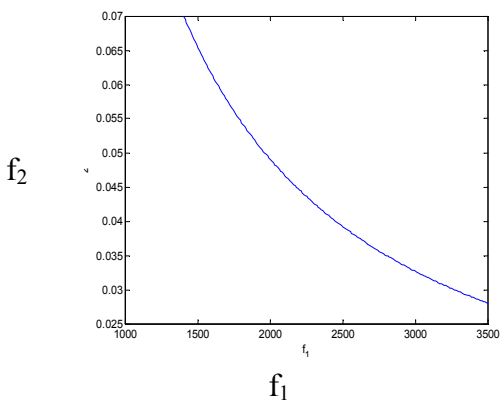

Figure 3a: Solution of problem 2 using proposed method

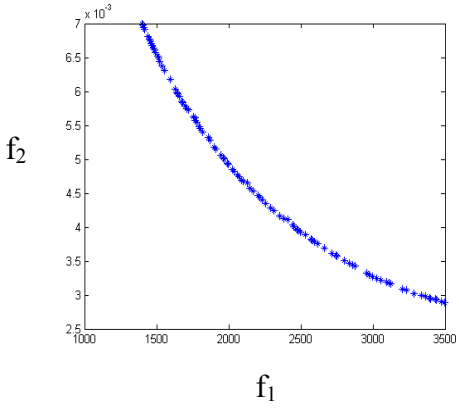

Figure 3b: Approximation of problem 2 using NSGA-II

Figure 2a shows the exact curve of the Pareto front for problem 1 by using the proposed approach. The equation of the Pareto front is $f_2 = 1 - \exp\left\{-\left(2 - \sqrt{-\ln(1 - f_1)}\right)^2\right\}$ and $0 \le f_1 \le 1 - \exp\left(-\left(4 - \frac{1}{\sqrt{2}}\right)^2\right)$. Figure 2b shows the existing results for problem 1 by using NSGA-II. The interesting observation here is the relationship between the decision variables that construct the curve of the Pareto front is $x_1 = x_2$. This means that not all the points in the decision space are used to construct the Pareto front. Figure 3a represents the solution of the equation of the Pareto front for problem 2. This equation has the formula $f_2 = \frac{49}{E} F L^2 \frac{1}{f_1}$ and $\frac{7LF}{\sigma} \le f_1 \le \frac{21FL}{\sigma}$. Figure 3b shows the results for problem 2 using NSGA-II. The important observation here is the relationship between the decision variables which

 Published by Cranfield University Press ISBN: 978-0-9557436-7-2 http://hdl.handle.net/1826/3832

is $x_1 = \sqrt{\frac{F\ \lambda_2}{E\ \lambda_1}} = x_4$, $x_2 = \sqrt{\frac{2F\ \lambda_2}{E\ \lambda_1}} = x_3$, where $\vec{\lambda} = (\lambda_1, \lambda_2) > 0$. This means that the engineering designer has to use bars with cross-sectional areas satisfying this relationship so as to get the best minimum values for both the volume V of the truss (f_1) and the displacement Δ of the joint (f_2). Knowing the exact relationship between the design variables which will be used in formulating the Pareto front helps the engineers to find exact and optimal solutions for manufacturing.

Conclusion

A mathematical approach to solve engineering design problems based on Karush-Kuhn-Tucker conditions was presented. The main advantage of this approach is that it gives the exact equation of the Pareto front in an analytical form. Furthermore, it guides to the relationship between the design variables which are responsible for formulating this equation. The approach also provided mathematically precise results and this is significantly different to the approximations yielded by numerical state-of-the-art algorithms.

References

1. Deb, K.: Multi-objective Optimisation Using Evolutionary Algorithms. Wiley, UK (2001)
2. Miettinen, K.: Nonlinear Multi-Objective Optimisation. Kluwer, Boston (1999)
3. Kuhn, H.W, and Tucker, A.W.: Nonlinear Programming. Proceedings of the Second Berkeley Symposium on Mathematical Statistics and Probability, 481-491 (1950)
4. Benson, H.P.: Existence of Efficient Solutions for Vector Maximisation Problems. Journal of Optimisation Theory and Applications, 26(4), 569-580 (1978)
5. Hanson, M.A.: A Generalisation of the Kuhn-Tucker Sufficiency Conditions. Journal of Mathematical Analysis and Applications, 184, 146-155 (1994)
6. Craven, B.D.: Modified Kuhn-Tucker Conditions When a minimum is Not Attained. Operations Research Letters, 3(1), 47-51 (1984)
7. Miettinen, K. and Makela, M. M.: On cone characterisations of weak, proper and Pareto optimality in multi-objective optimisation. Mathematical Methods of Operations Research, 53, 233-245 (2001)
8. Svanberg, K.: A class of globally convergent optimisation methods based on conservative convex separable Approximations. SIAM Journal of Optimisation, 12(2), 555-573 (2002)
9. Fonseca, C. M. and Fleming, P. J.: An overview of evolutionary algorithms in multi-objective optimisation. Evolutionary Computation Journal 3(1), 1-16, 1995.
10. Engau, A. and Wiecek, M. M.: Generating ε-efficient solutions in multi-objective programming. European Journal of Operational Research 177(2007) 1566-1579
11. Askar, S.S., Tiwari, A., Mehnen, J., and Ramsden, J.J.: A survey of state-of-the-art techniques to construct Pareto front analytically. JOTA (submitted, 2007)
12. Arora, J.S.: Introduction to optimum design. Elsevier Academic Press, UK (2004)

 Published by Cranfield University Press ISBN: 978-0-9557436-7-2 http://hdl.handle.net/1826/3832

Role of Acoustic Emission in condition based maintenance of slow speed bearings

M. Elforjani, D. Mba
School of Engineering, Cranfield University, Cranfield, Beds. MK43 0AL

Abstract

The principal aim of condition based maintenance is to improve system, and subsystem, life cycle costs, maintain system availability and reduce energy wastage due to non-optimum operation. To achieve these objectives the earliest detection of loss of mechanical integrity is of paramount importance. This paper demonstrates the use of Acoustic Emission (AE) measurements to detect natural defect initiation and propagation in a rolling element bearing. To facilitate the investigation a special purpose test-rig was built to allow for accelerated natural degradation of a bearing race. It was concluded that crack propagation is detectable with AE technology.

Introduction

Although rotating machinery has relatively little impact on the environment compared to other industrial applications, concerns can be raised over the energy losses due to any mechanical degradation that may occur in its vital components. Hence, failure detection of such vital components is important as any mechanical degradation or wear will often progress to more serious damage affecting the operational performance of the machine. This requires far more costly repairs than simply replacing a part. Reliable and robust monitoring systems can lead to scheduled corrective maintenance minimising collateral environmental impacts and the costs of failure.

Acoustic Emission (AE) is defined as the class of phenomena whereby transient elastic waves are generated by the rapid release of energy from localized sources within a material [1]; typical frequency content of AE is between 100 kHz to 1 MHz. A tremendous amount of work has been undertaken over the last 20-years in developing the application of the Acoustic Emission technology for bearing health monitoring [2]. Jamaludin et al [3] presented the challenges faced with using the vibration technology to monitor the mechanical integrity of slow speed bearings (less than 60rpm) and suggested that the AE technology could overcome such difficulties.

To date the only investigation on identification of the onset of natural degradation in bearings with AE was presented by Yoshioka [4]. This focused on detection of a rolling contact subsurface fatigue crack using AE technology. An acoustic emission source locating system was developed. Yoshioka presented results where cracks were actually found parallel to the surface. It is worth noting that Yoshioka employed a bearing with only three rolling elements which is not representative of a typical operational bearing. Moreover, Yoshioka terminated AE tests once AE

 Published by Cranfield University Press ISBN: 978-0-9557436-7-2 http://hdl.handle.net/1826/3832

activity increased as such the propagation of identified sub-surface defects to surface defects was not monitored. This work builds further on the work of Yoshioka by monitoring not only the initiation of cracks, but also its propagation to spalls or surface defects on a conventional bearing. The location of the AE source was also monitored throughout the test sequence in order to validate that the AE's generated throughout the test period can be eventually attributed to the surface defect noted at the end of the test.

Experimental procedure and equipment

One of the challenges is to enhance the crack signatures at the early stage of defect development. To implement this, bearing run to failure tests were performed under natural damage conditions on this specially designed test rig. To accelerate crack initiation, a combination of a thrust ball bearing and a thrust roller bearing was selected. One race of ball bearing (SKF 51210) was replaced with a flat race taken from the roller bearing (SKF 81210 TN) of the same size, see figure 1. Consequently, the rolling ball elements on a flat track caused very high contact pressure in excess of 6,000MPa. To determine the sub-surface stresses on the test bearing and thereby estimate the time to surface fatigue on the race the following theories were employed: the Hertizan theory for determining surface stresses and deformations, Thomas and Hoersh theory for sub-surface stress, and, the Lundberg and Palmgren theory for fatigue evaluation. For the grooved race the standard procedure, as described by BS 5512; 1991, was employed for determining dynamic load rating. The test rig rotational speed was 72 rpm and an axial load of 35kN was employed for this particular test. The test rig layout can be seen in figure 2.

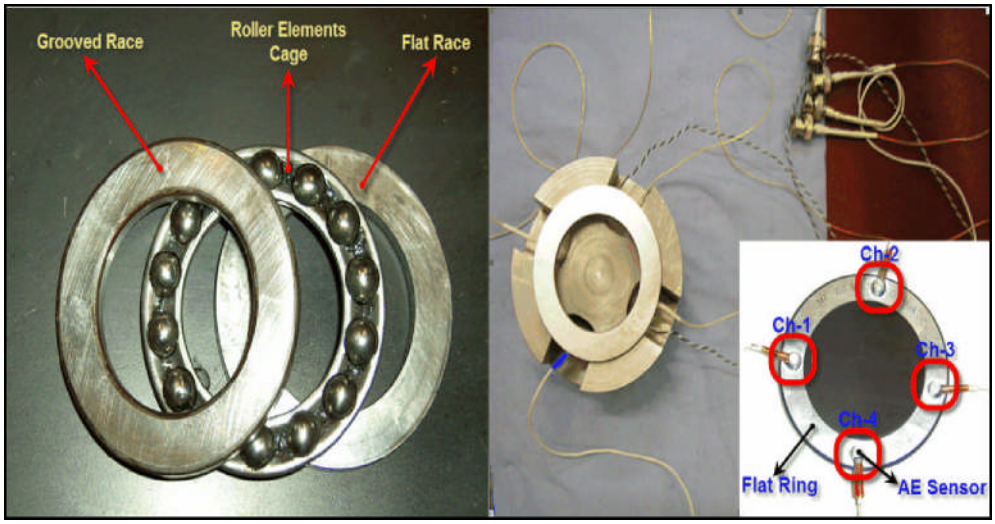

Figure 1Test bearing

 Published by Cranfield University Press ISBN: 978-0-9557436-7-2 http://hdl.handle.net/1826/3832

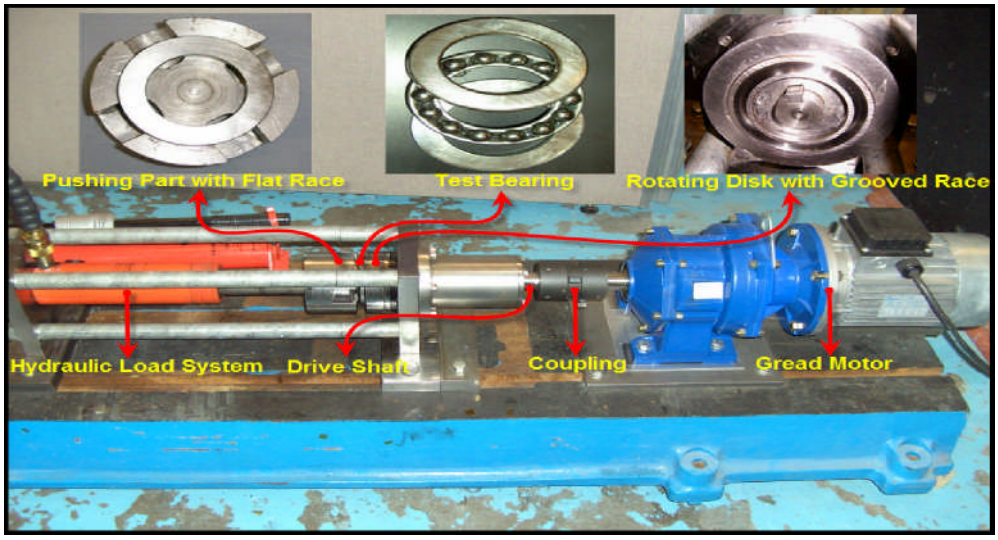

Figure 2 Experimental test-rig

A commercially available piezoelectric sensor (Physical Acoustic Corporation type "PICO") with an operating range of 200-1000 kHz was used. Four acoustic sensors, together with two thermocouples were attached to the back of the flat raceway using superglue. The acoustic sensors were connected a data acquisition system via a preamplifier, set at 40 db gain. The system was continuously set to acquire AE waveforms at a sampling rate of 2 MHz. The software (signal processing package "AEWIN") was incorporated within the PC to monitor AE parameters such as counts, r.m.s, amplitude, ASL and energy (recorded at a time constant of 10 ms and sampling rate of 100 Hz), see figure 3.

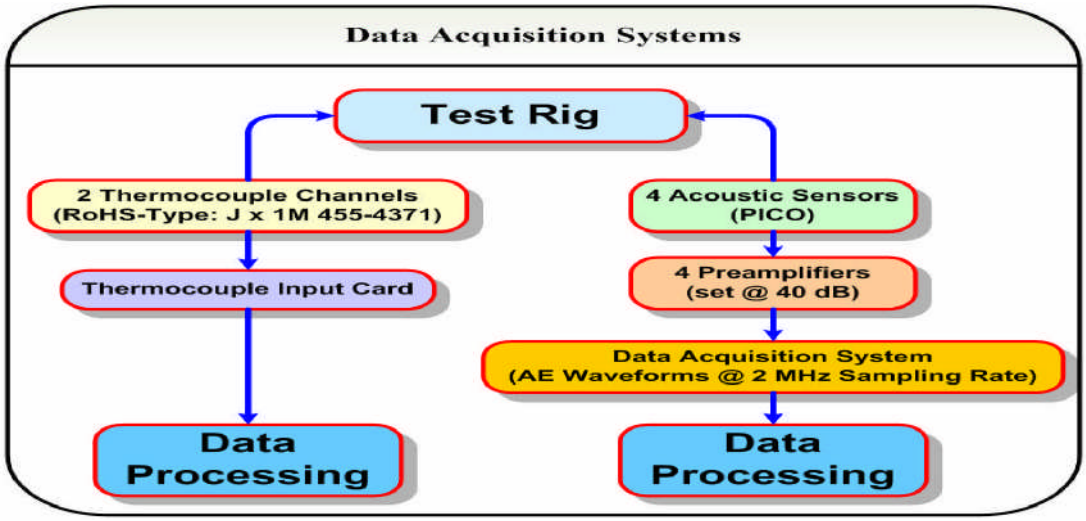

Figure 3 Schematic of the data acquisition systems

 Published by Cranfield University Press ISBN: 978-0-9557436-7-2 http://hdl.handle.net/1826/3832

Experimental results observations and discussions

Under normal conditions of load, rotational speed and good alignment, surface damage begins with small cracks, located between the surface of the flat track and the rolling elements, which gradually propagate to the surface generating detectable AE signals. During the first two hours of the test, an increase in AE activity levels and temperature was noted. This was attributed to run-in as after this period (2 hrs) all measured AE parameters and temperature remained constant. Figure 4 shows monitoring of the AE levels over 11-hours of bearing operation that reflect the general observations associated with over a dozen experimental tests. A relative increase in AE level was noted between 5- and 6-hrs of operation see figure 4. The initiation of the plastically deformed pathway was attributed to this sharp burst of AE activity, as visually observed at this period in the test. At 7-hrs into operation the AE levels returned to levels noted prior to the increase in AE activity. It was also observed that at approximately 9.5-hrs into the test AE showed significant increases in AE activity until the test was terminated (11 -hrs). Lubricant temperature was undertaken by two thermocouples channels attached to the back of the flat raceway. Following run-in (0- to 2-hr) the bearing temperature stabilized at 35 °C and after 1 1-hrs operation a maximum temperature of 37 °C was recorded, see figure 4. The surface damage observed on the termination of the test (11 -hrs) is presented in figure 5.

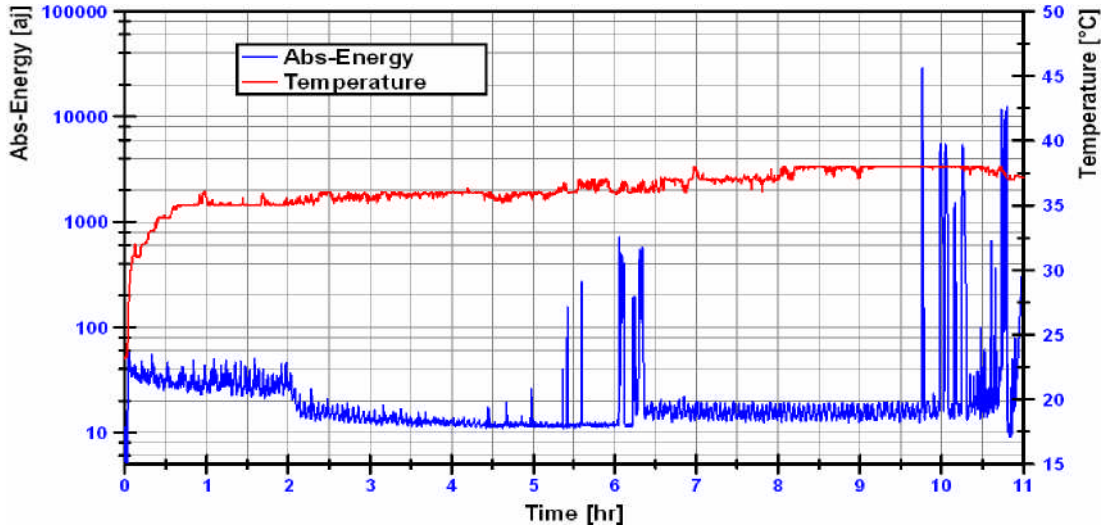

Figure 4 Observations of a run-to–failure bearing test.

 Published by Cranfield University Press ISBN: 978-0-9557436-7-2 http://hdl.handle.net/1826/3832

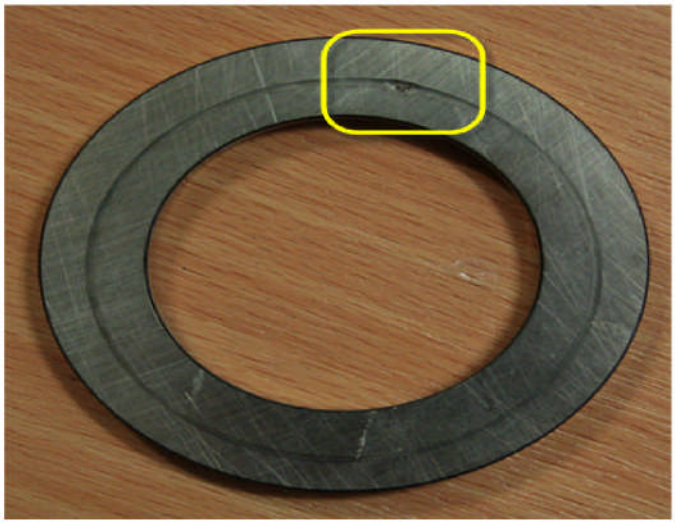

Figure 5 Surface damage on flat bearing race, see 'box' section

AE waveforms, recorded during the test, clearly showed high AE transient events after 6-hours. A strong evidence of 9Hz on the termination of the test (11 -hrs) indicating one defect on the flat race, see figure 6. This phenomenon had been noted by Al-Ghamdi et al [5].

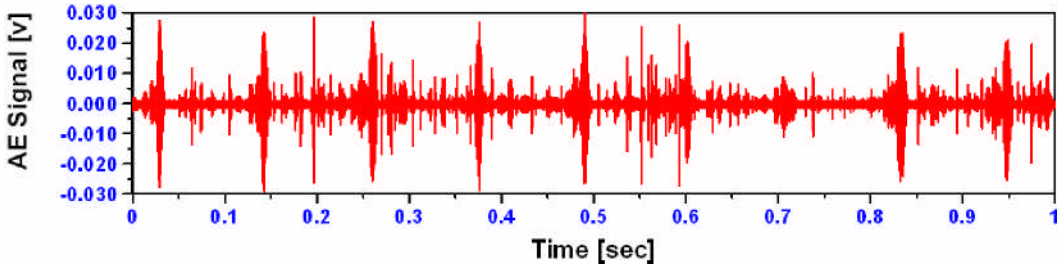

Figure 6 Waveform showing periodicity of bursts

Conclusion

The study has demonstrated that AE parameters such as energy are reliable, robust and sensitive to the detection of incipient cracks and surface spalls in slow speed bearing. It is concluded that condition monitoring of slow speed bearings using AE technology can complement other existing condition monitoring technologies all of which are aimed at reducing energy losses and improving life cycle costs.

Reference

1. ISO 22096; Condition monitoring and diagnosis of machines – Acoustic Emission. 2007.
2. Mba, D., Rao, Raj B. K. N. Development of Acoustic Emission Technology for Condition Monitoring and Diagnosis of Rotating Machines: Bearings, Pumps, Gearboxes, Engines, and Rotating Structures. The Shock and Vibration Digest 2006 38: 3-16.
3. Jamaludin N.; Mba D.; Bannister R. H., Condition Monitoring of Slow-Speed Rolling Element Bearings Using Stress Waves, Proceedings of the IMECHE Part E Journal of Process Mechanical Engineering, Volume 215, Number 4, 1 November 2001, pp. 245-271(27), Publisher: Professional Engineering Publishing.

 Published by Cranfield University Press ISBN: 978-0-9557436-7-2 http://hdl.handle.net/1826/3832

4. Yoshioka, T. Detection of rolling contact subsurface fatigue cracks using acoustic emission technique, Journal of the Society of Tribologists and Lubrication Engineers, Volume 49, June 1992.
5. Al-Ghamdi, Abdullah M.; Mba, David, A Comparative Experimental Study on the Use of Acoustic Emission and Vibration Analysis for Bearing Defect Identification and Estimation of Defect Size, Issue Date: 2005, Publisher: Elsevier Science.

 Published by Cranfield University Press ISBN: 978-0-9557436-7-2 http://hdl.handle.net/1826/3832

Business Process Mining: A Soft Computing Approach

Chris Turner and Ashutosh Tiwari
School of Applied Sciences, Cranfield University,
Cranfield, Bedfordshire, UK.

Abstract

Business processes are becoming ever more complex. Managers need to have an accurate picture of how a business process is operating in a live environment and guidance on how a process can be improved. For some time, Enterprise Resource Planning (ERP) software products have been able to record execution data for an organisation's live hosted processes in the form of an event log. This paper concerns the design of a business process mining algorithm to reconstruct processes from such event logs. The algorithm combines the power of Genetic Algorithms (GA) with hierarchical clustering techniques. In addition the algorithm will allow for the input of expert knowledge at an intermediate stage in the mining of complex processes. Outlines are provided of the combined GA clustering algorithm to be employed in this mining approach. This paper details the current strengths and weaknesses of the GA and hierarchical clustering approaches and concludes why the proposed approach will be more appropriate for the mining of complex processes from event logs containing noise and exhibiting common business process mining problems.

Introduction

Business processes are becoming ever more complex. Managers need to have an accurate picture on how a business process is operating in a live environment and guidance on how a process can be improved. For some time, Enterprise Resource Planning (ERP) software products have been able to record execution data for an organisation's live hosted processes. Such data typically contains detail on process tasks and the times at which they are executed. It is possible to manually reconstruct a flow chart of a process from this data showing how the tasks link together; however, this is a time consuming and error prone task. Automated process mining methods have been proposed by academic groups to solve this issue, though there are many challenges that a business process mining algorithm must address. The mining and analysis of complex business processes is difficult, along with the definition of what constitutes a complex process; Cardoso et al. [1] review the measurement of process complexity in detail. Taking the findings of [1] into account for the purposes of thispaper complexity can be thought of as a process exhibiting complex control flow (in effect a process that allows a large number of paths to completion). Business process mining algorithms must contend with a range of problems that may be found in

 Published by Cranfield University Press ISBN: 978-0-9557436-7-2 http://hdl.handle.net/1826/3832

event logs, such as loops, duplicate tasks and noise [2]. A range of business process mining approaches exist that are able to cope with different process mining problems. One particular mining algorithm is able to cope with an extensive range of problems [3]; the approach of Alves de Medeiros et al. [4] makes use of a Genetic Algorithm (GA) to render process representations from event logs containing noise and other difficult to mine constructs such as loops and duplicate tasks. However there are certain limitations of this particular algorithm in that while simple processes can be mined with relative ease more complex patterns, including those containing duplicate tasks and parallel constructs, present difficulties [5] [6]. The GA of [4] also takes a substantial amount of time to execute for more complex processes. The algorithm of Greco et al. [7] introduces a hierarchical clustering technique which is able to mine complex business processes from event logs in a relatively short time. The technique clusters together similar looking process traces from the event log and produces a schema for each cluster. The algorithm takes an iterative approach to schema refinement leading to the production of a process model based on the set of schemas (a disjunctive workflow schema) [7]. However this approach is limited as the process data to be mined must be free of noise; in addition process constructs such as loops and duplicate tasks cannot be mined effectively by the algorithm of [7]. This paper investigates the possible combination of a GA approach to process mining with a clustering approach and the potential role expert knowledge can play in the accurate and efficient mining of complex processes from noisy event logs.

Related Research

Early work by Agrawal et al. [8] introduced the use of mining techniques in the extraction of process flow graphs from workflow application data. Process mining as a practice also owes much to the work of Cook and Wolf [9], who conducted research into the extraction of process models from data logs. Cook and Wolf [9] while not directly relating their work to that of business process discovery did examine the use of three statistical analysis methods for use in the mining of software processes. One of the most popular business process mining algorithms is the α algorithm introduced by van der Aalst et al. [10]. These authors explore a group of workflow process models that can be discovered in full from a process log. The initial version of this algorithm was only able to mine on the basis of complete and noise free event logs. However several extensions have been made to this approach, to deal with common mining problems, such as one to enable the mining of short loops [11]. The use of GAs for the mining of business processes has been investigated by Alves de Medeiros [4]. While most current techniques can only overcome one or two mining problems the GA approach of [4] can address a much wider range of problems and mine a greater number of process types. Greco et al. [7] introduces a hierarchical clustering technique which is able to mine complex processes from noise free event

 Published by Cranfield University Press ISBN: 978-0-9557436-7-2 http://hdl.handle.net/1826/3832

logs in a relatively short time. This approach is limited in that it cannot tackle many of the problems inherent in process mining such as noise.

Combining GA and Hierarchical Clustering Approaches

This paper proposes that the approach of Greco et al. [7] could be used in combination with the GA of Alves de Medeiros et al. [4]. Both techniques present advantages and disadvantages, as demonstrated below in Table 1. The combination of the techniques may achieve a better mining outcome for complex processes contained in noisy problematic event logs.

Table 1. Advantages and disadvantages of the GA and Clustering mining approaches.

Genetic Algorithm approach [4] **Advantages**	**Disadvantages**
Able to mine noisy process logs	It is very slow to run
Can cope with many of the common mining problems when mining simple processes	The mining of complex processes including those with duplicate tasks and parallel constructs is not always accurate
Can mine complex sequences containing non-free choice and invisible task constructs	Low frequency process sequences can be missed
Hierarchical clustering approach [7] **Advantages**	**Disadvantages**
Can mine complex processes accurately given a perfect problem free event log	Not able to mine noisy process logs
It is fast to execute	Cannot cope with looping constructs and task duplicates
Can display a hierarchical view of a process	

The approach explained

There are several approaches that can be taken to combine the two techniques, though the approach proposed by this paper is to use the clustering algorithm to cluster event log traces by a common feature; the main steps of the approach are shown in Figure 1. A feature selection step is used to identify common features in the event log as a whole. Each trace in a cluster contains a feature common to all traces in that cluster. This is used in combination with a set of heuristics (used by the GA to generate an initial random population of individuals) to generate the initial population for each of the clusters. Expert users will then be able to select sequences of an identified common feature and assign a level of confidence to each construct within the sequence (at the intermediate mining view shown in Figure 1). This allows for pattern comparison between the selected sequences and process models produced by subsequent mining activities carried out by the GA. The level of matching will be fed into the fitness function of the GA and act as an extra weighting. The GA is then applied to each cluster for 500 generations each. The resulting process model from each cluster is then combined (proportionally by the amount of

 Published by Cranfield University Press ISBN: 978-0-9557436-7-2 http://hdl.handle.net/1826/3832

traces in the cluster) to give an overall process model. The ProM framework's [13] graph display capabilities will be utilised for this final stage. This approach is partly based on suggestions by Greco et al. [12] (when combining the clustering algorithm with another process mining algorithm) and has been selected for the proposed approach.

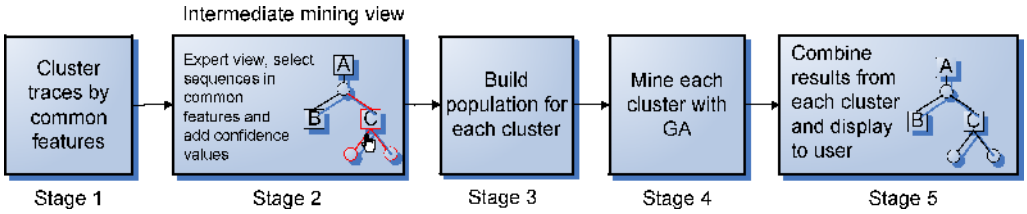

Figure 1: An outline of the proposed process mining approach

The approach will be programmed within the process mining framework ProM (van Dongen et al. [13]) and utilize the clustering algorithm of Greco et al. [7] and the GA of Alves de Medeiros [5], both available as plug-ins within ProM.

Additional amendments and experiments

The mutation and crossover functions of the GA will change in the proposed approach. Initially a decaying rate of mutation will be used as this has proved to be useful in the mining of simple processes [6]. Later experiments may involve the automated adjustment of mutation rate depending on the current fitness level during the running of the GA. Again further experimentation will also focus on the selection and swapping of process sequences based on encountered problems [4] and the selections made by experts at the intermediate mining stage.

The Role of Expert Knowledge in Process Mining

In the mining of complex processes there is often an advantage to introducing expert knowledge in the interpretation of certain sub process patterns. It could be advantageous for an expert, through a visual interface, to select certain sequences in identified common features and ask the algorithm to look for and accept similar sequences in the event log data. In doing this an expert may a have varying level of confidence in certain decision constructs and task edges (process task links) within a process. In the same way sequences that an expert does not hold so much confidence in may be negatively weighted.

Conclusion and Future Research

There is a need today for companies to be able to analyse how their processes actually operate in a live environment. The approach outlined in this paper addresses the need for organizations to be able to accurately mine complex processes from event logs containing noise, common mining

 Published by Cranfield University Press ISBN: 978-0-9557436-7-2 http://hdl.handle.net/1826/3832

problems and low frequency activities. The combination of the GA with its ability to mine in the presence of noise and other mining problems and the clustering algorithms accuracy and speed provides the potential to provide an improved process mining algorithm. The clustering of traces will also aid in the provision of an intermediate stage in the algorithm allowing experts to select sequences within identified common features. In this way importance may be given to certain sequences that might otherwise be ignored by independent use of the GA or the clustering algorithm. The approach will provide a tool that will mine complex processes in an accurate and time efficient manner and allow for the input of knowledge from an organisation's business process experts.

References

1. Cardoso, J., Mendling, J., Neumann, G., and Reijers, H.A.: A discourse on complexity of process models. In: Eder, J. and Dustdar et al. (eds.): BPM 2006 Workshops, LNCS 4103, Springer-Verlag, Berlin (1996) 117–128
2. Aalst, W. M. P. and Weijters, A.J.M.M.: Process mining: a research agenda. Computers in Industry (53) (2004) 231-244.
3. Tiwari, A., Turner, C.J., Majeed, B. (2008) A Review of Business Process Mining: State of the Art and Future Trends, Business Process Management Journal (BPMJ), 14 (1), pp 5-22.
4. Alves de Medeiros, A. K., Weijters, A.J.M.M., and van der Aalst, W.M.P.: Genetic process mining: A basic approach and Its Challenges. In: Bussler et al. (eds.): BPM 2005 Workshops, LNCS 3812, Springer-Verlag, Berlin (1995) 203–215
5. Alves de Medeiros, A. K,: Genetic process mining. Ph. D Thesis, Eindhoven Technical University, Eindhoven, The Netherlands, (2006).
6. Turner, C. .J and Tiwari, A.: An experimental evaluation of genetic process mining. Proceedings of the Genetic and Evolutionary Computation Conference (GECCO) London (2007) 2268.
7. Greco, G., Guzzo, A., and Pontieri, L.: Mining hierarchies of models: from abstract views to concrete specifications. In: van der Aalst et al. (eds.): BPM 2005 LNCS 3649, Springer-Verlag, Berlin (2005) 32–47.
8. Agrawal, R., Gunopulos, D., and Leymann, F.: Mining process models from workflow logs, in Schek, H. J., Proceedings of the 6th International Conference on Extending Database Technology: Advances in Database Technology. Heidelberg, Springer Verlag (1998) 469-483.
9. Cook, J. E. and Wolf, A. L.: Discovering models of software processes from event-based data, ACM Transactions on Software Engineering and Methodology, Vol. 7 No. 3, (1998) 215-249.
10. van der Aalst, W. M. P., Weijters, A.J.M.M. and Maruster, L.: Workflow mining: discovering process models from event logs. IEEE Transactions on Knowledge and Data Engineering 16, (9) (2004) 1128-1 142.
11. Alves de Medeiros, A. K.; van Dongen, B. F.; van der Aalst, W. M. P., and Weijters, A. J. M. M.: Process mining, extending the a-algorithm to mine short loops. BETA Working Paper Series WP1 13 Eindhoven University of Technology (2004).
12. Greco, G., Guzzo, A., Pontieri, L., and Sacca, D.: Discovering expressive process models by clustering log traces. IEEE Transactions on Knowledge and Data Engineering; 18, (8) (2006) 1010-1027.

 Published by Cranfield University Press ISBN: 978-0-9557436-7-2 http://hdl.handle.net/1826/3832

13. van Dongen, B. F.; Alves de Medeiros, A. K.; Verbeek, H. M. W.; Weijters, A. J. M. M., and van der Aalst, W. M. P.: The ProM framework: A new era in process mining tool support. Ciardo, G. and Darondeau, P. 26th International Conference on Applications and Theory of Petri Nets (ICATPN 2005). Heidelberg: Springer Verlag, (2005) 444-454.

 Published by Cranfield University Press ISBN: 978-0-9557436-7-2 http://hdl.handle.net/1826/3832

A Coevolutionary Perspective on Supply Networks

Liz Varga liz.varga@cranfield.ac.uk

This paper examines the contribution a coevolutionary perspective makes to the conception of a supply network as an complex adaptive system. The research in grounded in the aerospace manufacturing industry and in particular the supply networks which produce airplanes from design through to decommissioning. The need to understand the coevolution of supply networks is relevant to the current era of competing networks (Christopher, 2005); competition is no longer between organizations but between networks of interacting organizations involved in economic exchange, embedded in a particular structure (Powell, 1990). The definition of a supply network in the context of this paper is a network of organizational components which taken as a whole produce many instances of the same product model.

To demonstrate that evolutionary explanation is applicable to the population of supply networks, three requirements must be met (Murmann, 2003). Firstly, in order to introduce novelty into the economic system, there must exist a mechanism to create variants of existing structures. Secondly, new variants need to be created more often than the changes in selection criteria, otherwise evolutionary processes would not bring about new trial and error structures that are better adapted. Thirdly, there must be retention mechanisms that transmit economic structures from the present to the future. This paper shows that supply networks are evolutionary but, more importantly, this paper shows that supply networks are coevolutionary, emerging as complex adaptive systems, influencing and being influenced by their environments, in reciprocated evolution.

The case for a coevolutionary perspective on organizations as complex adaptive systems is well established (for example, Garnsey and McGlade, 2006). In complex systems terms, the environment is merely another layer in a nested system "*every system takes all other systems as its environment; systems co-evolve as they complexly adapt to their environment"* and which coevolves with the systems that constitute the environment "*the environment or landscape that each system faces is changed as a result of changes in the systems that constitute the landscape"* (Kauffman, 1993). Supply networks, which have emerged through the combination of organizations, are merely another layer of a nested system, so they too are complex adaptive systems. Coevolutionary theory extends evolutionary theory further and focuses on competitive leadership positions and how they are lost and gained over time (Murmann, 2003). Unlike static theories, coevolutionary theory is not bound by rules that require the same proportions of market share to apply consistently. Thus a supply network with a large leadership in market share need not have started out with a significant lead. This is explained by the butterfly effect (Lorenz,

 Published by Cranfield University Press ISBN: 978-0-9557436-7-2 http://hdl.handle.net/1826/3832

1963) in which the flap of a butterfly's wings in one region of the world could affect weather patterns in another. The current study examines from a coevolutionary perspective the nature of the supply network by considering two dimensions: structure and behaviour.

Structure

The structure of a supply network emerges from the underlying genetic code or internal diversity of the system. This genetic code is located within the components of each firm - its practices, routines, buildings, machinery and so on. The potential structures that might emerge are limited by the genetic codes of the firms. Unlike biological organisms, the genes of firms are not static, changes occurring more frequently in some firms than others. The extant form of an organization is the outcome of its components and its relationships with other organizations. This organizational history is carried into each supply network membership; the supply network becomes a confederation of many histories and thus has a unique character which is the consequence of irreversibility and path-dependency; the past co-produces the present and the future (Maguire, McKelvey, Mirabeau, and Õztas, 2006).

The context of the selection environment, locating the supply network within a particular space-time, is a fundamental coevolutionary perspective. Mutual adaptation of the evolving unit and the selection environment (Murmann, 2003). Global techno-economic paradigms, latterly the 3rd globalisation, have created new opportunities for supply networks, such as broadband for volume information flow and the global division of labour. And just as the environment enables the evolution of the supply network, so to does the growth of air-traffic affect the environment with its attendant infrastructure, CO_2 emissions, but also enabling of international cooperation and social mobility.

A number of supply network forms related to different types of governance can be qualitatively differentiated: the hierarchy, the heterarchy, the 4PL™, the Keiretsu (in the Far East). Hierarchies are created via vertical integration and thus ownership of firms; control and direction is possible at a strategic level. Heterarchies at the other extreme are found where the market is able to supply competing firms with requisite skills, for example, OEMs supplying electrical systems to many airframe integrators (and to other industries). The 4PL™ (fourth-party logistics service provider) is a hybrid organization typically formed from parts of organizations as a joint venture or long-term contract. The Keiretsu, originally from Japan, is a form of network structure in which a central bank exerts control over the supply network. Each of these network forms has appeared as a consequence of adapting to boundary conditions, consciously changing them to enable the teleological (goal

 Published by Cranfield University Press ISBN: 978-0-9557436-7-2 http://hdl.handle.net/1826/3832

oriented) nature of the supply network. These network forms can be described in more detail by considering their density and centrality (for example, Barabasi, 2002, Kauffman, 1993) and their

diversity, that is, their mix of organization types. Supply network membership and the mix of components (planned or otherwise) are critical to the performance of the supply network. Analyses of the most effective strategic alliances (or long term inter-organizational relationships) indicate that there needs to be some level of similarity but also some level of difference between components (Parkhe, 1991).

New layers or tiers have emerged within the supply network reflecting the creation of sub-systems. This appears to have been driven by the large and increasing numbers of components within the final aerospace products. Airframe integrators have responded by reducing, in some cases dramatically, the numbers of first tier supplier. A new layer or class of strategic first tier suppliers managing landing sub-systems, flight sub-systems and so on has been created and these firms are now managing many of the suppliers who were previously first tier suppliers. Whilst not fully decomposable (Simon, 2002), coordination within the supply network has been reduced reflecting the nature of the supply network as a complex adaptive system. The environment has facilitated the increased complexity of products driven by the current techno-economic paradigms (Tuomi, 2007). Supply network structures have become more layered and have organized into sub-systems which can more easily manage the increased complexity of products. Environment and supply network have coevolved, each affecting the other in a significant way.

Behaviour

Supply network structure thus emerges from the unique set of components within the supply network. These structures have emergent properties, for example, quality or agility emerge. These emergent capabilities may be planned (given some post-hoc rationalization) but unintended capabilities, desirable or otherwise, may also emerge. Importantly, structures emerge at many layers and one structure can be partially contained within a structure at the next layer; enabling and constraining the potential for new emergent properties at the next layer (Fuller and Warren, 2006).

Adaptive evolution of a complex system occurs as its states (variants) are modified in ways to enhance its chances for success (Capra, 1996; Kauffman, 1995). The supply network variant may be found to perform better than current variants of the supply network. New variants are found through testing. Without trial and error, new variants cannot emerge. Such adaptive evolution in the classical Darwinian mould is thought to stem from random mutations which are then subject to

 Published by Cranfield University Press ISBN: 978-0-9557436-7-2 http://hdl.handle.net/1826/3832

natural selection (Holland, 1995). For complex adaptive systems, it is the emergence of properties at various layers that create new order or structure, via a process of self-organization and autocatalysis (Kauffman, 1995). The structure with its unique emergent properties is then selected within the environment. New variants are created by changes to the existing components of the supply network; new variants are selected for their superior emergent properties.

But in a complex adaptive system the same emergent property may be produced from a different set of practices; the outcome may be produced in more than one way (Holling, 1986) and so the system is resilient. As the system is complex, we cannot say for certain which pathway produced the emergent property. The components are necessary but not sufficient to explain the emergent property. Interfering with the supply network may affect the properties of the system. If we reconfigure or remove components, then the desired property may not emerge. The behaviour of the supply network is limited by the components within the network, both locally and holistically. Coevolutionary processes create emergence through the combination of many components, including physical, informational and technological. Neo-classical methods would not allow the comparison of components of such different orders. By taking a coevolutionary approach we approach a more realist perspective of the components and mechanisms operating within the supply network. Decision-makers adopt new or replacement components (e.g. practices) in order to generate particular outcomes, such as cost efficiency, delivery performance and innovation. It is therefore important to have the right practices to stimulate the creation of intended emergent properties. And having the right components at the right time or stage in the product model life cycle is also critical. At different points within the life-cycle, different components are more important, such as freedom to experiment in order for innovation to emerge during the early stages and perhaps cost control and lean methods to extend the product life-span in later stages.

The organizations and the supply networks to which they belong are dynamic and need to adapt. An action may have varying effects on different parts of the complex system resulting in varying degrees of feedback, driving virtuous or vicious cycles (Holland, 1998). Adaptation can enhance positive feedback which are self-reinforcing processes of organizations and will allow small differences to be amplified (Arthur, 1994) so long as they dominate negative feedback which acts as a self-regulatory mechanism (Capra, 1996). At times there is a need to combat non-linearities, including the bull-whip effect which can spiral out of control between tiers in the supply network. Thus each organization in the supply network directly and indirectly affects the performance of all other supply network members as well as ultimate supply network performance (Cooper, Lambert and Pagh, 1997) in a non-equilibrium manner. A high rate of change in components may introduce greater diversity

 Published by Cranfield University Press ISBN: 978-0-9557436-7-2 http://hdl.handle.net/1826/3832

into the supply network which favours the creation of novel variants however supply network governance may limit flexibility for innovation.

Each organization contributes different components to the supply network. Mostly, these components are shared by many supply networks, for example, the same equipment may be used for another product-model or human resources may manage information relating to many product-models. In order for the supply network to evolve from its character at initial implementation stage, one or more components of the supply network must change causing a change in the supply network. This means that a change in a shared component can trigger a structural change in more than one supply network. Adaptability is enhanced among the system's components if there is a modest degree of interaction among the system's components (Ashby, 1960); this drives the need for standardization and the ability of shared low-level components to have consistent interfaces. The more 'shared' the component is, the more difficult it is to adapt, thus there is likely to be less evolutionary potential. If the component is wholly owned, or largely owned, the air-frame integrator can decide to allow it to change in favour of the product-model. This may have an effect (evolutionary or otherwise) upon the air-frame integrator's other product-model supply networks.

New supply network variants, replacing underperforming entities through a process of creative destruction (Schumpeter, 1942) are desirable if they can make better use of resources. Learning from past variants would be useful but because of the non-linear nature of interactions, this is likely to be limited. Miles and Snow (2007) identify a research gap for new models of inter-firm organization and collaboration which can exploit knowledge. If we recognize the supply network as a complex adaptive system, then we need to be aware of the limits of knowledge (Allen, 2001b) and very limited predictability within the supply network. Qualitative descriptions of the components and the emergent properties of supply networks can be of immense value in understanding the nature of the supply network and qualitatively similar supply network forms can then be compared and contrasted to develop knowledge in this area.

Summary

By looking at the structure and behaviour of supply networks, this paper has used a coevolutionary perspective to make sense of the creation, selection and retention of different variants of supply network and the coevolution of the supply network. It discussed the sources of variety as the components within the supply network, some of which are shared. It showed how new variants were created from existing variants via path-dependent evolution of supply networks, and that variants were selected for the superior emergent properties of the supply-network producing the

 Published by Cranfield University Press ISBN: 978-0-9557436-7-2 http://hdl.handle.net/1826/3832

product-model. Importantly, the coevolution of supply networks with the environment and the effect of one upon the other was demonstrated showing the non-linear and indeterminate nature of the evolution of the supply network.

References

1. Allen, P.M. (2001b), 'What Is Complexity Science? Knowledge of the Limits to Knowledge ',*Emergence,* Vol. 3, No. 1, pp. 24-42.
2. Arthur, W.B. (1994), *Increasing Returns and Path Dependence in the Economy,* University of Michigan Press, Ann Arbor.
3. Ashby, W.R. (1960), *Design for a Brain,* John Wiley & Sons, New York.
4. Barabasi, A-L. (2002), *Linked: The New Science ofNetworks* (1st edition), Perseus Books Group, New York.
5. Capra, F. (1996), *The Web ofLife: A New Scientific Understanding ofLiving Systems,* Anchor Books, New York, NY.
6. Christopher , M. (2005), *Logistics and Supply Chain Management: Creating Value-Adding Networks* (3rd edition), Pearson Education Ltd, Dorchester, England.
7. Cooper, M.C., Lambert, D. and Pagh, J.D. (1997), 'Supply Chain Management More Than a New Name for Logistics', *The International Journal ofLogistics Management,* Vol. 8, No. 1, pp. 1-13.
8. Fuller, T. and Warren, L. (2006), 'Entrepreneurship As Foresight: A Complex Social Network Perspective on Organisational Foresight', *Futures,* Vol. 38, pp. 956-97 1.
9. Garnsey, E. and McGlade, J. (Eds) (2006), *Complexity and Co-Evolution,* Edward Elgar Publishing, Cheltenham, UK.
10. Holland, J. (1995), *Hidden Order: How Adaptation Builds Complexity,* Perseus Books, Cambridge, MA.
11. Holland, J. (1998), *Emergence: From Chaos to Order,* Perseus Books, Cambridge, MA.
12. Holling, C.S. (1986), 'The Resilience of Terrestrial Ecosystems: Local Surprise and Global Change', in Clark, W.M. and Munn, R.E. (eds), *Sustainable Development in the Biosphere,* Cambridge University Press, Cambridge, pp. 292-320.
13. Kauffman, S.A. (1993), *The Origins of Order,* Oxford Univesity Press, New York.
14. Kauffman, S.A. (1995),*At Home in the Universe,* Oxford University Press, Oxford.
15. Lorenz, E.N. (1963), 'Deterministic Nonperiodic Flow', *Journal of the Atmospheric Sciences,* Vol. 20, 1,pp. 30-141.
16. Maguire, S., McKelvey, B., Mirabeau, L. and Őztas, N. (2006), 'Complexity Science and Organization Studies', in Clegg, S., Hardy, C., Lawrence, T. and Nord, W.R. (Eds), *The SAGE Handbook of Organization Studies,* Sage Publications Ltd, London,
17. Miles, R.E. and Snow, C.C. (2007), 'Organizational Theory and Supply Chain Management: An Evolving Research Perspective', *Journal of Operations Management,* Vol. 25, No. 2, March, pp. 459- 463.
18. Murmann, J.P. (2003), *Knowledge and Competitive Advantage: The Coevolution of Firms, Technology and National Institutions,* Cambridge University Press, Cambridge, UK.
19. Parkhe, A. (1991), 'Interfirm Diversity, Organizational Learning, and Longevity in Global Strategic Alliances', *Journal of International Business Studies,* Vol. 22, No. 4, pp. 579-601.

 Published by Cranfield University Press ISBN: 978-0-9557436-7-2 http://hdl.handle.net/1826/3832

20. Powell, W.W. (1990), *Neither Markets nor Hierarchy: Network Forms of Organization,* Kluwer Academic Publishers, USA.
21. Schumpeter, J.A. (1942), *Capitalism, Socialism and Democracy,* Routledge, New York.
22. Simon, H.A. (2002), 'Near Decomposability and the Speed of Evolution', *Industrial and Corporate Change,* Vol. 11, No. 3, June, pp. 587-599.
23. Tuomi, I. (2007), 'Learning in the Age of Networked Intelligence', *European Journal of Education,* Vol. 42, No. 2, Jun, pp. 235-254.

 Published by Cranfield University Press ISBN: 978-0-9557436-7-2 http://hdl.handle.net/1826/3832

Cognitive Analysis of Human-Human Interactions during Collaborative Decision Making

Matthias Groppe (matthias.groppe.ext@eurocontrol.int), Marc Bui (marc.bui@laisc.net),

Romano Pagliari (r.pagliari@cranfield.ac.uk)

Decision Making

Abstract

The objective of this study is to understand the cognitive mechanisms during Collaborative Decision Making (CDM) in typical Air Traffic Management (ATM) operation situations. It is based upon cognitive Human-Human Interactions (HHI) analysis in the asymmetric, distributed decision making environment with ATM domain characteristics.

In this paper, different flight and turn-round operation situations are compared and characterized by: (1) a face-to-face interaction mode, where all participating operators interact synchronously with each other through speech, and (2) an asynchronous or distributed interaction mode, where the participating operators interact with each other at different times and from different locations through a written text. Task and decision making for all situations is distributed between operators. The aircraft pilot's perspective and their information requirements during these flight and turn-round situations are used to identify critical information processing during CDM: All situations are usually time constrained, change quickly, and require a highly dynamic information transfer. Thereby, information sharing for decision making can be either homogenous having all operators the same information required or heterogeneous where information is not equally shared among operators.

This study relies on a structural model of team collaboration, developed for analysis on the cognitive mechanisms of CDM, and to handle both synchronous/ asynchronous and collocated/ distributed collaboration environments like in geographically distributed and time delayed situations of the military or flight operation.

Index Terms—Air traffic management, asynchronous distributed collaboration, collaborative decision making, human-human interaction

INTRODUCTION

CDM was initiated within ATM as a project of working together on operational level of aircraft operators, ground handling agents, airport,' air traffic control (ATC), and Central Flow Management Unit (CFMU) in order to challenge punctuality and reliability issues at increasingly congested airports. The CDM approach was introduced during field trials at selected European airports with the aim to achieve cooperation at *planning level* via information sharing and common situational awareness (CSA). However, from aircraft pilots' perspective on current air traffic operation, many problems

This study is conducted with the financial support from Eurocontrol Experimental Centre.

 Published by Cranfield University Press ISBN: 978-0-9557436-7-2 http://hdl.handle.net/1826/3832

encountered with CDM arise from human-human interactions (HHI) at *action level*; whereby HHI at *action level* refer to interactions with a shorter time span and less abstraction than HHI at *planning level* (Hoc, 2000). Further problems for CDM operation are conditioned on the specific situation of decision making in an *asynchronous*, *distributed* collaboration environment like it can be found in ATM operational decision making. Operators like aircraft pilots or ground handlers communicate with the operational centers of the airlines, ATC, and the airport through speech (e.g. via phone or radio = *synchronous interaction*) or written text (e.g. via ACARS = *asynchronous interaction*). Hence it will be addressed, how the airport CDM information sharing process is influenced by the following variables:

Cooperation Mode (face-to-face versus asynchronous-distributed)

Information Distribution (homogenous versus heterogenous)

Information Dynamics (static information content versus dynamic information content)

This cognitive analysis of flight situations also includes aspects of the *micro* level (neural-cognitive) on CDM. Even little understanding of operators think during CDM in asynchronous, distributed environment exists [25], an analysis of HHI within CDM via the perspective of a single operator (aircraft pilots) is used in order to cope with the still very inadequate mechanisms of collaborative problem solving during operators' decision making. According Ferber [1], HHI situations can be classified as antagonistic, cooperative, or indifferent depending on three main variable components like *aims, resources*, and *abilities,* hold by each participating operator. This classification is applied in order to understand the micro & macro level cognitive mechanisms of HHI in airport CDM flight operation situations. The advantage of using aircraft pilots as reference group is that there is a non punishment philosophy against pilots in dealing with punctuality problems. The presently use method of *delay assignment* intends to find out the reason of delay and assign the responsibility to a single operator via delay codes. Usually each operator tries to avoid assignment of a delay because a pay deduction has to be expected.

In this paper, prototypical HHI situations between all operators involved in flight and turn-round operation are introduced. They all take place in an asynchronous, distributed collaboration environment. Four proposed situations concern the turn-round of aircraft, where coordination of processes is necessary; processes include parking, ramp side, land side, and special ground handling processes. Within these situations, cooperative HHIs are mandatory: pilots have to coordinate processes with other operators like representatives of the ground handling companies, airport, airline, air traffic control, and Central Flow Management Unit. Cooperation and decision making is distributed between pilots and other operators: Decision making for the begin of all turn-round process which are in direct relation with the aircraft (e.g. boarding, de-boarding, refueling, cleaning..), is within responsibility of the pilots: other operators are concerned with decision making for coordination and execution of these processes, and again cooperate with each other. While any delayed process start can result in an overall delay of the subsequent flight, coordination of a standard turn-round (defined as a reference model) is usually predetermined.

During normal turn-round operation, *interactions* between pilots and other operators can be *asynchronous/ distributed* or *face-to-face*. Coordination takes place via predetermined key events (*milestones*) [8], organized as a sequence of interactions between operators within the airport operation centre; if a non-standard situation like aircraft change,

 Published by Cranfield University Press ISBN: 978-0-9557436-7-2 http://hdl.handle.net/1826/3832

technical repair adverse weather operation etc. occurs, interactions between pilots and other operators get mainly *synchronous* by ad hoc coordination of all necessary events *via face-to-face* communication between pilots and ramp agents or via radio/ phone between pilots and other operators coordinating from airport operation centre. The *milestone approach* used for CDM, includes *all* events which are necessary for an uninterrupted turn-round process, whereby some key events take place already far ahead of the turn-round itself. Information distribution during turn-round is *heterogeneous* between participating operators on *action* and *planning* level caused by the information dynamics in the highly dynamic environment of the turn-round operation and the varying tasks in the different domains itself. However, in order to cope with the usually limited time span for turn-round operation, CDM targets homogenous information processing to achieve a common situational awareness between all participating operators and to avoid departure delay caused by non-standard operation.

Another four proposed situations concern the flight, starting from aircraft leaving the parking position until reaching parking position at destination. Coordination here is also necessary for departure and arrival sequencing with other aircraft, usage of taxiways, airways and airspace/ sectors. It is pilots' responsibility to execute the flight according defined rules under consideration of highest degree of safety possible. Other operator involved during flight for coordination of traffic is air traffic control (ATC) by keeping safe separation distance between aircraft and managing air traffic flow by issuing clearances to the pilots. The different level of control between pilots and other operators like ATC in this situation is that ATC has authority about assigning the airspace in form of clearances to the pilots and again depend on cooperation from pilots, to adhere to these clearances. Decision making is shared between pilots and ATC within their domain relative to the situational need, but has to be executed under mentioned safety constraints. Other operators like the airline company or CFMU are only marginally involved in decision making during flight operation.

During flight operation, interactions between pilots and air traffic control are *synchronous* via radio during operation within present sector or when ATC issue clearances to the pilots. Interactions between ATC of different sectors can be *synchronous* or *asynchronous*, resulting in a non-coordinated flight through different sectors; interactions between pilots and other operators during flight are usually *asynchronous* and *distributed* by coordination of the *milestone events* within the airport control centre. Information distribution for clearances concerning airspace and routing is always homogenous, while information distribution for e.g. reasons of deviations from clearances can be homogenous or heterogeneous depending of the impartation willingness or time in hand from ATC and aircraft pilots.

Like during turn-round operation, the highly dynamic environment of the flight operation results in high dynamic information content. While some information dynamics like variations in flight progress occur on standard basis, changes are automatically accessible to all participating operators via human-computer interactions, but non-standard information dynamics like operational changes or technical issues are transferred by asynchronous interactions between aircraft pilots and other participating operators.

The overall goal of the study is to understand the cognitive mechanisms which are established during HHI between participating operators during turn-round and flight operation in order to optimize collaborative decision making activity in distributed and time-delayed ATM situations. The resulting objectives for the study are:

 Published by Cranfield University Press ISBN: 978-0-9557436-7-2 http://hdl.handle.net/1826/3832

To understand the cognitive processes of the HHI during day-to-day flight operation which are necessary in context of an asynchronous and distributed collaborative decision making environment.

To identify the information sharing components which should be employed to optimize the CDM concept in ATM typical standard & non-standard flight situations.

To understand how agents can support humans in achieving collaborative knowledge during asynchronous, distributed collaborative problem solving.

Theoretical Background

In our context of flight operation, HHI are seen as dynamic relations between pilots and other operators via a number of mutual actions. Each action by one operator has consequences which influence the behavior of the prospective behavior of the operators. Series of actions form events, and a number of events form the turn-round or flight situation (e.g. ATC assigns a parking position for the aircraft to the pilots (event) via mutual communication usually by two-way radio communication (HHI) in a turn-round situation). Ferber [9] defines interaction situations as *a number of behavioral patterns which evolves from a group of agents, who have to act in order to reach their targets and thereby have to regard their more or less limited resources and capabilities*. By using this definition, interaction situations can be described and analysed, because it defines abstract categories like cooperation, antagonism, and indifference via differentiation of observed key commonalities and different interaction situations. The relevant components for classification of interaction situations are the aims and intentions of the different agents, the relations of the agents to available resources, and abilities of the agents in regard to their assigned task. These criteria are used to define different types of interaction situations (*Figure 1*).

Aims	Ressources	Abilities	Type of Situation	Category
compatible	sufficient	sufficient	Independence	Indifference
compatible	sufficient	insufficient	simple working together	Indifference
compatible	insufficient	sufficient	blockade	Cooperation
compatible	insufficient	insufficient	Coordinated collaboration	Cooperation
incompatible	sufficient	sufficient	pure individual competition	Cooperation
incompatible	sufficient	insufficient	pure collective competition	Antagonism
incompatible	insufficient	sufficient	individual resource conflict	Antagonism
incompatible	insufficient	insufficient	collective resource conflict	Antagonism

Figure 1: Classification of Interaction Situations (Source: Ferber, 2001)

Each type of interaction situation has its own relation towards cooperation: In an *Indepence* situation, no interaction takes place and sufficient resources and abilities allow a coexistence of operators without any constraint. This situation has no relevance for ATM on congested airports. A *Simple Working Together situation* defines a collaboration situation which does not require coordination between operators, while a *Blockade, Coordinated Collaboration, Pure Individual/Collective Competition* and *Individual/Collective Resource Conflict* are situations which are expected to

 Published by Cranfield University Press ISBN: 978-0-9557436-7-2 http://hdl.handle.net/1826/3832

dominate in our contemplated HHI situations. These situations require coordination between operators and, depending on resources, aims, and abilities, can result in cooperative or antagonistic behavior.

During flight operation situations, HHI are usually not binding relations between involved actors and no mutual influence is exercised between pilots and other operators; therefore social components of the interactions are not contemplated.

According Hoc [12], cooperation can exist within various levels in terms of distance from the action itself: A cognitive architecture of cooperation model classifies cooperation in abstraction level and process time depending on the proximity to the action itself (*Figure 2*).

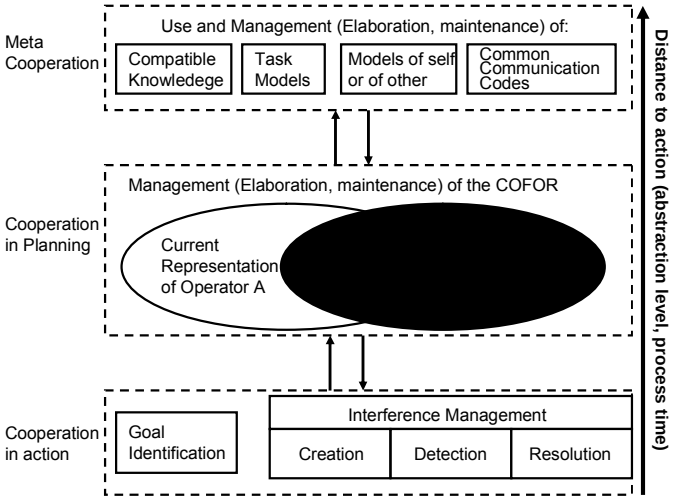

Figure 2: Processing Architecture of Cooperation (Source: Hoc 2000)

For the study of HHI situations, we focus on cooperation (or antagonism and indifference, if relevant) on action level. At *action level*, the operators perform operational activities related to their individual goals, resources, and abilities. Hoc [14] has defined four types of activities at action execution level which are interference creation (e.g. mutual control), interference detection, interference resolution, and goal identification (Goal identification also embodies identification of other operators goals). Cooperation at action level has short-term implications for the activity, as opposed to the more abstract type of cooperation at planning level. Interference creation relates to the deliberate creation of interactions; interference detection to the ability of detecting interferences, especially in non-deliberate interference situations; and interference resolution to the actual interaction in order to find a cooperative solution. Mutual domain knowledge is the basis for other operators' goal identification, to facilitate operator's own task, the other's task, or the common task.

At *planning level*, operators work to understand the situation by generating schematic representations that are organized hierarchically and used as an activity guide [13]. Schematic representations include the concept of situation awareness [23], and operators' goals, plans, and meta-knowledge [13]; therefore current approach to CDM operation in ATM is seen as an approach towards cooperation on planning level. De Terssac and Chabaud [7] use the term COFOR (Common frame of Reference) as a mental structure playing a functional role in cooperation and as a shared

 Published by Cranfield University Press ISBN: 978-0-9557436-7-2 http://hdl.handle.net/1826/3832

representation of the situation between operators likely to improve their mutual understanding [3]. The topmost level in Hoc's model, the meta-cooperation, as a level developed from knowledge of the other two levels, is not contemplated in the study.

Also Piaget [20] distinguishes between cooperation seen from structural (e.g. network organization) or functional point of view which looks at cooperation as activities performed by individuals within a team in real time. Two minimal conditions must be met in cooperative situations: (1) each actor strives towards goals and can interfere with other actors on goals, resources, and procedures. (2) Each actor tries to manage interference to facilitate individual activities or common task. Both conditions are not necessarily symmetric, because goal orientation or interference management depend on individual behavior or time constraints.

Hoc [12] argues that current air traffic management (ATM) is more concerned with operators' plans, goals, or role allocation instead of common situational awareness. But Lee [17] determines situational awareness, responsibilities and control, time, workload, and safety constraints as key factors driving collaborative behavior in air traffic control operation: *To have proper awareness of the situation, a controller and/or pilot needs to initiate or be informed of actions taken by other operators*. But time pressure and safety issues have negative effect on communicative behavior and therefore also cooperation or common situational awareness.

Share of responsibility and control are often different but determined through situation (e.g. air traffic controllers issue clearances which have to be executed by pilots). Nevertheless, *the more assistance, the more anticipative the mode of operation in controllers and the easier the human-human cooperation* [13].

Collaborative Decision Making means *applying principles of individual decision making on groups, whereby groups are established with the aim to show collectively a specific behavior* [15]. This implies that cooperation of participating individuals should be beneficial for CDM operation, also in air transport management. But how does cooperative work look like at day-to-day basis? Cooperation has *a wide variety of connotations in everyday usage* [24]. Do people only cooperate, if they are mutually dependant in their work or is mutual dependency sufficient for cooperation to emerge? In context of CDM operation, confrontation and combination of different perspectives of cooperation is an issue: how is pilot's perspective embedded in the current CDM approach? For Schmidt [24], the multifarious nature of the task can be matched by application of multiple perspectives on a given problem via articulation of the perspectives and transforming/ translating information of different domains.

The challenge of CDM operation in ATM is the unique cognitive mechanisms in a *distributed, asynchronous*, and highly dynamic environment like it can be found in flight operation. Similar situations can be found in military teams with asynchronous, distributed teams for mission planning and mission execution, but in general it is a relatively new area [16]. Other domains which have related aspects to asynchronous distributed collaboration are not contemplated. Warner [7] describes the major factors impacting collaborative teams which are the *collaborative problem environment, operational tasks, collaborative situation parameters,* and *team types (Figure 3)*.

 Published by Cranfield University Press ISBN: 978-0-9557436-7-2 http://hdl.handle.net/1826/3832

Problem Area Characteristics

Collaborative Situation Parameters:

time pressure
information/knowledge uncertainty
dynamic information
large amount of knowledge (cognitive overload)
human-agent interface complexity

Team Types

asynchronous
distributed
culturally diverse
heterogeneous knowledge
unique roles
command structure (hierarchical vs. flat)
rotating team members

Operational Tasks

team decision making
develop shared understanding
intelligence analysis (team data processing)

Figure 3: Problem Area Characteristics for Team Collaboration

His structural model of team collaboration focuses on *team decision making, course of action selection, developing shared understanding*, and *intelligence analysis*. Thereby, various parameters can influence the collaboration performance [26]. The collaborative decision parameters can be adapted to fit the specific environment of CDM in other domains using the respective characteristics under *operational tasks*, *collaborative situation parameters*, and *team types*. Werners' structural model of team collaboration uses the minimum number of unique stages identified in team collaboration literature and the results from a Collaboration and Knowledge Management Workshop *(Figure 4*).

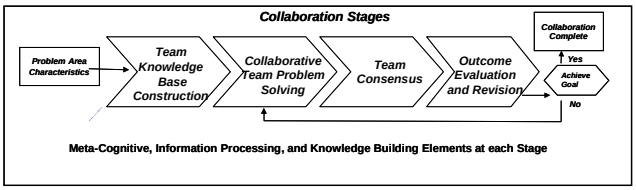

Figure 4: Structural Model of Team Collaboration

This structural model is based on the meta cognitive processes of an information processing and communication approach. For Davidsen [24], meta cognition is the knowledge of one's own cognitive processes in explaining how

 Published by Cranfield University Press ISBN: 978-0-9557436-7-2 http://hdl.handle.net/1826/3832

human cognitive processes are used for problem solving. According Werner, there is 'no generally recognized unified theory of human cognition'. By implementing Ferbers' component approach, a micro level cognitive perspective is applied into the structural collaboration model. This approach allows adapting the structural model of team collaboration to an asymmetric decision making environment under consideration of decision making with multiple objectives (e.g. like Airport CDM).

Methods

A methodological approach is used for the analysis of the cognitive mechanisms within HHI. First, all flight & turn-round situations which are seen as critical for CDM operation in terms of punctuality are determined via in-depth interviews with senior commanders of different airlines. All situations were decomposed in elementary activities and thereafter grouped into event classes. The classes within turn-round situations include the subclasses gate assignment, standard ramp services, standard land-side services, and non-standard turn-round services. Flight situations include the subclasses clearance variations 'ground', clearance variations 'flight', information processing, and information forwarding. Some event classes have only one possible event as problem cause.

For each event class, the collaboration stages analogous Werner's structural model were identified. To understand how participating operators think during each stage, a self-administered questionnaire was developed which aims to get knowledge about information processing (macro cognitive level) and interaction components (micro cognitive level) between participating CDM operators within distributed collaborative decision making. All questions were designed from the perspective of the airline pilots as distributive members of collaborative decision making, other operators perspectives could also be useful be researched. As reported by airline pilots, all event classes have critical elements concerning collaboration. Therefore the questions are designed to find the most problematic stage within the collaboration process.

Team Knowledge Base Construction is the first stage in team collaboration and includes steps like identifying relevant domain information, selecting team members, setting up the communication environment, individual team' members own mental model of the situation, and developing individual and team task knowledge. In ATM, information processing is established in day-to-day operation via various communication modes like phone, ACARS, or radio. Whereby, agreed methods of information sharing or filtering are established among all operators within the airport operation centre, while information sharing between distributed operators like airline pilots or air traffic control is not agreed. Therefore, an overall cognitive process of how to understand elements, relations, and conditions that compose the emerged problems, is not established among operators (meta cognitive), even some operators may have a mental model of situation parameters and their relationship. The airline pilots as operators of distributed site are asked to state, if information sharing for this stage is seen as sufficient for knowledge building and how important information sharing is for them. No further details like *how* or *which* information should be collected, how to understand problem task, or how communication mechanisms should be established, are analysed at this stage of research.

For the stage of *Collaborative Team Problem Solving* a closed-end question is designed to again catch the overall perspective from distributed participation in CDM. This stage can only successfully be accomplished, if a shared

 Published by Cranfield University Press ISBN: 978-0-9557436-7-2 http://hdl.handle.net/1826/3832

situational awareness of the emerged problem exists, because it builds on the identified and understood problem among all operators. This stage starts after information are processed among operators and has the aim to find a viable problem solution. Since each participating operator has its' unique domain constraints, the definition of a global goal and solution alternatives among all operators is the challenge for this collaboration stage. A micro level cognitive analysis is pursued and questions are developed analogous Ferbers' component model, which are *commonality of aims* among participating operators, *amount of resources available*, and *ability of function* to perform assigned task. All three components together form different interaction categories and give evidence about cooperation.

The stages of *Team Consensus* and *Outcome Evaluation and* Revision will not be used for this first phase of research.

The components from Ferber [9] which classify the interaction situations are:

Compatibility and Incompatibility of aims: Effect on cooperation can be negative, if aims are not compatible. Therefore critical activities during turn-round and flight are questioned for possible conflicting goals between pilots and other operators. Since holding of responsibility and possess of control for decision making can also be a reason for conflicting goals, pilots were also asked to assess aptitude of current state of decision making in all relevant event classes. Questions are out to test, if the decision maker in terms of responsibility and control issues is accepted by the pilots or if decision making is causing problems because of inappropriate decision maker.

Availability of resources: Resources are limited, therefore conflicts can arise which result in disturbances of HHI. Increasing airport congestion and abridged turn-round time of aircraft contribute to possible shortage of resources and result in reduced latitude of action or even individual competition between operators. Questions are out to test, if resources in terms of the time available for ground processes are aligned with the operational and safety requirements. Current approach on CDM operation is an attempt to challenge resource constraints via coordination of actions. Approaches for coordination of actions can also be used, to predict conflicts [9]. In this context, it will be analysed, how the current CDM approach is able to anticipate conflicts in order to resolve possible conflicting situations between pilots and other operators which are identified and quantified by occurrence and probability.

In this context of main components of interaction situations, information is also seen as a *resource* which has to be available to each operator in order to execute individual task: Information has to be shared between pilots and other operators to achieve common situational awareness. Initial data from interviews relate numerous problems regarding to cooperation on failures in information sharing. A number of elementary activities/ events are used to obtain data about possible reason for failed cooperation and effects on flight punctuality caused by information sharing problems. Questions are out to test, if there is a relation between failures in information sharing and delay (departure or arrival delay). Failure is seen, if a part of information is missing or if information is not delivered on-time.

Ability of operators in relation to their assigned task: It can not be assumed that knowledge and abilities of operators are automatically sufficient for executing assigned task. This is of course also appropriate for pilots, but it is unlikely to get realistic results from questioning of pilots, if the person asked has to determine or admits its' own inability. On the other hand it is unlikely that pilots are familiar with all other domains involved and can determine necessary abilities from other

 Published by Cranfield University Press ISBN: 978-0-9557436-7-2 http://hdl.handle.net/1826/3832

operators. Therefore only random questions are out to test pilots' perspective in a few events like failed information sharing or unpunctual process execution.

Overall, the questionnaire will examine, if pilot's perspective can be seen as contributing to CDM operation: This can be ascertained, if participation of pilot's information sharing and decision making can reduce current uncertainty in situational awareness and so increase flight punctuality.

Finally, semi-structured in-depth individual interviews with further representative commanders will be conducted to clarify the content of the questionnaire results. This is necessary to capture the meaning behind the essential results and to understand operators' attitude towards cooperation.

Demonstration

Data collection is still ongoing, only primary results are available to demonstrate usefulness and applicability of the survey.

The Environment of the Cockpit

Activity analysis on flight decks of commercial aircraft shows two pilots sharing flying and other duties like communication with ATC, monitoring flight instruments and all other tasks necessary. While pilot flying is responsible for steering and navigation of the aircraft, pilot not flying disburdens him with all other duties necessary in order to maximize safety by clear task sharing, since primary responsibility of the pilots is to steer the aircraft from departure to destination airport under maximum possible safety considerations.

In various situations they encounter interactions and interrelations with other actors involved in ATM operation. Flight relevant and operational information is shared with them.

The environment of the aircraft specifies a special case of decision making: the commander of the aircraft has the topmost responsibility of all decision making on board the aircraft. This can be compared as decision making with an individual decision maker and a group of advisers. He can either use his position to listen to his various advocates of different positions or actions or execute a structured analysis by the use of help from experts or advisers (airline company, ATC, ground handlers….). It is his final responsibility to identify key uncertainties in decision making and either adhere to objectives for the organization or his personal goal. Conflicts can arise through levels of authority and responsibility between advisers and the cockpit. Further losses of efficiency in this kind of decision making may result from other players' interactions, lack of information or limited ability of decision making. The advantage from this individual decision making is that a group of advocates is involved and therefore has more resources available [21]. Decision making seen from cockpits' perspective is also distributed since a number of decisions necessary for the flight operation remain in responsibility of the advisers (ATC, airline company, airport….).

Figure 5 shows a typical flow of HHI from cockpit's perspective identified from own experience: Aims, resources, and abilities form the basis for information exchange, decision making, and possible negotiation. Information exchange again

 Published by Cranfield University Press ISBN: 978-0-9557436-7-2 http://hdl.handle.net/1826/3832

is the basis for common situational awareness and coordination among operators. Decision making anticipates information exchange among actors which can also be used for mutual's goal identification.

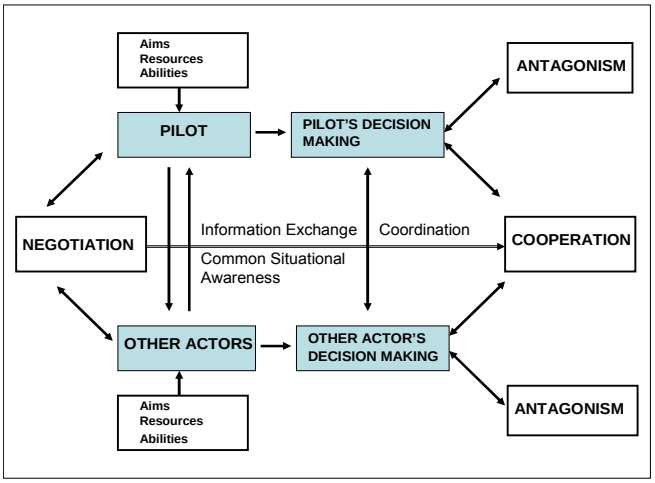

Figure 5: Cockpit's Perspective of Human-Human Interactions in ATM (Source: Own Illustration)

The Collaborative Decision Making Approach in ATM

The basic Airport CDM includes *Airport CDM Information Sharing* and the *CDM Turn-round Process* as a requirement for all subsequent airport CDM applications. Information sharing uses existing infrastructure at airports, but combines data from different sources and operators. Quality of information at each phase of flight is determined by defined rules in order to establish a common situational awareness between all operators involved.

The *Milestones Approach* defines the airport CDM turn-round process which links the flight and ground segments via a set of milestones in the aircraft turn-round process, ranging from planning of the inbound flight until the take off of the flight at the subject airport. Each milestone is monitored and allows participating operators to identify possible deviations from schedule by the use of an alarm system.

Subsequent Airport CDM levels are the *Variable Taxi Time Calculation* and the *Collaborative Management of Flight Updates (Level 2).* Variable taxi time calculation aims the introduction of a realistic taxi time in order to increase punctuality and slot adherence. Collaborative management of flight updates aims an improved operation and flexibility by slot swapping and slot shifting to take aircraft operators' preferences into account.

A *Collaborative Predeparture Sequence (Level 3)* aims to replace the present 'first come first serve' practice by consideration of aircrafts' and airport operators' requirements. [8].

Shared Situational Awareness between Pilots and Other Operators

Technological advances now allow communication and collaboration without being physically together. ATM systems today have adopted these technologies; however the highly dynamic environment of flight operation requires a fast and flexible adaptation to the changed situation. CDM is an answer to tackle problems with the short time span in hand for decision making, but no procedures are established to include interactions with airline pilots as standard CDM process.

 Published by Cranfield University Press ISBN: 978-0-9557436-7-2 http://hdl.handle.net/1826/3832

ACARS, phone, or radio are in place as possible collaboration support tools for synchronous or asynchronous decisions between airline pilots and other operators to contribute to the information sharing/ knowledge building process. Current approach to information sharing/ knowledge building is the issue of a Target Start Up Approval Time (TSAT) and a Target Off Block Time (TOBT). TSAT is a reference start up time for coping with air space constraints, TOBT has airport, airline and turn-round constraints as determining factors. Both should match as close as possible and be communicated to distributed decision makers. Constraining factors from airline pilots are not considered for calculation of TOBT or TSAT.

Critical Human-Human Interactions

Figure 6 provides an overview of critical HHI in day-to-day flight operation as reported by the airline pilots.

TURN-ROUND	COOPERATION/ NON-COOPERATION	COOPERATIVE COMPONENT	AIRPORT	FREQUENCY	RELEVANCE
Gate Assignment	Y/N	Aims/Resources/ Abilities	Hub/ Non Hub	Daily/Weekly/ Monthley	Avoidable Yes/No
Ground Handling/ Ramp	Y/N	Aims/Resources/ Abilities	Hub/ Non Hub	Daily/Weekly/ Monthley	Avoidable Yes/No
Ground Handling/ Land	Y/N	Aims/Resources/ Abilities	Hub/ Non Hub	Daily/Weekly/ Monthley	Avoidable Yes/No
Ground Handling/ Special	Y/N	Aims/ Resources/ Abilities	Hub/ Non Hub	Daily/Weekly/ Monthley	Avoidable Yes/No

FLIGHT	COOPERATION/ NON-COOPERATION	COOPERATIVE COMPONENT	AIRPORT	FREQUENCY	RELEVANCE
RWY/DEP Change	Y/N	Aims/Resources/ Abilities	Hub/ Non Hub	Daily/Weekly/ Monthley	Avoidable Yes/No
EAT	Y/N	Aims/Resources/ Abilities	Hub/ Non Hub	Daily/Weekly/ Monthley	Avoidable Yes/No
Clearnce Variation	Y/N	Aims/Resources/ Abilities	Hub/ Non Hub	Daily/Weekly/ Monthley	Avoidable Yes/No
Operational Change	Y/N	Aims/Resources/ Abilities	Hub/ Non Hub	Daily/Weekly/ Monthley	Avoidable Yes/No

PILOT	COOPERATION/ NON-COOPERATION	COOPERATIVE COMPONENT	AIRPORT	FREQUENCY	RELEVANCE
Information Forwarding	Y/N	Aims/Resources/ Abilities	Hub/ Non Hub	Daily/Weekly/ Monthley	Avoidable Yes/NO

Figure 6: Critical Information Sharing Situations (Source: Own Data 2007)

Responsibility and control allocation between pilots and other actors

'*The allocation of functions between humans and machines is a very old topic in human engineering'* [14]. Function allocation in terms of responsibilities and control has been identified as key factor for collaborative human-human behavior in ATM [17].

While air traffic controllers are responsible to separate the aircraft during flight, the responsibility of the pilots is the safety of the aircraft. The environment of the aircraft is a special case of interaction mode: final decision making on board of the aircraft is not shared between equitable partners, but is in the hand of the captain of the aircraft. Other actors take the role of advisers for an individual decision maker. Nevertheless all actions and decisions are obligatory on achievement of safety. The captain may either use his position to listen to his various advocates of different positions, or executes a structured analysis by the use of help from experts or advisers (airline company, air traffic control, ground

 Published by Cranfield University Press ISBN: 978-0-9557436-7-2 http://hdl.handle.net/1826/3832

handler…) It is his final responsibility to identify key uncertainties in decision making and either adhere to objectives for the organization or his personal goal.

The research shows that antagonistic or cooperative behavior can arise through different levels of authority and responsibility between the captain and his advisers [21].

Responsibilities on ground are shared among actors: the flight manager is responsible for boarding and check-in processes, ramp agent for delivery of flight documents and other operational information. To achieve cooperation, all actors should have the same aim [14] which implies that HHI take place between *equitable* partners.

Modes of Information Sharing in Pilot – Other Operators' Relationship

Central concern of CDM is information sharing and common situational awareness. Many studies have been devoted to information sharing at the airport control centre of CDM participating airports, but no focus has been made on exchange of information to the cockpit or receiving operational information from the cockpit.

Information sharing between airline pilots and other operators involves human activities, but as fare as humans are involved for information provision and creation, failures may occur and have obvious consequences on reliability [19]. Pilots were asked to identify different classes of information failures during all phases of turn-round and flight. From cockpit perspective, the main concern is how information sharing and common situational awareness between flight crews and ground parties is accomplished in order to achieve a predictability and punctuality during flight and ground operation. It has to be addressed:

How all necessary information is delivered to the cockpit or weather it is jammed at any interface.

If necessary information delivered on time.

How the information, forwarded from cockpit, is handled by other actors.

How much delay is encountered, if information delivery is late or not executed?

Which information not delivered has the greatest risk of producing delay.

Which information, forwarded by crew, has greatest risk of producing delay?

Time Constraints

Time pressure can have opposite effect on cooperative behavior. During peak traffic and short turnaround, pilot workload is very high for several reasons: Available time for coordination of necessary ground handling processes on ground is short or voice congestion over busy radio frequency demands high attention. Any failures in coordination or any retarded process on ground holds the risk of encountering delay. During flight on busy frequencies, issued clearances by air traffic control need to be executed promptly and often no time is left for negotiation. Especially during approach, high workload does not leave much time to gain situational awareness. Air traffic controllers' constraints are

 Published by Cranfield University Press ISBN: 978-0-9557436-7-2 http://hdl.handle.net/1826/3832

normally not visible to the pilot, but also controllers' time is very limited during busy approach hours, and therefore not much time is left, to share situational constraints or negotiate with the pilot. Especially in these situations, controllers depend on cooperation from pilots.

Conclusion

The analysis of micro level cooperative mechanisms represented by the airline pilots' perspective within a distributed collaborative decision making environment, is the first attempt to implement individual group members think into a structural decision making model within the domain characteristics of ATM operation. This study is expected to be useful, because the distributed CDM environment shows unique interaction characteristics and therefore requires a focus on operators' thoughts. The airline pilots' perspective is chosen because a non-punishment policy for pilots when causing flight delays is in place, opposite to other operators who have to expect pay deductions. De Ferbers' interaction classification reveals potential non-cooperative flight situations and results from questionnaire are expected to be useful for the design of experiments with further interactions in form of negotiations between operators. The unique situation of individual operators' domain constraints distinguishes decision making in ATM from decision making in other environments, e.g. military.

Further outcomes of the study are expected to be an empirically based theory for collaboration in an asynchronous, distributed decision making environment including information processing components. Empirical data can be used for development of an agent support in airside flight operation situations.

Acknowledgment

We would like to thank all participating pilots from Lufthansa and Lufthansa CityLine, Air Berlin, and Private Air for their collaboration in this research.

References

1. Amat, A.L. & Bellorini, A. (1996). The issue of ground/ cockpit integration: results from field studies, *8th European Conference on Cognitive Ergonomics*, ECCE-8, Granada, Spain
2. Bellorini, A. & Vanderhaegen, F. (1995). Communication and Cooperation Analysis in Air Traffic Control, *8th International Symposium on Aviation Psychology,* Columbus, Ohio, USA
3. Carlier, X. & Hoc, J.M. (2002). Role of Common Frame of Reference in Cognitive Cooperation: Sharing Tasks between Agents in Air Traffic Control. *Cognition, Technology & Work* 4, 37-47, Springer-Verlag London
4. Chavalarias, D. (2002). Emergence of cooperation and selection of interactions, *Center of Research of Applied Epistemology*, Ecole Polytechnique, Paris, France
5. Cox, G.; Sharples, S.; Stedmon, A. & Wilson, J. (2007). An observation tool to study air traffic control and flightdeck collaboration, *Applied Ergonomics* 38, 425-435
6. Dagaeff, Th.; Chantemargue, F. & Hirsbrunner, B. (1996). Emergence-Based Cooperation in a Multi-Agent System, *Computer Science Department,* University of Fribourg, Switzerland
7. De Terssac, G. & Chabaud, D. (1990). Réferentiel opératif commun et fiabilité. In J.Leplat & G.de Terssac (Eds.), *Les facteurs humains de la fiabilité dans les systems complexes* (pp. 110-139), Toulouse
8. Eurocontrol. (2003). *Airport CDM Applications Guide*, Eurocontrol, Belgium
9. Ferber, J. (1995). *Multi-Agent Sytems*, Addison-Wesley, Muenchen, Germany
10. Hamec, S.; Anceuax, F.; Pelayo, S.; Beuscart-Zéphir, M.-C. & Rogalski, J. (2002). Cooperation in Health Care – Theoretical and methodological issues. A Study of two situations: hospital and home care, *Le Travail Humain*, 65, 59-88

 Published by Cranfield University Press ISBN: 978-0-9557436-7-2 http://hdl.handle.net/1826/3832

11. Hoc, J.M. (1988). Cognitive psychology of planning, *Academic Press,* London, UK
12. Hoc, J.M. (2001). Towards a cognitive approach to human-machine cooperation in dynamic situations, *Human-Computer Studies* 54, 509-540
13. Hoc, J.M. & Lemoine, M.P. (1998). Cognitive evaluation of human-human and human-machine cooperation modes in air traffic control. *International Journal of Aviation Psychology* 8.1-32
14. Hoc, J.M. (2000). From human-human interaction to human-machine cooperation. *Ergonomics,* 43, 833-843
15. Jennings, N.R.; Norman, T.J. & Panzarasa, P. (2001). Formalizing Collaborative Decision Making and practical reasoning in Multi-Agent Systems, Journal of Logics & Communication 12 (1) 55-117
16. Keisler, S. & Cummings, J.N. (2002). What Do We Know About Proximity in Work Groups?, In P. Hinds and S.Keisler (Eds). *Distributed Work*, Cambridge, MA, MIT Press
17. Lee, P.U. (2005). Understanding Human-Human Collaboration to Guide Human-Computer Interaction Design in Air Traffic Control, *NASA Ames Research Center*, CA, USA
18. Millot, P. & Debernard, S. (1993). Men-machines cooperative organizations: methodological and practical attempts in air traffic control, *International Conference on Systems, Man, and Cybernetics*, Le Tourquet, France
19. Parasuraman, R., Mouloua, M. & Molloy, R. (1996). Effects od adaptive task allocation on monitoring of automated systems, *Human Factors*, 38, 665-679
20. Piaget, J. (1965). *Études sociologiques*, Genève, Switzerland
21. Raiffa, H.; Richardson, J. & Metcalfe, D. (2002). *Negotiation Analysis*, The Belknap Press of Harvard University Press, Cambridge, England
22. Rogers, Y. (2005). Distributed Cognition and Communication, *Encyclopedia of Language and Linguistics (2nd ed.),* Elsevier, GB
23. Salas, E.; Prince, C.; Baker, D. & Shrestha, L. (1995). Situation awareness in team performance: implications for measurement and training, *Human Factors,* 37, 123-136
24. Schmidt, K. (1994). Cooperative work and its articulation: requirements for computer support. *Le Travail Humain*, 57, 345-366
25. Terveen, L.G. (1995). An overview of human-computer collaboration, *Knowledge-Based Systems*, 8 (2-3), 67-81
26. Warner, N.W.; Vanderwalker, S. & Verma, N. (2002). State of the Art Review on Human-Human Collaboration Research: An Integrated, Multidisciplinary Perspective, *Naval Research Centre*, Arlington VA
27. Warner, N.W. & Wroblewski, E. (2003). The Cognitive Process Used in Team Collaboration During Asynchronous, Distributed Decision Making, Comand and Control Research and Technology Symposium, June 15-17, 2004, San Diego CA
28. Groppe, M. & Bui, M. (2007). Study of Cockpit's Perspective on Human-Human Interactions to Guide Collaborative Decision Making Decision, in IEEE Proceedings of ACHI 2008, Saint Luce, Martiniqué

 Published by Cranfield University Press ISBN: 978-0-9557436-7-2 http://hdl.handle.net/1826/3832

High Speed Marine Vehicles with Aerodynamic Surfaces: Development of a Dynamic Model for a Novel Configuration

M Collu, M H Patel, F Trarieux, Cranfield University, UK

SUMMARY

A research programme on high speed marine vehicles fitted with aerodynamic surfaces started in Cranfield University in 2005. One of the configurations analyzed is a high speed prismatic planing hull with one or more aerodynamic surfaces; it is called a hybrid vehicle (HV). Two mathematical models have been developed for the dynamic behavior which is a combination of the very different behaviors of aircraft and ships. The first model estimates the equilibrium attitude of the HV at a certain speed. A parametric analysis for the influence of the configuration on the performance of the HV has been conducted (1). With the second model, the authors propose a set of ordinary differential equations of motion, derived in the frame of small-disturbance stability theory which has been used to investigate the longitudinal dynamic stability of the HV (2).

Ref. (1) and (2) present a complete description of the mathematical models, while this article summarizes the methodology adopted to develop these dynamic models and gives a brief summary of the results.

NOMENCLATURE

HV	Hybrid Vehicle, having both aerodynamic and hydrodynamic surfaces
WIGe	Wing In Ground effect, aerodynamic effect experienced by wings flying near the ground (at a height above the ground about a fraction of the aerodynamic chord)
SPPO	Small Period Pitching Oscillation: oscillation mode of airplanes after a small disturbance
SPEoM	Small Perturbations system of Equations of Motion

CONTEXT

Several new high speed marine vehicle configurations have been developed during the last two decades (3). For 'very high speed vehicles' (~50 kts), the aerodynamic forces can become of the same order of magnitude compared to hydrodynamic forces, especially for small vehicles (weight < 10 tons). Although in some cases this can lead to stability issues, it offers a new range of possibilities to sustain the weight of the craft. High speed marine vehicles can be equipped with specifically designed aerodynamic surfaces and the aerodynamic lift can 'alleviate' the weight of the vehicle. This means less wetted length, less hydrodynamic drag and less required power. Such vehicles exploiting aerodynamic and hydrodynamic forces can find applications in several scenarios: high speed civil marine transport, military troop marine transport for littoral warfare and autonomous unmanned vehicles with airborne and seaborne capabilities.

PROBLEM STATEMENT

The dynamic models available in the literature focus either on marine vehicles or on 'Wing in Ground effect (WIGe)' vehicles. These models concentrate, respectively, on hydrostatic/hydrodynamic and aerodynamic forces; therefore they are not suitable for a vehicle experiencing hydrostatic, hydrodynamic and aerodynamic forces of the same order of magnitude.

 Published by Cranfield University Press ISBN: 978-0-9557436-7-2 http://hdl.handle.net/1826/3832

METHODOLOGY

First of all, a configuration was selected comprising a HV having aerodynamic surfaces, operating near the ground (wing in ground effect) and a high speed planing hull.

Since the HV shares the same dynamic characteristics as both WIGe vehicles and planing crafts, an analysis of the available dynamic models of these configurations has been conducted. A model for each has been implemented in Matlab, using a common template: xml file as input, graphical and excel files as output. The validity of these two dynamic simulation models has been tested against experimental and computational data and they have shown good agreement with previous work (4).

A mathematical framework to study the equilibrium state of the HV and its static stability has been developed by the authors, starting from the analysis of the static stability of WIGe vehicles and planing craft (1). Furthermore, a mathematical model has been developed to study the dynamic stability of the HV (2). Together, the static and the dynamic stability mathematical models constitute a useful tool for the conceptual and preliminary design of high speed marine vehicles having aerodynamic surfaces.

PROGRESS

SELECTED CONFIGURATION

The HV configuration combines the characteristics of a WIGe vehicle and a high speed marine vehicle:

The aerodynamic surfaces of the HV operate in WIGe, since they are very close to the ground,

The vehicle is in contact with the water at very high speed (>50 kts, 92.6 km/h or 57.5 mph), therefore it has to adopt a high speed marine configuration.

Among high speed marine vehicles, the planing craft configuration has been chosen as the authors considered that the HV should have also a free flight capability (or at least wing in ground flight), therefore the configuration with hydrofoils as hydrodynamic surfaces is not suitable. The selected HV configuration is shown in Figure 1.

WIGe VEHICLES AND PLANING HULL CRAFT DYNAMICS

A three step approach has been adopted for both WIGe vehicles and planing craft configurations:

investigation of the available mathematical models on the vehicle's dynamics,

selection of a mathematical model,

3. implementation of the selected mathematical model in MATLAB.

The implementation of mathematical models representing WIGe vehicles and planing craft dynamics needed to be validated against data available in the literature, therefore some previous works on WIGe vehicles dynamics (5), (6) and planing craft dynamics (7) have been selected. Two programs, developed in MATLAB, start from the geometrical, inertial, aerodynamic and hydrodynamic characteristics of the vehicle (input) and estimate the equilibrium attitude (1st output) and the modes of oscillation of the vehicle (2nd output). The results, as seen in (4), are in good agreement with the cited references; therefore they constitute a valid basis for the development of a HV dynamics model.

 Published by Cranfield University Press ISBN: 978-0-9557436-7-2 http://hdl.handle.net/1826/3832

System of equations of equilibrium (longitudinal plane)

An analysis of all the hydrostatic, hydrodynamic and aerodynamic forces and moments acting on the HV has been conducted to develop a system of equations of equilibrium in the longitudinal plane (Figure 1). The model can estimate the equilibrium attitude of the HV across a range of speeds. It has been implemented in Matlab and a parametric analysis of the influence of some key parameters of the configuration (such as the wing surface area, position of the CG) on the performance has been conducted. The complete analysis is illustrated in (1).

In Figure 2 the influence of the wing area on the resistance to weight ratio is illustrated. The three configurations are identical except for the area of the wing (this HV configuration has one wing). The speed range can be divided in two zones by the speed at which the curves cross each other (about Froude number 2.9, 40 knots), called V_X. In the speed range $V_0 < V_X$, the total drag of the planing craft configuration is lower than the total resistance of the HVs with wing. For $V_0 > V_X$, the HVs with wing experience less drag. If the requirement of the vehicle is to reach a speed $V > V_X$, the configurations with wing will require a power propulsion lower than the planing craft.

In Figure 3, the influence of η, the angle between the mean aerodynamic chord of the wing and the keel of the planing hull is presented. The three configuration used have $\eta=0$ deg (chord parallel to the keel), $\eta=5$ deg and $\eta=10$ deg. The resistance to weight ratio is lower for an increased η, due to the fact that increasing η, the angle of attack of the wing is increased.

In Figure 4, the influence of the longitudinal position of the CG (center of gravity) on the resistance to weight ratio is shown. This parameter has the most significant influence on the resistance. At high speed, a lower resistance to weight ratio is obtained when the CG is shifted rearward.

These results demonstrate how this mathematical model can be a useful in the conceptual and preliminary design phase of a hybrid vehicle.

System of equations of motion (small disturbances framework, longitudinal plane)

A mathematical model which can address the static and dynamic stability of the HV is required. Starting from the ordinary differential equations of motion used for WIGe vehicles and planing craft, the authors developed a model to describe the longitudinal motion of the HV after a small disturbance.

Static Stability

The static stability analysis is presented in (1). Briefly, starting from the developed system of equations of motion, the static stability of the HV has been derived using the Routh-Hurwitz criterion. A criterion to estimate the static stability of the HV has been identified, and a simplified version of the same condition has been derived for the reduced order system of equations of motion (reduced because the influence of the surge motion has been neglected). This condition for the HV is very similar to the static stability condition developed by Irodov for the WIGe vehicles (8). In fact, Irodov stated that a WIGe vehicle is stable if

"the (aerodynamic) center in height should be located upstream of the (aerodynamic) center in pitch"

 Published by Cranfield University Press ISBN: 978-0-9557436-7-2 http://hdl.handle.net/1826/3832

It means that dividing the total lift in two components, the lift due to a variation of the pitch angle (Lalpha) and the lift due to a variation of the height above the surface (Lheight), the point of action of force Lheight should be located upstream of the point of action of force Lalpha.

Similarly to Irodov, the authors (1) propose that a HV is stable if

"the hydrodynamic center in heave should be located upstream of the aerodynamic center in height"

It means that dividing the hydrodynamic lift due to a heave variation (Lhyd) from the lift due to a variation of the height above the surface (Lheight), the point of action of Lheight should be located upstream the point of action of Lhyd. This criterion requires validation against experimental data, but it constitutes a relatively straightforward 'thumbnail rule' to estimate the static stability of the novel hybrid configuration.

Dynamic Stability

To estimate the modes of oscillation of the HV the stability derivatives are needed. As described in (2), there are existing methods to estimate their values but experimental data are required to determine the dynamic behavior of the HV. The modes of oscllation of the HV can be determined once the stability derivatives have been estimated.

It is however possible to make a comparison between the dynamics of conventional airplanes, WIGe vehicles, planing craft and the HV (Table 1). With respect to the planing craft configuration, the HV also has to take into account the influence of the small changes of the height above the sea surface of the aerodynamic surfaces (h) and the surge velocity and acceleration disturbances (∂x/∂t and its derivative). With respect to WIGe vehicles, the HV also has to take into account the vertical position disturbance (z), since this greatly influences the hydrostatic and hydrodynamic forces acting on the HV.

BIBLIOGRAPHY

1. COLLU, M., PATEL, M. H., TRARIEUX, F., *A Mathematical Model to analyze the Static Stability of Hybrid (Aero-hydrodynamically supported) vehicles.,* 8th Symposium on High Speed Marine Vehicles 2008 (HSMV08), Naples, Italy, 2008.
2. COLLU, M., PATEL, M. H., TRARIEUX, F., *A Unified Mathematical Model for High Speed Hybrid (Air and Water-borne) Vehicles.,* 2nd International Conference on Marine Research and Transportation, 2007.
3. MEYER, J. R., CLARK, D. J., ELLSWORTH, W. M., *The Quest for Speed at Sea.,* Naval Surface Center, Carderock Division, 2004, Technical Digest, April.COLLU, M., *High Speed Marine Vehicles Exploiting Aerodynamic Lift: Dynamic Model.,* Cranfield University, Mid-Point Review Report, 2007.
4. CHUN, H. H., CHANG, C. H., *Longitudinal stability and dynamic motion of a small passenger WIG craft.,* Ocean Engineering, Vol. 29, pp.1145-1162,2002.
5. BELHAYE, H., *An Investigation into the Longitudinal Stability of Wing In Ground effect vehicles,* Master thesis, Cranfield University - College of Aeronautics, 1997.
6. SAVITSKY, B., Be LORME, M. F., BATLA, R., *Inclusion of Whisker Spray Drag in Performance Prediction Method for High-Speed Planing Hulls.,* Marine Technology, Vol. 44, pp. 35-56, 2007.
7. IROBOV, R. B., *WIG Longitudinal Stability Criteria (Kriterii prodol'noy ustoychivosti ekranoplana).,* TsAGI (Central Institute of Aerohydrodynamics im. N. Ye. Zhukovskij), 1970.

 Published by Cranfield University Press ISBN: 978-0-9557436-7-2 http://hdl.handle.net/1826/3832

Vehicle configuration	SPEoM equations (Longitudinal plane)	Characteristic polynomial	Roots of the SPEoM
Airplane	4 equations ($\partial x/\partial t$, $\partial z/\partial t$, $\partial\theta/\partial t$, θ)	4th degree	2 oscillatory solutions: phugoid and SPPO
Planing craft	4 equations ($\partial z/\partial t$, z, $\partial\theta/\partial t$, θ)	4th degree	2 oscillatory solutions: porpoising (least stable root)
WIGe vehicles	5 equations ($\partial x/\partial t$, $\partial z/\partial t$, $\partial\theta/\partial t$, θ, h)	5th degree	2 oscillatory solutions + 1 negative real root: Phugoid, SPPO and subsidence mode
Hybrid Vehicles	6 equations ($\partial x/\partial t$, $\partial z/\partial t$, z, $\partial\theta/\partial t$, θ, h)	6th degree	See 5.3 (b)

Table 1: comparison between the dynamics of conventional configurations and the HV

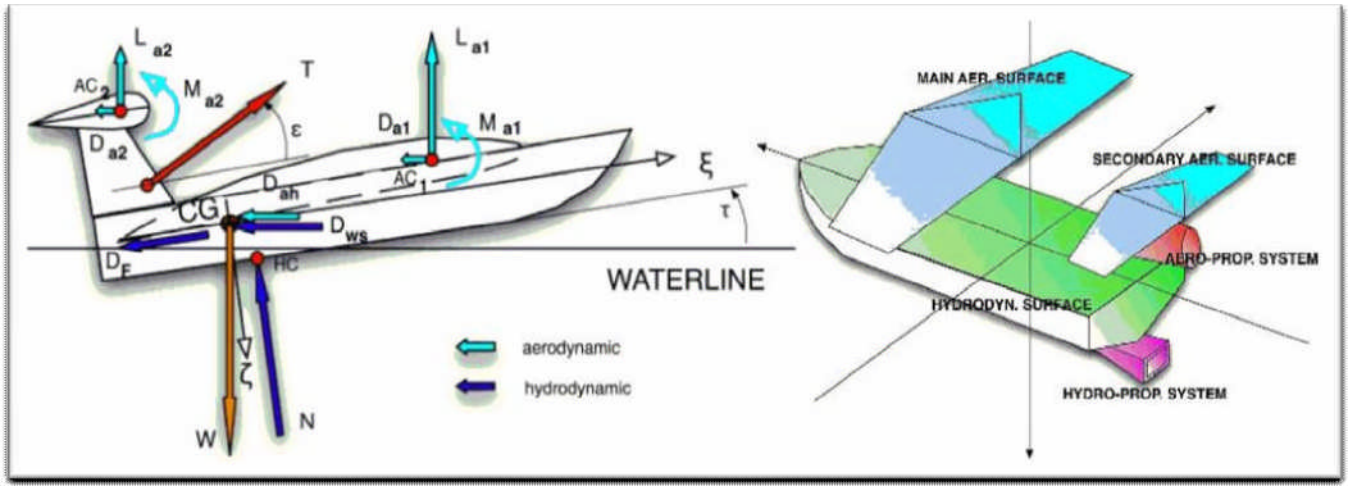

Figure 1: Hybrid Vehicle selected configuration

 Published by Cranfield University Press ISBN: 978-0-9557436-7-2 http://hdl.handle.net/1826/3832

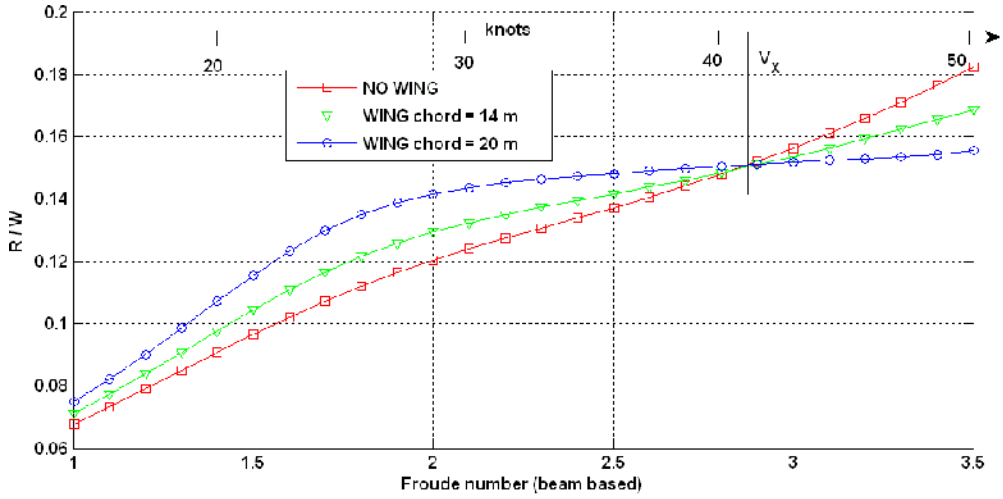

Figure 2: influence of the wing area on the resistance to weight ratio

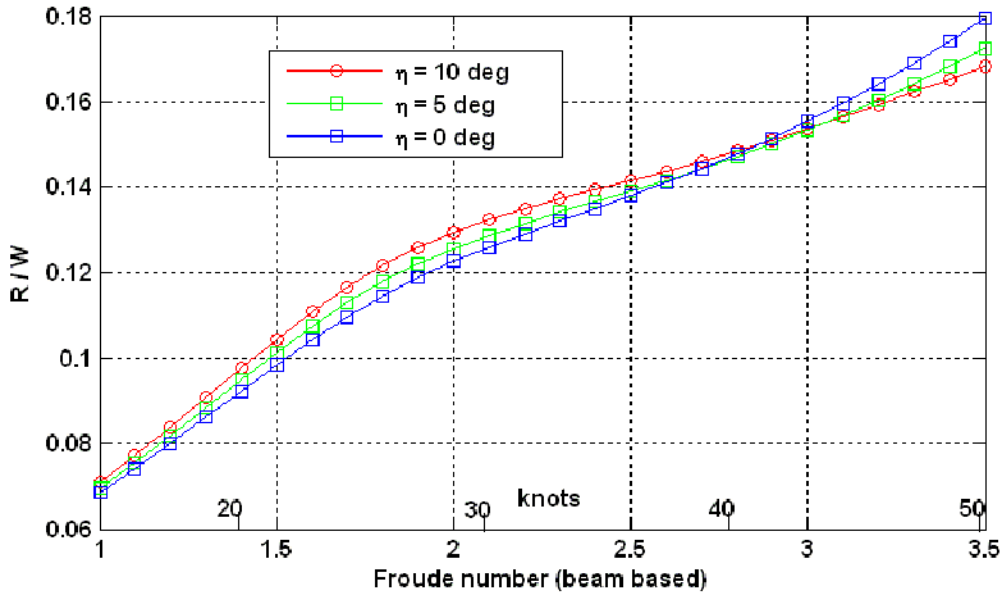

Figure 3: influence of η on the resistance to weight ratio

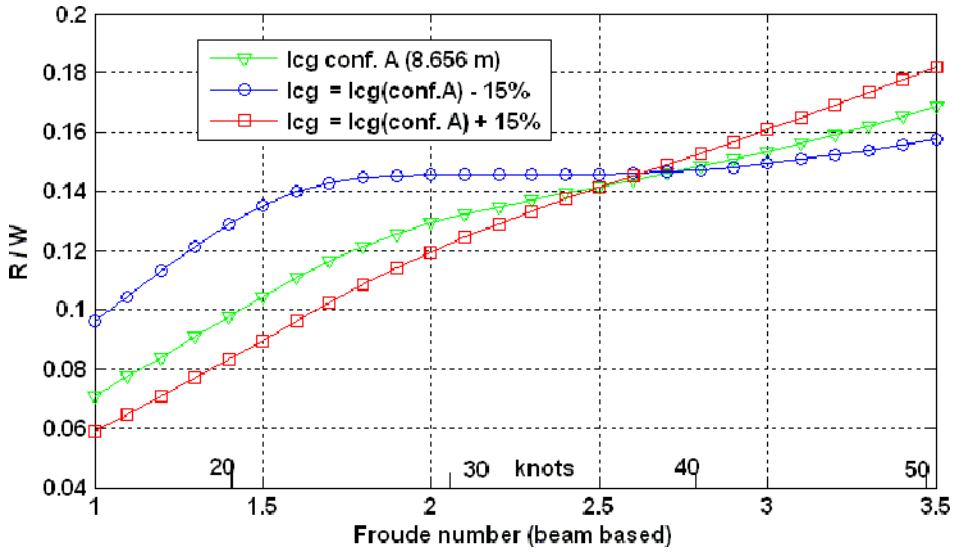

Figure 4: influence of the CG longitudinal position on the resistance to weight ratio

 Published by Cranfield University Press ISBN: 978-0-9557436-7-2 http://hdl.handle.net/1826/3832

The effect of internal surface roughness on the Gas Void Fraction measurements in two-phase Gas/Liquid flow using Acoustic Emission technology

A. Addali, S. Al-Lababidi, D. Mba, H Yeung
School of Engineering, Cranfield University, Cranfield, Beds. MK43 0AL.

Abstract

This paper demonstrates the use of the Acoustic Emission (AE) technique to the measurement of the gas void fraction GVF in two-phase air\water slug flow. Also, investigate the effect of the difference in the steel pipe wall surface roughness on the noninvasive AE measurements Two-phase air\water facility was employed to conduct the AE experiment. The experimental investigations were performed over a range of superficial water velocities from 0.3 to 2.0 ms^{-1} and 0.2 to 1.4 ms^{-1} superficial gas velocities. Based on the experimental investigations, it was found that the level of the AE absolute energy increases with the increase of the internal surface roughness; however, it maintained a linear correlation with gas void fraction that measured by conductive sensor.

Keywords: *Acoustic Emission, air\water flow, gas voidfraction, surface roughness*

Introduction

Two-phase gas-liquid flow commonly exists and dominates the chemical and petroleum industry. In this context, two parameters namely, superficial liquid and gas velocities (V_{SG} and V_{SL}) are required to calculate *liquid volume fraction* (liquid hold-up) and *Gas Void Fraction* GVF (Hewitt, 1978). The gas void fraction (*GVF)* is the ratio of the volumetric flow of gas to the total volumetric flow-rate. The measuring procedure of gas void fractions in multiphase flows is complex. Gamma-ray attenuation and electrical impedance such as conductivity sensor are the most commonly adopted techniques; other alternative techniques include microwave measurements, X-ray and gamma-ray tomography, magnetic resonance imaging and nuclear magnetic resonance (NMR), (Clayton,2005). However, most of the currently available measuring techniques are flow regime dependent. In this paper, the proposed non-invasive acoustic emission technique AE is based on the level of the acoustic energy generated from the gas\liquid phase's interaction regardless the developed flow regime.

Acoustic Emission (AE) is defined as the range of phenomena that results in the generation of structure borne and fluid-borne propagating waves due to the rapid release of energy from localised sources within and/or, on the surface of a material; typical frequency content of AE is between 100 kHz to 1 MHz (Alfayez *et al,* 2005). This investigation addresses the applicability of the Acoustic Emission (AE) technology for measurement of Gas Void Fraction GVF within a steel pipe. Furthermore, the effect of internal surface roughness of the pipe on AE activity was investigated. Despite the fact that Acoustic Emission (AE) is still under development; it has been used successfully to monitor the incipient cavitation in pumps where the principle source of AE was the collapse of gas bubbles associated with cavitation (Alfayez *et al,* 2005). Strasberg and Leighton (Strasberg, 1956 and Leighton, 1994), concluded that in

 Published by Cranfield University Press ISBN: 978-0-9557436-7-2 http://hdl.handle.net/1826/3832

two phase liquid/gas flow conditions, the amplitude of the bubbles oscillations, which generates sound, were influenced by several mechanisms such as; bubble formation, bubble coalescence or division, the flow of a free stream of liquid with entrained bubbles, and the flow of bubbles through a pipe past a constriction.

Experimental Setup

A purposely built two-phase experimental facility that allowed for investigations over a range of a superficial liquid velocities $_{VSL}$ (0.3 to 2.0 ms^{-1}) and superficial gas velocities $_{VSG}$ (0.2 to 1.4 ms^{-1}) was employed, see figure(1). Measurements of GVF were also undertaken with a conductive probe thereby allowing a direct correlation between AE and measured GVF. The experimental facility consisted of water and air supply systems, Perspex pipes, steel spacemen test sections, circulating pipes and fittings, Electrode rings for conductivity measurements associated with data acquisition system, and AE acquisition system, The pipeline used has 2-inch (ID ≈ 50mm) diameter and total length of 22 .5 m. The majority of the piping system was made from ABS (class E) pipe, and two Perspex sections were installed to allow for visual observations of the flow. Three stainless steel pipes of 750mm length, and 8mm thickness were investigated individually; each pipe was designated with different arbitrary internal surface roughness as following; Grade-1 (10μm Ra), Grade-2 (3.2μm Ra) and Grade-3 (1.6μm Ra).

A Commercially available AE acquisition system was used for acquiring the data from a Piezo-electric AE sensor, (PICO type) with broadband operating frequency range 150-750 kHz. The AE sensor was placed onto stainless steel pipe (Addali et al, 2007) as shown in the detailed picture associated with figure (1), The output AE signals from the sensor were pre-amplified at 60dB and AE waveforms were sampled at 2MHz. In addition, AE absolute energy (Joules) and r.m. s levels were sampled at 1 0ms over a time constant of 1 0msec.

Experimental Procedures

The experiments covered a rang of superficial water velocities $_{(VSL)}$ start from 0.3 ms^{-1} to 2.0 ms^{-1} at increments of 0.1 ms^{-1}; and superficial air velocities $_{(VSG)}$ start from 0.2 to 1.4 ms^{-1} at increments of 0.2 ms^{-1} at each $_{VSL.}$ The $_{VSL}$ and VSG values were achieved by throttling valves downstream of the flow meters, and every test condition was maintained for 120 seconds. Data were acquired and analysed for each test condition and comparisons between the conductivity sensor measurement and AE were presented for different GVF of the flow.

Results and Discussion

Results revealed from the mounted AE sensor on the three pipes, showed insignificant changes in the AE absolute energy (10^{-18} Joules) for single-phase water flow at velocity that ranges from 0.3 to 2.0 ms^{-1}. In single-phase water tests, the measured values of AE were higher than background noise levels of the system, see figure (2). This was ascribed to the absence of air bubbles. Conversely, at any constant $_{VSL,}$ and due to the presence of air bubbles and their associated activities such as; bubbles formation, coalescence, collapse, breaking-up and bubbles oscillation; the absolute energy of AE showed a gradual increase as superficial air velocities $_{VSG}$ ^{increased} (VSG =0.2 to 1.4 ms^{-1}), see figure(3). Figure (3) also

 Published by Cranfield University Press ISBN: 978-0-9557436-7-2 http://hdl.handle.net/1826/3832

shows that the surface roughness influenced the AE energy generated with the roughest internal surface generating the highest AE levels. This is attributed to the increase of the turbulent forces of the flow, which intensifying the bubble activities in the two phase flow. Figure (4) illustrates the observations of increasing AE energy levels with increasing $_{VSG}$ and V_{SL} levels. Similar observations were noted for Grade-2 and -3 pipes.

Additionally, the AE energy showed clear relationship with gas void fraction GVF measured by conductivity rings as shown in figures (5), and in order to quantify this relationship, a Pearson's Correlation Coefficient, (r) is introduced to calculate the degree of correlation between GVF and AE variables. The values of 'r' will always be between -1.0 (negative relationship) and +1.0 (positive relationship), see (addali *et al* 2008). Although, positive linear relationship between measured GVF and AE Energy at all velocities for the three different surface roughness were achieved, however, the effect of internal surface roughness is very obvious as shown in figures (3 and 6). In figure (3) the AE absolute energy increases with the increase of the surface roughness of the steel pipe. The increase of AE energy was attributed to the increase of turbulent intensity forces on the liquid phase and due to the increase of the rate of bubble activities on the pipe wall (collapse, formation, and ... etc). The turbulent intensity forces increased as a result of increasing the friction coefficient 'f' on the liquid phase. Typical friction values (Miler 1990) for $_{VSL}$ at 1.0 ms^{-1} for each internal surface roughness are seen in figure (3).

Conclusion

It can be concluded that the generated absolute energy of AE and measured GVF from two-phase flow are correlated. The gradual increase in the level of the AE energy was influenced by increases of both the superficial gas and liquid velocities. Furthermore the absolute energy of AE signal showed proportional increase with the internal surface roughness of the steel pipes, which may suggest the applicability of the AE technology for monitoring the condition of internal surface roughness of the pipes due to the effect of corrosion, erosion and material build-up. This investigation has shown the application of the non-intrusive measurement of AE can be used to assess the gas void fraction in pipes, offering a significant cost saving in comparison to traditionally employed measuring techniques.

 Published by Cranfield University Press ISBN: 978-0-9557436-7-2 http://hdl.handle.net/1826/3832

Figure 1 Lay out of the test rig facilities

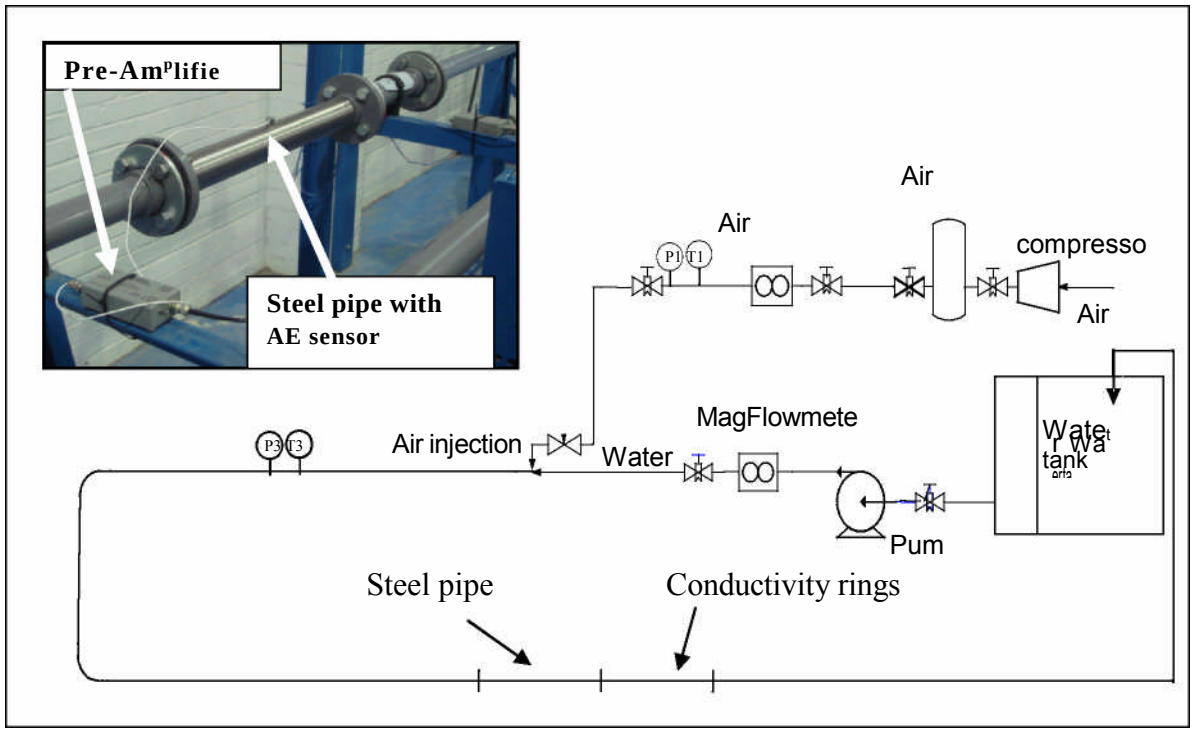

 Published by Cranfield University Press ISBN: 978-0-9557436-7-2 http://hdl.handle.net/1826/3832

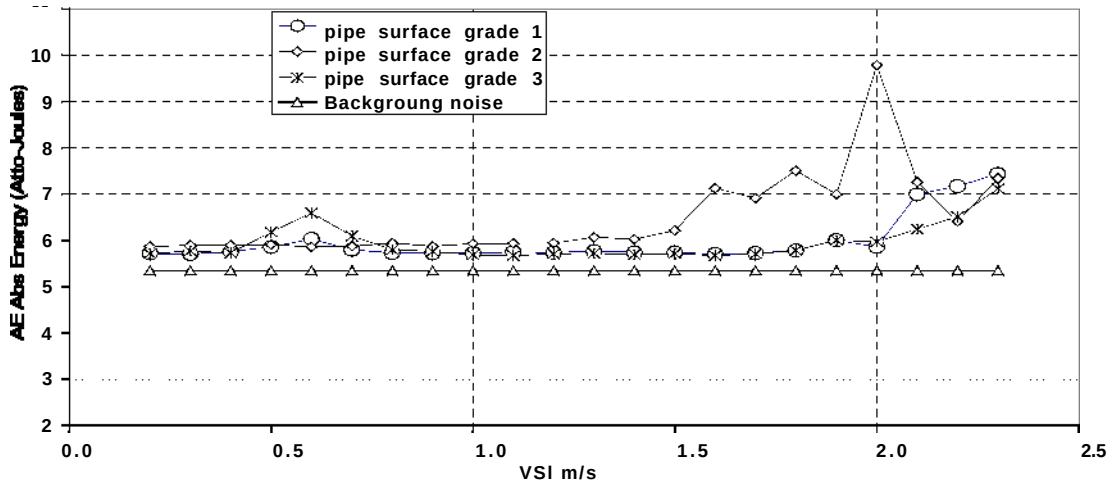

Figure 2 Observations of AE from pure liquid flow

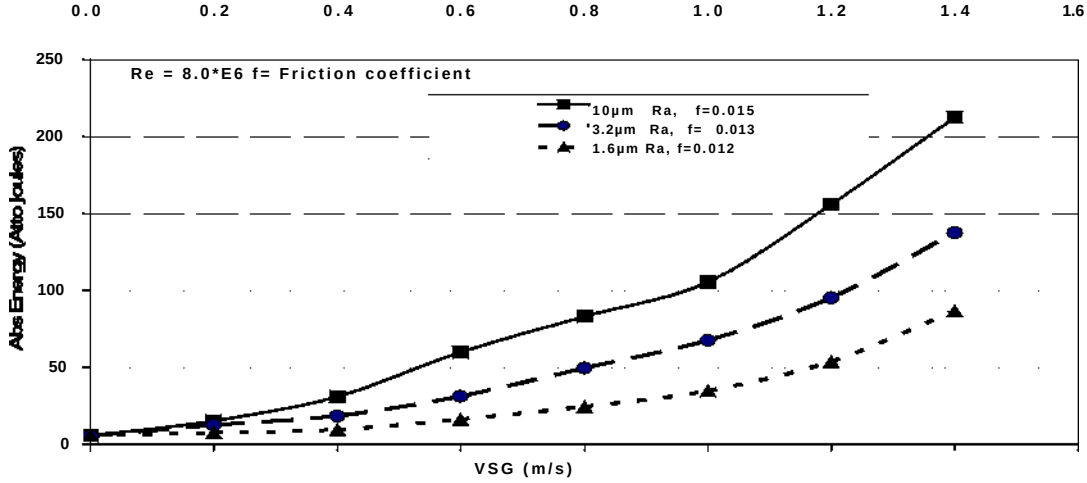

Figure 3 AE Absolute Energy level at $_{VSL}$ =1.0 m/s

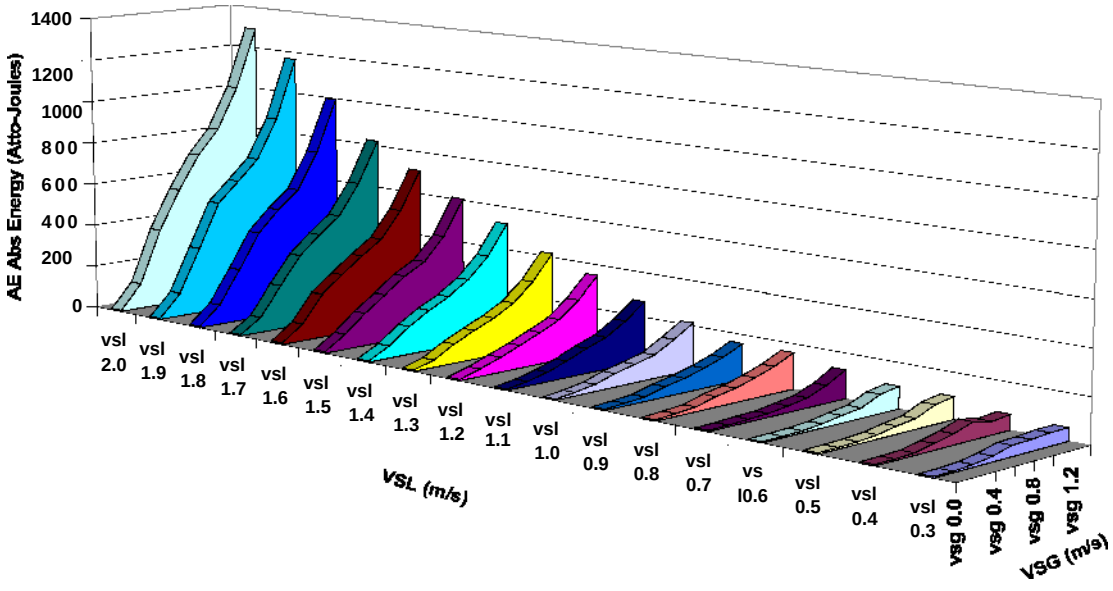

Figure 4 Increasing AE levels for varying VSG and VSL levels (grade-1 pipe)

 Published by Cranfield University Press ISBN: 978-0-9557436-7-2 http://hdl.handle.net/1826/3832

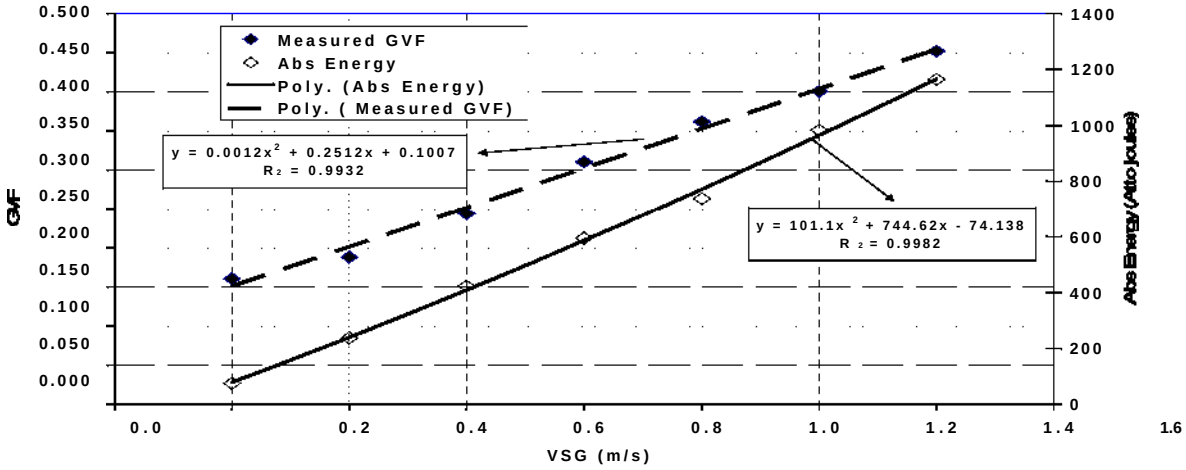

Figure 5 Correlation of measured GVF and Abs AE energy at $_{VSL}$=2.0 m/s

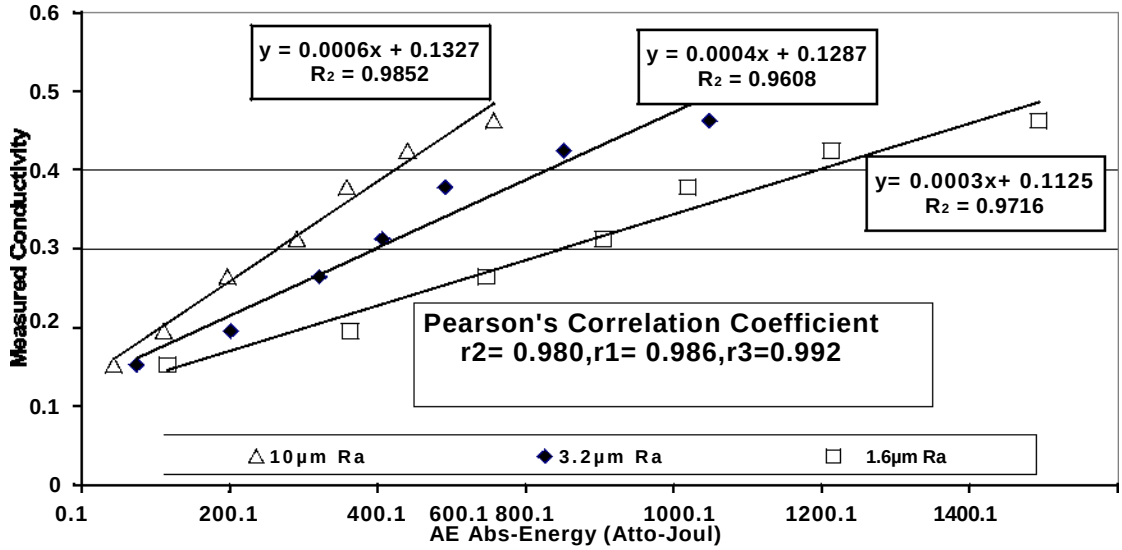

Figure 6 Correlation of measured GVF and Abs AE energy at $_{VSL}$ =2.0 m/s

References:

1. Addali A., Al-Lababidi S., Mba D. 2007. *Application ofAcoustic Emission to monitoring two phase flow.* Fourth International Conference on Condition Monitoring, UK
2. Addali A. Al-Lababidi S., D. Mba. 2008. *Gas Void Fraction Measurements Using Acoustic Emission Technique in Two-Phase Gas/Liquid Slug Flow.* The Fifth International Conference on Condition Monitoring and Machinery Failure Prevention Technologies. UK (under publication)
3. Alfayez, L. & Mba, D. 2005, "Detection of incipient cavitation and determination of the best efficiency point for centrifugal pumps using acoustic emission", *Proceedings of the Institution of Mechanical Engineers, Part E: Journal of Process Mechanical Engineering,* vol. 219, no. 4, pp. 327-344.
4. Clayton T. Crowe, 2005 .Multiphase Flow Handbook, Taylor and Francis
5. Hewitt, G. F. (1978), Measurements of Two Phase Flow Parameters, Academic Press, New York.
6. Leighton, T. G. (1994). *The acoustic bubble.* London: Academic Press.
7. Miller D. S. (1990). *Internal flow systems. BHR Group ,UK*
8. Strasberg M. *Gas Bubbles as Sources of Sound in Liquids.* The Journal of the Acoustic Society of America,28(1)1956

 Published by Cranfield University Press ISBN: 978-0-9557436-7-2 http://hdl.handle.net/1826/3832

Methodological Comparison of Electronic Noses for Headspace Analysis

HenriKnobloch[1§],Claire Turner[1], Andrew Spooner[1], Mark Chambers[2]

[1]Cranfield University, Cranfield Health, Silsoe, UK

[2]Veterinary Laboratory Agency (VLA, Weybridge)

§Corresponding author

Abstract

In past years, numerous electronic nose (e-nose) developments and applications have been published. However, little has been reported about methodological pitfalls that might be associated with e-nose technology. In this paper, some of these pitfalls such as temperature, filter application and mass flow are described and two different types of e-noses are compared. Reasons for a lack of stability and reproducibility are given explaining why e-noses cannot be considered as robust instruments for headspace analysis but also where the potential of e-noses lie.

Introduction

For more than 20 years, so-called electronic noses (e-noses) have been widely used for headspace- and trace gas analysis from solid-, liquid- and gaseous samples. During this time, different sensing methods have been developed but the e-nose principle remains the same and is described elsewhere (Mielle, 1996; Gardner et al., 2000; Nimmermark, 2001; Casalinuovo et al., 2006). However, little has been reported about e-nose methodology. In this paper, pitfalls regarding temperature, mass flow rates, filters and sampling methods will be addressed describing their impact on conducting polymer (CP)- and field effect transistor/ metal oxide semiconductor based e-noses (MOSFET/ MOS).

Methodology

In this study, CP e-noses (Bloodhound BH1 14 and BH214, Scensive Tech Ltd.) and MOSFET/MOS (NST 3220 Lab Emission analyzer) were assessed. Bloodhound BH1 14 and the BH214 e-noses contain 14 conducting polymer sensors (including 1 internal reference) and the MOS based devices housed ten MOSFET- and twelve MOS sensors working at 140°C and 170°C respectively. One MOSFET/MOS e-nose additionally contains a humidity sensor.

Two sampling methods were tested using CP e-noses; firstly so called static sampling in which a sample is headspaced within a variable sized sampling bag made from Nalophan (Kalle UK Ltd). Nalophan is used because it does not emit volatiles detectable by CP e-nose. One end of the bag is fitted with a polypropylene tube to enable attachment of the bag to the e-nose via SWAGELOK and LUER connectors. Once the sample has been placed in the bag, the other end of the bag is sealed. Hydrocarbon free air is added and after 10 minutes incubation, it is ready for analysis. Secondly, in dynamic sampling, a container with a liquid

 Published by Cranfield University Press ISBN: 978-0-9557436-7-2 http://hdl.handle.net/1826/3832

sample is attached to the e-nose which then "sucks" the headspace. The pressure difference causes an inflow of ambient air into the liquid via an inlet which bubbles through the sample.

The effect of temperature

Reverse osmosis water (ROW) and serum samples from clinically healthy cattle (breed "Holstein") were analysed at different temperatures to assess the effect on the BH214 sensor signal. The bag volume was 0.7L and the sample volume was 0.5ml leading to a sample- per bag volume ratio of 7E-04. The samples were incubated for 30 minutes in a water bath with a temperature range of 21°C to 40°C. The adsorption time for all analyses was 20 seconds.

Mass flow and filters

Both CP e-noses used in this study lack a flow controller for adjusting mass flow (entirety of all molecules in the gas phase and aerosols), and as this may lead to inconsistent results, the effect of flow rate was assessed.

Flow rates from both static and dynamic sampling configurations were measured by attaching a Honeywell AWM3300V mass flow sensor between sampling devices and CP e-noses. The impact of two different filters (0.45j.tm pore sized Sartorious Minisart, 0.20j.tm Whatman Acrodisc LC13) on the signal pattern and intensity was tested with the temperature kept constant at 25°C.

Selected ion flow tube mass spectrometry (SIFT-MS) assessed the change in concentration of water, acetone, methanol and ammonia with and without filter use (0.20µm PVDF filter; Whatman, Acrodisc LC13), and whole mass spectra were also taken to investigate qualitative differences of serum samples from clinically healthy cattle after passage through the filter. SIFT-MS is a real time mass spectrometry method that provides quantitative data on compounds present (Smith and Španel, 2005).

The mass flow stability for dynamic sampling and static sampling using large- (3.7L) and small bags (0.75L) were investigated by analysing 2% v/v 2-butanol and cyclohexane using two BH214 e-noses. Small bags (0.8L) were used to assess the mass flow stability across replicates at a constant temperature of 25°C.

E-nose characterisation

To assess the stability of two CP e-noses, serum from clinically healthy cattle were analysed 4 times a day in 2h intervals using small bag- (0.75L, sample volume 0.9mL) and large bag sampling (3.6L, sample volume 5mL). Small bags were used once and large bags were used for all time points. The temperature was kept constant at 25°C and incubated for 15 minutes.

SPSS (version 11.5) was used to analyse data via linear regression and multifactor ANOVA ($P \leq 0.05$). The e-noses were compared with each other and across time. Differences arising from the two sampling methods and the replicate reproducibility were investigated. Principal Component Analysis (PCA) was used to compare both devices using MATLAB 2006b.

 Published by Cranfield University Press ISBN: 978-0-9557436-7-2 http://hdl.handle.net/1826/3832

In MOSFET/MOS e-noses, the variation caused by different sample volumes and across the carousel was investigated. Twelve vials containing six different sample volumes (50j.tL, 100 j.tL, 150j.tL 200j.tL, 250j.tL and 500j.tL) of healthy cattle serum were equilibrated for 15 minutes and randomly sampled twice to test reproducibility.

Differences between MOS/MOSFET e-noses and over time were investigated. 200j.tL of serum was pipetted into three vials which were analysed randomly at four time points in a 2h interval. The adsorption phase time was 30 seconds at an air flow of 60mL per minute. Results were analysed using linear regression and multifactor ANOVA ($P \leq 0.05$).

Results

The effect of temperature

Linear regression and multifactor ANOVA discovered a significant influence of temperature on the sensor response of the BH214 e-nose covering the variation caused by two different substances (ROW and serum samples). Higher temperatures led to a bigger divergence expressed as a negative change in sensor response. A higher temperature increases the sensor response to ROW more than serum.

Mass flow andfilters

The CP e-nose had a mass flow rate of approximately 1 80ml/ min while the two BH2 14 e-noses had a flow of 200- and 240ml/min. The 0.45j.tm filter led to a drop in mass flow of approximately 1/3. In comparison to static sampling, dynamic sampling led to a drop in flow rates of about 1/4. When using a filter, a further reduction down to approximately 60% of the original flow was observed.

Addition of a 0.45j.tm Sartorious Minisart and the 0.20j.tm Whatman Acrodisc LC13 led to a decline in signal intensity of approximately 75% (ANOVA, $P \leq 0.001$, data not shown). There were also qualitative changes from filter application to sensors 1 and 7 to 11 using the 0.45j.tm filter and all sensors with the 0.20j.tm filter.

SIFT-MS analysis detected changes in the concentrations of water (-17%), ammonia (-19%), methanol (+126%) when analysed using the 0.20j.tm filter compared to no filter. Acetone concentrations remained unaffected. This and the SIFT-MS mass spectra (not shown) indicate and confirm quantitative and qualitative changes in the sample.

Analysis of small bag sampling revealed a 4% reduced flow for the first replicate and a significant drop after the 7^{th} or the 6^{th} replicate for e-nose 1 and e-nose 2, respectively. A second BH214 e-nose had a 20% higher flow rate compared to the first one, but using static sampling, 72% of the headspace contained in a bag could be analysed using both CP e-noses without any change of flow.

 Published by Cranfield University Press ISBN: 978-0-9557436-7-2 http://hdl.handle.net/1826/3832

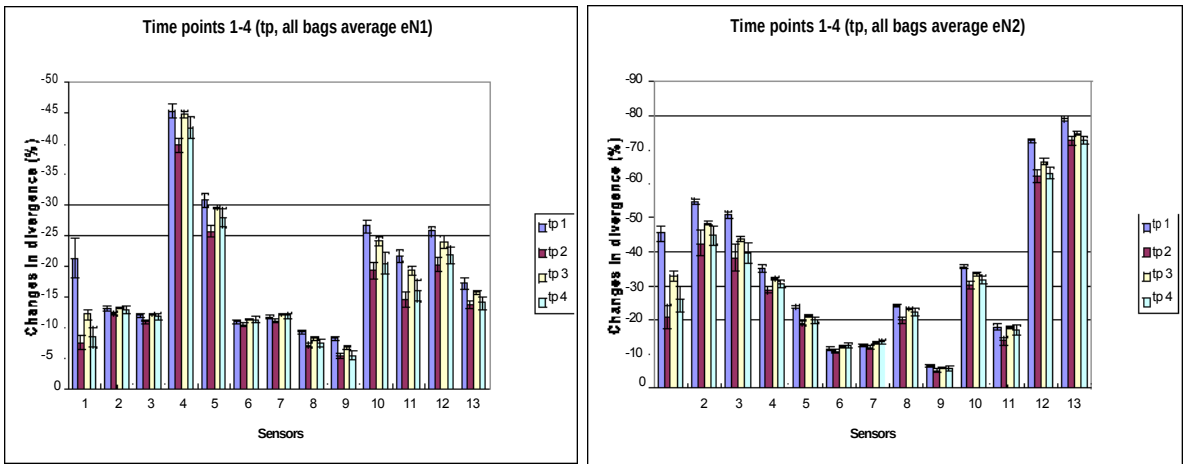

E-nose characterisation

Using PCA, 99.97% of all variance in the signals was covered by components 1 and 2 (data not shown). A clear discrimination between CP e-noses 1 and 2 due to qualitative and quantitative differences in sensor responses was revealed (see figure 1).

Figure 1: Replicate-averaged sensor responses for both CP e-noses and all 4 time points (tp) which appeared to be sine shaped for all sensors over the time. The two e-noses are qualitatively and quantitatively different.

A sine shaped change in sensor response over time was observed ($P \leq 0.05$). Changes in divergence for time point (TP) 1 were higher than TP 2. TP 3 had a bigger response again than TP 4 (see figure 2). Bag size had minor influence showing bigger sensor responses for large bags (5.5 and 5.3% for e-nose 1 and 2, respectively) while replicates taken for each samples showed no variation.

In the MOSFET/ MOS e-noses, the sample volume had no significant influence on the generated signal pattern within a range of 50 to 500μL. Analysing the same vial twice, only minor changes in sensor response were observed while random variation was found to affect vials in the carousel independent of their sample volume, with signals changing by 8.2 and 9.1% in each e-nose (referred to the baseline). Relative standard deviations referred to the sensor response the varied between 3.43% and 20.86% for one device and between 16.13% and 201.84% for the second e-nose, respectively. The e-noses gave significantly different responses for almost all sensors (see figure 2).

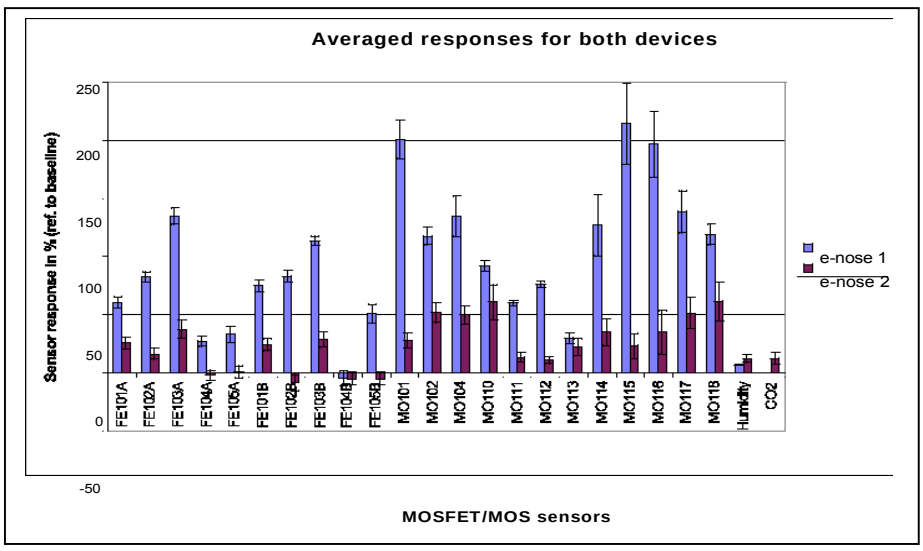

 Published by Cranfield University Press ISBN: 978-0-9557436-7-2 http://hdl.handle.net/1826/3832

Figure 2: Comparison between MOSFET/MOS e-noses. The first e-nose showed greater responses than the second one. Standard deviations of both devices were similar.

Almost all MOSFET sensors responses were dependent of replicate number for the first e-nose. All MOS sensors varied across all time points. For the second device, no sensors were replicate number dependent but 2 MOSFET and almost all MOS sensors varied at different time points ($P \leq 0.05$).

Discussion

The effect of temperature

Shifts in temperature significantly changed sensor responses since higher temperatures lead to more volatiles reacting with the sensor surface. The change in conductivity due to varying humidity and temperature has been described by various authors (Strike et al., 1999; Ampuero and Bosset, 2003; Kashwan et al., 2005; Nake et al., 2005). It is crucial for reproducible and reliable analysis to keep those parameters controlled and constant. A temperature and humidity controlled flow cell was described by Falcitelli et al. (2002) and Di Francesco et al. (2005) which may improve response reliability without losing e-nose portability.

Mass flow andfilters

Using filters for CP e-nose protection and dynamic sampling as suggested by Pavlou et al. (2002); Fend et al. (2005) and Bastos et al. (2006) yields changes in signal intensity. SIFT-MS confirmed the results. Pore size and mass flows are optimised to prevent water vapour destroying the sensing surface. However, filters change the composition of the samples and cannot be recommended. They lead to a drop in mass flow

During dynamic sampling, dilution of the sample can be expected (Misselbrook et al., 1997) which leads to a lack of reproducibility and sensitivity. In contrast, static sampling provides more stable responses and should therefore enhance discrimination. A difference in mass flow was observed between the same devices indicating a further lack of device reproducibility.

E-nose characterisation

The two CP e-noses were not qualitatively and quantitatively comparable. In addition, the temporal changes of sensor responses observed as a sine-like wave are possibly due to semi-reversible changes on the sensor surface since. The exact reason for this effect remains unclear. Memory effects were reported before (Kukla et al, 1996; Ampuero and Bosset, 2003).

The MOS and MOSFET/MOS e-noses were also different in sensor responses. High random standard variation was found when analysing different sample volumes (50-500μL). MOSFET sensors were partially replicate dependent while MOS sensors were mainly dependent on time of analysis. These results contradict other findings saying that dual needle sampling is a reliable method (Markelov et al. 2001). This might be also due to an insufficient desorption process as well as an “outgassing process” because headspace may be analysed faster than a new equilibrium has been established.

 Published by Cranfield University Press ISBN: 978-0-9557436-7-2 http://hdl.handle.net/1826/3832

Conclusion

An improvement in the devices including the sensing materials (sensitivity to water vapour, memory effects) is urgently required for both, CP- and MOSFET/MOS e-noses. However, static sampling and analysis without using a filter improve e-nose analyses significantly. A temperature controlled flow chamber with an improved desorption protocol (inert gas) could further improve results. However, if these sources of variance are eliminated, an improved and optimised e-nose sensor with enhanced data analysis methods may yield a device that is capable of living up to its promise.

References

1. Ampuero, S., Bosset, J.O. (2003). "The electronic nose applied to dairy products: a review." Sensors and Actuators B Vol. 94(1): pp 1-12.
2. Bastos, A. C., Magan, N. (2006). "Potential of an electronic nose for the early detection and differentiation between Streptomyces in potable water." Sensors and Actuators B Chemical Vol. 116(1-2): pp 15 1-155.
3. Casalinuovo, I. A., Di Pierro,D., Coletta, M., Di Francesco, P. (2006). "Application of Electronic Noses for Disease Diagnosis and Food Spoilage Detection." Sensors 6(11): pp 1428-1439.
4. Di Francesco, F., Falcitelli, M., Marano, L., Pioggia, G. (2005). "A radially symmetric measurement chamber for electronic noses." Sensors and Actuators B Chemical Vol. 105(2): pp 295-303.
5. Falcitelli, M., Benassi, A., Di Francesco, F., Domenici, C., Marano, L., Pioggia, G. (2002). "Fluid dynamic for simulation of a measurement chamber for electronic noses." Sensors and Actuators B Chemical Vol. 85(1-2): pp 166-174.
6. Fend, R., Geddes, R.,Lesellier, S., Vordermeier, H.-M., Corner, L. A. L. , Gormley, E., Costello, E., Hewinson, R. G., Marlin, D. J., Woodman, A.C., M.A. Chambers (2005). "Use of an Electronic Nose To Diagnose Mycobacterium bovis Infection in Badgers and cattle." Journal of Clinical Microbiology Vol. 43(4): pp 1745-1751.
7. Gardner, J. W. H. W. S., Hines, E.L. (2000). "An electronic nose system to diagnose illness." Sensors and Actuators B 70(1-3): pp 19-24.
8. Kashwan, K. R., Bhuyan, M. (2005). Robust Electronic-Nose System with Temperature and Humidity Drift Compensation for Tea and Spice Flavour Discrimination. Asian Conference on Sensors and the International Conference on New Techniques in Pharmaceutical and Biomedical Research.
9. Kukla, A. L., Shirshov, Y..M., Piletsky, S.A. (1996). "Ammonia sensors based on sensitive polyaniline films." Sensors and Actuators B Chemical Vol. 37(3): pp 135-140.
10. Markelov, M., Bershevits, O. A. (2001). "Methodologies of quantitative headspace analysis using vapor phase sweeping." Analytica Chimica Acta vol. 432(2): pp 2 13-227.
11. Mielle, P. (1996). "Electronic noses: Towards the objective instrumental characterization of food aroma." Trends in Food Science and Technology Vol.7: pp 432-438.
12. Misselbrook, T. H. H., P . J ., Persaud, K. C. (1997). "Use of an Electronic Nose to Measure Odour Concentration Following Application of Cattle Slurry to Grassland." Journal of Agricultural Engineering Research Vol. 66(3): pp 2 13-220.
13. Nake, A., Dubreuil, B., Raynaud, C.,Talou, T. (2005). "Outdoor in situ monitoring of volatile emissions from treatment plants with two portable technologies of electronic." Sensors and Actuators B Chemical Vol. 106(1): pp 36-39.
14. Nimmermark, S. (2001). "Use of electronic noses for detection of odour from animal production facilities: a review." Water Science and Technology Vol. 44(No 9): pp 33–41.
15. Pavlou, A. K., Magan, N., McNulty, C., Jones, J.M., Sharp, D., Brown, J., Turner, A.P.F. (2002). "Use of an electronic nose system for diagnoses of urinary tract infections." Biosensors and Bioelectronics Vol. 17(10): pp 893-899.

 Published by Cranfield University Press ISBN: 978-0-9557436-7-2 http://hdl.handle.net/1826/3832

16. Smith, D. and Španel., P. (2005). "Selected ion flow tube mass spectrometry (SIFT-MS) for on-line trace gas analysis" Mass Spectrometry Reviews **24:** 661-700.
17. Strike, D. J., Meijerink, M. G. H., Koudelka-Hep, M (1999). "Electronic noses – A mini-review." Fresenius Journal of Analytical Chemistry **vol. 364** (6): pp 499–505.

 Published by Cranfield University Press ISBN: 978-0-9557436-7-2 http://hdl.handle.net/1826/3832

IPR: Intellectual Property Rights or Responsibilities?

Brian Stevens(b.stevens@cranfield.ac.uk), Department of Information Systems, Cranfield University

Abstract

Intellectual Property (IP) has expanded from the traditional areas ofpatents, literature and music and is now considered an important tradable asset and some companies now derive the majority of their revenue from IP licences. Whilst there are internationally agreements that guarantee protection of these rights many companies attempt to limit their responsibilities via restrictive licence agreements. This paper presents the rights and responsibilities that exist for software vendors (and are likely to exist) and aims to promote discussion of the ways that the software industry can come to terms with these responsibilities.

INTRODUCTION

The decline of heavy industry in the western world coupled with the growth of a consumer society has seen western countries embrace the concept of a knowledge economy. Because of this interest in Intellectual Property (IP)[1] has expanded from the traditional fields of literature, music and industrial patents to embrace pharmaceuticals, plant breeds, processor designs and software. Whilst organisations have been keen to exploit their Intellectual Property Rights (IPR) in order to receive recompense for their efforts there has been little discussion of the corresponding responsibilities that suppliers must accept.

This paper outlines the responsibilities that software vendors must accept and aims to promote discussion about them. However, unlike science and engineering, legal matters are not a universal truth and may even be reversed according to the whims of legislators.

1 IP is an intangible asset that has been defined as "*The non-tangible products of human inventiveness and endeavour."[1]* or more simply as "*The product of creative works."*

INTELLECTUAL PROPERTY RIGHTS

Within the UK intellectual property issues are the responsibility of the UK Intellectual Property Office (UKIPO) (formerly the Patent Office) which cooperates with both the European Patent Office and the World Intellectual Property Organization . The UKIPO identifies four main types of intellectual property[2] [3] and these rights and protections offered differ according to the type of work and are summarised below (partially taken from [4]).

 Published by Cranfield University Press ISBN: 978-0-9557436-7-2 http://hdl.handle.net/1826/3832

Right	Works Protected	Duration
Patent	New inventions.	20 years
Copyright	Original literary works.	until 70 years after death of the author
	Literary, dramatic, musical and artistic works.	70 years
	Sound recordings, films, broadcasts or cable programs.	50 years
	Typographical arrangements.	20 years
Trade Mark	A distinctive distinguishing mark.	Indefinitely (renewable every 10 years)
Registered Design	The shape and appearance of a product.	25 years
Unregistered Design	The shape and appearance of a product.	10 years from 1st marketing
Database right	A collection of information made accessible.	15 years
Moral rights	The right to be identified as the creator of the work, to object to derogatory treatment of the work and not to be incorrectly identified as the creator of the work.	Indefinitely
Artist's Resale Rights (Droite de Suite)	The right to a royalty on the professional resale of any original work of art.	The lifetime of the artist.

Protection of Software

1) Copyright

Software (computer programs) is considered to be a literary work and as such is automatically protected when published until 70 years from the death of the author. This means that software is unlikely to fall out of protection within its useful life time.

2) Patents

The patent office reports that approximately 15% of patent applications are now related to computer implemented inventions (Patent Office 2004). However, computer programmes have been considered excluded inventions, yet over time this exclusion has been relaxed as patents for software controlled inventions have been accepted. The European Commission has been investigating the granting of patents to software and in 2002 produced a draft proposal. This proposal has been through many stages, but was finally rejected by the European Parliament in July 2005. However, in the

 Published by Cranfield University Press ISBN: 978-0-9557436-7-2 http://hdl.handle.net/1826/3832

United Stated it is possible to patent software and the United States Patent and Trademark Office have several categories under which a data processing application may be filed.

III. Intellectual Property Responsibilities

Whilst software vendors make much of their intellectual property rights and take steps to ensure that they are not infringed they also attempt to limit their responsibilities in the event of failure. However, consumers in England and Wales have some protection under both the Sale of Goods Act (SGA)[5] and the Supply of Goods and Services Act (SGSA)[6] such that any goods are:

as described;

fit for purpose;

of satisfactory quality;

and for services:

the supplier uses reasonable care;

they are completed within the time agreed;

they are for the agreed cost.

Despite the best efforts of software vendors to absolve themselves from liability there may still be liable because of:

the terms of the contract;

negligence;

negligent misstatement;

product liability;

liability to consumers can not be removed by contract and covers death, personal injury and damage to property.

The Consumer Protection Act[7][8] extends to “all consumer goods and goods used at a place of work.” and includes “ components and raw materials”. However, the act does not include pure information or services. A defence to producers is the “state of the art” defence which allows a defendant to show that the “state of the art” knowledge at the time was such that a producer might not be expected to have discovered the defect. This is an objective test and it is left to the courts to determine the “state of the art”.

A. Software as Goods or services

When software is purchased the person acquiring the software normally receives a copy of the software on some media (or possibly an electronic download via the internet) and a licence to use the software from the copyright holder. As copyright is an intangible asset the sale of a licence to exploit it is unlikely to be covered by the sale of goods act and will

 Published by Cranfield University Press ISBN: 978-0-9557436-7-2 http://hdl.handle.net/1826/3832

thus fall under the auspices of the supply of goods and services act. However, there are some conditions under which software may be consider as a tangible asset and thus come under the SGA, these are summarised in the table below:

Type of Software	Responsibility
Off the shelf / Shrink wrapped	Service – the supplier must have used reasonable care
Specialist software	Service - the supplier must have used reasonable care and this level of care may be different to that for general shrink wrapped software. e.g. software intended for use in avionics should be produced to the accepted standard.
Bespoke software	A reasonable level of care and as specified in the contract.
Open Source Software	Service - although this often obtained off the shelf as it is supplied free it is likely to have been developed with sufficient care given the costs.
Embedded Software	A hybrid between goods and services but as they are inseparable within the device then it is likely that they will be treated as goods.

As software is intellectual property it is generally supplied in the form of a licence rather than a physical entity and thus is likely to be covered by the SGSA rather than the SGA (unless embedded within a device). However, a recent green paper by the European Commission[7] has noted that *"The exclusion of software and data from the scope of the Consumer Sales Directive may prompt professionals to try to avoid responsibility for possible damages/non conformity of such products through conditions in End User Licence Agreements (EULA), preventing consumers from making use of remedies for non conformity and invoking damages."* it goes on to suggest that consumer protection be extended to digital content (e.g. on-line music), and it is thought by others[10] that it should also include packaged software as they are sold as *goods.* The green paper draws a distinction between a c*onsumer* and a p*rofessional* and this means that potentially a vendor may have different responsibilities for the same software depending on the end user and although it is only a consultation document, the European Parliament has reviewed the green paper and accepts that the inclusion of software as goods be considered.

IV. DISCUSSION

Although currently purchasers have little protection against defects within software consumers expect to have similar rights as they do with any tangible product and the interest of the European Commission and Parliament in software being treated as goods suggests that in future software vendors (and producers) will be liable for defective products. If the SGA is extend to apply to software then it will have to be of satisfactory quality and fit for the purpose intended, this means that software will have to "do what it says on the tin" or consumers will be able to ask for their money back. This leads to some interesting problems:

How will consumers prove that they have uninstall the software – will it have to have a code generated at the end of the uninstall process that matches the licence key?;

 Published by Cranfield University Press ISBN: 978-0-9557436-7-2 http://hdl.handle.net/1826/3832

If consumers accept patches will this suffice as a repair.

How long will software have to work for – a consumer is able to request their money back if there are inherent faults that effect its use, even if they are not initially apparent. With manufactured good the burden of prove rests with the consumer after 6 months. However, as software does not age or wear out any defects will have been present at manufacture;

Will software maintenance periods have to be extended? With goods a consumer can seek redress for up to 6 years from purchase.

The industry will need to change the way it sells and promotes software and this may lead to a tiered market in which the software available to consumers is markedly different to that available to businesses. However, perhaps the biggest impact will be felt by retailers such as PC World as the SGA directs consumers to seek redress from them.

V. Concluding Remarks

The author does not claim to have the answers to these questions but would welcome feedback and suggests that the industry will need to improve both the quality of its products and the way in which it sells and distributes them.

VI. Limitations

This work has been produced as an engineer's view of intellectual property rights and responsibilities and should not be considered a legal opinion. IPR is a legal concept and may change (even reverse) depening on the views of legislators.

References

1. P. Marret, *Information Law in Practice* Ashgate Publishing, ISBN 0-566-08390-6 2nd edition 2002.
2. UK Intellectual Property Office *What is Intellectual Property* available via www.ipo.gov.uk/whatis.htm accessed 3rd February 2008.
3. UK Intellectual Property Office *Intellectual Property Explained* available via www.ipo.gov.uk/myip.pdf accessed 3rd February 2008.
4. D. Bainbridge, *Introduction to Computer Law* Pearson Education, ISBN 0-582-47365-9 5th edition 2004
5. Department for Business Enterprise and Regulatory Reform *Sale of Goods Act Quick Facts* available via www.dti.gov.uk/consumers/fact-sheets/page38311.html accessed 3rd February 2008
6. Department for Business Enterprise and Regulatory Reform *Sale of Goods and Services Act 1982 Quick Facts* available via www.berr.gov.uk/consumers/fact-sheets/page38337.html accessed 3rd February 2008
7. Department for Business Enterprise and Regulatory Reform *Product Liability, Defective Products, Unsafe Products Quick Facts* available via www.berr.gov.uk/consumers/fact-sheets/page38253.html accessed 3rd February 2008
8. Department for Business Enterprise and Regulatory Reform *Guide to the Consumer Protection Act 1987* available via www.berr.gov.uk/files/file22866.pdf accessed 3rd February 2008
9. European Commission *Green paper on the review of the Consumer Acquis* available via ec.europa.eu/consumers/cons_int/safe_shop/acquis/gree-paper_cons_acquis_en.pdf accessed 3rd February 2008
10. Pinsent Mason *Consumer guarantee law may extend to software under EU plans* available via http://www.out-law.com/page-8458 accessed 16th September 2007

 Published by Cranfield University Press ISBN: 978-0-9557436-7-2 http://hdl.handle.net/1826/3832

CRANFIELD MULTI-STRAND CONFERENCE 6-7 MAY 2008

Methodology stream

Methodological Issues in the Design of a Study of a Regulated Market: the Case of the UK Retail Pensions Industry

David Slattery

Cranfield School of Management

david.slattery.phd.02@cranfield.ac.uk 01234 349645

February 2008

Abstract

Creating a research design is not a linear process. It is an iterative process which involves a constant appraisal and reappraisal of a number of issues: the phenomenon being studied, the research question, the literature to which a contribution is to be made, the models and analytical techniques adopted and above all the data which is being collected. Solutions to problems emerge during the research process. Examination of the data may show that a perceived design problem is not significant in the context being studied or the solution may become apparent by immersion in the data. A research design is not finished until the thesis or the journal paper is written.

Introduction

In September 2006 Sir Callum McCarthy, Chairman of the UK Financial Services Authority (FSA) addressed the Savings and Pensions Industry Leaders' Summit, asking the question 'Is the present business model bust?' (McCarthy, 2006). The business model McCarthy was referring to is the distribution system for financial services to retail customers, the system under which an individual buys a pension plan or savings product (other than a simple interest bearing deposit) from a provider such as an insurance company or a unit trust company. In his speech, McCarthy answers his question in the affirmative and then sets out what the FSA, as industry regulator, proposes to do about it. But the business model in question has been subject to strict regulation since 1988, so what has gone wrong? Why is the business model now bust? Did the regulators fail to foresee the effect of regulation? Why do we think that more regulation will fix the business model now?

These questions belong within the discipline of regulatory economics which involves the study of the rationale, process and outcomes of government intervention in markets. These questions

 Published by Cranfield University Press ISBN: 978-0-9557436-7-2 http://hdl.handle.net/1826/3832

are also addressed to a lesser extent within the discipline of strategic management where the focus is on the effect of regulation on firms' strategic choices. Within these two literatures there are a limited number of studies into the outcomes of government regulation of competitive markets over the longer term. The UK retail pensions market presents an ideal laboratory for research into the effect of regulation on the behaviour of firms and the development of a competitive market.

The UK retail pensions industry - a pilot study

At the time of McCarthy's speech my research into the impact of regulation in this market was well advanced. My pilot study revealed a wealth of contemporaneous data on the regulatory regime, about the products launched by producers, about the distribution channels used, about the industry costs and sales etc. Financial data is available from companies regulatory returns at a lower level than that found in companies' annual accounts. There is also copious commentary in companies' annual reports, the practitioner journals and the mainstream press (e.g. the Financial Times) about what was happening, or perceived to be happening at any point in time. This data is available back at least to 1985 and is increasingly detailed in more recent years. An examination of this data reveals a complex ever changing regulatory and commercial environment. There is a vigorous discourse among government departments, regulators, companies and their industry bodies, consumer groups and industry observers such as financial journalists. Alongside this discourse is a changing market as companies launch new products, compete for distribution channels, attempt to boost market share and to control costs, and to defend themselves against the reputational damage of regular regulatory criticism. A rapid phase of market exit and consolidation takes place from 1997 onward, with the number of active companies reducing by more than half. Companies abandon active marketing of their products to lower-middle income earners as these customers are unprofitable. The friendly man from the Pru has gone. There is plenty of evidence to support the view that this is a very dysfunctional market.

The research questions

A number of research questions arise in the context outlined above and it is useful to examine these from the perspective of the two main interested parties, the public policymakers (the government and the regulators) on the one hand and the strategic managers in firms on the other hand. This in turn reflects the perspectives of the two literatures, regulatory economics and strategic management respectively. From the point of view of the public policymaker the questions are: what was the effect of regulation on the evolution of the market? did the regulation achieve its objectives or were there unintended consequences? The public policymaker is interested in whether the policy objective of protecting consumers was met and also whether other policy objectives, such as ensuring that adequate provision is made by the citizen for retirement, were affected. From the point of view of the strategic manager the question is: what was the effect of

 Published by Cranfield University Press ISBN: 978-0-9557436-7-2 http://hdl.handle.net/1826/3832

regulation on the strategies adopted by firms? The strategic manager is interested in the effect of regulation on strategic choice and the creation of competitive advantage. These different perspectives may require different designs.

Methodologies used in reported studies of regulated markets

A typical research design within the regulatory economics literature addressing the public policy questions involves creating a mathematical model and testing hypotheses under different regulatory conditions or before and after a regulatory change. But this methodology is problematic within the insurance industry as there is no consensus on how to define the inputs and outputs for the model and studies produce inconsistent results (Berger *et al,* 1993).

Within the strategic management literature, there are reported studies using statistical modelling techniques where the strategies adopted by firms are identified by a simple typology such as Porter's (1980) generic strategies: cost leadership, differentiation and focus. Hypotheses that changes in regulation lead to changes in strategy are tested, and effects on profitability are assessed. But it is difficult to type a firm's strategy especially retrospectively (Golden, 1992) and these studies tend to produce inconsistent results.

An alternative to the modelling approach is to use historical techniques as pioneered by Chandler (1962) in the strategic management field and used by Vietor (1989, 1994) in his studies of the public policy and strategic management issues raised by the regulations introduced by Roosevelt in the US in the 1930s. The work of both Chandler and Vietor produced some rich insights into organisational and market change but their work was very resource intensive; they each report a major programme of research and not just a study. There is much to be said however for longitudinal studies and there are calls in the literature for more such studies. Webb and Pettigrew (1999) point out that much writing in the field of strategic management (and a good deal of the social sciences) remains an exercise in comparative statics, a tradition which is increasingly regarded as inadequate. Porter (1991) calls for research which uses historic data to reveal the chains of causality that help to create a more dynamic theory of strategic development.

Issues in the research design for the regulated UK retail pensions market

It is clear from the pilot study that the introduction of the regulatory regime in 1988, and its subsequent development, had a profound effect on the behaviour of firms and the evolution of the market. First and foremost, there is a story to tell here and it begins in the mid-1980s. This suggests a longitudinal study which is designed to make sense of what has happened from the perspective of either the public policymaker or the strategic manager or both. In the context of the existing literature, this study will make a contribution if it is explanatory and sufficiently rigorous. A number of questions arise in the design of the study which I now address.

 Published by Cranfield University Press ISBN: 978-0-9557436-7-2 http://hdl.handle.net/1826/3832

Should the research question be focused on just one perspective: either public policy or strategic management?

Focusing on just one question is almost imperative if the study is to be well bounded but it also creates problems as changes in the regulatory regime, in firms' strategic decisions and in the market are inextricably intertwined. The problem is relating microstate (firm level) change and macrostate (market level) change (McKelvey, 1997). A research design could focus on one perspective but it cannot ignore the other. Any model of how this system works must show the actors in the market with feedback loops between the actions of regulators and response of participants with links to the structural dimensions of the market such as the product range on offer, the distribution channels in use, the industry cost structure, barriers to entry and exit and industry concentration. The models in the economics literature could form the basis of a model for the regulated pensions market, but adopting these models leads to the decision to focus on the public policy issues which are the focus of this literature. The research question then becomes: what was the effect of regulation on the evolution of the market?

At what level is the analysis to be done:market/industry level or firm level?

A decision to focus on the public policy issues leads to a decision to focus on the market! industry level and not the firm level. The challenge then becomes showing the link between regulatory change and market!industry level change given that the mechanism must inevitably involve strategic decisions by firms. An assumption may be made that firm level actors are homogeneous, or perhaps a degree of heterogeneity may be admitted by identifying the strategic groups within the industry. As it happens however, it can be shown that the regulation introduced had the effect of reducing firms' strategic choices about products and distribution channels, so in the context of this study, the issue is not as difficult as it might at first seem. The link between the regulations introduced on the one hand and the products launched into!removed from the market and the distribution channels which developed on the other hand, emerges clearly from the data and can be modelled more simply than may at first be imagined.

How may regulation be analysed given that it is constantly changing?

There is no ready made framework in the literature to enable an analysis of regulatory change so I have created a framework using concepts within the literature and from an iterative analysis of my empirical data. This framework identifies the subject matter of the regulations, their purpose, the key events and the contemporaneous perceptions of market participants and observers. While it is specific to the context it also has generic features which will allow it to be used in other contexts.

How is the market/industry defined?

 Published by Cranfield University Press ISBN: 978-0-9557436-7-2 http://hdl.handle.net/1826/3832

The economics literature defines a number of structural variables for a market including the products on offer and the degree of differentiation between them, the distribution channels used, the cost structure, economies of scale, the barriers to entry and exit, and the firm concentration. The literature also indicates how the extent and boundaries of a market may be defined.

How are distinctions to be made between the effects of regulation and the more normal effects of economic, social and technological change?

The analysis will need to take into account the effects of economic, social and technological change and to distinguish the effects of regulatory change from the other factors which affect the evolution of markets without regulation. Ideally, a comparison should be made between a regulated situation and an unregulated situation but there is no obvious comparator for the retail pensions market. Economic change can however be assessed from time series data on the level of growth, inflation, interest rates, stock market levels etc. Data is available on the level of household incomes and savings so assessments can be made of individuals' changing propensity to save. Some modelling is therefore possible to identify market change which can be attributed to non-regulatory factors.

Is an econometric analysis possible?

An econometric study of the UK retail pensions market would make a contribution to the economics literature if it could overcome the particular problem of defining output variables and if the heterogeneity of firm behaviour could be modelled in some way. A full scale econometric study of this market is however impractical and would not in my view help to answer the research question. But close examination of the data shows that it is possible to construct a more focused econometric study on the process that firms use to win new business, where the major part of the costs are to be found. A reliable output variable can be defined in this context and the relationship between a major regulatory change (which can be clearly dated) and changes in marketing costs can be established. This study provides good evidence to answer the research question.

Are there any epistemological issues from using both "objective" and "subjective" data in the same study, i.e. "hard" evidence (both quantitative and qualitative) and the contemporaneous perceptions/interpretations of market participants and observers?

It may be argued that a researcher must make clear his/her ontological and epistemological positions and that it is not possible to mix different approaches. One cannot adopt a positivist and an interpretivist approach at the same time. An alternative view is that there is paradigm war within the social sciences, much of it stemming from a misattribution of one position by another (Moldoveanu and Baum, 2002). I argue elsewhere (in a paper submitted to the Cranfield School of Management Research Paper Series) that the current epistemological

 Published by Cranfield University Press ISBN: 978-0-9557436-7-2 http://hdl.handle.net/1826/3832

literature is of no assistance to a researcher. A historian would not have a problem here. A historian assesses the various sources at his/her disposal and prefers multiple sources for cross-checking. Opinions expressed by observers in contemporaneous sources are not accepted without investigation but are often starting points for the historian's own search for causes (Howell and Prevenier, 2001, p128). In my study, it may be that a number of different market participants and observers express the same view of unfolding events, and even if this view is mistaken it may influence the behaviour of firms or regulators and therefore explain events. Such contemporaneous perceptions and observations may assist understanding the changes observed in products launched or distribution channels used; it may assist understanding the market exit and consolidation observed. The use of "subjective" data is not therefore incompatible with the use of "objective" data. All data, from whatever source, needs to be evaluated for its relevance to the research question and for its probative value in answering that research question. The weight of each piece of evidence needs to be assessed, and conflicts between evidence resolved. Such assessment of data is not helped by adopting a prior epistemological position.

Conclusions

During the course of my research I oscillated between the public policy perspective and the strategic management perspective before deciding to focus on the public policy issues. I have continuously grappled with the methodological issues as I have collected my data. Decisions needed to be taken to focus the data collection, but I have found it useful to keep my options open wherever possible. Many of the issues I have faced turn out to be tractable within the context of the study and solutions have emerged as I have become immersed in the data. My research design has evolved rather than being created. It is still evolving and will not be finished until I have finished my thesis and am satisfied that I have presented a logical and coherent narrative explaining the work that I have done and my contribution to knowledge.

References

1. Berger, A.N., Hunter, W.C. and Timme, S.G. (1993), 'The Efficiency of Financial Institutions', *Journal ofBanking and Finance,* Vol. 17, pp. 22 1-249.
2. Chandler, A.D. (1962), *Strategy and Structure. Chapters in the History of the American Industrial Enterprise,* MIT, Massachusetts.
3. Golden, B.R. (1992), 'The Past Is the Past - or Is It? The Use of Retrospective Accounts As Indicators of Past Strategy', *Academy ofManagement Journal,* Vol. 35, No. 4, pp. 848-860.
4. Howell, M. and Prevenier, W. (2001), *From Reliable Sources. An Introduction to Historical Methods,* Cornell,
5. McCarthy, C. (2006), 'Is the Present Business Model Bust?', in Savings and Pensions Industry Leaders Summit Gleneagles 16 September 2006, www.fsa.gov.uk,
6. McKelvey, B. (1997), 'Quasi-Natural Organisational Science', *Organisational Science,* Vol. 8, No. 4, pp. 352-380.

 Published by Cranfield University Press ISBN: 978-0-9557436-7-2 http://hdl.handle.net/1826/3832

7. Moldoveanu, M.C. and Baum, J.A.C. (2002), 'Contemporary Debates in Organizational Epistemology', in Baum, J.A.C. (Ed), *Companion to Organizations,* Blackwell, MA USA,
8. Porter, M.E. (1980), *Competitive Strategy,* Free Press, New York.
9. Porter, M.E. (1991), 'Towards a Dynamic Theory of Strategy', *Strategic Management Journal,* Vol. 12, No. Special Issue, Winter, pp. 95-117.
10. Vietor, R.H.K. (1989), *Strategic Management in the Regulatory Environment,* Prentice Hall, New Jersey.
11. Vietor, R.H.K. (1994), *Contrived Competition.Regulation and Deregulation in America,* Harvard,
12. Webb, D. and Pettigrew, A. (1999), 'The Temporal Development of Strategy: Patterns in the UK Insurance Industry', *Organization Science,* Vol. 10, No. 5, pp. 601-621.

 Published by Cranfield University Press ISBN: 978-0-9557436-7-2 http://hdl.handle.net/1826/3832

Feasibility Study and Optimum Design of Functionally Graded Structures

O. Oyekoya1, D. Mba, A. El-Zafrany

Summary

Two new Mindlin-type elements were formulated in a previous publication by the author [1]. A summarised result of the previous work has been presented in this paper. The major contributions of the previous work to the current functionally graded technology include considerations of geometrical nonlinearity, material nonlinearity, economical meshing using smooth fibre distribution technique, structural integrity enhancement and strength maximisation. In order to investigate the commercialisation of the previous work, a literature review on the functionally graded technology applications, its commercialisation feasibility and optimum structural design have been undertaken in this paper. This study was able to show that the functionally graded technology has rapidly expanded its area of applications and it still has a promising future. This technology expansion is due to the strong government and private investments by the major pioneers of the technology (i.e. Japan and USA). The reason for the interest in this technology is due to its economical and environmental benefits. The economical benefits include low cost and quality product for customers; reduction in energy consumption for manufacturer and manufacturing cost for manufacturer. The environmental benefits are due to weight minimisation which results in reduction of carbon emission in various functionally graded technology applications such as automotive, aerospace, industrial applications etc.

Introduction

 Published by Cranfield University Press ISBN: 978-0-9557436-7-2 http://hdl.handle.net/1826/3832

Composite materials are often used in different engineering fields, especially in the aerospace field. The advantage of composite materials is the high stiffness-to-weight and strength-to-weight ratios. The limitations of composite materials are the following: the weakness of interfaces between layers may lead to de-lamination, extreme thermal loads may lead to de-bonding between matrix and fibre due to mismatch of mechanical properties, and residual stresses may be present due to difference in coefficients of thermal expansion of the fibre and the matrix. In order to overcome the limitations, functionally graded materials (FGMs) were proposed. The FGMs are made in such a way that the volume fractions of two or more materials are varied continuously along a certain dimension. The FGMs can be made as required for different applications. For example, thermal barrier plate structures can be made from a mixture of ceramic and metal for high temperature application. The advantage of the FGM plate is that its material properties vary continuously from one surface to the other, hence avoiding the interface problem that exists in homogeneous composites.

Applications

This section presents the evolution of the functionally graded technology. This technology has already started revolutionising the science and technology world due to the vastness of its application. In this paper, a literature review of some sample applications of the technology was undertaken.

In 1996, Watari et al [2] have developed a functionally gradient dental implant as a typical example of the FGM application to biomaterials. The dental implant is used for restoring the function of chewing and biting, and therefore eating, which is the most fundamental activity of human beings required for living. Humans are living in an era of longer life expectancy, and thus dental care becomes especially important for better quality of life in old age.

 Published by Cranfield University Press ISBN: 978-0-9557436-7-2 http://hdl.handle.net/1826/3832

In 1999, Chin [3] presented key technologies necessary for prompt delivery of FGAC technology to the war-fighter. With the emphasis on smaller but more mobile combat forces to meet a broad range of mission requirements, future weapon platforms and upgrades will require materials to do better, do more, weigh less, size less and cost less. Metal matrix composites (MMCs) are such material candidates for niche Army applications such as armour, armaments, and vehicle structures. Under the shadow of shrinking resources, a focused research team (FRT) composed of the US Army Research Laboratory (ARL), academia, and small business was assembled to address MMC issues for Army applications. The immediate focus of this team is on the development of MMCs with a tailored ceramic-to-metal through-thickness gradient known as functionally graded armour composites (FGACs). The goal is to provide the science and technology to deliver a high space and mass efficient armour material for ballistic protection against light to medium threats.

In 2001, Chan [4] studied the performance and emissions characteristics of a partially [1]insulated gasoline engine. Instead of using a single-property yttria-stabilized zirconia (YSZ) coating to achieve the thermal barrier for the piston crown, a varying-properties functionally graded material (FGM) was used in this study. Extensive experiments were conducted on a 3- cylinder SI Daihatsu engine with all piston crowns coated with a layer of ceramic, which consists of zirconia and yttria with varying compositions along its thickness. Measurements of engine performance, in particular its fuel consumption and emissions characteristics, were made before and after the application of FGM coatings onto the piston crowns.

In order to lengthen rocket engine's life-expectancy, it is important that the heat- and acid-resisting properties of the materials used in fabricating the combustion chamber be improved and, to this end, the development of a new heat-resistant

[1] 1 Corresponding Author. School of Engineering, Cranfield University, Cranfield, Bedfordshire, England, MK43 0AL

 Published by Cranfield University Press ISBN: 978-0-9557436-7-2 http://hdl.handle.net/1826/3832

material is essential. In order to respond to these needs, Moro et al [5] from the Kakuda Research Centre of the National Aerospace Laboratory have, since 1994, been engaged in the research and test evaluation of the reusable engines for use in conjunction with H-II Orbiting Plane-Experimental (HOPE) and other future reusable engines. In 2002, Moro et al [5] described the background of the development of the two kinds of reusable high-performance engine. One of these two is the re-generatively cooled 1200N thrust engine composed of two kinds of ZrO2/Ni functionally graded materials (FGMs) chambers. The other is the Reaction Control System (RCS) engine with chambers that are made of carbon-Aber-reinforced carbon matrix (C/C) composites coated with SiC FGMs.

In 2002, U.S. Department of Defense, Manufacturing Technology Program [6] researched on F135 engine and PW J52 engine by applying functional graded thermal barrier coatings on turbine components, which will increase component life under severe environment and reduce the down-time for the repair of components and enhance readiness of the fleet. These were run in two engine tests for qualification: (1) F402 engine (AV-8B) test as test engine for insertion in F135 engine (JSF) and (2) PW J52 (EA-6B) engine test.

This application study was able to show that the functionally graded technology has rapidly expanded its area of applications and it still has a promising future. Though this technology is still in its infant stage of development, it has already gained its reputation in various areas of science and technology such as medical, defence, manufacturing, aerospace and automotive applications as shown in this paper.

Feasibility Study on the Commercialisation of FGMs

The functionally graded technology is quite a remarkable technology and it is expected to revolutionise the science and technology world. The key driving forces

 Published by Cranfield University Press ISBN: 978-0-9557436-7-2 http://hdl.handle.net/1826/3832

are cost effectiveness, structural weight minimisation, structural strength maximisation, improved heat resistance, improved wear resistance and improved corrosion resistance. In order to show the commercialisation feasibility of this technology, a literature review of the commercialisation of functionally graded technology was undertaken.

In the heavy manufacturing industry, strength, resilience, and reliability are vital characteristics in products. In the early 1990s, Caterpillar [7] developed a research plan to apply functionally gradient material (FGM) coatings onto wear parts in a cost-effective manner so that the coated parts would last several times longer than parts currently available. Caterpillar and its five subcontractors (four companies and one university laboratory) submitted a proposal to the Advanced Technology Program (ATP). In 1994, ATP awarded Caterpillar $1.9 million in cost-shared funds to pursue FGM research. Through this three-year ATP project, the team developed new FGM systems that improve contact fatigue and wear and corrosion resistance of components such as gears, undercarriages for heavy earth-moving equipment, and rolls for steel mills. Because Caterpillar used the new technology to enhance several of its products, end users are now realising the benefits of lower costs and higher quality products. In addition, several firms are marketing the technology for other applications within large mining operations and high deposition thermal spraying.

On March 2004, some US industries formed a collaboration called the FGM team [8] to investigate the implementation of FGM solutions into manufacturing environments associated with hot forming applications in the forging, die casting and glass industries. The targets for success in the project are to reduce energy consumption by 25 percent, increase tooling lives by a minimum of five times that of current materials and provide a globally competitive cost edge to U.S. forging, die casting and glass manufacturing industries. All the project partners agree that

 Published by Cranfield University Press ISBN: 978-0-9557436-7-2 http://hdl.handle.net/1826/3832

a 5X increase in tool life will greatly improve manufacturing efficiency and reduce energy consumption. One forging company purchases over 80,000 pounds of tooling per month, while the project's glass partner purchases over one million plungers per year, all of which could potentially be minimized with new FGM tooling. Plans include testing of FGM tooling in commercial hot forming operations at each industrial partner and comparing the results with baseline material currently being used. All of the industrial partners have committed to implement new tooling that reduces energy consumption and manufacturing costs.

The case studies considered in this feasibility study were able to highlight the strong government and private investment by the major pioneers of the technology (i.e. Japan and USA). This feasibility study highlighted low cost and quality product for customers. It also highlighted reduction in energy consumption and cost for manufacturers.

Theory of Mindlin-Type Elements

The author [1] has previously written a paper on structural integrity of functionally graded composite structure using Mindlin-type finite elements. Further details of the Mindlintype element theory can be found in the paper [1]. The theory includes the formulation of the displacement equation, strain equation, stress equation, strain energy variation and generalised equation of equilibrium. The generalised equation of equilibrium is then linearised, in-order to obtain the Mindin-type element equation.

In the paper [1], two new Mindlin-type plate bending elements were derived for the modelling of functionally graded plate subjected to various loading conditions such as tensile loading, in-plane bending and out-of-plane bending. The properties of the first Mindlin-type element (i.e. Average Mindlin-type element) are computed by using an average fibre distribution technique which averages the

 Published by Cranfield University Press ISBN: 978-0-9557436-7-2 http://hdl.handle.net/1826/3832

macro-mechanical properties over each element. The properties of the second Mindlin-type element (i.e. Smooth Mindlin-type element) are computed by using a smooth fibre distribution technique, which directly uses the macro-mechanical properties at Gaussian quadrature points of each element. There were two types of non-linearity considered in the modelling of the plate, which include finite strain and material degradation.

Finite Element Modelling

A rectangular plate made of a typical FGM with its midplane as shown in Figure 1 was considered. A 72 element mesh was employed for all the three validation case studies. The elements used in the validation exercise include 4-noded Average Mindlin element, 4-noded Smooth Mindlin element and 4-noded Ordinary Mindlin element. The boundary condition applied in the three case studies is that edge x=0 is a clamped edge. A load of 0.1kN was applied as an equivalent nodal loading at edge x=2 for all load cases.

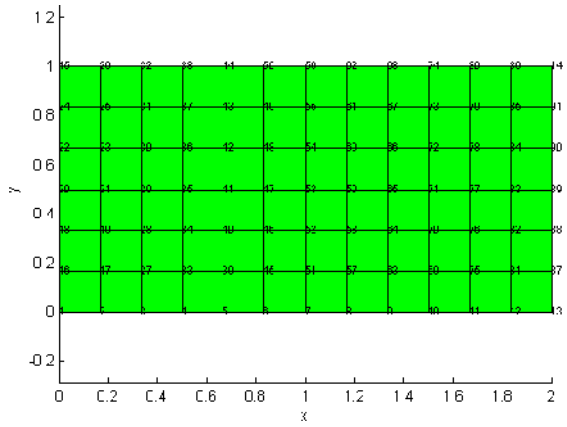

Figure 1: Mesh

 Published by Cranfield University Press ISBN: 978-0-9557436-7-2 http://hdl.handle.net/1826/3832

Optimum Design

The optimum design criterion employed in this paper can be described as minimum deflection criterion.

The equation used for fibre distribution is as given below.

$$V_{f(\xi)} \; V_{\square} \; . \; (V_2 \quad V_1)\xi_p$$

$$\text{where} \quad \xi = \frac{x_1}{\tilde{x}\ \tilde{x}_2} \qquad (1)$$

 Published by Cranfield University Press ISBN: 978-0-9557436-7-2 http://hdl.handle.net/1826/3832

V_1, V_2 fibre ratio at x_1 and x_2

Nine fibre distribution cases were considered, where P could assume a value of 0.5, 1 and 2. Also V_1 could assume the value 0.5, 0.55 and 0.6. It must be noted that all cases have the same amount of fibre as in the P=0 case but different fibre distributions across the composite domain. The P=0 case represents the traditional composite case with uniform fibre distribution.

Figure 2 shows a displacement plot of out-of-plane bending cases with P=0 and P=2. This plot shows the most pronounced fibre distribution effect in all fibre distribution cases and all loading cases. The fibre distribution case P=2 and V_1=0.55 satisfies the minimum deflection criterion for the out-of-plane bending case with 59% w_{max}-deflection relative to the traditional composite case. This fibre distribution case also satisfies the minimum deflection criterion for the in-plane bending case with 84% v_{max}-deflection relative to the traditional composite case. But this fibre distribution case results in an adverse u_{max}-deflection result for the tension case with 125% u_{max}-deflection relative to the traditional case. Hence it can be deduced that the fibre distribution case with P=2 and V_1=0.55 gives the optimum design for most load cases. The prioritisation of the load cases need to be undertaken for a given design in determining whether this adverse result is a good enough trade-off.

 Published by Cranfield University Press ISBN: 978-0-9557436-7-2 http://hdl.handle.net/1826/3832

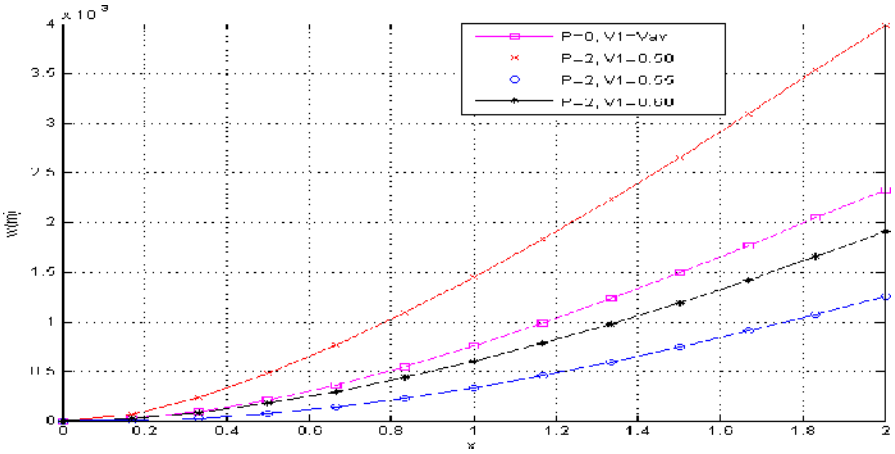

Figure 2: Displacement results for out-of-plane bending cases with P=0 and P=2

Conclusion

The author's previous work [1] made some contributions to the current functionally graded technology. These contributions include considerations of geometrical nonlinearity, material nonlinearity, economical meshing using smooth fibre distribution technique, structural integrity enhancement and strength maximisation. A methodical approach was used to achieve the objectives in this paper by learning from previous publications on functionally graded technology applications and commercialisations. The major lessons learnt include low cost and quality product for customers. Also manufacturers benefited from reduction in energy consumption and manufacturing cost. This paper has succeeded in its objective by applying the lessons learnt from current success stories of functional graded

 Published by Cranfield University Press ISBN: 978-0-9557436-7-2 http://hdl.handle.net/1826/3832

technology applications and commercialisations to justify the commercialisation feasibility of this technology.

Reference

1. 1 O.Oyekoya, D. Mba and A. El-Zafrany; Structural integrity of functionally graded composite structure using Mindlin-type finite elements; ICCES, vol.172, no.1, pp.1 -6, 2008
2. 2 Watari F., Yokoyama A., Saso F., Uo M. and Kawasaki T.; Fabrication and properties of functionally graded dental implant, Composites Part B, 28B, 1997
3. 3 Chin E. S. C.; Army focused research team on functionally graded armor composites, Materials Science and Engineering, 1999
4. 4 Chan S. H.; Performance and emissions characteristics of a partially insulated gasoline engine, Int. J. Therm. Sci., 2001
5. 5 Moro A., Kuroda Y. and Kusaka K; Development status of the reusable high performance engines with functionally graded materials, Acta Astronautica Vol. 50, No. 7, pp. 427– 432,2002
6. 6 U.S. Department of Defense; Functionally graded thermal barrier coating, Manufacturing Technology Program, Fiscal Year 2002
7. 7 NIST; Performance of 50 completed ATP projects, Status Report Number 3, August 2002.
8. 8 Lherbier L. W.: Development of Functionally Graded Material for Manufacturing Tools and Dies and Industrial Processing Equipment; 2006

 Published by Cranfield University Press ISBN: 978-0-9557436-7-2 http://hdl.handle.net/1826/3832

Determination of the elastic modulus of piezoelectric films using self-supported cantilever structures

G. Leighton, Z. Huang and R. Dorey

Department of Materials, School of Applied Sciences,
Cranfield University, Beds MK43 0AL, UK

Piezoelectric lead zirconate titanate $_{(PbZrxTi1-xO3,}$ PZT) thin and thick films have received considerable interest for their use as the functional material within microelectromechanical systems (MEMS). Accurate knowledge of the electrical and mechanical properties of these materials is essential for the effective modelling and design of novel MEMS devices. With macro-scale devices this can be accomplished, as all properties can be determined for a given bulk material. In MEMS devices this is not true due to the difficulties involved in measuring properties such as the elastic modulus of thick/thin films, which is why most modelling results are considered acceptable if they are within 10% of experimental values. The main difficulties in measuring the elastic modulus of piezoelectric ceramic films are the influence of the substrate and any additional layers required to grow them e.g. electrodes and seeding layers. We report here the preparation of self-supported PZT cantilevers about 10 μm in thickness and the determination of their elastic coefficients using vibrometry techniques.

Using this method we have determined the elastic modulus of a thick film PZT cantilever without electrodes to be about 57 GPa. We have found that 100 nm thick electrodes increase the apparent elastic modulus by as much as 38%. The effect of poling on the elastic coefficient has also been investigated.

 Published by Cranfield University Press ISBN: 978-0-9557436-7-2 http://hdl.handle.net/1826/3832

GPA Diagnostics: An Application to an Industrial Gas Turbine

E. Tsoutsanis* Y.G. Li* P. Pilidis* M. Newby**
*School of Engineering, Cranfield University, Bedfordshire, MK43 0AL, England
**Manx Electricity Authority, Isle of Man, England

ABSTRACT

In the competitive power generation market, in which the gas turbine works, accurate engine performance simulation and diagnostics have a deep impact in the plant's operational and maintenance strategy. Gas path analysis (GPA) developed at Cranfield University is a powerful diagnostic technique that has been extensively used to predict the health of a gas turbine. This paper presents an application of the GPA technique to a GE LM2500+ gas turbine engine operating in the Manx Electricity Authority (MEA), Isle of Man, for estimating its degradation over a three month period. The application shows that the GPA approach can provide a fast and accurate assessment of a gas turbine's health condition.

KEYWORDS

Gas turbine, Engine, Gas Path analysis, Diagnostics, GPA Index,

INTRODUCTION

Gas path analysis (GPA) is a powerful diagnostic technique that has been extensively used to predict the health of a gas turbine, by implementing the variety of measurements located in the engine's gas path. This technique enables the gas turbine users to construct a reliable and robust maintenance strategy. Therefore the highly considerable maintenance and operational costs of gas turbines are reduced.

Comprehensive reviews of gas path diagnostics techniques have been provided by Li [1] and Singh [2]. The gas path analysis initiated as a linear approach introduced by Urban [3] and followed by Stamatis et al [4] approach which considered the non-linearity effects of the problem. However the limitations addressed by the repeatable uncertainties of the gas turbine system like measurement noise and variable ambient conditions, motivated the development of various conventional and artificial optimisation techniques like neural networks [5-9], genetic algorithms [10], hybrid systems [11,12] and fuzzy expert systems [6,13].

 Published by Cranfield University Press ISBN: 978-0-9557436-7-2 http://hdl.handle.net/1826/3832

Since the GPA is a model-based performance diagnostic technique thence the accuracy of the diagnostic analysis is dependent on extremely accurate performance simulation. The development of techniques to adapt a performance engine model to the measurements of a particular gas turbine engine is highly pursued. A design point performance adaptation method has been developed by Li [14].

Many performance software, that can handle a series of the repeatable uncertainties, have been developed based on a family of diagnostic techniques [15]. One of these programmes is PYTHIA [16]; a user friendly performance simulation and diagnostic system, which is built around gas path analysis theory developed at Cranfield University.

In this paper a gas path analysis method will be employed, through the use of PYTHIA software, in order to determine the actual degradation of an aeroderivative gas turbine. This application procedure commences with the development of an engine performance model, continues with the performance adaptation for matching the real engine measurements, pre-processes ambient and operating condition correction and concludes with the prediction of the engine component degradation using the concept of GPA index.

THEORY OF GAS PATH ANALYSIS

A linear and non-linear GPA approach developed at Cranfield [17] is an effective tool for inverse mathematical problems such a gas turbine performance adaptation and performance diagnostics. The idea of the method is as follows. The thermodynamic relationship among performance parameters, component parameters and ambient, operating condition parameters can be represented with Equation (1).

$$\vec{z} = h(\vec{x}, \vec{y}) \qquad (1)$$

Where $\vec{z} \in \Re^M$ is a measurable performance parameter vector and M is the number of performance parameters, $\vec{x} \in \Re^N$ is the component parameter vector (or called to-be-adapted parameter vector for adaptation and health parameter vector for diagnostics) and N the number of component parameters, $\vec{y} \in \Re^{N'}$ is the ambient and operating condition parameter vector and N' the number of these parameters, and $h()$ is a vector-valued function. At a given operating point which is denoted by subscript $"0"$, Equation (1) can be expanded in a Taylor series

$$\vec{z} = \vec{z}_0 + \left.\frac{\partial h(\vec{x}, \vec{y})}{\partial \vec{x}}\right|_0 (\vec{x} - \vec{x}_0) + \left.\frac{\partial h(\vec{x}, \vec{y})}{\partial \vec{y}}\right|_0 (\vec{y} - \vec{y}_0) + HOT \qquad (2)$$

 Published by Cranfield University Press ISBN: 978-0-9557436-7-2 http://hdl.handle.net/1826/3832

HOT represents higher order terms of the expansion and can be neglected. Therefore, a linearised relationship gas turbine performance model, by assuming no deviation from standard ambient and nominal operating conditions, can be expressed with Equation (3).

$$\Delta\vec{z} = H \cdot \Delta\vec{x} \tag{3}$$

The deviation of component parameters can be predicted by inverting the influence coefficient matrix (ICM), H, to a fault coefficient matrix (FCM) for diagnostic problems, H^{-1}, leading to Equation (4).

$$\Delta\vec{x} = H^{-1} \cdot \Delta\vec{z} \tag{4}$$

The non-linearity of the engine behaviour is taken into account by using an iterative Newton-Raphson process where linear GPA is applied iteratively until a converged solution is obtained, Figures 1, 2. The number of performance parameters, M, may not be equal to the number of component parameters N. Therefore, a pseudoinverse matrix is defined depending on whether $N > M$ or $N < M$. Typically such a situation leads to an infinite number of least-squares solutions. The solution resulting from the pseudoinverse which is best in a least-squares sense is the following

$$\vec{x} = H^{\#} \cdot \vec{z} \tag{5}$$

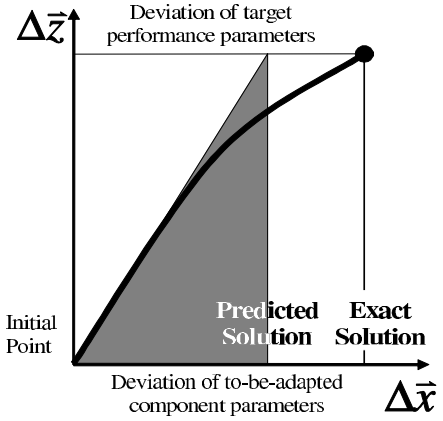

Figure 1: Linear GPA

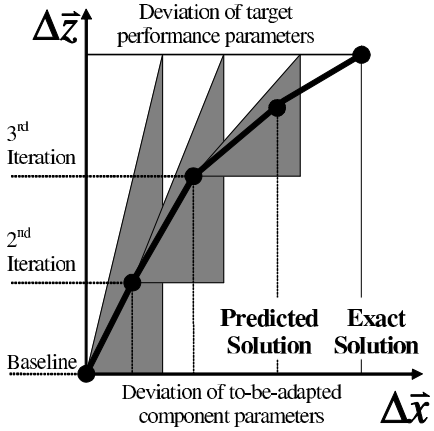

Figure 2: Non Linear GPA

This diagnostic method is simple and fast in prediction although it has certain requirements that must be met. One of them is that the ICM is an accurate mathematical description of gas turbine performance at a specific operating point. The second requirement involves measurement bias and noise free sensors and the third the un-correlated measurements being sensitive to engine degradation. The GPA is dependent on the apriori information of degraded components. To effectively isolate the deteriorated components GPA index is introduced. The GPA index is a measure of the diagnostic accuracy and is defined as:

$$\lambda = \frac{1}{1+\varepsilon} \tag{7}$$

 Published by Cranfield University Press ISBN: 978-0-9557436-7-2 http://hdl.handle.net/1826/3832

where λ is the GPA index and ε is the difference between measured and predicted deviations of engine gas path measurements expressed with equation 8.

$$\varepsilon = \sum w_i \left| \frac{\Delta z_i}{z_{0,i}} - \frac{\Delta z_{m,i}}{z_{0,i}} \right| \qquad (8)$$

where w_i are the weighting factors taking into account the relative importance of the measurements. To apply the GPA index effectively to gas turbine component fault diagnosis, the maximum number of simultaneously degraded engine components and the component fault cases (CFC) should be assumed. In a situation where more than one CFC cases are likely, weighted degradation is suggested and calculated as follows

$$\bar{x}_i = \sum_{j=1}^{S_f} x_{i,j} \cdot \lambda_j \Big/ \sum_{j=1}^{S_f} \lambda_j \qquad (9)$$

where $\bar{x}_i$ is a weighted health parameter, $x_{i,j}$ the i_{th} health parameter predicted in CFC case j, λ_j the GPA index in CFC case j and S_f the total number of the most likely faults. Summarising this diagnostic system which is based on GPA has been implemented into Cranfield gas turbine performance analysis software PYTHIA [17] developed from TURBOMATCH, the validity of which has been tested over many years.

APPLICATION AND ANALYSIS

The engine chosen for the application of this GPA analysis is the GE LM2500+ aeroderivative gas turbine operating at Manx Electricity Authority. A pair of these engines along with two steam generators and a steam turbine produces a total power of 87 MW in a combined cycle configuration [18]. This engine consists of a variable geometry compressor [19], a single annular combustor, a two stage high pressure turbine and a two stage high speed power turbine as illustrated in Figure 3.

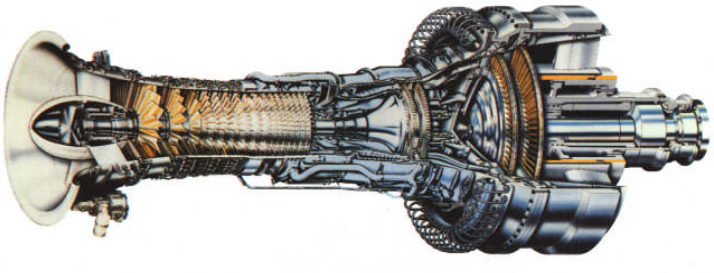

Figure 3: GE LM2500+ HSPT [23], Courtesy of GE

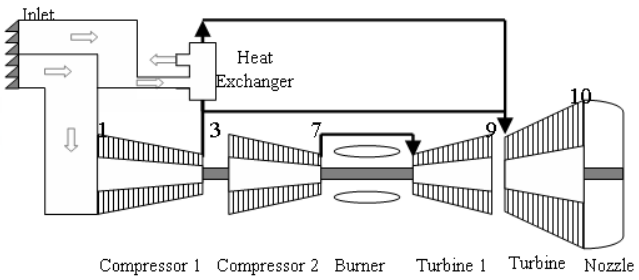

Figure 4: Model gas turbine configuration

 Published by Cranfield University Press ISBN: 978-0-9557436-7-2 http://hdl.handle.net/1826/3832

Engine Performance Model

When the engine is operating at certain conditions, the power output is used as the control parameter and kept constant as environmental conditions change and degradation happens. At the 9th stage of the compressor the bleed flow passes through a heat exchanger for further reducing the temperature of the flow fed to the power turbine Figure 4. The developed engine model accurately matches the design point performance of the real engine. The selected instrumentation set for diagnostic analysis of the model engine is described in Table 1.

Table 1: Engine gas path measurement

No	Symbol	Parameter
1	T_1 (K)	Ambient temperature
2	P_1 (atm)	Ambient pressure
3	P (MW)	Power output
4	PCN (%)	Compressor shaft speed
5	T_7 (K)	Compressor discharge total temperature
6	P_7 (atm)	Compressor discharge total pressure
7	T_9 (K)	Compressor turbine exit total temperature
8	P_9 (atm)	Compressor turbine exit total pressure

Table 2: Measurement Conditions

Parameters	Jan 2007	Mar 2007
T_1 (K)	283.45	285.0
P_1 (atm)	0.996	0.990
P (MW)	29.3	29.3

From a series of available measurements the selected set for this analysis had the same power output at slightly different ambient conditions as described in Table 2. Both set of measurements were very close to the design point performance of the engine and the reason for that will be amplified later on the paper.

Analysis

The objective of this analysis is the application of the diagnostic system described throughout the paper to a real scenario to determine the degradation that this gas turbine has experienced during this period. Performance wise the main focus of this diagnosis is to determine the deterioration that the first stages of the compressor have experienced due to fouling since the degradation of the other engine hot end components will be negligible. The considered assumptions of this procedure are enlisted here.

 Published by Cranfield University Press ISBN: 978-0-9557436-7-2 http://hdl.handle.net/1826/3832

Up to two components can be simultaneously degraded

The components among which faulty compressor will be searched for is Compressor 1 and Turbine 1.

Adapted engine model for matching the set of measurements close to design point

Ambient condition shift present

Performance Adaptation

Performance adaptation was employed to adapt the engine model to the real engine measurements. Since both set of data were taken close to the design point of the engine's performance it becomes clear that design point performance adaptation could be applied for matching the engine model to the January measurements.

Measurement Correction

All the available measurements of March were corrected to the same ambient conditions of the earlier January measurements. The apparent deviation between the two set of measurements was due to degradation and mainly due to compressor fouling. A comparison between the deviation of the engine performance parameters with and without ambient conditions correction is presented in Figure 5.

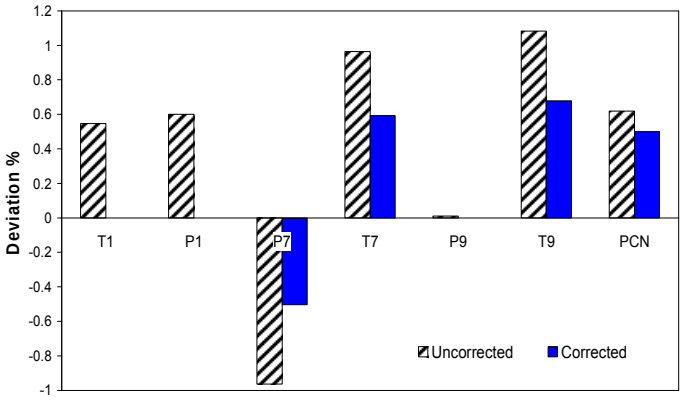

Figure 5: Uncorrected and corrected measurement deviation

Table 3: Engine component fault classes

Component Fault Case	Pre-defined faulty components
CFC1	Compressor 1
CFC2	Turbine 1
CFC3	Compressor 1 + Turbine 1

Engine Component Fault Detection

To identify which engine component is responsible for the observed deviation the GPA Index is used. Assuming that the maximum number of simultaneously degraded components can be up to

 Published by Cranfield University Press ISBN: 978-0-9557436-7-2 http://hdl.handle.net/1826/3832

two the component fault cases are listed in Table 3. The Component Fault Cases with their corresponding GPA index is represented in Fig 6.

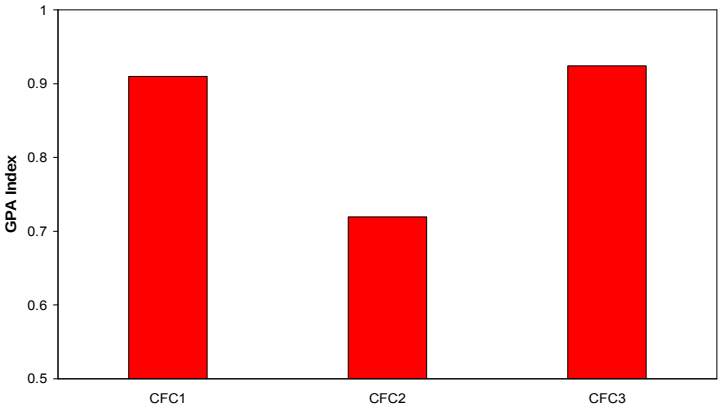

Figure 6: Engine fault detection with GPA Index

Table 4: Degradation results

Compressor 1	$\Delta\eta_c$ (%)	$\Delta\Gamma_c$ (%)
Degradation	-0.79	-0.67
Turbine 1	$\Delta\eta_t$ (%)	$\Delta\Gamma_t$ (%)
Degradation	-0.09	0.02

It is evident from Figure 6 that CFC 1 and CFC3 present the highest GPA index therefore there is a deterioration of the compressor and a very small deterioration of the compressor turbine. In order to determine the actual degradation of each component and since two of the CFC are likely responsible for the apparent parameter deviation, the weighted solution is applied. This provides the diagnostic results tabulated in Table 4.

As expected the first stages of the compressor had a drop of 0.79% in isentropic efficiency and a 0.67% reduction in mass flow capacity. The degradation of the compressor turbine is negligible compared to that of the compressor's. The compressor fouling has an immediate effect on the performance of the gas turbine which results in lost power. The engine's control reaction to the above degradation was to add more fuel and run at slightly higher rotational speed to satisfy the power output.

CONCLUSIONS

In this paper a Gas Path Analysis technique has been applied through the use of PYTHIA, a diagnostic software developed at Cranfield University, for accessing the deterioration of an aeroderivative gas turbine engine used for power generation at the Isle of Man. Gas path analysis is a powerful diagnostic technique and its dependencies on accurate performance simulation and a-priori information about degraded components are compensated by performance adaptation and GPA index respectively.

From the development of an engine model and its adaptation to real engine measurements, which is considered fundamental for such kind of analysis, to the consideration of practical issues of

 Published by Cranfield University Press ISBN: 978-0-9557436-7-2 http://hdl.handle.net/1826/3832

measurement correction and instrumentation selection this GPA method has the capacity to predict component degradation at a reliable level.

The analysis showed that during a continuous operation of three months and close to the date of the engine's major overhaul the first stages of the compressor have deteriorated due to fouling. The application of this technique to this real case scenario facilitates gas turbine users with the operation and maintenance decision making of the power plant.

AKNOWLEDGEMENTS

The present research is supported by the Manx Electricity Authority (MEA) and the Engineering and Physical Sciences Research Council (EPSRC). The authors also thank the MEA for allowing us to use their test data and providing valuable technical information.

REFERENCES

1. Y. G. Li. Performance-analysis-based gas turbine diagnostics: A review. *Proceedings of the Institution of Mechanical Engineers, Part A: Journal of Power and Energy,* 216(5):363–377, 2002.
2. R. Singh. Advances and opportunities in gas path diagnostics. *ISABE-2003-1008, 15th:ISABE*, 2003.
3. L. A. Urban. Parameter Selection for multiple fault diagnostics of gas turbine engines, *AGARD-CP-165 ASME Paper 74-GT-62, J. Eng. Power*, 225-230, April 1975
    A. Stamatis, K. Mathioudakis, M. Smith and K. Papailiou. Gas turbine component fault identification by means of adaptive performance modeling. *ASME Paper 90-GT-376*, 1990.
    B. Whitehead, E. Kiech. and M. Ali. Neural network approach to space shuttle main engine health monitoring. *AIAA 90-2259*, 1990
4. H. R. DePold and F. D. Gass. The application of expert systems and neural networks to gas turbine prognostics and diagnostics. *Journal of Engineering for Gas Turbines and Power* 121 (4), pp. 607-612, 1999
5. S. O. T. Ogaji and R. Singh. Advanced engine diagnostics using artificial neural networks. *Applied Soft Computing Journal* 3 (3), pp. 259-271, 2003
6. G. Romesis and K. Mathioudakis. Setting up of a probabilistic neural network for sensor fault detection including operation with component faults. *Journal of Engineering for Gas Turbines and Power* 125 (3), pp. 634-641, 2003
7. Y.-J Zhai, X.-W. Dai and Q. Zhou. Fault detection for gas turbines based on long-term prediction using self-organizing fuzzy neural networks. *Proceedings of the Sixth International Conference on Machine Learning and Cybernetics, ICMLC 2007*, art. no. 4370312, pp. 1120-1125, 2007
8. M. Zedda and R. Singh. Gas turbine engine and sensor fault diagnosis using optimization techniques. *Journal of Propulsion and Power* 18 (5), pp. 1019-1025, 2002
9. S. Sampath and R. Singh. An integrated fault diagnostics model using genetic algorithm and neural networks. *Proceedings of the ASME Turbo Expo 2004* 2, pp. 749-758, 2004
10. T. Kobayashi and D. L. Simon. Hybrid neural-network genetic-algorithm technique for aircraft engine performance diagnostics. *Journal of Propulsion and Power* 21 (4), pp. 751-758, 2005
11. S. O. T. Ogaji, L. Marinai, S. Sampath, R. Singh and S. D. Prober. Gas-turbine fault diagnostics: A fuzzy-logic approach. *Applied Energy* 82 (1), pp. 81-89, 2005

 Published by Cranfield University Press ISBN: 978-0-9557436-7-2 http://hdl.handle.net/1826/3832

12. Y. G. Li, P. Pilidis, and M. A. Newby. An adaptation approach for gas turbine design-point performance simulation. *Journal of Engineering for Gas Turbines and Power*, 128(4):789–795, 2006.
13. NATO Technical Report, Performance Prediction and Simulation of Gas Turbine Engine Operation for Aircraft, Marine, Vehicular, and Power Generation. *Final Report of the RTO Applied Vehicle Technology*, 2007.
14. P. Escher and R. Singh. An object-oriented diagnostics computer program suitable for industrial gas turbines. *21st (CIMAC) International Congress of Combustion Engines, Switzerland*, 1995.
15. Y. G. Li and R. Singh. An advanced gas turbine gas path diagnostic system-pythia, *ISABE paper 2005-1284*, 2005
16. Manx Electricity Authority Leaflet "Pulrose Power Station"
    A. R. Wadia, D. P. Wolf, and F. G. Haaser. Aerodynamic design and testing of an axial flow compressor with pressure ratio of 23.3:1 for the LM2500+ gas turbine. *Journal of Turbomachinery* 124 (3), pp. 331-340, 2002.
17. GE Leaflet "PGT25+ Aeroderivative gas turbine" or http://www.geoilandgas.com

 Published by Cranfield University Press ISBN: 978-0-9557436-7-2 http://hdl.handle.net/1826/3832

A survey of applications of coalitional game theory in reliability of systems

Haris Aziz[1]

[1]Computer Science Department, University of Warwick, Coventry, CV4 7AL, UK

Haris.aziz@warwick.ac.uk

The reliability of a system is the ability of a system and its components to perform the required functions under stated conditions for a specified period of time. Reliability of systems has been vastly studied in engineering and computer science. This paper provides a survey of application of coalitional game theory and social choice in reliability of systems. The conclusion is that further developments in computational and theoretical aspects of coalitional game theory should have bearing on advancements in reliability theory.

Index Terms — reliability, game theory, voting systems and mutual exclusion.

INTRODUCTION

THE IEEE (Institute of Electrical and Electronics Engineers) defines reliability as ``. . . the ability of a system or component to perform its required functions under stated conditions for a specified period of time." The reliability measurement of a component based system comprises of two main activities. Firstly, the reliability measurement of individual component and secondly, the reliability measurement of the whole system based on the component context model. Social choice is the study of voting rules for aggregating preferences. Game theory concerns the behavior of rational agents in strategic situations. This paper highlights the links between aspects of reliability of systems and coalitional game theory and social choice theory in general. This includes the correspondence between coherent structures in reliability theory and simple games in the voting theory literature. Moreover we show how concepts from social choice methods are utilized in permission based mutual exclusion mechanisms.

Voting algorithms are prevalent in reliability of systems. Parhami [1] outlines voting schemes which are used in fault tolerant computing and to obtain reliable data. Latif-Shabgahi et al. [2] show how voting algorithms are used to provide an error masking capability in software and hardware systems with commercial and research applications. hey provide a taxonomy of those voting algorithms. They classify voters into three categories: generic, hybrid, and purpose-built voters. Voting algorithms are compared on the criteria of acceptability of voter behavior, based on statistical considerations or probabilistic calculation.

RELIABILITY STRUCTURES AND SIMPLE GAMES

A structure is made of various components the failure of which can lead to the failure of the overall structure. Ramamurthy [3] shows how Boolean structure are useful to model reliability theory. For a system with components $N = \{1, \ldots, n\}$ the Boolean value of x_i indicates whether component I is functioning or not. The overall reliability of a structure can be considered a function $f(x)$ where $x = (x_1, \ldots, x_n)$.

 Published by Cranfield University Press ISBN: 978-0-9557436-7-2 http://hdl.handle.net/1826/3832

A component *i* is considered irrelevant if it does not affect the reliability of the over all system. A dual f^d is defined by $f^d(x) = 1 - f(1-x)$. Many of the definitions are due to Ramamurthy [3]. The notation and terminology has previously been used by Barlow and Proschan [6].

A structure f is *coherent* if it is

Monotone.

$f(0) = 0$ and $f(1) = 1$.

all the components of N are relevant to f.

We denote $x_J \in \{0,1\}^{|J|}$ as the states of a components in the set $J \subseteq N$. Moreover 1^J denotes that the components in J are all functioning and 0^J denotes that the components in J are failed. Let f be a structure on N, $A \subseteq N$ and $J=N\backslash A$. Then A is a *path set* of f if $f(1^A, 0^J) = 1$ and a *cut set* if $f(0^A, 1^J) = 1$.

Cooperative games are based on a set *N*. A simple game is a form of a cooperative game, where the possible gain is either '0' or '1'. A simple game is couple *(N, W),* where *W* is the list of winning coalitions. *Weighted voting games* are coalitional games in which each player has a weight and a coalition is successful if the sum of its weights exceeds a given threshold. Ramamurthy [3] draws links between the standard coherent structures and simple voting games. (See Appendix).

In reliability of systems, the level of dependence of the system on the reliability of its components is a crucial issue. Birnbaum [5] and Barlow and Proschan [6] examined the a priori importance of components in a reliability of systems. Similarly the ability of a voter to affect elections is gauged by standard voting power indices such as *Banzhaf index* and *Shapley-Shubik index.* Ramamurthy et al. [7] and Freixas and Puente [8] show how voting power measures are a useful way to gauge the importance of components in a reliability of systems. They point out that in fact Birnbaum rediscovered the Banzhaf index and Barlow and Proschan rediscovered the Shapley-Shubik index.

RELIABILITY OPTIMIZATION IN WEIGHTED VOTING MODELS

Weighted voting games (also known as weighted voting systems) are useful models for analyzing reliability engineering and system safety. In the reliability literature the voting players are also termed as voting units or components. The work of Levitin demonstrates how analysis of voting systems can directly help in reliability design. Levitin suggests a method to maximize system reliability by choosing proper unit weights and threshold values [9]; analyses asymmetric weighted voting systems in which each player or unit has one weight when it votes no and another weight if it votes yes [10] and shows how to enhance the survivability of a system by choosing appropriate weights, threshold and by separating its voting units [11]. Levitin [12] demonstrates that reliability of a system can be improved by grouping players into voting subsystems and tallying the votes of the subsystems in decision making. He [13] also shows a method to incorporate information of a player's availability into a procedure for determining the optimal reliability of the overall system. The approach in all the papers is using a universal generating function for evaluating system reliability.

PERMISSION BASED DISTRIBUTED MUTUAL EXCLUSION ALGORITHMS

 Published by Cranfield University Press ISBN: 978-0-9557436-7-2 http://hdl.handle.net/1826/3832

In a distributed system, sometimes nodes cannot communicate with each other due to failures and the network may be partitioned into isolated components. In such a situation, a mutual exclusion mechanism is needed so that different groups do not update the same data. The requirement of the problem is that only one process can enter the critical section at one time. Most of the algorithms can be termed as token-based or permission based. A good mutual exclusion approach also avoids deadlocks and starvation. A comprehensive survey on mutual exclusion mechanism is provided by Saxena and Rai in [14]. Gifford [15] and Thomas [16] pointed out that weighted voting can be used in this situation: each node is given a number of votes and only that component of nodes which has votes more than a specified majority can update data. This may lead to situations in which none of the groups can update data. In this case *dynamic voting* may be applied [17, 18].

Mutual exclusion was first confronted by Dijkstra [19] and Knuth [20] when they outlined natural criteria for mutual exclusion such as communication complexity, synchronization delay, fault tolerance and fairness.

In token-based algorithms, a node can enter the critical section if it has a token. In permission-based algorithms, nodes exchange rounds of messages to obtain permission to enter the critical section. Permission-based algorithms can be either voting based or coterie based. A site requiring access to the critical section needs permission from a set of nodes whose total votes is a majority. The permission does not depend on which nodes give the permission but only on the total number of votes of the permitting nodes.

In weighted voting, a coalition of nodes which can enter the critical section is one which has total votes more than the majority votes. Agrawal and Abbadi [21] and Kumar [22] use a logical tree structures or hierarchical along with weighted voting assignment to make the system more efficient. Multidimensional voting is more general to multiple weighted voting games which are a generalization of weighted voting games. In order for a coalition to win in a (*l*,*k*)-multidimensional voting game, a coalition must win in at least *l* of the total of *k* weighted voting games. Dynamic versions of voting algorithms minimize the number of halted states by reassigning the number of votes [23]. The effect of network topology and the node numbers on the distributed system is studied in [24]. Barbara and Garcia-Molina [25] examine the effect of voting assignments on reliability of the system.

Molina and Barbara [26] introduces a more powerful concept of coteries to ensure mutual exclusion. A coterie is a set of set of nodes which satisfies the minimality and intersection conditions. A set of groups ^{SN}

$\subseteq 2$ is a coterie iff

- $G \in S \Rightarrow G \neq \{\} \wedge G \subseteq N$.
- For $G, H \in S, \exists\ x \in S : x \in G \wedge x \in H$.
- $\neg\exists\ G, H \in S$ such that $G \subseteq H$.

Coterie *R dominates* coterie *S* iff $R \neq S$ and for each $H \in S$, there exists a $G \in R$ such that $G \subseteq H$. Coteries which are dominated are not desirable because they can result in lack of action if mutual exclusion is applied on the basis of coteries. Molina and Barbara [26] prove that coteries are a more powerful concept than vote assignment and in fact there are non-dominate coteries for which there are no vote assignments. They also formulate an algorithm to enumerate

 Published by Cranfield University Press ISBN: 978-0-9557436-7-2 http://hdl.handle.net/1826/3832

non-dominated coteries. For every vote assignment, the set of minimal winning coalition is the equivalent coterie for that system. However, for more than five nodes, every coterie does not necessarily have to have a corresponding vote assignment.

Quorum sets have a similar definition as coteries but without the intersection condition. Coteries are more general than voting-based methods. However voting is more flexible and easier in implementation. [27] covers one of the earliest algorithm for mutual exclusion but in [28] one of the earliest algorithm using coteries for mutual exclusion is introduced.

CONCLUSION

We see that voting theory and coalitional game theory in general is crucial in reliability of systems. Computational voting theory and social choice include aspects such as elicitation, representation and aggregation of preferences, resource allocation and fair division algorithms, ranking systems, logics for collective decision making and using complexity as a barrier to control and manipulation in voting. For a recent survey of the developments in computational issues in social choice, refer to [29]. Developments in computational social choice include using logic and mechanism design to specify the behavior of protocols. This can then enable design of desirable properties of systems. Compact representation of preferences and voting scenarios may enable more advanced voting mechanisms in reliability of systems. Therefore recent and future advances in coalitional game theory and computational social choice should have increasing bearing on reliability of systems.

APPENDIX

Reliability Theory	Voting theory
Component	Player
Semi-coherent structure	Simple game
Structure function	characteristic function
Irrelevant component	Dummy player
Path set	Winning coalition
Cut set	Blocking coalition
Series structure	Unanimity game
Parallel structure	Rule of individual initiative
Reliability function	Multilinear extension
path vector for component i	Swing for player
Importance of a component	Power of a player
Proschan measure of importance	Shapley-Shubik index
Birnbaum measure of importance	Absolute Banzhaf index
Module	committee

 Published by Cranfield University Press ISBN: 978-0-9557436-7-2 http://hdl.handle.net/1826/3832

REFERENCES

1. B. Parhami, “Voting algorithms,” IEEE Transactions on Reliability, vol. 43, no. 4, pp. 617–629, Dec 1994.
2. G. Latif-Shabgahi, J. Bass, and S. Bennett, “A taxonomy for software voting algorithms used in safety-critical systems,”
3. Reliability, IEEE Transactions on, vol. 53, no. 3, pp. 3 19–328, Sept. 2004.
4. K. Ramamurthy, Coherent structures and simple games (Theory and Decision Library), first edition ed. Netherlands: Kluwer Academic Publishers, 1990.
5. R. E. Barlow and F. Proschan, Mathematical Theory of Reliability, first edition ed. John Wiley & Sons Inc, 1965.
6. Z. Birnbaum, “On the importance of different components in a multicomponent system,” Multivariate Analysis II ed. P.R.Krishnaiah, 1969.
7. R. Barlow and F. Proschan, “Importance of system components and fault tree event,” Stochastic Processes and Their Applications, vol. 3, p. 153172, 1975.
8. K. G. Ramamurthy, A. Seth, and M. K. Sadegh, “A combinatorial approach for component importance,” Communications in Statistics - Theory and Methods, vol. 32, p. 497 507, 2003.
9. J. Freixas and M. Puente, “Reliability importance measures of the components in a system based on semivalues and probabilistic values,” Annals of Operations Research, vol. 109, pp. 33 1–342, 2002.
10. G. Levitin and A. Lisnianski, “Reliability optimization for weighted voting system,” Reliability Engineering & System Safety, vol. 71, 2001.
11. G. Levitin, “Asymmetric weighted voting systems,” Reliability Engineering & System Safety, vol. 76, pp. 205–212, 2002.
12. ——, “Maximizing survivability of vulnerable weighted voting system,” Reliability Engineering & System Safety, vol. 83, pp. 17–26, 2004.
13. ——, “Optimal unit grouping in weighted voting systems,” Reliability Engineering & System Safety, vol. 72, pp. 179–191, 2001.
14. [13] ——, “Analysis and optimization of weighted voting systems consisting of voting units with limited availability,” Reliability Engineering & System Safety, vol. 73, pp. 9 1–100, 2001.
15. P. C. Saxena and J. Rai, “A survey of permission-based distributed mutual exclusion algorithms,” Comput. Stand. Interfaces, vol. 25, no. 2, pp. 159–18 1, 2003.
16. D. K. Gifford, “Weighted voting for replicated data,” in Proceedings of the 7th ACM Symposium on Operating Systems Principles (SOSP), 1979, pp. 150– 162.
17. R. H. Thomas, “A majority consensus approach to concurrency control for multiple copy databases,” ACM Trans. Database Syst., vol. 4, no. 2, pp. 180–209, 1979.
18. D. Barbara, H. Garcia-Molina, and A. Spauster, “Increasing availability under mutual exclusion constraints with dynamic vote reassignment,” ACM Trans. Comput. Syst., vol. 7, no. 4, pp. 394–426, 1989.
19. S. Jajodia and D. Mutchler, “Dynamic voting algorithms for maintaining the consistency of a replicated database,” ACM Trans. Database Syst., vol. 15, no. 2, pp. 230–280, 1990.
20. E. W. Dijkstra, “Cooperating sequential processes, technical report ewd-123,” Tech. Rep., 1965.
21. D. E. Knuth, “Additional comments on a problem in concurrent programming control,” Commun. ACM, vol. 9, no. 5, pp. 32 1–322, 1966.
22. D. Agrawal and A. E. Abbadi, “The generalized tree quorum protocol: an efficient approach for managing replicated data,” ACM Trans. Database Syst., vol. 17, no. 4, pp. 689–7 17, 1992.
    A. Kumar, “Hierarchical quorum consensus: A new algorithm for managing replicated data,” IEEE Trans. Comput., vol. 40, no. 9, pp. 996–1004, 1991.
23. S. Jajodia and D. Mutchler, “Dynamic voting algorithms for maintaining the consistency of a replicated database,” ACM Trans. Database Syst., vol. 15, no. 2, pp. 230–280, 1990.
24. D. Barbara and H. Garcia-Molina, “The reliability of voting mechanisms,” IEEE Trans. Comput., vol. 36, no. 10, pp. 1197–1208, 1987.
25. ——, “The vulnerability of vote assignments,” ACM Trans. Comput. Syst., vol. 4, no. 3, pp. 187–213, 1986.
26. H. Garcia-Molina and D. Barbara, “How to assign votes in a
27. distributed system,” J. ACM, vol. 32, no. 4, pp. 841– 860, 1985.
28. G. Ricart and A. K. Agrawala, “An optimal algorithm for mutual exclusion in computer networks,” Commun. ACM, vol. 24, no. 1, pp. 9–17, 1981.

 Published by Cranfield University Press ISBN: 978-0-9557436-7-2 http://hdl.handle.net/1826/3832

29. M. Maekawa, “An algorithm for mutual exclusion in decentralized systems,” ACM Trans. Comput. Syst., vol. 3, no. 2, pp. 145–159, 1985.
30. Y. Chevaleyre, U. Endriss, J. Lang, and N. Maudet, “A short introduction to computational social choice,” in Proceedings of the 33rd Conference on Current Trends in Theory and Practice of Computer Science (SOFSEM-2007), ser. LNCS, vol. 4362. Springer-Verlag, January 2007.

 Published by Cranfield University Press ISBN: 978-0-9557436-7-2 http://hdl.handle.net/1826/3832

Immersed membrane bioreactors for nitrate removal from drinking water: Cost and feasibility

E.J. McAdam*, S.J. Judd

* Centre for Water Science, Cranfield University, Bedfordshire MK43 0AL, UK

(E-mail: *e.j.mcadam.2003@cranfield.ac.uk*)

Abstract

Brine disposal remains a key consideration when employing ion exchange (IEX) for nitrate removal. To circumvent this issue, research was conducted into developing an immersed membrane bioreactor (MBR) as a replacement for ion-exchange. This paper compares the economics of the two process options whilst also considering MBR for brine treatment. At a blend flow rate of 3000 $m^3.d^{-1}$, total life cycle costs were £0.095, 0.128 and 0.064.m^{-3} for IEX, MBR and IEX with brine recycle MBR respectively. Capital and O&M costs associated with MBR were extremely sensitive to membrane price variation. For blend flows >700 $m^3.d^{-1}$, IEX with brine recycle MBR proved the most cost effective option (total life cycle cost £0.044-0.087.m^{-3}, 1500-30000 $m^3.d^{-1}$) when assuming similar hydrodynamic efficiencies to the IEX replacement MBR. Further cost reductions (≤17%) can be found by operating Brine recycle MBR at higher salinity (~100 gNaCl.L^{-1}), provided an appropriate halo-tolerant community can be established.

Keywords Cost; Drinking Water; Membrane Bioreactor; Nitrate

INTRODUCTION

Several technologies are commercially available to treat nitrate-contaminated raw water to meet drinking water standards including reverse osmosis, electro dialysis, biological denitrification and ion exchange (IEX). IEX is typically selected due to its low cost and simplicity. However, costs primarily associated with brine disposal (but also with salt consumption) significantly impact on process cost with increasing stringent restrictions on disposal options. Biological nitrate removal presents a viable alternative to ion-exchange since it effectively destroys the nitrate ion (Matějů et al., 1992). However, when compared to ion exchange, construction has been found to be 2.5-3 times that of an IEX plant (Richard et al., 1989) and to extensive post-treatment was required o remove micro-organisms, turbidity and nitrites (Clifford and Liu, 1993a). Membrane bioreactors (MBRs) offer well known advantages over traditional biological processes and have been reported for this duty at full scale by Urbain et al. (1996), who used a pressure driven (externally configured) MBR for groundwater nitrate removal. Various authors (Clifford and Liu, 1993b; Chung et al, 2007) have also considered biological processing of the brine regenerant in conjunction with IEX, significantly reducing waste volumes and salt costs. Following a technical study into immersed MBRs as a replacement for ion exchange, this paper uses the data

 Published by Cranfield University Press ISBN: 978-0-9557436-7-2 http://hdl.handle.net/1826/3832

obtained to evaluate possible cost reduction by replacing IEX completely or, combining MBR with IEX to limit reduce brine disposal.

METHODS

Ion Exchange - IEX Blend

The calculation was based on nitrate-selective resin with an assumed maximum specific exchange capacity 0.9 Eq.L^{-1} and a Cl^-/NO_3^- equivalent ratio of 3.5. Optimum nitrate selectivity was assumed to be 0.89. Exhaustion was determined on the basis of influent NO_3^--N concentration and flow. Brine regenerant concentration was 100gNaCl.L^{-1}. Brine disposal volume was calculated using the regenerant concentration and equivalent ratio. A resin life of 7 years was assumed, and the feed nitrate concentration was set as 14.67 mgNO_3^--N.L^{-1} with a target N of 10 mgNO_3^--N.L^{-1} (blended).

Membrane Bioreactor - MBR Blend

Immersed membranes were used in this study (Table 1) for their low specific energy demand (Cornel and Kraus, 2006) and operational flexibility. In this current study, the authors have found that at relatively low suspended solids concentrations, it is possible to operate immersed hollow fibres sustainably with limited air injections. Due to the limited gas injection, low air flow and limited oxygen mass transfer associated with coarse bubble aerators, dissolved oxygen concentration recovered to <0.1 mg.L^{-1} quickly with no noticeable impact on biological activity. Specific biomass activity (mg N.g MLSS.h^{-1}) was calculated according to predicted average temperature and operating pH using data from this current investigation and the relationship proposed by Timmermans and van Haute (1983):

$$SA = SA\max,20\left(\frac{10^{0.052(t-20)}}{1+0.0502(10^{(8.3-pH)}-1)}\right) \quad (1)$$

Hydraulic residence time (hence tank size) is based upon specific activity, influent N concentration and assumed mixed liquor suspended solids (MLSS) concentration at the set solids residence time (SRT, 40 days). Power for mixing (Eq. 2), blowers (Eq. 3) and pumps (Eq. 4) were determined according to the design equations below (Metcalf and Eddy, 2003):

$$P = G^2 \mu V \quad (2)$$

$$P_w = \frac{wRT_1}{29.7ne}\left[\left(\frac{p_2}{p_1}\right)^{0.283} - 1\right] \quad (3)$$

$$P_w = \frac{\rho g H}{1000\xi}.\frac{Q_{pump}}{Q_p} \quad (4)$$

where G is (s^{-1}), μ is viscosity (N.s.m^{-2}), V is tank volume (m^3), w is air flow (kg.s^{-1}), R is air gas constant (8.314 J.K^{-1}.mol^{-1}), T is temperature (K), n is (0.283 for air), e is blower efficiency, ρ is density (kg.m^{-3}), g is gravity (m.s^-

 Published by Cranfield University Press ISBN: 978-0-9557436-7-2 http://hdl.handle.net/1826/3832

^{2}), H is pump head (m of water), ξ is pump efficiency. When MBR is configured to process brine regenerant, salt concentration is reduced to 30gNaCl.L^{-1} (3%) and consequently flow of brine regenerant to the brine MBR is increased. Under these conditions, biomass *SA* is assumed to fall to 90% of the MBR blend process (Clifford and Liu, 1993a).

Table 1. Membrane Bioreactor (MBR) operating conditions.

Parameter	**MBR**	**Brine MBR**
Influent N (mg N.L^{-1})	14.67 (*mean*)	600-1400
Target N (mg N.L^{-1})	10 (*once blended*)	<60
Blend Ratio	0.31 (Based on the above)	N/a
NaCl Concentration (%)	N/a	3
Net flux (L.m^{-2}.h^{-1})	17.1	17.1
SAD_m (SAD_m *net*) (m^3.m^{-2}.h^{-1})	0.77 (0.01)	0.77 (0.01)
Permeability (LMH.bar^{-1})	150	150
Backflush: Frequency (mins)	30	30
Backflush: Duration (secs)	30	30
Clean-in-place: Frequency (d)	14	14
Complete Chemical Clean (d)	180	180
HRT (hours)	1.4	13.65 (Influent 586.3mgN.L^{-1})
SRT (d)	40	40

Costs

All costs are given either as installed capital cost (£.m^{-3}.d^{-1}), operating cost (£.m^{-3}) or total life cycle cost (£.m^{-3}). All of these produced values refer to the blend stream product cost rather than the total site flow. Breakdown of costs and assumptions are listed below (Table 2). For further item specific costs refer to Fletcher et al. (2007). Membrane material cost is scaled down with increasing blend flow to £40.m^{-2} (minimum). Labour (hours) is scaled according to total treatment works flow (Adham, 2004).

Table 2 . Summary of costing assumptions used.

Capital Items		Design data	
Brine disposal	£11.m^{-3}	Power	£0.12 kWh
Membrane cost	£40-80.m^{-2}	Plant life expectancy	20 years
		Maintenance	0.5% Capital
		Interest + Inflation	8%
		Labour	Scaled[a]
		Conversion	$/£0.51; €/£0.68[b]

[a]Taken from Adham, 2004. [b]As of March 2007.

RESULTS AND DISCUSSION

Capital cost

Calculated installed costs for the IEX replacement MBR are highly competitive (Figure 1) versus other MBR capital costs reported for more typical applications such as re-use and reclamation (Côté et al., 2004) and

 Published by Cranfield University Press ISBN: 978-0-9557436-7-2 http://hdl.handle.net/1826/3832

municipal wastewater (Hanft, 2006; Adham et al., 2000), ranging from £325.$m^{-3}.d^{-1}$ (Q, 1709 $m^3.d^{-1}$) to £157.$m^{-3}.d^{-1}$ (Q, 34188 $m^3.d^{-1}$). This is due to smaller tank capacity per unit flow (i.e. no aeration or anaerobic basins) coupled with zero screening or biological aeration requirements. Furthermore, due to the aeration strategy adopted, cassettes are gassed sequentially and intermittently, and thus the number of blowers required for membrane gasification is limited yielding a capital saving ~7.3% (blend flow, 3400$m^3.d^{-1}$). Civil structures were the dominant cost when constructing the early heterotrophic nitrate removal plants (Kapoor and Viraraghavan, 1997). Process intensification provided by MBR limits these costs. However, membrane material constitutes a significant fraction of the total capital (>50%), resulting in significant sensitivity (Table 3) to fluctuations in membrane cost and material requirements. Consequently, whilst the MBR design is cost competitive versus standard MBR designs, the total cost is between 1.2 and 3.6 times the cost for IEX plant construction. Specific costs for the brine recycle MBR are high (£2923-£503.$m^3.d^{-1}$ for brine recycle flows of 7.7-770 $m^3.d^{-1}$). However, for plant sizes >500 $m^3.d^{-1}$ capital costs for IEX with MBR for brine recycling were much less than those for MBR alone (Figure 2) and only slightly more expensive than IEX (1.3-1.03 times the cost).

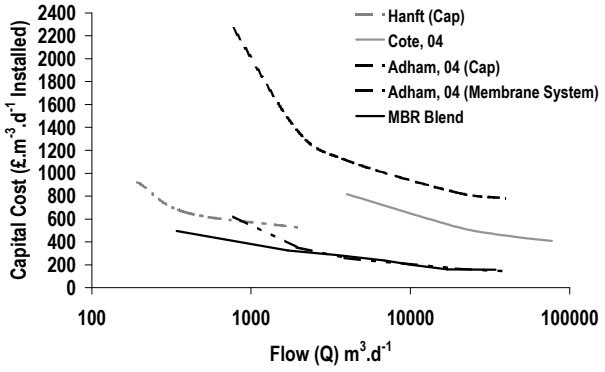

Figure 1. MBR installed capital costs (£.$m^{-3}.d^{-1}$) from several authors compared to the MBR blend.

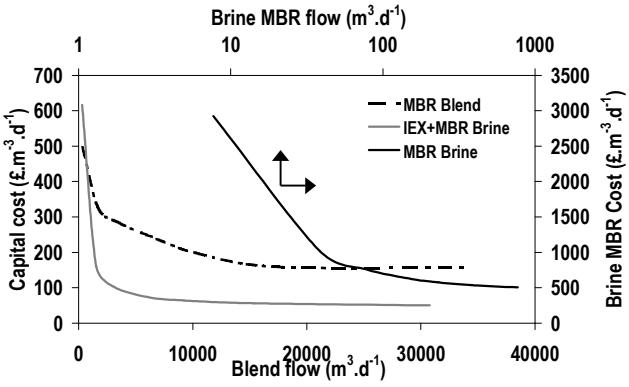

Figure 2. Installed capital cost comparison between MBR blend and IEX combined with MBR brine (MBR Brine costs also shown independently).

Due to the scale of the brine MBR, capital cost for IEX and brine recycle combined is relatively insensitive to membrane cost variations compared to MBR alone. However, both processes are sensitive to specific bacterial activity (*SA*, mgN.gMLVSS.h^{-1}). A factor of safety (*fos* 1.5) was therefore assigned to oversize the brine and replacement MBR tanks to offset influent concentration variation. Limited research has been conducted on the influence of salinity on denitrifying communities. Clifford and Liu (1993a) reported that *SA* of denitrifiers derived from activated sludge declined by only 10% at 30gNaCl.L^{-1} (3%) concentration however, significant effects have been reported at higher concentrations. Investigators have made use of Halo-type bacteria (e.g. *Halomonas campisalis*) typically derived from marine sediments which provide similar *SA*s at high salinities (12.5%, or 125gNaCl.L^{-1}) to denitrifiers (e.g. *Pseudomonas denitrificans*) in non-saline environments (Peyton et al., 2001). In this costing, use of a low salinity bacterial community has been assumed. If operation was switched to highly saline conditions (100gNaCl.L^{-1}), flow in the MBR brine recycle loop would decrease from 231 to 97.5 $m^3.d^{-1}$

 Published by Cranfield University Press ISBN: 978-0-9557436-7-2 http://hdl.handle.net/1826/3832

(blend flow 9230 $m^3.d^{-1}$) reducing capital and operating costs (IEX and brine MBR combined) by £4.54.$m^{-3}.d^{-1}$ (~7%) and £0.015.m^{-3} (~22%) treated respectively.

Operating and Maintenance

Nitrate selective resins have reduced waste brine generation by limiting sulphate and bicarbonate adsorption and reducing the chloride/ nitrate (Cl^-/NO_3^-) equivalency ratio required for regeneration (Clifford and Liu, 1993a). However, costs associated with tankering or alternative methods of disposal (literature range £4-13.m^{-3} brine disposal) remain cost intensive (Figure 4). Consequently both the replacement MBR and IEX with brine recycle MBR have significantly lower O&M cost (Figure 3). Salt replenishment and brine disposal are still required when operating the brine recycle MBR due to concentration amendment (NaCl) post bio-treatment, water losses over time and to avoid anionic (sulphate and bicarbonate) accumulation. A net loss of 7.5% brine regenerant volume was assumed based on a study by Cifford and Liu (1993a) which corresponds to a reduction in salt mass of ~93%. Although salt requirements are lower for the two alternative processes, chemical costs remain higher than for IEX primarily due to electron donor consumption (ethanol), owing to either process scale (throughput of product water relative to total flow (MBR Blend)) or influent strength (600-1400 mgNO_3^--N.L^{-1} (MBR Brine)). However, both processes show similarly low to moderate operating cost sensitivity to ethanol bulk purchase price (Jonsson, 2004) variation.

Table 3. Sensitivity analysis. Basis: total flow 30 MLD, influent NO_3^- 14.67mg NO_3^--N.L^{-1}.

Parameter	+/-	MBR Blend		IEX Blend		IEX & MBR Brine	
	(%)	Cap[a]	Op (£.m^{-3})	Cap[a]	Op (£.m^{-3})	Cap[a]	Op (£.m^{-3})
Pre-analysis		198.36	0.087	58.97	0.144	64.06	0.067
SA[b]	20	4.24	0.005	N/a	N/a	1.15	0.0012
Resin[d]	20	N/a	N/a	3.32	0.0013	1.43	0.0004
Salt[d]	10	N/a	N/a	N/a	0.0014	N/a	0.0001
Brine[d]	10	N/a	N/a	N/a	0.0227	N/a	0.00247
Sludge[d]	10	N/a	0.002	N/a	N/a	N/a	0.00047
Ethanol[d]	10	N/a	0.002	N/a	N/a	N/a	0.00188
Membrane	10	16.44	0.003	N/a	N/a	0.64	0.00014
Flux[e]	10	19.63	0.004	N/a	N/a	0.87	0.00015
Resin Life	20	N/a	N/a	N/a	0.002	N/a	0.00069
Mem. Life	20	N/a	0.012	N/a	N/a	N/a	0.00046
SAD_m	50	0.4	0.0005	N/a	N/a	0.3125	0.00005

[a](£.$m^{-3}.d^{-1}$). [b]Specific activity. [c]Capacity. [d]Consumption/ disposal costs.[e]Variation ($L.m^{-2}.h^{-1}$). [f]Based on lifetime projection. N/a – Not applicable.

Côté et al. (1997) reported low specific energy requirements for immersed (0.3 kWh.m^{-3}) compared with externally configured MBRs (1-4 kWh.m^{-3}, Cornel and Kraus, 2006). Due to the extended gassing intermittency (30 seconds/30minutes) adopted in this study, specific energy requirements associated with near constant gassing (0.29 kWh.m^{-3}, SAD_m 0.77$m^3.m^{-2}.h^{-1}$) were reduced to 0.025 kWh.m^{-3} (SAD_m 0.01 $m^3.m^{-2}.h^{-1}$) through experimental optimisation for the MBR blended process.

 Published by Cranfield University Press ISBN: 978-0-9557436-7-2 http://hdl.handle.net/1826/3832

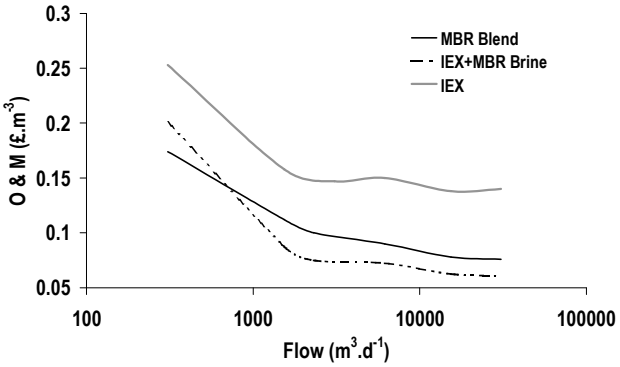

Figure 3. O&M Costs.

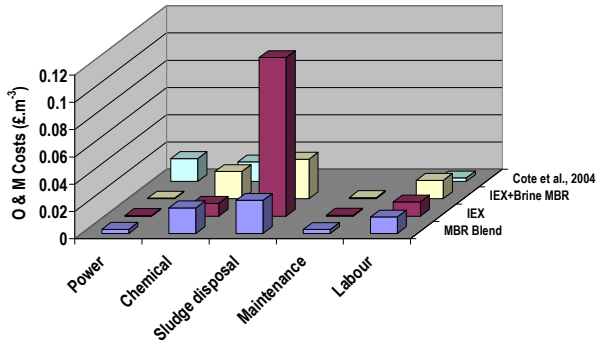

Figure 4. O&M Cost breakdown.

Replacement costs are dominated by the IEX resin and membrane material costs. Due to the scale of the replacement MBR, cost, flux and most notably life expectancy (membrane 8 years; resin 7 years), impact heavily on O&M cost. Membrane replacement costs constitute 33% of total O&M (due to the low specific energy demand), 93% of which is attributable to membrane replacement. In comparison, replacement costs constitute only 4.8% of the total O&M for IEX coupled with brine MBR even when operating with low salinity (30gNaCl.L^{-1}) regenerant (hence higher brine MBR flows). Côté et al. (2004) assumed low labour costs in their MBR cost analysis on the basis of complete automation. In the current study, low level automation has been assumed and labour 'contact time' has been scaled according to plant scale (Adham, 2004) thus labour cost is equal when comparing processes at set flows (Figure 4).

Total life cycle costs (TLCC)

Total costs were assessed based on a 20 year life expectancy and 8% combined interest (*PV*=9.818) and inflation rate. Although the replacement MBR O&M costs were significantly below IEX with brine disposal, the saving was insufficient to off-set the significant capital cost. As such the replacement MBR was only cost competitive on total life cycle costs at flow rates $<$700 $m^3.d^{-1}$, equating to $\sim$£0.032.m^{-3} below IEX with brine disposal (*TLCC* £0.26-0.082.m^{-3}). Therefore if membrane cost continues to fall for small-scale applications, the process could be competitive at low flow rates. For blending flow rates $>$700$m^3.d^{-1}$, *TLCC* for IEX with brine recycle MBR ranged from £0.087 to £0.044.m^{-3} (Blend flow, 1500-30000 $m^3.d^{-1}$) dependent upon scale which constitutes a saving of £0.038-0.059.m^{-3} compared to IEX with brine disposal. Total life cycle costs could be further reduced by $\leq$17% by optimising brine regeneration for high salinity processing (Figure 5).

 Published by Cranfield University Press ISBN: 978-0-9557436-7-2 http://hdl.handle.net/1826/3832

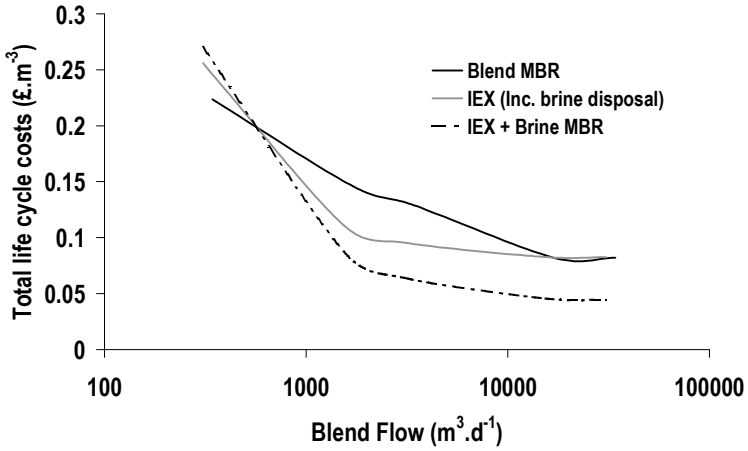

Figure 5. Comparison of total life cycle costs for IEX, replacing IEX with MBR and combining MBR to treat brine. Project period 20 years. Interest rate 8%.

CONCLUSIONS

MBR designed for IEX replacement exerts a very low specific energy demand compared to conventional MBRs and a low specific O&M relative to conventional IEX. However, membrane cost renders the process uncompetitive versus IEX with brine disposal at flows >700 $m^3.d^{-1}$. IEX with brine recycle MBR is cost competitive with total life cycle cost savings of £0.038-0.059.m^{-3} over IEX with brine disposal. The process is less sensitive to membrane costs and a further total life cycle cost reduction of $\leq$17% is possible by operating at considerably higher salinities. To validate process viability, research is required to assess the impact of varying saline concentrations on nitrate removal. Furthermore, although the influence of salinity shocking on fouling propensity in municipal wastewater MBR has been documented (Reid et al., 2006), fouling for a permanently high saline environment is less well understood which also needs to be addressed.

REFERENCES

1. Adham S., Merlo R.P., Gagliardo P. (2000). *Membrane bioreactors for water reclamation-phase II*. Metropolitan Wastewater-Public Works, San Diego CA, USA. http://www.usbr.gov/pmts/water/media/pdfs/report060.pdf (accessed 12 March 2007)
2. Adham S., Decarolis J.F., Pearce W. (2004). *Optimisation of various MBR systems for water reclamation – phase III*. Report No. 103, City of San Diego Water Department, Montgomery Watson Harza. http://www.usbr.gov/pmts/water/media/pdfs/report103.pdf (accessed 12 March 2007).
3. Clifford D., Liu X. (1993a). Ion exchange for nitrate removal. *J. Am. Water Works Assoc.*, **85**(4), 135-143.
4. Clifford D., Liu X. (1993b). Biological denitrification of spent regenerant brine using a sequencing batch reactor. *Water Res.,* **27**(9), 1477-1484.
5. Cornel P., Kraus S. (2006). Membrane bioreactors in industrial wastewater treatment-European experiences, examples and trends. *Water Sci. Technol.,* **53**(3), 37-44.
6. Côté P., Masini M., Mourato, D. (2004). Comparison of membrane options for water reuse and reclamation. *Desalination,* **167**(1), 1-11.
7. Côté P., Buisson H., Pound C., Arakaki G. (1997). Immersed Membrane Activated Sludge for the Reuse of Municipal Wastewater. *Desalination,* **113**(2-3), 189-196.
8. Chung J., Nerenberg R., Rittmann B.E. (2007). Evaluation for biological reduction of nitrate and perchlorate in brine water using the hydrogen based membrane biofilm reactor. *J. Environ. Eng.,* **133**(2), 157-164.

 Published by Cranfield University Press ISBN: 978-0-9557436-7-2 http://hdl.handle.net/1826/3832

9. Fletcher H., Mackley T., Judd, S. (2007). The cost of a package plant membrane bioreactor. W*ater Res.* 41 2627-2635 (2007).
10. Glass C., Silverstein J., Oh J. (1997). Inhibition of denitrification in activated sludge by nitrite. *Water Environ. Res.,* 69(6), 1086-1093.
11. Hanft S. (2006). Membrane bioreactors in the changing world water market. Report ID MST047A, Business Communications Company.
12. Jonsson L. (2004). Denitrification rate and carbon source consumption in full-scale wastewater filtration. *Water Sci. Technol.*, 50(7), 105-112.
13. Kapoor A., Viraraghavan, T. (1997). Nitrate removal from drinking water – review. *J. Environ. Eng.*, 123(4), 371-380.
14. Matějů V., Čižinská S., Krejčí J., Janoch T. (1992). Biological water denitrification – A review. *Enzyme Microb. Technol.*, 14, 170-182.
15. Metcalf and Eddy Inc. (2003). *Wastewater Engineering – Treatment and Reuse*. 3rd edn, McGraw-Hill, New York.
16. Montgomery Watson (1999). Application of ion-exchange technology for perchlorate removal from San Gabriel basin groundwater. Final Research Report, Montgomery Watson, Applied research department, Pasadena CA, USA. http://jplwater.nasa.gov/nmoweb/AdminRecord/docs/NAS70216.PDF (accessed 12 March 2007).
17. Peyton B.M., Mormile M.R., Petersen J.N. (2001). Nitrate reduction with *Halomonas campisalis*: Kinetics of denitrification at pH 9 and 12.5% NaCl. *Water Res.,* 35(17), 4237-4242.
18. Reid E., Liu X., Judd S.J. (2006). Effect of high salinity on activated sludge characteristics and membrane permeability in an immersed membrane bioreactor. *J. Membr. Sci.,* 283(1-2), 164-171.
19. Richard Y.R. (1989). Operating experiences of full scale biological and ion-exchange denitrification plants in France. *J. Inst. Water Environ. Mgmt.*, 3, 154-167.
20. Timmermans P. and van Haute A. (1983). Denitrification with methanol. *Water Res.*, 17(10), 1249-1255.
21. Urbain V., Benoit R., Manem J. (1996). Membrane bioreactor: a new treatment tool. *J. Am. Water Works Assoc.*, 88(5), 75-86.

 Published by Cranfield University Press ISBN: 978-0-9557436-7-2 http://hdl.handle.net/1826/3832

Virtualisation of Grid Services for Multidisciplinary Optimisation in Aerospace Industry

Gokop Goteng, Ashutosh Tiwari and Rajkumar Roy
School of Applied Sciences, Manufacturing Department, Cranfield University, UK
{g.l.goteng, a.tiwari and r.roy@cranfield.ac.uk}

Abstract

The design of complex products such as aircraft requires the participation of multidisciplinary experts from different application domains. These experts need to collaborate and use various tools during optimisation process. Unfortunately, these experts are often located in different geographical locations and may have to work separately on different copies of the design. In this paper, we developed a grid problem solving environment called DECGrid (Decision Engineering Centre Grid) for multidisciplinary experts to collaborate and work on a single copy of a design as well as share tools and optimisation resources. The Globus Toolkit is used to publish resources as services while Condor is used for collaborating experts to schedule jobs and take advantage of the computational synergy in the Condor pool. This prototype shows that multidisciplinary optimisation (MDO) is time and resource efficient within secure collaborative grid virtual organisation.

Introduction

Multidisciplinary optimisation (MDO) problems consist of multi-objective functions for different disciplines or domain areas each subject to various constraints and conditions. Mathematical modelling is the core activity in MDO and requires inputs from different experts in many fields and also the use of different techniques to compare optimum solutions. In this paper, we developed a framework in which optimisation resources (objective functions, constraints, data, design parameters, etc) and tools (evolutionary algorithms, search strategies, visualisation devises, applications, etc) are published in the Globus Web Monitoring and Discovery Service (WebMDS) Index Service so that MDO experts can view these resources within a virtual organisation (VO) and subscribes for MDO services that help them to perform optimisation collaboratively. Apart from performing optimisation, the system also guides users to create math models from input data streams, optimisation workflow and output data streams which is facilitated by the WebMDS (Nguyen and Selmin, 2006).

This paper is organised into 5 sections. Section 1 is a brief introduction of the paper. Section 2 is the background and literature on MDO. Section 3 describes the framework and DECGrid architecture. Section 4 highlights the distributed collaborative process of optimisation among multidisciplinary experts. Section 5 is summary and conclusions.

Industrial MDO Background

Multidisciplinary optimisation (MDO) is a methodology for the design of systems in which tightly coupled interaction between disciplines motivates designers to concurrently manipulate variables in several disciplines (Sobieszczanski-Sobieski and Haftka, 1997). This interdisciplinary coupling presents a tough computational and organisational domain challenges for MDO experts. For example, one discipline in the design of airframe contributes thousands of analysis variables with different dimensionalities (Berkes, 1990). In the bit to produce quality products at competitive costs and

 Published by Cranfield University Press ISBN: 978-0-9557436-7-2 http://hdl.handle.net/1826/3832

time, companies are increasingly using MDO techniques. MDO techniques use problem solving environments to allow different experts to collaborate and work on a design concurrently thereby reducing the time of design as well as improving the quality of the product (Song et al., 2003). In addition, novel designs could evolve as a result of this collaboration. MDO also uses CFD (Computational Fluid Dynamics) and FEA (Finite Element Analysis) methods to produce the CAD (Computer Aided Design) model, mesh and produce the solutions. CFD and FEA are computationally and data intensive even when using state-of-the-art parallel distributed computing (Grauer et al., 2004). Companies and researchers are exploring grid technology capabilities to efficiently perform feature-based parametric CAD modelling which has proved to improve speed of computation and integration of other tools for performing CFD and FEA (Song et al., 2004).

MDO has played significant role in aerospace industry over the years. The MDO Aerospace Vehicles European Union Project uses multidisciplinary analysis and design optimisation tools to minimise the direct operating cost of the design of and construction of aerodynamic and design of a wing of A3xx (Airbus) concept aircraft (Bartholomew, 1998). Concurrent engineering played key role in this project. Substantially minimised cost and improved performance of aircrafts is increasingly becoming important and these trade-offs can be enhanced using MDO methods (Willcox and Wakayama, 2003). Techniques that ensure reusability of aircraft optimisation resources (data, geometry, area, shape, etc) are used to further minimise cost of design and production of new versions of the same family of aircrafts (Brown and Olds, 2006). Uncertainties are also incorporated along side other constraints in MDO to ensure high reliability of aircrafts (Pettit and Grandhi, 2000).

High fidelity aerospace structural design, analysis and configurations are better done within MDO environment when distributed experts need to simultaneously work on a copy of the design (Alonso et al., 2004). For this reason, the NASA Langley Research Centre uses HPC (High Performance Computing) and virtualisation programs to demonstrate the multidisciplinary shape and sizing optimisation of a complete aerospace vehicle using high-fidelity, FEA and CFD (Walsh et al., 2000). Algorithms such as particle swarm (PS) and evolutionary algorithms (EA) are currently used for MDO in aircraft designs to tackle high-fidelity problems (Venter and Sobieszczanski-Sobieski, 2004). Grid computing research activities are in line with developing problem solving environments to handle the computations that produce multiple optimum solutions using PS and EA (Ng et al., 2005). Non-technical barriers to MDO in aerospace industry such as interaction complexity which involves experts and organisations (Belie, 2002) can be improved through virtualised service-oriented architecture (Alpdemir et al., 2004). Computational synergy may also reduce cost of optimisation simulation using Condor software to perform cycle-stealing and distributed resource management (Ferris et al., 2000).

Framework and Architecture of DECGrid

A framework for the DECGrid is designed in such a way that optimisation resources are published as services and these services in turn are subscribed for by optimisation engineers or companies that want to use them. The DECGrid architecture consists of 8 computers running CentOS 4 Linux, Globus and Condor.

Service Framework

The framework is the process of service specifications. This is a document that shows the functionalities of the optimisation resources and quality of service. This document represents the bond between the two parties and

 Published by Cranfield University Press ISBN: 978-0-9557436-7-2 http://hdl.handle.net/1826/3832

ensures the delivery and review of services. Figure 1 is the class diagram of the framework. The initial interaction is between the service provider and requestor based on service level agreement. After which the service provider uses the functionality of Globus Toolkit to register MDO resources in WebMDS (Web Monitoring and Discovery Service). All resources are aggregated in the MDO Aggregator Source. A search strategy interface is provided for optimisation engineers to perform search using deterministic or stochastic search algorithms. After subscription, requestors execute the MultiDisplinaryOptimisationService which has interfaces for step by step process for building a math model for optimisation in a particular field. The first interface is the main domain. This allows the optimisation engineer to select the domain (FEA, CFD, etc) that the math model is needed. The criteria, design parameters and constraints are obtained to generate the math model. The MDO Collaboratory allows distributed optimisation engineers to securely share data, make queries and collaborate.

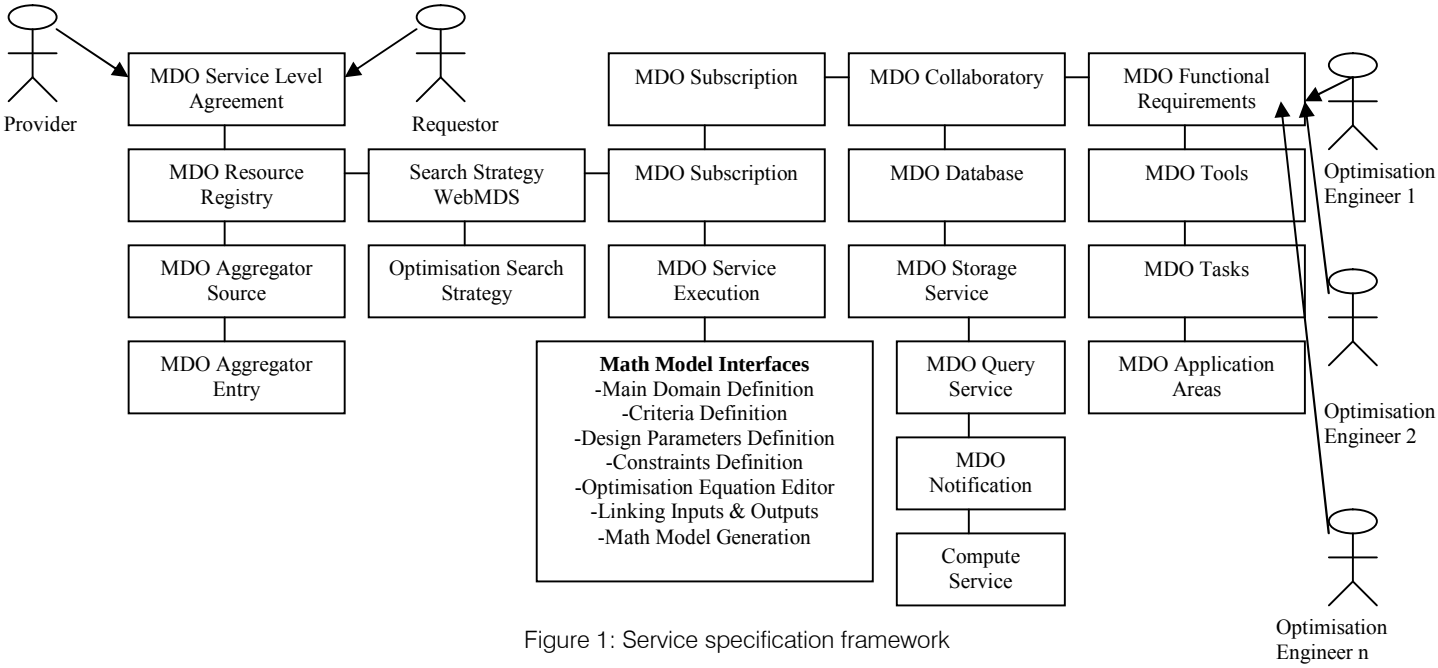

Figure 1: Service specification framework

 Published by Cranfield University Press ISBN: 978-0-9557436-7-2 http://hdl.handle.net/1826/3832

DECGrid Architecture

The framework is implemented using 8 computers that served as grid nodes. CentOS 4.0 Linux is used as the operating system. Globus Toolkit 4.0.4 (GT4) is used as the middleware and Condor 7.0.0 as the resource scheduler. Apache web server and WSRF (Web Services Resource Framework) are used to allow the application run both as grid services and web services. Figure 2 describes the architecture. Service provider publishes optimisation resources and requestors (optimisation engineers) subscribed for the resources as they also collaborate.

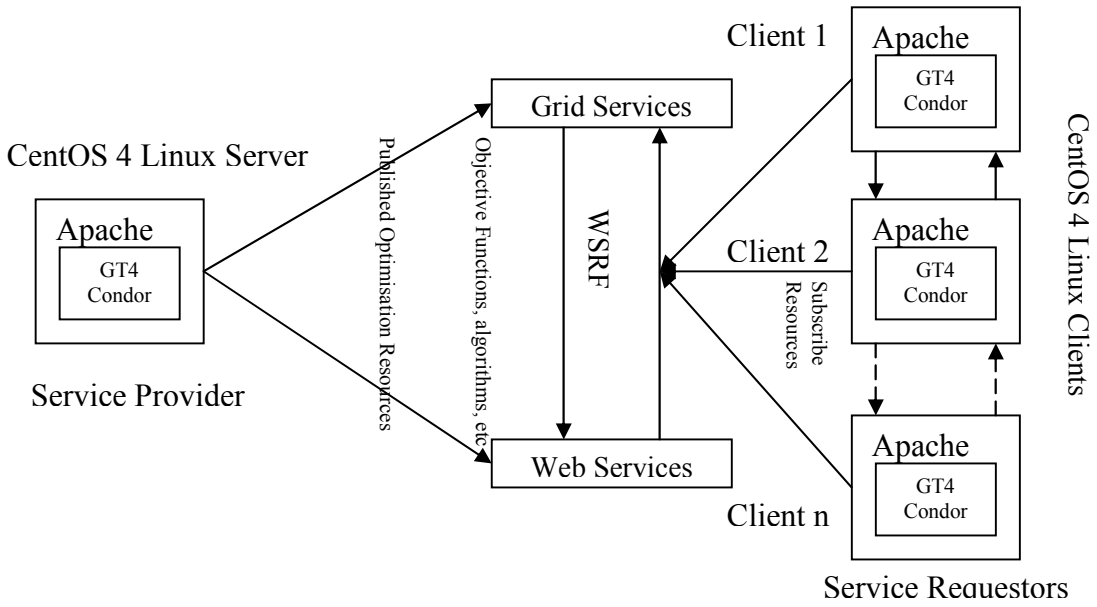

Figure 2: DECGrid Architecture

Virtualisation of Optimisation Resources

The resources for optimisation and math model building such as objective function, constraints, parameters, algorithms and boundary conditions are published within the virtual organisation. Virtualisation of resources in grid systems eliminates the multiple problems of resource naming, resource discovery, resource monitoring and resource organisation (Nebro eta l., 2007). This provides seamless and uniform access to multiple experts making inputs for optimisation and math model creation simultaneously. Another innovative advantage of using virtualised resources is the efficient use of idle computer power of collaborating parties. Condor scheduler spreads jobs to idle machines or takes the computing power of idle machines to add it to machines that are doing optimisation thereby increasing the speed of optimisation process. Duplication of resources for optimisation are minimised through resource virtualisation in DECGrid.

Discussion and Conclusions

Optimisation of complex products such as aircrafts requires the collaboration of multidisciplinary experts. The grid platform provides a secure and distributed environment for computational virtualised resources to be provided for distributed engineers working on optimisation problem. This research developed a prototype called the DECGrid to demonstrate how virtualised grid resources can enhance performance and efficiency in the optimisation process in

 Published by Cranfield University Press ISBN: 978-0-9557436-7-2 http://hdl.handle.net/1826/3832

aerospace industry. The major challenges in service development are security control of user access to resources, service reliability, quality control of services and dynamic service discovery on a real time basis by users.

References

1. Alonso, J. J., LeGresley, P., Weide, E., Martins, J. R. R. A. and Reuther, J. J. pyMDO: A Framework for High-Fidelity Muilti-Disciplinary Optimization. 10th AIAA/ISSMO Multidisciplinary Analysis and Optimization Conference. USA: AIAA; 2004; 2004-4480.
2. Alpdemir, M. N., Mukherjee, A., Gounaris, A., Paton, N. W., Watson, P., Fernandes, A. A. A. and Fitzgerald, D. J. OGSA-DQP: A Service for Distributed Querying on the Grid2004; 2992/2004858-861.
3. Bartholomew, P. The Role of MDO Within Aerospace Design and Progress Towards an MDO Capability. AIAA; 1998; 98-4705.
4. Belie, R. Non-Technical Barriers to Multidisciplinary Optimization in the Aerospace Industry. 9th AIAA/ISSMO Symposium on Multidisciplinary Analysis and Optimization. USA: AIAA; 2002; 2002-5439.
5. Berkes, U. L. Efficient Optimization of Aircraft Structures with a Large Number of Design Variables. Journal of Aircraft. 1990; 271073-1078.
6. Brown, N. F. and Olds, J. R. Evaluation of Multidisciplinary Optimization Techniques Applied to a Reusable Launch Vehicle. Journal of Spacecraft and Rockets. 2006; 43(6):1289-1300.
7. Ferris, M. C. , Mesnier, M. P. and More, J. J. NEOS and Condor: Solving Optimization Problems Over the Internet. ACM Transactions on Mathematical Software. 2000; 26(1):1-18.
8. Grauer, M., Barth, T. and Thilo, F. Grid-Based Computing for Multidisciplinary Analysis and Optimization. 10th AIAA/ISSMO Multidisciplinary Analysis and Optimization Conference. USA: AIAA; 2004; 2004-4456.
9. Nebro, A. J., Alba, E. and Luna, F. Multi-Objective Optimization using Grid Computing. Soft Computing. 2007; 11531-540.
10. Ng, H., Lim, D., Ong, Y., Lee, B., Freund, L., Parvez, S. and Sendhoff, B. A Multi-Cluster Grid Enabled Evolution Framework for Aerodynamic Airfoil Design Optimization2005; 3611/20051112-1121.
11. Pettit, C. L. and Grandhi, R. V. Multidisciplinary Optimization of Aerospace Structures with High Reliability. 8th ASCE Speciality Conference on Probabilistic Mechanics and structural Reliability. 2000; PMC2000-132.
12. Sobieszczanski-Sobieski, J. and Haftka, R. T. Multidisciplinary Aerospace Design Optimization: Suevey of Recent Developments. Structural Optimization. 1997; 141-23.
13. Song, W., Keane, A. and Cox, S. CFD-Based Shape Optimization with Grid-Enabled Design Search Toolkits. Proceedings of UK e-Science All Hands Meeting 2003 . UK: UK e-Science AHM; 2003: 619-626.
14. Song, W., Keane, A., Eres, H., Pound, G. and Cox, S. Two Dimensional Airfoil Optimisation using CFD in a Grid Computing Environment2004; 2790/2004525-532.
15. Venter, G. and Sobieszczanski-Sobieski, J. Multidisciplinary Optimization of a Transport Aircraft Wing using Particle Swarm Optimization. Industrial Applications Abd Design Case Study: Structural Multidisciplinary Optimization. 2004; 26121-131.
16. Walsh, J. L. , Townsend, J. C., Salas, A. O., Samareh, J. A., Mukhopadhyay, V. and Barthelemy, J. F. Multidisciplinary High-Fidelity Analysis and Optimization of Aerospace Vehicles, Part 1: Formulation. AIAA; 2000; 2000-0418.
17. Willcox, K. and Wakayama, S. Simultaneous Optimization of a Multiple-Aircraft Family. Journal of Aircraft. 2003; 40(4):616-622.

 Published by Cranfield University Press ISBN: 978-0-9557436-7-2 http://hdl.handle.net/1826/3832

Using Bioinformatics to Increase Speed and Reduce Uncertainty in Protein Biomarker Discovery

JenniferA. Mead, Luca Bianco and Conrad Bessant

Bioinformatics Group, Cranfield Health, Cranfield University, Bedfordshire, UK. MK43 0AL

Abstract

Biomarkers – biological molecules indicative of specific diseases – have great potential value as targets for novel pharmaceuticals and as analytes for diagnostic devices. The identification of a biomarker, or pattern of biomarkers, for a specific disease can ultimately lead to product lines generating billions of dollars. With such rewards on offer, recent years have seen the development of high throughput bioanalytical techniques capable of looking at differential expression of molecules at the genomic, proteomic and metabolomic levels. Although these new developments have vastly increased the capability to generate large amounts of data from a given study, reliable identification of biomarkers from such data remains a major challenge due to the data volumes and sheer complexity of biological samples. In this paper, we outline methodologies developed at Cranfield to assist in this process, with particular emphasis on proteomic biomarkers.

Introduction

Biomarkers are a major part of the drug development lifecycle. To design a novel medicine, the mechanism of disease may be elucidated by characterising changes in protein expression. A drug can then be designed to counteract the shift and rebalance the system to produce a healthy state. Biomarkers provide the objective measure required to indicate normal biological processes, pathogenic processes or pharmacological responses to a therapeutic intervention. In this way, they may be used to identify profiles characteristic of unwanted toxicity in early drug candidate screening and provide evidence of drug efficacy and safety in early trials. In commercial terms, this provides a means to make better clinical trial decisions earlier and hence avoid expensive late-stage failure. The other major application of biomarkers is diagnostics, where the presence or absence of certain molecules can indicate deviation from a healthy state.

The tool of choice for differential protein profiling comparing healthy versus diseased or drug-treated samples, is currently proteomic mass spectrometry (MS). Although complex and expensive, this is a powerful approach that has already been used to identify biomarkers of diseases including as cancer (1,2), atherosclerosis (3) and viral-induced transformation (4).

The challenge of proteomic MS is the complexity of biological samples, and the resulting large quantity of data acquired (6,000 spectra from a single sample is not unusual). Deriving meaningful protein

 Published by Cranfield University Press ISBN: 978-0-9557436-7-2 http://hdl.handle.net/1826/3832

identifications from this data with sufficient confidence to propose novel biomarkers is extremely difficult (5), and it is this challenge that we tackle in this paper.

Methodology

In simple terms, the first step in the proteomic MS workflow is to separate the proteins in a sample and enzymatically break these down into much smaller peptides. Mass spectra are obtained from each peptide, and by using characteristic features present in these spectra it is possible to postulate which proteins the sample contains. Traditionally this is achieved in two ways: data can be interpreted manually by expert practitioners, or by using peptide identification software such as Mascot (6) to identify the proteins sample by sample.

The novel methodology developed by Cranfield is a fully automated data analysis system, called the Genome Annotating Proteomic Pipeline (GAPP). GAPP takes as its input a series of MS/MS peak lists from a given experimental sample, with accompanying experimental and biological metadata, and produces a series of database entries corresponding to the peptides observed within the sample, along with related confidence scores (Figure 1). These identifications are then mapped back to the genome using sequence identifiers. The peptide identifications are made using a search-engine type algorithm called X!Tandem (7), which attempts to match acquired spectra with theoretically derived spectra using a parallel computing approach optimised for speed. From peptide identifications the presence of corresponding proteins are inferred. The similarity of the spectral matches forms the basis of a score for each protein, which is used to assess the confidence of the protein identification.

Methodological Challenges

Several challenges arise when developing an integrated system such as GAPP - some of which are easily resolved and others remain ongoing difficulties. In this section, the problems faced are explored and the solutions and work in progress explained.

Integration

The process of integrating discrete processing steps into a pipeline is the first challenge. Deciding on an optimal workflow depends both on user requirements and available resources. Speed of processing, data security, data visualisation, data-mining functionality and platform compatibility are all important for potential users. A key resource constraint is the existing software landscape. GAPP exploits open source software including X!Tandem (spectral search engine) and MySQL (database server). Use of such software reduces development time and avoids licensing issues, while still providing results within acceptable timeframes.

In response to increasing interest in the research community, the pipeline was also designed to allow automated identification and visualisation of proteins with post-translational modifications (PTMs), which

 Published by Cranfield University Press ISBN: 978-0-9557436-7-2 http://hdl.handle.net/1826/3832

are believed to play a role in biological regulation, such as in cell signalling, and disease aetiology, making them promising biomarker candidates.

Figure 1: The core of the Genome Annotating Proteomic Pipeline (GAPP).

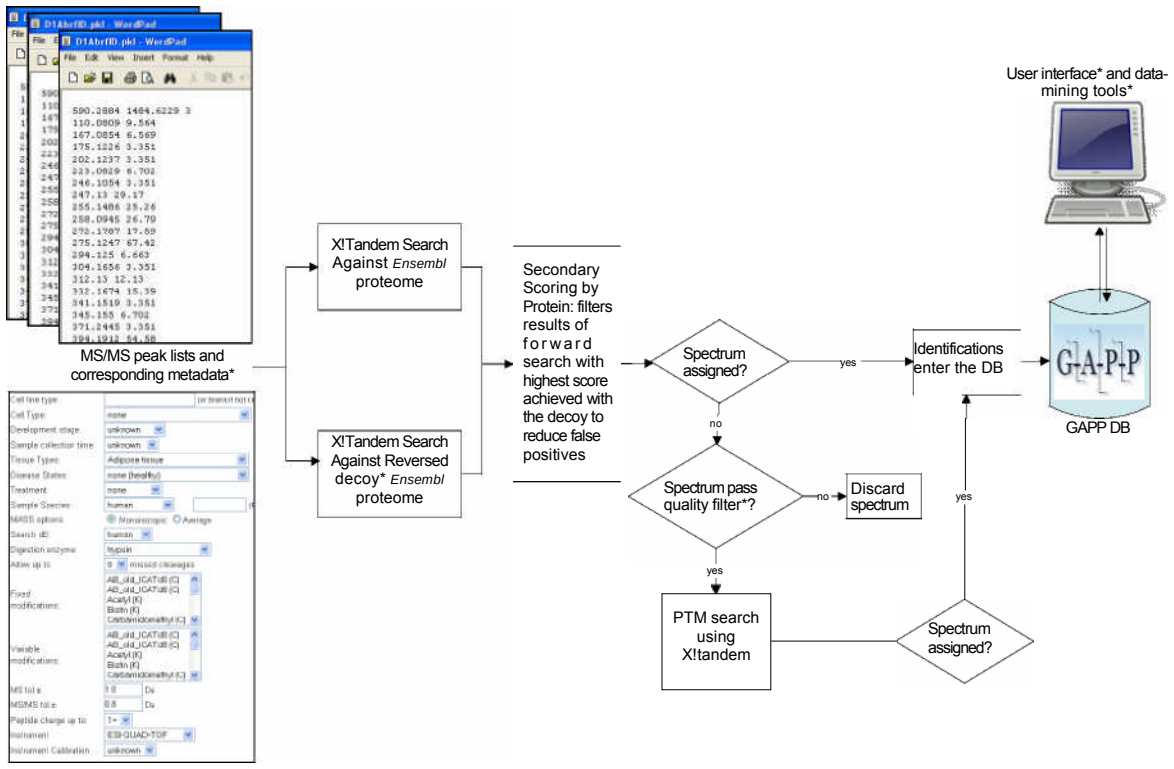

Increasing Confidence in Results by Reducing False Positives

In high throughput proteomics, human judgement cannot be relied upon to interpret the data.

This is an important challenge to consider, since studies have shown that the experience and skill of the researchers involved in generating and interpreting MS/MS data has the greatest impact on the accuracy of the results. A big danger in proteomics is a false positive (FP) – a protein identification which is made when the protein in question was not actually in the sample. Such bogus identifications are very common in proteomics, for example when background noise happens by chance to make a spectrum look like a genuine peptide. It is obviously disastrous if a falsely identified protein is taken forward as a biomarker.

 Published by Cranfield University Press ISBN: 978-0-9557436-7-2 http://hdl.handle.net/1826/3832

FPs are avoided in GAPP by using advanced average peptide score (APS) methodology (8). APS is a validative step performed after each X!Tandem search. In essence, it results in a confidence score for each protein from which peptides were observed. Protein assignments with an APS score below a defined threshold are discarded. The threshold is derived *ab initio* by setting it to the maximum score achieved when searching the acquired spectra against a decoy database. A decoy database search provides a null model against which identifications are tested - if matches are found with the null model the match is assumed to be incorrect and the highest score achieved is used as the threshold described above. We have undertaken a thorough and objective study to determine the most effective decoy database.

Data Mining and Data Visualisation

Data-mining is the process by which valuable information (in our case potential biomarkers) are extracted from data in a repository (our protein identifications). Tools to interrogate the GAPP identifications database and present complex results to users were needed to make the numerous protein identifications available to the user in a convenient form. Such tools help the user to spot significant differences that are indicative of biomarkers. This is a formidable and ongoing challenge as requirements vary between individual studies and individual users, but progress has been made by scanning published literature, attending proteomics meeting and through discussions with proteomics groups in industry and academia.

Protein Quantitation

Once potential protein biomarkers have been tentatively identified by high throughput analysis, the next step is to validate these biomarkers by conducting further experiments, ideally quantifying the differences in abundance of proteins between disease samples and controls. Such validation often needs to be carried out for multiple protein biomarkers, as it is now widely recognized that multiple biomarkers must be characterized if mechanisms of regulation, and hence diagnosis, of complex diseases is to be possible. One approach to achieve this goal is a targetted proteomic MS protocol called multiple reaction monitoring (MRM). Compared to other biomarker discovery and validation methods, such as antibody-based ELISAs, MRM has the advantage of being cost effective, quicker to design and suitable for multiplexed analysis (9). Due to the increasing use of this approach, support for MRM experiments has recently been built into GAPP. This support takes the form of a modular tool that helps users to design MRM experiments for peptides of interest by exploiting all the experimental proteomic information contained in GAPP.

Data Volume and Data Quality

The value of GAPP to its users is obviously totally dependent on the quality and quantity of the data fed to it. Increasing quantities of proteomic data are now available in public domain repositories (10), and even organisations collecting large amounts of their own data are keen to directly compare their results with those from public projects. We have therefore proposed to add automated data harvesting to GAPP to suck in and process all publicly available data as it becomes available. The danger of taking data from multiple distributed sources is that the classic *garbage in – garbage out* axiom applies as much to

 Published by Cranfield University Press ISBN: 978-0-9557436-7-2 http://hdl.handle.net/1826/3832

proteomics as to any other science. We will therefore also be seeking to apply automated quality filtering, both to the incoming data and to verify the resulting protein identifications.

Unforeseen Methodological Challenges

When building an automated pipeline such as GAPP, we are faced with the difficulty of operationalising complex processes that are subject to bias and subjectivity. Proteomics researchers are not used to expressing their approach for interpreting mass spectra in the form of rules suitable for automation. In fact, communicating to a third party how any multifaceted process is performed, particularly one that requires rules of thumb, intuition and experience, is a challenging feat. This is because human reasoning is a very complex, often subtle, process. For this reason, we have faced substantial difficulties in extracting programmable rules, and forming consensus on an approach, after consulting multiple experts. To address this issue, several strategies have been adopted. Firstly, where possible, we allow the user to specify the action of the program according to their own requirements, but this must be strictly controlled so as not to limit the ability to directly compare results. Where possible, targeted and structured questioning is used to capture expert knowledge, and prototypes are developed for live demonstration to communicate our intentions and stimulate discussion of ideas. Inviting several experts to attend the same demonstration drives the conversation towards consensus, or if necessary highlights strong divergence of ideas.

Obtaining metadata – the data describing an experiment – is another major challenge. Locating data resources that are suitable for GAPP is not difficult *per se,* but finding those that have sufficient metadata to allow a meaningful analysis is currently problematic. If metadata is totally absent, spectra cannot be processed at all, but if the minimal metadata is provided (e.g. the species from which the sample was taken) it is possible to identify proteins, but information required for mining the results will be absent – essentially preventing the conversion of data into commercially valuable conclusions. It is hoped that all data will

eventually be available in PSI (Proteomics Standards Initiative) standard formats which include detailed metadata, but this is not the case at present. The only way we can begin to address this issue at a high level is by supporting proteomics practitioners, journal editors and research funders in their efforts to embrace data standards.

Conclusions

The GAPP framework provides a high throughput platform for protein biomarker discovery by supporting analysis of differential proteomic studies. The system also provides a platform on which to build new tools, such as the MRM tool to validate and refine biomarkers for developing novel medicines. By capturing large volumes of data more candidates may be analysed, in less time, and through consensus across many datasets uncertainty may be reduced. Tools such as the GAPP system described here make a major impact on the amount and quality of biomarker candidates that an organisation can discover, but there remains much scope to further smooth the journey from data to commercially exploitable biomarker.

 Published by Cranfield University Press ISBN: 978-0-9557436-7-2 http://hdl.handle.net/1826/3832

Acknowledgements

The work described in this paper is being funded by BBSRC, ESPRC, GSK and Oxford Genome Sciences.

References

1. Ahmed, N., Oliva, K. T., Barker, G., Hoffmann, P., Reeve, S., Smith, I. A., Quinn, M. A., and Rice, G. E. (2005) Proteomic tracking of serum protein isoforms as screening biomarkers of ovarian cancer. *Proteomics* 5, 4625-4636.
1. 2 Cheng, A.-J., Chen, L.-C., Chien, K.-Y., Chen, Y.-J., Chang, J. T.-C., Wang, H.-M., Liao, C.-T., and Chen, I. H. (2005) Oral Cancer Plasma Tumor Marker Identified with Bead-Based Affinity-Fractionated Proteomic Technology. *Clin Chem* 51, 223 6-2244.
2. Donners, M., Verluyten, M. J., Bouwman, F. G., Mariman, E. C. M., Devreese, B., Vanrobaeys, F., van Beeumen, J., van den Akker, L. H., Daemen, M. J., and Heeneman, S. (2005) Proteomic analysis of differential protein expression in human atherosclerotic plaque progression. *J. Pathology* 206, 39-45.
3. Go, E. P., Wikoff, W. R., Shen, Z., O'Maille, G., Morita, H., Conrads, T. P., Nordstrom, A., Trauger, S. A., Uritboonthai, W., Lucas, D. A., Chan, K. C., Veenstra, T. D., Lewicki, H., Oldstone, M. B., Schneemann, A., and Siuzdak, G. (2006) Mass Spectrometry Reveals Specific and Global Molecular Transformations during Viral Infection. *J. Proteome Res.* 5, 2405-2416.
4. Rifai, N., Gillette, M. A., and Carr, S. A. (2006) Protein biomarker discovery and validation: the long and uncertain path to clinical utility. *Nat Biotech* 24, 97 1-983.
5. Perkins, D., Pappin, D., Creasy, D., and Cottrell, J. (1999) Probability-based protein identification by searching sequence databases using mass spectrometry data. *Electrophoresis* 20, 3551-3567.
6. Craig, R., and Beavis, R., C, (2003) A method for reducing the time required to match protein sequences with tandem mass spectra. *Rapid Communications in Mass Spectrometry* 17, 2310-2316.
7. Shadforth, I., Dunkley, T., Lilley, K., Crowther, D., and Bessant, C. (2005) Confident protein identification using the average peptide score method coupled with search-specific, ab initio thresholds. *Rapid Communications in Mass Spectrometry* 19, 3363-3368.
8. Stahl-Zeng, J., Lange, V., Ossola, R., Eckhardt, K., Krek, W., Aebersold, R., and Domon, B. (2007) High Sensitivity Detection of Plasma Proteins by Multiple Reaction Monitoring of N-Glycosites. *Mol Cell Proteomics* 6, 1809-18 17.
9. Mead, J. A., Shadforth, I. P., and Bessant, C. (2007) Public proteomic MS repositories and pipelines: available tools and biological applications. *Proteomics* 7, 2769-2786.

 Published by Cranfield University Press ISBN: 978-0-9557436-7-2 http://hdl.handle.net/1826/3832

Fabrication and characterization of magnetic Fe_3O_4 nanoparticles

Farahnaz Ansari[1]*, Zsuzsanna Libor[1], Jeremy J. Ramsden[1]

[1] *Microsystems & Nanotechnology Centre, Dept of Materials, Cranfield University, Bedfordshire, MK43 0AL, UK*

* Corresponding author. Tel.: +44 (0)1234 750111 ext 2465; fax: +44(0) 751346.
E-mail address: f.ansari@cranfield.ac.uk

Abstract

Spherical shaped magnetic nanoparticles with a narrow size distribution ≈ 10 nm in diameter were prepared by a thermochemical method. These particles were characterized by means of transmission electron microscopy (TEM) and X-ray diffraction (XRD). Nanoparticles exhibited superparamagnetic behavior as measured by a Magnetic Measurements Variable Field Translation Balance (MMVFTB). Saturation magnetization was calculated from hysteresis loops with applied magnetic fields from 0 up to 8000 Oe.

Keywords: Synthesis; Iron oxide; Magnetic Nanoparticles;

1. Introduction

Nanoparticles are the end products of a wide variety of physical, chemical and biological processes, some of which are novel and thoroughly different, others are quite routine. Among them, iron oxide nanoparticles have attracted considerable attention during the last decade and they have been of great interest in clinical uses[1-4]. Although there are many kinds of interesting magnetic nanoparticles such as iron, cobalt or ferrites, we have focused our study on iron oxide particles, namely magnetic (Fe_3O_4) because they are biocompatible and less susceptible to changes due to oxidation and also for their chemical stability, compared to nanoparticles of pure Fe[5,6]. For nanoparticles to produce an effective magnetic enrichment and exhibit superparamagnetism, they must be small enough that each particle becomes a single domain. Morrish and Yu[7] determined that Fe_3O_4 particles are single domains when the diameter is 50 nm or less.

The possibility of synthesizing nanoparticles and the utilization of commercially available mass-produced nanoparticles with properties on demand is taken into account. Therefore simplicity of production would be a main criterion in this case. A

 Published by Cranfield University Press ISBN: 978-0-9557436-7-2 http://hdl.handle.net/1826/3832

number of techniques have been developed in order to synthesise magnetic nano-particles including: hydrothermal[8,9], micro-emulsion[8,10], ball milling[11,12], mechano-chemical[13,14],microwave heating[15,16], sonochemical preparations[17], and chemical co-percipitation[18,19]. Compared to other methods, chemical methods have been found the better methods in order to get high quality nanoparticles.

In this study, a chemical method for producing magnetic ferrofluid has been used because it is accessible and the materials are commercially and inexpensively available in large quantities (order of grams). In this approach; stable dispersion of magnetite fluid was obtained with particles in the range of less than 10 nm. The main characteristics of this methods is to obtain an ultrafine magnetic oxide by a chemical reaction from the aqueous solution containing ferrous (Fe^{2+}) and ferric (Fe^{3+}) ions. A constant temperature and pH adjustment is needed to ensure particle formation and stabilization.

2. Experimental

2.1Materials

Ferrous sulphate $FeSO_4$, ferric nitrate Fe $(NO_3)_3$, and all other chemicals were from Fisher Scientific (UK). Water used was purified by ion exchange and reverse osmosis (ELGA-PRIMA- option3-15 mega ohm, UK).

2.2 Synthesis procedure

In a 100 mL 3-neck flask, ferric salt, $Fe(NO_3)_3$, was dissolved in 12.5 mL of ultrapure water to make a solution with a concentration of 0.9 mM and purged with nitrogen for at least 30 minutes. Ferrous salt was then added in the form of $FeSO_4$ with a concentration of 0.9 mM, while the nitrogen purge was continued. In a 500mL 3-neck flask, NaOH was dissolved in 125 mL of distilled water to achieve the desired concentration (0.5 M).The basic solution was purged with nitrogen and then heated in a mantel. When the reaction temperature was reached to 65°C, the solution of iron salts was added dropwise into the basic solution. Black precipitates formed immediately upon addition of the iron salt solution. The reaction solution was mixed vigorously for 30 minutes (from where the iron salt was added). At the end of the 30 minutes, the flask was removed from the mantel and centrifuged for 15 minutes at 3000 g. Separation of catalysts was achieved by applying an external permanent magnet to one side of the vessel. The supernatant was discarded by decantation and the particles were rinsed three times with approximately 150 mL of distilled and

 Published by Cranfield University Press ISBN: 978-0-9557436-7-2 http://hdl.handle.net/1826/3832

deoxygenated water by centrifugation at 3000 g for 10 min to remove excess ions in the suspension. Finally the particles were rinsed with approximately 100 mL of 0.01 M HCl to neutralize them. The particles were then collected, and were dried in an oven at 80 °C for overnight. The magnetic nanoparticle concentration was expressed in terms of dry weight per volume of suspension medium.

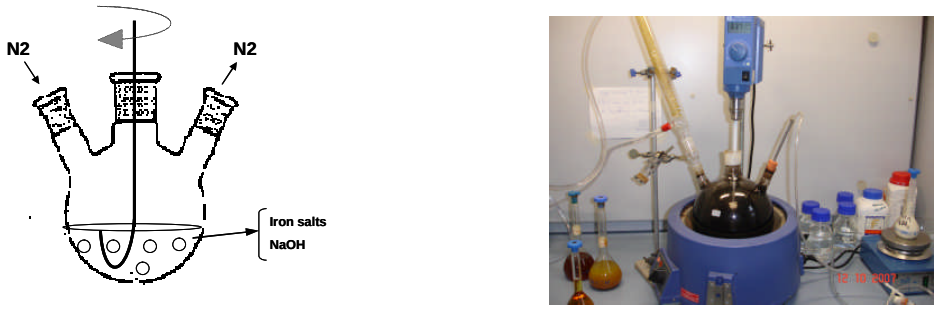

Fig 1. Dispersing of ferrite nanoparticles and embedding them in a three neck flask under nitrogen. The displacement of air by N_2 gas during preparation prevented oxidation of ferrous ion in the aqueous solution and also controlled the particle size.

Fig 2. Photograph of fabricated nanoparticles. Nanoparticles were gradually concentrated and collected on one side of the vessel by an external permanent magnet.

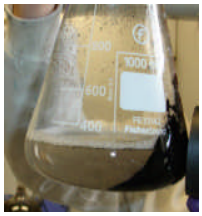

3. Results and discussion

3.1 Transmission electron microscopy

TEM provided a method for viewing the shape of the particles and determining the particle size. To prepare TEM samples, dispersion was prepared by first collecting a small amount of nanoparticle slurry at the final rinsing step just prior to the filtration step and followed by sonication for approximately 5 minutes to disperse the nanoparticles. A drop of solution containing the dispersed nanoparticles was placed on a TEM grid and then left to dry in air. The best results were obtained using carbon-coated copper grids (200-300 mesh). Fig. 3 shows the particles are almost spherically shaped with particle size of 10 nm and exhibiting good, stable and long-lasting water dispersibility.

Fig 3. (a)TEM image of a 10 nm Fe3O4 particle. (b) is a low resolution image of the synthesized partivcles.

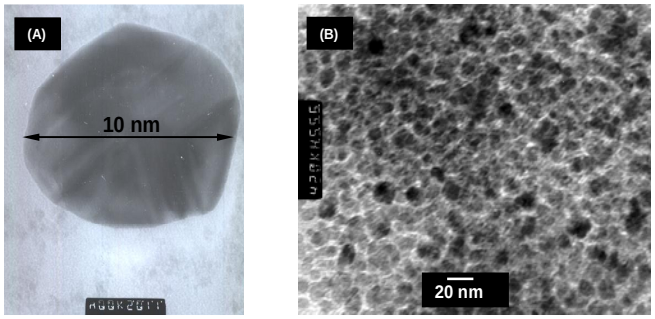

 Published by Cranfield University Press ISBN: 978-0-9557436-7-2 http://hdl.handle.net/1826/3832

3.2 X-ray diffraction (XRD)

Powder X-ray diffraction (XRD) studies were performed between 10° and 80° on a Cupper x-ray source, Siemens. The XRD pattern of dark brown powder collected from vessel indicates the formation of Fe_3O_4 crystals because of the peaks at 30, 35,43,53,57 and 63° which can be clearly identified in the angular (2θ) and it reflected by the well matching of the diffraction peaks with the magnetic pattern (vertical lines) (Fig.4).

Fig 4 X-ray diffraction pattern of a sample collected with decantation.

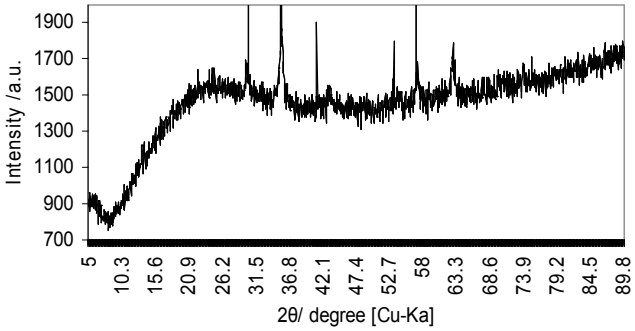

3.3 Magnetization study

Magnetic properties of the nanoparticles were measured at room temperature. Saturation magnetization was obtained from magnetization curves by applying magnetic fields from 0 up to 8000 Oe. The hysteresis loop of synthesized magnetics indicates a superparamagnetic behavior (Fig. 5). It should be emphasized here that the residual magnetization is almost negligible for the present magnetic nanoparticles, which might have contributed to their good dispersibility.

Fig5. Hysteresis loop of magnetic Fe_3O_4 nanoparticles measured at room temperature. δ_S = 50.07 , saturation magnetization.

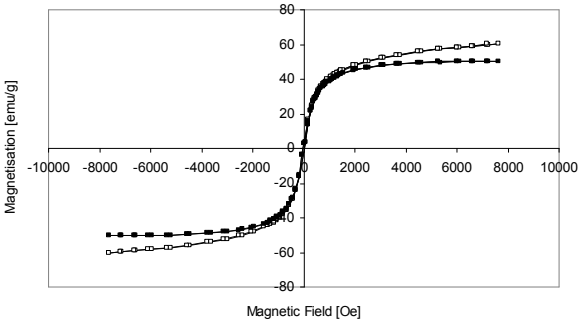

3.4 Zetapotantial measurements

The fabricated nanoparticles suspended in deionized water (100 μg/mL) and their size distribution and zeta potential of the prepared nanoparticles were measured using a Zetasizer (3000HS, Malvern Instruments Ltd., Worcestershire, UK).

 Published by Cranfield University Press ISBN: 978-0-9557436-7-2 http://hdl.handle.net/1826/3832

Fig 6. Surface charges of Fe_3O_4 magnetic nanoparticles as a function of pH in water at 25°C.

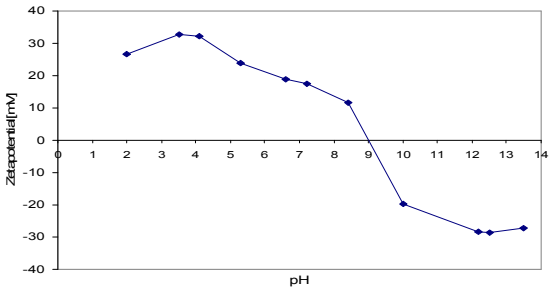

4. Conclusions

For magnetic nanoparticles, current and future research is geared towards size distribution control. For most applications it is critical to have a specific size as well as a very tight size distribution. Current research is pushing to synthesize superlattices of magnetic nanoparticles which show size distribution of less than 10 nm.

We propose a chemical method to synthesize Fe_3O_4 nanoparticles of 10 nm diameter using ferrous and ferric ions magnetite nanoparticles. This method is easy, highly reproducible and allows obtaining a large amount of particles in a one-pot short synthesis procedure. Their characters were determined by TEM, XRD, magnetization and zetapotential measurement. The nanomagnetic Fe_3O_4 particles are superparamagnetic and have a good stability.

References

1. Berry, C.C., Curtis, A.S.G. Fictionalization of magnetic nanoparticles for application in biomedicine. *Journal of Physics. D: Applied Physics.* **36**(2003) R198.

2. Chastellain1, M., Petri1, A.., Hofmann, M., Hofmann, H. Synthesis and patterning of magnetic nanostructures. *European Cells and Materials*. **3** (2002) 1, 11.

3. Willard, M. A., Kulrihara, L. K., Carpenter, E. E., Calvin, S., and Harris, V.G. Chemically prepared magnetic nanoparticles. *International Material Reviews*. **49**(2004) 3.

4. Pankhurst, Q. A., Connolly, J., Jones, J, S. K., and Dobson, J. Applications of magnetic nanoparticles in biomedicine. *Journal of Physics D: Applied Physics*. **36** (2003) R167.

5. Pankhurst, Q. A., Connolly, J., Jones, J, S. K., and Dobson, J. Applications of magnetic nanoparticles in biomedicine. *Journal of Physics D: Applied Physics*. **36** (2003) R167.

6. Fu, L., Dravid, V.P., Klug, K., Liu, X., and Mirkin, C.A. Synthesis and patterning of magnetic nanostructures. *European Cell and Materials*. 3 Suppl. **2**(2002) 156.

 Published by Cranfield University Press ISBN: 978-0-9557436-7-2 http://hdl.handle.net/1826/3832

7. Morrish, A. H., Yu, S. P. Magnetic Measurements on Individual Microscopic Ferrite Particles Near the Single-Domain. *Physical Review*. **102** (1956) 670-673.

8. Christy R, Vestal and Z. John Zhang. Magnetic spinel ferrite nanoparticles from microemulsions" *International Journal of Nanotechnology* **1** (2004) 1-2.

9. Ji, G. B., Tang, S.L., Ren, S.K., Zhang, F.M., Gu, B.X., Du,Y.W. Simplified synthesis of single-crystalline magnetic CoFe2O4 nanorods by a surfactant assisted hydrothermal process. Journal of Crystal Growth. **270** (2004)156.

10. Xinyong Li, Charles Kutal. Synthesis and characterization of superparamagnetic CoxFe3-xO4 nanoparticles. *Journal of Alloys and Compounds*. **349**(2003) 264.

11. Bid,S., Banerjee, A., Kumar,S., Pradhan,S. K., Udaya De, D. Banerjee. Nanophase iron oxides by ball-mill grinding and their Mössbauer characterization. *Journal of Alloys and Compounds*. **326** (2001) 292.

12. Gerardo F. Goya, F. Handling the particles size and distribution of Fe3O4 nanoparticles through ball milling. *Solid state communications*. **130** (2004) 783.

13. Liu, W., McCormick, P.G. Synthesis of Sm2Co17 alloy nanoparticles by mechanical processing. *Journal of magnetism and magnetic materials*. **195** (1999) L297.

14. Shi, Y., Ding, J., Yin, H.CoFe2O4 nanoparticles by the mechanochemical Method. *Journal of Alloys and Compounds*.**303** (2002) 290.

15. Bensebaa, F., Zavaliche,F., Ecuyer, P. L., Cochrane, R.W., Veres, T. Microwave synthesis and characterization of Co-ferrite nanoparticles *Journal of Colliod and Interface Science*, 277, 104(2004).

16. Hrpensess, R., Gedanken, A. The microwave-assited polyol synthesis of nanosized hard magnetic material, FePt. *Journal of Material Chemistry*, **15** (2005) 698.

17. Kurikka V.P.M., Shafi, Aharon Gedanken, Ruslan Prozorov, Judit Balohgh. Sonochemical Preparation and Size-Dependent Properties of Nanostructured CoFe2O4 Particles. *Chemical Material*.**10** (1998) 3445.

18. Rajendran, M., Pullar, R. C., Bhattacharya, A. K., Das, D., Chintalapudi, S. N. and Majumdar, C.K. Magnetic properties of nanocrystalline CoFe2O4 powders prepared at room temperature: variation with crystallite size. *Journal of Magnetism and Magnetic Materials*. **232** (2001) 71.

19. Yeh, Ch. Sh., Cheng, F.Y., Shieh, D.B., Wu, Ch.L. Method for preparation of water-soluble and dispersed iron oxide nanoparticles and application thereof. *United States Patent* (2004) 20050271593.

 Published by Cranfield University Press ISBN: 978-0-9557436-7-2 http://hdl.handle.net/1826/3832

CFD & Turbulence Modelling of Contaminant Dispersion in Environmental Flows

C. Papachristou, E. Shapiro and D. Drikakis

Fluid Mechanics and Computational Science (FMaCS) Group, Department of Aerospace Sciences, Cranfield University, Cranfield, Bedfordshire, MK43 0AL

Abstract

Detailed information about dispersion patterns of contaminants is important in a number of applications ranging from the sustained pollution impact analysis to industrial accident modelling. In this paper simulations of dispersion of nitrogen from a roof vent of a single building at high Reynolds number are presented. The sensitivity of the results to the choice of the turbulence modelling approach, within the time-averaged family of models is investigated for widely used k-ω and k-e model families. The validation against available wind tunnel experimental data demonstrates that the Renormalisation Group k-e turbulence model provides best results. Moreover, it is shown that application of the standard k-ω model to this case leads to a converged solution with different arrangement of recirculation zones.

Introduction

The dispersion pattern of a contaminant within a built up area can be affected by different factors such as the outdoor environment (wind velocity, wind direction, and ambient temperature), the contaminant characteristics (locations of the sources and emission characteristics) and building configuration [1]. A combination of the above could lead to rapid spreading of the contaminant and resulting increase of the exposure level to this contaminant. For the purposes of prevention and regulation of industrial pollution, it is necessary to understand the dispersion patterns associated with emittance of particular contaminants under various wind conditions.

The dispersion of toxic gases resulting from either accidental or permanent releases (cases of industrial fumes or motorways) within a built up area has been the subject of many investigations. Experimental studies conducted by Li and Meroney [2], Wilson and Chui [3] and Saathoff *et al.* [4] focused on the contaminant dispersion patterns and their dependency on the location of the source and the building height. Over the

 Published by Cranfield University Press ISBN: 978-0-9557436-7-2 http://hdl.handle.net/1826/3832

past decade CFD has rapidly emerged as an analysis tool of choice supplementing and in many cases replacing wind tunnel experiments. The benefits of CFD in this context include extensive data output, relatively low cost and the ease of handling unscaled models and dangerous contaminant substances. The two turbulent modelling approaches, most frequently encountered for problems of contaminant dispersion in environmental flows, are the Reynolds Averaged Navier Stokes (RANS) approach and, in particular, Standard $k-\varepsilon$ turbulence model and Large Eddy Simulation (LES) approach. Chan et al. [5] and Smith *et al*. [6] compared these approaches and concluded that LES is able to predict with accuracy the dispersion patterns whereas Standard $k-\varepsilon$ RANS is less accurate but more cost-effective and less time consuming. While LES rapidly gains grounds as an engineering modelling tool, high computational costs associated with LES simulations lead to RANS models still being widely applied. Confidence in the performance of RANS models, particularly those implemented in leading commercial CFD solvers is essential to industries relying on commercial CFD modelling software or utilising it in conjunction with in-house analysis tools.

In this paper, the dispersion of nitrogen (N_2) emitted from the roof of a cubical model was simulated using three different turbulent models, the Standard $k-\varepsilon$, the Standard k-ω RANS model and the RNG $k-\varepsilon$ model implemented in the commercial CFD solver FLUENT 6.1. The performance of these turbulence models is analysed based on the qualitative and quantitative comparisons against available wind tunnel data by Saathoff *et al*. [4].

Problem Formulation

The motion of a fluid is described by the standard set of Navier-Stokes equations representing conservation laws [7]. Addition of other species to the fluid flow results in an additional advection-diffusion equation per specie which has to be solved in conjunction with the initial set of Navier-Stokes equations:

$$\frac{\partial}{\partial t}(\rho Y_i) + \nabla \cdot (\rho \vec{v} Y_i) = -\nabla \cdot \vec{J}_i \qquad \text{(eq.1)}$$

Where Y_i is the local mass fraction of i th species.

 Published by Cranfield University Press ISBN: 978-0-9557436-7-2 http://hdl.handle.net/1826/3832

The computation domain consists of a channel in the spanwise centre of which the building is located (Figure 1). The side dimension of the building $D = 60\,mm$ corresponds to a full scale building with a height of 15m at a scale reduction of 1:250. Nitrogen was released from a flush vent located at the centre of the roof. The vent's diameter was $D_0 = 0.1 * D$.

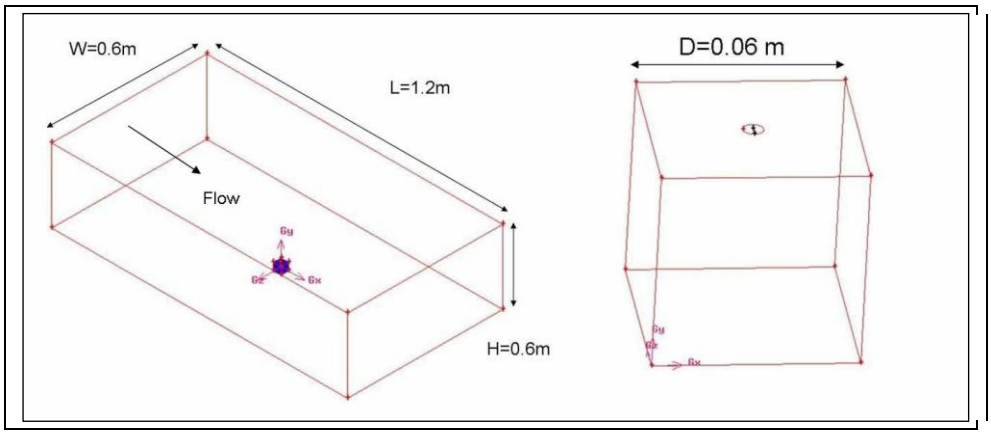

Fig.1 Computational Domain

The mesh of the complete computational domain is non-uniform and consists of 479.913 nodes in total. In order to be able to capture the near wall effects at the regions of the vent and the faces of the cube, the mesh density was increased at those specific areas. The mesh was generated using GAMBIT 2.2 software package.

The experimental case simulated corresponds to the constant velocity of air of 4.7 m/s and constant velocity of nitrogen emitted from the roof of 0.24 m/s. Temperature remained constant at 300K throughout all simulations and the amount of the nitrogen emitted was calculated in terms of the mass flux.

Results

Figure 4 illustrates the flow topology using velocity vectors (coloured by velocity magnitude) along the symmetry plane XY and plane XZ (y=0, centre of the building). The typical flow pattern observed in computations and experiments [4] consists of the front recirculation region, side recirculation zones, detached wake and a separation and reattachment on the top of the building leading to a vortical structure attached to the roof.

Out of these structures, the roof top vortex is of most importance for the contaminant dispersion pattern, as the emitted nitrogen gets entrained in the roof top vortex and

 Published by Cranfield University Press ISBN: 978-0-9557436-7-2 http://hdl.handle.net/1826/3832

dissipates, which prevents dangerous concentrations of nitrogen from reaching the ground level. Further discussion focuses on the resolution of this flow feature.

While both Standard and RNG $k-\varepsilon$ models captured the flow topology properly, the standard k-ω model leads to the opposing sign of the vorticity for the roof top vortex. Figures 4a and 4b show the flow topology obtained with the Standard $k-\varepsilon$ model and the Standard k-ω model results are illustrated by Figures 4c and 4d respectively.

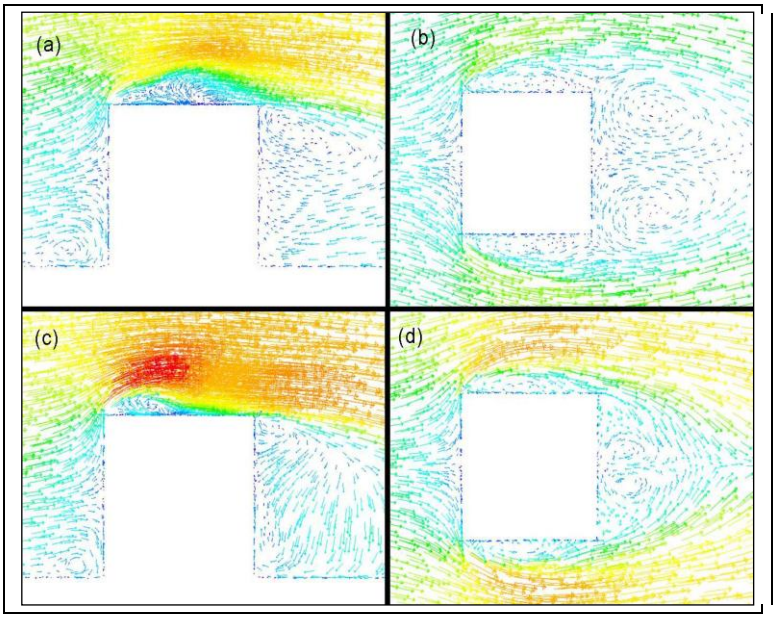

Fig.4 Flow structure obtained with different turbulence models

As a result of the different vorticity signs, the direction of the contaminant propagation changes, which is clearly indicated by the concentration levels on the top of the building (Figures 5 and 6). The upstream nitrogen propagation observed in the experiments is correctly captured by the $k-\varepsilon$ model while the k-ω model leads to unphysical downstream propagation of nitrogen on the roof.

 Published by Cranfield University Press ISBN: 978-0-9557436-7-2 http://hdl.handle.net/1826/3832

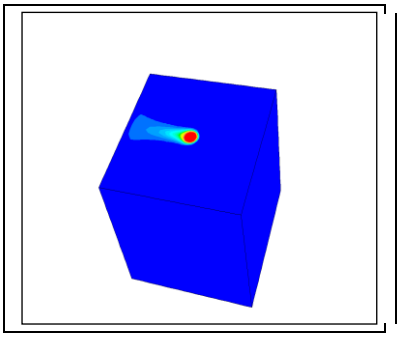

Fig.5 Dispersion of nitrogen modelled with the Standard $k-\varepsilon$ RANS model

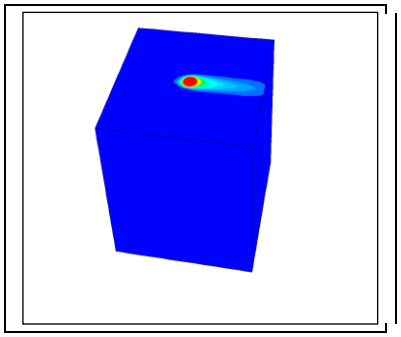

Fig. 6 Dispersion of nitrogen modelled with the Standard k-ω RANS model

In the reference paper [4], the concentration levels are expressed in terms of the non-dimensional concentration coefficient $K=CH^2U_h/Q$ where C is the concentration, H the dimension of the cube, U_h the mean wind speed at building height and Q the realise rate of nitrogen. Figure 7 shows the distribution of the concentration coefficient along the centreline of the roof of the building with three studied turbulence models.

In accordance with the experiment [4], the maximum concentration of nitrogen is located on the vent surface and reduces as it moves upstream of the vent. On the other hand, downstream of the vent, concentration of nitrogen is negligible. The concentration distribution comparisons indicate that both Standard and RNG $k-\varepsilon$ models correctly capture the upstream propagation of nitrogen on the roof of the cube whereas the Standard k-ω model fails to predict the distribution of nitrogen correctly.

 Published by Cranfield University Press ISBN: 978-0-9557436-7-2 http://hdl.handle.net/1826/3832

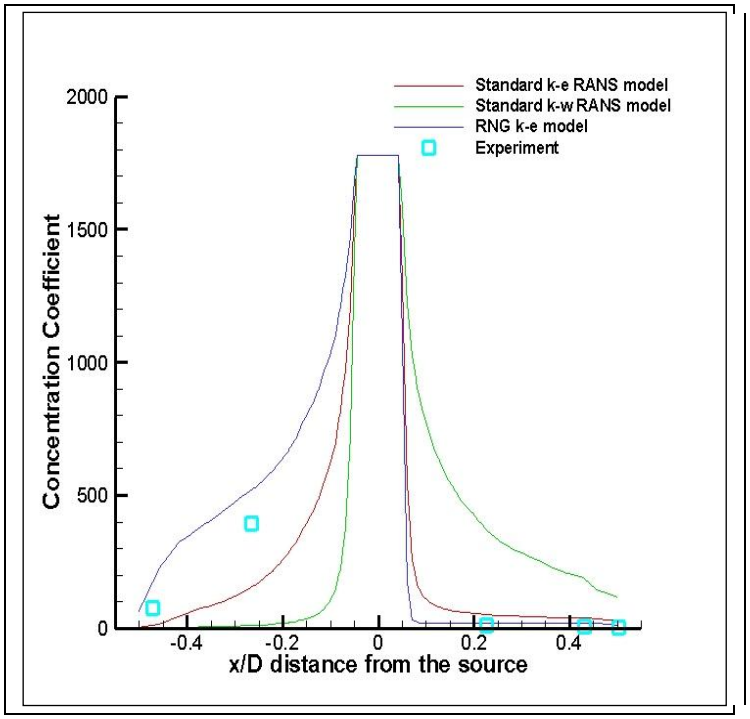

Fig.7 Comparison between the numerical studies and the experiment [4]

Based on the above comparisons, it is clear that among all three turbulent models, the most appropriate model in predicting the flow characteristics of the emitted nitrogen, is the RNG $k-\varepsilon$.

Conclusions

The dispersion pattern of emitted nitrogen around the surfaces of a cubical model was examined. Simulations were performed using three turbulent models the Standard $k-\varepsilon$ RANS model, the Standard k-ω RANS model and the RNG $k-\varepsilon$. While all three turbulence models should be applicable for the flow speeds in consideration, the computations indicate that only the $k-\varepsilon$ model family captures the flow topology and determines the contaminant dispersion pattern correctly. The fully converged solution with standard k-ω turbulence model exhibits opposite sign of the roof top vortex rotation and hence, opposite direction of the contaminant propagation.

Furthermore the comparisons of the concentration distribution versus experimental data indicate that RNG model leads to more accurate results for the contaminant concentration coefficient.

 Published by Cranfield University Press ISBN: 978-0-9557436-7-2 http://hdl.handle.net/1826/3832

References

1. LI, Y. STAFOPOULOS T. Computational evaluation of pollutant dispersion around buildings: Estimation of numerical errors. *Journal of Wind Engineering and Industrial Aerodynamics*, Vol.77&78, pp. 619-630 (1998).
2. LI, W., MERONEY R. Gas dispersion near a cubical model building part: 1. *Journal of Wind Engineering and Industrial Aerodynamics*, Vol.12, pp.15- 33 (1983).
3. WILSON, D *et al*., Effect of turbulence from upwind buildings on dilution of exhaust gases. *ASHRAE* Trans. 93, Part 2 pp. 2186-2197 (1987).
4. SAATHOFF, P.J. *et al*., Effects of model scale in estimating pollutant dispersion near buildings. *Journal of Wind Engineering and Industrial Aerodynamics,* 54/55, 549-559 (1995).
5. CHAN S.T., STEVENS , S.E. Validation of two CFD urban dispersion models using high resolution wind tunnel data.*3rd International Symposium on Environmental Hydraulics Conference, Tempe, AZ*, December 5-8 (2001)
6. SMITH W., et al. A CFD model intercomparison and validation using high resolution wind tunnel data. *11th Joint AMS/AWMA Applications of Air Pollution Meteorology*, Jan 2000.
7. DRIKAKIS, D. RIDER, W. High Resolution methods for incompressible and Low-speed Flows. *Springer,* 2004

 Published by Cranfield University Press ISBN: 978-0-9557436-7-2 http://hdl.handle.net/1826/3832

Multiscale Modelling for Flows & Materials

N. Asproulis, E. Shapiro, M. Kalweit & D. Drikakis

Fluid Mechanics & Computational Science Group

Department of Aerospace Sciences

Cranfield University,

Cranfield, Bedfordshire MK43 0AL, UK

Abstract

Over the past decade Micro and Nanofluidics emerged as vital tools in the ongoing drive towards the development of nano-scale analysis and manufacturing systems. Accurate numerical modelling of the phenomena involved at these scales is essential in order to speed up the industrial design process for nanotechnology, which is in a nascent phase. The key challenge of the numerical modelling of micro and nanofluidics is associated with inherently multiscale nature of the problem and the absence of a unified approach capable of tackling molecular, continuum and mesoscales without incurring unrealistic computational costs. In this paper we propose a novel multiscale approach in the hybrid continuum-molecular framework designed to deliver computational efficiency superior to that of currently available methods. The new approach is implemented in the in-house fluid flow HIRECOM solver and validated for a classic solid-liquid slip boundary problem.

Keywords: Hybrid Continuum-Molecular, Multiscale Modelling, Slip Boundary Condition, Micro/Nanofluidics, Nanotechnology.

Introduction

Micro and Nanofluidic devices have emerged as effective and promising tools for a wide range of applications in many different disciplines including bioengineering and chemistry [1]. Over the last years there has been an explosion of work in the area with the market for such devices growing from $400M in 2000 to $2bn in 2004 [2]. The main benefits of downscaling include improved accuracy and reduced process times and volume samples [3].

The precise fabrication of devices at those scales necessitates optimal design. Hence, efficient and accurate modelling of the phenomena involved in flow in nanochannels is of paramount importance. Numerical modelling is the cornerstone for obtaining better understanding of the processes involved in the operation of small devices [4].

The fluid flows in micro and especially nanofluidic devices present significant differences from those in larger scale devices. Fluid flow in a variety of microelectromechanical (MEMS) systems, including valves, nozzles, turbomachines, etc, cannot be predicted based on continuum flow models like the Navier-Stokes equations with no-slip boundary conditions at the solid-liquid interface [4]. As the dimensions of the system shrink to small scales, the assumptions of the continuum approximation break down. Particularly, the macroscopic constitutive relations and boundary conditions

 Published by Cranfield University Press ISBN: 978-0-9557436-7-2 http://hdl.handle.net/1826/3832

became inadequate [5]. In the cases where the continuum models cannot fully capture the physics of the system, molecular models based on the motion of molecules governed by the laws of classical mechanics have to be employed.

The Achilles heel of the molecular models is their computational cost. To illustrate the computational limitations, consider a microscopic MD simulation of pure water with fixed $O-H$ bonds and $H-O-H$ angles. The time step in a MD simulation is dictated by the faster frequency one needs to resolve. Estimating for the aforementioned simulation a typical time step to be $\delta t \sim 2\ fs$, one can see that in order to simulate a period of of $1\mu s$ a total number of 500 million time steps is required. Assuming that that the execution of a single time step takes at least 0.1 s, a total of some 19 months of CPU time is required [6]. Consequently, modelling phenomena at micro and nanofluidic devices presents significant difficulties due to the inaccuracy of the continuum models and inefficiency of the molecular ones. In order to address this challenge multiscale hybrid frameworks have been developed to couple the microscopic and macroscopic description of a system and facilitate the exchange of information [7]. Hybrid methods bring in the balance between the accuracy of the multiscale phenomena description and the computationally efficiency, bridging the gap between the macroscopic and microscopic length scales and providing a unifying description of liquid flows from nanoscale to larger scales. Hybrid methods can be broadly classified into the following three groups:

- Domain Decomposition Techniques [6-14]
- Embedding Based Techniques [15, 16]
- Patch Dynamics [17-19]

Domain decomposition methods are appropriate for problems where continuum equations are still valid in large regions of the system, but fail to fully describe the phenomenon in a particular area. In this case two regions are defined, where the one is solved by the continuum solver and the other one is solved by molecular dynamics [7, 8]. The advantage of this approach is that computationally slow molecular dynamics technique is employed in a small region, which is essential, whereas the rest of the domain is treated with the several orders faster CFD solvers [8]. The idea of domain decomposition was initially introduced in 1995 by O'Connell [7]. Since then several coupling approaches based on this idea have been developed, including the relaxation method [7, 13, 20], coupling through state- Schwarz Method [6, 11, 21-23] and coupling through fluxes method [10, 24-26].

In the embedding multiscale methods, the whole domain is covered with the macroscopic solver and the microscale model is used to obtain macroscopic properties. This method was introduced to handle the time scale constraints imposed by the geometrical coupling. The Heterogeneous Multiscale Method when applied to the moving contact line and the Marangoni flow problems inherits the characteristics of the "embedding based" framework [15].

The patch dynamics method was initially developed by Yiannis Kevrekidis and James Hyman [27]. The objective of patch dynamics method is to bridge the time and length scales and predict the macroscale dynamics by performing molecular simulations in a limited number of small "patches" only. The averaged properties obtained for a short period of time and for a small region, are used in order to advance and predict long space-time scale dynamics [17-19]. The

 Published by Cranfield University Press ISBN: 978-0-9557436-7-2 http://hdl.handle.net/1826/3832

general framework of the patch dynamics circumvents the need for a closed analytical description of the macroscale systems and delivers macroscopic information.

In this paper we present a novel Point Wise Coupling (PWC) method based on the ideas of patch dynamics. PWC approach couples the molecular dynamics (MD) simulations with continuum CFD simulations by performing MD simulations around a grid point for a number of time steps at every time step of the macroscopic computation fluid dynamics (CFD) solver. In this approach the molecular model is treated as a refinement of properties obtained by the macroscopic solver. The method is verified by the application to the classical Couette slip flow problem.

Point Wise Coupling Methodology

In the proposed Point Wise Coupling method MD simulations constrained from the macroscale by the velocity gradient are performed in the beginning of each macroscopic time step. MD simulations are performed using LAMMPS software developed by S. Plimpton [28]. CFD simulations were performed using the in-house high-resolution HIRECOM solver [29]. The results of the MD simulation in terms of either shear stresses or velocities are fed back into the CFD solver through the boundary conditions. Microscale simulations are performed using Non Equilibrium Molecular Dynamics (NEMD) techniques, in particular, the Parrinello-Rahman method for deformation boxes is utilised in order to maintain constant shear in the performed simulations. This method enables the use of periodic boundary conditions and at the same time a linear velocity profile is obtained. The schematic representation of PWC is shown in Figure 1.

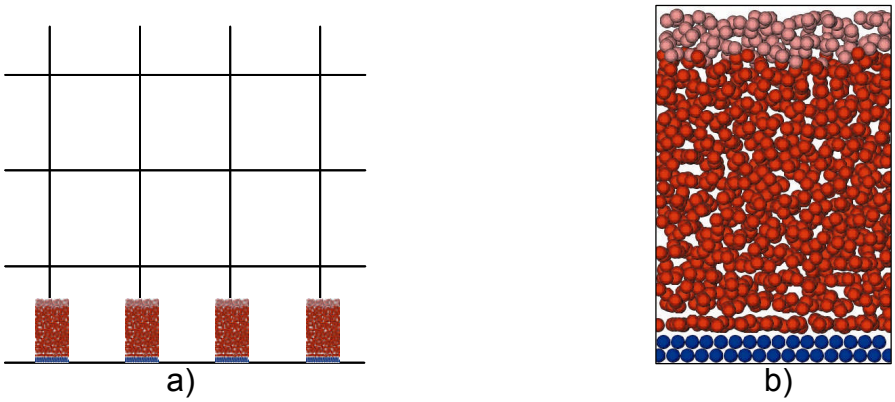

Fig. 1: a) Schematic representation of a grid with the MD Simulations b) The representation of the molecular domain. Here blue corresponds to the solid wall molecules, red to the fluid molecules and pink to the constrained region from the continuum representation

Results

The flow of a fluid inside a micro or nanochannel can be significantly influenced by liquid slip at the solid boundary conditions. The liquid flows are described by the incompressible Navier-Stokes equations under most circumstances [4]. However there are fundamental open questions related to the successful applicability of the no-slip Navier-Stokes equations, for example. Liquids can be considered as the “Holy Grail” of micro and nanofluidic modelling [30] due to the lack of a well advanced molecular based theory like the one for dilute gases. Furthermore the conditions under which the

 Published by Cranfield University Press ISBN: 978-0-9557436-7-2 http://hdl.handle.net/1826/3832

no-slip boundary assumption becomes inaccurate and the relationship of stress and strain rate becomes non linear are not known from first principles [30].

In the current application the Point Wise Coupling technique is used in order to investigate the influences of the channel height on the slip predictions. Multiscale computations are performed for Couette flow of liquid argon in a channel with height H varying from 50 to $500\,\sigma$, where σ is the molecular length scale (for liquid argon $\sigma \sim 0.34\,nm$ [22]). For MD simulations the liquid used has the following physical parameters: mass of each atom m, density $\rho = 0.81\,m \cdot \sigma^{-3}$, potential cut-off distance equal to 2.2σ and temperature of the liquid equal to $T = 1.1\varepsilon/k_B$, where k_B is the Boltzmann's constant and ε is the characteristic energy scale. The heat exchange is controlled by a Langevin thermostat with a random uncorrelated force and a friction term $\Gamma = 1.0\,\tau^{-1}$, where τ is the characteristic time $\tau = (m \cdot \sigma^2/\varepsilon)^{1/2}$ [31, 32].

In this particular application we consider that there is a slip condition on the lower stationary wall. Around the grid point on the lower wall MD simulations are performed constrained from the continuum solver via the strain rate and from those simulations the slip velocity is estimated and is passed as a boundary condition to the continuum solver. The size of the domain for the molecular simulations is 10σ in each x, y, z direction. The solid wall is modelled as two planes of a (111) face-centred cubic lattice that interact with the fluid particles through the shifted Lennard-Jones 6-12 potential:

$$V^{LJ} = 4 \cdot \varepsilon \cdot \left[\left(\frac{\sigma}{r} \right)^{12} - \left(\frac{\sigma}{r} \right)^{6} - \left(\frac{\sigma}{r_c} \right)^{12} + \left(\frac{\sigma}{r_c} \right)^{6} \right]$$

where r_c is the cut-off distance ($r_c = 2.2\sigma$). The parameters for the wall-fluid interaction ε^{wf} and σ^{wf} with the density of the solid particles determine the amount of slip in the boundary conditions. Particularly, in our simulations the following sets of parameters have been employed for modelling the slip and the non-slip boundary conditions: 1) $\varepsilon_{wf} = 0.6\varepsilon$, $\sigma_{wf} = \sigma$, $\rho_w = \rho$, 2) $\varepsilon_{wf} = 0.6\varepsilon$, $\sigma_{wf} = 0.75\sigma$, $\rho_w = 4\rho$ and 3) $\varepsilon_{wf} = 0.2\varepsilon$, $\sigma_{wf} = 0.75\sigma$, $\rho_w = 4\rho$. The first set of parameters is used to creating non-slip boundary conditions and the other two correspond to slip boundary conditions [31].

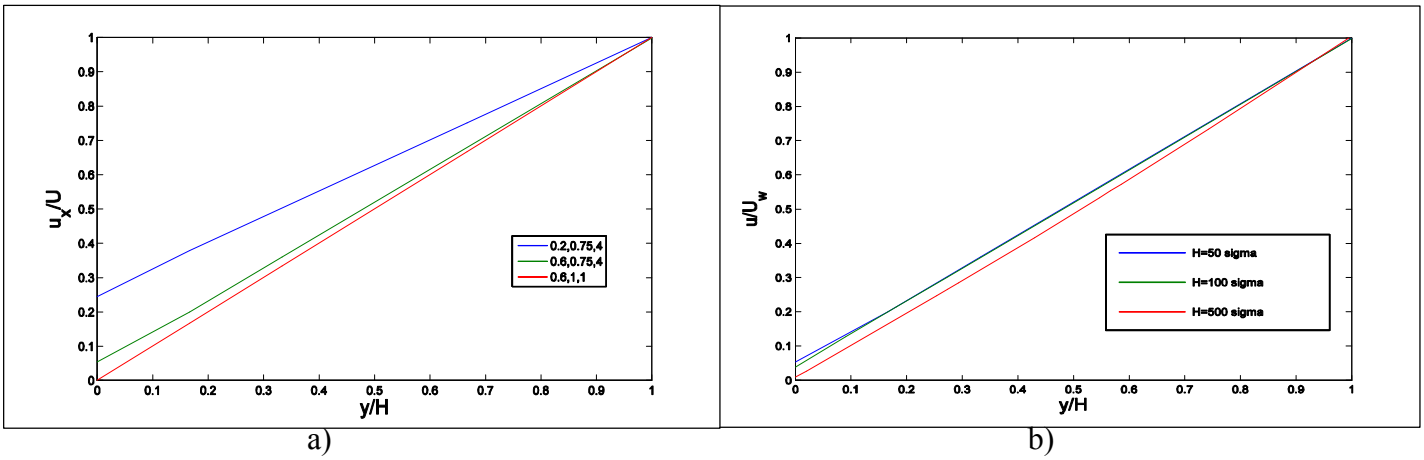

a) b)

Fig. 2: a)Velocity profiles for H = 50σ under slip and no-slip boundary conditions b) Velocity distribution for Couette flow in different

 Published by Cranfield University Press ISBN: 978-0-9557436-7-2 http://hdl.handle.net/1826/3832

channels under constant shear rate,εwf = 0.6ε, σwf = 0.75σ, ρw = 4ρ

In Figure 2a the velocity profiles for the channel with height H = 50σ are presented. The results obtained from the Point Wise Coupling are in full agreement with those obtained from other hybrid methods based on the domain decomposition [13], as it is presented in Figure 3, and those obtained from full MD simulations [31] where the maximum deviation for the slip velocity is from 0 to 0.24 $\cdot U_{Wall}$ for the non-slip and slip boundary conditions respectively. In Figure 2b the normalised velocity profiles are presented for the Couette flow under constant shear rate $U_w\tau/H = 0.02$. Comparing the results with continuum analytical solution for the non-slip flows $u/U_w = y/H$ it is noticed that for the narrower channels of 50σ and 100σ the deviation in the velocity profile is apparent whereas for the channels with height 500σ it can be assumed that the no-slip condition still holds. Comparing the results of the current hybrid method with other hybrid frameworks in the literature it has been found that the developed framework had one order of magnitude greater range of applicability in terms of channel height than most of the published models [32].

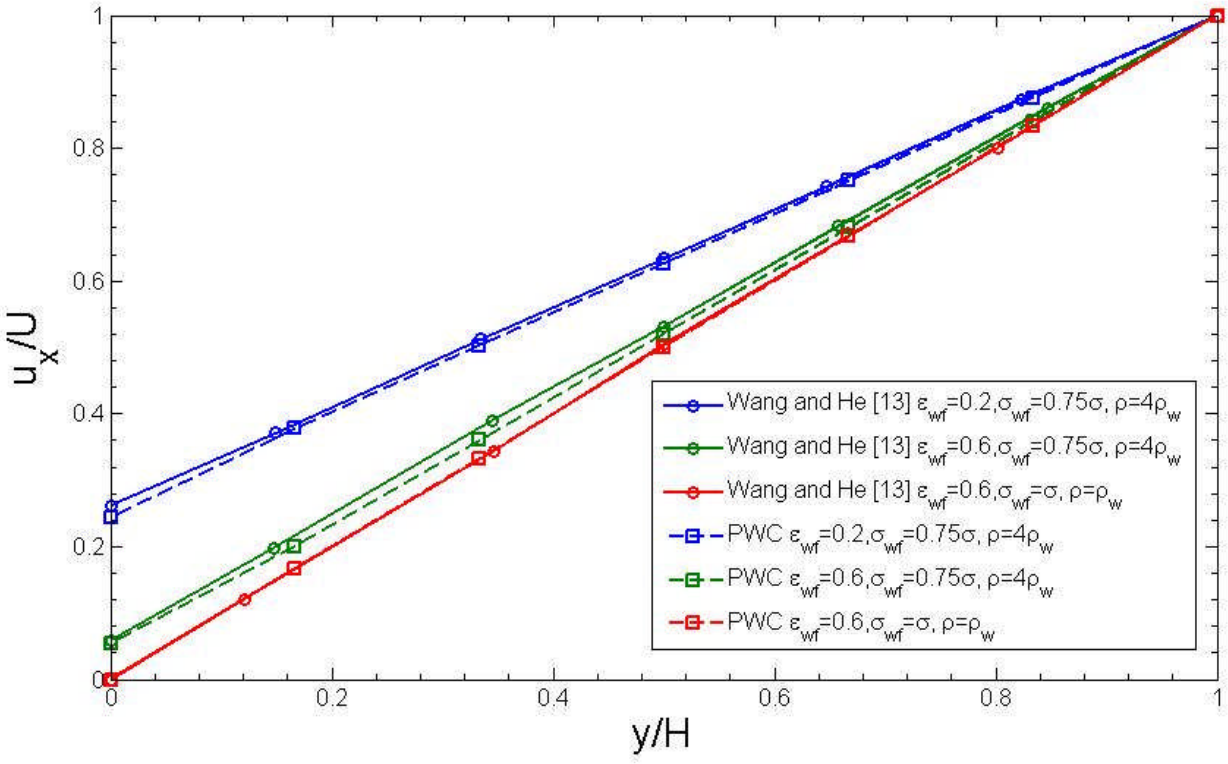

Fig. 3: Velocity profiles for $H = 50\sigma$ under slip and no-slip boundary conditions as obtained with PWC and domain decomposition developed by Wang and He [13]

 Published by Cranfield University Press ISBN: 978-0-9557436-7-2 http://hdl.handle.net/1826/3832

Conclusions

In this study a new Point Wise Coupling multiscale method is presented and applied to nanoscale and mesoscale fluid flows with slip at the liquid solid interface. The PWC method effectively decouples the timescales and employs smaller domains for the MD simulations which lead to increased efficiency in comparison with the classic domain decomposition approach. To further illustrate the efficiency benefits, the PWC method is compared to the domain decomposition method as implemented by Yen [32] in the slip Couette flow study. Considering the minimum size of the MD domain in both cases to be of order 10-12 σ and taking into account the overlapping region of at least 10-12σ necessary for the convergence of the domain decomposition [32], it is possible to state that the costs associated with the PWC MD simulations are halved in comparison with the domain decomposition. Furthermore in both cases the time step of the MD simulation is equal to $0.005\,\tau$ and the time step employed in the PWC simulation for the continuum flow is equal to $10\,\tau$. For the PWC method, an MD simulation of 10000 time steps is performed every 20 continuum time steps in order to calculate the boundary slip. In order to simulate the same system with the domain decomposition method for the same number of 20 continuum time steps a total number of 40000 molecular time steps is required. In addition, the PWC method requires MD simulations to be performed in a domain with half the size of that required for the domain decomposition and for four times smaller number of time steps. Consequently, taking into account that the computational time per time step per unit area is the same in both methods, in this particular example PWC is leading to ~8x speedup factor.

Acknowledgements

This work has been supported in part by the European Commission under the 6th Framework Program (Project: DINAMICS, NMP4-CT-2007-026804).

References

1. [1] A. E. Kamholz, B. H. Weigl, B. A. Finlayson, and P. Yager. Quantitative analysis of molecular interaction in a microfluidic channel: The t-sensor. *Analytical Chemistry*, 71(23):5340–5347, 1999.
2. [2] S. Wiggins J.M. Ottino. Introduction: mixing in microfluidics. *Phil. Trans. R. Soc. Lond. A*, 362:923–935, 2004.
3. [3] Z. Wu and N.. Nguyen. Hydrodynamic focusing in microchannels under consideration of diffusive dispersion: Theories and experiments. *Sensors and Actuators, B: Chemical*, 107(2):965–974, 2005.
4. [4] M. Gad-El-Hak. Gas and liquid transport at the microscale. *Heat Transfer Engineering*, 27(4):13–29, 2006.
5. [5] J. Liu, S. Chen, X. Nie, and M. O. Robbins. A continuum-atomistic simulation of heat transfer in micro- and nano-flows. *Journal of Computational Physics*, 227(1):279–291, 2007.
6. [6] T. Werder, J. H. Walther, and P. Koumoutsakos. Hybrid atomistic-continuum method for the simulation of dense fluid flows. *Journal of Computational Physics*, 205(1):373–390, 2005.
7. [7] S.T. O'connell and P.A. Thompson. Molecular dynamics-continuum hybrid computations: A tool for studying complex fluid flows. *Physical Review E - Statistical, Nonlinear, and Soft Matter Physics*, 52(6):R5792–R5795, 1995.
8. [8] Kalweit Marco and Drikakis Dimitris. Hybrid molecular dynamics and continuum. In *Proceedings of "Micro and Nano-scale Flows: Advancing Engineering Science and Design", Glasgow*, 2006.
9. [9] E. G. Flekkoy, G. Wagner, and J. Feder. Hybrid model for combined particle and continuum dynamics. *Europhysics Letters*, 52(3):271–276, 2000.
10. [10] E. G. Flekkoy, R. Delgado-Buscalioni, and P. V. Coveney. Flux boundary conditions in particle simulations. *Physical Review E - Statistical, Nonlinear, and Soft Matter Physics*, 72(2):1–9, 2005.

 Published by Cranfield University Press ISBN: 978-0-9557436-7-2 http://hdl.handle.net/1826/3832

11. [11] N. G. Hadjiconstantinou and A. T. Patera. Heterogeneous atomistic-continuum representations for dense fluid systems. *International Journal of Modern Physics C*, 8(4):967–976, 1997.
12. [12] X. Nie, M. O. Robbins, and S. Chen. Resolving singular forces in cavity flow: Multiscale modeling from atomic to millimeter scales. *Physical Review Letters*, 96(13):1–4, 2006.
13. [13] Y. c Wang and G. w He. A dynamic coupling model for hybrid atomistic-continuum computations. *Chemical Engineering Science*, 62(13):3574–3579, 2007.
14. [14] J. Li, D. Liao, and S. Yip. Nearly exact solution for coupled continuum/md fluid simulation. *Journal of Computer-Aided Materials Design*, 6(2):95–102, 1999.
15. [15] W. Ren and E. Weinan. Heterogeneous multiscale method for the modeling of complex fluids and micro-fluidics. *Journal of Computational Physics*, 204(1):1–26, 2005.
16. [16] G. Karniadakis, A. Beskok, and N. Aluru. *Microflows and Nanoflows: Fundamentals and Simulation*. Springer, New York, 2005.
17. [17] G. Samaey, I. G. Kevrekidis, and D. Roose. Patch dynamics with buffers for homogenization problems. *Journal of Computational Physics*, 213(1):264–287, 2006.
18. [18] C. W. Gear, J. Li, and I. G. Kevrekidis. The gap-tooth method in particle simulations. *Physics Letters, Section A: General, Atomic and Solid State Physics*, 316(3-4):190–195, 2003.
19. [19] J. M. Hyman. Patch dynamics for multiscale problems. *Computing in Science and Engineering*, 7(3):47–53, 2005.
20. [20] X. B. Nie, S. Y. Chen, W. N. E, and M. O. Robbins. A continuum and molecular dynamics hybrid method for micro- and nano-fluid flow. *Journal of Fluid Mechanics*, (500):55–64, 2004.
21. [21] N. G. Hadjiconstantinou. Discussion of recent developments in hybrid atomistic-continuum methods for multiscale hydrodynamics. *Bulletin of the Polish Academy of Sciences: Technical Sciences*, 53(4):335–342, 2005.
22. [22] N. G. Hadjiconstantinou. Hybrid atomistic-continuum formulations and the moving contact-line problem. *Journal of Computational Physics*, 154(2):245–265, 1999.
23. [23] P. Koumoutsakos. Multiscale flow simulations using particles. *Annual Review of Fluid Mechanics*, 37:457–487, 2005.
24. [24] G. Wagner and E. G. Flekkoy. Hybrid computations with flux exchange. *Philosophical Transactions: Mathematical, Physical and Engineering Sciences (Series A)*, 362(1821):1655–1665, 2004.
25. [25] R. Delgado-Buscalioni and P. V. Coveney. Hybrid molecular-continuum fluid dynamics. *Philosophical Transactions: Mathematical, Physical and Engineering Sciences (Series A)*, 362(1821):1639–1654, 2004.
26. [26] R. Delgado-Buscalioni and P. V. Coveney. Continuum-particle hybrid coupling for mass, momentum, and energy transfers in unsteady fluid flow. *Physical Review E - Statistical, Nonlinear, and Soft Matter Physics*, 67(4 2):467041–4670413, 2003.
27. [27] Ioannis G. Kevrekidis,et. al. Equation-free multiscale computation: enabling microscopic simulators to perform system-level tasks, 2002.
28. [28] S. J. Plimpton. Fast parallel algorithms for short-range molecular dynamics. *J. Comput. Phys.*, 117:1–19, 1995. lammps.sandia.gov.
29. [29] E. Shapiro and D. Drikakis. Artificial compressibility, characteristics-based schemes for variable density, incompressible, multi-species flows. *Journal of Computational Physics*, 210(2):584–607, 2005
30. [30] M. Gad el Hak. Liquids: The holy grail of microfluidic modeling. *Phys. Fluids*, 17:100612, 2005.
31. [31] P. A. Thompson and S. M. Troian. A general boundary condition for liquid flow at solid surfaces. *Nature*, 389(6649):360–362, 1997.
32. [32] T. H. Yen, C. Y. Soong, and P. Y. Tzeng. Hybrid molecular dynamics-continuum simulation for nano/mesoscale channel flows. *Microfluidics and Nanofluidics*, 3(6):665–675, 2007.

 Published by Cranfield University Press ISBN: 978-0-9557436-7-2 http://hdl.handle.net/1826/3832

Hydrothermal synthesis of potassium -sodium niobates for piezoelectric applications

Sophie d'ASTORG, Qi ZHANG

Cranfield University, School ofApplied Sciences, Bld 70, Cranfield, Bedfordshire, MK43 0AL, United Kingdom.

$Pb(Zr_{1-x}Ti_x)O_3$ (PZT) and related compositions have been the mainstay for high performance actuators and transducers, owing to their superior dielectric, piezoelectric and electromechanical coupling coefficients. But the increasing consciousness for health and environment protection, related to using lead, encourages the research on lead-free piezoelectric ceramics. Perovskites like $BaTiO_3$ or $(K, Na)NbO_3$, $Ba_2NaNb_5O_{15}$ tungsten bronze or layer structure like $Bi_4Ti_3O_{12}$ are the three main kinds of Pb-free piezoelectric. $(K,Na)NbO_3$-based ceramics are believed to be one of the most promising systems among the lead-free piezoelectric ceramics, due to their high piezoelectric properties.

The difficulties related to synthesis, sintering, control of microstructure and/or stoichiometry are well known for these $(K,Na)NbO_3$-based ceramics. Hydrothermal synthesis has been widely used for producing fine oxide powders. In this study we report $K_xNa_{1-x}NbO_3$ compounds synthesized by this method ($0<x<1$). Fine-grained microstructures are preferable for most of the applications. The study is more particularly focused on the interesting $K_{0.5}Na_{0.5}NbO_3$ compound, due to its morphotropic phase boundary and its excellent piezoelectric properties ($d_{33}>100$pC/N for a well dense ceramic). The aim of this study is first to determine the initial K^+/Na^+ ratio (>1) in order to obtain the $K_{0.5}Na_{0.5}NbO_3$ phase. Then the influence of the synthesis conditions (time, temperature...) on the piezoceramic powder (crystallinity, grain size...) will be discussed.

 Published by Cranfield University Press ISBN: 978-0-9557436-7-2 http://hdl.handle.net/1826/3832

CFD evaluation of water injection for industrial compressor washing

D. Fouflias, A. Gannan, K. Ramsden and P. Lambart.

Department of Power and Propulsion

Cranfield University, England

Abstract

Computational fluid dynamics (CFD) results are used to provide a basis of optimizing the position, droplet diameter and velocity of injecting water within an industrial gas turbine intake. The intake of an industrial gas turbine (98 MW) located at an altitude of 240 m with 27 °C ambient temperature was investigated via CFD tools in terms of on-line water injection for compressor washing. Three water nozzle position arrangements were investigated involving conical sprays of different droplet size and injection velocities.

Introduction

In order to combat fouling, industrial gas turbines are subjected to on-line compressor cleaning while they run at full load via injection of washing fluid or water from nozzles positioned around the air intake duct of the gas turbine. According to Bromley et al (2004), output losses can reach values of 15% to 20% under adverse conditions and the droplet size for safe and effective online washing must be in the range between 50 to 250 microns. Droplets of too small sizes can be easily deflected from the air stream and there are possibilities not to reach the inlet guide vanes (IGVs), however large droplet sizes can cause blade erosion. Injection velocities up to 200 m/s were suggested according to Mund et al (2005) simulating compressor cleaning of an industrial gas turbine. Water-air mass flow ratios between 0.8 to 2% were suggested for aero-engines according to Syverud et al (2005). In the present case the water-air mass flow ratio comes out to be of lower value about 0.2 %. In order to explore the parameters influencing on-line compressor cleaning, water injection simulations using Fluent 6.3 (2007) took place involving an intake of an industrial gas turbine (9 8MW).

 Published by Cranfield University Press ISBN: 978-0-9557436-7-2 http://hdl.handle.net/1826/3832

Industrial intake geometry and meshing

The geometry of the gas turbine intake (5 m height, 2.8 m length and 5.6 m width) was eliminated in the volume just after the filters (intake flange) and the inlet guide vane plane (see figure 1). The volume of the intake was filled with structured fine mesh (12 million hexahedral cells) close to the important IGVs area and with unstructured course mesh outside the IGV and strut area (see figure 2). Different meshes were examined and grid independency was achieved after 10 million grid cells by checking the aerodynamic total pressure loss coefficient (Y) between the intake flange and the IGV plane according to Biesinger 2002 (see figure 3).

$$Y = \frac{'_F - '_{IGV}}{'_{IGV} - P_{IGV}}$$

$'_F$: flange total pressure

$'_{IGV}$: total pressure on the IGV plane

P_{IGV}: static pressure on the IGV plane

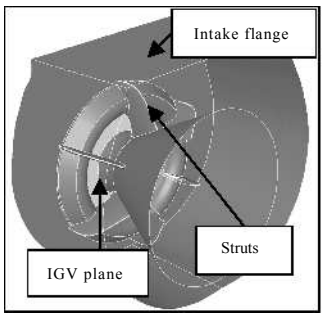

Figure 1: Engine intake.

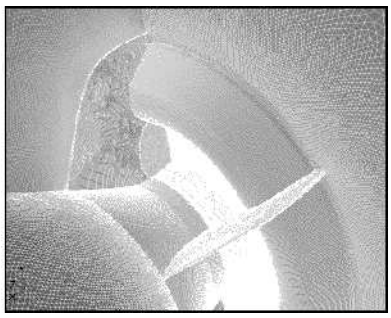

Figure 2: Intake mesh.

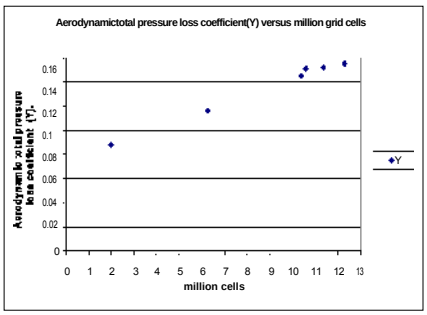

Figure 3: Y parameter versus number of grid cells.

Simulation settings

For the simulation the standard k-ε model was selected, characterized by it's robustness, economy, and reasonable accuracy for a wide range of turbulent flows which explain its popularity in industrial flow simulations. The pressure based solver of Fluent was used for solving the continuous phase and the second order discretization scheme was implemented for the flow equations. In order to set the inlet boundary conditions the total pressure at the intake flange was calculated to be 97900 Pa at 27 °C total temperature

 Published by Cranfield University Press ISBN: 978-0-9557436-7-2 http://hdl.handle.net/1826/3832

assuming that the filters are high velocity filters and the pressure drop along them to be 400 Pa according to Mund et al (2004). Assuming that the flow between the inlet and the outlet of the volume simulated is adiabatic, the static pressure on the IGV plane was calculated to be 84082 Pa. The two phase flow for the simulation was assumed to be sufficiently diluted meaning so that particle-particle interactions and the effects of the dispersed phase (droplets) on the continuous phase (air) are negligible. The water droplets for the simulation were modelled as spherical inert particles not subjected to evaporation since the temperature rises halfway within the engine intake duct. The simulation was run using default wall boundary conditions reflecting the droplets.

Nozzle Injection arrangements and CFD analysis

The first simulation (normal set) involved 19 nozzles positioned on the wall opposite to the IGVs (see figure 4). The upper nozzles 1, 2, 3, 4, 5, 16, 17, 18 and 19 were pointing 5 degrees upwards away from the shaft cone surface with respect to the engine centerline. Nozzles 6 and 15 were pointing horizontally while all the remaining nozzles were pointing at 13 degrees towards the cone surface. Arrangement 1 involved 19 nozzles projecting towards the IGVs and between the struts (see figure 5). Nozzles 1, 2, 3, 18 and 19 were set at zero degrees with respect to the engine centerline while all the other nozzles were pointing towards the mid span area of the IGV plane. Arrangement 2 involved 18 nozzles and different nozzle positions with four upper nozzles injecting parallel to the engine centreline and all the others towards the IGVs mid span area (figure6).

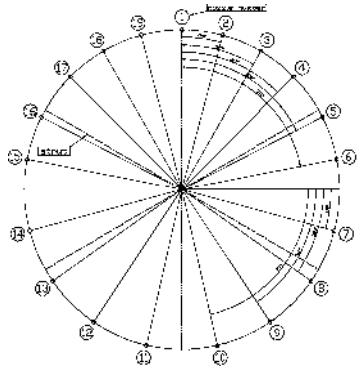

Figure 4: Normal set.

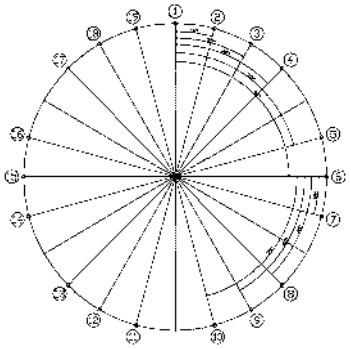

Figure 5: Arrangement 1.

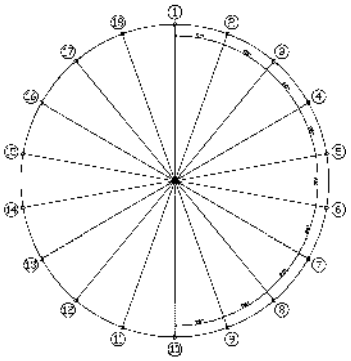

Figure 6: Arrangement 2.

 Published by Cranfield University Press ISBN: 978-0-9557436-7-2 http://hdl.handle.net/1826/3832

Initially, the simulation involved the gas turbine subjected to water injection of 135 litters in 4 minutes time (33.75 litters / min). Spray angles of 40 degrees, injection velocity of 143 m/s and droplet diameters of 150, 300 and 400 pm were used. From figures 7, 8 and 9 it can be seen that the IGV plane is covered more efficiently as the droplet diameter increases. This can be attributed to the fact that the momentum of the larger droplets is higher and as a result they are deflected less than the smaller droplets from the air flow towards the bottom of the intake.

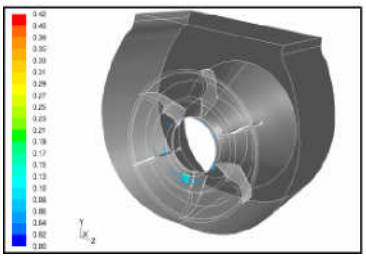

Figure 7: Normal set droplet concentration contours (kg/m^3), droplet diameter 150 pm.

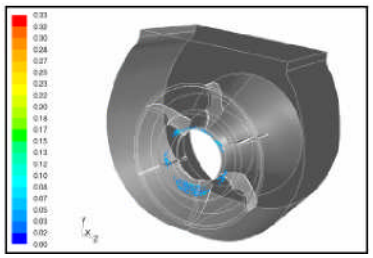

Figure 8: Normal set droplet concentration contours (kg/m^3), droplet diameter 300 pm.

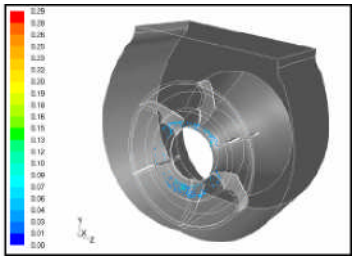

Figure 9: Normal set droplet concentration contours (kg/m^3), droplet diameter 400 pm.

However, for all the cases there was unavoidable water spillage on the walls around the IGV plane (see figure 10). Then keeping an average droplet size of 300 pm according to Mund (2006), arrangement 1 was examined and not much differences were found in terms of IGV plane coverage (see figure 11), however less waste of water on the walls around the IGV plane was achieved (see figures 12).

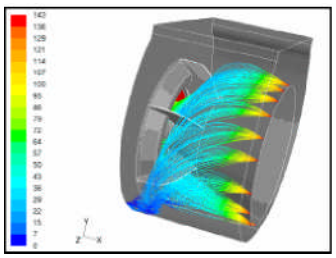

Figure 10: Normal set particle tracks coloured by velocity magnitude (m/s), droplet diameter 300 pm.

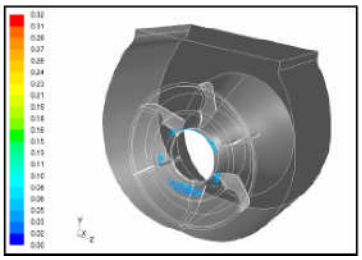

Figure 11: Arrangement 1 droplet concentration, contours (kg/m^3), 40 deg cone angle.

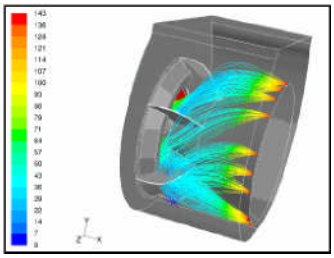

Figure 12: Arrangement 1 particle tracks coloured by velocity magnitude (m/s).

 Published by Cranfield University Press ISBN: 978-0-9557436-7-2 http://hdl.handle.net/1826/3832

Arrangement 2 gave similar results to arrangement 1 (see figure 13). Running arrangement 1 with water supply of 50 litters per min and increased injection velocity, better IGV coverage was obtained (see figure 14) especially on the upper part of the shaft cone area. Running arrangement 1 with 80 degrees spray cone angle (33.75 litters per min) the simulation gave no better results in terms of IGV water coverage, however the spillage of water on the walls around the IGV plane was higher (see figure 15).

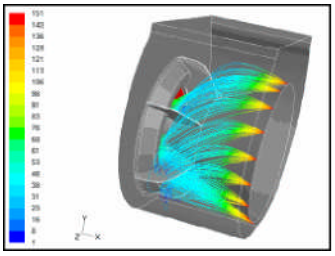

Figure 13 : Arrangement 2 particle tracks coloured by velocity magnitude (m/s).

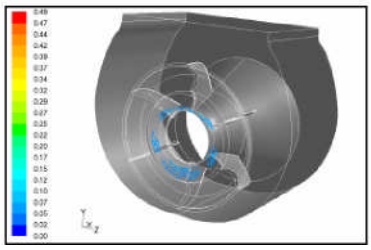

Figure 14: Arrangement 1 droplet concentration contours (kg/m^3), injection velocity 212 m/s.

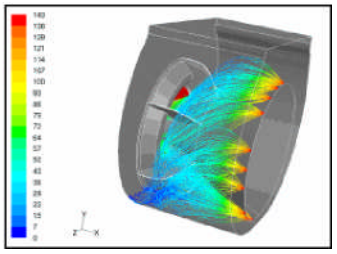

Figure 15: Arrangement 1 particle tracks coloured by velocity magnitude (m/s), 80 deg cone angle.

In parallel, the first trajectory of the nozzle number 0 according to the normal nozzle setting was analysed for the case of 80 degrees spray angle. As figure 16 shows, along this trajectory the droplets leave the nozzle with a velocity magnitude of 143 m/s which falls to 39 m/s at approximately half way between the injection point and the IGV plane. The droplets then start to accelerate reaching a value of around 80 m/s at the IGV plane.

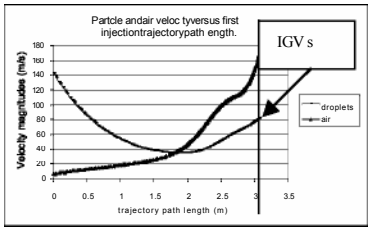

Figure 16: Particle and air velocity distribution along the first injection trajectory path.

The loss of droplet kinetic energy can be attributed to the gravity force and to the fact that the air trajectories coming from the top of the intake are directed vertically downwards opposing the droplet trajectories of the nozzle directed upwards prohibiting them to accelerate. Beyond the halfway point the droplets start to approach the low pressure IGV

 Published by Cranfield University Press ISBN: 978-0-9557436-7-2 http://hdl.handle.net/1826/3832

region and the flow area is reducing due to the struts and curved walls around the IGVs so, the air flow is accelerating encouraging the particles to accelerate too. This air acceleration is obvious by the sudden increase after the halfway point of the slope of the line corresponding to the air velocity distribution along the same water trajectory. The air reaches the IGVs at 165 m/s hence at a Mach number of 0.5 typical for industrial engines.

Conclusions

In this paper an investigation of the main parameters affecting industrial gas turbine water injection has been undertaken. The results obtained illustrated that projecting the nozzles towards the midspan of the IGVs and increasing the droplet diameter and velocity better IGV coverage is obtained. However, the most sensitive upper part of the IGV plane to air deflection was treated more efficiently with nozzles projecting horizontally with respect to the engine centreline.

References

1. Biesinger T. and Lepel M. (2002). Flow field Investigations in intake manifolds of industrial gas turbines including CFD matching. 5th European Turbomachinery Conference, Prague.
2. Bromley Andrew F. and Meher-Homji Cyrus B. (2004). Gain a competitive edge with a better understanding of GT compressor fouling, washing. Combined Cycle Journal, Fourth Quarter 2004.
3. Fluent (2007). Fluent 6.3 Documentation, Fluent Inc.
4. Mund, F.C. (2006). Coordinated application of CFD and gas turbine performance methods. PhD thesis, Cranfield University.
5. Mund, F.C. and Pilidis, P. (2005). Online compressor washing: a numerical survey of influencing parameters. J. Power and Energy. Proc. IMechE Vol.2 19 Part A. Mund, F.C., Pilidis, P. (2004). Effects of spray parameters and operating conditions on an industrial gas turbine washing system. Paper No GT2004-53551, ASME Turbo expo 2004, Power for land, sea and air, June 14-17, Vienna, 2004, Austria.
6. Syverud, E., Bakken E.L. (2005). Online water wash tests of GE J85-13. Paper No GT2005-68702, ASME Turbo expo 2005, Power for land, sea and air, June 6-9, 2005, Reno-Tahoe, Nevada, USA.

 Published by Cranfield University Press ISBN: 978-0-9557436-7-2 http://hdl.handle.net/1826/3832

Labeless Immunosensor Assays based upon an AC Impedance Protocol

Frank Davis[1], Goulielmos-Zois Garifallou[1], Georgios Tsekenis[1], Paul A. Millner[2] Daniel G. Pinacho[3], Francisco Sanchez-Baeza[3], M.-Pilar Marco[3], Tim D. Gibson[4] and Séamus P. J. Higson[*1].

[1]Cranfield Health, Cranfield University, Silsoe, Beds, MK45 4DT, UK.

[2]School of Biochemistry and Molecular Biology, University of Leeds, Leeds, LS2 9JT, UK.

[3]Applied Molecular Receptors Group (AMRg). Department of Biological Organic Chemistry. IIQAB-CSIC. Jorge Girona, 18-26, 08034-Barcelona, Spain

[4]T and D Technology, Wakefield, W. Yorks, WF3 4AA, UK.

*.Corresponding author. Fax (+44) 01525 863433, email s.p.j.higson@cranfield.ac.uk

Abstract

This paper describes the construction of labeless immunosensors for the selective determination of an antigen, of which two immunosensors for ciprofloxacin and myelin basic protein are described in more detail. Commercial screen-printed carbon electrodes were used as the basis for the sensor. Polyaniline was electrodeposited onto the sensors and then utilised to immobilise biotinylated antibodies for ciprofloxacin and myelin basic protein using avidin-biotin interactions.

Electrodes containing the antibodies were exposed to solutions of antigen and the AC impedance of the electrodes measured over a range of frequencies. The faradaic component of the impedance of the electrodes was found to increase with increasing concentration of antigen. Control samples containing a non-specific IgG antibody were also studied and calibration curves obtained by subtraction of the responses for specific and non-specific antibody based sensors, thereby eliminating the effects of non-specific adsorption of antigen.

Introduction

The principle of immunoassays was established in 1959 (Yalow & Berson, 1959) and led to the development of the widely used technique. Later in 1962 the concept of a biosensor was pioneered (Clark & Lyons, 1962). The original methodology was to immobilise enzymes on the surface of electrochemical sensors-assuming that this would enhance the ability of a sensor to

 Published by Cranfield University Press ISBN: 978-0-9557436-7-2 http://hdl.handle.net/1826/3832

detect specific analytes. This idea has remained virtually unchanged since this original design, however, technological advances have allowed for the expansion of this field of science.

The incorporation of antibodies into conducting polymer films was first reported in 1991 (John *et al* 1991). Anti-human serum albumin (anti-HSA) was incorporated into a polypyrrole film, polymerised onto a platinum wire substrate. When the pyrrole anti-HSA electrode was exposed to 50 μg ml^{-1} HSA for ten minutes, a new reduction peak was observed at a potential of approximately +600mV vs. Ag/AgCl, increasing in magnitude after a further thirty minutes in the same solution This was thought to be due to an antibody/antigen interaction with the polymer. Other work utilised a pulsed amperometric detection technique for other analytes, including p-cresol (Barnett *et al* 1994), Thaumatin (Sadik *et al* 1994) and polychlorinated biphenyls (Bender and Sadik 1994). Since this work there has been a huge increase in the development of electrochemical immunosensors as detailed in several recent reviews (Rodriguez-Mozaz *et al* 2006, Diaz-Gonzalez *et al* 2005, Cosnier 2005).

We have previously shown that up to 2-3 μg antibodies for BSA and digoxin may be successfully incorporated into conducting polymer films by entrapment in a electrochemically deposited polypyrrole film with no detrimental effect to antibody activity (Grant *et al* 2003). Measuring the electrochemical properties of these films demonstrated selective interactions with the target antigens. Further work utilised an AC impedance protocol (Grant *et al* 2005) as the method of interrogation for these films and led to the development of immunosensors for digoxin and bovine serum albumin. The AC protocol consisted of measuring the AC impedance of the system across a frequency range of 1-10000 Hz, peak amplitude 5 mV.

We review within this work our studies on immunosensors for ciprofloxacin (Garifallou *et al* 2007) and myelin basic protein (Tsekenis *et al* 2008). Ciprofloxacin is a member of the fluoroquinolone family of broad-spectrum antibiotics, widely used within adult patients because of excellent tissue penetration which makes them extremely effective against bacteria that grow intracellularly such as salmonella (Gendrei *et al* 2003) and anthrax (Torriero *et al* 2006). The monitoring of fluoroquinolones within both food and the environment is important since these antibiotics have potential health and environmental damaging effects. Ciprofloxacin concentrations in hospital wastewaters were monitored and correlations with DNA damaging effects made (Hartmann *et al* 1999). Levels of ciprofloxacin in hospital outflow water between 0.7-124.5 ng ml^{-1} were measured using HPLC (Hartmann *et al* 1999) and shown to display genotoxicity at levels as low as 5.2 ng ml^{-1}. Levels *in vivo* have also been widely studied with the therapeutic ranges typically being between 0.57-2.30 μg ml^{-1} in serum and 1.26-4.03 μg g^{-1} in tissue (Licitra *et al* 1987).

 Published by Cranfield University Press ISBN: 978-0-9557436-7-2 http://hdl.handle.net/1826/3832

Myelin basic protein (MBP) is a cytoplasmic protein important in the process of myelination of nerves in the central nervous system since it comprises the bulk of the main line of compact myelin (Arroyo and Scherer 2000) and up to 30% of the protein content of myelin overall (Baumann and Pham-Dinh 2001). A demyelinating disease is any disease of the nervous system in which the myelin sheath of neurons becomes damaged. This impairs the conduction of signals in the affected nerves, causing impairment in sensation, movement, cognition, or other functions, depending on which nerves are involved. Examples are multiple sclerosis, transverse myelitis, Guillain-Barré syndrome, and progressive multifocal leukoencephalopathy. The normal level of MBP in cerebrospinal fluid is less than 4 ng ml^{-1}, levels between 4 and 8 ng ml^{-1} in cerebrospinal fluid may indicate a chronic breakdown of myelin, or recovery from an acute episode. MBP levels greater than 9 ng ml^{-1} indicate that active demyelination may be occurring.

Ciprofloxacin is usually measured by HPLC and commercial ELISA tests exist for myelin basic protein; Diagnostic Systems Laboratories (Texas) for example manufacture an ELISA which can measure levels of MBP in cerebrospinal fluid in four hours. These methods both require expensive equipment and trained personnel in a laboratory setting. The development of inexpensive single use immunosensors will reduce costs and increase the speed and simplicity of testing.

Results of the study

The sensors described within this work utilise screen-printed carbon electrodes, modified by deposition of first, a conducting polymer (polyaniline) which is then modified with biotinylating reagent. Complexion of the immobilised biotin with avidin allows the further binding of biotinylated antibodies via standard avidin-biotin interactions (Figure 1). Control electrodes containing non-specific IgG have also been fabricated and allow the subtraction out of unspecific interactions.

Polycolonal antibodies for ciprofloxacin, raised in rabbit by the Applied Molecular Receptors Group (AMRg). Department of Biological Organic Chemistry. University of Barcelona (Garifallou *et al* 2007), and MBP (monoclonal anti-MBP from rat, Sigma catalogue number M9434) incorporated within the immunosensors as described previously (Garifallou *et al* 2007, Tsekenis *et al* 2008). Commercial (Sigma) IgG antibodies from the same species were used as controls. As described within these papers, the sensors were then exposed to various concentrations of antigen in solutions containing a ferri/ferrocyanide redox couple. It was found for both antigens that there were large changes in the faradaic component of the ac impedance spectrum, especially at low frequencies. In both cases, control electrodes were fashioned using a non-specific IgG antibody. The control electrodes provide a measure of the non-specific binding within the system and allow for its subtraction.

 Published by Cranfield University Press ISBN: 978-0-9557436-7-2 http://hdl.handle.net/1826/3832

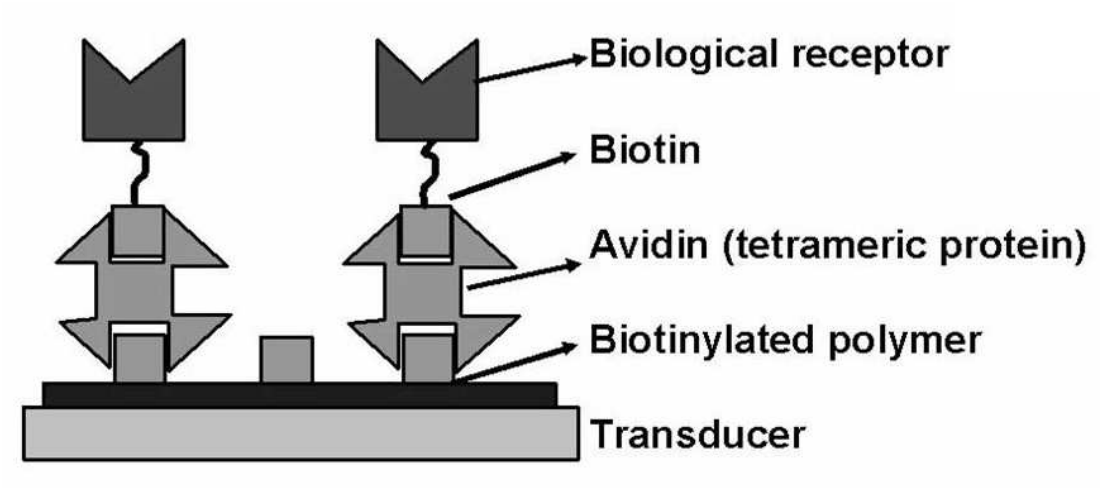

Figure 1. Schematic of antibody modified electrodes.

Figure 2a shows the Nyquist plots for the anti-ciprofloxacin electrodes upon exposure to the antigen. These plots show the increases in faradaic (x-axis) and capacitive (y-axis) impedance with decreasing frequency. As can be seen, there is a steady decrease in the impedance of the electrodes with increasing antigen concentration and it is most pronounced at the lower frequencies. Previous work by our group found that the real component offers far greater reproducibility in comparison to the imaginary contribution. Therefore it was decided that changes in impedance at 1 Hz would be used as a measurement of antigen binding.

Figure 2b shows the percentage decrease in Z' across a range of antigen concentrations. As can be seen, there is a steady decrease in impedance as antigen concentration increases up to a concentration of about 100 ng ml^{-1}, above which concentration there is a tend towards a plateau, possibly indicating saturation of the specific binding sites. Results for the IgG electrodes were obtained in exactly the same way and the calibration plot is shown (Figure 2c). As can be seen, there is a much lower response for the non-specific antibody, showing that although there are non-specific interactions, between the ranges of 1-100 ng ml^{-1}, they comprise a minor component of the detected response. Figure 2d shows the subtracted responses and this demonstrates linearity between the response and the $\log_{10}$ of ciprofloxacin concentration between 1-100 ng ml^{-1} (R^2=0.96). The limit of detection (three times the standard deviation of the baseline) was 1 ng ml^{-1}, suitable for testing environmental levels of ciprofloxacin and with sample dilution, physiological levels.

 Published by Cranfield University Press ISBN: 978-0-9557436-7-2 http://hdl.handle.net/1826/3832

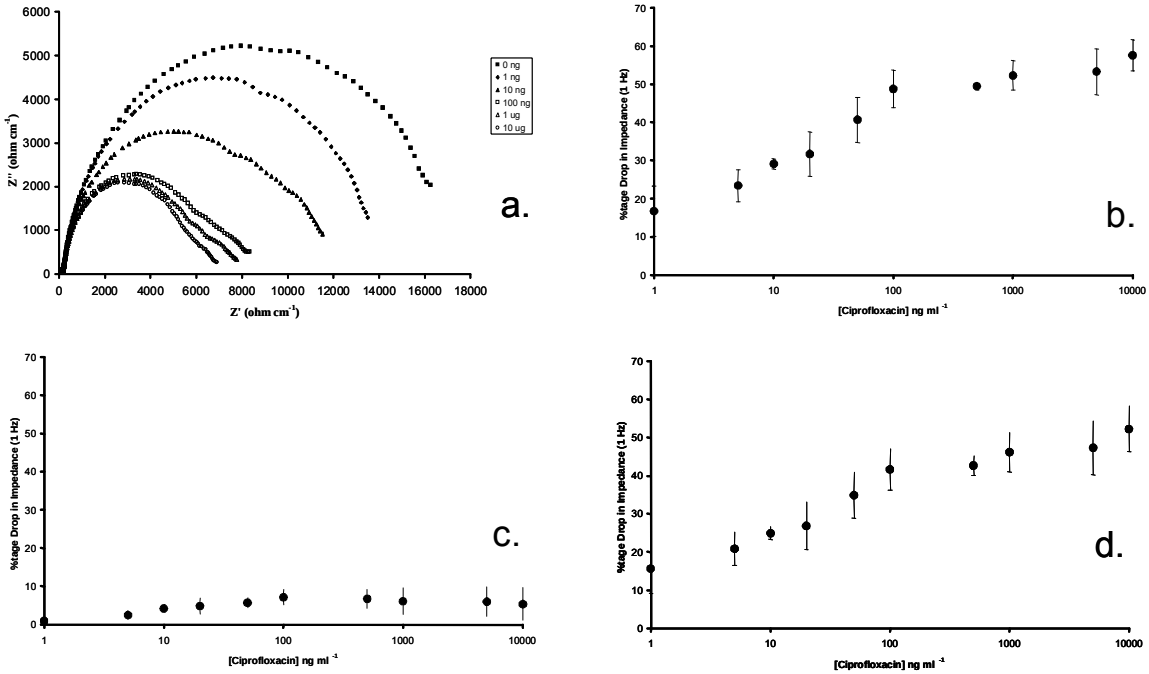

Figure 2. (a) Nyquist plots of a typical antibody modified electrode exposed to various concentrations of antigen, calibration curves for (b) anti-ciprofloxacin modified electrodes (c) IgG modified electrodes (d) corrected calibration curves. Points are means of responses of three electrodes; error bars show standard deviation.

Using an identical method, electrodes containing antibodies to MBP were constructed and interrogated as above. Figure 3a shows the Nyquist plots for this system. In this case exposure to the antigen led to increases in the ac impedance, probably because MBP is a large molecule and binding of this protein leads to formation of a resistive layer at the surface of the electrode. Figure 3b shows there is a steady increase in impedance as antigen concentration increases up to a concentration of about 100 ng ml^{-1}, above which concentration there is a tend towards a plateau, possibly indicating saturation of the specific binding sites. The calibration plot for the control electrodes is shown (Figure 3c) again displaying a much lower response for the non-specific antibody. Figure 3d shows the subtracted responses and this demonstrates linearity between the response and the $\log_{10}$ of MBP concentration between 1-100 ng ml^{-1} (R^2=0.98). Within the lower range of 1-15 ng ml^{-1} (which covers the physiological range) the correlation of the impedance change with the $\log_{10}$ of concentration is further improved (R^2=0.99). Limit of detection (3 x standard deviation of baseline) was 1 ng ml^{-1}.

Conclusions

We have demonstrated the construction of an immunosensor for the antibiotic ciprofloxacin and for MBP using a combination of screen-printed electrodes coated with conducting polyaniline and an immobilised antibody. Interrogation of the electrodes by AC

 Published by Cranfield University Press ISBN: 978-0-9557436-7-2 http://hdl.handle.net/1826/3832

impedance demonstrated the detection of the antigen. Linear correlation of the impedance change with the $\log_{10}$ of antigen concentration was observed between concentrations of 1-100 ng ml^{-1}. Commercialisation of this research is proceeding through a new spin-out company ELISHA Systems Ltd., who are developing a range of labeless immunosensors for a number of different antigens.

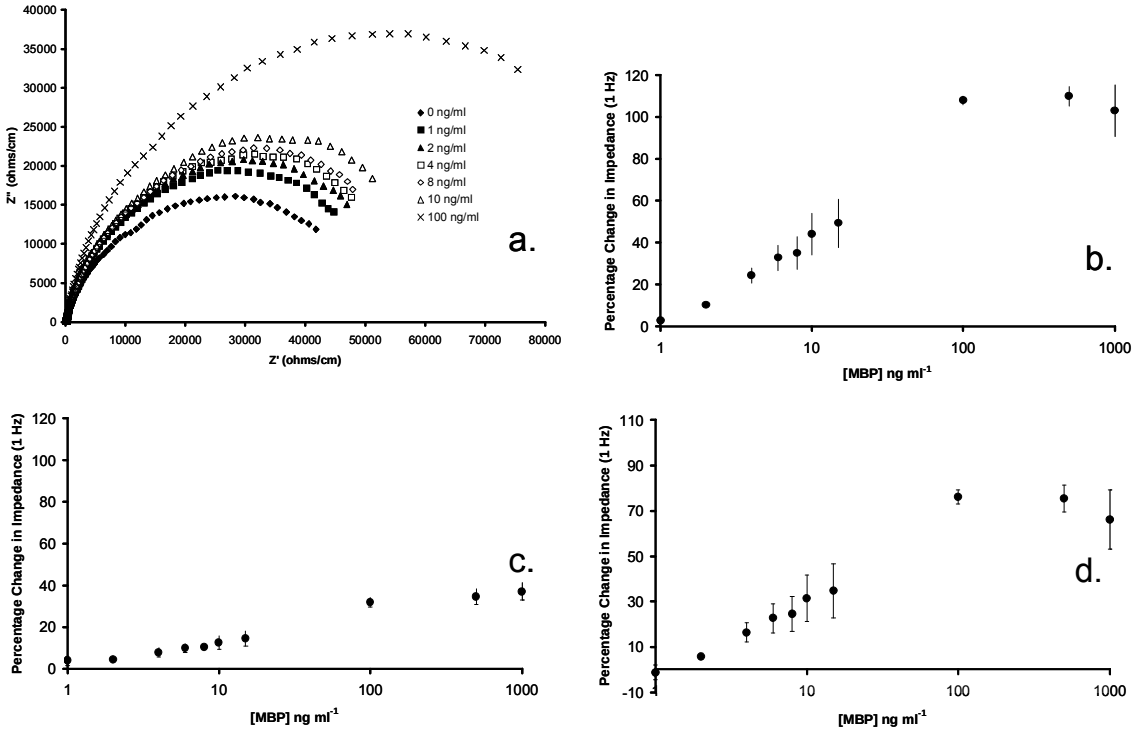

Figure 3. (a) Nyquist plots of a anti-MBP modified electrode exposed to various concentrations of MBP, calibration curves for (b) anti-MBP modified electrodes (c) IgG modified electrodes (d) corrected calibration curves. Points are means of responses of three electrodes; error bars show standard deviation.

REFERENCES

1. Arroyo E. G., Scherer S. S., 2000, *Cell Biol.* 113, 1-18.
2. Barnett, D. Laing, D. G. Skopec, S. Sadik, O. A. Wallace, G. G. 1994, *Anal. Lett*. 27: 2417-2429.
3. Baumann N., Pham-Dinh D., 2001, *Physiol. Rev.,* 81, 871-927.
4. Bender, S. Sadik, O. A. 1998, *Environ. Sci. Tech.*, 32: 788-797.
5. Clark, L.C and Lyons, I.R. 1962, *Ann New York Academy Sci*. 102: 29.
6. Cosnier, S., 2005, *Electroanalysis,* 17: 1701-1715.
7. Diaz-Gonzalez, M., Gonzalez-Garcia, M. B., Costa-Garcia, A. 2005*Electroanalysis,* 17: 1901-1918.
8. G-Z. Garifallou G. Z., Tsekenis G., Davis F., Millner P. A., Pinacho D. G., Sanchez-Baeza F., Marco M.P., Gibson T. D., Higson S. P. J., 2007 *Anal. Lett.,* 40, 1412-1442.
9. Gendrei, D., Chalumeau, M., Moulin, F., Raymond, J., 2003, *Lancet Inf. Dis.,* 3: 537-546.
10. Grant, S., Davis, F.,. Pritchard, J. A., Law, K. A.,. Higson S. P. J.,. Gibson, T. D. 2003, , *Anal. Chim. Acta.,* 495: 21-32.

 Published by Cranfield University Press ISBN: 978-0-9557436-7-2 http://hdl.handle.net/1826/3832

11. Grant, S., Davis, F.,. Law, K. A.,. Barton, A. C., Collyer, S. D., Higson S. P. J.,. Gibson, T. D. 2005, *Anal. Chim. Acta*., 537: 163-168.
12. Hartmann, A. Golet, E. M. Gartiser, S. Alder, A. C. Koller, T. Widmer, R. M. 1999, *Ach. Environ. Contam. Toxicol.,* 115-119.
13. John, R. Spencer, M. Wallace, G. G. Smyth, M. R. (1991) *Anal. Chim. Acta*. 249: 381-385.
14. Licitra, C. M., Brooks, R. G., Sieger, B. E. (1987), *Antimicrobial Agents And Chemotherapy,* 31: 805-807.
15. Rodriguez-Mozaz, S., de Alda, M. J. L., Barcelo, D. 2006, *Anal. Bioanal. Chem.,* 386: 1025-1041.
16. Sadik, O. A. John, M. J. Wallace, G. G. Barnett, D. Clarke, C. Laing, D. G. (1994), *Analyst*. 119: 1997-2000.
17. Tsekenis G., Garifallou G-Z., Davis F., Millner P. A., Gibson T. D., Higson S. P. J., 2008, *Anal. Chem.,* 20: 2058-2062.
18. Torriero, A. A. J., Ruiz-Dıaz J. J. J., Salinas, E., Marchevsky, E. J., Sanz, M. I., Raba, J., 2006, *Talanta,* 69: 691-699.
19. Yalow, R. S. Berson, S. A 1959, *Nature.* 184: 1648-1649.

 Published by Cranfield University Press ISBN: 978-0-9557436-7-2 http://hdl.handle.net/1826/3832

Interactions of DNA at surfaces - electrical and optical characterization

Frank Davis', W. S. Roberts', A. V. Nabok[2], M. A. Hughes[3], A. R. Cossins[3], Séamus P.J. Higson'*

[1]Cranfield Health, Cranfield University, Silsoe, MK45 4DT, U.K. [2] Sheffield Hallam University, Materials and Engineering Research Institute, Sheffield, S1 1 WB, UK[3] School ofBiological Sciences, University ofLiverpool, Liverpool L69 7ZB, UK.

Correspondence should be addressed to s.p.j.higson@cranfield.ac.uk.

Abstract

This paper presents a review of our work on the adsorption of genomic and single gene DNA on carbon electrodes modified with cationic polymers and subsequent interactions between adsorbed and solvated DNA. Initial investigations were conducted using electrochemical measurements and the adsorption kinetics and film structure studied using a novel sensitive optical method of total internal reflection ellipsometry (TIRE), which combines spectroscopic ellipsometry with surface plasmon resonance (SPR). Initially single stranded DNA from either herring or salmon was adsorbed onto screen printed carbon electrodes. The further adsorption of single stranded DNA from an identical source, i.e. herring ss-DNA on herring ss-DNA or salmon ss-DNA on salmon ss-DNA, on the surface was observed to give a large drop in the impedance of the electrodes. Studies using TIRE on gold surfaces showed adsorption of complementary DNA gave rise to substantial film thickness increases at the surface of about 20-2 1 nm. Conversely adsorption of DNA from alternate species, i.e. salmon ss-DNA on herring ss-DNA or herring ss-DNA on salmon ss-DNA, yielded much smaller changes in thickness of 3-5 nm and only minimal changes in impedance. Limits of detection of genomic DNA were of the order of 10 ng/ml, however when DNA from single genes was utilized, the levels of detection were of the order of fg/ml.

Introduction

There is a great demand that needs to be met for simple portable analytical tools for DNA characterization. Biosensing approaches for DNA analysis could offer a cost-effective alternative to expensive contemporary methods requiring the use of enzyme, fluorescent or radioisotope labels. DNA biosensors are based on the concept of specific hybridization between nucleic acids in solution - and those immobilized on solid substrates[1]. For example, a number of DNA sensors exploiting immobilization of nucleic acids on conjugated polymers and different transducing techniques have been reported[2-5].

 Published by Cranfield University Press ISBN: 978-0-9557436-7-2 http://hdl.handle.net/1826/3832

The method of electrostatic layer-by-layer adsorption of DNA, which was first reported in the early 1 990's[6,7] has later become widely used in DNA sensors for immobilization of oligonucleotides[8-10] and whole DNA molecules[11,12]. The concept of using a single strand DNA immobilized on solid support for further hybridization with its counterpart in the solution and the subsequent formation of DNA double helices on the surface has been exploited previously[13-15], although the formation of the ideal DNA double helix is not obvious because of a limited mobility of the adsorbed single strand DNA.

Most of the work reported earlier has utilized short DNA fragments, usually containing <50 bases and of perfectly matched or a few base pair mismatched sequences, although cDNA arrays often use DNA of similar lengths for detection. Our work however has tended towards the use of genomic DNA rather than specific sequences since that is the form in which DNA naturally occurs. Genomic DNA can be easily denatured to form single-stranded DNA by heating, however upon cooling, hybridization back to the double-stranded form is a complex procedure. This is probably because genomic DNA contains a wide variety of individual chains with different lengths and sequences and the statistical probability of two complementary chains meeting and hybridizing is very low. Even when DNA from a single species is allowed to reassociate, measurements have showed that nucleotide pairing is imprecise[16]. The extent of reassociation between DNA of different species has been shown to be a measure of the relationship between the species[17].

This led us to attempt to determine whether adsorbed genomic DNA would display increased interactions with genomic DNA from the same species compared to DNA from a different species. Although it is very unlikely that we would see complete hybridization due to the reasons given above, it was thought that there may still be more interaction between two samples of single stranded DNA of similar composition than two samples from different species[17]. This could potentially lead to a simple DNA sensor capable of quickly and inexpensively determining the identity of components in, for example, foodstuffs and/or fabrics made from natural materials.

Our initial studies[18] utilized a layer of single stranded DNA electrostatically adsorbed onto screen-printed carbon electrodes which had been modified by a monolayer of polyethylenimine for use as a recognition template in electrochemical DNA sensors. We monitored the ac impedance spectra of these electrodes in solutions of complementary DNA, non-complementary DNA and phosphate buffer as a control. Figure 1a shows the relative changes in impedance of a typical electrode with immobilized herring single stranded genomic DNA upon exposure to solutions of identical DNA. As can be seen there is a clear drop in the relative impedance, especially noticeable at lower frequencies. It was therefore decided to monitor the behaviour of the electrodes in solutions of various concentrations of complementary DNA. As can be seen (Figure 1b) there is a noticeable drop in impedance over 2 hours for solutions with concentrations as low as 0.01 mg/ml DNA. Higher concentrations of DNA gave more rapid drops in impedance until a saturation point after about 2 hours exposure was reached.

The drop in impedance could be due to several factors: formation of regions of double stranded DNA could lead to a drop in impedance, other authors have reported double stranded DNA to be much more conductive than single stranded. The change in the charge characteristics of the surface due to adsorption of a second layer of anionic DNA could also lead to facilitated electron transfer between the electrode and solution. Figure 1c shows the changes in impedance when electrodes modified with single stranded herring DNA were exposed to 0.2 mg/ml solutions of

 Published by Cranfield University Press ISBN: 978-0-9557436-7-2 http://hdl.handle.net/1826/3832

complementary and non-complementary DNA. As can be seen exposure to complementary DNA led to large drops in impedance whereas exposure to non-complementary DNA led to small increases in impedance.

Figure 1. (a). Plot of relative impedances at different frequencies for a polyethylenimine/herring ss-DNA modified electrode scanned whilst immersed in 0.2% herring ss-DNA/buffer solution for differing periods of time compared to the same electrode immediately after immersion in the solution,

(•) 4 min, (•) 8 min, (□) 21 min, (X) 36 min, (*)57 min, (.)77 min, (+) 100 min, (□)141 min (□)

188 min. (b) Plot of mean relative impedances over the range of frequencies for an polyethylenimine/herring ss-DNA modified electrode scanned after exposure to pH 7 buffer (X), 0.01% complementary DNA (•), 0.1% complementary DNA (•), 0.2% complementary DNA (□), 1% complementary DNA (•), (c) Plot of mean relative impedances over the range of frequencies for an polyethylenimine/herring ss-DNA modified electrode scanned after exposure to pH 7 buffer (•), 0.2% complementary DNA (•), 0.2% non-complementary DNA (□).

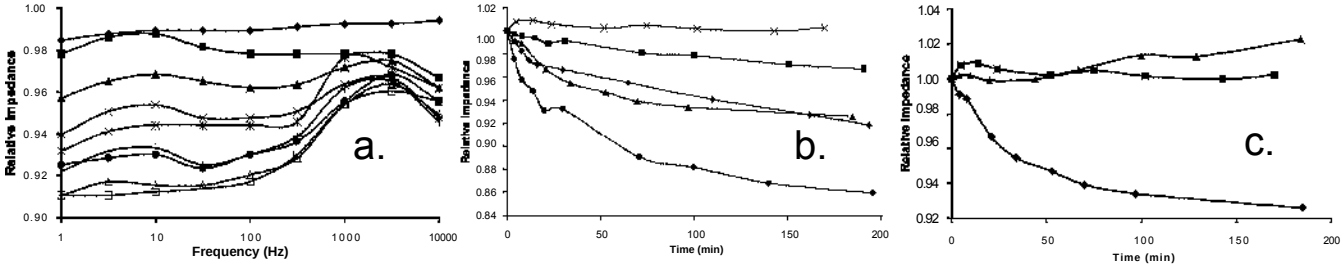

A detailed study of DNA electrostatic immobilization and further DNA interactions was carried out using an advanced optical technique of total internal reflection ellipsometry (TIRE). The sensitivity of TIRE is approximately ten times greater than that of conventional ellipsometry[19], potentially making small changes in film thickness and morphology much easier to detect. Gold coated glass microscope slides were used as the substrate in this case and coated with polyethylenimine as before. They were then exposed to 0.2 mg/ml of DNA (denatured by boiling) and then further exposure to single stranded DNA (complementary and non-complementary). A typical TIRE spectra of DNA adsorption is shown in Fig. 2. As can be seen, adsorption of a very thin monolayer of PEI causes a tiny shift of the TIRE □(□) spectra. Adsorption of a layer of either herring ss-DNA or salmon ss-DNA causes an additional shift[19] (still small) of the □(□) spectrum. Adsorption of a second layer of complementary ss-DNA, i.e. salmon ss-DNA on top of salmon ss-DNA (Fig. 2a) or herring ss-DNA on top of herring ss-DNA causes a large spectral shift of about 80-100 nm. At the same time, the adsorption of non-complementary ss-DNA, i.e. herring ss-DNA on top of salmon ss-DNA (Fig. 2b) or salmon ss-DNA on top of herring ss-DNA yields much smaller spectral shift of 40-60 nm. Table 1 shows the changes in thickness which occur at each stage.

 Published by Cranfield University Press ISBN: 978-0-9557436-7-2 http://hdl.handle.net/1826/3832

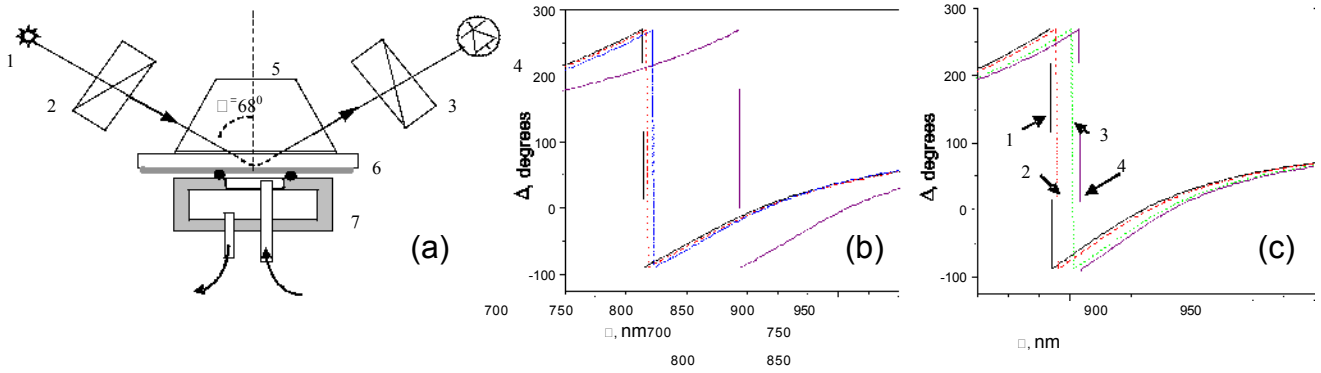

Figure 2. (a) Schematic of TIRE experimental set-up comprising white light sourse (1), polariser (2), analyser (3), photodetector array (4), 68^0 prism (5), Cr/Au coated glass slide (6), reaction cell (7). Series of Δ(λ) spectra taken after following adsorption sequences: (b) (left-to-right) bare Cr/Au, PEI, salmon ss-DNA, salmon ss-DNA; (c) bare Cr/Au (1), PEI (2), salmon ss-DNA (3), herring ss-DNA (4).

Adsorbed layers	**Thickness changes (nm) (TIRE)**
Adsorption initial PEI layer (layer 1)	2.87 ± 1.24
Adsorption of herring ss-DNA on PEI (layer 2)	4.22 ± 1.72
Adsorption herring ss-DNA on herring ss-DNA/PEI (layer 3)	21.81 ± 1.09
Adsorption salmon ss-DNA on herring ss-DNA/PEI (layer 3)	4.36± 0.36
Adsorption of salmon ss-DNA on PEI (layer 2)	4.08 ± 1.56
Adsorption salmon ss-DNA on salmon ss-DNA/PEI (layer 3)	20.47± 0.53
Adsorption herring ss-DNA on salmon ss-DNA/PEI (layer 3)	3.02± 1.15
Adsorption herring ds-DNA on PEI (layer 2)	9.75± 1.97
Adsorption salmon ds-DNA on PEI (layer 2)	8.52± 2.37

Table 1. Increases in thickness (TIRE data) of different adsorbed layers.

 Published by Cranfield University Press ISBN: 978-0-9557436-7-2 http://hdl.handle.net/1826/3832

For herring DNA, the thickness of the adsorbed single strand DNA was found to be of 4.22 ± 1.72 nm, somewhat higher than expected, indicating that we do not have a simple compact monolayer at the surface. It should be remembered however that our measurements take place with the film submerged in buffer, meaning that it will be fully hydrated. Other workers[20] have shown that the thicknesses of DNA layers on a gold surface are much greater in a hydrated state than in a dry state. Longer DNA chains have been shown to have a quite flexible structure[21] and there is also the possibility of looping of the DNA chains from the surface which would also have the effect of increasing the thickness of the adsorbed layer. When undenatured herring ds-DNA was utilized, the film thickness was much greater (9.75 ± 1.97 nm). This cannot be a simple monolayer of double-stranded DNA lying flat on the surface since this would only have a thickness of about 2 nm. Again however the layers are fully hydrated and there is also potential for supercoiling to occur, as observed by other workers on silicon surfaces[21].

Figure 3. DNA adsorption on Au/PEI.

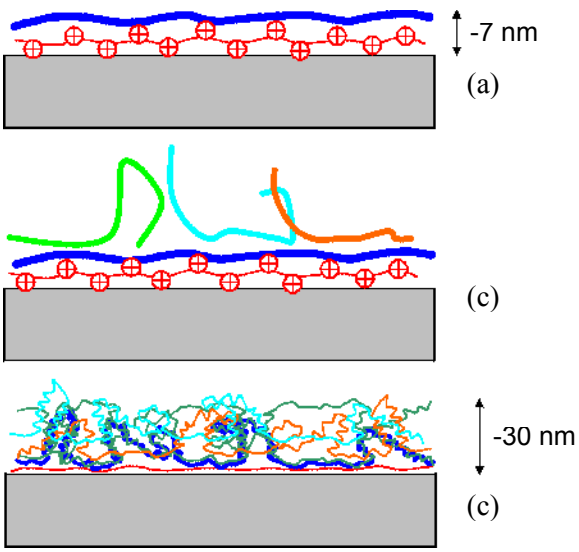

Adsorption of a second layer of herring ss-DNA causes substantial increase in the layer thickness of 21.81 ± 1.09 nm. We believe we first have a hydrated layer of DNA electrostatically adsorbed onto the substrate. Interaction between complementary short sequences of bases on adsorbed and solvated DNA cause adsorption of a second layer of DNA, although it is certain that hybridization to a double helix will not occur. Since this interaction will only occur along a relatively short part of the DNA chain, there will be extensive looping out into the solution of the rest of the chain. These unbound chains could then further interact with each other or with other strands in solution. The final structure is that of a loosely bound, crosslinked multilayer. Figure 3 illustrates schematically main stages of adsorption, (a) electrostatic adsorption ss-DNA onto the PEI layer, (b) adsorption of complementary ss-DNA on top with parts of the strands pendant to the surface, (c) adsorption of further ss-DNA accompanied with cros slinking and tangling. The adsorption of non-complementary ss-DNA (salmon) on top of adsorbed layer of herring ss-DNA has resulted in much smaller changes in the thickness (4.36 ± 0.36 nm) corresponding to a much lower level of adsorption. There will always be some degree of interaction between long DNA strands because there will always be small sequences of a few bases that will match and cause some interaction, however, as this work shows, genomic DNA strands from the same source display a higher degree of interaction, leading to formation of thicker films. Similar results occurred when salmon ss-DNA layers were exposed to complementary and non-complementary DNA.

 Published by Cranfield University Press ISBN: 978-0-9557436-7-2 http://hdl.handle.net/1826/3832

Surprisingly large thickness changes of 20-2 1 nm, which were observed after adsorption of complementary ss-DNA, can be explained by initial interaction to form a loosely bound second layer with extensive looping out of unbound chains. Further interaction could then stabilize the formation of a crosslinked multilayer structure. Super-coiling of DNA, which was reported recently to occur on a silicon surface could also have an effect[21].

The limits of detection of these systems were comparatively low (0.01 mg/ml). Therefore single gene monodisperse DNA was utilized instead since it was thought much more selective binding would occur than for genomic DNA[22]. Carbon/PEI electrodes were formulated as before and coated with single stranded DNA from the pyruvate kinase gene. As before the electrodes were then exposed to single stranded DNA from the same source. Figure 4a shows the drops in impedance that occur. They clearly show that single stranded DNA sensors display much higher sensitivity than genomic DNA sensors, with detection limits of the order of fg/ml. Electrodes were also exposed to DNA from the genes for actin or chymotrypsin (figure 4b) and showed much lower changes in impedance. It is thought that these could be due to the solvated DNA chains displacing the bound pyruvate kinase DNA.

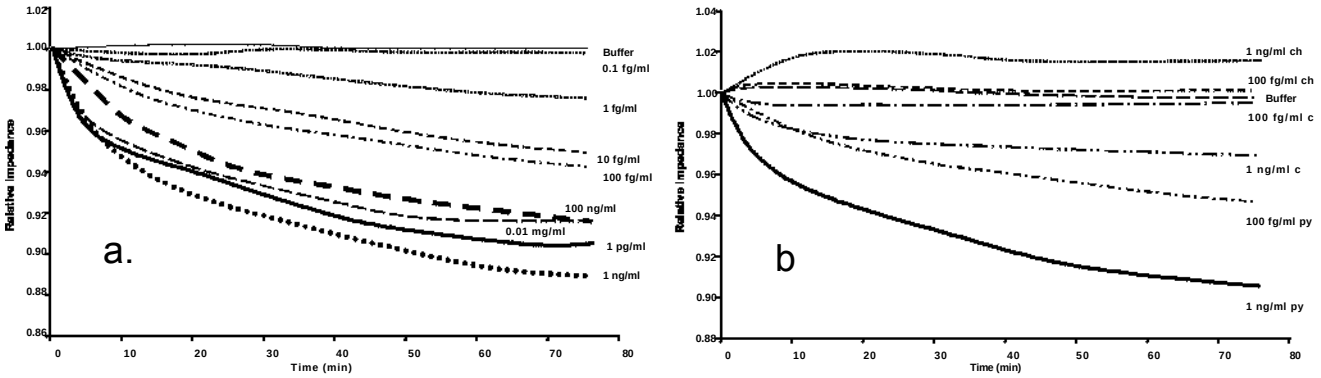

Figure 4. Adsorption of single gene DNA on carbon electrodes measured by ac impedance.

Conclusions

The method of electrostatic self-assembly was successfully implemented for adsorption of both single strand and double stranded DNA, as well as RNA. Single stranded DNA electrostatically adsorbed on the solid substrates, (despite the limited degree of freedom), is capable of binding further ss-DNA subsequently forming a DNA multilayer structure with some degree of species selectivity. The results obtained by a sensitive optical technique of total internal reflection ellipsometry proved this concept: the observed changes in thickness due to binding of complementary ss-DNA layers are 5-6 times larger than those observed for non-complementary binding of ss-DNA. The results allow a better understanding of the binding processes that are occurring and combined with our previous electrochemical results show a possibility for the development of rapid and inexpensive electrochemical DNA analyses of natural substances

 Published by Cranfield University Press ISBN: 978-0-9557436-7-2 http://hdl.handle.net/1826/3832

of food, drinks, fabric, wool and other biologically derived materials with sensitivities for genomic DNA in the 0.01 mg ml^{-1} to 1 mg ml^{-1} range and down to 1 fg ml^{-1} for single gene DNA.

References

1. Ausubel, F.M., Brent, R., Kingston, R E., Moore, D.D., Sedman, G.G., Smith, J.A., Struhl, K.S., 1993, Current Protocols in Molecular Biology, Vol. 1-2; John Wiley & Sons, New York,.
2. Korri-Youssufi, H., Garnie, F., Srivastava, P., Godillot, P., Yassar, A., 1997, J. Am. Chem. Soc., 119, 73 88-73 89.
3. Kumpubu-Kalemba, L., Leclerc, M. 2000, Chem. Comm., 19, 1847-1848.
4. Leclerc, M., 1999, Adv. Mater., 11, 1491-1498.
5. McQuade, D.T., Pullen, A.E., Swager, T.M., 2000, Chem. Rev., 100, 2537-2574.
6. Lvov, Yu., Decher. G., Sukhorukov. G., 1993, Macromolecules, 26, 5396-5399.
7. Sukhorukov. G., Mohwald, H., Decher, G., Lvov, Y.M., 1996, Thin Solid Films, 284-285, 220-223.
8. Xi Chun Zhou; Li Qun Huang; Sam Fong Yau Li., 2000, Biosens. Bioelec, 16, 85-95.
9. Bjork, P., Persson, N.K., Peter, K., Nilsson, R., Asberg, P., Inganas, O., 2005, Biosens. Bioelec, 20, 1764-1771.
10. Travas-Sejdic, J., Soman, R., Peng, H., 2005, Thin Solid Films, 497, 96-102.
11. Cardenas, M., Braem, A., Nylander, T., Lindman, B., 2003, Langmuir, 19, 7712-7718.
12. Sato, Y., Kobayashi. Y., Kamiya, T., Watanabe, H., Akaike, T., Yoshikawa,. K., Maruyama, A., 2005, Biomaterials, 26, 703-711.
13. Nicollini, C., Erokhin, V., Facci, P., Guerzoni, S., Ross, A., Pashkevich, P., 1997, Biosens. Bioelec,, 12, 613-618.
14. Mascini, M., Palchetti, H., Marazza,. G. J., 2001, Anal. Chem., 369, 15-21.
15. Lemeshko, S.V., Powdrill, T., Belosludsev, Y.Y., Hogan, M., 2001, Nucleic Acids Res., 29, 305 1- 3058.
16. Britten, R.E., Kohne, D.E., 1968, Science, 161, 529-540.
17. Martin, M.A., Hoyer, B.H., 1966, Biochemistry, 5, 2706-2713.
18. Davis, F., Nabok, A.V., Higson, S.P.J., 2005, Biosens. Bioelec, 20, 1531-1538.
19. Nabok, A.V., Tsargorodskaya, Davis, F., Higson S. P. J., 2007, Biosens. Bioelec., 23, 1531-1538.
20. Legay, G., Finota, E., Meunier-Prest, R., Cherkaoui-Malki, M., Latruffe, N., Dereux, A., 2005, Biosens. Bioelec, 21, 627-636.
21. Steel, A.B., Levicky, R.L., Herne, T.M., Tarlov, M.J., 2000, Biophys. J., 79, 975-981.
22. Rippe, K., Mucke, N., Langowski, J., 1997, Nucleic Acid Research, 25, 1736-1744. 23. Davis, F., Hughes, M A., Cossins, A.R., Higson, S.P.J., 2007, Anal. Chem, 79, 1153-1157.

 Published by Cranfield University Press ISBN: 978-0-9557436-7-2 http://hdl.handle.net/1826/3832

A Framework for Surveying Patent Infringement Clearance Practice in UK and German Companies

Ian P. Hartwell
European Patent Attorney, Visiting Research Fellow
Centre for Intellectual Property Policy and Management, Bournemouth University

Introduction

Funding has been received from the European Patent Organisation to support a survey of UK and German companies regarding their patent infringement clearance practice. This paper considers the background to this project and describes a framework that, once populated with survey data, will enable company Intellectual Property Managers to manage the risk of patent infringement more cost-effectively, thereby releasing resources for the technical and marketing work that is vital for company success.

Background

Intellectual property (IP) rights encompass copyright, patent rights, design rights and trademark rights. IP rights – particularly patent rights – are generally acknowledged to be a key element in the creation of wealth from research and innovation. One route to value from technical IP is the Single Technology Company, previously defined by Hartwell (2004) as a company having the fundamental patent rights to a new technology and having development of that technology as its core competence. Since most of the value of such companies resides – at least in the early years – in their IP rights, such companies typically designate someone in-house to take responsibility for this key asset. Such a person must of course understand the technology as well as understanding IP and will occasionally have an IP legal qualification, e.g. European Patent Attorney. They will be referred to hereafter as the 'IP Manager'.

If, as is to be hoped, a company is operating in a technical field having commercial potential, then there will inevitably be competitors. The role of the IP Manager is twofold: firstly to use the IP system to secure competitive advantage over those competitors and secondly to avoid infringing IP rights belonging to those competitors. There is also a third requirement, namely to achieve the first two objectives within budget: government fees, legal bills and translation charges make IP a costly tool.

Patent Infringement Clearance

Many organisations, for example the UK Intellectual Property Office, offer detailed advice on the task of using the IP system to secure competitive advantage. However, there is much less guidance on the task of avoiding infringement of IP rights belonging to third parties (otherwise known as 'infringement clearance' or 'freedom to operate'). Such detailed advice as is available is chiefly in the form of commercial seminars given by IP attorneys and focuses very much

 Published by Cranfield University Press ISBN: 978-0-9557436-7-2 http://hdl.handle.net/1826/3832

on the legal analysis of individual third party patents, particularly in the pharma and biotech industries.

Moreover, the significant cost of such legal analysis risks being wasted if the technology in development subsequently changes (e.g. as a result of technical problems) so that a particular third party patent is no longer relevant. At the other extreme, there is a risk of the cost of technology development being wasted should a third party patent block the technology from reaching the market. The challenge for the IP Manager is to find the balance between these two extremes: in the words of IPAC (2003), infringement clearance should be '*not too early or too late'.*

There is also the question of what infringement clearance measures to take. A particular dilemma when faced with a potentially blocking third party patent is whether to invest resource in trying to invalidate the patent or instead invest resource in redesigning the technology so as not to infringe the patent. Patent invalidation requires searches to be carried out to identify earlier public disclosures that are pertinent to the invention of the patent. However, as noted by Simmons (1984), one can never know in advance whether searches will actually yield any pertinent earlier disclosures, although Hartwell (2002) discusses factors that may increase the likelihood of a patent being invalidated. The alternative approach of redesigning the technology carries its own risk of infringing other third party patents, not to mention the costs associated with such redesign.

In the event that searches are carried out and pertinent earlier disclosures are found, a further question is exactly what to do next: although the patent law of most countries allows for the invalidation of a patent to be requested, anecdotal evidence suggests that the use of such 'opposition' procedures is far from uniform. In particular, it is believed that German companies prefer opposition while UK companies prefer the higher-risk, lower-cost approach of reserving their defensive arguments until such time as infringement proceedings are launched by the patent proprietor.

A final question concerns the amount of resource, in particular the personnel, allocated to each step of the infringement clearance process. In the large Japanese chemical corporation interviewed by Granstrand (1999), patent clearance would appear to be the sole responsibility of a dedicated IP department. However, such departments are the exception rather than the rule and, in England, a decision of the Patents Court (2006) suggests that a company's engineering team should be aware of third party patents.

This dearth of guidance and data on patent clearance, particularly outside of the pharmaceutical and biotech fields, inevitably results in some companies spending too much on their clearance and other companies spending too little. The former will divert precious resource from the development and marketing activities that are core to generating wealth from research and innovation, while the latter has serious corporate governance implications. The proposed survey seeks to remedy this deficit.

 Published by Cranfield University Press ISBN: 978-0-9557436-7-2 http://hdl.handle.net/1826/3832

Survey Framework

To address question of what infringement clearance measures are used, there is proposed a survey framework based on three stages:

A Identification of potentially problematic third party patents

B Assessment of infringement of valid scope of potentially problematic patent

C Action

There is general agreement between the previously mentioned IPAC (2003) and Grandstrand (1999), as well as Sweeney (1997) regarding these three stages, the first of which may be considered as operating at the patent landscape level while the second and third operate at the individual patent level.

Stage A: Identification of potentially problematic third party patents

There is also general agreement on the available measures in stage A, namely (a) a one-off search for third party patents, (b) regular searches for new patent publications

in the technical field of interest, (c) regular searches for new patent publications by competitors, and (d) review of any third party patents that are cited against a company's own patent applications. These measures are included in the framework.

A key question is who carries out the various searches, e.g. technologists or IP personnel with their additional costs. A further layer of complexity results from the fact that a search typically involves two skills: (i) using search systems to find patent documents of relevance to the technical field and (ii) assessing whether a found document is relevant to product plans. As a result a search could require two people. Accordingly, for each kind of search (a) to (d), the survey framework asks (i) who operates the search system and (ii) who assesses the search hits.

As previously mentioned, the question of 'who' is in essence a question of cost. Thus, the framework offers five response options, ranked in order of cost, namely: (1) nobody, (2) automated, (3) technologist, (4) searcher, (5) attorney, (6) counsel.

Timing

To capture information about when in the product development process a particular measure is implemented, the survey framework uses the Stage-Gate™ model of the new product development process proposed by Cooper (1993). This defines six stages: Ideation, Preliminary Investigation, Detailed Investigation, Development, Testing & Validation, Full Production & Market Launch. To this has been added an additional preliminary stage of 'Identifying General Technology Field' during which it may be appropriate e.g. to carry out certain preliminary searches.

 Published by Cranfield University Press ISBN: 978-0-9557436-7-2 http://hdl.handle.net/1826/3832

Stage B: Assessment of infringement of valid scope of problematic patent

Stage B again involves two skills, viz: (i) searching for earlier public disclosures that might reduce the valid scope of the patent, and (ii) assessing whether product plans infringe this – possibly reduced – valid scope. Again, each skill can be exercised at different levels with their associated different costs.

Stage C: Action

The available measures depend on the outcome of the previous stage B. Where there is infringement of the valid scope of a problematic patent, many of the available measures are identified by Granstrand (1999), namely (1) decide to wilfully infringe the patent, (2) design around the patent, (3) develop a bargaining position with the patent owner, (4) acquire or take a license to the patent, (5) halt the project until the patent has expired, and (6) abandon the project entirely.

However, since the survey also plans to establish the timing of such measures, a further measure needs to be added to the framework, namely (7) defer action. Such deferral may be appropriate in view of the early stage of technology development. Another reason may be the stage of the problematic patent: it can take a number of years for a patent application to go through the stages of being searched, examined and finally granted, during which time the valid scope of the application can shrink, potentially to a scope that no longer encompasses product plans. These three stages of examination are accordingly also included in the survey framework.

The survey framework also contains a section corresponding to the event that the problematic patent is found to be infringed but invalid. Options include (1) seeking invalidation of the patent or (2) deciding to reserve arguments, as discussed previously. Another option is again to (3) defer action, either to a later stage in the project and/or a later stage in the examination of the problematic patent filing.

Implementation of the Survey Framework

It is planned to survey German companies in addition to UK companies. Not only will this significantly increase the survey base compared to the UK alone, it will hopefully also shed light on the aforementioned differences in opposition behaviour between the two countries. Moreover, inclusion of German companies should allow data to be collected for two particular technical fields of interest to the author, namely automotive and microtechnology. Both fields contribute to the creation of wealth from research and innovation but differ significantly from pharmaceuticals and biotech where most IP management guidance has been focused to date.

Although the Stage-Gate™ process has, according to Cooper (1993), already been used in engineering companies, it is anticipated that not all companies surveyed will fit within the framework, which will consequently require adjustment. Additional clearance measures may similarly become apparent during surveying and require

 Published by Cranfield University Press ISBN: 978-0-9557436-7-2 http://hdl.handle.net/1826/3832

incorporation into the framework. Moreover, surveyed companies are unlikely to adopt the same approach to all third party patents: for example, Gassman and Bader (2007) note that Alcatel varies its patent watching strategy depending on whether it already has a cross-licence with the company to be watched. Such differences and the underlying factors will be recorded as part of the survey.

Conclusion

Once populated with survey data, the framework described in this paper should provide IP Managers – particularly those in single technology companies in the automotive and microtechnology fields - with a tool with which to optimise their patent clearance process in respect of measures, timing and cost. For the company as a whole, the framework should demonstrate to outsiders that third party patent infringement risk is being managed according to industry standards.

References

1. Cooper, R.G. *Winning at New Products.* Addison-Wesley Publishing. 1993 Gassmann, O. and Bader, M. *Patentmanagement. Innovationen erfolgreich nutzen und schützen.* Springer Verlag. 2007.
2. Granstrand, O. *The Economics and Management ofIntellectual Property. Towards Intellectual Capitalism.* Cheltenham: Edward Elgar Publishing, 1999.
3. Hartwell, I.P. The Vulnerability of Granted Patents, *Managing Intellectual Property.* October 2002, 65-69.
4. Hartwell, I.P. Patent Portfolio Structure for Single Technology Companies, PhD Thesis, School of Engineering, Cranfield University. July 2004.
5. Intellectual Property Advisory Committee (IPAC), UK Patent Office. Seminar: Freedom to Operate. London, 11 July 2003
6. Patents Court Judgement: Tamglass v. Luong North Glass, [2006] EWHC 65 (Ch). Simmons, E.S. The Paradox of Patentability Searching, *J. Chem. Inf. Comput. Sci.* 1985, 25-28
7. Sweeney, A. Effective Risk Management, *Conference. Exploiting and Protecting your Intellectual Property Rights.* London: 4 and 5 December 1997.

 Published by Cranfield University Press ISBN: 978-0-9557436-7-2 http://hdl.handle.net/1826/3832

High Volume Automated Testing of Relational Database Management Systems

Jeremy Gardiner
Cranfield University
Defence College ofManagement and Technology
Department ofInformation Systems
jgardiner@woomerang.com

Abstract

Methodological challenges during empirical research into High Volume Automated Testing (HVA T) of a Relational Database Management System (DBMS) are described. A fundamental problem in software testing is that only a small fraction of possible program inputs can be tested in the time available; HVAT addresses this problem by automatic generation of very large numbers of test cases. Manual testing ofDBMS is insufficient due to the complexity of this type of software. HVATofDBMS using random testing and genetic algorithm techniques may be a more suitable approach, although more empirical research into the effectiveness of these techniques is needed. Initial results using MySQL and random generation of SQL appear to support the hypothesis that the DBMS enters an invalid state as a consequence of accepting an invalid SQL statement, resulting in delayed failure; however further work is needed to overcome the methodological challenges encountered. Future work will introduce another DBMS and a genetic algorithm testing technique in a full twoby-two factorial design.

Keywords: Automated Testing, DBMS, Empirical Research, Genetic Algorithm, HVAT, Methodology, Random Testing, Relational Database Management System.

Introduction

This paper describes some methodological challenges encountered during empirical research into High Volume Automated Testing of a Relational Database Management System; an abstract of this research was previously presented in [1].

High Volume Automated Testing

A fundamental problem in software testing is how to do sufficient testing to give adequate confidence and appropriate fault coverage. Only a small fraction of possible program inputs can be tested in the time available for testing; even with automatic test execution, manual generation of test cases limits the number of tests that can reasonably be performed in a given time. High Volume Automated Testing (HVAT) addresses this problem by automatic generation of very large numbers of test cases (tens of thousands) combined with automatic test execution and automated comparison of results [2].

 Published by Cranfield University Press ISBN: 978-0-9557436-7-2 http://hdl.handle.net/1826/3832

Database Management Systems

Database Management Systems (DBMS) are an important component of many software systems, however manual testing of DBMS is insufficient due to the complexity of this type of software. HVAT of DBMS using techniques such as random testing and genetic algorithms may be a more suitable approach although there is a need for empirical research into the effectiveness of different testing techniques [3].

Related Work

Slutz describes a system for Random Generation of SQL (RAGS). The RAGS system combines a random testing approach with grammar–based generation to generate large numbers of valid Structured Query Language (SQL) statements. This has been used successfully for testing SQL database systems [4].

Bati et al describe a random test case generation technique for database systems based on a genetic approach that uses execution feedback to guide the test generation process toward specific DBMS subcomponents and rarely exercised code paths. Experiments with Microsoft SQL Server have indicated that the technique can outperform other methods of random testing (e.g. RAGS) in terms of efficiency and code coverage [3].

Software Under Test

The Software Under Test (SUT) should ideally be a real software product rather than a 'toy' program and should be freely available along with source code and information about known bugs. The SUT should also have a well-documented standard interface that facilitates creation of an automatic test harness. The Open-Source RDBMS MySQL meets these criteria.

Method

Experimental Design

A two-by-two factorial design is planned as shown in figure 1. This allows comparison of different testing techniques for the same SUT and comparison of different SUT for the same testing technique. Experimental results have so far been obtained for a single SUT S_1 (MySQL) and a single testing technique T_1 (random generation of SQL).

 Published by Cranfield University Press ISBN: 978-0-9557436-7-2 http://hdl.handle.net/1826/3832

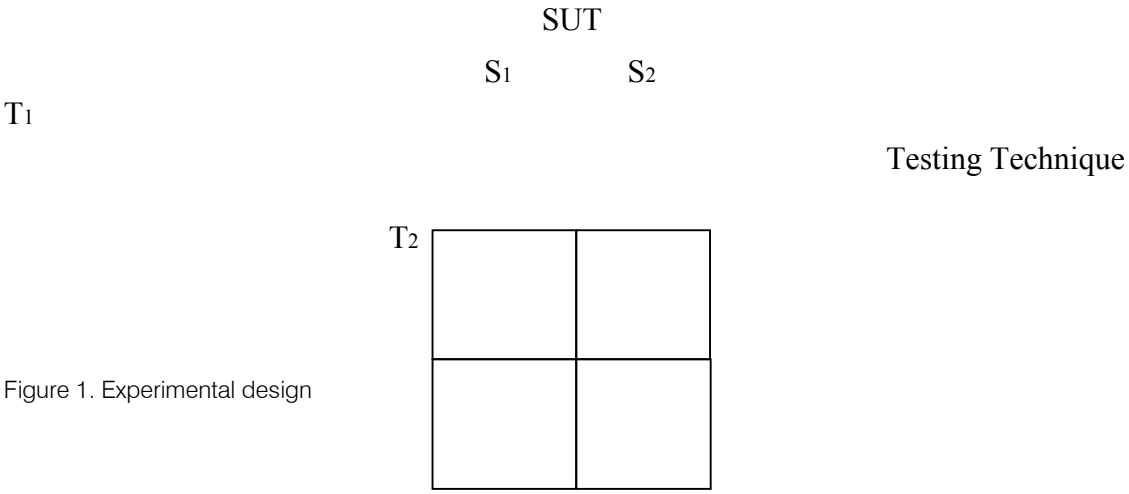

Figure 1. Experimental design

Experimental Procedure

Table 1 shows the steps of the experimental procedure and the resulting database state after each step. It is assumed that the SUT fails in step (3) of the procedure, but does not fail in step (6). The same sequence of randomly generated valid SQL statements is executed in step (3) and in step (6); therefore the failure of the SUT in step (3) can be attributed to the sequence of invalid (mutated) SQL statements executed in step (2).

The hypothesis is that the SUT enters an invalid state s_2 due to accepting an invalid SQL statement in step (2) and that this eventually leads to the failure in step (3) (delayed failure). The type of software failure most easily detected in this experiment is a crash (loss of connection to the MySQL server).

 Published by Cranfield University Press ISBN: 978-0-9557436-7-2 http://hdl.handle.net/1826/3832

Table 1. Experimental procedure

Step (0)	Start up SUT	(state s_0)
Step (1)	Initialise database	(state s_1)
Step (2)	Execute sequence of invalid (mutated) SQL statements	(state s_2)
Step (3)	Execute sequence of valid SQL statements □ Failure	(state s_3)
Step (4)	Restart SUT	(state s_0)
Step (5)	Initialise database	(state s_1)
Step (6)	Execute sequence of valid SQL statements □ No failure	(state s_4)

Generation of SQL Statements

The sequences of SQL statements used in the experimental procedure were generated using a similar technique to that used in the Random Generation of SQL (RAGS) system described by Slutz [4]. The basic approach is to generate a syntax tree from an SQL syntax specification in Backus Naur Form (BNF) and to descend the syntax tree, choosing branches of the tree at random. This produces a random distribution of SQL statements determined by the contents of the BNF specification. The sequence of valid SQL statements was generated from a valid BNF specification and the sequence of invalid SQL statements was generated from a mutated version of the BNF specification produced by randomly inserting invalid terms into the BNF rules. Not all of the SQL statements generated from the mutated version of the BNF specification are invalid, however, since random choices are made during descent of the syntax tree.

Results and Methodological Challenges

The experimental procedure shown in Table 1 was repeated several times with different sequences of randomly generated SQL statements (generated using different random seed values). This produced 4 positive outcomes (appearing to support the hypothesis) in 21 runs of the procedure. Further analysis of positive outcomes is required to confirm if an invalid SQL statement was actually accepted by the SUT in each case. Analysis of results is complicated by the fact that SQL statements generated from the mutated version of the BNF specification are not guaranteed to be invalid.

The stability of MySQL when executing a sequence of randomly generated valid SQL statements was unexpectedly poor: the mean number of randomly generated valid MySQL statements executed before MySQL crashed (lost connection to the server) was 28,620 with a standard deviation of 12,412. This places a practical limit on the length of sequence of valid SQL statements that can be executed in step (6) of the procedure.

Results obtained immediately after a 'cold start' of MySQL when the PC is first started up differ from results obtained after a 'warm start' of MySQL with NET START and this suggests that the start-up state of MySQL is different in these two cases.

 Published by Cranfield University Press ISBN: 978-0-9557436-7-2 http://hdl.handle.net/1826/3832

The number of SQL statements accepted by the SUT for different sequences of randomly generated SQL statements (using different random seed values) varied although the variation was not statistically significant.

However, the number of SQL statements accepted by the SUT on repeated execution of the same sequence of valid SQL statements was not identical; the results were essentially identical up to shortly before the point of failure, but subsequently failure occurred at a different point in each run. This suggests the existence of a variable delay period before failure.

Conclusions

Initial results appear to support the hypothesis that the SUT suffers a delayed failure after entering an invalid state as a consequence of accepting an invalid SQL statement; however further work is needed to overcome the methodological challenges encountered before outcomes appearing to support the hypothesis can be accepted as meaningful.

Future Work

Future work will introduce another DBMS as SUT S_2 and will introduce a genetic algorithm technique T_2 in a full two-by-two factorial design as shown in Figure 1.

References

1. Gardiner, J, “Delayed Failures in Software Using High Volume Automated Testing”, Testing: Academic and Industrial Conference - Practice And Research Techniques (TAIC PART), 2006.
2. Kaner, C, Bond, P, McGee, P, “High Volume Test Automation”, Florida Institute of Technology Computer Science Department, 2003.
3. Bati, H, Giakoumakis, L, Herbert, S, Surna, A, “A genetic approach for random testing of database systems”, Microsoft Corporation, 2007.
4. Slutz, D, “Massive Stochastic Testing of SQL”, VLDB'98, Proceedings of the 24th International Conference on Very Large Data Bases, 1998.

 Published by Cranfield University Press ISBN: 978-0-9557436-7-2 http://hdl.handle.net/1826/3832

The Influence of Desert Environment on Gas Turbine Compressor Fouling

A. Gannan, D. Fouflias, K.W. Ramsden

Department of Power and Propulsion, School of Engineering
Cranfield University, England

Abstract

Industrial gas turbines suffer from a common problem which is compressor fouling. It occurs when there are large deposits of sand and oil present. In an oil field in a desert environment the problem is intensified due to dust and sand. Fine sand particles and hydrocarbon emissions when combined with oil vapour invade the engine and settle on the compressor blades. This paper discusses how the desert environment influences engine performance and investigates the effect of engine degradation at different ambient temperatures. The performance deterioration was simulated for an industrial gas turbine of 8 MW (approximate) output power sited in an oil field in a desert environment.

Introduction

Gas turbine users face genuine problems with both performance and cost penalties due to compressor fouling. Analysis of the effects of this problem and suggested solutions has been studied at Cranfield University. The recent increase in fuel prices has exaggerated the economic effect of compressor fouling. This is due, of course, to the fact that compressor fouling requires an increased fuel flow to recover the power reduction occurring with compressor fouling. In addition, whilst retaining the required power output by increasing fuel flow, the corresponding increase in gas temperatures cause hot gas components to suffer reduced creep life. Some estimates show that 85% of the total performance loss is caused by fouling during operation [1]. A cost estimate of the performance loss is given by Diakunchak [2]. Other forms of deterioration can occur such as corrosion and erosion where both compressor and turbine components suffer fouling, foreign body damage, and thermal distortion. These contributions are discussed in References 3 and 4. Fouling has been described as the deterioration which is caused by the deposits of particles on the compressor airfoil and annulus surfaces [5]. The shape of the airfoils and the incidence angles change due to the build up of foreign material, the blade surface roughness increases, the boundary layer thickness increases and the throat area of the compressor blade passages reduces [6]. 70-85% of the performance loss has been accredited to compressor fouling [7]. This loss of power can be substantially reduced by cleaning. The impact of fouling typically results in a reduced mass flow of up to 3% [8,9], a reduced

 Published by Cranfield University Press ISBN: 978-0-9557436-7-2 http://hdl.handle.net/1826/3832

power output of 3% and a reduction of the overall pressure ratio of 2% [10]. Two methods may be introduced to reduce compressor fouling, air intake filtration and compressor washing.

Engine Working Environment

This paper considers a typical gas turbine installation sited in an oil field in a desert environment. In the case considered, the climate in the summer months is hot and dry

with ambient temperatures of up to 5 0°C. Conversely during the winter months, ambient temperatures of as low as -2°C are experienced during the night. At the same time, from January to April typically very windy and sandy conditions can be experienced. These environmental changes have huge effects on the performance of gas turbine engines. The variation of ambient temperatures and the presence of dust and sand can cause severe fouling of the compressor as well as corrosion and erosion. In addition, hydrocarbon particles are present in the air.

The Influence of Ambient Temperature on Engine Performance

The performance of the engine in the gas turbine is at its best when the ambient temperatures are low since air density is then highest. Figure 1 illustrates the influence of ambient temperature on the engine performance based on calculations undertaken using the Turbomatch performance deck at Cranfield.

 Published by Cranfield University Press ISBN: 978-0-9557436-7-2 http://hdl.handle.net/1826/3832

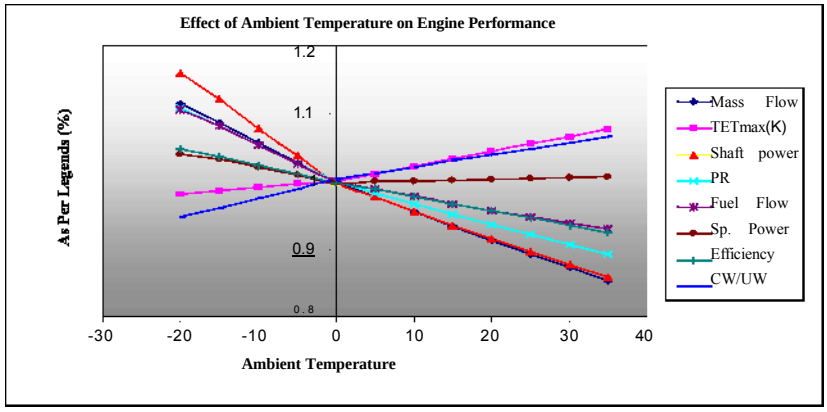

Figure 1:

Effect of Ambient Temperature on Engine Performance

There are increases of the inlet mass flow in proportion with the increase in TET, at different ambient temperatures as shown in figure 2. In order to recover the engine power loss, TET must be increased with fuel flow increases. The mass flow loss happens because of reduced air density as the ambient temperature increases. More power is needed to compress the hot air. As a result fuel flow must be increased. In consequence, the thermal efficiency will drop due to reduction in compressor pressure ratio. Figure 3 shows the effect of changes in ambient temperatures on TET for a variety of performance parameters.

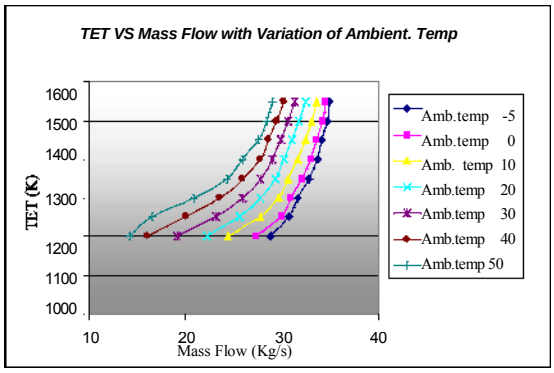

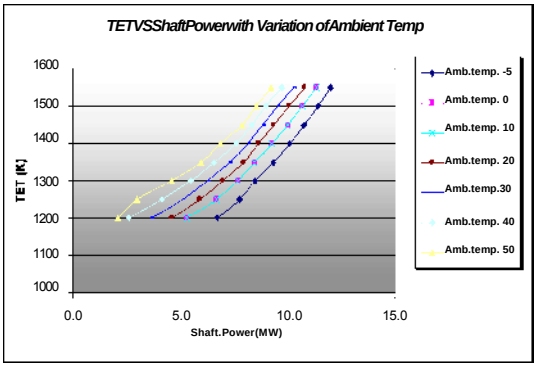

 Published by Cranfield University Press ISBN: 978-0-9557436-7-2 http://hdl.handle.net/1826/3832

Figure 2: Mass Flow and TET Variation with Ambient Temperature

Figure 3: Shaft Power and TET with Variation Ambient Temperature

The shaft power is decreased when the ambient temperature is increased. It is shown that increasing the TET allows power output to be maintained.

The effect on thermal cycle efficiency as a function of ambient temperature is shown in Figure 4. In figure 5 specific fuel consumption (SFC) versus specific power is illustrated for different engines working at design point conditions. Different pressure ratios with a steady TET are shown by the straight lines. The curved lines represent different TET at a constant pressure ratio. From the above Figures it is shown that as the TET increases with constant pressure ratio, a reduction in SFC and an increase in specific power can is obtained. Keeping the TET constant, as the pressure ratio increases, the SFC falls, however the specific power at low pressure ratios remains almost constant. However, once the pressure ratio increases above the value of 12, power reduces.

 Published by Cranfield University Press ISBN: 978-0-9557436-7-2 http://hdl.handle.net/1826/3832

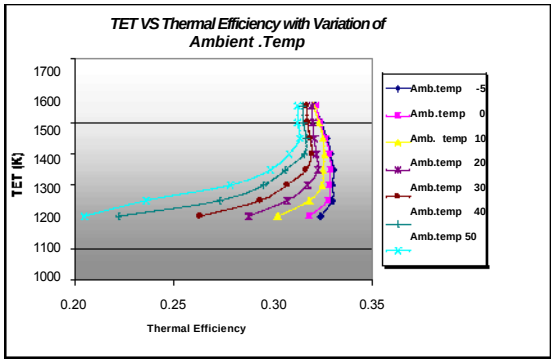

Figure 4: Thermal Efficiency and TET with Variation in Ambient Temp

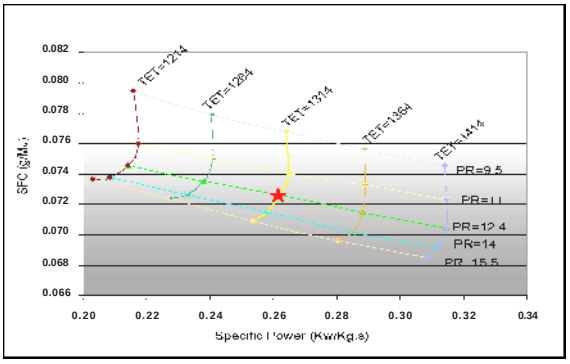

Figure 5: Specific Power and Specific Fuel Consumption Variation with different PR and TET

Degraded Engine Simulation

The performance of the gas turbine engine can be seriously affected by deterioration of parts such as the compressor, combustor and turbine. The first time the engine is started from new, deterioration of performance will begin. In particular, the mass flow and the isentropic efficiency will both reduce. Studies of component degradation have been undertaken using Cranfield performance software (PYTHIA) to ascertain the affect that fouling and erosion have on engine performance.

Compressor Isentropic Efficiency Loss

For example Figure 6 shows that engine degradations can cause an isentropic efficiency loss of 2.5%, and a mass reduction 5%. This results in a reduction in power output of almost 6%.

Compressor Non Dimensional Mass Flow Reduction

Non-dimensional mass flow deterioration has a strong effect on the engine performance especially the power output which drops by about 10.6% as can be seen in Figure 7.

 Published by Cranfield University Press ISBN: 978-0-9557436-7-2 http://hdl.handle.net/1826/3832

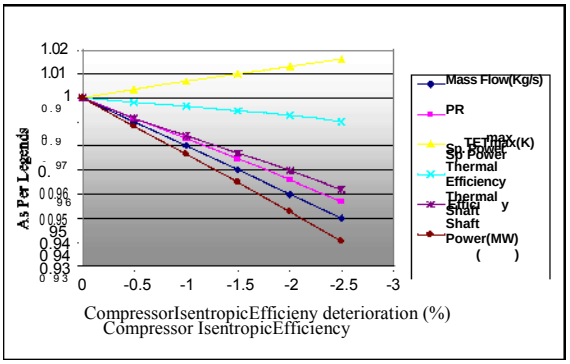

Figure 6: Engine Performance Deterioration by Isentropic Efficiency

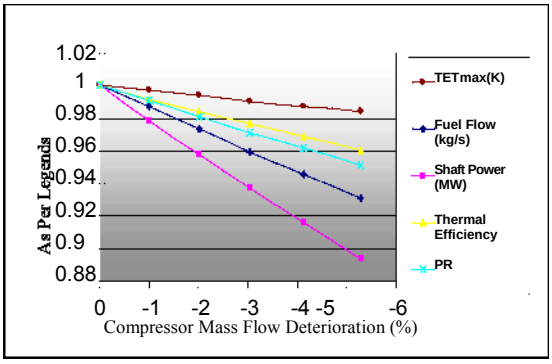

Figure 7: Engine Performance Deterioration by NDMF

Compressor Fouling and Erosion

Using PYTHIA software compressor NDMF and isentropic efficiency are stored together in one simulation. Less air enters the compressor when the compressors are fouled due to erosion causing rough surfaces. The mass flow and shaft power is reduced as can be seen in Figure 8. Because of the acute sensitivity of the engine to fouling, the shaft power drops very quickly.

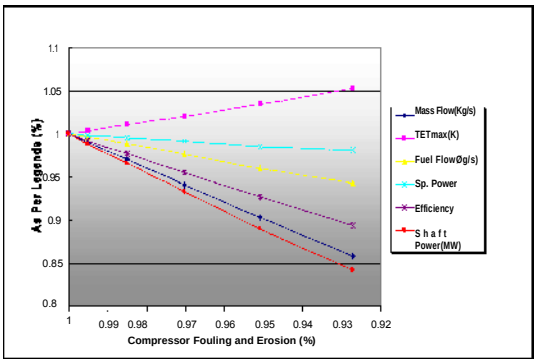

Figure 8: Engine Performance Deterioration by Compressor Fouling

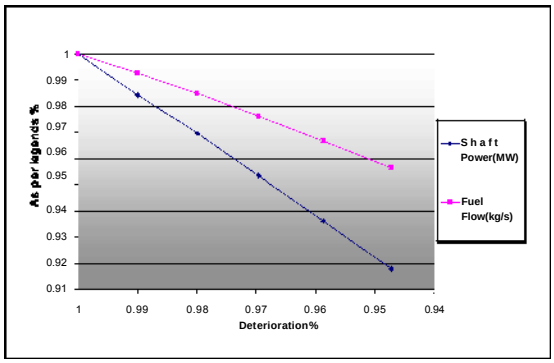

Figure 9: Compressor Performance Deterioration

 Published by Cranfield University Press ISBN: 978-0-9557436-7-2 http://hdl.handle.net/1826/3832

Figure 9 shows that the power output will drop by 8.2% and the fuel flow will reduce by 4.36% if the compressor efficiency deteriorates by 5.3%. I fact, power output falls much quicker than the fuel consumption.

Conclusions

In can be concluded that fouling rates vary from engine to engine and are dependant upon different factors like plant location, design and layout and climate. Weather conditions have the largest impact on fouling rates and performance deterioration. By carefully checking compressor performance, atmospheric changes and the gas turbine, evaluations

and histograms will help to decide on the best washing regimes and through fouling predictive methods be able to initiate the use of on line washing when necessary. As a result, with an effective maintenance schedule, plant profitability will improve with a corresponding reduction in production costs. The net result will also be to create a cleaner environment.

References

1. Meher-Homji, C. B., 2000, ''Compressor Fouling. . . Causes and Solutions,'' *Global Gas Turbine News,* IGTI, 40(3).
2. Diakunchak, I. S., 1991, ''Performance Deterioration in Industrial Gas Turbines,'' *ASME Paper* 91 -GT-228.
3. Kurz, R., and Brun, K., 2000, ''Degradation of Gas Turbine Systems,'' *ASME Paper* 2000-GT-345.
4. Zwebek, A. I., and Pilidis, P., 2001, ''Degradation Effects on Combined Cycle Power Plants Performance, Part 1: Gas Turbine Cycle Component Degradation Effects,'' *ASME paper* 2001 -GT-388.
5. Mund, F. C. and Pilidis, P., 2006, "Gas Turbine Compressor Washing: Historical Developments, Trends and Main Design Parameters for Online Systems", *ASME J. Eng. Gas Turbines Power,* 128, pp. 344-3 53.
6. Diakunchak, I. S., 1992, "Performance Deterioration in Industrial Gas Turbines," *ASMEJ. Eng. Gas Turbines Power,* 114, pp. 161–168.
7. Scheper, G. W., Mayoral, A. J., and Hipp, E. J., 1978, "Maintaining Gas Turbine Compressors for High Efficiency," *Power Eng.,* 82(8), pp. 54–57.
8. Mezheritsky, A. D., and Sudarev, A. V., 1990, "The Mechanism of Fouling and the Cleaning Technique in Application to Flow Parts of the Power Generation Plant Compressors," *ASME Paper* No. 90-GT- 103.
9. Becker, B., and Bohn, D., 1984, "Operating Experience with Compressors of Large Heavy-Duty Gas Turbines," *ASME Paper* No. 84-GT- 133.
10. Bagshaw, K. W., 1974, "Maintaining Cleanliness in Axial Compressors," *Gas Turbine Operation and Maintenance Symposium 1974, National Research*
11. *Council (eds.),* Toronto, Canada, pp. 247–2 64.

 Published by Cranfield University Press ISBN: 978-0-9557436-7-2 http://hdl.handle.net/1826/3832

Supply Chain Relationship Management Research in a Sino-West Context

Methodological paper for Multiple Strands Conference

Fu Jia
Centre for Logistics and Supply Chain Management
Cranfield School of Management
Cranfield, Bedfordshire
MK43 0AL
U.K.

Introduction of the research

Based on the literature review, one of the problems facing Western buyers and their Chinese suppliers hinges on the differences between *Guanxi,* one of the most important dynamics of Chinese society and a major influence on Chinese business, and Western forms of relationship management. The first phase of my research based on literature review has led to the identification of three root differences:

- The Chinese are family orientated whereas Westerners are individualistic. In contrast to Western culture, Guanxi puts group interests above the interests of the individual.
- The Guanxi network is based on family connections and provides a support network for individuals and businesses. In the West institutionalisation has created a more formal support network of regulated associations and institutions.
- Guanxi building takes place between individuals and is based on the interplay of face (*mianzi)* and favour (*renqing),* and the principle of Yin-yang, i.e. when there is conflict in a relationship, only two movements are available to either party: 'to pull or push the door'. As Chinese individuals will not confront others directly, when the other party pushes, Chinese will pull and vice versa. This is called complementary response or yielding. Western relationship building on the other hand tends to begin at an organisational level and follows a more structured step-by-step approach based on economic principles. The Guanxi building process is also based on a long term orientation whereas Western relationships are by contrast built with a short term orientation.

Cultural adaptation is proposed as the solution to above problems (Powell, 1998; Boisot and Child, 1999, Lin, 2004); however, very little has been done on how both parties adapt to each other in terms of above three root differences. Based on the literature review, two research questions are proposed and a conceptual framework has been developed:

 Published by Cranfield University Press ISBN: 978-0-9557436-7-2 http://hdl.handle.net/1826/3832

- How do Western buyers and their Chinese suppliers adapt to each other in terms of the differences between Western forms of supply chain relationship management and Guanxi?
- How do the mutual benefits achieved relate to the cultural adaptation process?

Conceptual framework

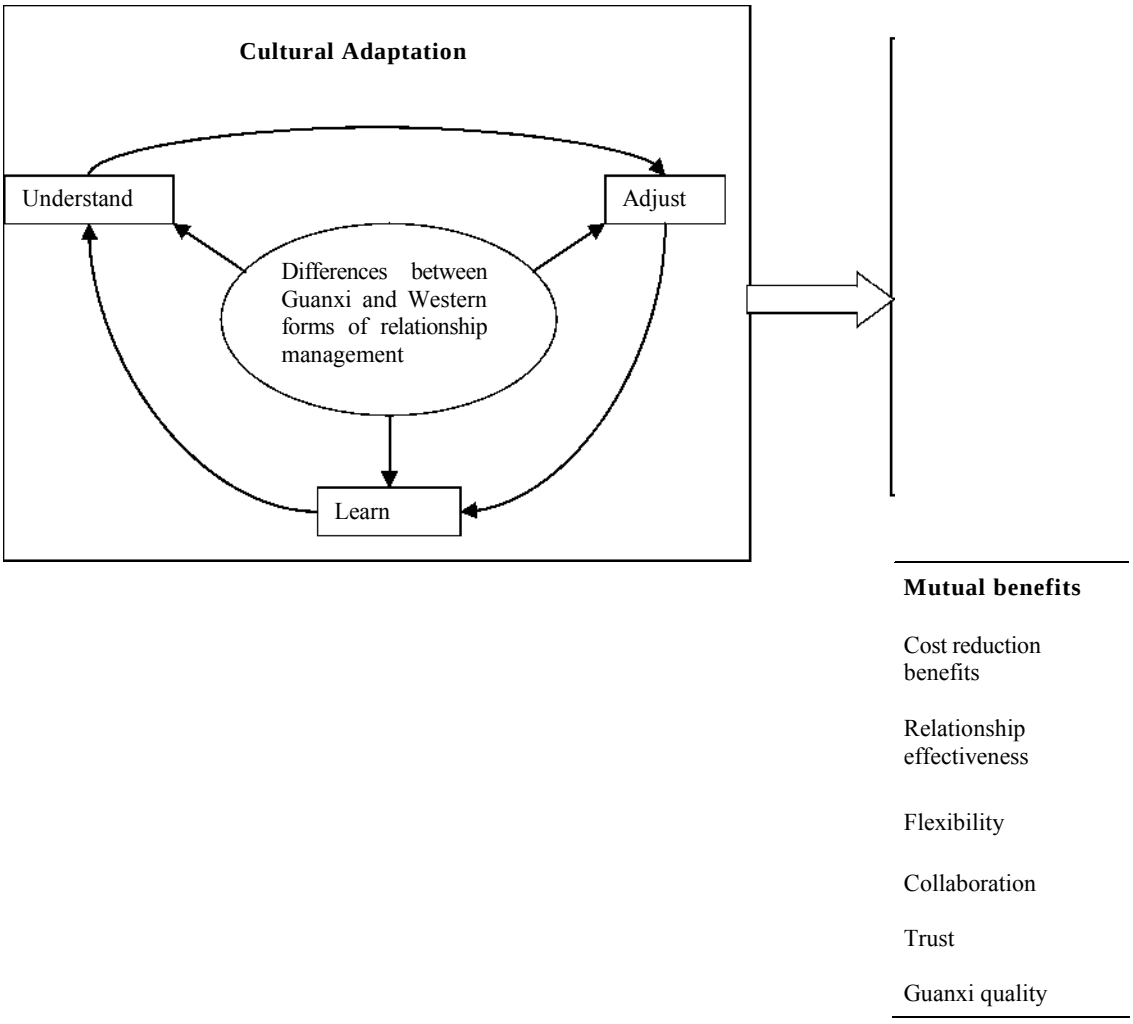

 Published by Cranfield University Press ISBN: 978-0-9557436-7-2 http://hdl.handle.net/1826/3832

Figure 1: Conceptual framework

In the development of a conceptual framework (Figure 1), Lin's (2004) cultural adaptation process is adopted as the basis of cultural adaptation. This dynamic process includes three elements: to understand, to adjust and to learn. The three root differences between Western forms of supply chain relationship management and Guanxi identified are the inputs or content of this cultural adaptation process. From an inter-firm learning perspective, the differences are areas of learning. KoulikoffSouviron and Harrison (2007) claim that the adaptation between a buyer and a supplier may range from unilateral (one partner dominates) to reciprocal (a bilateral or mutual process).

The right side of the model shows the mutual benefits for the partnership. Cultural adaptation (supply chain relational risk mitigation) results in mutual benefits for both members of the partnership.

Methodology used in this research

This research employs a multiple case studies methodology. Since one of the aims of my research is to find out how Western buyers and Chinese suppliers adapt to each other and, the research questions are two "how" questions about a contemporary phenomena (Yin, 2003) that has not yet been thoroughly researched, multiple case studies method is the logical methodology. Ellram (1996) argues that the case study method provides depth and insight into a little known phenomenon.

Ghauri (2004) argues that the case study method is particularly well suited to international business research, where data is collected from cross-border and cross-cultural settings. Surveys and/or experiments raise serious questions about equivalence and comparability of data collected from different countries. The case study method provides excellent opportunities for respondents and researchers to check their understanding and keep on asking questions until they obtain sufficient answers and interpretations.

Marschan-Piekkari and Welch (2004) claim that qualitative research allows for deeper cross-cultural understanding and is less likely to suffer from cultural bias and ethnocentric assumptions on the part of the researcher than survey instruments. Qualitative research takes an "emic" perspective investigating other organizations and societies on their own terms rather than imposing one's own culturally bound concepts and theories. Compared to quantitative methods,

 Published by Cranfield University Press ISBN: 978-0-9557436-7-2 http://hdl.handle.net/1826/3832

qualitative research takes a more holistic approach to the research project and studies a phenomenon in its context.

He continues to explain that case study is particularly useful when phenomenon under investigation is difficult to study outside its national settings, as typically occurs in international business research, since researchers are often studying the impact of different national contexts. This is the case for this research. It is impossible to separate the phenomenon from the context of Chinese culture.

Unit of analysis

Based on the two research questions, the unit of analysis of this research is neither Western buyers nor Chinese suppliers, but is the relationship between them. Therefore the unit of analysis will be the relational dyads between Western buyers and their Chinese suppliers. However as the idea develops, it seems that the above unit of analysis is not accurate. The more accurate description of the unit of analysis is different forms of relationship management of the dyadic relationship.

Data collection instruments include:

- In-depth interviews with Western sourcing managers and Chinese account managers
- Observations of the informants
- Documentation

Documentation is not the main instrument of this research since the adaptation process is hardly formalized in the companies' documents.

Sample/case selection

Based on the literature review, a number of factors, which influence the partnership performance, other than different forms of relationship management have been identified. These factors are control variables in this research.

- The cases will be chosen from those relationships, the aim of which is to form partnership.

Discussion

 Published by Cranfield University Press ISBN: 978-0-9557436-7-2 http://hdl.handle.net/1826/3832

- In terms of Western buyers sourcing in China, those which have IPOs (International Purchasing Office) or sourcing department in China will be selected. Having IPO/sourcing department in China proves that first the Western buyer has entered a mature stage of China sourcing; second the
- purchase scale of the Western firms has justified the presence of IPO or sourcing department (Rajagopal and Bernard, 1993).
- The Western buyers and Chinese suppliers should fit with each other. The inter-partner fit has four dimensions according to Yan and Duan (2003):
- Both parties have good track record on reputation and prior experiences with Chinese suppliers or Western buyers (Arino *et al.,* 2005).
- All case companies will be selected from manufacturing industry. This is because manufacturing has distinct characteristics from service industry.
- Select U.K. based companies only to reduce the error caused by variation of Western cultures (Pirie, 2007).

The research context

The context of this research is the partnership between a Western buyer and a Chinese supplier. Eckhardt (2004) claims that engaging in qualitative business research in China has many challenges. One of the most prominent is gaining a thorough cultural grounding in the lived experience of the people under investigation. To do this, a general understanding of some of the nuances of Chinese culture and psychology is needed. In China, Westerners are often seen as high in the social hierarchy simply by virtue of being from the West, even by business elites. Because of the high social hierarchy of Chinese societies, subordinates do not want to say anything negative about their superiors.

In the case of this research, Chinese informants may not tell me the truth of how they deal with Western buyers. Because of the group orientation of Chinese people, people feel much more comfortable opening up when they are in a group. This could be a method for me to use when interviewing informants from Chinese suppliers.

 Published by Cranfield University Press ISBN: 978-0-9557436-7-2 http://hdl.handle.net/1826/3832

However, it is notable that Chinese psyche is typically very interdependent. Chinese do not want to "offend" others verbally when they are together and tend to consider other's attitude, feelings and actions and then act accordingly. Therefore the focus group method may not work so well (Eckhardt, 2004). It may be better to ask questions that are not linked to specific persons in the group in the focus group and ask sensible questions in the individual interview situation.

China is a high context country. It is difficult for respondents to respond to issues acontextually. Therefore questions have to be couched in context. Being specific is much more appropriate and will lead to meaningful interpretable results (Eckhardt, 2004). Based on my experiences in the pilot study, setting up a scenario for each question may be a good way to deal with Chinese informants.

Eckhardt (2004) argues that China is characterized by holistic thinking, meaning that respondents do not typically speak in the straightforward and logic manner many researchers expect. Thus being flexible in terms of implementation of an interview protocol becomes quite important. A group orientation also implies that if one is a member of the out-group, it is notoriously difficult to break into the strictly defined in-groups in China.

Ideally the local research partner will be fluent in English as well as local language and also a qualitative methods specialist. This helps not only to ensure the smooth

communication during the interview but to assist with the interpretation of the data thanks to the researcher's local cultural background. In this research, it is crucial for the researcher to be an in-group member before getting the "true story" for the adaptation process.

Marschan-Piekkari *et al.* (2004) suggest collecting data in both headquarters and subsidiary unit to avoid "methodological separatism", meaning the tendency to study either headquarters or subsidiary units but not both. It may obscure an understanding of the complexity of the MNCs (Multinational Corporations). The foreign subsidiary unit may have a different perception of the researcher to that held by the headquarters and treat researchers as VIP therefore provide additional interview opportunities. They also recommend that access to a clear diagram showing the organizational hierarchy, reporting lines and business units often facilitates locating appropriate informants for the study. One category of elite interviewees in the MNCs consists of the expatriate specialist or manager. Expatriates often possess large informal networks spanning

Discussion

 Published by Cranfield University Press ISBN: 978-0-9557436-7-2 http://hdl.handle.net/1826/3832

different countries and units and can answer questions from the viewpoint of both headquarters and subsidiary. In this research, expatriate managers are the key informants.

Learning and discussion points

There are some learning points from the pilot study. They are broken down into two categories: those associated with interviews and those associated with research process.

Interviews

Setting up a scenario for each question is a good way to deal with Chinese informants. During the interviews, I have to try very hard to set up such scenarios. For example, I ask them to give me an example of how they adapt to Chinese suppliers.

Respondents do not typically speak in the straightforward and logic manner than I expect. Thus being flexible in terms of implementation of an interview protocol becomes quite important. I have to jump back and forth of the interview questions. It is very easy to miss some questions out if I do not have them in my mind.

I should have allowed the natural flow of the speech by the interviewees. Sometimes I interrupted their speech several times during the interviews, which I feel I should allow them to continue when I did the transcriptions.

I need to develop more experiences on interview, because I felt it is a challenge for me to interview both Chinese and Westerners. The ways dealing with Western informants and Chinese informants are different. Those Westerners based in China are especially difficult to handle in a way that they are not kind to students. I think this is because the competition in China is quite tough for everybody and they also form a different working style in China from the one they work in the West. Westerners based in the U.K. are very nice. Westerners in both U.K. and China are easy to communicate comparing to Chinese and answer my questions frankly. However if I have not built up Guanxi with Chinese, it is very difficult to get any data. It is said that if a Westerners interview Chinese, it is easy for Chinese to open up.

At least one expatriate sourcing manager/director should be interviewed for each case because expatriate managers are the good representative of cultural adaptation of Western firms. There is much less problem for the Chinese staff of the Western firms to adapt to Chinese suppliers.

 Published by Cranfield University Press ISBN: 978-0-9557436-7-2 http://hdl.handle.net/1826/3832

It is anticipated that the interviews to be conducted with Chinese suppliers will be more difficult than those in Western firms since the indigenous Chinese are expected to be more "Chinese" than those in Western firms.

Research process

After the pre-pilot study, I found I should go back to do more literature review on antecedents to partnership performance and adaptation. This is the value of pilot study. Sometimes one will never know what is needed by the practitioners until he or she conducts the field research.

When I did the data analysis, I found coding is one of the most important techniques. I have to go back to interview transcripts again and again to explore the themes and code them. The process is iterative one.

One should know as much information as possible about the case company he/she will investigate before doing interviews. I was blamed by one interviewee that I know little about what they are manufacturing. The experts want to talk to people who understand them well. So the rule of thumb is that getting as much as one can about the company, no matter it is relevant to the research topic or not.

The major limitation of the research is that cross cultural studies require researchers from the cultures being studied to form a collaborative team. It is advantageous to have different interpretation from different cultural perspectives to complement with each other. Easterby-Smith and Malina (1999) argue that the problem for researchers from one culture or context wishing to conduct research on another culture is that the outsiders' past experiences will not have equipped them to make sense of events in the same way that insiders would. No one researcher can be an insider in multiple cultures. The fact that I have been studying and working in the U.K for four and half years or so to some extent helps me understand Western culture. In another hand, my supervisor and PhD review panel are from Western cultural background and can also to some extent compensate the lack of field investigators from Western cultural background. However as the only field investigator of this research, I lose the chance of discussing with co-investigators, which is a very important stage of a reflective process.

Another limitation is the research design. It is best to do a longitudinal study to answer the research questions. However first of all it may takes 2-3 years for a relationship to enter the stage of

Discussion

 Published by Cranfield University Press ISBN: 978-0-9557436-7-2 http://hdl.handle.net/1826/3832

commitment, it is not feasible to implement as a PhD project. What I will do is to do a retrospective study, which asks informants to recall what happens in the past of the relationship. The limitation of this method is that I may not get the information I want since the high employee's turnover in China. People who negotiated with suppliers quite often move to other companies therefore the information for that period is not retrievable.

Is it necessary to select U.K. based companies only or I can select MNCs based in the West for the Western firms of the partnership? For example, I have got access to Volvo (Shanghai IPO), Sweden's scores are very similar to the U.K. in terms of Hofstede's five dimensions, and can I use it as a case company?

References:

1. Arino, A., De la Torre, J. and Ring, P.S. (2005), "Relational quality and inter-personal trust in strategic alliances", *European Management* Review, Vol. 2, pp. 15.
2. Boisot, M. and Child, J. (1999), "Organizations as adaptive systems in complex environments: The case of China", *Organization Science,* Vol. 10, pp. 237.
3. Easterby-Smith, Mark and Malina, Danusia. (1999), Cross-cultural collaborative research: Toward reflexivity. *Academy ofManagement Journal* 42(1), 76.
4. Eckhardt, G. M. (2004), "The role of culture in conducting trustworthy and credible qualitative business research in China", in Marschan, P.R. and Welch, C. (Eds.), *Handbook of Qualitative Research Methods for International Business,* Edward Elgar Publishing, U.K. and USA.
5. Ellram, L.M. (1996), "The use of the case study method in logistics research", *Journal ofBusiness Logistics,* Vol. 17, pp. 93.
6. Ghauri, P. (2004), "Designing and conducting case studies in international business research", in Marschan-Piekkari, R. and Welch, C. (Eds.), *Handbook of Qualitative Research Methods for International Business,* pp. 109-124, Edward Elgar Publishing, UK and USA.
7. Lin, X.H. (2004), "Determinations of cultural adaptation in Chinese-U.S. joint ventures", *Cross Cultural Management,* Vol. 11 No. 1, pp. 35.
8. Marschan, P.R. and Welch, C. (2004), "Qualitative research methods in international business", in Marschan,P.R. and Welch, C. (Eds.), *Handbook of Qualitative Research Methods for International Business,* Edward Elgar Publishing, U.K. and USA.
9. Marschan-Piekkari, R., Welch, C., Penttinen, H., and Tahvanainen, M. (2004), Interviewing in the Mutinational Corporation: Chanllenges of the Organizational Context. Marschan-Piekkari, R. and Welch, C. *Handbook of Qualitative Research Methods for International Business.* U.K. and USA, Edward Elgar Publishing.
10. Pirie, M., 2007. The Anglo-Saxon model of capitalism.
11. Powell, W.W. (1998), "Learning from collaboration: Knowledge and networks in the biotechnology and pharmaceutical industries", *California Management Review,* Vol. 40 No. 3, pp. 228.

 Published by Cranfield University Press ISBN: 978-0-9557436-7-2 http://hdl.handle.net/1826/3832

12. Rajagopal, S. and Bernard, K.N. (1993), "Globalization of the procurement process", *Marketing Intelligence & Planning,* Vol. 11, pp. 44.
13. Yan, A. and Duan, J. (2003), "Interpartner fit and its performance implications: A four-case study of U.S.-China joint ventures", *Asia Pacific Journal ofManagement,* Vol. 20, pp. 541.
14. Yin, R. (2003), *Case study research: design and methods,* 3rd Ed., Sage, London.

Discussion

 Published by Cranfield University Press ISBN: 978-0-9557436-7-2 http://hdl.handle.net/1826/3832

Development of an Immunosensor for the detection of *Salmonella typhimurium*

F. Salam and I.E. Tothill
Cranfield Health, Cranfield University, Silsoe, Bedfordshire, MK45 4DT, UK
f.salam.s06@cranfield.ac.uk
i.tothill@cranfield.ac.uk

Introduction

Salmonella serotypes are among the most common bacteria responsible for foodborne gastroenteritis. In the United States approximately 76 million food-borne illnesses resulting in 5000 deaths have been reported (Mead *et. al.,* 1999). The World Health Organization (WHO) reports that salmonellosis caused by Salmonella sp. is the most frequently reported food-borne disease worldwide (Schlundt, 2002). The two most commonly found types of salmonella are Salmonella typhimurium and Salmonella enteritidis (Schlundt, 2002). In addition to the problem of food-borne illness, losses due to microbial spoilage and contamination in food and agricultural products usually have a significant economical impact on the country producing these products. At present many of the currently used methods of detection are time consuming. Food safety and quality management is crucial in production and distribution of food products. In order to avoid the sale of contaminated products, expensive inventories are held at the production site while samples are tested for microbial contamination, which often takes more than 3 days. Since the food products have a short shelf life, they are released before microbial results are available. Rapid detection of pathogens, spoilage microorganisms and other microbial contaminants in foods is critical to ensure the safety of consumers and quality of the food (Oliver *et al,* 2007).

Different methods have been developed and are used for the detection of Salmonella spp. Conventional culture methods for detection of Salmonella in foods involve blending of the food product in a non-selective medium to increase the population of the target organism, followed by plating onto selective or differential agar plates to isolate pure cultures (June *et al.,* 1996). Phenotypic analysis or metabolic markers detection is then conducted to examine the cultures. A major drawback in these techniques is that these methods are labor-intensive, and take 2–3 days to receive the results and up to 7–10 days for confirmation (June *et al.,* 1996). Enzyme-linked immunosorbent assays (ELISA),

 Published by Cranfield University Press ISBN: 978-0-9557436-7-2 http://hdl.handle.net/1826/3832

though faster than the conventional culturing methods, still take up to 3 h. (Schneid, *et al.,* 2006). Although recently more rapid and specific immunological assays and methods based on nucleic acid probes and polymerase chain reaction (PCR) have been used, the total time frame is still several hours and requires trained personnel (Mozola, 2006). Recent developments make microbial detection and identification faster, more convenient, more sensitive and specific with novel biosensors technologies. These technologies come with unique capabilities for direct, sensitive and real-time detection. Biosensors are analytical instruments possessing a capturing biological molecule as a reactive surface in close contact to a transducer, which converts the binding of the analyte to the capturing molecule into a measurable signal (Tothill & Turner, 2003). The use of biosensors for microbial detection is very appealing especially when the sample is minimally processed and detection is carried out in real-time or near real-time. Real-time detection of pathogenic contaminants is important because it provides immediate interactive information regarding the sample being tested and enabling food facilities to take corrective measures before the product is released for consumption.

This paper focuses on the development of an electrochemical immunosensor for salmonella analysis. Electrochemical immunosensors present the advantages of sensitivity and selectivity inherent to the use of immunochemical interactions (Tothill, 2003). In these applications, catalysis of substrates by an enzyme conjugated to an antibody produces products such as ions, pH change or oxygen consumption. These products are capable of generating electrical signal on a transducer. In this work a sandwich ELISA format was developed where the capture antibody was immobilized to the gold electrode surface (mouse monoclonal antibody with physical absorption on the gold surface working electrode). A second antibody conjugated to an enzyme marker is used as the detection antibody which will recognise the captured antigen. The detection of the enzyme is then conducted using an electrochemical system. The reduction of an electroactive species (an electron transfer mediator) in the presence of a substrate for the enzyme takes place. In this format, the enzyme horseradish peroxidase (HRP) was conjugated to a second antibody (rabbit polyclonal antibody against Salmonella). The electron transfer mediator used is 3,3',5,5'-tetramethylbenzidine (TMB) and it's a preferred mediator for amperometry determination of HRP activity. TMB has been

 Published by Cranfield University Press ISBN: 978-0-9557436-7-2 http://hdl.handle.net/1826/3832

reported to be a good mediator for the electrochemical detection of low levels of HRP when TMB-H_2O_2 is used as the substrate system (Volpe *et al.,* 1998). The concept of the developed electrochemical immunosensor system for Salmonella detection is illustrated in Figure 1.

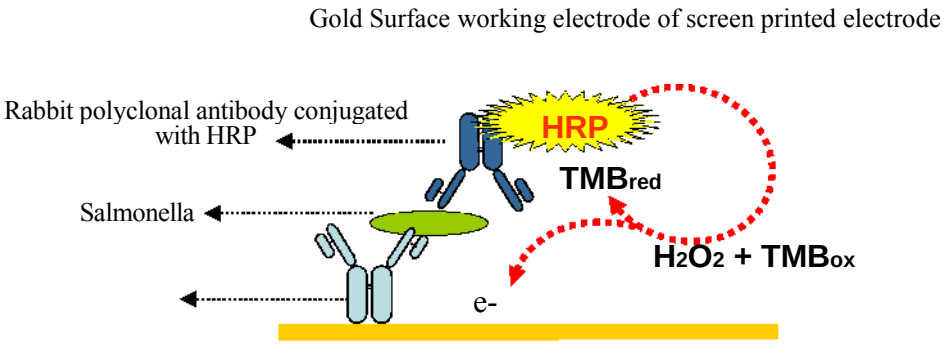

Figure 1: The sandwich assay format conducted on the gold electrode surface. The capture antibody is immobilised on the gold electrode surface. The sample is then added followed by the detection antibody (antibody-conjugate). The current generated through the TMB-H_2O_2 system and is proportional to the amount of HRP conjugate bound to the Salmonella cells captured by the immobilised antibody.

Results and discussions

The first approach applied in the development of the immunosensor was to use physical immobilization of the mouse monoclonal antibody (Abcam Ltd, UK, against lipopolysacaride of *Salmonella typhiumurium)* with optimal concentration of 25 □g mL^{-1} coated on the gold working electrode followed by the addition of heat kill Salmonella cell (10^1 to 10^7 CFU mL^{-1}) and rabbit polyclonal antibody-HRP conjugate (IgG-HRP) at 250 □g mL^{-1}. The mixture of TMB and $_{H2O2}$ in citrate-phosphate buffer in 0.1M KCl was added to the sensor surface and the change in current was observed versus time for different Salmonella cell concentrations at a constant current of -200mV (*vs* Ag/AgCl) using GPES AUTOLAB software (Figure 2). Figure 3a showed chronoamperometry measurement at -200mV for each concentration of *Salmonella typhimurium* standard using physical absorption of mouse monoclonal antibody on the gold sensor surface. Figure 3b, demonstrate an increase in signal with increasing Salmonella cells number and the detection limit was determined at 100 cell mL-1.

 Published by Cranfield University Press ISBN: 978-0-9557436-7-2 http://hdl.handle.net/1826/3832

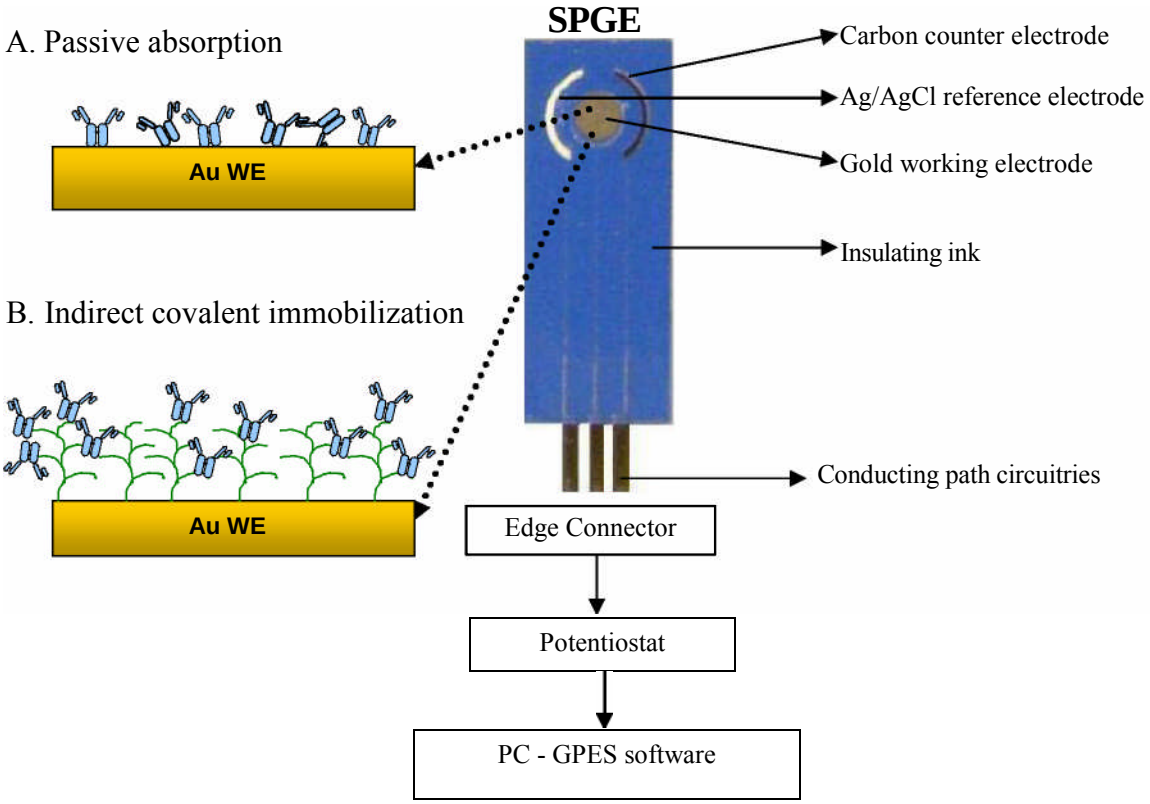

Figure 2: Schematic diagram of the antibody immobilization using the fabricated Screen Printed Gold Electrode in the development of immunosensor for *Salmonella typhimurium.*

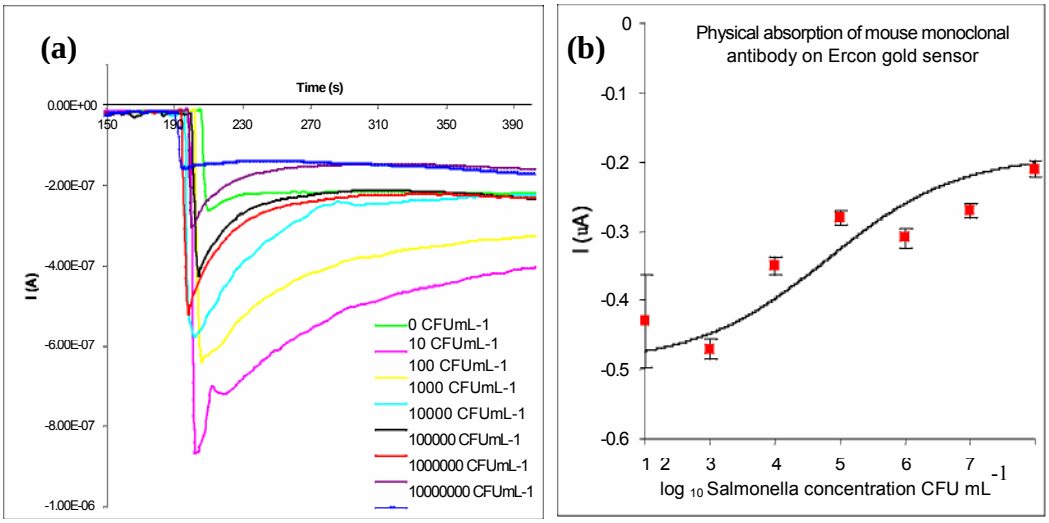

Figure 3: Direct ELISA format was applied in the electrochemical immunosensor for Salmonella detection (a) Chronoamperometry measurement at -200mV vs Ag/AgCl for each of Salmonella concentration from 10 to 10^7 CFU mL^{-1}, CFU=Colony Forming Unit (b) Current (I, μA) versus Salmonella concentration, measurement taken after 250s, error bar = standard deviation, n=3, CV=12.07%

 Published by Cranfield University Press ISBN: 978-0-9557436-7-2 http://hdl.handle.net/1826/3832

Using physical absorption method for antibody immobilization, the attachment of the antibodies is random on the sensor surface and the correct orientation of the binding sites cannot be controlled. The adsorption is non-specific and the biosensor performance is seldom very good.

To enhance the sensitivity of electrochemical immunosensor, covalent antibody immobilisation using amine-coupling via carboxy-methyldextran was carried out. The main target for this approach is to lower the background current or to decrease the nonspecific binding. This was achieved by immobilising carboxy-methyldextran on the gold surface which can also help in preventing non-specific binding of the antibody-HRP conjugate. At the same time this will increase the surface sensitivity by increasing the antibody binding to carboxy-methyldextran which will lower the detection limit. Figure 4, shows chronoamperometry measurement at -200mV potential for each concentration of *Salmonella typhimurium* standard using covalent immobilization of mouse monoclonal antibody on the gold sensor surface. An increase in the current is achieved with increasing the cell concentration and the detection limit was determined at 50 CFU mL^{-1}.

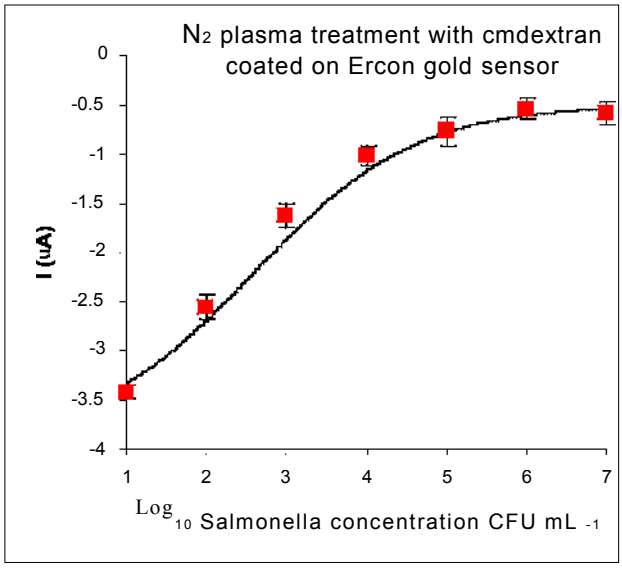

Figure 4: Direct ELISA format with covalent immobilization of mouse monoclonal antibody via amine coupling with CM-Dextran was applied in electrochemical immunosensor for Salmonella detection from 10 to 10^7 CFU mL^{-1}, CFU=Colony Forming Unit. Salmonella standard plot, Current (I, μA) versus Salmonella concentration, measurement taken after 200s, error bar = standard deviation, n=3, CV=6.04%

 Published by Cranfield University Press ISBN: 978-0-9557436-7-2 http://hdl.handle.net/1826/3832

This figure showed that the sensitivity was increased and better detection limit can be achieved using this method. Therefore, covalent antibody immobilization will be used in future works. Further optimisation of the assay system will also take place to increase the sensitivity of the immunosensor.

Conclusion

We have demonstrated a promising approach for Salmonella detection using an electrochemical immunosensor based on the immobilization of antibodies via covalent bonding with carboxymethyldextran on gold substrates. This gives rapid and sensitive sensing system for on-site analysis. The work is in progress and further optimization and sample analysis need to be conducted in future work.

References

1. June, G. A.; Sherrod, P. S.; Hammack, T. S.; Amaguana, R. M.; Andrews W. H. Relative effectiveness of selenite cystine broth, tetrathionate broth, and rappaport-vassiliadis medium for recovery of Salmonella spp. from raw flesh, highly contaminated foods, and poultry feed: Collaborative study. J. AOACInt. 1996, 79 (6), 1307-1323.
2. Mead, P.S., Slutsker, L., Dietz, V., Mccaig, L.F., Bresee, J.S., Hapiro, C., Griffin, P.M. and Tauxe, R.V. (1999). Food related illness and death in the United States. Emerg. Infect. 5, 607–625.
3. Mozola M. A. Genetics-based methods for detection of Salmonella spp. in foods. J. AOACInt.2006, 89 (2), 517-529.
4. Olivier Lazcka, F. Javier Del Campo, F. Xavier Mu˜noz (2007). Pathogen detection: A perspective of traditional methods and biosensors Biosensors and Bioelectronics 22 (2007) 1205–12 17
5. Schlundt, J. (2002). New directions in foodborne disease prevention. Int. J. Food Microbiol. 78, 3–17
6. Schneid, A. D.; Rodrigues, K. L.; Chemello, D.; Tondo, E. C.; Ayub, M. A. Z.; Aleixo, J. A. G. Evaluation of an indirect ELISA for the detection of Salmonella in chicken meat. Braz. J.Microbiol. 2006, 37 (3), 350-355.
7. Tothill, I.E., Turner, A.P.F., (2003), Biosensors. Encyclopaedia of food sciences and nutrition (second edition), 489-499, ISBN 0-12-227055-X.
8. Tothill, I.E (2003). On-line Immunochemical Assays for Contaminants Analysis, In: Rapid and on-line Instrumentation for Food Quality Assurance, Ibtisam E. Tothill (Editor). Woodhead Publishing Limited, ISBN: 1-85573-674-8.
9. Volpe, G., Draisci, R., Palleschi. G., Compagnone. D., (1998), 3,3 ,5,5 - Tetramethylbenzidine as electrochemical substrate for horseradish peroxidase based enzyme immunoassays. A comparative study. Analyst. 1303-1307.

 Published by Cranfield University Press ISBN: 978-0-9557436-7-2 http://hdl.handle.net/1826/3832

Analysis and Synthesis of the Identity Problem

by Rebecca Gauci-Maistre, PhD Candidate, Cranfield University DCMT

Introduction

Research into Identity Management Systems (IdM S) development led to the deduction that it was not the 'traditional systems development lifecycle' that was encountering obstacles per se, but the understanding of the problem situation which eventually shapes that same SDLC. The research became focused within the research cloud of the 'problem space' (fig 1 below), and results will be applied to an architectural framework within the 'solution space'. Several traditional development lifecycle methodologies were too restrictive for the particular research and a more flexible approach that allowed primary focus to be on discovery, without hindering iteration or application of knowledge directly to the design stage was required. Challenges of IdMS Identity management systems are a specific form of information systems that process data pertaining to the identity of a human being, and therefore held in a sensitive view by users, governed by state regulations and other standards, in addition to providing a service to all stakeholders (owners to users); and without becoming an obvious intervention during communication with the system within which it is embedded (e.g, the Oyster Card within the London transport system). All information systems may be regarded as meta-systems, that is, a series of collaborative systems communicating to produce the results required. Every factor, agent, or view-point within these systems are information systems themselves. Fig 5 depicts the 11 elements of an IdMS, as well as impact directionality, and herein lies the importance of understanding the problem space. IdMS elements range from law to security to organizational culture, and each is a discipline rather distinct from the other. It is a very rare occasion where there is a project manager expert in all disciplines, and that lack of knowledge could become the Achilles' heel of the project, leading to several issues later in the system's life, such as lack of compliance, flaws in security or lack of user uptake, potentially resulting in serious situations for the system stakeholders.

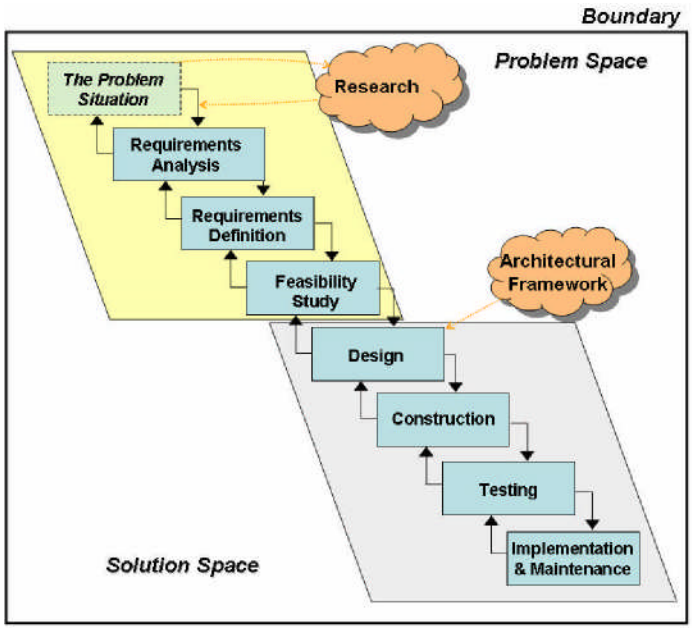

Figure 1 Problem space vs Solution space

Analysis and synthesis of the identity problem

Allen and Varga explain that "each agent has their own. . epistemology, which is their. . IS, and is wider than the IT systems they use. The IS of each agent co-evolves by interaction with other agents, based on the agent's view of reality"[i]. Thus, an IdMS could also be classified as a form of complex systems. Despite

 Published by Cranfield University Press ISBN: 978-0-9557436-7-2 http://hdl.handle.net/1826/3832

there being a lack of consensus, scholars agree that complex systems comprise a number of entities, which in their own right may not fall into the same discipline as each other or as the whole they collaboratively produce. It is clear that true complexity modelling, falls somewhere in between the extremes of the "science spectrum", and is a compromise between very hard science and very soft philosophy. Figure 2 attempts to define the complexity 'space' on (what the author terms) the science spectrum.

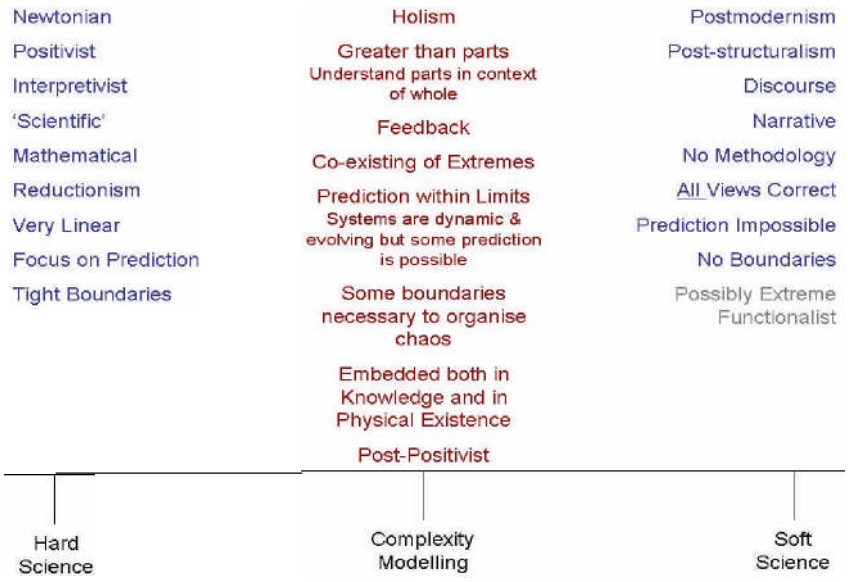

Figure 2 Complexity falls in between the hard and soft sciences

Allen and Varga are clearly in agreement, stating that "complexity science concerns both the nature of the systems and the nature of its interpretation. It is about both ontology and epistemology."[ii]

If one then considers the Functionalist and Interpretivist paradigms of the Burrell and Morgan's Paradigm Matrix[iii], and their potential joint evolution into Pragmatism, one may deduce that complexity falls squarely into the latter domain of thought.

This is the contention that dominance of a single paradigm does not fully reflect the "multifaceted nature of social, organisational, and phenomenological reality."[iiv] It encourages "methodological pluralism - a diversity of methods, theories and even philosophies"[iv]. The argument for this is that a combination of methodologies will lead to 'holism', or what Peter Checkland calls "Holon", meaning whole in a complete or holistic sense, and it is evident from the above discussion that these are also the issues put forward by complexity science.

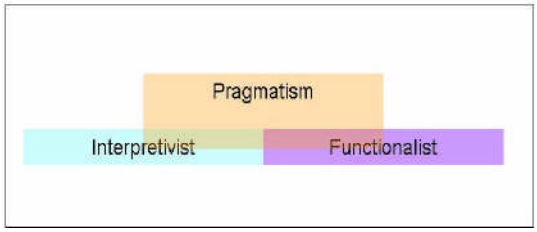

Figure 3 A relative view of pragmatism in relations to the lower portion of the Paradigm Matrix

However, Pragmatism is somewhat subjective in itself. With reference to the above diagram, the

 Published by Cranfield University Press ISBN: 978-0-9557436-7-2 http://hdl.handle.net/1826/3832

Pragmatism block could easily move up, down, left or right. This would depend very much on the practitioner's previous grounding. For example, if one is more firmly grounded in the Interpretivist approach, then the Pragmatism block would move substantially to the right and possible further down. Conversely, if the grounding is more Functionalist with a distinctive awareness of Interpretivism, then the Pragmatism block will move to the right and upwards. A "Pragmatic Idealist"[vi] would attempt to place themselves in the domain as depicted above.[1]

Carson and Flood describe the pragmatic approach as "a single container in which all methodologies are stored."[viii] The pragmatist, they argue, will use a mixture of tools to provide a diversity of ways to deal with problems and problematic situations, without being constrained to using tools specifically attributed to a particular method or methodology. However, they describe 'critics' concern' with the heuristic approach of pragmatism, and have created a "complementarist approach", which is "critical systems thinking and the practical output."

Total Systems Intervention (TSI) was discounted as being suitable for the author's current research for several reasons, and was further affirmed by Flood, who maintains that TSI is a meta-methodology, and that all problem-solving methods are complementary, where the key is to "get problem solvers to 'choose' the best methods to deal with the problems taking circumstances into account"[vii].

Pragmatism endorses the use of multiple methodologies to reach the intended goal. Figure 4 is the author's broad representation of this issue. The use of soft systems methodology in conjunction with complexity theory and architecture design is a demonstration of this.

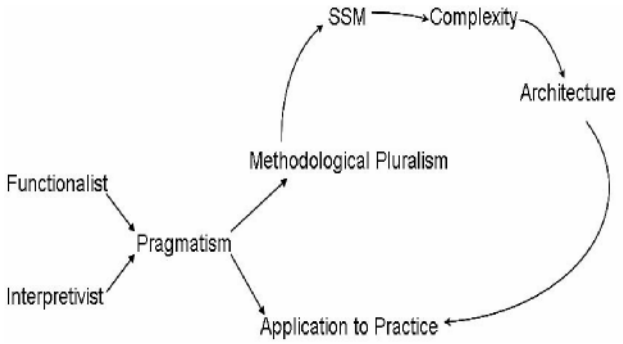

Figure 4 An overview of the application of pragmatism

The application of SSM in this research is as a learning tool. Especial merit is given to the concept of "world-views" in discovering the pertinent elements of an IdMS, and then using the rich picture concept. This process assisted in determining the 'bigger picture' of an IdMS, which, as stated, had become the focus of the research. Later, conceptual modelling (and possibly Entity-Relationship Modelling) to investigate the relationships and inter-play between them. Holism is imperative in IdMS development because most systems exist as a layer, and not in isolation. The implementation of several identity-related ah-hoc systems tends to create

more complexity and less stability for the owning enterprise, and in the long term could potentially defeat the purpose they were implemented for.

1 This field is heavily dominated by the work of Charles Pierce (Pragmatic Maxim).

 Published by Cranfield University Press ISBN: 978-0-9557436-7-2 http://hdl.handle.net/1826/3832

Beyond this point, SSM as such was no longer as constructive since the product of this research will not attempt to create a 'radical change' (or 'bettering') solution to the system itself, but to the manner in which a system is developed and implemented. That is, the aim is to provide a deeper *understanding* of the problem space that will then prove beneficial to system *developers.* Thus, at this stage complexity modelling becomes a more appropriate method. Understanding factor dependencies, for example such as in hardware and software, and their interactions (cumulatively known as coupling) should be one of the major aims of this phase of such research (see fig. 1 for overview). Moreover, complexity theories and modelling will also achieve a better understanding of the "organisation and behaviour that may occur when elements are related." [viii] It is important to note here, that the term "organisation" indicates the systemic order and not the enterprise. Whilst understanding the enterprise in which the system is living is vital (factors such as culture, policies and the environment) to the successful investigation, development and implementation of a system, it is necessary to be very clear on the distinction between those two very different definitions. These distinctions should be painstakingly defined within the discovery stage, and become the 'language', so to speak, of the remainder of the project. Figure 5 provides an example of these distinctions and the need for the move into complexity modelling.

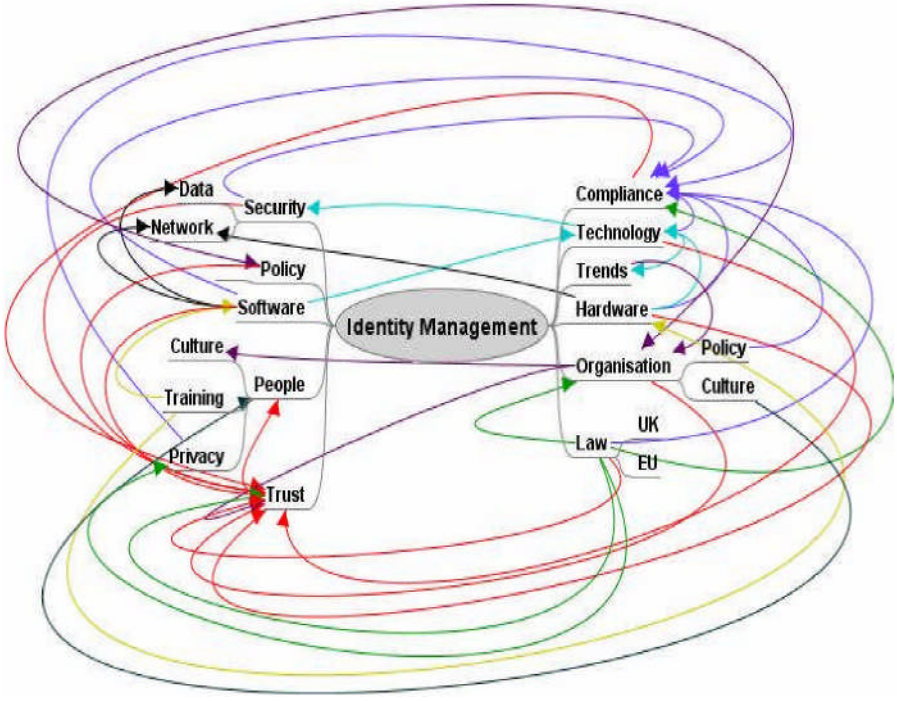

Figure 5 An attempt at obtaining a holistic view of IdMS

In order to provide *knowledge* to the problem space, a combination of qualitative and quantitative studies would be required. These would vary depending on the type of system being explored. Using tools such as questionnaires could provide some weighting for some agents, but it is not always possible to weight agents. How does one, for example, place a value of culture, or similar 'people issues'? To compensate, allowing for feedback in the questionnaires and conducting interviews can broaden understanding further. For the current research, a combination of 'top-down' and 'bottom-up' approaches are being used. After questionnaires with feedback space are completed by several system users, system managers, developers and owners, possibly even administrators are interviewed. These 'top-side' interviews provide 3 very different perspectives of the system's requirements and usage-expectations, and conducting the interviews with the knowledge of the questionnaires provides the ability to uncover potential discrepancies that may result in 'agent adversaries'. The 'bottom-side' users are also split into two camps, the users and non-users, and users are further split into the full-time and part-time users. These 3 differ

 Published by Cranfield University Press ISBN: 978-0-9557436-7-2 http://hdl.handle.net/1826/3832

substantially from each other and have provided interesting knowledge for the understanding of the problem space.

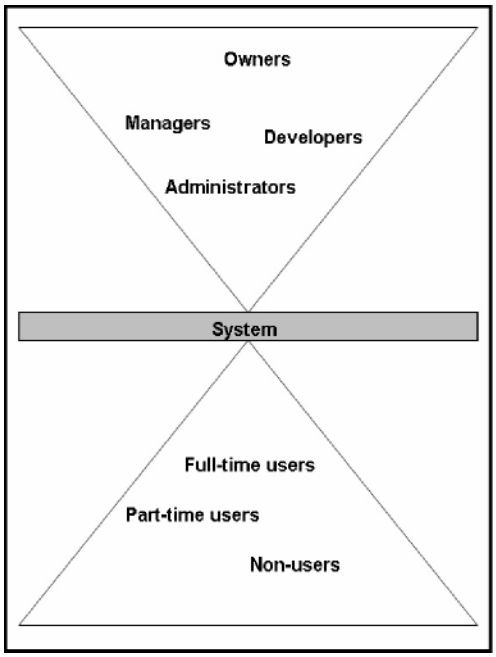

Figure 6 An overview of how the case study is being conducted

This variety of analysis would benefit substantially from what Weinberg (ref) terms a “systems synthesist”. This is not necessarily one person who knows all there is to know about the systems, environment, and with an in-depth knowledge of each and every factor, but more appropriately an attempt to be an unbiased chair-person cum project manager. Weinberg explains how a synthesist shouldn’t be biased to one world-view or another, and whose primary duty is to “circumscribe the affecting and affected factors”. One would also be assigned the task of creating very specific action plans from the conception of the lifecycle, and carry the role right through until the implementation so as to be able to assist in any adjustments that may be required due to a changing reality through their knowledge of environment politics, communication procedures, economics of information, and so on. Weinberg proposes the role of synthesist as he is aware that it is impossible to be a systems theorist, but merely one who adopts a general systems approach. That is, one can not be completely unbiased, but merely attempt to be.

It is indeed the case that the research project had to be drastically scaled-down so as to fit in with the constraints provided, and remain as balanced as would benefit the analysis. This made the necessity for a synthesist on a larger-scale project even more apparent, and Weinberg’s theories draw close parallels to the pragmatic and complexity approaches, which in turn, made

the term and role of synthesist even more appropriate than the varied terms of systems analyst and/or investigator. Those are actually different roles entirely, though of no lesser importance. Finally, the previous

 Published by Cranfield University Press ISBN: 978-0-9557436-7-2 http://hdl.handle.net/1826/3832

stages, overseen by the synthesist, will provide results which will be of direct use to the system developers, providing a more profound view of complimentaries and adversaries, politics, usage and so on. One possible product may be an architectural framework for the solution phase.

Conclusion

A fundamental understanding of the intricate mechanisms of a system requires a careful study of the problem space, and in turn necessitates the role of a systems synthesist. Identity management systems are particularly sensitive as they process data pertaining to the identification of a human being – a human being entitled to privacy, data protection and so on. Additionally, IdMS must appeal to the aimed users, comply with several laws, comply with standards that increase reliability and trust, ensure adequate security, portray said security appropriately, and many, many other tasks that range across a spectrum of disciplines that cannot be managed by one 'expert'. Adopting a pragmatic approach allows the implementation of a variety of methods that are more suitable to the project in-hand. This emphasises that whilst there is no one formula for an SDLC, the history and 'holistic' knowledge of the problem space will provide a solid foundation for any methods or 'methodologies' applied during the solution space.

References

i Allen, P., Varga, L. (2006) Social and Economic Complexity: The co-evolution of Reality, Knowledge and Values. Presented in session Social and Economic Systems 2 during ECCS06, Oxford.
ii Allen, P., Varga, L. (2006) A co-evolutionary complex systems perspective on information systems. Journal of Information Technology 00, 1–10. JIT Palgrave Macmillan Ltd.
iii Burrell, G. & Morgan, G. (1979) Sociological paradigms and Organisational analysis. London. Heinemann
iv Goles T.& Hirschheim R. (2000) The paradigm is dead, the paradigm is dead...long live the paradigm: the legacy of Burrell and Morgan. USA: Elsevier Science
v Landry, M., Banville, C. A., In: Goles T.& Hirschheim R. (2000) The paradigm is dead, the paradigm is dead...long live the paradigm: the legacy of Burrell and Morgan. USA: Elsevier Science
vi Lewis, D. (2004) Operation Certain Death. UK: Century
vii Flood, R.L. (1995) An improved version of the Process of Total Systems Intervention (TSI). Systems Practice Vol 8 No 3
viii Flood, R. L., Carson E. R., (1993) Dealing with Complexity (2nd edition). New York: Plenum

 Published by Cranfield University Press ISBN: 978-0-9557436-7-2 http://hdl.handle.net/1826/3832

The properties of tapered optical fibres with nanostructured coatings

R. Jarzebinska[a], C. S. Cheung[a], S. W. James[a*], G. J. Ashwell[b] and R. P. Tatam[a]

[a]Engineering Photonics Group, School of Engineering, Cranfield University, MK 43 0AL, UK

[b]School of Chemistry, Bangor University, Bangor, Gwynedd, LL57 2UW, UK

ABSTRACT

The influence of nanostructured coatings on the transmission spectrum of the tapered fibres has been analysed and exploited to demonstrate an optical fibre chemical sensor.

Keywords: tapered optical fibre, nanocoating, Langmuir Blodgett

INTRODUCTION

The coating of optical fibres with nanomaterials that change their optical properties in response to an external stimulus offers an exciting new platform for the development of chemical sensors. Nanostructured coatings may deposited onto optical fibre devices using the electrostatic self-assembly [1], Langmuir Blodgett [2] and dip coating [3] techniques. A number of means for facilitating the interaction of the light propagating within the optical fibre with the nanostructured coating have been investigated. Coating may be deposited onto the end face of the optical fibres to create Fresnel interferometers [4], onto side polished optical fibres to create coupled waveguide structures [5], or onto optical fibre grating based core-cladding mode coupling devices, such as long period gratings [2,3,6], tilted fibre Bragg gratings [7] and tapered optical fibres [8]. Sensors for pH [5], copper [9], humidity [1] and chloroform [10] have been demonstrated using these approaches [11].

Tapered optical fibres facilitate a strong interaction between the coating and the propagating modes of the fibre. Tapering allows the evanescent field of the propagating mode to penetrate into the surrounding environment and thus to interact with the coating, with the proportion of the power in the evanescent field increasing with decreasing diameter of the tapered region.

A biconical fiber taper consists of a conical segment where the diameter of the fibre decreases, a taper waist section with uniform diameter and a second conical segment where the fibre diameter increases. The optical properties of the fibre taper are influenced by the taper angle and by the diameter of the taper waist. The taper waist determines the number of modes that may propagate

 Published by Cranfield University Press ISBN: 978-0-9557436-7-2 http://hdl.handle.net/1826/3832

within the tapered region, where the core may be considered to be the silica fibre and the cladding is formed by the surrounding medium. The taper angle controls the coupling of light between the propagating mode of the single mode fibre and the modes of the tapered section. For small taper angles the coupling is adiabatic, such that there is little loss from the $_{LP01}$ mode of the single mode fibre over the conical tapering region by coupling to higher order modes of the tapered region [12]. This is an important consideration in the fabrication of tapered fused couplers.

In a non-adiabatic taper, the $_{LP01}$ mode of the single mode fibre may couple to the numerous modes of the tapered waist that exists because of the high index contrast between the silica and the surrounding medium. In general, this coupling occurs only to the $_{HE11}$ ^{and} HE12 modes of the tapered waist [13, 14]. These two modes propagate, with different effective refractive indices, to the end of the tapered waist, and then will couple back to the $_{LP01}$ mode of the fibre through the second conical region. As a result of their different propagation constants the coupling will also result in interference between the modes, which is observable as a channeled spectrum. This effect has been used previously to demonstrate sensors for temperature and surrounding refractive index, based upon the differential response of the two modes of the tapered region [14]. In this paper the response of the transmission spectrum of a non-adiabatic tapered optical fibre of taper diameter 5 □m to the deposition of a nanostructured coating is reported, and its use as a pH sensor demonstrated.

EXPERIMENT

Tapering a single-mode optical fiber involves the reduction of the cladding diameter by heating a section of the fibre and pulling the fibre's ends. In these experiments, the heat source used was a gas burner containing a butane (65%) / propane (3 5%) mixture. The burner was equipped with a nozzle enabling manual flame control. The size of a flame was ~6mm. During the tapering process both ends of a fibre were attached to rotation stages which were set to rotate in opposite directions to pull the fibre with constant velocity of 30μm/s. The tapers were formed in an optical fibre with a cut-off wavelength of 635nm (Fibercore SM750). The transmission spectrum of the optical fibre taper was recorded by coupling the output from a tungsten-halogen lamp into the fibre, and analyzing the transmitted light using a fibre coupled CCD spectrometer.

The evolution of the transmission spectrum in response to increasing coating thickness was investigated by depositing a film of 4-[2-(4-dimethylamino-naphthalen- 1 -yl)-vinyl] -1 -octadecyl-

 Published by Cranfield University Press ISBN: 978-0-9557436-7-2 http://hdl.handle.net/1826/3832

quinolinium iodide using the Langmuir-Blodgett (LB) technique [11]. This material is known to change its absorption spectrum and thus refractive index when protonated, and thus may be used for pH measurement. The LB technique facilitates deposition of the material one molecular layer at a time onto a substrate. A chloroform solution of the iodide salt (0.1 mg mL^{-1}) was spread onto the pure water subphase of one compartment of a Nima Technology LB trough. The deposition was carried at a surface pressure of 26 m Nm^{-1} and a transfer rate of 8 mm min^{-1}. The fibre containing the taper was positioned vertically so its long axis was aligned with the dipping direction and was alternately raised and lowered through the floating monolayer at the air–water interface to deposit the coating. Transmission spectra were recorded after the deposition of each monolayer, with the taper below and above the water subphase for alternate layers.

RESULTS AND DISCUSSION

3.1 5□m diameter fibre taper

The transmission spectrum of the 5□m diameter fibre taper is shown in figure 1. The sinusoidal channeled spectrum indicates that this taper is non-adiabatic.

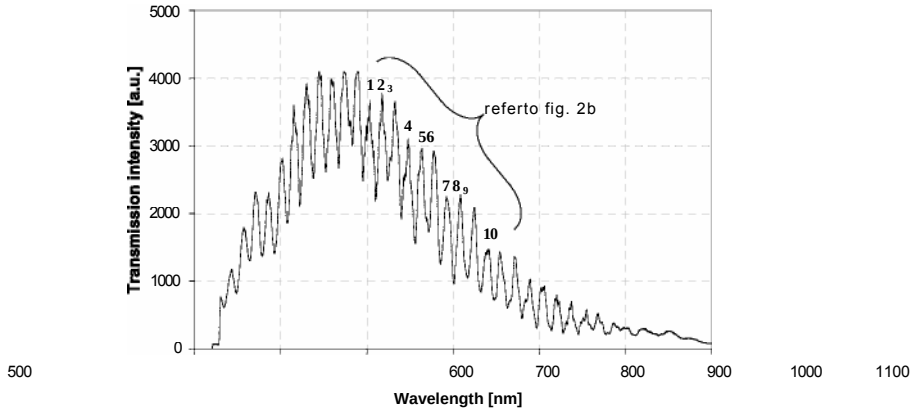

Fig. 1. The transmission spectrum of the 5□m diameter fibre taper, without coating. The sinusoidal channeled spectrum indicates that this taper is non-adiabatic. (Labeling numbers refer to fig. 2b.)

The response of the transmission spectrum to the deposition of the nanostructured coating is shown in figure 2 (a) and (b), where the wavelengths of the channeled spectrum features can be seen to vary with increasing coating thickness. The visibility of the spectrum was observed to decrease and the

 Published by Cranfield University Press ISBN: 978-0-9557436-7-2 http://hdl.handle.net/1826/3832

attenuation of the spectrum increase for coating thicknesses of 100 bilayers. The channeled spectrum reappears as the coating thickness increases further, but with reduced visibility.

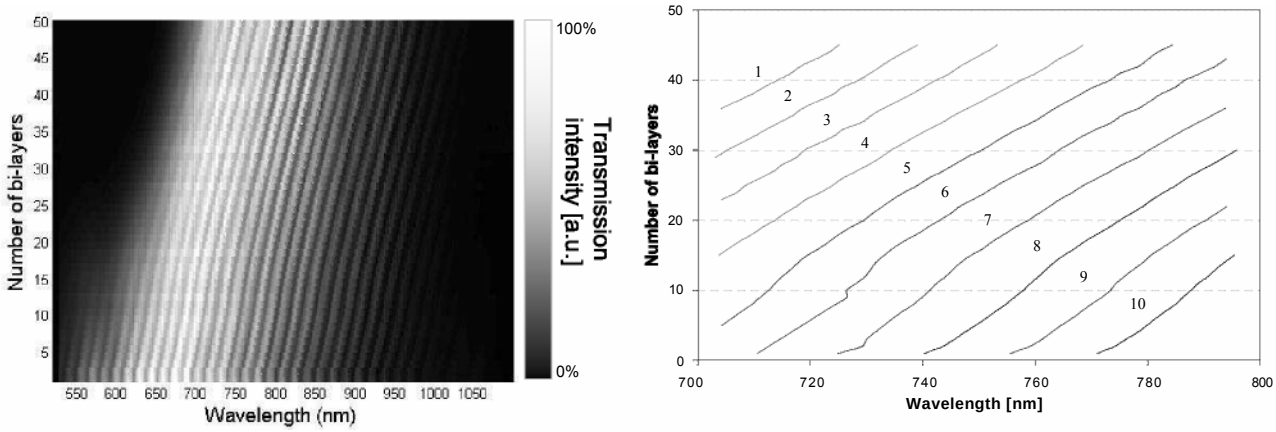

(a) (b)

Fig. 2. (a) Evolution of the transmission spectrum of a 5 □m diameter fibre taper in response to an increase in the nanocoating thickness, (b) plot of the wavelength shift of a selection of the spectral features as a function of the number of coating bilayers. (Line labels: 1-10 correlate with features in fig. 1.)

The change in wavelength of the channeled spectrum features in response to increasing coating thickness is a result of a differential change in the propagation constants of the two modes of the tapered region, which can be predicted using a simple slab waveguide approximation for the tapered region. As the film thickness increases it acts as a waveguide. The reduction in visibility and disappearance of the channeled spectrum may be a result of increased attenuation of one of the modes, which may occur and the mode of the tapered region is phase matched to a mode of the overlay waveguide. This is the subject of current investigation.

To characterise the pH sensitivity, the tapered fibre with a 60nm thick coating of 4-[2-(4- dimethylamino-naphthalen-1 -yl)-vinyl] -1 -octadecyl-quinolinium iodide was immersed in of buffer solutions within the pH range 3-11. The results are shown in Figure 3.

 Published by Cranfield University Press ISBN: 978-0-9557436-7-2 http://hdl.handle.net/1826/3832

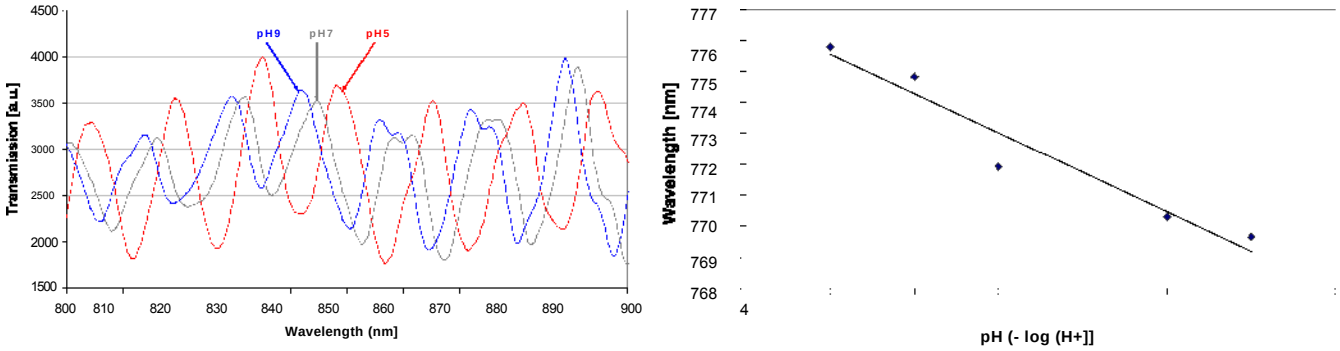

(a) (b)

Fig. 3 (a) Changes in the transmission spectrum of the 5μm diameter fiber taper with a 60 nm thick coating in response to a change in the pH of the surrounding environment. (b)

SUMMARY

The evolution of features within the transmission spectra of an optical fibre taper of diameter 5 μm

in response to the deposition of a nanostructured coating has been reported. The taper exhibited a channeled spectrum that was indicative of a non-adiabatic taper and of interference between two modes of the tapered region. The phase of the channeled spectrum was dependent on the optical thickness of the overlay. To demonstrate the potential of the use of tapered optical fibres with nanostructured coatings as a chemical sensing platform, a pH sensor was characterised.

The authors would like to acknowledge the support of the Engineering and Physical Science Research Council (EPSRC) UK.

REFERENCES

1. J. M. Corres , F. J. Arregui and I. R. Matıas, “Sensitivity optimization of tapered optical fiber humidity sensors by means of tuning the thickness of nanostructured sensitive coatings” Sens. Actuators B, **122,** 442–449 (2007).
2. N D Rees, S W James, R P Tatam, and G J Ashwell, “Optical Fiber Long Period Gratings With Langmuir-Blodgett Thin Film Overlays,” Opt. Lett. **9,** 686-688 (2002).
3. A. Cusano, P. Pilla, L. Contessa, A. Iadicicco, S. Campopiano, A. Cutolo, M. Giordano and G. Guerra, “High sensitivity optical chemosensor based on coated long-period gratings for sub-ppm chemical detection in water,” Appl. Phys. Lett. **87,** Art. No. 234105 (2005).

 Published by Cranfield University Press ISBN: 978-0-9557436-7-2 http://hdl.handle.net/1826/3832

4. F. J. Arregui, I. R, Matias, Y. J. Liu Y, K. M. Lenahan and R.O. Claus, "Optical fibre nanometrescale Fabry–Perot interferometer formed by the ionic self-assembly monolayer process" Opt. Lett. **24,** 596-598 (1999)
5. D. Flannery, S. W. James, R. P. Tatam and G. J Ashwell, "Fibre optic chemical sensing using Langmuir–Blodgett overlay waveguides "Appl. Opt. **38,** 7370–7374 (1999).
   I. Del Villar, M. Achaerandio, I. R. Matias and F. J .Arregui "Deposition of overlays by electrostatic self assembly in long-period fibre gratings," Opt. Lett. **30,** 720–722 (2005).
6. E. Chehura, R. P. Murphy, S. W. James and R. P. Tatam, "Tilted fibre Bragg gratings with nanostructured overlays" Presented at OFS-18, Mexico, 2006. Published in the proceedings, OSA, 2006.
7. J. Keith, L. C. Hess, W. U. Spendel, J. A. Cox and G. E. Pacey, "The investigation of the behavior of a long period grating sensor with a copper sensitive coating fabricated by layer-by-layer electrostatic adsorption," Tatanta **70,** 818-822 (2006).
8. J. M. Corres, F. J. Arregui, and I. R. Matias, "Design of Humidity Sensors Based on Tapered Optical Fibers," J. Lightwave Technol. 24, 4329-4336 (2006)
   A. Cusano, A. Iadicicco, P. Pilla, L. Contessa, S. Campopiano, A. Cutolo, M. Giordano and G. Guerra, "Coated
9. long-period fiber gratings as high-sensitivity opto-chemical sensors," J. Lightwave Technol. 24, 1776- 1786, 2006
10. S.W. James and R.P. Tatam "Fibre Optic Sensors with Nano-Structured Coatings", Journal of Optics A: Pure and Applied Optics, **8** S340, 2006
11. J. D. Love, W. M. Henry, W. J. Stewart, R. J. Black, S. Lacroix and F. Gonthier, "Tapered single-mode fibres and devices, Part 1: Adiabaticity criteria" IEE Proc. J, **138,** 343-3 54 (1991).
12. R. J. Black, J. Bures and J. Lapierre "Finite-cladding fibres: $_{HE11}$ and local-normal-mode coupling evolution", IEE Proc. J, **138,** 343-354 (1991).
13. K. Q. Kieu and M. Mansuripur, "Biconical Fiber Taper Sensors" IEEE Photonic. Tech. Lett. **18,** 2239-224 1 (2006).

 Published by Cranfield University Press ISBN: 978-0-9557436-7-2 http://hdl.handle.net/1826/3832

Micro-injection moulding of three-dimensional microfluidic devices for a medical application

Usama M. Attia [a] and Jeffrey Alcock [a]

[a] *Materials Department, Cranfield University, Beds, MK43 0AL, UK*

Abstract

This paper investigates the use of micro-injection moulding as a high-volume, cost-efficient process for producing three-dimensional microfluidic devices. The application demonstrated in this paper is a microfluidic blood-plasma separator intended to act as a preliminary step in a fully integrated blood analysis system. Micro-injection moulding is applied as a step in a proposed process chain for mass-production of disposable microfluidic devices. The design criteria and manufacturing limitations are presented, and the replication accuracy of the process is investigated. The replication of a micro-featured insert is presented as an example to demonstrate the strengths and limitations of the process. Research challenges and opportunities are highlighted and discussed.

Introduction

Recently, microfluidic devices have gained special attention owing to their potential benefits in fields such as medicine, chemistry and biomedical research. Several companies are already producing such devices, known as Lab-on-a-chip (LOC) devices or micro Total Analysis Systems (μTAS), for commercial use.

However, several obstacles still face the technology before it can become more widely commercialized. Firstly, the fabrication techniques, largely inherited from the silicon industry, are relatively expensive. This limits many of microfluidic applications to lab prototyping. Secondly, fabrication techniques limit the geometry of most of the developed microfluidic prototypes to 2½ dimensional structures (flat 2D structures with a vertical thickness). The ability to produce three-dimensional microfluidic devices would allow greater flexibility in structural design, in built-in leak-proof sealing of microfluidic devices and also in integration of additional functionality.

One strategy to overcome the cost challenge is to develop cost-efficient, high-volume production techniques for fabricating microfluidic devices. These techniques would be particularly appropriate for the production of disposable systems required for medical applications. The challenge of fabricating 3D-spatial structures could be overcome by redesigning the microfluidic device such that it might be fabricated in several parts, which can then be assembled into more complex shapes. Ideally, future manufacturing processes would combine both these capabilities.

Micro-injection moulding (μIM) is an example of a micromoulding technique, which is the process of transferring the micron or submicron scale precision of micro-structured features to moulded polymeric parts

 Published by Cranfield University Press ISBN: 978-0-9557436-7-2 http://hdl.handle.net/1826/3832

[1,2]. μIM has rapidly developed over the past decade due to its notable advantages. It is a fully automated, mass-production, cost-efficient process that is especially useful for disposable products [2-5]. In addition, it has accurate shape replication and good dimension control [3,4,6]. Therefore, it is a strong candidate as a base–process for low cost microfluidic device production. However, as yet, it is not well suited for producing, 3-D sealed devices. This paper represents an attempt an attempt to overcome this limitation by designing and fabricating a three-dimensional microfluidic device constructed by lamination. The function of the prototype device is to separate red blood cells (RBS) from plasma. The device is intended to act as a preliminary step in an integrated blood analysis system.

Device Design

Designing for functionality

The device is designed in the form of an enclosed microfluidic system (Figure 1). It connects externally via one input channel, where the whole-blood sample is delivered to the device, and two separate outputs from which an RBC-rich phase and a plasma-rich phase of the blood are collected. Within the device, the 400 μm input channel narrows in diameter in the form of a cylindrical constriction (100 – 150 μm in diameter), which acts as a flow-focusing channel. The blood flow through the constriction tends to concentrate the red blood-cells into the middle of the flow stream, whereas the plasma is concentrated near the sides of the stream [7]. After this constriction the main channel is intersected by a set of 50 μm high, disc-shaped cavities that act as separation layers. Each act as an output for the plasma, while the RBC-rich fluid tends to continue through the main channel.

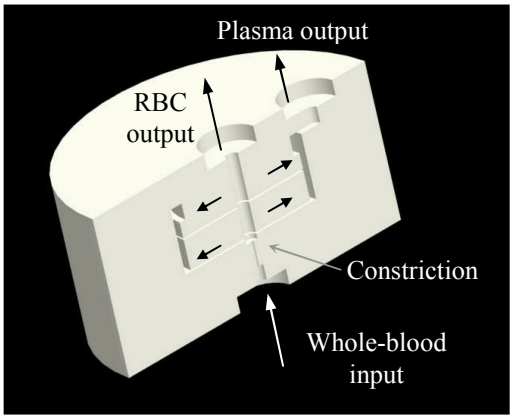

Fig. 1: A half cross-section in the separator

Designing for manufacturability

Micro-injection moulding, similar to most net-shape manufacturing techniques, has a limited capability of producing geometrical shapes with three-dimensional complex cavities. In particular, the technique is not suited to manufacturing devices with “undercuts”, i.e. elements that prevent, either the core mould half from being extracted after the component has been formed, or the component from being ejected out of the cavity [8] . Consequently, the design of the device was adapted for this manufacturing process to one that could be manufactured as a laminated structure (Figure 2). Each device layer carries a section of the microfluidic system, with each section designed to be free from undercuts. The sections are then subsequently joined with one of

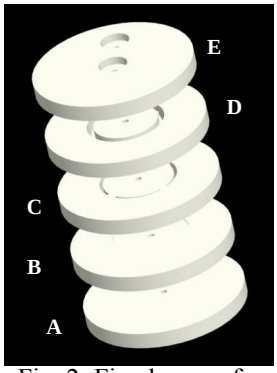

Fig. 2: Five layers of the blood separator.

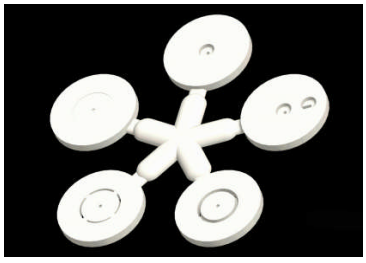
Fig. 3: Plastic part structure including the five layers and the runner and gate system.

 Published by Cranfield University Press ISBN: 978-0-9557436-7-2 http://hdl.handle.net/1826/3832

the commonly know techniques for joining polymers. The five main sections of the device are marked from A to E for identification purposes.

In an optimised manufacturing process all five sections of an individual device would be fabricated from one single shot of polymer (Figure 3). This would reduce tolerance build-up on assembly, as all device sections would, for example, be expected to possess the same shrinkage in the mould. However, a single mould system for such a complex part would not allow for any flexibility during characterisation of the process. Therefore, a replaceable-mould system was devised in which the mould for each of the five sections formed its own insert in the mould. This offered several advantages: flexibility in changing the inserts' features or in optimisation of insert machining without affecting the rest of the mould parts, low manufacturing costs and time consumption, and the ability to either mould all the five inserts together, or selected ones, for the purposes of process optimization.

Designing for assembly

The size of each section layer was designed to allow for a free area allocated for joining. Each layer is 10 mm in diameter and 1 mm in thickness with microstructures centred in the middle of the part. Several polymer joining techniques are to be tested including, but not limited to, ultrasonic welding and laser welding. When selecting a joining technique, special attention is to be directed to the alignment between the different layers to ensure a convenient, leak-proof laminated device. The symmetry in the design allows the layer to be assembled in any axial orientation without affecting the functionality of the device.

Manufacturing Processes

A potential process chain for replicating disposable microfluidic devices on a mass-manufacturing scale involves two main steps: mould manufacturing and replication/assembly.

Mould manufacture by micromilling

The five mould inserts (figure 4) were each manufactured separately from an aluminium alloy (Alumold) using a five-axis micromilling machine KERN Evo. During manufacturing the fitting and alignment between the inserts and the rest of the mould was monitored.

Micro-injection moulding

The machine used in this process was a Battenfeld Microsystems, 50-kN, micro-injection moulding machine. The polymer chosen was a Polymethyl methacrylate (PMMA), (Altuglas VS UVT). This PMMA was selected because of its high transparency (light transmittance above 90%), which enables the observation of

 Published by Cranfield University Press ISBN: 978-0-9557436-7-2 http://hdl.handle.net/1826/3832

flow during testing, and low shrinkage (0.2 to 0.6%). The grade selected possessed a relatively high melt-flow index of 24 in order to facilitate the flow of the polymer inside the micro-cavities of the mould.

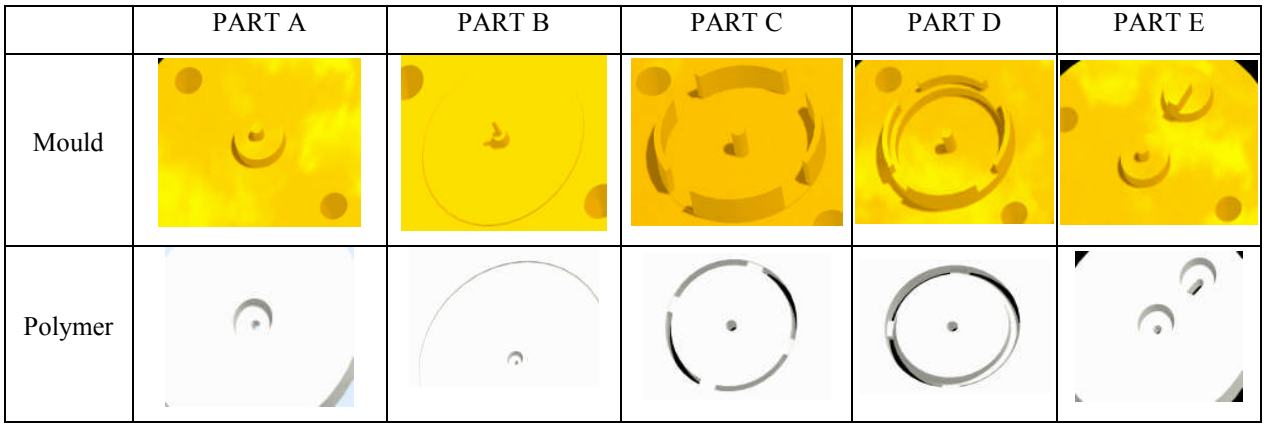

Fig. 4: The five insert moulds and five moulded device sections.

In this initial investigation, each of the five insert moulds was replicated during separate injection moulding trials. Four main processing parameters were adjusted: polymer-melt temperature (T_p), mould temperature (T_m), holding pressure (P_h) and injection speed (V_i). In the experimental design each parameter was varied separately while holding the rest constant. Table 1 shows the optimized parameters of each insert. For all the inserts, the cycle time was less than 20 seconds. Melt-temperature and holding pressure both show significant variations between device sections. For a production mould, the challenge would be to alter the section and mould insert design so that each moulded part moulds optimally at the same processing conditions.

Part Code	A	B	C	D	E
Volume [mm^3]	200	200	200	193	200
T_p [°C]	250	255	265	265	265
T_m [°C]	84	84	84	84	84
P_h [bar]	400	800	600	600	400
V_i [mm/s]	700	700	700	700	700

Table 1: Volume and operation conditions for the device parts. Volume includes both the part and the runner and gate system.

Results and Discussion

Figures 5 and 6 show the different parts of the mould dismantled and combined, respectively. Figure 7 shows a scanning electron microscope (SEM) image of insert A as an example. Most micro-milled features could be produced with tolerances below 2%. The achievable tolerances and surface-finishes are factors of several machining parameters including cutting speed, feed rate, tool type and substrate materials. Unless carefully controlled, they can affect the tolerances on the device fluid constrictors, efficiency of fluid flow through the device and the ease of device sealing during assembly. A considerable improvement in the fine-control of surface features can be achieved by combining into the mould-forming process other machining processes, such as diamond turning.

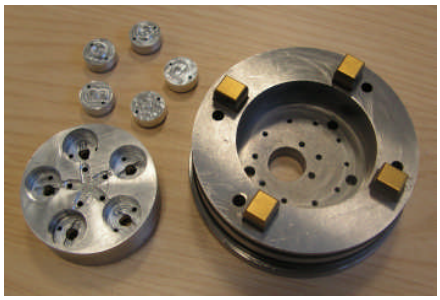

Fig. 5: Dismantled mould pieces.

 Published by Cranfield University Press ISBN: 978-0-9557436-7-2 http://hdl.handle.net/1826/3832

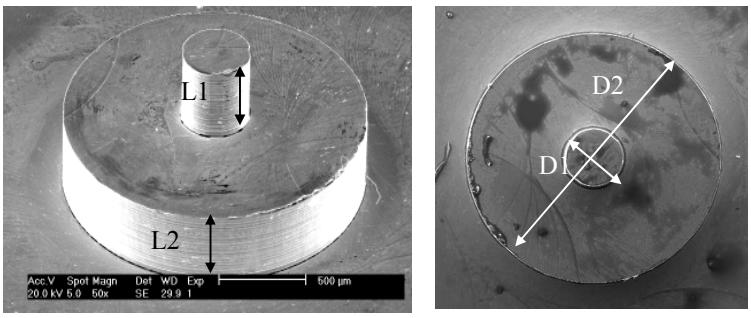

Fig. 7: Isometric and top-view SEM-images of insert A

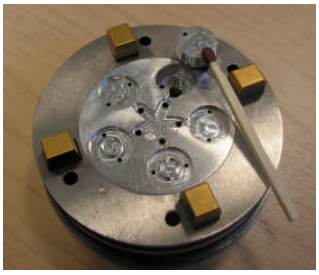

Fig.6: Assembled mould.

Fig 8 shows optical micrographs of several replicated PMMA parts of different device sections. Figure 9 shows environmental scanning electron micrographs (ESEM) for device section A. Table 2 shows measured accuracies for moulded parts of device section A. An example of a complete, clamped and assembled device is shown in Figure 10.

As well as having to achieve the required dimensional tolerances, polymer micro-moulding requires optimisation to avoid errors caused by flashing of material and by weld lines. These can block off through-fluid parts of the sections or introduce leakage points or section weaknesses. Producing high-quality micro-featured parts is a factor of both good design and effective control of processing conditions. Owing to the many interacting processing parameters, significant improvement can be achieved by investigating the process within a designed experiment scheme. This identifies the significant processing parameters and the interaction, if any, between them.

	Mould [µm]	Poly. [µm]	Err. %	SD
D1	392	391	0.25	3.88
D2	1730	1784	3.13	6.82
L2	492	524	6.58	14.17

Table 2. Comparison between mould dimensions and polymer dimensions for device section A.

Metrology remains a challenge in moulding and assembly of such 3-D fluidic devices. In-process dimensional measurement at the micro-scale is currently severely limited in its capabilities, especially for complex 3-D parts.

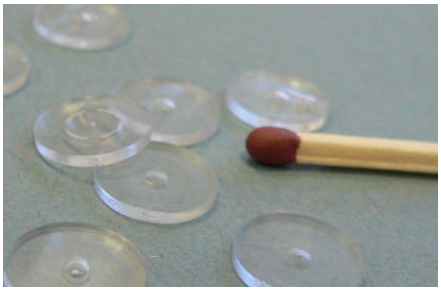

Fig. 8: Replicated PMMA parts with microstructures.

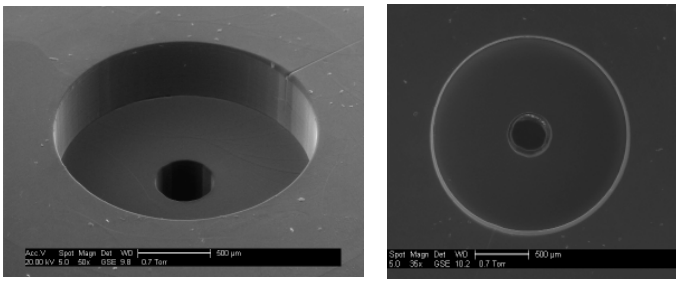

Fig. 9: Isometric and top-view E-SEM images of plastic part A.

 Published by Cranfield University Press ISBN: 978-0-9557436-7-2 http://hdl.handle.net/1826/3832

The measurements recorded in this work (Table 2) were obtained by ESEM, which offers good visualization of micro-scaled features but has severe limitations as a numerical measurement technique. Micro-coordinate measuring machines (CMM) appear to be better suited to this type of measurement: however, as yet, the necessary measurement protocols are still in their infancy.

The results presented above indicate that micromilling and micro-injection moulding have the potential to form the basis of a process chain for mass-producing three-dimensional microfluidic devices. A process chain that combines both processes should offer considerable potential for producing microfluidic devices with complex shapes, accurate dimensions, in a large variety of materials and at low cost.

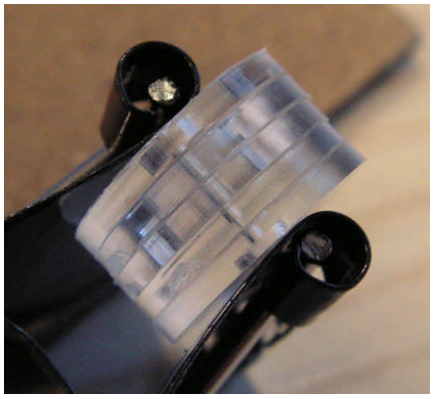

Fig. 10: An assembled structure of the device. Microfluidic channels can be observed within the structure.

Conclusions

This paper aimed at presenting a process chain for mass-producing three-dimensional microfluidic devices, using a medical application as an example. The initial experiments show that the chain is suitable for producing micro-features down to tens of microns. Design techniques such as lamination are required to adapt micro-injection moulding to true three-dimensional geometries. Metrology techniques capable of recording measurements of 3D geometries are necessary for accurate replication evaluation.

References

[1] Weber L., Ehrfeld W. Molding of microstructures for high-tech applications. Proceedings of the 1998 56th Annual Technical Conference, ANTEC. Part 3 (of 3); 26 April 1998 through 30 April 1998; Atlanta, GA, USA: Soc Plast Eng; 1998.
[2] Smith J.H., editor. Fabrication of miniaturized biotechnical devices. Proceedings of SPIE - The International Society for Optical Engineering; 21 September 1998 through 22 September 1998; Santa Clara, CA; 1998.
[3] Wimberger-Friedl R. Injection molding of sub-μm grating optical elements. J Inject Molding Technol 2000;4 (2): 78-83.
[4] Yao D, Kim B. Injection molding high aspect ratio microfeatures. J Inject Molding Technol 2002;6(1): 11-7.
[5] Piotter V, Guber AE, Heckele M, Gerlach A. Micro Moulding of Medical Device Components. Business Briefing: Medical Device Manufacturing & Technology 2004; Feb. 2007.
[6] De Mello A. Plastic fantastic? Lab Chip Miniaturisation Chem.Biol. 2002; 2(2).
[7] Yang S, Ündar A, Zahn JD. A Microfluidic Device for Continuous, Real Time Blood Plasma Separation. Lab Chip Miniaturisation Chem. Biol. 2006; 6(7):871-80.
[8] Anon, editor. Features and Algorithms for Tooling Cost Evaluation in Injection Molding and Die Casting. Proceedings of the 1992 ASME International Computers in Engineering Conference and Exposition; 2 August 1992 through 6 August 1992; New York, NY, United States: Publ by ASME; 1992.

 Published by Cranfield University Press ISBN: 978-0-9557436-7-2 http://hdl.handle.net/1826/3832

Uncertainty in Cost Estimation at the Bid Stage: An Introductory Industry Review

Sirish Parekh, Rajkumar Roy and Paul Baguley
Decision Engineering Centre, Cranfield University

Abstract

This paper presents the technical work that was part of an industry survey investigating cost estimation techniques and uncertainty at the bid stage within industries that typically have long term contracts. The initial results were derived from the industry survey across a series of manufacturing industries. The results are analysed to provide an overview and the key observations within a manufacturing environment. Also the participated companies are involved with a significant number of bids per year thus they require an efficient and smooth bidding process in place. However, most of the participants cannot define uncertainty in a consistent manner, nor highlight its possible sources in relation to cost estimation and bidding process.

Introduction

This paper presents an overview of the cost estimation practices within the manufacturing industry. Uncertainty is also considered during this study due to its volatility at the bid stage and its relative impact on the project. Cost estimating itself is a process of predicting or forecasting the cost of a work activity or work output (Stewart et al., 1995) and its difficulties are well recognised (Rush and Roy, 2000). A more detailed definition from Greves and Journier (2003) suggests that cost estimation is an assessment of the likely costs and risks to occur on a project or product, taking account of past experience with similar activities and the assessment of associated trends, and of any changes in working practices and productivity gains.

Methodology

The industry survey was carried out using fully structured interviews. A face-to-face interview approach with mixture of open and closed questions was adopted to enable a clear understanding of the problems faced in a qualitative manner, as described by Robson (2002). The results presented here involve the responses of 14 experts from 5 different organisations for various sectors including: aerospace (9), automotive (2), oil & gas (1) and consultancy (1). Figure 1 shows the nature of projects that each of the participants is responsible for.

 Published by Cranfield University Press ISBN: 978-0-9557436-7-2 http://hdl.handle.net/1826/3832

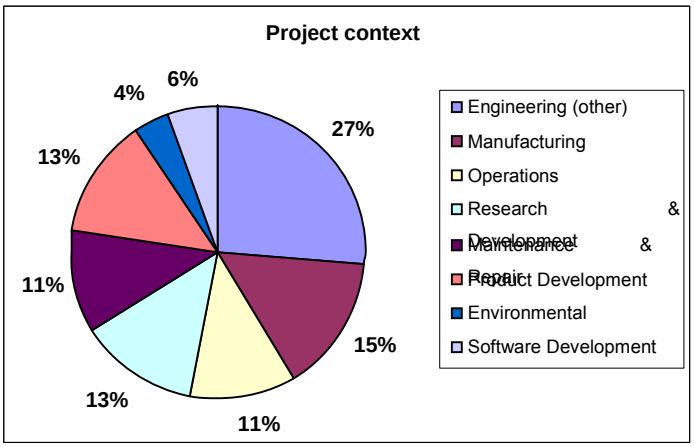

Figure 1. The project context for the participants

The average duration of each interview was approximately 90 minutes. The questionnaire was segmented into three main categories: bidding, cost estimation and uncertainty as described in table 1.

Questionnaire Section	Description
Bidding	The main function of this section is to acquire a solid understanding of the bid process of the organisation. This allows a graphical representation of what is done and when.
Cost Estimation	This section aims to identify the cost estimation techniques, their accuracy and impact on the various industries. An approach of how projects are estimated, who is involved in the process and why is also aimed to be understood from this section.
Uncertainty	The section entailed questions aimed at the understanding and perception of uncertainty. Once identified, a crucial aspect was to comprehend what measures were taken to deal with uncertainty. Other aspects investigated include modelling techniques, mitigation procedures, focussing on sources of uncertainty and its relative impact.

Table 1: Main sections of the industry survey questionnaire

 Published by Cranfield University Press ISBN: 978-0-9557436-7-2 http://hdl.handle.net/1826/3832

The results are described in the next section. For the closed questions of the questionnaire, the answers are visualised in charts. For the open questions, the responses of the participants were recorded and the common elements are identified, analysed and further discussed.

Results

Bid Projects

This sub-section presents the analysis of results. The analysis focuses on specific questions that are of significant interest. In order to appreciate the project scope, several questions were focused towards surrounding issues. One such question investigated the average project size in the participating companies. The responses regarding the average size of projects (in monetary terms) usually undertaken by the companies were recorded. Here, the majority (49%) of the projects are above £10million and 25% between £1m and £10m. This indicates the importance and the benefits of having an effective bidding process. Errors made within the pre-concept phase of a project may have critical impact on cost, performance and schedule and since the project deals with such issues at such large scale in terms of cost, it is important to ensure that projects are estimated and bid for in an efficient way. The next question was concerned with the number of the bids that each company has to prepare on an annual basis. With the exception of the 3 respondents who prepare a significantly large number of bids (between 40 and 50), the average bids per participant lies around 10. One respondent is also an exception with zero bids as he comes from an insurance position. Having to prepare and bid for ten projects per year can be a frustrating process where each successful case can play an important role as the department's performance indicator. Therefore, it is important to have a robust and effective bidding process into place that limits uncertainty and ensures successful cases. The participants were also asked to propose any improvements on the current bidding process that they follow. Many of them proposed a framework which will provide organised feedback of lessons learned, data and benchmarking. Also an accurate statistical analysis of the main risk factors and a clear understanding of the bidding purpose along with clear focus from the customer were proposed. The overall feeling was that there is a need for better data capture and metrics.

Cost Estimation

Cost estimation is an important element of the bidding process. The survey investigated the range of cost estimation techniques that are used across the industry. The most commonly used techniques are: Activity based costing (23%), Parametric models (23%), and the 3 point estimate (21%). Feature based costing and Monte Carlo simulation techniques are each used by the 12% of the participants. Monte Carlo simulation is not strictly a cost estimation methodology but a tool for modelling uncertainty. This was included due to its popularity and an important aspect in cost estimation techniques. The diversity in the cost estimation techniques shows that none has clearly gained strong acceptance by industries as the state-of-the-art standard, though it can be argued that each company has selected the one that best

 Published by Cranfield University Press ISBN: 978-0-9557436-7-2 http://hdl.handle.net/1826/3832

suits the individual requirements. Cost estimation at the bidding stage requires accurate and competitive cost estimation in a timely fashion. The vast majority of respondents (63%) reported that their cost estimates are completed in less than six months. However 37% of respondents require longer than 6 months, with 16% taking more than a year. Delaying a cost estimate can prove highly ineffective when it comes to preparing and winning a bid. Therefore these results indicate a requirement for further awareness towards reduction in cost estimation preparation time. An encouraging outcome of the survey is that 10 out of 14 participants consider the cost estimates that they produce as successful. The participants that rated the produced cost estimates as moderate, they attributed their quality to uncertain factors that were not taken into account when the cost estimate was originally produced. The majority of the interviewees implied cost estimates to be reasonable but deviations from these are due to ill projected assumptions. This may also be due to a lack of uncertainty inclusion.

Expert judgment is crucial when it comes to cost estimation, particularly within a cost engineering context (Hollman, 2007). Two particular questions of the questionnaire targeted that. The first open question sought to identify experts involved in the cost estimation process. The second was a closed question aiming at understanding the degree to which the expert judgment is utilised and incorporated in the cost estimation process. Regarding the first question the majority of participants mentioned qualified cost engineers as the key stakeholders of the process. Other experts involved project managers, procurement/supplier managers, finance, and manufacturing engineers. Some of the respondents have specific estimators that are involved and some mentioned that the cost estimation process involves experts from all aspects of the firm that all need to sign the estimate. Results relating cost estimation to expert judgment and the quality of cost estimates showed that two of the participants sit on the opposite sides of this spectrum. One stated that there is little utilisation of expert judgment in preparing cost estimates, and the other stated that there is excessive use of expert judgment. The majority of participants claimed that there is substantial (8) or moderate (3) input from the experts in order to produce a cost estimate. Using experts to form or validate a cost estimate can contribute towards taking into account many uncertainties that are likely to occur based on the expert's opinion.

Uncertainty

The last two questions discussed here related to uncertainty, and both were open-ended. The first involves the perception and definition of the participants towards uncertainty. The second seeks to investigate the sources of uncertainty at the bidding stage. The definitions given about uncertainty reveal the diversity of understanding around the subject. A common denominator in all the answers was related to unknown events. Uncertainty towards an event's impact was a frequent occurrence from the interviewees. The responses provide a wide range of explanations but not confident definitions. The respondents' definitions often referred to risk rather than uncertainty itself. Several answers were very generic and vague, whilst some were expressed in the context of cost estimation although that was not required. Five responses referred to the impact of an occurring event, which is related to project risks and

 Published by Cranfield University Press ISBN: 978-0-9557436-7-2 http://hdl.handle.net/1826/3832

not uncertainty. The respondents were more specific on the sources of uncertainty. According to a significant number of participants, the sources of uncertainty are identified by a risk management process using brainstorming and/or multi-discipline workshops to identify risks and evaluate probability & impact. Also in terms of the bidding process, the bid team are asked to identify the level of uncertainty associated with the bid. Regarding the sources of uncertainty, it is interesting that although the respondents were specific, very few responses have common elements. Costs, technology and future are identified as three of the factors that were mentioned by most of the respondents.

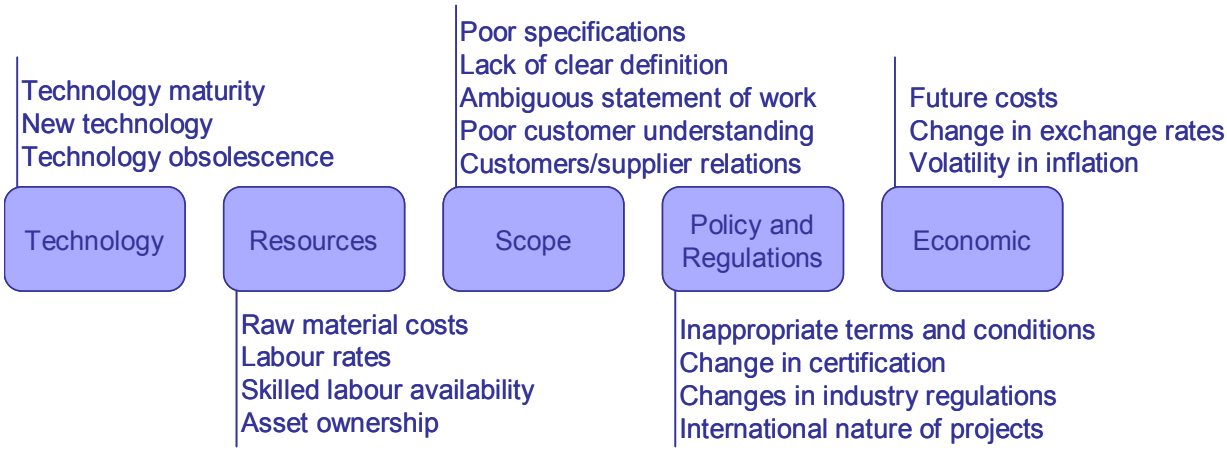

Figure 2: Types of uncertainties from participants' responses

Figure 2 shows these responses along with types of uncertainties in groups. These are typical uncertainties involved in long term contracts/projects at the bidding stage. Hastings (2004) presents an alternative uncertainty classification method, which is part of a framework developed to help decision making. Thunnissen (2005) presents various classifications from several industry perspectives.

Conclusions

The initial results of the industry survey revealed a range of important facts. First, the study is concerned with companies that undertake large and costly projects. Another attribute of the participating companies is that they place a considerable number of bids per year. The cost estimation processes used for these bids vary to a great degree among the participants with Activity-Based Costing and Parametric cost estimation to be the most common. Although most cost estimates are completed within a six month period, they still are not considered as successful and accurate as they should. One of the major factors for that is uncertainty. Uncertainty can affect factors such as cost and technology thus making it an important aspect to understand and manage, particularly at the bid stage.

References

1. Hastings, D. and McManus, H. (2004) 'A Framework for Understanding Uncertainty and its

 Published by Cranfield University Press ISBN: 978-0-9557436-7-2 http://hdl.handle.net/1826/3832

	Mitigation and Exploitation in Complex Systems', *2004 Engineering Systems Symposium*
2.	Hollmann, J.K. (2007) 'What is Cost Engineering', AACE – Association for the Advancement of Cost Engineering.
3.	Greves, D. and Journier, H. (2003) 'Cost Engineering for cost-effective space programmes', ESA bulletin 115.
4.	Rush, C. and Roy, R. (2000), 'Analysis of Cost Estimating Processes Used Within a Concurrent Engineering Environment Throughout a Product Life Cycle', *CE2000 Conference,* Lyon, France, pp. 58-67.
5.	Stewart, R., Wyskidsa, R. and Johannes, J. (1995), Cost *Estimator's Reference Manual: 2nd Edition*, Wiley Interscience, Chichester.
6.	Thunnissen, D.P. (2005) 'Propagating and Mitigating Uncertainty in the Design of Complex Multidisciplinary Systems', *California Institute of Technology Pasadena, California*, Thesis.

 Published by Cranfield University Press ISBN: 978-0-9557436-7-2 http://hdl.handle.net/1826/3832

Re-Sourcing Using Competitive Bids and Virtual Baskets

Mr. Kieron Younis and Dr. Ashutosh Tiwari

Manufacturing Department, School of Applied Sciences, Cranfield University, Bedfordshire, MK43 0AL Email: { k.younis, a.tiwari }@cranfield.ac.uk

1 Abstract

Automotive manufacturers have achieved productivity and efficiency improvement by paying particular attention to their operational and production areas. However, many of these production practices no longer offer strategic advantage and today's automotive manufacturers are seeking new ways to improve their overall performance. One business area coming into focus is corporate purchasing. This study has paid particular attention to the purchasing of key consumable parts sourced from the far-east and used in the production of cars. The work shows how structured competitive bids (with virtual baskets of parts) can allow a manufacturer to make costs savings while strengthening its supplier base.

Keywords: Purchasing, Supply Management, Continuous Improvement, Kaizen.

Pertinent Literature

Kraljic's purchasing portfolio model illustrates the use of different purchasing strategies dependant upon where a purchasing department is placed in the model.

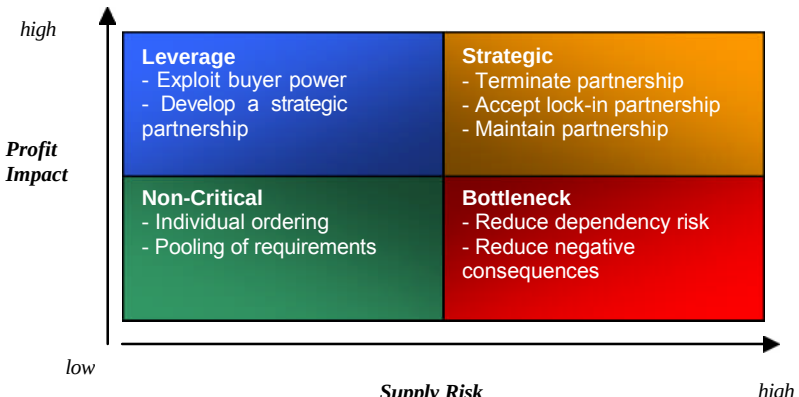

Figure 1. Purchasing Strategies for Portfolio Quadrants reproduced from Caniels and Gelderman (2005)

 Published by Cranfield University Press ISBN: 978-0-9557436-7-2 http://hdl.handle.net/1826/3832

It was found by (Caniels and Gelderman, 2005) that purchasers tend to prefer a scenario where they can maintain their leverage. Selecting the right suppliers to work with is a vital component of achieving competitive advantage, however the ambiguity over what constitutes a fair and reasonable measure makes the process complicated (Amid et al, 2006). Ruiz-Torres and Mahmoodi (2007) found that under experimental conditions the optimal approach to making cost savings with highly reliable suppliers was to single source inputs. Taking this as the optimum quality of supplier, should the quality supply base deteriorate then multi-sourcing becomes more effective (Ruiz-Torres and Mahmoodi, 2007). Even under such conditions it does not become economically prudent to extend the supply base further until the reliability of each supplier is considered extremely low and losses are beginning to accrue (Ruiz-Torres and Mahmoodi, 2007). Kauffman and Popkowski Leszczyc (2005) state that the majority of companies know of suppliers that offers inputs at a rate lower than that being currently paid or better quality than that being currently received. As Schiele (2006) points out a buyer may wish to become the preferred customer of the most valuable suppliers. When considering the value of the supply base it is useful to distinguish between the strategically relevant and the replaceable. Where as business does not have a competent pool of suppliers it may miss the benefits of continuous innovation, it will therefore need to invest to create such a pool of suppliers (Schiele, 2006). However, trying to prioritise suppliers by weighting the relevance of each performance measure is very difficult (Talluri and Narasimhan, 2004) and therefore efforts may be better spent elsewhere.

"The optimal number of suppliers for a buyer to consider should be analytically evaluated rather than be determined by some historical rule of thumb" (Kauffman and Popkowski Leszczyc, 2005). De Boer et al (2001) reason that any one method of supplier selection is not applicable across all contexts. They identified the following generic characteristics that will assist in assessing supplier performance:

- The number of suppliers available to purchase the inputs from.
- The availability of historic information on past transactions with the supplier
- The importance of the buy to key business processes.

 Published by Cranfield University Press ISBN: 978-0-9557436-7-2 http://hdl.handle.net/1826/3832

Method

The work has been comprised of stages of problem identification, data mining, data analysis, strategy formulation, presentations, practitioner interviews and supplier negotiations. The general method can be summarised as being made up of three key stages.

1. Data analysis and dissemination
2. Formulation of initial recommendations
3. Results synthesis and best practice strategy development

Parts from Japan were investigated in more detail in order to gain more understanding of the problem domain and inform future strategies. A list of 35 parts bought by the UK plant were compared against prices paid by the company's plants in Japan (Figure 2).

In the next stage of work a list of 96 parts complete with details was given to five suppliers (plus one manufacturer/supplier) who were asked to offer quotes for the list of parts with the possibility that they might gain the business. Virtual baskets were used to compare across supplier quotes where the number of parts quoted for differed on a supplier by supplier basis. This method allowed for all quotes to be taken into account regardless of whether another supplier had quoted on that specific part. A relative performance index was then developed from this study (see Table 2).

Results

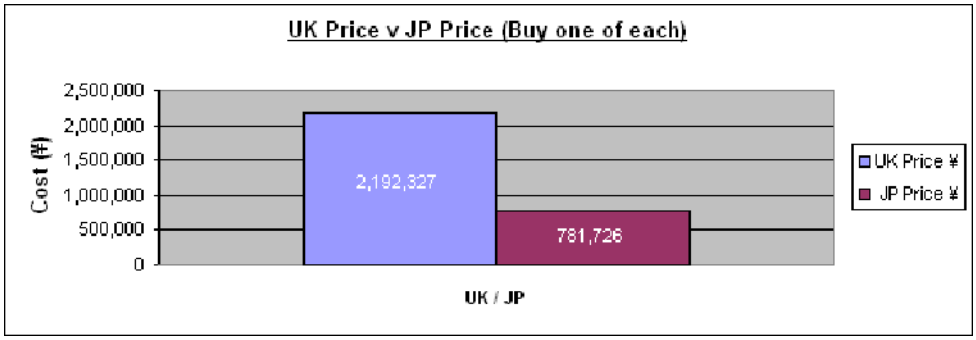

Figure 2. The cost for a basket of parts

35 parts from 3 manufacturers had an average price difference of 280.4% in favour of Japanese buyers.

 Published by Cranfield University Press ISBN: 978-0-9557436-7-2 http://hdl.handle.net/1826/3832

Table 1. Supplier quotations / response rate

SUPPLIER	Number of Returned Quotes
S1	36
S2	34
S3	85
S4	36
S5/M4	28
S6	22

None of the suppliers returned a complete list of parts with quotations.

Table 2. Project savings (extrapolated from quotes, using virtual baskets)

PROJECTED SAVING(£)	M9	M5	S5/M4	M8	M7
Current Spend (£)	126,358	47,647	93,336	277,810	290,570
S1	0	-5,572	1,083	0	0
S2	0	9,737	31,883	0	0
S3	**-11,247**	19,008	27,472	**32,373**	**-17,057**
S 4	0	-6,899	26,693	0	0
S5/M4	0	0	37,170	0	0
S6	0	**22,878**	**39,058**	0	0

PROJECTING SAVING IN TOTAL (£)	Business Quoted For	Total Savings	% Saving
Take Only Savings	835,721	94,310	11.3
Take Good and Bad	835,721	66,006	7.9

Table 3. Projected annual savings for quoted business

RE-SOURCE PROPOSAL	M9 Parts to:	M5 Parts to:	S5/M4 Parts to:	M8 Parts to:	M7 Parts to:
	S3	S6	S5/M4	S3	S3
result:	increase	saving	saving	saving	increase

Table 4. Proposed re-sourcing structure

Discussion / Conclusion

Japan parts are those sourced from Japanese manufacturers (either directly or through intermediary suppliers) and can be shipped directly from Japan or from regional distribution

 Published by Cranfield University Press ISBN: 978-0-9557436-7-2 http://hdl.handle.net/1826/3832

centres in Europe. Japan parts represent around L1m of spend per year and are therefore a significant contributor to overall expenditure. The comparison of prices paid in the UK compared to those in Japanese domestic market supported this move.

None of 6 suppliers selected for the study returned quotes for all the parts requested. The most common reasons they gave for this include; not being able to identify the parts, conflicts with management priorities and/or no explanation was given. Given that a simple like for like comparison was not going to be possible the most accurate means of assessment was to use 'virtual baskets', showing the relative performance for each of the suppliers against current spend. The performance of each supplier against current costs is shown in Table 2.

It was found that S5/M4 was the cheapest supplier over a larger data set of their own parts, but not over the smaller data set quoted for by S6. However, given the advantages offered by direct supply it was felt that they still offered the optimum balance of cost saving and performance.

The research has led to the conclusion that entire business for a manufacturer's parts should be single sourced and reviewed on a 1 to 3 year basis. In addition it is felt fair that short-term cost increases be taken as well the savings. Re-sourcing business to a single competitive supplier will prove advantageous over the medium to long-term. Corporate Services will be better able to manage part-supplier-manufacturer relationships. Suppliers will be incentivised to maintain/offer competitive prices in order to retain/gain business. The process of managing price changes will be more transparent and future negotiations for re-sourcing simpler.

The exact makeup of the proposal can be viewed in Table 4. As can be seen it has been recommended that the company take on some cost increases at this stage. There is a real need to demonstrate to suppliers that the company operates in a socially responsible manner and avoiding increases, particularly given the assistance suppliers have offered, would undermine this. Even so the study has delivered a significant predicted saving on next years spend for Japanese machine spares of approximately 8% or around £66,000.

The study has demonstrated how using virtual baskets at the competitive bid stage can allow a manufacturer to compare the relative performance of its supply base, even where there is a lack of direct competition on a part by part basis. The cost savings achieved here represent only a small fraction of the annual spend the company invests in new machine spares and consumable goods annually. However, if a similar programme of activities were to be applied across the board, cost savings could run in to single digit millions.

References

1. CANIELS, M.C.J. and GELDERMAN, C.J., 2005/0. Purchasing strategies in the Kraljic matrix--A power and dependence perspective. Journal of Purchasing and Supply Management, 11(2-3), pp. 141-155.
2. DE BOER, L., LABRO, E. and MORLACCHI, P., 2001/6. A review of methods supporting supplier selection. European Journal of Purchasing & Supply Management, 7(2), pp. 75-89.

 Published by Cranfield University Press ISBN: 978-0-9557436-7-2 http://hdl.handle.net/1826/3832

3. KAUFFMAN, R.G. and POPKOWSKI LESZCZYC, P.T.L., 2005/1. An optimization approach to business buyer choice sets: How many suppliers should be included? Industrial Marketing Management, 34(1), pp. 3-12.
4. RUIZ-TORRES, A.J. and MAHMOODI, F., 2007/2. The optimal number of suppliers considering the costs of individual supplier failures. Omega, 35(1), pp. 104-115.
5. SCHIELE, H., 2006/11. How to distinguish innovative suppliers? Identifying innovative suppliers as new task for purchasing. Industrial Marketing Management, 35(8), pp. 925-935.
6. TALLURI, S. and NARASIMHAN, R., 2004/4/1. A methodology for strategic sourcing. European Journal of Operational Research, 154(1), pp. 236-250.

 Published by Cranfield University Press ISBN: 978-0-9557436-7-2 http://hdl.handle.net/1826/3832

Operationalising Luxury in the Premium Automotive Industry: Research Methodology.

Bernie Law, Research Engineer
Cranfield University, School of Applied Science
29th February 2008
Supervisors: Professor Steven Evans, Dr Joe Jaina

Executive Summary

This report presents a review of the research methodology for an EngD research project investigating the perception of luxury in the automotive industry.

The research is driven by the need to bridge the gap between how a customer experiences luxury in cars, and how luxury is embedded into the new product development process.

The main aims of this research are to understand and communicate luxury, and to get luxury into the brand. The research objectives have been developed into a model that has aided communication and understanding within the sponsoring firm.

A research methodology has been developed that formalises the phenomenological, inductive approach that has been adopted for this project, and appropriate research tools have been selected. Primary data sources include primary customer car clinic data, internal design and development team assessments Secondary data is obtained from syndicated automotive surveys.

Analysis of these data and interviews with company personnel has identified the difficulty in relating internal measures of luxury with the customer experience, both from primary and secondary data.

The research plan has evolved to recognise these difficulties and incorporate additional activities to better understand and resolve them.

INTRODUCTION

The research is driven by the need to bridge the gap between how a customer experiences luxury in cars, and how luxury is embedded into the new product development process. The main aims of this research are to understand and communicate luxury, and to get luxury into the brand. A research objectives communication tool has been developed (Figure 1); this has been invaluable in fostering an understanding of both the research and the EngD process within the company.

 Published by Cranfield University Press ISBN: 978-0-9557436-7-2 http://hdl.handle.net/1826/3832

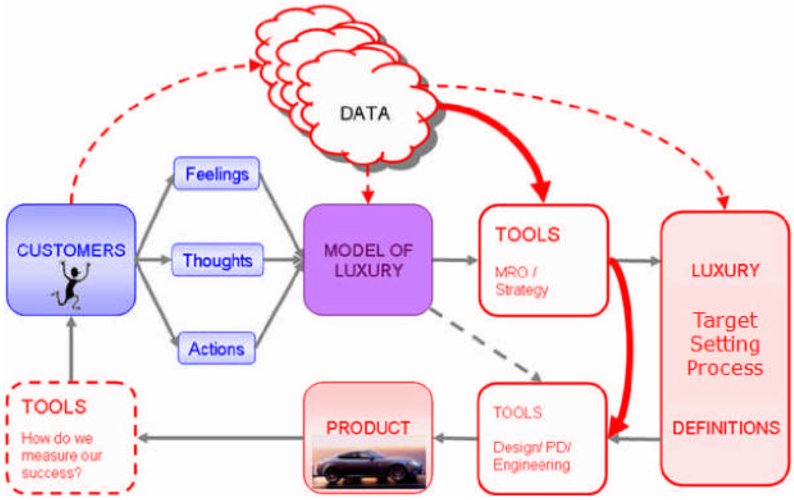

Figure 1 Project Objectives

Research questions (not discussed in this paper) have been developed to facilitate achievement of these objectives.

This paper discusses the development of the research design and evolving research methodology that supports this EngD project.

RESEARCH DESIGN

Blaikie [1] identified several areas in which choices must be made when designing a research project, including the problem to be investigated, the questions to be answered, the strategy to be used answering the questions and the research paradigm.

Thomas Khun [2] defined the concept of the research paradigm as the "*underlying assumptions and intellectual structure on which research in a field of inquiry is based".* It has also been described as an interpretive framework guided by a "*set of beliefs and feelings about the world and how it should be understood and studied" [3].* These beliefs can be categorised by [4] [5]:

- ontology: "the science or study of being" (the nature of reality);
- epistemology: "the theory or science of the method or grounds of knowledge" (how to gain knowledge of this reality – what can be known and what criteria must be satisfied to distinguish knowledge from belief);
- methodology: the analysis of how research should proceed (as opposed to method – the actual techniques or procedures used to gather and analyse data).

Guldbrandsen [6] summarised different aspects of research design, adapting the works of Gill and Johnson [7], Robson [8] and Blaikie [1] (Figure 2):

 Published by Cranfield University Press ISBN: 978-0-9557436-7-2 http://hdl.handle.net/1826/3832

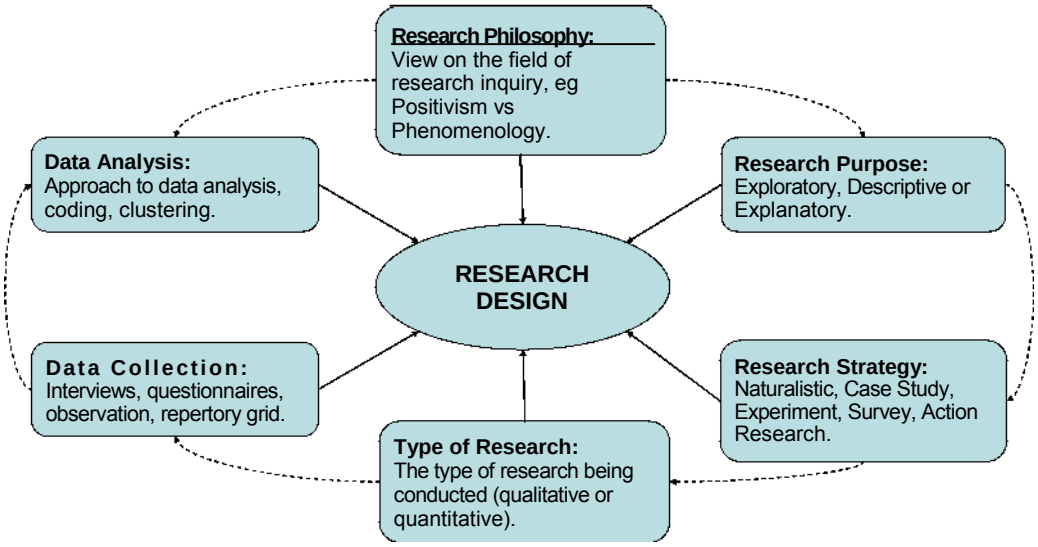

Figure 2 Issues in Research Design (adapted from Guldbrandsen [6])

RESEARCH PHILOSOPHY

The research philosophy reflects the researcher's ontological and epistemological stance, the research approach and reasoning process adopted.

Ontology

According to Blaikie [5], research approaches fall into two ontological groups: realist or constructivist. The realist ontology assumes that reality exists independently of the observer and that this reality is ordered, can be observed and be explained. The constructivist ontology assumes that reality is produced by actors, and is an intersubjective world of cultural objects and meanings [5].

Epistemology

Research approaches can fall into the internalism or externalism camps. Internalism is the idea that everything necessary to provide justification for a belief is immediately available in consciousness. Externalism in this context is the view that there are factors other than those which are internal to the believer which can affect the justificatory status of a belief. [9]

Specific theories of knowledge include Empiricism, Rationalism and Constructivism [10]:

- Empiricism emphasises the role of experience, especially experience based on perceptual observations by the five senses.
- Rationalists believe that knowledge is primarily (at least in some areas) acquired by a priori processes or is innate—e.g., in the form of concepts not derivedfrom experience.
- Constructivism is a view in which all knowledge is contingent on convention, human perception, and social experience. Constructivism proposes new definitions for knowledge and truth that forms a new paradigm, based on inter-subjectivity instead of the classical objectivity and viability instead of truth.

Philosophical Approaches

Blaikie identified a number of research approaches (Figure 3):

 Published by Cranfield University Press ISBN: 978-0-9557436-7-2 http://hdl.handle.net/1826/3832

Approach	Ontology
Positivism	Realist
Critical Rationalism	Realist
Interpretivism	Constructivist
Critical Theory	Constructivist
Realism	Realist
Structuration Theory	Constructivist
Feminism	Constructivist

(adapted from Blaikie [1])

Figure 3 Research Approaches

The two major research paradigms to be considered here are Positivism and Phenomenology (the new paradigm).

Positivism views the world as existing externally: its properties should only be measured through the use of objective measures [11].

Phenomenology advocates the study of direct experience, in which behaviour is seen as being determined by the phenomena of experience rather than external, objective and physically described reality [12]. Phenomenology is sometimes referred to as interpretivism, constructivism and naturalistic enquiry [11]. Key differences between the paradigms are highlighted in Figure 4 below:

	Positivism	Phenomenology
Assumptions / Beliefs	Reality is tangible, external and objective Observers are independent of the enquiry Science is value-free	Realities are multiple, holistic, socially constructed and subjective Observers are part of what is observed Science drive by human interest
Approach	Focus on facts and truths Explanation through analysis of causal relationships and fundamental laws Reduce phenomena to simplest elements Formulate and test hypotheses based on theory (statistical probability)	Focus on meanings Explanation of subjective meaning held by subjects through understanding Describe totality of situations Generate theory from data through induction (theoretical abstraction)
Preferred Methods	Quantitative Measurement Large samples Generalisation Rigour and validity	Qualitative Multiple methods/viewpoints Small samples/in depth Context-bound understanding. Trustworthiness, utility and triangulation.

(adapted from Burns [11] and Guldbrandsen [6])

Figure 4 Positivism vs Phenomenology

Reasoning Process

Blaikie [1] identifies four distinct types of reasoning: inductive, deductive, retroductive, and abductive. Their differences are described briefly in Figure 5 below.

Each of the research strategies contain ontological and epistemological assumptions about the nature of reality and how that reality can be known [1].

 Published by Cranfield University Press ISBN: 978-0-9557436-7-2 http://hdl.handle.net/1826/3832

	Inductive	Deductive	Retroductive	Abductive
Aim:	To establish universal generalisations to be used as pattern explanations	To test theories, to eliminate false ones and corroborate the survivor	To discover underlying mechanisms to explain observed regularities	To describe and understand social life in terms of social actors' motives and understanding
Start:	Accumulate observations or data	Identify a regularity to be explained	Document and model a regularity	Discover everyday lay concepts, meanings and motives
	Produce generalisations	Construct and theory and deduce hypotheses	Construct a hypothetical model of a mechanism	Produce a technical account from lay accounts
Finish:	Use these 'laws' as patterns to explain further observations	Test the hypotheses by matching them with data	Find the real mechanism by observation and/ or experiment	Develop a theory and test it iteratively
Use	For answering "what" questions	For answering "why" questions	For answering "why" questions	For answering both "what" and "why" questions

(adapted from Blaikie [1])

Figure 5 Types of Reasoning

Adopted Research Philosophy

This project concerns the understanding of a deeply subjective phenomenon. A phenomenological, inductive approach therefore represents the most appropriate stance for this research by generating theory that can be used to embed luxury into the mindset of the company and its NPD processes. However, the field of inquiry is in an environment that has a very positivist outlook, and the contrast between how the business views the world and the nature of this research is a potential area of conflict.

RESEARCH PURPOSE

Robson [8] suggests that research can be distinguished according to its purpose, and lists three categories (exploratory, descriptive or explanatory). Blaikie [5] expands this list to include understanding, change and evaluation, but these do not seem to be sufficiently different to warrant separation.

Figure 6 [8] distinguishes the three main categories:

Exploratory	Descriptive	Explanatory
To find out what is happening	To portray an accurate profile of persons, events or situations	Seeks causal explanation of a situation or problem
To seek new insights	Requires extensive knowledge of the situation to be researched	
To ask questions		
To assess phenomena in a new light		
Usually, but not necessarily,	May be qualitative and/or quantitative	May be qualitative and/or quantitative

(adapted from Robson [8])

Figure 6 Research Purpose

This research project combines elements of each of these. Luxury is a subjective construct that is not well described, suggesting that an exploratory study is appropriate to develop a new theoretical understanding of this phenomenon. Theory emerging from this initial study can then be used to drive a descriptive study from which a model of luxury can be generated. The primary aim of this research is to generate new theory: these two phases may be sufficient to support the

 Published by Cranfield University Press ISBN: 978-0-9557436-7-2 http://hdl.handle.net/1826/3832

phenomenological stance of this research. However, a further explanatory exercise may be appropriate to satisfy the company's positivist needs by empirically testing the new theory, through the develop of new tools.

 Published by Cranfield University Press ISBN: 978-0-9557436-7-2 http://hdl.handle.net/1826/3832

RESEARCH STRATEGY

It is suggested that there is a relationship between the strategy chosen for a piece of research and its purpose (Figure 7 Figure 7) [8]:

Purpose		Strategy
Exploratory	--	Case Studies
Descriptive	--	Surveys
Explanatory	--	Experiments

Figure 7 Research Strategies

Yin [13] defines a case study as an *empirical inquiry that investigates a phenomenon in its real-life context.* They can be based on both qualitative and quantitative evidence, and can establish cause and effects, where context is recognised as a powerful determinant of both [12]. Case study methods include interviews, observation, documentary analysis and action research. Tellis [14] describes how the case study strategy can be used for exploratory, descriptive and explanatory purposes.

Robson [8] describes surveys as the *"collection of information in standardised form from groups of people".* Data can then be presented in quantitative or statistical form. This strategy suits a positivistic approach. Survey methods include questionnaires and structured interviews.

Robson [8] characterises experiments as *"measuring the effects of manipulating one variable on another variable",* that are used to test hypotheses derived from the theory under consideration.

This research is fundamentally based on a case study approach, but uses elements of the survey strategy within that framework. Specifically, the survey method is used for both primary and secondary data collection from luxury car customers.

Action Research is a special instance of case study research [15], described as an *iterative collaborative inquiry process that balances problem solving actions with data-driven research to understand underlying causes enabling prediction and change* [16]. It seeks to bring together action and reflection, theory and practice [16]. The researcher works in collaboration with the firm to effect real changes within the organisation. Reason [16] highlights five characteristics of action research (Figure 8).

(from Reason [16])

Figure 8 Characteristics of Action Research

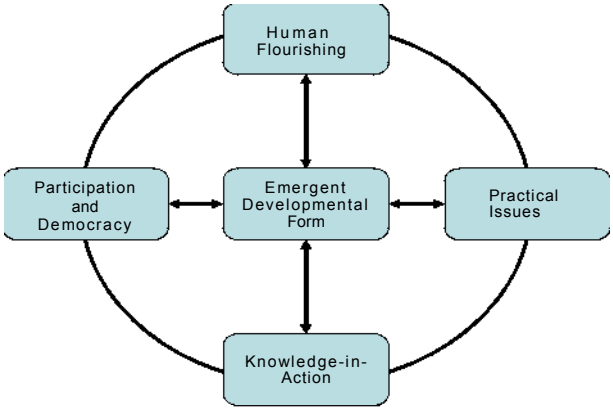

Action research has two key goals: to solve problems and contribute to knowledge. The researcher and company personnel learn from each other to develop their competences and an holistic understanding of the problem. This is an action research project: the researcher is embedded within the sponsoring firm, working within and as part of the organisation to develop and embed an understanding of luxury into the company's mind-set and actions.

Published by Cranfield University Press ISBN: 978-0-9557436-7-2 http://hdl.handle.net/1826/3832

TYPE OF RESEARCH

The research strategy above will yield both qualitative and quantitative data, and there is a distinction between the two (Figure 9):

(adapted from Robson [8])

Figure 9 Quantitative vs Qualitative Research

This research will use both quantitative and qualitative techniques to answer the research questions, using a multi-method approach that includes interviews, observation, surveys and document analysis.

DATA COLLECTION

Data will be collected from two different directions: from the customers (to understand how they view and experience luxury) and from within the company (to understand the company mind-set and how luxury can be incorporated into everyday practice).

Quantitative Research	Qualitative Research
Used in research that requires facts and figures in order to answer the research question (through verification of hypotheses)	Deals with exploration of issues and the generation of theories within emerging subject areas Used to develop insight and understanding
Seeks to measure, test, and quantify elements in order to explain or describe something	Seeks to create gestalt and holistic interpretations

In view of the considerations of purpose and strategy above, and to enable the induction of grounded theory, the following data collection methods will be used (Figure 10).

Data Collection Method	Description	Progress
Interviews	Combination of informal and semi-structured interviews with key stakeholders within the business.	On-going. Interviews and discussion meetings held with brand, product planning, perceived quality and product quality team members (6 people to date)
Questionnaires	Short, open questions to elicit customers' emotional responses (stream of consciousness) when evaluating cars in a pre-purchase environment.	Customer car clinic was described in earlier report [17]. Repeat exercise for different vehicles conducted Dec 07.
Survey	Customers rate vehicles viewed on a 10 point scale (emotionally positive to emotionally negative) on subjective vehicle attributes.	Customer car clinic was described in earlier report [17]. Repeat exercise for different vehicles conducted Dec 07.
Observation	Attendance of team briefings, work shadowing personnel.	On-going. Worked with Market Research team three days per week for last year. Now working with Perceived Quality team one day per week.
Documentation Analysis	Company documentation relating to luxury message, brand, product specification, both internal and published, will be analysed	On-going on an ad-hoc basis.
Literature Review	Exploration of themes including definition of luxury, relationship between people and product, and evaluation and measurement of luxury.	Initial literature review reported [17]. Additional sources identified and under review.

Figure 10 Data Collection Methods

DATA ANALYSIS

The data analysis techniques to be used on this project are driven by the needs of the data as it emerges.

The data generated so far has been subject to content analysis (customer verbatims from customer car clinics) and regression analysis (comparing internal perceived quality ratings with customer ratings for a range of product attributes).

 Published by Cranfield University Press ISBN: 978-0-9557436-7-2 http://hdl.handle.net/1826/3832

The findings to date are not discussed in this paper for reasons of confidentiality.

REFERENCES

1. Blaikie, N; *Approaches to Social Enquiry,* 2nd Edition. Polity Press, Cambridge, 2007.
2. Kuhn,TS; *The Structure of Scientific Revolutions.* 2nd Edition. Univ. of Chicago Press, Chicago, 1970.
3. Guba, E; *The Paradigm Dialogue.* Sage Publications, Newbury Park, CA, 1990.
4. Denzin, K & Lincoln, Y (eds.); *Handbook of Qualitative Research.* 2nd Edition. Sage Publications, Inc, Thousand Oaks, CA, 2000.
5. Blaikie, N; *Approaches to Social Enquiry.* Blackwell Publishers, Cambridge, 1993.
6. Guldbrandsen, M; *How Companies embed Non-Quantifiable Product Qualities through their Product Development Process.* PhD Thesis, Cranfield University, 2006.
7. Gill, J. & Johnson, P; *Research Methods for Managers,* 3rd edition. Sage Publications, London, 2002.
8. Robson, C; *Real World Research.* Blackwell Publishers Ltd, Oxford, 1993.
9. Anon; *Internalism and Externalism.* http://en.wikipedia.org/wiki/Internalism and externalism. Accessed 09/11/07.
10. Anon; *Epistemology.* http://en.wikipedia.org/wiki/Epistemology. Accessed 09/11/07.
11. Burns, A; *The Phenomenology of Customer Delight: a case study ofproduct evaluation.* PhD Thesis, Cranfield University, 2004.
12. Cohen, l, Manion, L, & Morrison, K; *Research Methods in Education,* 6th Edition. Routledge, Oxon, 2007.
13. Yin, RK; *Case Study Research –Design and Methods,* 3rd Edition. Applied social research method series Volume 5. Sage Publications. California, 2002.
14. Tellis, W; Introduction to Case Study. The Qualitative Report, Vol 3, No 2, July 97. http://www.nova.edu/ssss/QR/QR3-2/tellis1.html. Accessed 10/11/07.
15. Evans, S; *Action Research.* Presentation, Manufacturing and Technology Management Research Methodology Workshop 2007, University of Cambridge, March 2007.
16. Reason, P & Bradbury, R (eds); *Handbook ofAction Research.* Sage Publications, London, 2001.
17. [17] Law, Bernie; Operationalising Luxury in the Premium Automotive Industry. EngD First Year Report. Cranfield University, 2 1/12/06 (unpublished).

 Published by Cranfield University Press ISBN: 978-0-9557436-7-2 http://hdl.handle.net/1826/3832

A steady state neural network model predicting separation efficiency of a compact Cyclonic separator

Nadeem Qazi, Dr Hoi Yeung.

Introduction

Separation of dense phase in multi phase flow is one of the major and challenging tasks of the oil and gas industry. Separators are widely used for this purpose however Compact Centrifugal separators are becoming a better choice due to their low cost, lightweight, easy handling and simple installation over bulky gravitational separator.

There are several models available in literature that defines the separation efficiency and performance of the separators. A fluid mechanical model [2] is developed for the axial cyclone by defining a relation for the liquid, liquid separation efficiency. However these models mainly estimate the cut size diameter of the heavy particles in the separator. The performance of a newly designed gas liquid compact centrifugal separator is being studied in the department of process and system engineering at Cranfield University. The idea is to build an intelligent agent base system that can assist and guide plant operator. The first and important task in this case is to predict the separation efficiency at varying operating conditions along with development of an optimal control strategy to increase the performance of the separator. Neural network has not been used so far to predict the separation efficiency of the compact separator at least according to literature survey done by the author. This paper describes an empirical model for the gas liquid compact separator, using artificial neural network at different inlet conditions. The paper is organised in four sections the first section describes in general the compact separator, its efficiency and working principle. The experimental rig and model development & optimisation are discussed in second and third section respectively followed by result and conclusion.

The ISEP

ISEP is the name given to a new design of axial flow cyclone by its inventor Caltec, Ltd UK. It is a lightweight, low cost dual involutes cyclonic separator that converts rotational energy in to centrifugal force to separate particle of different density from air, water and oil. It is different from other axial flow cyclones as it uses inlet involute to produces the swirl inside the separator .The fluid is entered in ISEP through an involute device where it is made to spin, then it progress up to the separating chamber where separation takes place and heavier fluid moves radially outwards through

 Published by Cranfield University Press ISBN: 978-0-9557436-7-2 http://hdl.handle.net/1826/3832

tangential outlet or underflow, while lighter fluid is moved towards axial outlet also known as overflow and collected via vortex finder.

The separation efficiency of the separator could be defined as a ratio of mass flow rate of the lighter and heavier phase at axial and tangential outlet respectively to the total input mass of the both liquid and gas. The separation efficiency and hence the performance of the separator is measured by percentage of Liquid carry over and Gas carry under in the separated liquid and gas at their respective outlets.

The Separator Rig

The two-phase separator rig used for experiments is consisting of a gravity separator (HISEP) along with the compact gas liquid separator (ISEP). Gas and liquid inlet stream is measured with single-phase-meters, are commingled to form gas-liquid mixture and then passed to 15-meter long pipe before entering in to ISEP. The air is introduced in to the rig by the compressor and flow rate of air is controlled automatically through the controlled valve handled by the Delta V system. The flow rate of the water is controlled using a control valve named as CV2 in the rig. This two-phase mixture is separated by the I-Sep into a liquid-rich mixture and a gas-rich mixture, which are then further purified from their contents by passing them through gravity separators. Liquid and gas flow rates are measured after complete separation with single-phase meters and then sent back to they supply/receiver tank. The performance of the separator is a function of both its geometry and inlet operating conditions but in the present work due to fixed geometry of ISEP, it is investigated by changing inlet flow condition only i.e. gas volume fraction, mixture velocity gas and liquid flow rate, and inlet pressure. The experiments covering mainly slug flow are performed at room temperature in two sets of constant GVF and constant velocity as shown in experimental matrix in table 1.0. The data is recorded for two minutes after the steady state is achieved.

Experiment Type	GVF %	Mixture Velocity m/s	Inlet Pressure $bara$	Inlet Gas Flow rate $std\ m^3/hr$	Inlet liquid Flow rate l/s
Fixed GVF	90	15-40	1.25-4.25	37.5-425	1-3.3
	98	7.5-67.5	1.1-4.75	22.5-850	0.1-1
Fixedvelocity	82.5-97.5	15-30	1-2.75	45-230	0.6-4.1
	87.5-97.5	35	1.75-3.5	152-290	0.7-3.5

Table 1.0 experimental matrix

 Published by Cranfield University Press ISBN: 978-0-9557436-7-2 http://hdl.handle.net/1826/3832

Model Development

A Non-linear relationship was observed between the separation efficiency parameters

and the inlet operating conditions during the experiments analysis that lead to use non-linear neural network to model the separator efficiency. The widely used network architecture for this purpose is Multiple Layer perception (MLP) as reported in [3, 4], recurrent neural network [5, 6] and radial basic networks [7]. This work uses a variant of MLP neural network due to the large number of activation functions provided in this architecture. The model development process is shown in the figure 1.

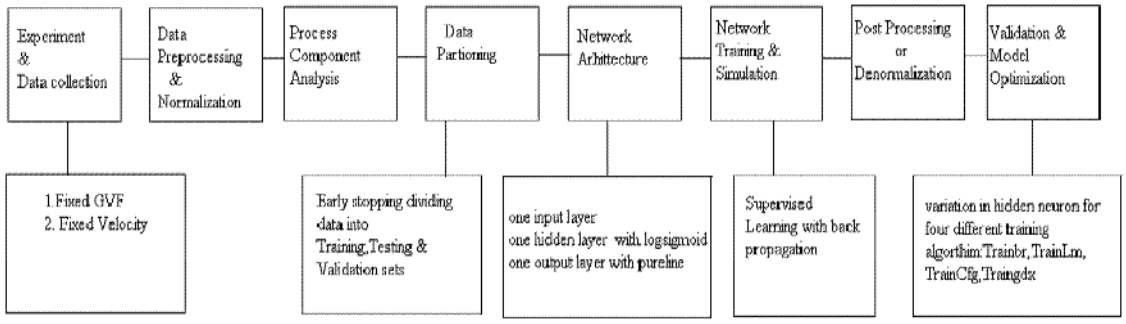

Figure 1. Procedural algorithm for developing a neural network model.

The experimental data is pre-processed before passing it to the neural network to remove any noise and outliers from the data. It is scaled down using the Z score normalization followed by process component analysis to remove multicollinearity and redundant data. The leading problem of generalization or over-fitting which occurs during training of a neural network can be resolved by using early stopping approach, Bayesian regularization and exhaustive search method. Early stopping procedure is used here to avoid the over-fitting by dividing the data set into three sets training, validation and testing. This technique continuously monitors the validation error and stops the training if validation error begins to rise.

A total number of 241 data sets were collected during the experiments. One half of the data is used for the training set and the remaining half is divided in to validation and testing, thus these two data sets takes one fourth of the input data. Four different algorithms are selected from MATLAB neural network tool box and network is trained with each of this algorithm changing the hidden neurons, using log sigmoid in the hidden layer and purline as activation function in the output layer. The whole process is repeated for each of the four algorithms.

 Published by Cranfield University Press ISBN: 978-0-9557436-7-2 http://hdl.handle.net/1826/3832

Input and Output Parameter of Models

The out put variables of the model are very obvious i.e. it should be liquid and gas separation efficiency with gas carry under and liquid carry over. However choice of the input or predictor variables is not very straightforward. It is due to complexity of the neural network model that depends upon the number of predictor variables, hidden neurons and hidden layers. The choice of the input variable is based upon the requirement specifications of the model, the strength of relation ship between the predicator variables with the output parameters of the model. Experimental results have shown that the gas separation efficiency decreases with increasing GVF and inlet mixture velocity whereas the liquid separation increases with inlet mixture velocity but decreases with the GVF in non linear manner. The Gas flow rate, liquid flow rate and inlet pressure had shown a direct relationship with the gas and liquid separation efficiency at fixed velocity, however during the fixed GVF experiments while the liquid flow rate maintained this trend, the gas flow rate and inlet pressure was found to have reverse relationship i.e. an increase in the gas flow rate caused to decreased in the gas separation efficiency at fixed GVF. A correlation analysis is done to establish the strength of the relationships between predicator and predicted variables, which has produced the following sets of suitable predicator candidates for the network model as shown in figure 2.

Predicator variables						Predicted Variables
No	Set_A	Set_B	Set_C	Set_D	Set_E	
1	Gas volume fraction	Inlet liquid volumetric flow rate	Gas volume fraction	Liquid superficial velocity	Liquid superficial velocity	Liquid Efficiency
2	Inlet liquid volumetric flow rate	Inlet Gas volumetric flow rate	Inlet mixture velocity	Pressure drop across ISEP	Pressure drop across ISEP	Gas Efficiency
3	Pressure drop across ISEP	Pressure drop across ISEP	Inlet Pressure	Gas residence time.	Stoke's number	Liquid carry over
4	Pressure drop b/w HISEP inlet and HISEP axial outlet	Pressure drop b/w HISEP inlet and HISEP axial outlet	Pressure drop b/w HISEP inlet and HISEP axial outlet	Pressure drop b/w HISEP inlet and HISEP axial outlet	Pressure drop b/w HISEP inlet and HISEP axial outlet	Gas carry under

Figure 2 Input and out parameters of the separator used in the model

Multicollinearity among the predictor variable effects the accuracy of the model hence should be kept lower if not possibly removed. Partial correlation coefficients are calculated for all the possible predicators listed in figure 2 and it is found that Set_A and Set_C of the predicators bear significant relation ship with gas and liquid

 Published by Cranfield University Press ISBN: 978-0-9557436-7-2 http://hdl.handle.net/1826/3832

separation efficiency and at the same time also have relatively less multicollinearity among them selves and hence can be regarded more suitable choice for the input parameters. Software is developed using MATLAB to train the network for all the five sets of predictor variables. This software automatically selects best possible training algorithm by comparing the validation error during training and average absolute percentage error during the testing for given set of input condition and can be used to forecast the efficiency parameter like liquid carry over and Gas carry under at varying inlet flow condition.

Network Architecture and optimisation

The developed network model is consist of one input layer of four neurons, one hidden layer and one out put layer of four neurons. The number of hidden layers and activation function in the hidden layer was decided after doing some preliminary experiments with the network architecture. It was observed that more than one hidden layer does not produce good result hence it was decided to use one hidden layer in the model. There is no hard and fast rule to define the hidden neurons in hidden layers although some guidelines are available in literature. This critical problem is tackled by following the constructive algorithms approach. The smallest possible network with one hidden neuron in the hidden layer is used at the start of the training and then number of neuron is added in the hidden layer to improve the performance. The number of neurons initially has varied from 1 to 50 for all four chosen training algorithms but then reduced to 15 hidden neurons as the testing, validation and training error was found almost unchanged after 10 hidden neurons. The validation error being an indicator of over-fitting is used to choose the best trained network among 60 possible trained networks for every given input set.

Figure 3 shows the effect of adding neurons of all used training algorithms for input Set_A, same trend is observed for other inputs sets. Looking at the figure it can be seen that the training, testing and validation errors are decreasing with the increasing hidden neurons. These errors have become almost constant in Trainbr, Trainlm and Traincfg after 10 hidden neurons but start increasing in Traingdx. It can also be noted that the validation and training error are not significantly differ from each other which also indicates absence of any over fitting, as according to Master (1993) If the difference in the error obtained using the validation set is markedly different than that obtained using the training data, it is likely that the model has been over-fitted.

 Published by Cranfield University Press ISBN: 978-0-9557436-7-2 http://hdl.handle.net/1826/3832

Result

The performance and accuracy of all the neural network is evaluated by analysing statistical parameters such as average relative percent error, root mean square error, correlation coefficient on the error between predicated network output and the measured out. For Set_A. Figure 3 shows the best train algorithms for all the five input sets along with the average percentage error for all the output parameters. It can be seen that TrainLm is found to be most suitable training algorithm for all the five input sets. On the basis of the over fitting, the least validation has occurred in Set_E. However the accuracy error i.e. average percentage error for all the output parameters are found low in set_C and set_A and since this two sets contains all measurable inputs and also have less multicollinearity exist b/w them hence on this basic Set_A and Set_C can be regarded as more suitable input parameter of the developed neural network model. The residual analysis for the best select neural network is shown in figure 4.

	Set_A	Set_B	Set_C	Set_D	Set_E
Training algorithm	Trainlm	Trainlm	Trainlm	Trainlm	Trainlm
Hidden Neurons	15	15	7	10	15
Validation Error	0.0174	0.0186	0.0168	0.0156	0.0140
APE Err Liq_efficiency	0.140	0.1446	0.1496	0.1817	0.1831
APE Err_Gas efficiency	0.459	0.5185	0.5184	0.5732	0.5248
APE Err_GCU	3.160	4.2354	3.7650	4.2812	3.6839
APE Err_LCO	13.575	13.0120	13.4103	17.3316	16.8848

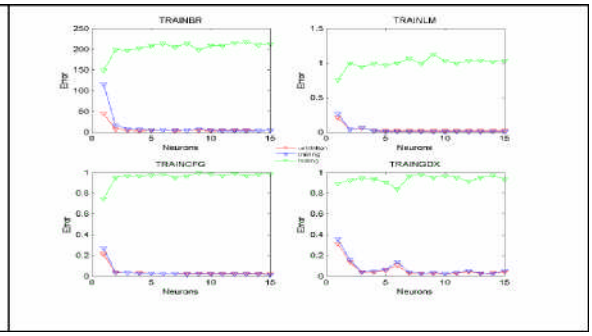

Figure 3: Effects of hidden Neurons on Absolute percentage error & validation error

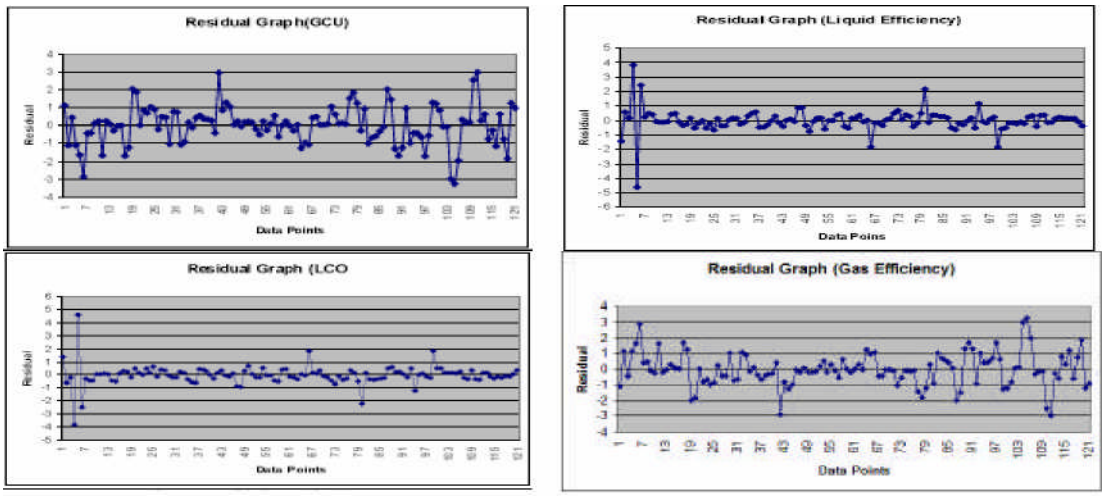

Figure 4 Residual analysis of the trained neural net for output efficiency parameters.

 Published by Cranfield University Press ISBN: 978-0-9557436-7-2 http://hdl.handle.net/1826/3832

Conclusion

Neural networks with several training algorithm and varying hidden neurons are trained to predict the separation efficiency of a compact separator at different inlet conditions. All the trained networks are then simulated on the physical data. Trainlm is found to be most accurate model to predict the separation efficiency The developed model is compared with the physical data and is found to work reasonable well with unseen data.

References

1. Frans T.M. Niewstadt and Maarten dirkzwager A fluid Mechanics Model for an Axial Cyclone Separator Ind Eng,chem..Res 1995.
2. Lingjuan Wang,Calvin B. Parnell, Analysis of Cyclone Collection Efficiency 2003 ASAE Annual International Meeting.
3. Sharda, R., Patil, R.B., 1992. Connectionist approach to time series prediction: An empirical test. Journal of Intelligent Manufacturing 3, 3 17–323.
4. Fishwick, P.A., 1989. Neural network models in simulation: A comparison with traditional modelling approaches. In: Proceedings of Winter Simulation Conference, Washington, D.C., pp. 702–710.
5. Connor, J.T., Martin, R.D., Atlas, L.E., 1994. Recurrent neural networks and robust time series prediction. IEEE Transaction on Neural Networks 51(2), 240–254. 6.Gent, C.R., Sheppard, C.P., 1992. Predicting time series by a fully connected neural network trained by back propagation. Computing and Control Engineering Journal 3 (3),May, 109–112.

 Published by Cranfield University Press ISBN: 978-0-9557436-7-2 http://hdl.handle.net/1826/3832

Characterising the level of crashworthiness for impacts on hard ground and water surfaces for a metallic helicopter under floor structure: What lessons can be learned?

K. Hughes

Crashworthiness, Impact and Structural Mechanics Group (CISM),
School of Engineering, Cranfield University, Cranfield, BEDS, MK43 0AL, UK

Abstract

Helicopters are seen by the petroleum industry as the only viable way of transportation between on and offshore platforms. At present, there exists no certification requirement to ensure a high level of survivability in the event of a water impact. Within the literature, there exists a body of information related to the post crash analysis of accident data, which supports the finding that a conventional metallic under floor design performs poorly during a water impact, in relation to the transmission of water pressure and the absorption of energy.

In order to characterise this behaviour, this paper concerns the crashworthiness of helicopters to two extremes in loading, namely hard ground and water surfaces, for an impact speed of $8ms^{-1}$, for a simple box-beam construction common to metallic helicopters. The experimental findings were used to validate finite element simulations, with a view for assessing the level of crashworthiness currently offered, together with identifying potential design improvements. To improve the level of crashworthiness, careful redesign of frames, joints and skin is required, together with developing a passive next generation floor that can cater for both hard surface and water impacts, by being able to degrade its localised strength, depending upon the type of surface encountered.

Introduction

The earliest recorded work that investigates the effects of a man made object impacting on water can be traced back to 1929, where Von Karman developed the first theoretical model to calculate the forces encountered during rigid seaplane floats impacting onto water [1]. This approach utilised the concept of added mass, which was a difficult parameter to quantify, but provided a good starting point for developing understanding in this field, which was subsequently extended and adopted during later works.

 Published by Cranfield University Press ISBN: 978-0-9557436-7-2 http://hdl.handle.net/1826/3832

In the early days of helicopter crashworthiness development, a small cross-section of experimental data was available. Typically, these were reviewed by separate agencies and the information was generally fragmented, making it difficult to identify potential design improvements, or amend current regulations.

This problem was first addressed in 1986 by providing a historical review of civil helicopter accidents occurring between 1974 and 1978, which was later followed by a review of US Navy and Army accidents in the same year [2, 3]. This was again reviewed in 1993 for helicopter ditchings onto water that occurred between 1982 and 1989. This was performed in two phases, where part I dealt with the analysis of the impact and post impact conditions [4], and part II provided an assessment of the structural response on occupant injury, the identification of ways of alleviating injury, together with an evaluation of current numerical techniques for modelling impacts onto water [5]. Several full-scale helicopter drop tests have also been performed in recent years in order to provide a greater understanding of the phenomena associated with fluid-structure interactions [6-9].

This research has identified that the water environment poses a unique design case, for which conventional designs perform poorly, in terms of transmitting the water pressure and the absorption of energy. The poor transmission of these loads, coupled with a high failure strength of the surrounding structure, means that frame collapse does not occur and high forces and accelerations are passed through the airframe. This in turn can lead to the distortion of the passenger floor and preventing the energy absorbing seats from operating effectively, through to the jamming or loss of the doors. A more serious problem concerns loss in floatation capability if skin integrity fails and the resulting internal damage that will occur.

This paper concerns the crashworthiness of helicopters onto water and provides a complete section-by-section analysis of a representative sub floor section that was dropped as part of an EU project (*CAST,* whose aim was to develop simulation tools and a design methodology that will permit cost effective design and entry into service of crashworthy helicopters for impacts onto both ground and water [9].

This paper is split into two parts, with the first providing a description of the test facilities, the choice of boundary conditions and the instrumentation applied to the structure, and the second part will provide a detailed classification of the different failure modes observed. The assessment of the crashworthy response will enable limitations to be identified, which will have a profound impact on future metallic helicopter design and significantly improve occupant survivability during an impact on water. For further information, the reader is directed towards reference [10].

 Published by Cranfield University Press ISBN: 978-0-9557436-7-2 http://hdl.handle.net/1826/3832

Helicopter crashworthiness

Due to the facilities available within CAST, a novel and dedicated instrumented experimental campaign was performed to investigate water impact phenomena, ranging from material and joint testing, right through to helicopter sub structure and full-scale helicopter drop tests onto hard and water surfaces. A Westland WG30 helicopter was supplied by Agusta-Westland, as this airframe was considered to be typical of a metallic design. Two sections of floor were cut from the main passenger section, which saw the aft section sent to the water impact facility at CIRA, Italy, and the forward section to Eurocopter Deutschland who performed the hard surface drop test, as shown in figure 1.

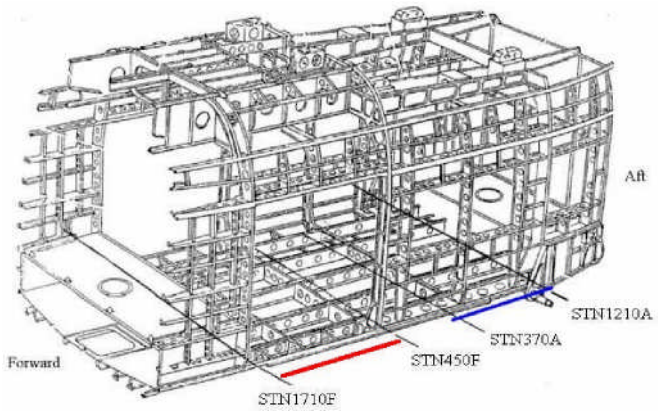

Figure 1 Location of the component sub floors in relation to the main passenger section of the WG30

Hard surface drop test

This section of floor was cut between STN1710F and 450F, which is located in the forward part of the main passenger section and corresponds to the full width of the port and starboard doors. This component weighed 44kg and was 2.25m wide, 1 .26m long and 0.1 65m high. This section was chosen to investigate the damage that occurs where the main lift frames are directly attached, together with incorporating the influence of at least one other major cross-member. The floor is primarily constructed from aluminium 2014-T6, whilst the passenger floor is constructed from a fibrelam composite.

The floor was dropped via a guided descent at $8ms^{-1}$, to which a 1 ton ballast plate was added. Instrumentation included eight accelerometers positioned on the main longitudinal frames, together with strain gauges and three force transducers. The main features of damage can be found in figure 2, where the passenger floor has been removed for clarity. As can be seen, all the frames contribute to energy absorption, as failure in the form of hinge lines in both transverse and longitudinal frames is observed. The skin plays no part in the energy absorbing process. Good agreement was obtained for the locations of frame collapse and force-time histories with the

 Published by Cranfield University Press ISBN: 978-0-9557436-7-2 http://hdl.handle.net/1826/3832

numerical results. The existing structure is capable of absorbing the impact energy, but achieves this in an inefficient manner due to the limited use of the available stroke.

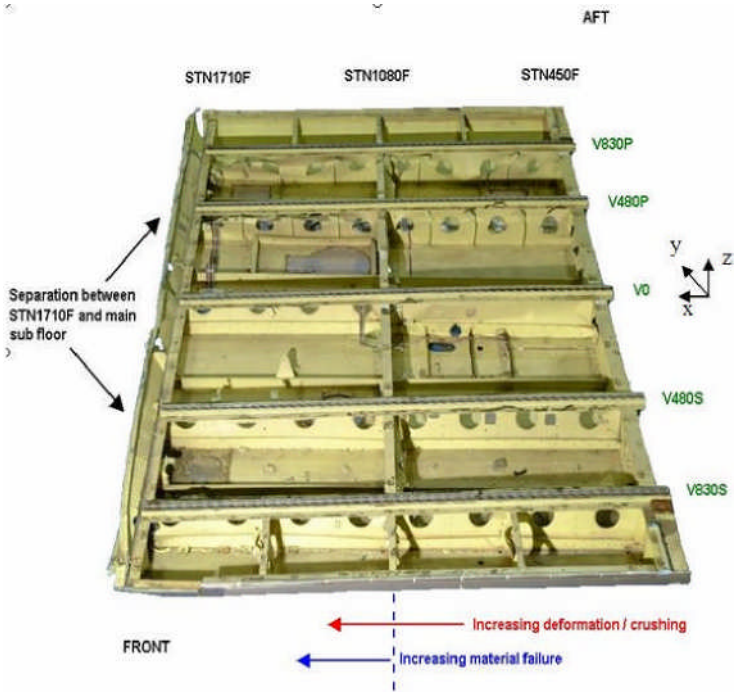

Figure 2 Overall view of the post test specimen, where the floor has been removed for clarity

Water drop test

This under floor construction is based upon simple box-beams and was cut between STN370A and 1210A, resulting in a floor with a mass of 41 kg, with dimensions 2170mm wide, 970mm long and 163mm high. An $8ms^{-1}$ guided descent was performed via a trolley assembly, to which ballast of 600kg was applied through 18 seat rail attachment points in order to represent the lift frames, seats and passengers.

 Published by Cranfield University Press ISBN: 978-0-9557436-7-2 http://hdl.handle.net/1826/3832

The post impact specimen can be found in figure 3, where the passenger floor has been removed for clarity. As can be seen, the floor retains its global integrity, as the main longitudinal frames remain undamaged, with the skin deflecting quite significantly in between these longitudinal frames. There are two main locations of skin and rivet failure, which would result in the ingress of water and the resulting secondary damage. The curved end sections remain relatively undamaged, as their shape minimises loading at these locations, due to the redirection of the water.

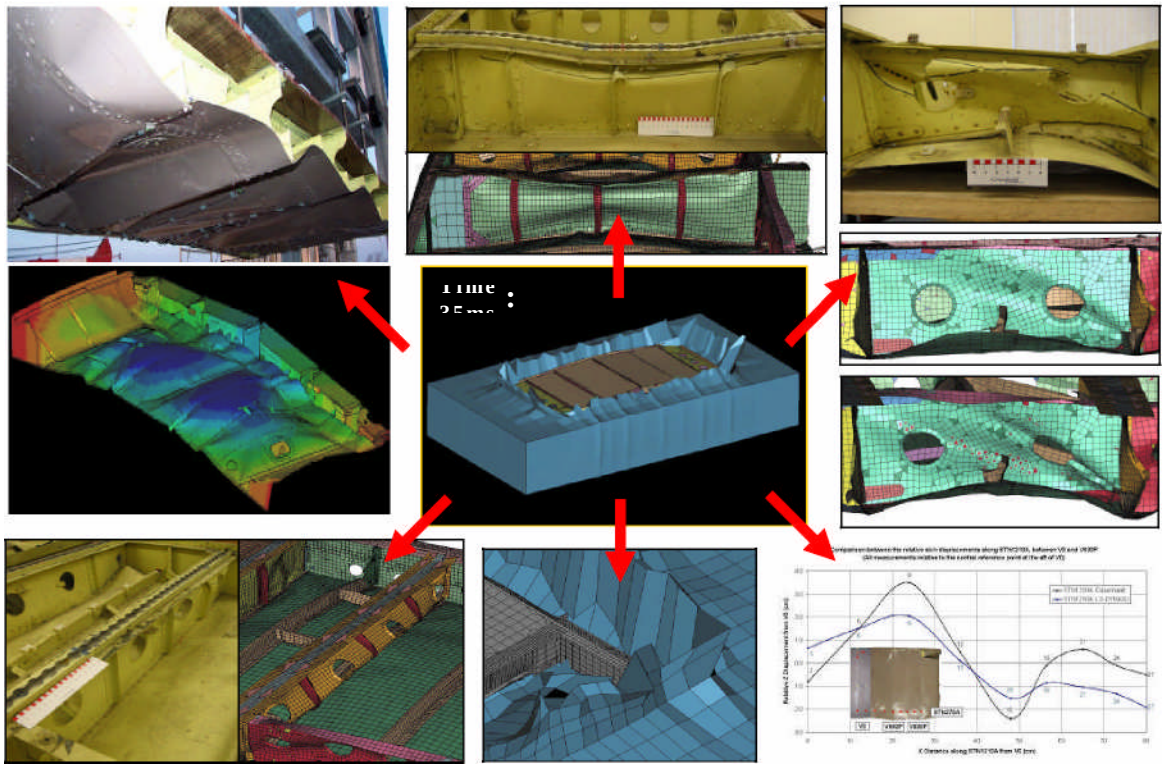

Figure 3 The finite element analysis allowed detailed comparisons with experiment for hinge location, skin deformation and collapsed height of the frames

To recreate numerically, a purely Lagrangian approach was used. The code was able to predict a representative response when compared to test, as good agreement for limited frame collapse, the deflections of the skin (within 10% of test), together with the locations of potential skin failure. Limited joint collapse is predicted, which is also consistent with test. The skin deflects in-between the frames, causing localised material and rivet failure, in the form of tensile pull-out from the surrounding frames.

 Published by Cranfield University Press ISBN: 978-0-9557436-7-2 http://hdl.handle.net/1826/3832

Design Limitations

The key issues for developing helicopter crashworthiness for impacts on both hard ground and water surfaces depend upon developing a passive energy absorbing structure that incorporates the following recommendations;

Reduce failure strength of the existing design

The first observation concerns limited utilisation of the available frame stroke, so consideration should be given to frame construction to ensure progressive collapse through the careful selection of geometry, material type and possible inclusion of a trigger, and the second is through the redesign of the joints, as progressive joint failure will be critical in order to allow for increased and controlled frame collapse.

The current metallic design has been developed based upon hard ground crash regulations, so the structure has been designed to collapse at relatively higher loads than are typically encountered during a water impact, which are insufficient to trigger frame collapse. Reducing the failure strength of the existing design is a difficult engineering problem, as if the strength of the structure is too low, this will result in a degradation in performance during a hard surface impact.

Development of skin

During a water impact, the dominant membrane behaviour of the skin is the only mechanism to transfer the water pressure to other energy absorbing components. Therefore, skin integrity is essential if the loads generated are to be transferred to enable frame collapse to occur, without the skin failing. This in turn will increase the floatation capabilities and post impact survivability for the occupants. Therefore, the deflection of the skin needs to be encouraged, as this forms a significant passive energy absorber during an impact on water. This will require a move away from conventional metallic skins towards the use of composite materials.

Conclusions

The experimental and numerical results have demonstrated that a water impact is a critical design scenario, where crash requirements from both hard and soft surfaces must be taken into account during the preliminary design phase.

 Published by Cranfield University Press ISBN: 978-0-9557436-7-2 http://hdl.handle.net/1826/3832

To improve the crashworthy response on water requires an improvement in the membrane behaviour of the skin in order to utilise the infinite stroke offered by the water, together with incorporating a dual failure mode capability for the surrounding structure that can degrade its strength depending upon the type of surface impacted. This will lead to a next generation under floor structure that offers improved crash protection for occupants and crew.

References

1. Von Karman, Th. The impact of seaplane floats during landing, NACA Technical Note 321, October 1929
2. Coltman, J.W., Neri, L.M., Analysis of US civil rotorcraft accidents for
3. development of improved design criteria, National specialists meeting on crashworthy design of rotorcraft, American Helicopter Society, 1986
4. Coltman, J.W., Domzalski, L., Arndt, S.M., Evaluation of the crash environment
5. for US Navy helicopters the hazards and Navy response, National specialists meeting on crashworthy design of rotorcraft, American Helicopter Society, Atlanta, Georgia, 1986
6. Chen, C.C.T., Muller, M., Fogary, K.M., Rotorcraft ditchings and water related impacts that occurred from 1982 to 1989 – Phase I, US Department of Transportation, FAA Technical Center, Atlantic City, DOT/FAA/CT-92/13, October, 1993
7. Muller, M., Rotorcraft ditchings and water related impacts that occurred from 1982 to 1989 – Phase II, US Department of Transportation, FAA Technical Center, Atlantic City, DOT/FAA/CT-92/14, October, 1993
8. Fasanella, E.L., Jackson, K.E., Lyle, K.H., Finite element simulation of a full scale crash test of a composite helicopter, AHS 56th Annual Forum, Virginia, USA, 2000
9. Wittlin, G., Smith, M., Sareen, A., Richards, M., Airframe water impact analysis using a combined MSC/DYTRAN – DRI/KRASH approach, AHS 53rd Annual Forum, Virginia Beach, Virginia, April 29- May 1, 1997
10. Wittlin, G., Schultz, M., Smith, M.R., Rotary wing aircraft water impact test and analyses correlation, AHS 56th Annual Forum, Virginia, USA, May 2-4, 2000
11. CAST – Crashworthiness of Helicopters onto Water – Design of Structures using Advanced Simulation Tools, funded by the European Community under the "Competitive and Sustainable Growth" programme (Contract G4RD-CT1999- 0172), 2000-2003.
12. Hughes, K, Application of improved Lagrangian techniques for helicopter crashworthiness on water. *Phd Thesis,* Cranfield University, 2005

 Published by Cranfield University Press ISBN: 978-0-9557436-7-2 http://hdl.handle.net/1826/3832

Estimating the Ultrasonic Doppler Flowmeter Performance under Multi-phase Well-homogeneous Flow

K. M. Khalifa, Akinyemi Seun and Sanderson M. L.

Department of Process and Systems Engineering, Cranfield University. UK

Abstract

Existing accurate techniques for multi-phase flow measurement may cause process interruptions and flow restrictions which affect the oil and gas field's production and profitability. However the developments in areas of non-intrusive / non-invasive flow metering have reasonably overcome the challenges of measuring multi-phase flow to improve online flow measurement and offer a measurement solution for limited flow regimes that occur within oil production systems. However, multiphase flow regimes associated with high gas and liquid velocities existing in oil and gas systems are yet to be accurately measured.

A Doppler ultrasonic technique has been used in conjunction with a static on line mixer in a water/air system to measure the mixture flowrate from which the liquid flow rate was used in combination with a conductivity ring to measure the fraction. The gas flowrate was then obtained using mass balance between the mixture and liquid flow rates within this section. The results were compared with the reference measurements and good agreement between these two measurements was obtained with accuracy ranges from 6% to 10%. Also the gas measurement was compared with the reference measurements with 10% accuracy.

Nomenclature

α	Void fraction
V_{sl}	Superficial liquid velocity ($m.s^{-1}$)
V_{sg}	Superficial gas velocity ($m.s^{-1}$)
V_m	Mixture velocity ($m.s^{-1}$)
$V_{(doppler)}$	Velocity of mixture ($m.s^{-1}$)
T	Temperature ^oC
P_s	Static pressure ($bar.abs$)
Q_m	Volumetric mixture flowrate ($m^3.s^{-1}$)
Q_l	Volumetric liquid flowrate ($m^3.s^{-1}$)
Q_g	Volumetric gas flowrate ($m^3.s^{-1}$)
A	Cross section area (m^2)
A_l	Liquid area (m^2)

 Published by Cranfield University Press ISBN: 978-0-9557436-7-2 http://hdl.handle.net/1826/3832

A_g Gas area (m^2)

Introduction

The problem of how to measure with high accuracy the flowrate of multiphase mixtures has been considered by many researchers in order to meet the oil and gas industries needs. The conventional method of measuring a multi-phase flow accurately is to separate the flow of each phase and measure the individual phases using well known single phase flow-meters. This is the method used for fiscal measurements. However, when the purpose of separating oil-water-gas is to control and monitor the oil production, or to monitor and test each well in production field, the test separation method will be costly (interrupted production and time) and require bulky equipment (Thorn R, et al 1997). As a result online measurement using accurate multi-phase flow meters are emerging employing partial separation homogenisation and pattern recognition. These methods can also be used in volume allocations for companies producing from the same reservoir or injecting into the same pipeline.

Two-phase Homogeneous Flow

In two-phase flow the behaviour of the gas and liquid in a flowing pipe reveals various flow characteristics, which depend on the gas pressure, gas and liquid velocity, as well as the geometry and inclination of the piping. Homogeneous flow is associated with good bubble distribution within the flowing liquid; however, this distribution depends very much on the Gas Void Fraction. (Norwegian Society for Oil & Gas Measurement 2005)

In order to achieve an accurate performance of the multi-phase flow metering, a STATIFLO Motionless mixer was used to homogenize the flow thereby eliminating the slip between gas and liquid. A clamp-on ultrasonic Doppler flowmeter and a pair of conductivity rings (flush-mounted in the pipe internals) were installed within the homogeneous two-phase flow region to measure the volumetric flow rates and determine the gas void fraction.

Doppler Ultrasonic Flow Meter

The Doppler ultrasonic flow meter principle is based on the reflection of acoustic waves from a moving scatterer back to the source; the frequency shift is proportional to the velocity component of the object parallel to the acoustic beam. The frequency shift is given as: $\Delta f = 2\,ft(V/c)\cos\theta$, where V is the velocity of the scatterers, and c the acoustic velocity.

However, The Doppler flow meters performance is limited as a result of the nature, size, and spatial distribution of the scatterers which varies the attenuation of ultrasonic beam. Since the measured velocity is as a result of scatterers, slippage might not correspond to the actual fluid

 Published by Cranfield University Press ISBN: 978-0-9557436-7-2 http://hdl.handle.net/1826/3832

velocity (Sanderson M.L, Young H, 2002). Normally, the wall section near the transducer is the only section that is monitored. The zone of reflection is in a region of variable velocity (Bernard C.J. 1988).

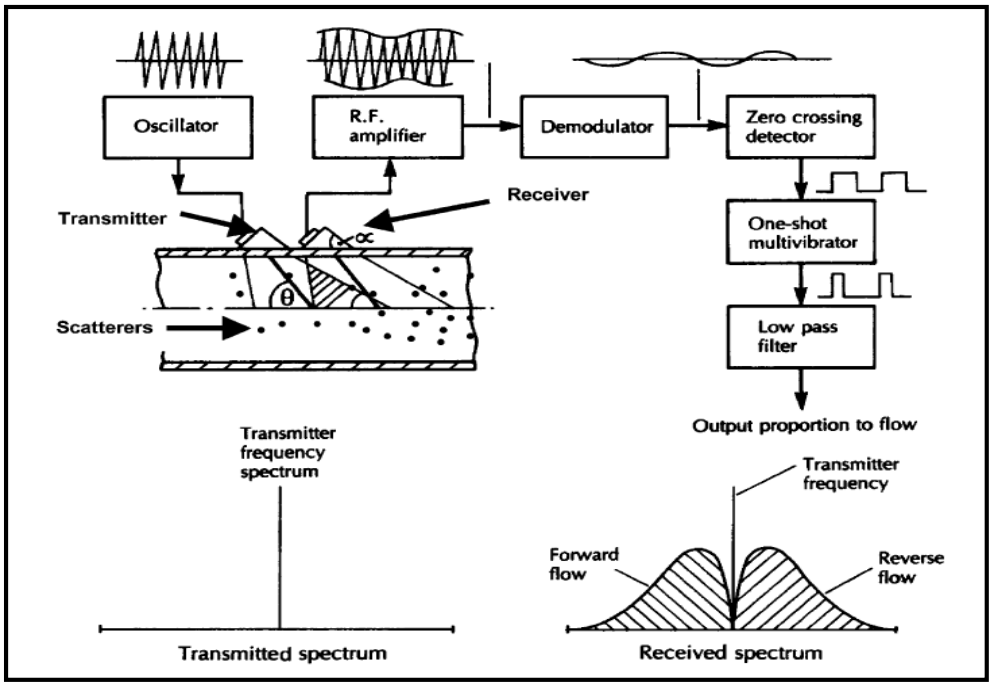

Figure 1, Doppler ultrasonic flow meter, taken from (M.L. Sanderson and H. Yeung)

The Experimental Pipe Loop

The two-phase (water, air) rig situated in the Process and Systems Engineering Flow Laboratory in Cranfield University is made of a 22 m long plastic ABS (class E) horizontal pipe of 50 mm inner diameter. The pipeline length is sufficient for forming fully developed slugs. The reference measurements are made using a Khrone Altoflux Electromagnetic flow meter (0 - 4.524m^3/hr) installed downstream of the water pump. The air flow is measured with a Quadrina Turbine flow meter with a calibrated flow range of 6-60m^3/hr and an uncertainty greater than +/- 1% of full scale at very low flow rates.

The water is pumped to the test section by a centrifugal pump with 40 m^3/hr and discharge pressure of 5 barg. Gas is supplied from a screw engineering compressor with a maximum supply capacity of 400 m^3/ hr free air delivery and a maximum discharge pressure of 10 barg.

 Published by Cranfield University Press ISBN: 978-0-9557436-7-2 http://hdl.handle.net/1826/3832

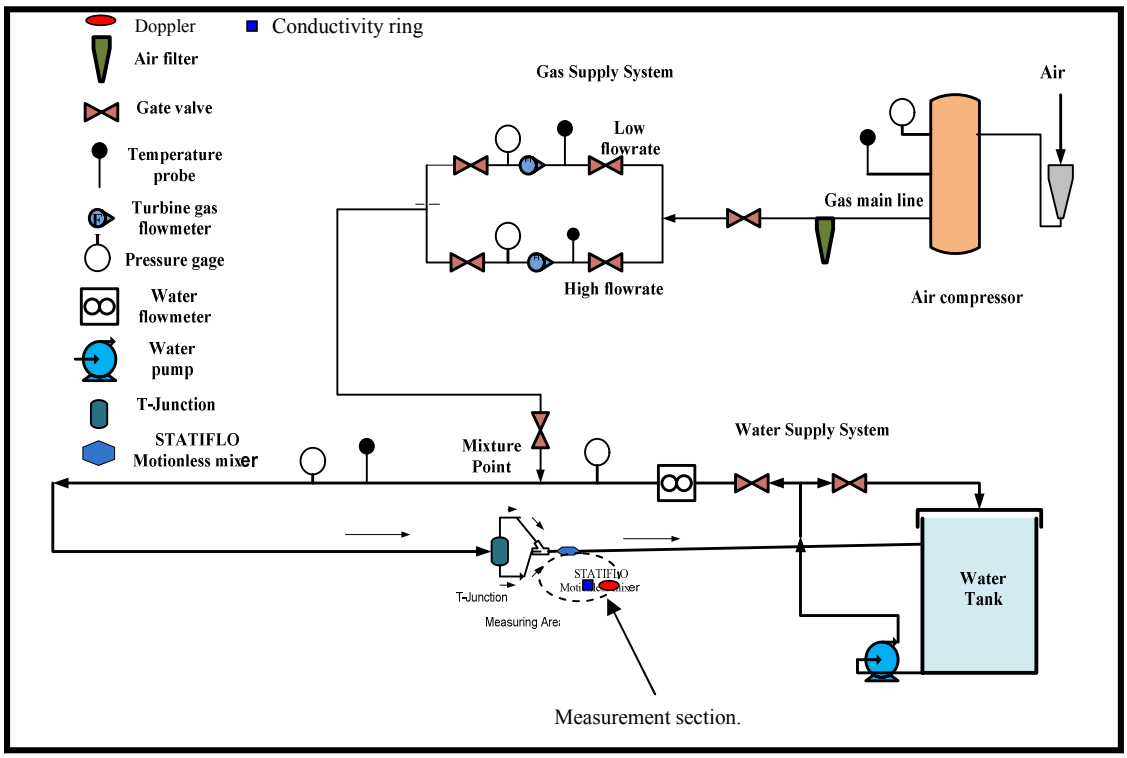

Figure 2, Schematic of two-phase test rig.

The test section consists of 6-inch T-junction with 2-inch gas and liquid outlets. These two outlets were joined into 2-inch pipeline where the STATIFLO Static Kenics Mixer device is installed. This mixer has 6 identical left and right helical elements. The mixer homogenises the two-phase flow before ultrasonic Doppler flowmeter measurement section where the mixture flow velocity is measured, and then the two-phase flow is returned to the water tank. The pipe loop and instrumentation are shown schematically (not to scale) in Figure 2. A flush-mounted conductivity ring was calibrated and installed to measure the fraction in the homogeneous flow.

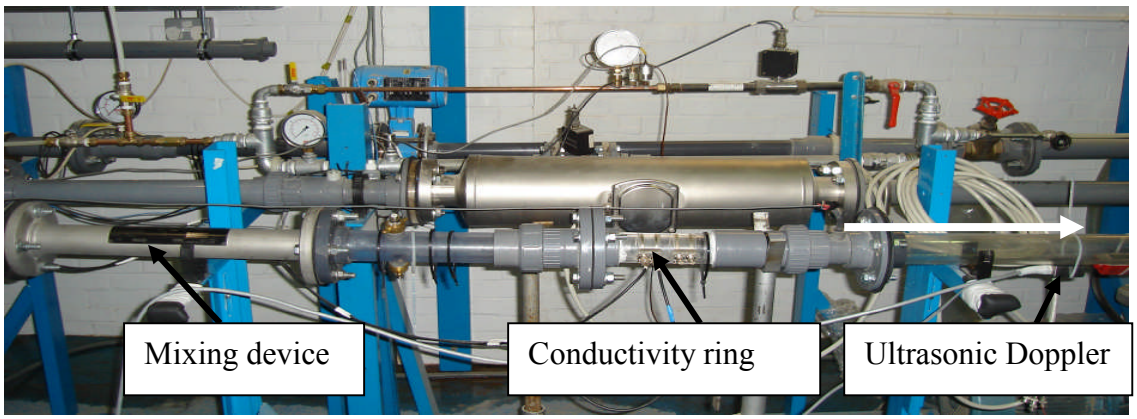

Figure 3, Homogenized flow section.

 Published by Cranfield University Press ISBN: 978-0-9557436-7-2 http://hdl.handle.net/1826/3832

Experimental Results and Analysis

The assumptions used in the analysis of the results obtained are that there is no slip between the gas and liquid phases downstream of the mixer, the flow stream is well homogenized at the measurement points and the mixture volumetric flow rate is corrected for the working temperature and pressure. The experimental test conditions ranges were as follows:

- V_{sl} $1\, m.s^{-1}$.
- V_{sg} 0.5 to $8\, m.s^{-1}$.
- α 38% to 88 %.
- P_s 1.02 bar abs.
- T 23^{o}C.

Total Volumetric Flowrate Measurement

The mixture velocity measurement in the measuring section is based on the ultrasonic Doppler flowmeter reading. The total volumetric flowrate of mixture is obtained as the product of the mixture velocity $m.s^{-1}$ and the pipe cross section area which is 0.002 m^2.

$$Q_m = V_{(doppler)} * A$$

For this test, V_{sl} is fixed at1 $m.s^{-1}$ and V_{sg}, was in increased from 0.5 to 8 $m.s^{-1}$.This results in an increase in the value of α. From graph 4 it may be seen that the mixture flowrate error increases as V_m increases.

Liquid Volumetric Flowrate Measurement

The liquid's volumetric flow rate within the homogeneous flow region was obtained by using flush-mounted conductivity rings to measure the liquid fraction and the Doppler flowmeter to measure the mixture velocity. So, $Q_l = V_{(doppler)} * A_l$

Figure 5 shows the accuracy measurement of liquid flowrate. The error of this measurement is a combination of the mixture velocity measurement and conductivity measurement error. This arises because the conductivity rings were calibrated in static stratified flow and are employed in homogenous flow regime. These errors can be reduced by carrying out dynamic calibration of the rings within homogeneous flow.

Gas Flowrate Calculation

The gas flowrate was obtained by discounting the measured liquid flow rate from the mixture flowrate measured by the ultrasonic Doppler.

$Q_m = Q_l + Q_g .so, Q_g = Q_m - Q_l$.

 Published by Cranfield University Press ISBN: 978-0-9557436-7-2 http://hdl.handle.net/1826/3832

Figure 6 illustrates the gas flowrate calculated from mixture flowrate and liquid flowrate within the homogeneous section. The error in this measurement is a combination of the liquid fraction error and mixture velocity error.

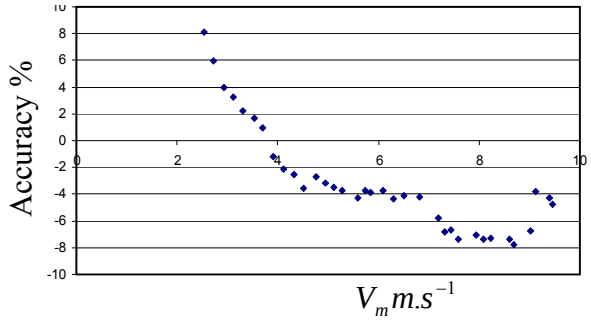

Figure 4, homogeneous flowrate accuracy

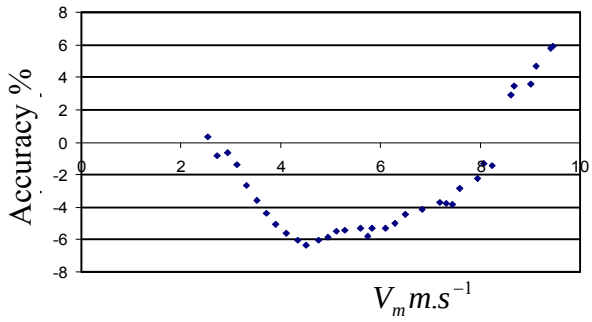

Figure 5, Liquid flowrate in homogeneous

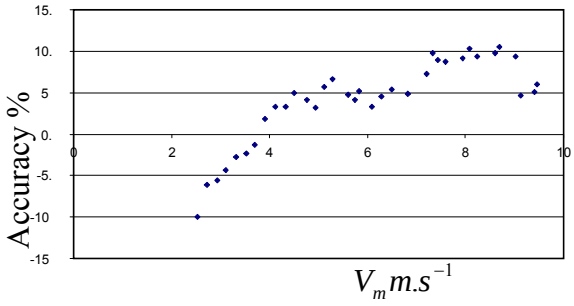

Figure 6, calculated gas flowrate

Conclusions and Scope for Future Work

The experimental results shown above give some measure of success in this investigation. The Doppler flow meter reading, combined with the void fraction measurements is capable of giving reasonably accurate measurements of the individual phase flows in the multiphase system. These results were obtained at a strictly controlled temperature range. Further studies will be carried out with the following aims:

- Perform a homogeneous calibration for the used conductivity ring.
- Improve the accuracy of the results under different flow regimes.
- Replace the liquid phase with higher a viscosity liquid and determine the conditions for accurate measurements.

References

1. Benard, C.J. (1988), Handbook of Fluid Flow-metering, the Trade & Technical Press Limited, Surrey, England.
2. Handbook of Multiphase Flow Metering, Norwegian Society for Oil and Gas
3. Measurement, March 2005.

 Published by Cranfield University Press ISBN: 978-0-9557436-7-2 http://hdl.handle.net/1826/3832

4. Sanderson M.L. and Young H., Guidelines for the Use of Ultrasonic Non-invasive Metering techniques, Flow Measurement and Instrumentation 13 (2002) 125-142.
5. Thorn R, Johansen G A and Hammer EA 1997 Recent Developments in three-phase Flow Measurement, Meas. Sci. Technol., Vol 8, No. 7, pp.691-701.

 Published by Cranfield University Press ISBN: 978-0-9557436-7-2 http://hdl.handle.net/1826/3832

Fabricating diamond microtools with focused ion beam machining

R.W.Evans, D.M.Allen, Precision Engineering Centre.

R.Evans@cranfield.ac.uk

Abstract

Diamond tooling is commonly used in Precision Engineering to achieve accurate form and sub-micrometre surface finishes in a wide range of materials. Such applications include electroless nickel lens moulds and diamond-turned embossing rolls of substantial (metre) dimensions.

This paper describes the challenges of fabricating single crystal diamond microtools with demanding geometries and tolerances. The microtools need to be small, durable and capable of machining precise features such as 20μm wide, 20μm deep channels that are not possible to machine with conventional, bulky single-point diamonds. The products of the machining process are typically micromoulds for health diagnostic microfluidic polymer devices. In this feasibility study, the starting tool is a diamond tool that has already been sculpted to the rough shape by laser beam machining by the tool supplier, a UK industrial collaborator. The laser-sculpted shape is machined rapidly by a focused gallium ion beam orientated at approximately 70° to the normal of the diamond surface leaving characteristic striations as a result of this first “roughing” process. The diamond is then machined to a much smoother surface finish by orienting the beam at $< 40°$ to the diamond surface, resulting in an amorphous surface with Ra $<$ 1nm.

Focused ion beam (FIB) machining

FIB is a subtractive process involving the removal of material by a directed beam of ions (positively charged atoms). Many different ions have been used for this purpose in the past but argon and gallium are two of the most frequently used. The research described herein has used a stream of gallium ions (Ga^+) 10-50nm in cross-section, using FEI hardware and Raith software, to remove carbon atoms from the diamond crystal lattice. This results in the ability to sculpt diamond into any desired 3D shape with a resolution of a few tens of nanometres.

 Published by Cranfield University Press ISBN: 978-0-9557436-7-2 http://hdl.handle.net/1826/3832

Effects of the beam orientation

The orientation of the beam to the surface to be machined is of fundamental importance. As the beam changes from a surface normal to an oblique angle, the resulting surface finish changes from smooth to rippled to stepped, as shown in Figure 1 [1] [2].

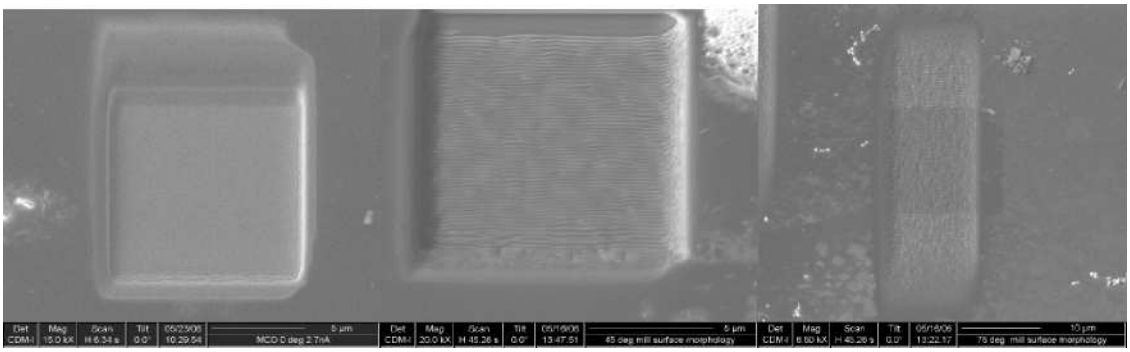

Figure 1: Surface finish on (100) diamond with the FIB at 0° (left), 45° (centre) and 75° (right) with respect to the normal to the surface. Ra values for the surfaces, obtained by AFM, are 0.58, 13.6 and 7.2nm respectively compared to 0.59nm for the unmilled diamond.

The dependence of surface finish on beam angle is an important aspect of the cutting methodology. This is illustrated in Figure 2 where, in the initial experiments, the laser-roughed out tool shape has been modified by milling a flat cutting edge at the tip. The rough surface finish can be seen in the intermediate state but can be finished satisfactorily when adjustments are made to the beam orientation.

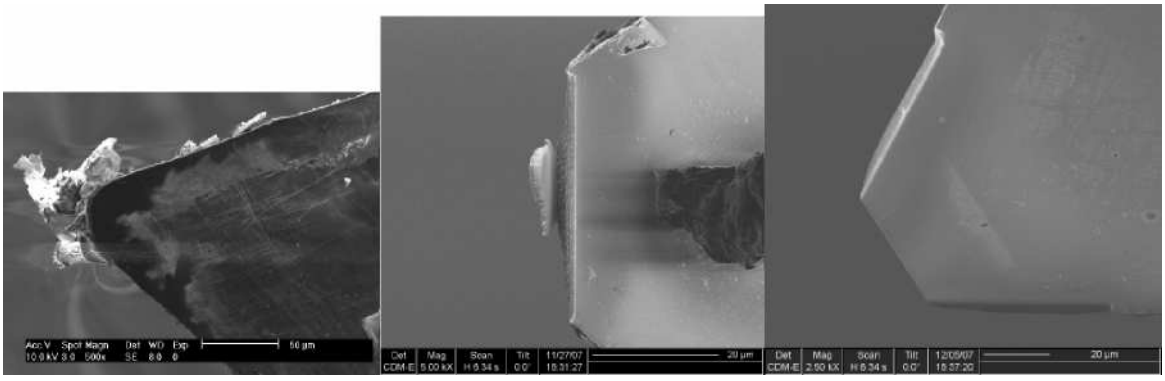

Figure 2: Roughed-out laser-cut tool before FIB machining (left), intermediate state showing surface ripples caused by beam reflections (centre) and finished smooth tool (right).

 Published by Cranfield University Press ISBN: 978-0-9557436-7-2 http://hdl.handle.net/1826/3832

FIB technique for edge creation

The diamond tool is made by Chemical Vapour Deposition (CVD) of carbon which has then been laser-cut to the rough outline of the desired tool shape. CVD diamond (which is polycrystalline) has no single crystal orientation and consequently no orientation dependence of its bulk hardness which has been measured as 81±18 GPa [3]. The advantage of the laser cutting is that most of the tool shaping can be done quickly, leaving the fine detail work for the FIB. The laser cannot give a sharp cutting edge, so the tool tip is left rounded, as shown in Figures 3 and 4.

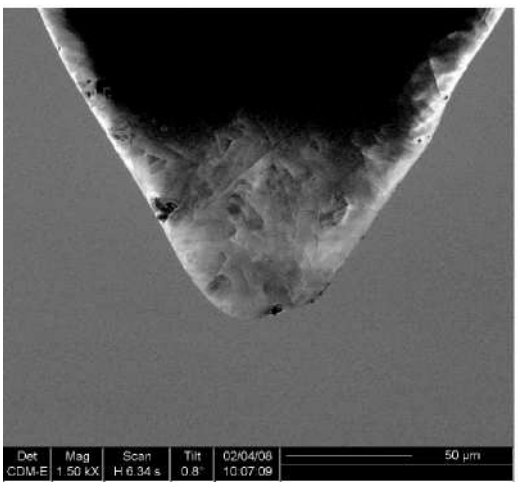

Figure 3: Laser cut tool (top view)

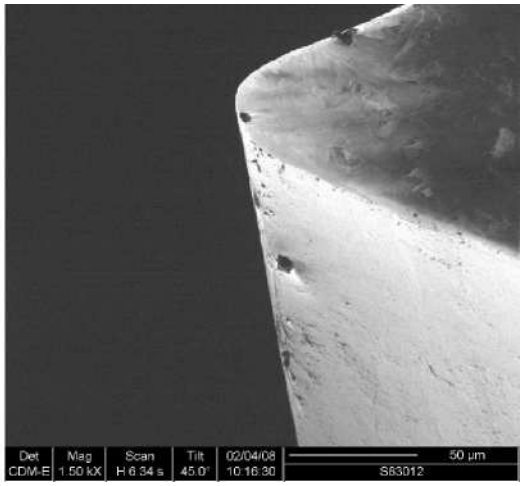

Figure 4: Laser cut tool (side view)

The rounded tip is FIB milled to give a straight edge. When milling a nominally flat edge with a FIB, the resulting surface will be angled at ~ 5 degrees. This is due to ions hitting the face at glancing angles with a high probability of being reflected, rather than removing any carbon atoms. Angling the tool to the beam can account for this and eliminate the unwanted slope.

To get the required clearance on the tool face the tool has to be angled when milling so that there is a negative angle on the front face. Figures 5 and 6 show a tool edge with a slope on the front face of 4 degrees. The debris on the tool rake was left untouched during edge milling because it is a visual aid when focusing the beam. Further milling at higher angles and milling directly onto the tool face are used to give tip clearance. To achieve a smooth finish on the tool, low angle milling is needed after the main processing to remove roughness from the tool face (see Figures 7 and 8). A finished tool is shown in Figure 9.

 Published by Cranfield University Press ISBN: 978-0-9557436-7-2 http://hdl.handle.net/1826/3832

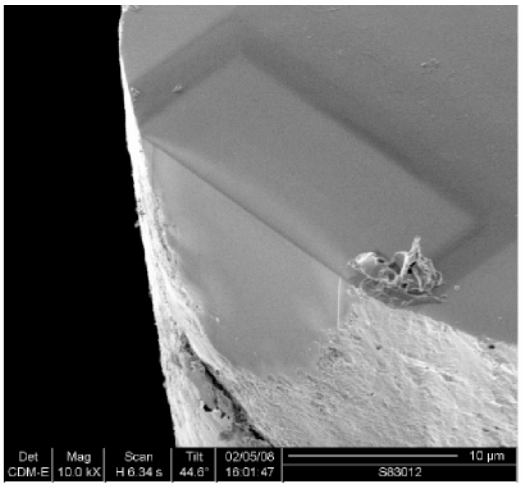

Figure 5: Milled straight edge

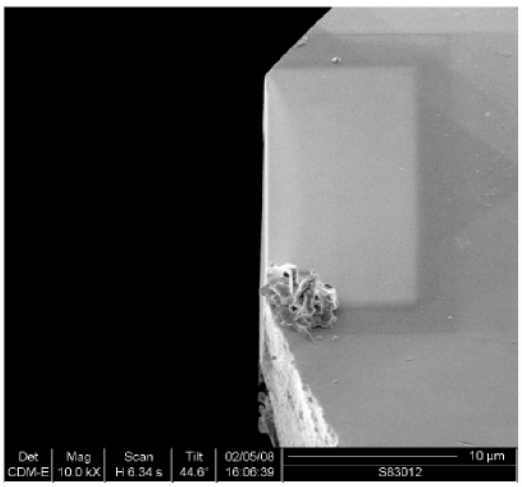

Figure 6: Four degree slope on front face

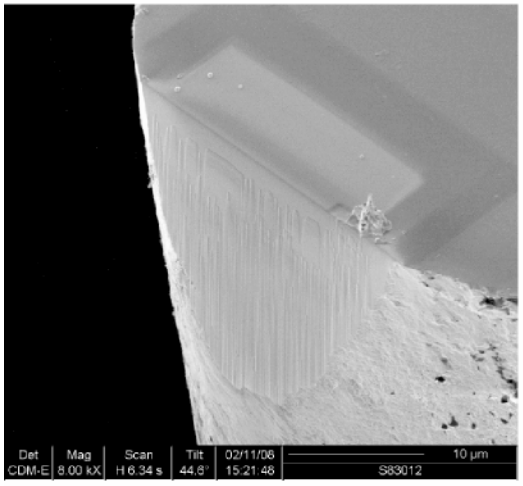

Figure 7: Corrugated front face

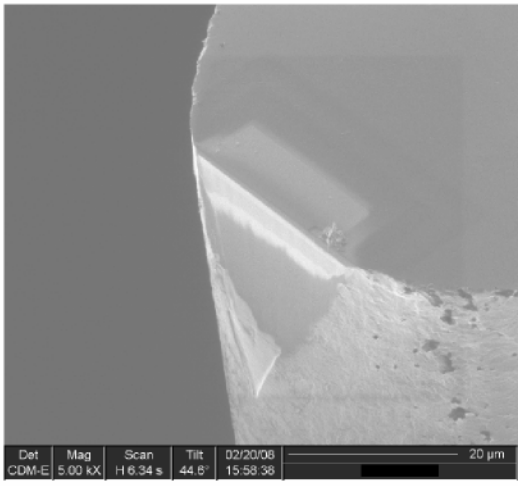

Figure 8: Smooth front face

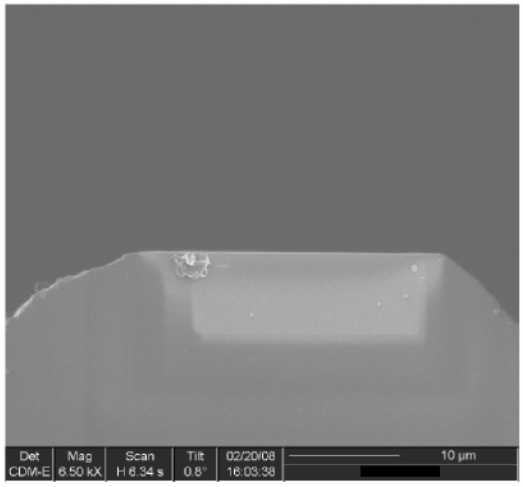

Figure 9:Finished tool

 Published by Cranfield University Press ISBN: 978-0-9557436-7-2 http://hdl.handle.net/1826/3832

Conclusions

FIB is capable of putting sub-micron features onto diamond tool tips. The angle of milling is important to achieve the correct angle on the front face of the tool and to give a smooth surface to the milled diamond. Simple-shaped tools are relatively easy to produce. The creation of non-standard shaped tools for bespoke applications is the objective of future research, either putting a parabolic or a sine wave pattern on the end of a laser-cut tool.

Acknowledgement

This work is part of the Engineering and Physical Sciences Research Council funded Grand Challenge project EP/C534212/1 investigating "3D-Mintegration". Thanks to Mr Andrew Cox, General Manager of Contour Fine Tooling, UK for supplying the roughed out laser-cut diamond tools as starting material.

References:

1. R.W. Evans, S. Marson and D.M. Allen, A review of focused ion beam technology for the fabrication of ultra precision diamond cutting tools, Proceedings of the $_{6}$th International Conference on Materials for Microelectronics and Nanoengineering, 29th-31st October, Cranfield, UK, 9-12, 2006.
2. Chan.W.L and Chanson.E, Making waves: kinetic processes causing surface evolution during low energy ion sputtering, J.Appl.Phys. 101. 121301-121346, (2007).
3. [3] www.e6.com

 Published by Cranfield University Press ISBN: 978-0-9557436-7-2 http://hdl.handle.net/1826/3832

Micro Milling Force Prediction by Coupling FE and Analytical Modelling Approaches

T Jin, D Zdebski, D M Allen and D J Stephenson

Precision Engineering Centre, Cranfield University, Bedford MK43 0AL, UK

e-mail:t.jin@cranfield.ac.uk

Abstract

The complex material removal mechanism at the micro tool tip was investigated in detailed FE simulation and the knowledge was used in a mathematical model to derive the cutting forces in both the feed and normal directions. The new approach has been proved to provide quick and reliable milling force predictions for selecting the appropriate cutting parameters. Good agreement has been achieved between the measured and predicted forces.

Key words: cutting force, micro end milling, prediction, finite element, monitoring

INTRODUCTION

The micro end milling process provides a cost effective and flexible means for making 3D micro features on miniature parts. Micro milling force prediction is crucial to avoid premature tool breakage. The existing cutting force models, such as Tlusty and Macneil's model [Tlusty et al., 1975], were developed for the conventional end milling (CEM) process, with the assumption that the cutting forces are proportional to the cross-sectional area of the un-deformed chip. When moving down to the micro cutting domain, it is often invalid to use such simple assumptions. The specific cutting energy (SCE) level in micro milling can be significantly higher than that in the macro milling regime. By using a new approach in determining the variation of SCE and force ratio, based on the finite element simulation of the micro cutting process [Jin, 2007], the milling forces in feed and normal directions can be predicted. The advantage of this new approach is the significant reduction of computing time and reliable estimation of SCE and force ratio, which can be obtained conventionally only by matching the theoretical and measured results of cutting forces.

CUTTING FORCE MODEL IN END MILLING PROCESS

Cutting force model

The cutting forces can be calculated from a predictive force model. A cutting tooth on the tool is subject to a tangential cutting force and also a radial force. It is assumed that the tangential force, F_t, is proportional to the cutting area [Tlusty et al., 1975 and Bao et al., 2000] :

 Published by Cranfield University Press ISBN: 978-0-9557436-7-2 http://hdl.handle.net/1826/3832

$$F_t = K_m \cdot b \cdot h \tag{1}$$

Where b is the axial cutting depth and h is the chip thickness, and

$$h = f_t \cdot \sin\theta \tag{2}$$

f_t is the feed per tooth and θ is the tool cutting angle (Figure 1). K_m is a proportional constant, referred to as specific cutting energy (SCE), and is dependant on the cutting tool geometry, cutting parameters and workpiece properties.

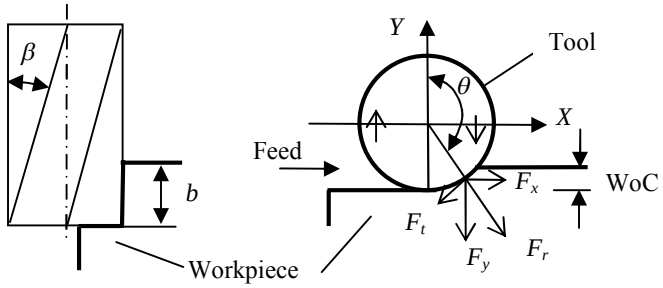

Figure 1; Schematic of end milling process

The radial cutting force is assumed to be proportional to the tangential cutting force:

$$F_r = p \cdot F_t \tag{3}$$

p is the cutting force ratio constant and is mainly dependent on the cutter geometry. For a certain tool cutting angle θ, the chip thickness is not a constant value, it varies along the tool axial direction due to the existence of tool helix angle β. The cutting forces in feed and normal directions are derived as: [1, 5]:

$$F_x = -F_u \cdot \left[\left(\sin^2\theta_e - \sin^2\theta_s\right) - 0.5 \cdot p \cdot \left(\sin 2\theta_e - \sin 2\theta_s\right) + p\left(\theta_e - \theta_s\right)\right] \tag{4}$$

$$F_y = F_u \cdot \left[-p\left(\sin^2\theta_e - \sin^2\theta_s\right) - 0.5 \cdot \left(\sin 2\theta_e - \sin 2\theta_s\right) + \left(\theta_e - \theta_s\right)\right] \tag{5}$$

where $F_u = 2 \cdot K_m \cdot R \cdot f_t / \tan\beta$. θ_s and θ_e are the start and end cutting angles along the tool axis due to the existence of the tool helix angle β, at a certain tool cutting angle θ .

 Published by Cranfield University Press ISBN: 978-0-9557436-7-2 http://hdl.handle.net/1826/3832

2D Finite element simulation of down milling process

Two-dimensional FE simulations of end milling have been carried out (Figure 2). The chip thickness varies with the tool cutting angle according to Equation 2 (see Figures 1 and 2). The cutting chips are generated by using adaptive remeshing of the finite element mesh.

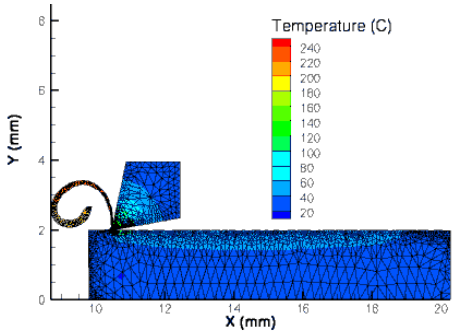

Figure 2; 2D FE mesh and temperature contour for down milling (Chip thickness decreases from the start to end position)

The radial and tangential force signals obtained from FE simulations (Figure 3) are used to derive the variation of SCE and force ratio with tool cutting angle. This information is then correlated to the analytical milling force model mentioned above, to finally predict the milling forces in feed and normal directions.:

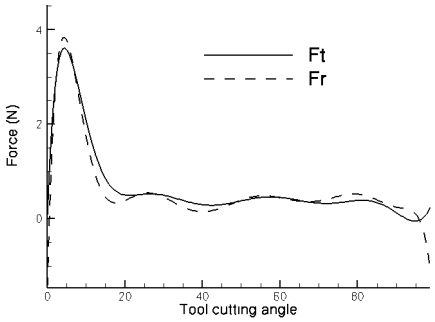

Figure 3; Tangential and radial forces F_t and F_r from the 2D FE simulation (tool diameter 1mm, cutting edge radius r =0.003mm)

The Johnson-Cook model is used for the two workpiece materials, Toolox 33 and Al6061 T6, in which the effects of strain hardening, strain rate sensitivity and thermal softening are included.

FORCE PREDICTIONS FOR MICRO END MILLING PROCESS

A 0.3 mm and a 1mm diameter tungsten carbide tools have been used in the study. The cutting forces were monitored by using a high resolution Kistler Dynamometer Model 9256C2. The cutting conditions are listed in Table I. Based on the observation under SEM, the cutting edge radius for the 1mm diameter tungsten carbide (TC) tool was estimated as r = 3μm. For the 0.3mm diameter tool, the

 Published by Cranfield University Press ISBN: 978-0-9557436-7-2 http://hdl.handle.net/1826/3832

cutting edge was much sharper, about r=0.001mm. The predicted milling forces in feed (F_x) and normal (F_y) directions show reasonably good agreement with the measured forces for the 1mm TC tool (see Table II). For the 0.3mm TC tool, the predicted forces, F_x and F_y, do not match exactly with those measured from the cutting tests, whilst the predicted principle forces, R, show rather good agreement with those obtained from measured forces(Table 2):

$$R = \sqrt{F_x^2 + F_y^2} \tag{6}$$

R is the force responsible for the tool loading and premature breakage, as it is the combined effects of F_x and F_y. It provides important information for evaluating the selection of cutting parameters to avoid overloading the micro milling tool.

Table I: Conditions for the micro end milling

Cutter Diameter D	0.3 mm	1 mm
Rake Angle	5 deg	
Clearance Angle	10 deg	
Tool helix angle β	30 deg	
Cutting Edge Radius r	1 μm	3 μm
Work material	Al 6061	Al 6061 and Toolox 33
Width of Cut	0.025 mm	0.1 mm
Axial depth of cut b	0.06 mm	0.5 mm
Feed Per Tooth f_t	0.5 um and 1 um	3.25 um
Spindle speed	10000 rpm	

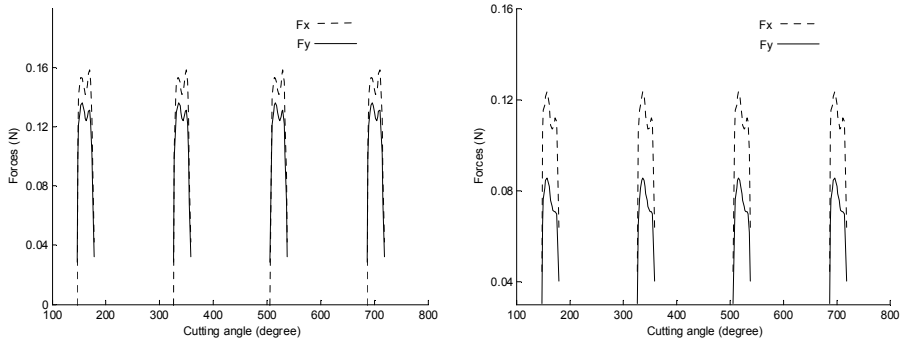

a. f_t=1μm *b.* f_t=0.5 μm

Figure 4; Predicted forces in feed (F_x) and normal direction (F_y)

(Tool diameter D=0.3mm, cutting edge radius r=0.001mm)

 Published by Cranfield University Press ISBN: 978-0-9557436-7-2 http://hdl.handle.net/1826/3832

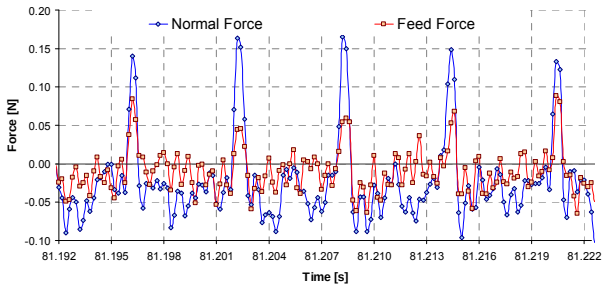

Figure 5; Measured forces in feed and normal direction

(Tool diameter D=0.3mm, cutting edge radius r=0.001mm, $f_t = 1\mu m$)

Table II: Predicted and measured forces (workpiece:)

D(mm)	r (μm)	ft(um)	F_x (N)	F_y (N)	R (N)	$F_{x,\,measured}$ (N)	$F_{y,\,measured}$ (N)	$R_{measured}$ (N)	workpiece
1 mm	3	3.25	4.5	3.9	**5.95**	4.2	4.3	**6.01**	Toolox 33
1 mm	3	3.25	2.1	2.9	**3.58**	1.5	2.3	**2.75**	Al6061
0.3 mm	1	1	0.16	0.14	**0.21**	0.08	0.16	**0.18**	Al6061
0.3 mm	1	0.5	0.125	0.084	**0.15**	0.11	0.16	**0.19**	Al6061

CONCLUSIONS

By using the new approach in modelling the end milling process, the variations of specific cutting energy and force ratio (radial over tangential) with the tool cutting angle can be obtained from detailed 2D finite element micro cutting simulations. The micro milling forces can then be predicted by using an analytical milling force model. The advantage of this new approach is the reliable estimation of SGE and *p* values and significant reduction of computing time, and it also significantly reduces the demands for running micro cutting tests and thus reduces the costs for machining time and micro tools.

The predicted micro milling forces show relatively good agreement with the experimental measurements. Further work is needed to investigate the main factors affecting the cutting force ratio, F_x / F_y, under the micro cutting regime of submicron chip thickness, as the actual chip thickness is much smaller than the feed per tooth and the mechanism controlling the variation of the force ratio, F_x / F_y, becomes much more complicated when compared to that of a large width of cut, factors such as the spindle run-out and process dynamics may have direct impact on the variation of chip thickness and need to be further investigated.

ACKNOWLEDGMENT

The authors would like to thank the Engineering and Physical Sciences Research Council for supporting the Grand Challenge project: *3D-Mintegration: the design and manufacture of 3D integrated miniaturised products* (EP/C534212/1).

 Published by Cranfield University Press ISBN: 978-0-9557436-7-2 http://hdl.handle.net/1826/3832

REFERENCES

1. [Bao et al., 2000] Bao, W. Y.; Tansel, I. N.; "Modelling micro-end-milling operations Part I: analytical cutting force model", Int. J. Machine Tool and Manufacture, 40, 2155-2173
2. [Cygax, 1979] Cygax, P. E.; "Dynamics of single-tooth milling", Annals of the CIRP, 28/1, 65-70
3. [Jemlelniak, 1992] Jemlelniak, K.; "Modelling of dynamic cutting coefficients in three-dimensional cutting", Int. J. Machine Tool and Manufacture, 32/4, 509-519
4. [Jin, 2007] Jin, T.; Stephenson, D. J.; Allen, D. M.; "A new approach in modelling the micro end milling process using variable specific cutting energy and force ratio", Proceedings of ICRM2007 – 4th International Conference on Responsive Manufacturing, Nottingham
5. [Kline et al., 1983] Kline, W. A.; DeVor, R. E.; "The effect of cutter runout geometry on cutting geometry and forces in end milling", Int. J. Machine Tool Des. and Res. 23, 123-148
6. [Palanisamy, 2006] Palanisamy, P.; Rajendran, I.; et al.; "Prediction of cutting force and temperature rise in the end-milling operation", Proc. IMechE Vol. 220 Part B: J. Engineering Manufacture, 1577-1587
7. [Tlusty et al., 1975] Tlusty, J.; Macneil, P.; "Dynamics of cutting forces in end milling", Annals of the CIRP, 24/1, 21-25
8. [Yucesan et al., 1990] Yucesan, G.; Bayoumi, A. E.; et al.; "An analytical cutting force model for milling", Transactions of the North American Manufacturing Research Institution of SME 1990, 137-145

 Published by Cranfield University Press ISBN: 978-0-9557436-7-2 http://hdl.handle.net/1826/3832

A Coupled FE-SPH approach for Simulation of Structural Response to Extreme Wave and Green Water Loading

J.C. Campbell, R. Vignjevic and M. Patel,

School of Engineering, Cranfield University

Introduction

Green water loading and wave impact are major sources of damage in the marine industry. Design for such eventualities is based on empirical considerations and on model test data in the absence of reliable theoretical models for predicting the relevant loads. The objective of this research is to develop and demonstrate an analysis tool capable of predicting the response of structures to extreme wave loading. To achieve this objective the tool must be capable of representing the following important features of this problem:

- The behaviour of extreme waves, including breaking,
- The response of a floating structure to waves,
- The interaction of the water with a structure,
- The response of the structure to the fluid loading including large deformations and non-linear material behaviour (including plasticity, damage and failure).

Together these features form a time dependent and highly non-linear problem.

Smooth Particle Hydrodynamics (SPH) is a numerical technique for the approximate integration of the governing partial differential equations of continuum mechanics. It is a meshless Lagrangian method that uses a pseudo-particle interpolation method to compute smooth field variables. The application of SPH to water waves and related free-surface hydrodynamics problems was begun by Monaghan [1], who performed two-dimensional simulations of a dam break problem and wave propagation onto a shallow beach. Recently SPH methods have been successfully applied to 2D simulations of green water overtopping [2] and wave overtopping [3] using rigid representations of the impacted structure.

Other approaches for wave impact simulations typically use Eulerian or ALE methods to solve the Navier-Stokes equations. For example, Buchner, Kleefsman and co-workers [4,5] have developed an Eulerian code and applied it to wave run-up and green water loading on Floating Production Storage and Offloading (FPSO) systems. Their results show good agreement with experiment for structural loads, but the structures are modelled as rigid.

The explicit finite element (FE) method is the established method for simulating the crash and impact response of structures and is implemented in numerous commercial and development codes. This approach is well suited to modelling the structural response to fluid loading. However due to the known problems with mesh-tangling FE is not appropriate for modelling the fluid. In order to simulate the

 Published by Cranfield University Press ISBN: 978-0-9557436-7-2 http://hdl.handle.net/1826/3832

structural response to extreme wave loading the method must be coupled with another method, here SPH, appropriate for the fluid behavior.

In this work the SPH particles interact with the FE mesh through a contact algorithm developed at Cranfield based on the use of a contact potential [6]. This approach avoids the requirement to construct a surface geometry from the SPH nodes and provides a simple and robust coupling between the solvers.

SPH for wave loading

Under the conditions of wave loading the water can be considered incompressible. The SPH solver used assumes that all materials are compressible and therefore a bulk stiffness, in the form of an equation of state (EOS), must be defined. In this paper, unless stated otherwise, the Murnaghan is used for the water. This defines the pressure P as

$$P = B\left[\left(\frac{\rho}{\rho_0}\right)^{\gamma} - 1\right], \qquad (1)$$

where B and γ are user supplied material coefficients and ρ_0 is the reference density of the material. For an incompressible fluid the parameter B can be chosen to give an artificially low speed of sound, while keeping the density changes small. This is valid provided the flow velocities are small compared with the speed of sound [1]. The advantage of this is that a lowered speed of sound increases the critical stable time step size for the explicit time integration algorithm, potentially reducing the CPU cost of a simulation.

Initial conditions

At the start of the simulation the model must be under static equilibrium, otherwise the initial behaviour of the model will be governed by this lack of equilibrium, potentially changing the overall behaviour of the model. The initial equilibrium must be determined for the pressure vs. depth in the water and for the contact forces between structure and water.

The dynamic relaxation method was selected to solve the initial static problem. Dynamic relaxation is a commonly used method that allows an explicit transient solver to approximate the solution to a static problem [7].

Boundary conditions

During the simulation an appropriate boundary condition is required to generate the waves in the water. If the simulation is required to progress beyond the interaction of the first wave with the structure a non-reflective boundary condition is necessary. Otherwise the CPU cost of a 3D simulation quickly becomes prohibitive due to the size of the water domain required.

 Published by Cranfield University Press ISBN: 978-0-9557436-7-2 http://hdl.handle.net/1826/3832

Where only a single wave is required, and it is not necessary for the structure to be in initial contact equilibrium with the fluid, the initial conditions in the water can be determined from standard wave theory [8]. Where multiple waves are required or the fluid and structure must be in initial equilibrium the wave have to be generated during the transient analysis. This is achieved through the use of an oscillating plate. This is a copy of wave makers commonly used in experimental wave tanks and in previous wave simulations [1,2,3].

Non-reflecting boundary conditions for pressure waves are well established for Lagrangian hydrocodes, but can not be adapted for water surface waves as the propagation of these waves involves large fluid motion. For deep water a marker particle at the water surface would travel a circular path, with diameter equal to the amplitude of the wave, and any absorbing boundary condition must not prevent this motion.

A non-reflecting boundary condition for water waves has been developed that consist of an additional region of fluid where the motion is damped, the damping coefficient being proportional to the distance from the boundary. SPH particles are free to enter and leave the volume, so it does not prevent the circular motion of the water particles. The volume of the damping region should remain small compared with the overall domain.

Results for a rigid boundary are compared to a non-reflective boundary in figure 1. For the non-reflecting boundary the marker particle shows the expected circular motion throughout the simulation, while reflection off the rigid boundary significantly changes the wave behavior later in the simulation.

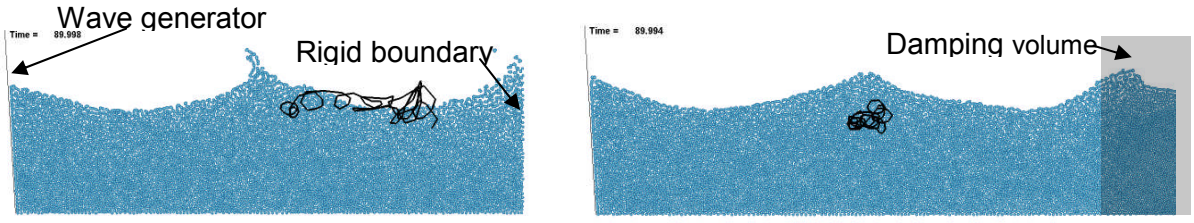

Figure 1. (a) 2D wave tank results with a rigid boundary showing the motion of a marker particle. (b) Results for the same problem using a non-reflective damping layer. The motion of the marker particle remains circular.

Numerical tests and demonstrations

A set of test cases of varying complexity have been performed to validate the capability of the coupled FE-SPH approach to simulate floating bodies and impact on water. This section presents some main tests cases from this process.

 Published by Cranfield University Press ISBN: 978-0-9557436-7-2 http://hdl.handle.net/1826/3832

Equilibrium of floating objects

A useful verification of the method's ability to simulate the response of a floating body is to demonstrate that it will reach its correct equilibrium state. Simulations have been performed using rigid 2D shapes, and results compared with published results [9]. The results from these tests show that the coupled FE-SPH approach will correctly predict the equilibrium floating behaviour of a floating body.

An example of one of these tests is the simulation of a rectangular float, 10 cm x 5 cm, with density half the density of the fluid. The initial position of the float is with the long axis vertical. In the simulation the float rotates to the stable equilibrium position with the long axis horizontal, figures 2 and 3.

Figure 2: Rotation of the rectangular float during the simulation.

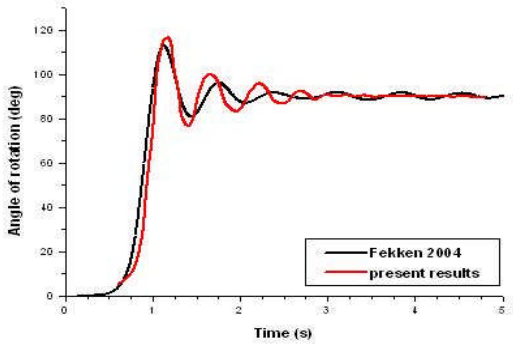

Figure 3: Time history for rotation angle of rectangular float

CALM buoy model

The objective of the main test problem is to demonstrate the capability of the coupled approach to perform a 3D simulation of wave interaction with a floating body. The problem consists of a cylindrical buoy with an outer diameter of 12 m and mass 400 tonnes. The buoy is moored to the sea bed with 6 mooring lines. The state of the model at the start of the transient simulation is shown in figure 4, dynamic relaxation has been used to solve the initial equilibrium state. Model scale tank test data is available for comparison with the predicted buoy motion.

 Published by Cranfield University Press ISBN: 978-0-9557436-7-2 http://hdl.handle.net/1826/3832

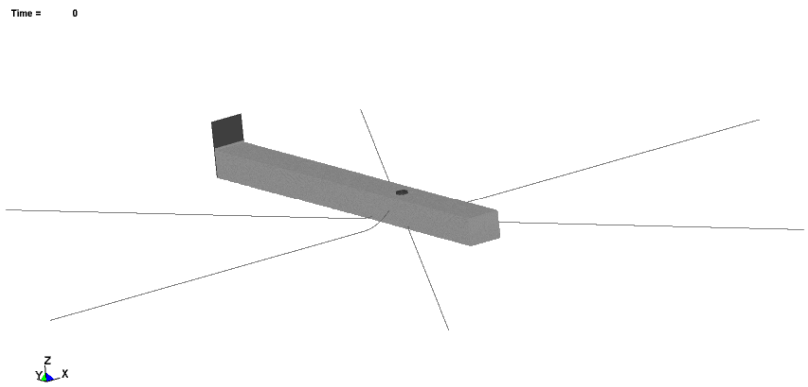

Figure 4: Complete model at start of transient simulation.

The water component is modelled with 1,045,436 SPH particles, representing a domain 430.5 m long, 36 m wide and 28.5 m deep. The initial particle spacing is 0.75 m, the initial particle spacing is the equivalent of the mesh size in FE. Symmetry boundary conditions are used on the long and the wave generator is placed at one end, 293 m from the buoy centre.

The buoy is modelled as a rigid body, with correct mass and inertial properties defined. A rigid body is used as this is consistent with the test data and the fluid resolution would need to be significantly increased for a deformable structural model. The six mooring lines are each represented with truss elements, for a total of 1200 truss elements. Simulating the mooring line interaction with the water would require the use of a far higher fluid resolution to capture the hydrodynamic behaviour, impractical without a fully parallelized code and the use of a large super-computer. The cable interaction with the water is therefore ignored.

In this model the computational cost of one SPH time step is approximately three orders of magnitude greater than one FE step due to the comparatively large number of SPH particles. As the stable time-step size of the FE model, controlled by the cable elements, is an order of magnitude below the SPH stable step size, a subcycling algorithm was developed and implemented, allowing multiple FE steps per SPH step and resulting in a significant saving in computation time.

A simplified simulation of a free floating buoy has been completed, showing a sensible response of the buoy, figure 4. Simulations of the moored buoy will be completed shortly.

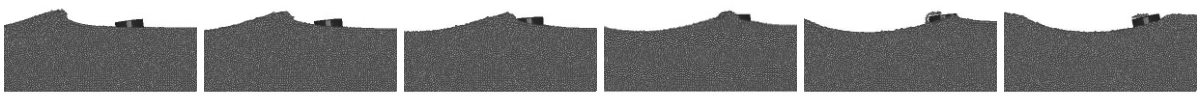

Figure 4: Sequence showing the interaction of a wave with a free-floating buoy. The images should be read from left to right, the time interval between each image is one second.

 Published by Cranfield University Press ISBN: 978-0-9557436-7-2 http://hdl.handle.net/1826/3832

Conclusions

Extreme waves can cause significant damage to ships and offshore structures. Currently there is no reliable theoretical or numerical technique available to predict the relevant loads and structural response.

The coupled Finite Element – Smoothed Particle Hydrodynamics approach has been developed for treating fluid-structure interaction problems where the structural response is potentially highly non-linear. This paper demonstrates that the approach can be extended to the treatment of extreme wave loading of floating structures though the addition of appropriate initial and boundary conditions.

A set of simulation results are shown to demonstrate that the approach allows:

- the correct behavior of a floating body,
- the prediction of structural collapse under water loading,
- 3D simulation of wave interaction with a floating body.

Acknowledgement

The authors would like to acknowledge the support of the UK Engineering and Physical Sciences Research Council (EPSRC) under project GR/S95435/01.

References

1. Monaghan, J.J. : “Simulating free surface flows with SPH” Journal of Computational Physics (1994) **110**, 399.
2. Gómez-Gesteira, G., Cerqueiro, D., Crespo, C. and Dalrymple, R.A. : “Green water overtopping analyzed with a SPH model” Ocean Engineering (2005) **32**, 223.
3. Shao, S., Ji, C., Graham, D.I., Reeve, D.E., James, P.W. and Chadwick, A.J. : “Simulation of wave overtopping by an incompressible SPH model” Coastal Engineering (2006) **53**, 723.
4. Buchner, B., Bunnik, T.H.J., Fekken, G. and Veldman, A.E.P. : ‘A numerical study on wave run up on an FPSO bow.’ Presented at the 20th international conference on offshore mechanics and arctic engineering. Rio de Janeiro, Brazil (2001).
5. Kleefsman, K.M.T, Fekken, G., Veldman, A.E.P., Bunnik, T.H.J., Buchner, B. and Iwanowski, B. : “Prediction of green water and wave loading using a Navier-Stokes based simulation tool” Presented at the 2002 ASME Offshore Mechanics and Arctic Engineering conference , Oslo, Norway
6. Vignjevic, R., De Vuyst, T. and Campbell, J.C. : “A frictionless contact algorithm for meshless methods” Computer Modeling in Engineering and Sciences (2006) **13**, 35.
7. Lin, J.I. : “DYNA3D: A Nonlinear, Explicit, Three-Dimensional Finite Element Code for Solid and Structural Mechanics. User Manual” Lawrence Livermore National Laboratory, USA (1999).
8. Tucker, M.J. and Pitt, E.G.: “Waves in Ocean Engineering” Elsevier Science Ltd, Oxford, UK (2001).
9. Fekken, G.: “Numerical simulation of free-surface flow with moving rigid bodies” PhD Thesis, Groningen University, Netherlands (2004).

 Published by Cranfield University Press ISBN: 978-0-9557436-7-2 http://hdl.handle.net/1826/3832

Use of volatile fingerprints for antifungal efficacy against common dermatophytes

Natasha Sahgal and Naresh Magan

Applied Mycology, Cranfield Health, Cranfield University, Bedford, MK43 0AL

Email: n.sahgal.s03@cranfield.ac.uk

Abstract

This study assessed the potential of volatile fingerprints to screen for antifungal susceptibility with a hybrid sensor array electronic nose (e-nose). Antifungal treatments with itraconazole (ITZ) against Trichophyton mentagrophytes and T. rubrum showed that the e-nose could differentiate between untreated/treated fungal species at 25-30°C. However, intermediate concentrations (LD50 values) and 2 ppm of ITZ could not be easily separated from each other or the controls based on their volatiles. Volatile fingerprints may be a good tool for screening efficacy of novel anti-microbial compounds and for early warning of a build up of resistance within populations.

Introduction

Dermatophytes are mainly responsible for superficial and to some extent deep-seated infections of the keratinised tissue (skin, hair and nails) that constitute a public health concern worldwide. Appropriate administration of antifungal therapy, i.e. topical or systemic treatments, is of vital importance and depends particularly on the species, the site and severity of infection. Other contributing factors include the cost of drugs (oral therapy being more expensive), treatment duration (longer for nails) and increasing resistant species[1,2].

Current methods for detecting antifungal susceptibility against dermatophytes are based on modifications of the reference methods for filamentous fungi or yeasts as specified by the NCCLS. Thus due to the lack of a standardised protocol numerous investigations have resulted in developing suitable reproducible assays using broth micro-dilution, agar diffusion or commercial systems[3-5]. However, due to the risks associated with current commercial therapeutics - drug-drug interactions, unpleasant side-effects, rising fungal resistance there is a focus on natural sources (plant products, essential oils) for antifungal activity, although the techniques used were similar to those mentioned previously[6,7].

These techniques are tedious because of the difficulty in determining the end point for the inhibitory concentrations. Therefore, the objective of the present study was to determine the potential of an e-nose system to screen antifungal agents (e.g. concentrations and temperatures) based on their generated volatile profile patterns.

 Published by Cranfield University Press ISBN: 978-0-9557436-7-2 http://hdl.handle.net/1826/3832

Materials and Methods

Strains and antifungal agent

Type cultures of two *Trichophyton* species, *T. mentagrophytes* (NCPF-224) obtained from the National Collection of Pathogenic Fungi and *T. rubrum* (strain D12) kindly provided by the University of Oxford were used. The antifungal selected for the screening study, Itraconazole (ITZ), was kindly provided by Janssen Pharmaceutica, Belgium. The cultures were grown and maintained on Sabouraud Dextrose Agar (SDA) with 0.05 g l^{-1} of the antibiotic, Chloramphenicol (Sigma) at 25°C. The antifungal stock solution was prepared in dimethyl sulfoxide (DMSO) (Sigma).

Temporal growth

The efficacy of the antifungal was tested by measurements of effects on growth rates. The antifungal was screened at 0.25-2 ppm on SDA at 25 and 30°C. Controls included afar media alone and that inoculated with the test species. Plates were centrally inoculated (4mm agar plug) from three week old cultures of both fungi. Three replicates per treatment were incubated at 25/30°C. Colony growth was measured for 2 weeks.

Sample preparation, e-nose and data analysis

Spore suspensions of three-four week old cultures were prepared in sterile 10 ml Tween 80 and RO water. The inoculum concentrations were approx. 10^7 spores ml^{-1} for both species. Five replicate agar plates for each treatment (LD_{50}[1] values, controls and/or 2ppm) per species were inoculated with 250 μl of the inoculum, spread plate on the surface, and then incubated at 25 and 30°C for 96-120 h respectively and then destructively sampled. Blank agar plates including some containing the antifungal were used as negative controls.

Four 2 cm diameter agar plugs were placed in 25 ml vials and set aside to equilibrate for 1 h at 25 and 30°C for headspace generation. These were then placed in the e-nose (NST 3320, Applied Sensors, Sweden) carousel system and analysed randomly. The data (mean-centred) were analysed with the accompanying software NSTSenstool and Statistica 7 using multivariate statistics such as principal component analysis (PCA) and cluster analysis (CA) respectively. Fungal growth rate measurements against the antifungal were used to determine the lethal dose at which the fungi were 50% inhibited (LD_{50} value) using Microsoft® Excel.

Results

[1] LD_{50} – the effective concentration of the antifungal at which the fungal growth is 50% inhibited.

 Published by Cranfield University Press ISBN: 978-0-9557436-7-2 http://hdl.handle.net/1826/3832

Temperature and concentration of the antifungal agent affected the growth rates of the two fungal species, where the controls appeared to grow slightly faster at 30 than 25°C. The growth of both fungi was almost completely inhibited by the antifungal concentration of 2 ppm at 25°C. The effective concentrations at which 50% of fungal growth was inhibited was determined from these data and shown in Table 1.

Table 1: Antifungal (ITZ) concentrations at which 50% growth is inhibited at different temperatures.

Temperature	ITZ LD_{50} concentration (ppm)	
	T. mentagrophytes	*T. rubrum*
25 °C	0.16	0.18
30 °C	0.22	0.14

For the e-nose study of the two dermatophytic fungi at 25°C, the antifungal concentrations of 0.16 and 0.18 ppm was used respectively. Cluster analysis (using Euclidean distance and Ward's linkage) after 96 h analysis on the data showed two main clusters segregating antifungal treatments from non-antifungal treatments. In the latter case, however, only the *T. mentagrophytes* samples formed a distinct cluster that differentiated them from the controls (Figure 1). The two species without the antifungal could almost be differentiated from each other and the controls.

Similar experiments at 30°C after 96 h growth and based on PC1 and PC2 indicated that the species, especially *T. rubrum*, in the absence of the antifungal could be differentiated from each other and the controls. The other treatments with ITZ were dispersed among the controls and one fungal species. In contrast, when observing the first and fourth PCs except for the *T. mentagrophytes* samples treated with the antifungal that were scattered, the remaining treatments appeared to be differentiated from each other (Figure 2).

In either case, over 90% of the variance in the data was accounted for. Subsequent analysis on data from two ITZ treatments - LD_{50} and 2 ppm and controls after 96 h at 25°C showed that the fungal treatments exclusive of itraconazole could be discriminated from the remaining treatments. After 120 h, the two fungi without ITZ could be differentiated from each other more clearly and from the remaining treatments (Figure 3).

Discussion

The efficacy of the antifungal agent, ITZ, was determined *in vitro* on the two main dermatophyte species at two different temperatures. Initial screening was based on temporal studies, thereafter the susceptibility of the fungi to ITZ was determined by their *in vitro* volatile profile patterns with/without the

 Published by Cranfield University Press ISBN: 978-0-9557436-7-2 http://hdl.handle.net/1826/3832

antifungal agent. E-nose analyses after 96 h at either temperature differentiated between treatments. However, at 25°C the discrimination was more prominent than at 30°C because there was a greater spread in some of the treatments at 30°C (e.g. *T. mentagrophytes* + antifungal).

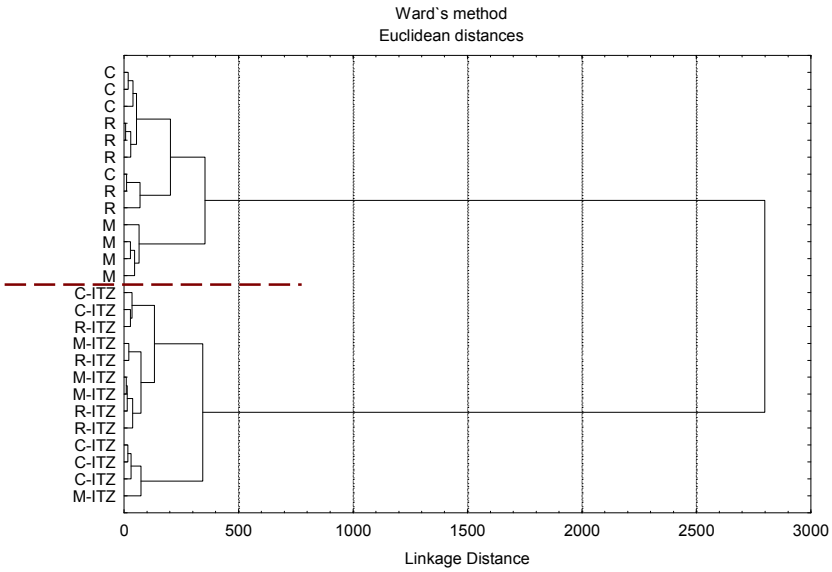

Fig 1: Dendrogram depicting two distinct clusters separating antifungal treatments from those without antifungal including only *T. mentagrophytes* (without antifungal) being clearly differentiated (at 25°C). (*Key:* C – Controls; M – *T. mentagrophytes*; R – *T. rubrum*; X-ITZ – Treatments + antifungal)

The fact that there was no discrimination between the controls and treatments containing two antifungal concentrations could be explained by virtually no growth or inhibition of the fungi at 2 ppm of the antifungal (after 96-120 h), thus being very similar to the uninoculated controls. The inability to distinguish the second antifungal concentration (LD_{50} inhibition) which was still similar to the controls implies that a longer incubation time was required. Previous studies by Fernandez-Torres *et al.*[4] have indicated an optimum incubation period of seven days before visual inspection when traditionally screening antifungals against dermatophytes. However, at 120 h, both the fungal controls were clearly distinguished from the negative controls and treatments with antifungals.

 Published by Cranfield University Press ISBN: 978-0-9557436-7-2 http://hdl.handle.net/1826/3832

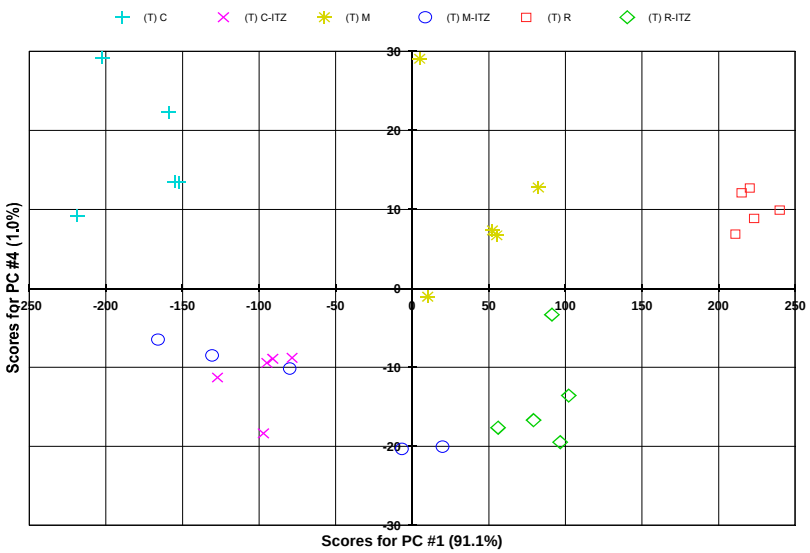

Fig 2: PCA analysis of fungal samples treated with and without an antifungal at 30°C after 96 h indicating differentiation between treatments. (*Key:* C – Controls; M – *T. mentagrophytes*; R – *T. rubrum*; X-ITZ – Treatments + antifungal)

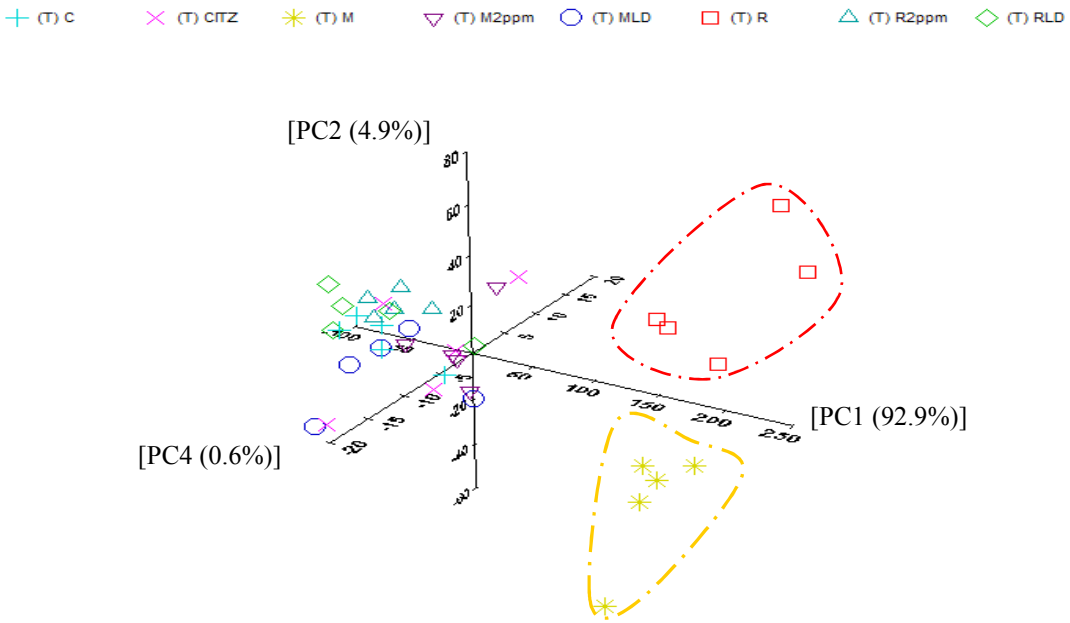

Fig 3: 3D PCA plot illustrating discrimination between the two fungal species, after 120 h at 25°C, in the absence of itraconazole from each other and the remaining treatments including controls. (*Key:* C – Controls; CITZ – Controls with 2ppm antifungal; M – *T. mentagrophytes*; R – *T. rubrum*; M/R-LD – Fungi with LD_{50} concentration; M/R-2ppm – Fungi with 2 ppm antifungal concentration)

Needham[8] used an e-nose to screen the efficacy of antioxidants/preservatives *in vitro* for use in the food industry. Her study indicated the ability of the e-nose to discriminate between treatments containing antioxidants, responsible for at least 50-70% inhibition in growth, from those without these treatments for spoilage bacteria and fungi. Antifungal screening for dermatophytes, to date has been

 Published by Cranfield University Press ISBN: 978-0-9557436-7-2 http://hdl.handle.net/1826/3832

performed using variations of the technique specified by the NCCLS by using different dermatophyte strains, temperatures (28-30°C) and incubation periods (3-7 days)[3-5]. Similar adaptations were carried out for screening plant extracts and essential oils as antifungals against various dermatophytes using the traditional tests[9,10]. Reports have also indicated different plant extracts to have a lower or similar efficacy when compared with commercial antifungals such as griseofulvin[6,9]. However, Silva *et al.* [10] showed eugenol extract from *Ocimum gratissimum* to have a higher antifungal activity than ITZ at the same concentration because the former inhibited the growth of other dermatophytic isolates.

This is the first study to assess the use of volatile fingerprints to screen for antifungal susceptibility with an e-nose. It could distinguish between fungal control treatments and those containing ITZ. It may also serve as a useful tool for monitoring resistance build up against the antimicrobials generally.

References

1 Gupta AK, Tu LQ. Dermatophytes: Diagnosis and treatment. *J Am Acad Derm* 2006; **54**: 1050-5.

2 Hiruma M, Yamaguchi H. Dermatophytes. In: *Clinical Mycology* (Anaissie EJ, McGinnis MR, Pfaller MA, eds), 1st edn. Philadelphia, USA: Churchill Livingstone. 2003; 370-9.

3 Favre B, Hofbauer B, Hildering K-S *et al.* Comparison of In Vitro Activities of 17 Antifungal Drugs against a Panel of 20 Dermatophytes by Using a Microdilution Assay. *J Clin Microbiol* 2003; **41**: 4817-9.

4 Fernandez-Torres B, Cabanes FJ, Carrillo-Munoz AJ *et al.* Collaborative evaluation of optimal antifungal susceptibility testing conditions for dermatophytes. *J Clin Microbiol* 2002; **40**: 3999-4003.

5 Santos DA, Barros MES, Hamdan JS. Establishing a method of inoculum preparation for susceptibility testing of *T. rubrum* and *T. mentagrophytes. J Clin Microbiol* 2006; **44**: 98-101.

6 Gurgel LA, Sidrim JJC, Martins DT *et al.* In vitro antifungal activity of dragon's blood from *Croton urucurana* against dermatophytes. *J Ethnopharmacol* 2005; **97**: 409-12.

7 Koc AN, Silici S, Ayangil D *et al.* Comparison of in vitro activities of antifungal drugs and ethanolic extract of propolis against *Trichophyton rubrum* and *T. mentagrophytes* by using a microdilution assay. *Mycoses* 2005; **48**: 205-10.

8 Needham R. Early detection and differentiation of microbial spoilage of bread using electronic nose technology. *PhD Thesis.* Silsoe: Cranfield University. 2004.

9 Ali-Shtayeh MS, Abu Ghdeib SI. Antifungal activity of plant extracts against dermatophytes. *Mycoses* 1999; **42**: 665-72.

10 Silva MRR, Oliveira JG, Fernandes OFL *et al.* Antifungal activity of *Ocimum gratissimum* towards dermatophytes. *Mycoses* 2005; **48**: 172-5.

 Published by Cranfield University Press ISBN: 978-0-9557436-7-2 http://hdl.handle.net/1826/3832

An analysis of the effects of nanolayered nitride coatings on the lifetimes and wear of tungsten carbide micromilling tools

a Precision Engineering Centre, Cranfield University, Bedford MK43 0AL, UK

D. Zdebski[a], D.M. Allen[a], D.J.Stephenson[a], J. Hedge[a], C. Ducros[b] and F. Sanchette[b]

b *CEA Grenoble, Labatoire des Technologies des Surfaces, 17 rue des Martyrs 38054 Grenoble CEDEX , France*

Abstract

Micromilling is becoming increasingly important for a wide range of manufacturing tasks in the general field of microengineering, such as milling small channels in micromoulds designed for the fabrication of microfluidic devices by microinjection moulding of polymers. However, micromilling tools, often <1mm in diameter, are rather delicate, fracturing when forces become excessive and, consequently, micromilling can become an expensive process. In an attempt to increase tool lifetimes and reduce costs, micromilling forces have been measured with a microdynamometer and the effects of chromium nitride/titanium nitride and titanium aluminium nitride/titanium nitride coatings have been evaluated as an aid to decreasing tool wear and extending the lifetime of tungsten carbide micromilling tools. The surface finish of the milled workpiece has also been measured to monitor how tool wear affects the resultant milled surface.

Keywords: coatings, micromills, wear

Introduction

The cost of micromilling can be reduced if the lifetime of the delicate microtools used in cutting processes can be extended. This research aims at improving tool-lifetime by coating micro endmills with wear-resistant materials. Two coatings have been investigated and compared with an uncoated tool and a tool with a commercially-available coating.

 Published by Cranfield University Press ISBN: 978-0-9557436-7-2 http://hdl.handle.net/1826/3832

Experimental

Two types of 1mm and 0.2mm diameter Unimax tungsten carbide (WC) endmills were purchased from Union Tools, Japan. The first type (Carbide Endmill) was uncoated and the second type (UT Dry) had been coated with a commercial material of unknown composition. Energy dispersive X-ray analysis (EDX) was used to analyse the UT Dry tool coating that was determined to contain aluminium, titanium and nitrogen.

A number of the uncoated tools were coated at CEA by cathodic arc evaporation to produce two other coatings for comparison. The first comprised nanolayers of CrN and TiN and the second comprised nanolayers of AlTiN and TiN. Both coatings have a total thickness of approximately 2μm.

It was noted that the CrN/TiN coatings were gold-coloured, whilst the AlTiN/TiN coatings were grey-coloured, thus making visual identification of the coatings easy for the machine operator and researcher.

Micromilling was carried out on an Evo type Kern CNC ultra precision machining centre, installed in the temperature-controlled (20.0 ± 1.0°C), humidity-controlled (50 ± 5% RH) Hexagon Loxham Precision Laboratory at Cranfield University.

Measurement of the micromilling forces was carried out with a Kistler microdynamometer (model 9256C2) positioned as shown in Figure 1.

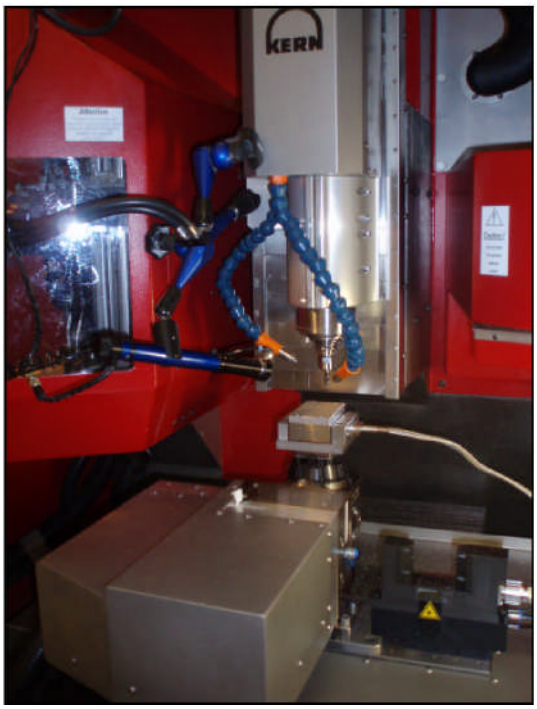

Figure 1. Kistler microdynamometer in the Evo Kern CNC machinining centre

 Published by Cranfield University Press ISBN: 978-0-9557436-7-2 http://hdl.handle.net/1826/3832

Examinations of the machined steel (Toolox 33, a prehardened tool steel) surfaces were carried out by white light interferometery (WLI) and scanning electron microscopy (SEM). The tool was also examined by SEM and, in addition, EDX was also used to monitor the chemical changes on the surfaces of the tools during the cutting process.

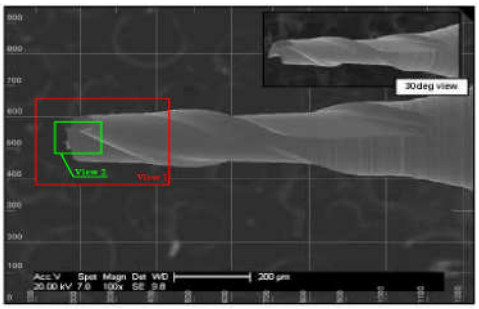

Figure 2. SEM of the uncoated 200µm diameter WC endmill

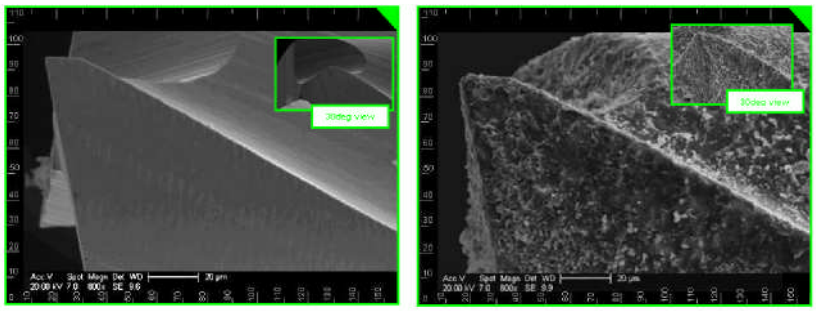

(a) *(b)*

Figure 3. High magnification SEM of the cutting edges of the uncoated 200µm diameter WC endmill (a) uncoated tool , (b) coated with 2µm of nanolayered AlTiN/TiN

Figure 2 shows an SEM image of a 200µm diameter uncoated tungsten carbide tool prior to cutting. Figures 3a and 3b show higher magnifications of the flute areas where cutting mainly occurs. Comparison of these images also illustrates the rougher tool surface produced by the CEA coating process.

The new uncoated tools (Figures 2 and 3) had very sharp flute edges with no visible damage. However, the CEA coatings tended to reduce the sharpness of the cutting edges. A good indicator of tool sharpness is the ratio of feed force to normal force. The ratio is usually higher when the tool is sharper. In Table 1 are shown cutting forces and ratios for cutting steps 100µm wide and 500µm deep in Toolox 33 blocks by 1mm diameter WC tools with different coatings. The cutting speed was 10,000 rpm and the feed rate was 65mm/min. No coolant was applied to minimise external influences for future simulations. Tests with different cooling and lubrication

 Published by Cranfield University Press ISBN: 978-0-9557436-7-2 http://hdl.handle.net/1826/3832

conditions are planned to be undertaken in future work. The cutting forces are roughly the same. However, the ratio of F_{feed} to F_{normal} is slightly lower for the coated tools, indicating a reduction in sharpness.

	Feed force	Normal force	Ratio F_f/F_n
Uncoated tool	*6.2 N*	*6.6 N*	*0.94*
UT Dry	*5.7N*	*6.9N*	*0.83*
CEA CrN/TiN	*6.2 N*	*8.3 N*	*0.75*
CEA AlTiN/TiN	*6.1 N*	*7.1 N*	*0.87*

Table 1. Cutting forces and $F_{f/Fn}$ ratio of 1mm diameter WC tools with different coatings

Wear tests of 1mm diameter tools were carried out under the conditions described before.

The tool radius was measured at 250μm and 500μm from the tool tip. Analysis of both measurements shows similar trends. The measurements at 500μm are plotted in Figure 4.

Figure 4. Dependence of tool radius reduction vs. number of cuts for 1mm diameter tools with different coatings

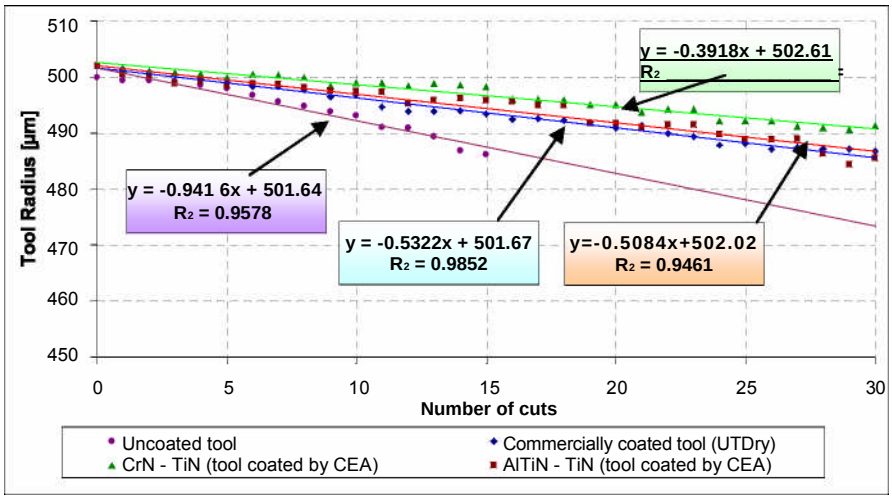

All the coated tools tend to show a linear trend in tool radius decrease with the number of cuts. The uncoated tool wears almost twice as fast as the commercially-coated tool and the AlTiN/TiN tool coated by CEA. The AlTiN/TiN-coated tool tends to have a similar trend to wear as the commercially-coated tool that has a very similar type of coating composition.

The best coating material for reducing wear is CrN/TiN, as the change in tool radius is about 20% slower than tools coated with AlTiN/TiN.

The main tool wear mechanism for the specified conditions was abrasion [1]. The EDX shows that some steel has also adhered to the inside surfaces of the flutes.

 Published by Cranfield University Press ISBN: 978-0-9557436-7-2 http://hdl.handle.net/1826/3832

Figure 5 shows areas where the coating was worn away after 10 cuts. The green colour signifies areas where the coating has been removed, the red colour signifies coated areas and the blue colour signifies areas covered by adherent workpiece material.

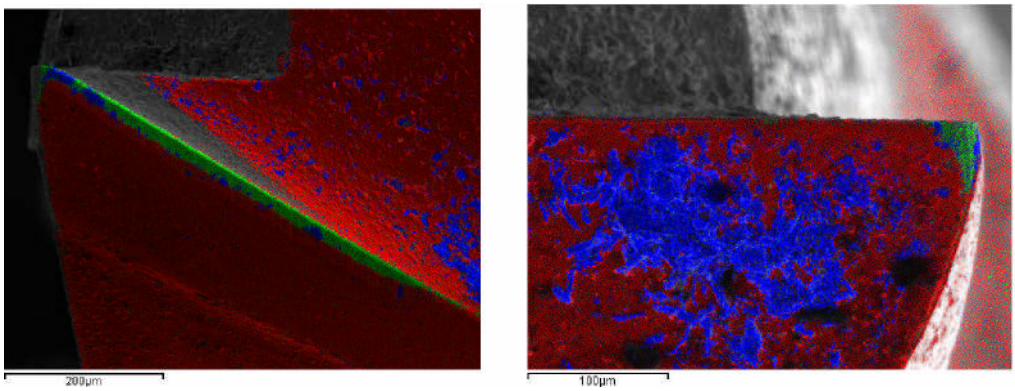

(a) (b)

Figure 5. High magnification, false colour EDXof the cutting edges of a 1mm diameter WC endmill coated with 2µm of CrN/TiN after 10 cuts, (a) side view, (b) front view

(c) (d)

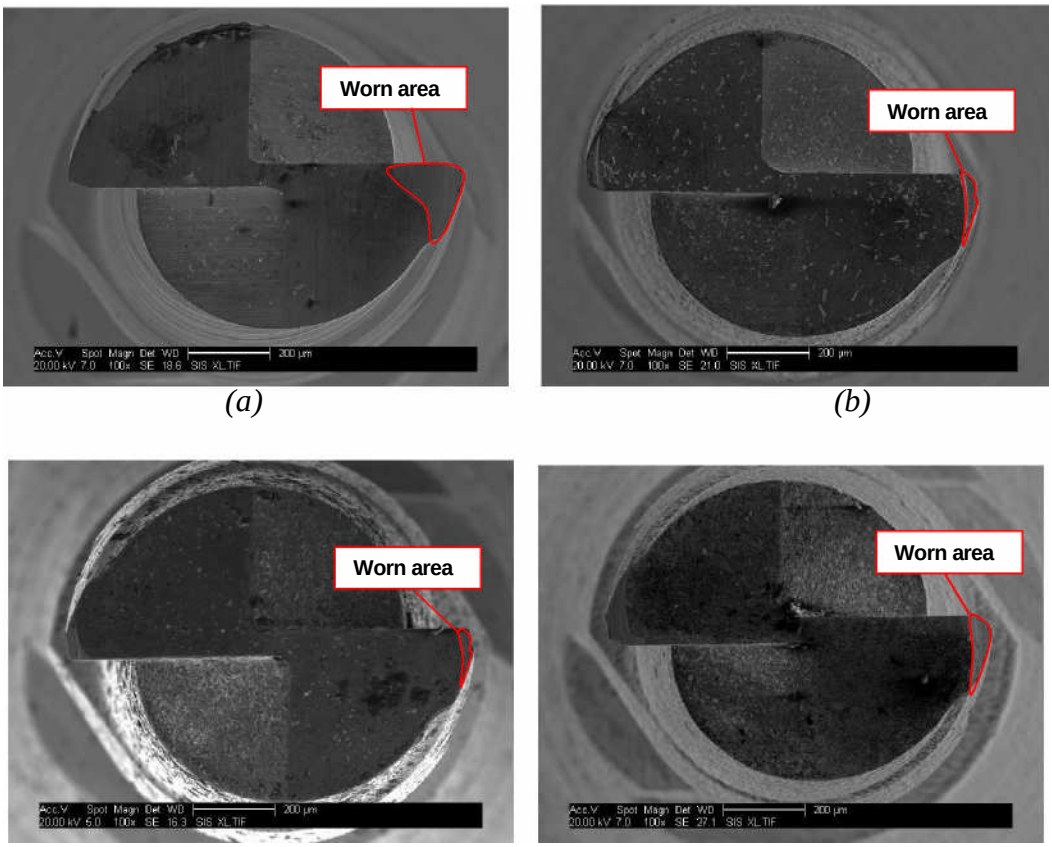

(a) (b)

Figure 4. End-on views of the 1mm diameter tools (a) uncoated tool after 15 cuts, (b) commercially-coated tool (UTDry) after 30 cuts, (c) CrN/TiN-coated tool after 30 cuts, (d) AlTiN/TiN-coated tool after 30 cuts

 Published by Cranfield University Press ISBN: 978-0-9557436-7-2 http://hdl.handle.net/1826/3832

It is clear that the wear of the tool, appearing in the areas of green colour, is mainly on the tip of the flutes and along the sides of the cutting edges [2]. The green colour also shows indirectly the areas which are in contact with the workpiece during the cutting process. The contact areas grow as the tool wears.

Figure 6 shows the end-on views of the 1mm diameter tools after machining for a certain number of 100μm wide, 500μm deep and 80mm long cuts. Figure 6a shows the uncoated tool after 15 cuts (having removed approximately 60mm^3 from the workpiece material) and Figures 6b-6d show coated tools after 30 cuts (having removed approximately 120mm^3 from the workpiece material). It is apparent that, even on visual inspection, the uncoated tool wears much faster at the cutting edges than the coated tools.

It was also observed that the CrN/TiN-coated tool is more resistant against wear than the two coated tools containing aluminum, titanium and nitrogen.

Conclusions

The choice of coating method and materials seems to have a significant influence on tool wear. Our preliminary investigations have indicated that all the coatings examined have a beneficial effect on reducing endmill wear. The most efficient coating tested to date is the nanolayered CrN/TiN coating but other coatings will be investigated in future research.

Acknowledgements

DMA and DJS wish to acknowledge the financial support of EPSRC for DZ and JH employed on Grant EP/C534212/1 (“3D-Mintegration”), Cranfield University IMRC (Grant 110) and the invaluable contribution of CEA in coating the tungsten carbide endmills through the 4M Consortium programme.

References

1. Zhang J.-H., Theory and Technique of Precision Cutting, Pergamon Press, 1991, Chapter 4, The wear characteristics of precision cutting tools, ISBN 0 08 035891 8
2. Woon K.S. et al, Investigations of tool edge radius effect in micromachining: a FEM simulation approach, Journal of Materials Processing Technology (in the press)

 Published by Cranfield University Press ISBN: 978-0-9557436-7-2 http://hdl.handle.net/1826/3832

Key Service Issues in Two UK Manufacturing Companies from a PSS Perspective

Athanasia Doultsinou*, Rajkumar Roy*, David Baxter*, James Gao**

* Decision Engineering Centre, Cranfield University, Cranfield, MK43 0AL, UK

** Innovative Product Development Centre, School of Engineering, University of Greenwich, Chatham Maritime, Kent, ME4 4TB, UK

Abstract

This paper illustrates the key service issues within two UK manufacturing companies, which belong to two different industrial domains, and highlights the main points of difference. It draws also on the literature on Product-Service Systems regarding their definition, types, benefits and difficulties in their implementation.

Keywords

Technical product-service systems, service issues

Introduction

Nowadays, services represent 74% of the UK's gross domestic product (National statistics, 2007) and 80% of US economic activity is service-sector based (BBC news, 2008). Thus, understanding service issues faced in industry seems to be essential. In addition, the traditional distinction between manufacturing and services is becoming increasingly blurred, with the concept of Product-Service Systems arising.

Literature findings

A theoretical insight is essential before exploring issues in real-life conditions. This section discusses the definition and characteristics of services, and PSS concepts including their definition, types, conditions for success, and barriers to development. A service can be defined as "a change in the condition of a person or a good belonging to some economic entity, brought about as the result of the activity of some other economic entity, with the approval of the first person or economic entity" (Hill, 1977). Gronroos (2000) defines service as an activity or series of activities provided as a solution to customer problems (www.ibm.com). According to Cowell (1991) there are a number of characteristics that distinguish goods and services, including: intangibility, inseparability, heterogeneity, perishability, and ownership.

 Published by Cranfield University Press ISBN: 978-0-9557436-7-2 http://hdl.handle.net/1826/3832

This research will focus on technical PSS (t-PSS). Technical PSS are defined as PSS having the following characteristics:

- A physical product core (e.g. an aircraft engine) enhanced and customised by a mainly non-physical service shell (e.g. maintenance, training, operation, disposal);
- Relatively higher monetary value and importance of the physical PSS core;
- A 'business to business' relationship between PSS providers and users (Aurich et. al., 2006).

Three types of PSS are typically presented: product-oriented, use-oriented and result-oriented. A comprehensive description of all the possible approaches has been carried out by Tukker (2006). A description of the various PSS types is shown in Fig.1.

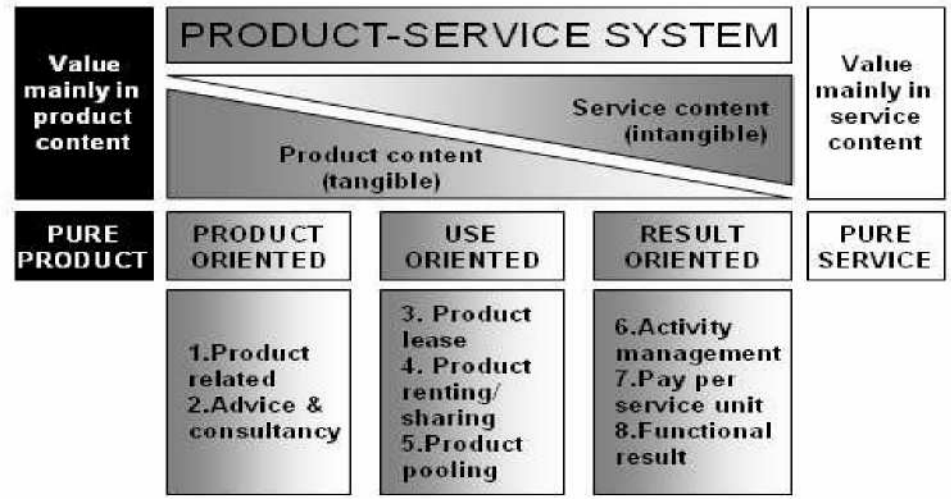

Figure 1: Main and subcategories of PSS (Source: Tukker, 2006)

These models can be applicable to most industrial sectors. Each model is evaluated from both economic and environmental perspectives. The designers need to consider the correlation between value/costs and eco-aspects of the system. Therefore, a number of points are outlined: tangible and intangible value for the user, tangible costs and risk premium for the provider, investments needed, and synergy and responsibilities between users and providers.

There are certain conditions under which PSS might be profitable. Firstly, the costs of use and disposal phases should be internalized. Secondly, the product should have a high market value at the disposal stage. Thirdly, the alternative scenario of product use should generate additional profit (Mont, 2002).

 Published by Cranfield University Press ISBN: 978-0-9557436-7-2 http://hdl.handle.net/1826/3832

Despite the benefits of the PSS, some barriers to their development and application should be examined. These are the following (Mont, 2002):

- Difficult development of alternative scenarios of product use.
- Resistance of companies to extend involvement with a product beyond pointof-sale.
- Need for time and resources for the reorientation of the companies.
- Customers' demands and purchasing behavior appears to be more complicated than expected.
- Environmental characteristics of PSS are not yet studied.
- Need for new infrastructure.

Industrial research

After having studied the key PSS themes in the literature, the researchers conducted a case study in a UK pump manufacturing company, whose main characteristics are the provision of availability contacts and short-lead times (Company 1). This case study which comprises of three parts: 10 interviews with New Product Development (NPD) personnel in the UK, 5 phone interviews with service personnel in a company's service centre in the USA and 6 interviews with service personnel, who provide on-site service to a customer in Germany. As a result, service issues were identified and a deep understanding of the service operation was gained. After this case study, an interview, which lasted two hours, was conducted in order for the researcher to gain broader and richer understanding of the service issues that might exist in UK manufacturing companies. Company 2 belongs to the aerospace industry sector, with long-lead times and provision of capability contracts as the main characteristics .This section presents a part of the research protocol that was used for this interview. The whole document consisted of the following subsections: research aim, research stage and current insight, subjects to be covered, case description, case justification, questions to be covered and any specific data required, and analysis techniques and plan; it described the points of interest and the questions of the semi-structured interview and was designed and sent to the interviewee in advance.

Research aim

Investigation of service issues in Company 2, UK.

Case justification: why this company? How does this company match the research aim? Why this business unit?

 Published by Cranfield University Press ISBN: 978-0-9557436-7-2 http://hdl.handle.net/1826/3832

Company 2 represents a capital intensive, mature and complex aerospace domain, which is suited to a formal knowledge reuse methodology.

Questions to be covered in the interview

1 .	How important is service to Company 2 as a business?
2 .	Types of service carried out.
3 .	What does PSS mean to Company 2?
4 .	How is service taken into account into the design process?

Snapshot interview results

The results mentioned in this section derive from a 2-hour semi-structured interview with an experienced engineer from the cost estimating team within Company 2. The company focuses on selling capability rather than selling equipment. They supply equipment, they are responsible for having it working (repair and upgrades), they supply spare parts, and they train the crew. Their service agreements focus on the application of the service rather than just the product.

Two examples of PSS that are used in Company 2 could be a helicopter or an aircraft carrier. If the example of the aircraft carrier is used, then the end user of the aircraft carrier will have a rough idea of the mission. Based on this knowledge, they specify service requirements in the contract, such as commercial requirements, statement of work (design reviews, deliverable documentation, and requirements specification).

The difficulty stems from the fact that the lifecycle is long and some factors cannot be taken into account. The most important thing in an extended enterprise is the sharing of information about obsolescence and anything that can affect PSS long-term across the company. In terms of technology update and obsolescence it would be good for manufacturing and design to focus on the high-value components and make sure that there is always an alternative. Also, the system should be as modular as possible and the components should be more standardised, so that the availability is increased.

In terms of service quality, it is assessed by technical criteria related to the performance of the equipment and by criteria related to ‘abilities’. The term ‘abilities’ is used to describe reliability, availability (proportion of time that the system is available), maintainability, supportability (how easily you keep the system working), failure rates and mean time to repair.

It has been also stated that there is a feedback process from service to design and manufacturing. Typically the customer records problems that occur. There are always periodic review meetings, depending on the type of contract that each customer has. Therefore, the responsibility is shared between the end user and the supplier. If there

 Published by Cranfield University Press ISBN: 978-0-9557436-7-2 http://hdl.handle.net/1826/3832

is a high rate of failures on specific equipment, then the service level agreement places the emphasis on the supplier to rectify it. Condition monitoring also takes place especially for components that are expensive to be replaced. So, they have introduced innovation to detect the time when the equipment is likely to fail in its design. They also have built-in tests to warn the operator about a fault that can happen. The issue is that these systems are very complex and when a function is off, you cannot notice a problem until you use this specific function.

Finally a definition for service was provided by the interviewee: "Understanding of the customer's mission requirements and the need to make sure that they are addressed successfully."

The main issues mentioned in Company 2 interview and in Company 1 case study are illustrated here, along with a comparison between the two. The main observation is that the need for cooperation between the service, design and manufacturing departments is vital for the design of serviceable products. In Company 2, the feedback process is better established and the major difficulties stem from the long life-cycle of the products and as a result the high unpredictability of the factors that can affect the life-cycle; whereas, in Company 1 the main difficulties exist due to the lack of resources (service people) in the NPD team and, as a result, the lack of time spent in the provision of feedback from service to design and manufacturing.

Key issues (Company 1 case study, Doultsinou et al, 2007):

- Need for cooperation between service, design and manufacturing.
- Lack of service personnel in the NPD team.
- No special tooling required for the majority of the service activities.
- Lack of formal customer feedback procedure.

Key issues (Company 2 interview):

- Long product life-cycles: there is danger for parts' obsolescence and difficulty in predicting the factors that will affect the PSS in long term.
- Necessity for high modularity of the systems and standardisation of the components so that the availability is increased.
- Regular review meetings with the customers during the design phase.
- Condition monitoring on expensive components.
- Cooperation between service, design and manufacturing is essential for the design of serviceable products.

 Published by Cranfield University Press ISBN: 978-0-9557436-7-2 http://hdl.handle.net/1826/3832

Conclusions

A brief overview of the literature in the domain of PSS was provided to set the theoretical basis for the exploration of service issues that arise within UK manufacturing companies. Emphasis should be given on the crucial theme of cooperation between service, design and manufacturing, which appears to be of high importance for manufacturing companies judging from their current concerns regarding the provision of PSS and service more specifically.

Acknowledgements

This paper is based on a research project funded by Cranfield IMRC/EPSRC, Rolls-Royce Plc and Edwards Ltd. The researchers are also grateful to Company 2 that kindly agreed collaborate for the purposes of this research.

References

1. T. P. Hill, (1977), On Goods and Services, *Review ofIncome and Wealth,* Vol. 23, No.4, pp 315- 338
2. www.ibm.com, Accessed 23rd October 2006
3. Donald W. Cowell, (1991), *The marketing of services,* Butterworth-Heinemann Ltd, Oxford, UK
4. J.C. Aurich et al (2006) Life cycle oriented design of technical Product-Service
5. Systems, *Journal of Cleaner Production,* Vol.14, Issue 17, pp 1480-1494 Tukker Arnold and Ursula Tischner, (2006), *New Business for Old Europe,* 1st
6. edition, Greenleaf Publishing Ltd, UK
   . K. Mont (2002) Clarifying the concept of product-service system, *Journal of cleaner production,* Vol. 10, pp 237-245
7. N. Doultsinou et al (2007) Identification of service knowledge types for technical Product-Service Systems Proceedings of4th International Conference on Digital Enterprise Technology, 19-2 1 September 2007, Bath, UK
8. "US service sector growth slowing", http://news.bbc.co.uk, Accessed 15th April 2007 "The monthly index of services: movements in GVA for service industries", http://www.statistics.gov.uk, Accessed 9th July 2007

 Published by Cranfield University Press ISBN: 978-0-9557436-7-2 http://hdl.handle.net/1826/3832

High Power Density Permanent-Magnet Generators for Portable Power Supplies

W. Fei, P.C.K. Luk

Power and Drive Systems Group, Engineering Systems Department

Defence College of Management and Technology, Cranfield University

Shrivenham, SN6 8LA, United Kingdom

Contact Email: p.c.k.luk@cranfield.ac.uk

Abstract

This paper reports initial findings of the design and analysis of a high-power density air-cored surface mounted axial flux permanent magnet (AFPM) synchronous machine intended to be used as a man-portable power supply. Both analytical equations and three dimensional (3-D) electromagnetic finite element analysis (FEA) models are developed for the design and analysis of the machine performance. The FEA results confirm the validity of the analytical model and show excellent efficiency and power density of the proposed machine.

Introduction

High-speed permanent magnet (PM) machines generally benefit from superior power-to-weight ratios, higher efficiency, and compact structures to their lower speed counterparts. These machines can be directly coupled to high speed gas turbines with no gear box involved, resulting in increased overall system efficiency and compactness. Thus, they are particularly suitable for mission-critical power supply applications where weight and space are critical factors. Recently, there are increased interests in the development of man-portable power platforms suitable for humanitarian and defence applications. The main design challenge in these machines lies in preventing overheating rather than achieving optimum performance. Axial flux design with its disc type geometry is conducive to better cooling because of higher stator surface area and lower electrical losses when compared with other radial flux designs [1]. However, there are still many design challenges due to the high speed operation, which are not addressed methodologically in the literature. This paper concerns the derivation of the analytical formula for a multi-pole axial flux PM machine. The formula is then used to design a 1kW 3-phase 8-pole 50,000rpm machine. A 3-D finite element (FE) model is built to validate the formula.

Machine Structure

Fig.1 shows the 3-D structure of the high speed air-cored AFPM synchronous machine under study. The machine consists of two rotor discs and one stator disc sandwiched in between. Circular axially magnetized

 Published by Cranfield University Press ISBN: 978-0-9557436-7-2 http://hdl.handle.net/1826/3832

high strength neodymium-iron-boron (NdFeB) permanent magnets, evenly spaced, are circumferentially mounted on the surface of the steel back iron in an N-S-N-S arrangement for each rotor disc. The rotor discs are assembled such that the magnets on each rotor disc are directly aligned and faced with the opposite polarity. Fig.2 shows some of the primary electromagnetic design parameters such as circular magnet radius R_m, circular winding coil inner radius R_i, outer radius R_o, and machine mean radius R_c. From the figure, it can easily be seen that:

$$R_o = R_c \sin(\pi/p_s) \qquad (1)$$

$$R_i < R_m < R_c \sin(\pi/p) \qquad (2)$$

where p_s and p are the stator coil number and rotor's magnet pole number respectively.

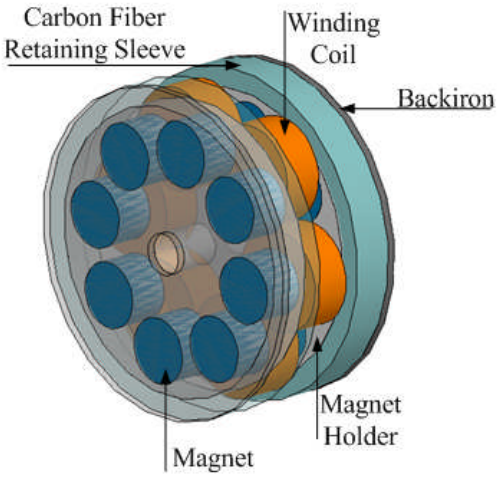

Fig.1. Machine structure under study

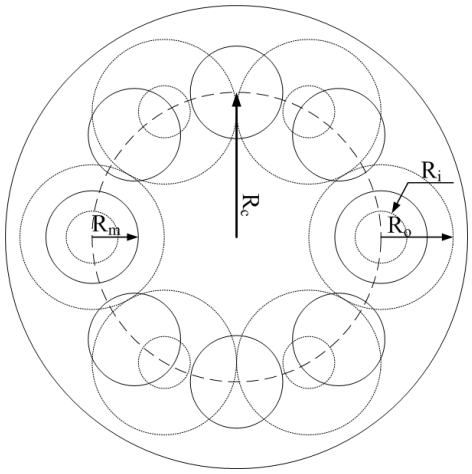

Fig.2. Machine's main geometric parameters corresponding to Fig.1.

Machine Modelling and Design

Analytical Sizing Equation

In Fig.2, the flux density produced by the circular permanent magnets appears to fall in all directions from the centre of the magnet in an approximate sinusoidal shape. A similar machine structure is introduced as a low-speed small-scale wind turbine direct-drive generator in [5], with an assumption that at the axial middle point of the stator the flux density produced by the magnets takes the form of a 'sinusoidal hill' with a radius half

 Published by Cranfield University Press ISBN: 978-0-9557436-7-2 http://hdl.handle.net/1826/3832

that of the machine pole pitch. The peak flux density at the centre of the magnet can be derived analytically with reasonable accuracy as [2]:

$$B_{peak} = \frac{4B_r}{\pi\mu_r} \frac{\sin\left(pR_m/2R_c\right)\sinh\left(pl_m/2R_c\right)}{\sinh\left(p\left(2l_m+g\right)/4R_c\right)} \qquad (3)$$

where B_r is the magnet residual flux density, and μ_r is the magnet's relative recoil permeability.

By the aforementioned 'sinusoidal hill' assumption and with the machine structure under study, an analytical machine sizing equations can be derived as:

$$P = \frac{8k_1k_p n\pi p_s J B_r \left(g-2c\right)R_c^3 \sinh\left(pl_m/2R_c\right)}{15\sqrt{2}p^2\mu_r \sinh\left(p\left(2l_m+g\right)/4R_c\right)} \left(\begin{array}{l} 4\left(\sin\left(pR_o/2R_c\right)-\sin\left(pR_i/2R_c\right)\right) \\ -pR_o\left(1+\cos\left(pR_o/2R_c\right)\right)/R_c \\ +pR_i\left(1+\cos\left(pR_i/2R_c\right)\right)/R_c \end{array} \right) \sin\left(\frac{pR_m}{2R_c}\right) \qquad (4)$$

where P is the machine output power, k_1 is the flux enhancement factor to compensate the flux density in radial direction that is not exactly sinusoidal distribution, which normally has a value slightly larger than 1 (k_1=1.05 is used here), n is the machine speed, k_p is the winding fill factor and J is the winding's root mean square current density.

Machine Design

Although 2-pole or 4-pole rotor configurations are generally considered for high speed applications, they are often not conducive to effective start-up due to poor torque capability. It is therefore necessary to consider a higher pole number configuration. Since the circular concentrated winding is employed in the proposed machine structure, the electrical angle θ_c between adjacent armature coils is given as:

$$\theta_c = \frac{p\pi}{p_s} \qquad (5)$$

where p_s and p are defined previously in (1) and (2).

Since the machine is designed as three-phase, in which angle θ_c must be 120°, 240° etc, thus the most common pole numbers p_s=6 or p_s=12 can be used. Higher numbers are not considered due to higher eddy current losses and assembly complexity, among others. Considering the geometric structure of the stator, and inspecting equation (1), it can be concluded that more winding space and better machine performance can be

 Published by Cranfield University Press ISBN: 978-0-9557436-7-2 http://hdl.handle.net/1826/3832

achieved with p_s=6. From (5), with p_s = 6, then p = 8. This means there are 8 magnets per rotor disc and the preferred coil number is 6, as already illustrated in Fig.1. The 8-pole rotor configuration offers better magnet utilisation and smaller outer diameter, which is critical for mechanical integrity at high speed. Based on the sizing equation (4), a 1kW AFPM machine with a rated speed 50,000rpm is designed with key parameters as shown in Table 1.

Machine Rated Power Output (P)	1000W	Permanent Magnet Axial Length (l_m)	10mm
Machine Rated Phase RMS Voltage (U)	40V	Winding Coil number (P_s)	6
Machine Rated Phase RMS Current (I)	8.4A	Winding Coil Inner Radius (R_i)	4.5mm
Machine Rated Speed (n)	50,000rpm	Winding Coil Outer Radius (R_o)	12.5mm
Machine Mean Radius (R_c)	25mm	Winding Package Factor(k_p)	0.5
Permanent Magnet Residual Flux Density (B_r)	1.21T	Winding RMS Current Density (J)	5A/mm^2
Permanent Magnet Recoil Permeability ($\mu_r\mu_0$)	1.1μ_0	Airgap axial Length (g)	12mm
Permanent Magnet pole number (p)	8	Running clearance (c)	1mm
Permanent Magnet Radius (R_m)	8mm	Back Iron Thickness (l_b)	3mm

Table 1: Key design parameters of machine under study

FEM Validation

A 3-D FEA model of the proposed machine is developed to validate the analytical sizing equation and predict the machine performance more accurately. The simulated no load flux density in the air gap is shown in Fig.3. The 3-D flux density distribution from the FEA model confirms the earlier presumption that it follows a 'sinusoidal hill' shape. The flux density is seen sinusoidally distributed circumferentially around the machine, and reduces sinusoidally to zero both radially inwards and outwards from the centre of the magnet. Close inspection however reveals that flux density decreases more rapidly when moving outwardly than moving inwardly. This discrepancy can, however, be easily compensated by employing a flux enhancement factor k1 as in equation (4). Thus, the assumption of a sinusoidal flux density 'hill' is still justified in the analytical model. FEA models with the same parameters but varying winding coil inner radius Ri are built in order to investigate the effect of Ri on the machine performance. The per turn back EMF times phase winding area of the machine with different Ri calculated by the FEA models, are displayed in Fig.4. It can be seen that the machine back EMF waveforms are essentially sinusoidal which make the machine especially suitable for use as a brushless AC motor drive. The machine power output for different Ri based on the same winding fill factor and current density, from both 3-D FEA simulation and analytical equation (4), are shown as in Fig.5. It can be seen that there are good agreements between the two

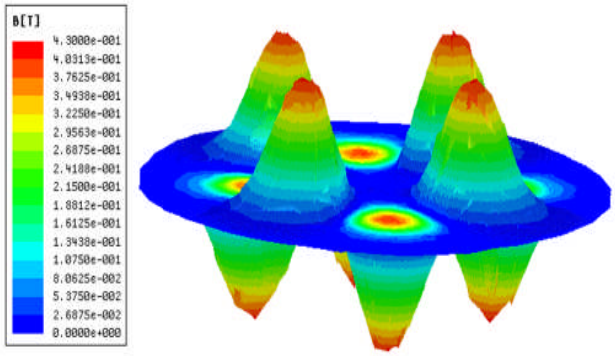

Fig.3. Flux density distribution at stator from FEA model

 Published by Cranfield University Press ISBN: 978-0-9557436-7-2 http://hdl.handle.net/1826/3832

results, in particular when Ri is low. The discrepancy is higher when Ri becomes bigger, which can be explained by the assumption made for the analytical equation. The impact of the non-sinusoidal radial components is stronger for bigger Ri, which means a bigger flux enhancement factor k1 for bigger Ri is indeed necessary. From Fig.4 and Fig.5, it follows that smaller Ri can deliver better performance and higher output. However, it should also be noted that smaller Ri means more stator winding copper, and thus higher copper losses and eddy current losses based on the same current density.

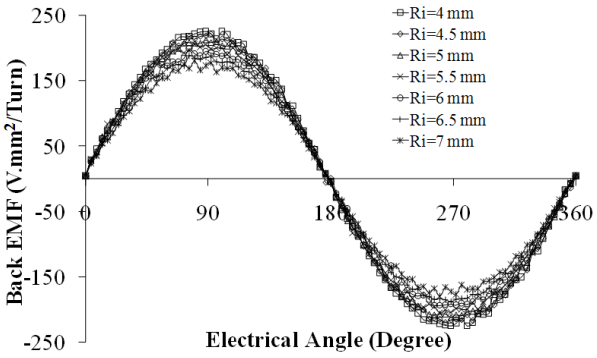

Fig.4. Back EMF versus position for different R_i

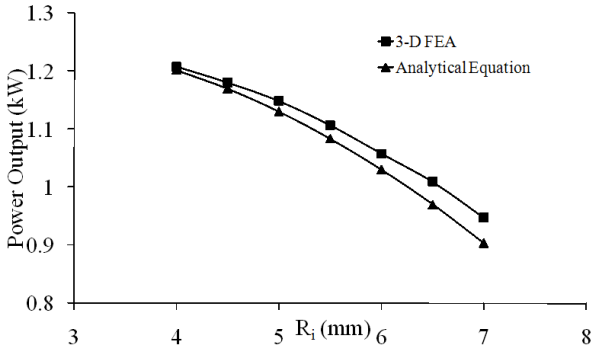

Fig.5. Machine power output for different R_i

Conclusion and Further Work

Multi-fuel high speed gensets present an attractive alternative to future power sources for man-portable power platforms, due to its shorter and more certain development time, and minimum logistics compared with other competitive technologies such as fuel cells. This paper concerns the initial findings on the design of a 1 kW PM machine to be used in these high speed gensets. The analytical sizing equations for a surface mounted AFPM machine with a double-rotor, single slot-less stator structure, is developed and validated by 3-D FEA results. The machine losses and efficiency are investigated for an optimised design of the proposed machine. Due to the high rotational speed, the machine windage losses are identified as the dominant components of the total machine losses. This makes the machine electromagnetic design much less critical than thermal management of these high speed machines. However, if proper cooling method is employed to ensure no excessive heating of the machine, the proposed machine structure presents an excellent over-load capability, with efficiency at over 92% at 3 times of overload. At rated load, the machine has an efficiency of 85% at rated speed, which compares very favourably with other power conversion at this low power level and high power density. Further work will involve integrated design to reduce windage losses, and special means such as heat pumps to remove the heat generated within the machine. Extensive experimentation will also be undertaken for the prototype machine, shown in Fig.6. Although the prototype has been designed for a top speed of up to 20,000 rpm in order to minimise development costs, it is envisaged that with extensive experimental results at up to 20,000rpm, vital information and key operational challenges such as windage losses at the rated speed of 50,000rpm can be identified by extrapolations.

 Published by Cranfield University Press ISBN: 978-0-9557436-7-2 http://hdl.handle.net/1826/3832

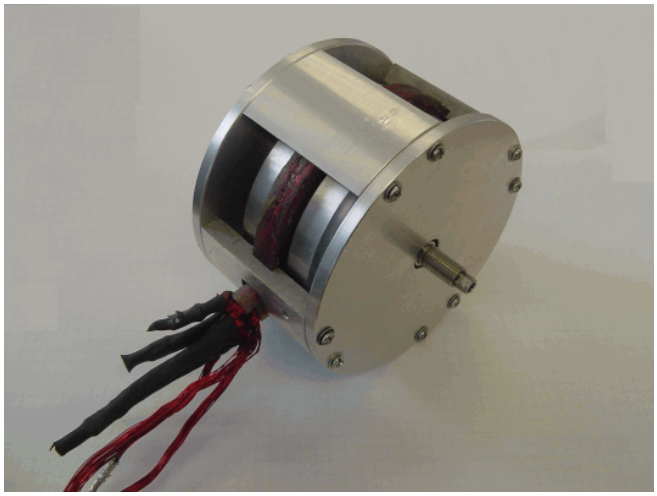

Fig.6 Prototype of the high speed machine with designed top speed of 20,000rpm

References

1. K. R. Pullen, M. R. Etemad, A. Fenocchi, “The high speed axial flux disc generator-unlocking the potential of the automotive gas turbine,” *Proc. IEE Colloq. Machines and Drives for Electric and Hybrid Vehicles*, pp. 8/1 -8/4, 1996.
2. J. R. Bumby, R. Martin, “Axial-flux permanent-magnet air-cored generator for small-scale wind turbines,” *IEE Proc.-Electr. Power Appl.*, No. 5, Vol. 152, pp.1065-1075, Sept. 2005.

 Published by Cranfield University Press ISBN: 978-0-9557436-7-2 http://hdl.handle.net/1826/3832

Cranfield University Multi-Strand Conference
May 6-7, 2008, Cranfield, United Kingdom

Advanced Low Carbon Power Systems: the TERA Approach

Giuseppina Di Lorenzo
Email: g.dilorenzo@cranfield.ac.uk

Pericles Pilidis
Email: p.pilidis@cranfield.ac.uk

Department of Power and Propulsion

Cranfield University

Bedfordshire, MK43 0AL, United Kingdom

Abstract

This paper presents the application of TERA (Technoeconomical Environmental and Risk Analysis) for the emerging low carbon power concepts. The challenge of moving towards a low carbon future requires the development and the deployment of a portfolio of low carbon technologies for the power generation sector. The TERA methodology, used for the European aviation industry under the leadership of Cranfield University, can represent a useful guide to support the strategic-decision making process for future investments in the UK energy sector. The purpose of the methodology is described here, whereas its steps are also analyzed. A review of the literature is also presented to highlight the beneficial use of TERA in the power generation case.

Background

It has been widely recognized that climate change is one of the largest environmental issues of our time. Levels of carbon dioxide (CO_2) in the global atmosphere have been increasing in recent years and are now rising faster than ever before. This has already led to environmental changes through the global warming. Significant actions are urgently required to reduce and stabilise the CO_2 and other greenhouse gases (GHGs) emissions before their effects become even more severe [1].

Efforts have been made internationally to try to reduce CO_2 emissions. An example is represented by the Kyoto protocol (December 1997), through which most industrialised countries have agreed to reduce their CO_2 emissions by 8% from the release level (1990 to 2010).

The power generation sector is a major source of GHGs emissions, especially in the UK where it accounts for about a third of the total CO_2 release [2]. According to the Stern Review “the power sector around the world will have to be at least 60%, and perhaps as much as 75%, decarbonised by 2050” to stabilise CO_2 emissions [1]. On the other hand, in the UK the next 10-15 years will be critical in terms of energy supply, as many nuclear power stations and coal-fired power stations will be decommissioned, leaving an estimated energy gap of 20

 Published by Cranfield University Press ISBN: 978-0-9557436-7-2 http://hdl.handle.net/1826/3832

GW to be met by 2020 and requiring significant investments in new power plants [3]. Therefore, reducing CO_2 emissions has become a major challenge for the power generation industry.

Novel Low Carbon Power Systems

In order to reduce the CO_2 emissions from power generation plants and to support future investment strategies a wide variety of techniques is being proposed, among which three different types of concepts have emerged as the most interesting possibilities: increasing the thermodynamic efficiency of energy conversion and utilization; using power sources with intrinsically very low CO_2 emissions, as renewable or nuclear energy and designing new fossil fuel fired power plants for the capture and storage of carbon dioxide (CCS) [4]. Regarding the latter, several concepts are proposed: oxy-fuel combustion concepts, post-combustion concepts and pre-combustion concepts.

The development and deployment of novel low carbon power systems is strongly stimulated [1]. They represent a major business opportunity for the UK, as demand for these technologies is forecasted to expand in the next years. Moreover they will contribute significantly to the UK's climate change commitments and energy security goals.

A key question is which options to pursue. These options, quite different with each other, have been extensively studied and investigated in the scientific literature, but the selection of best candidates is difficult and uncertain. They could be compared by means of different criteria. Plant efficiency is of course one of them, but not necessarily the most decisive selection criterion. Bolland et al. [5] have presented benchmarking results based on plant performance in terms of plant efficiency for nine different concepts for power plants with CO_2 capture. A quantitative comparison of the same concepts based on net plant efficiency and CO_2 emissions level has been carried out by the same authors [6]. A common challenge for all these approaches is the reduced plant efficiency compared to conventional power plants. Nevertheless the plant efficiency and the CO_2 emissions avoided alone can not rule out any of the proposed concepts.

The systems envisaged are larger and more complex than the current state-of-the-art technology. All approaches will imply an increase in the first cost of the plant, an increased challenge in reliability and availability and more complex operating procedures. Both qualitative aspects, such as technology maturity, and costs for investment and operation and maintenance will have an impact on the selection of low carbon technologies. These aspects will need to be addressed when evaluating investment performance, enabling a fair estimation of the actual benefit from each concept and how large this benefit can be. Several economic data concerning the new low CO_2 emission power generation processes are available. Due to the absence of a standard framework for the economic assessments, it is difficult to compare them in a reliable way [7]. In addition, various projects have been conducted to draft the improvement potential of specific CO_2 capture technologies [8, 9]. A qualitative analysis based on issues such as technology maturity and process complexity has been presented by Bolland et al. [10].

 Published by Cranfield University Press ISBN: 978-0-9557436-7-2 http://hdl.handle.net/1826/3832

A novel method has been developed [11] that compares power plant concepts including CO_2 capturing. Instead of using extensive thermodynamic calculations for these concepts, reaction equations for the conservation of molecular species together with specific energy consumption numbers for the different process sections are used to characterize the concepts with respect to fuel-to-electricity conversion efficiency.

Lombardi [12] has proposed an environmental life cycle assessment (LCA) focussed on CO_2 production during the three phases of construction, operation and dismantling of the plants to verify whether the process is effective in terms of CO_2 reduction. Besides the classic LCA, also an exergetic life cycle assessment (ELCA) has been performed by the same author to assess the cost, in terms of exergy losses, of the life cycle of the plants.

During the last years much effort has been directed towards comparative assessments of novel low carbon power plants concepts in terms of many criteria. Many studies have been carried out to attempt a techno-economic comparison of some concepts [4, 7, 8, 13]. To take into account the most significant costs and emissions factors in comparison of CCS concepts, the Carnegie Mellon University has developed the Integrated Environmental Control Model tool [14].

Along this route, TERA provides a method approach for this kind of investigation because it allows to incorporate multidisciplinary aspects for modelling gas turbine and power plant performance, estimation of emissions, environmental impact and economic aspects, so as to draw a big picture of these technologies, among which the most secure, reliable, efficient technologies need to be identified.

The TERA approach and its application to Power Systems

TERA is an acronym for “Technoeconomical Environmental and Risk Analysis”. The origins of the TERA in Cranfield University are traced back to work in the environmental impact and engine conceptual design choices for civil aircraft: it is a decision-making framework formulated for the investigation and application of long-term and short-term strategies to improve the overall efficiency of aero-engine aircraft systems. Within the European projects VITAL and NEWAC TERA can be used for the evaluation of advanced aircraft engine concepts designed to meet the ACARE goals [15].

 Published by Cranfield University Press ISBN: 978-0-9557436-7-2 http://hdl.handle.net/1826/3832

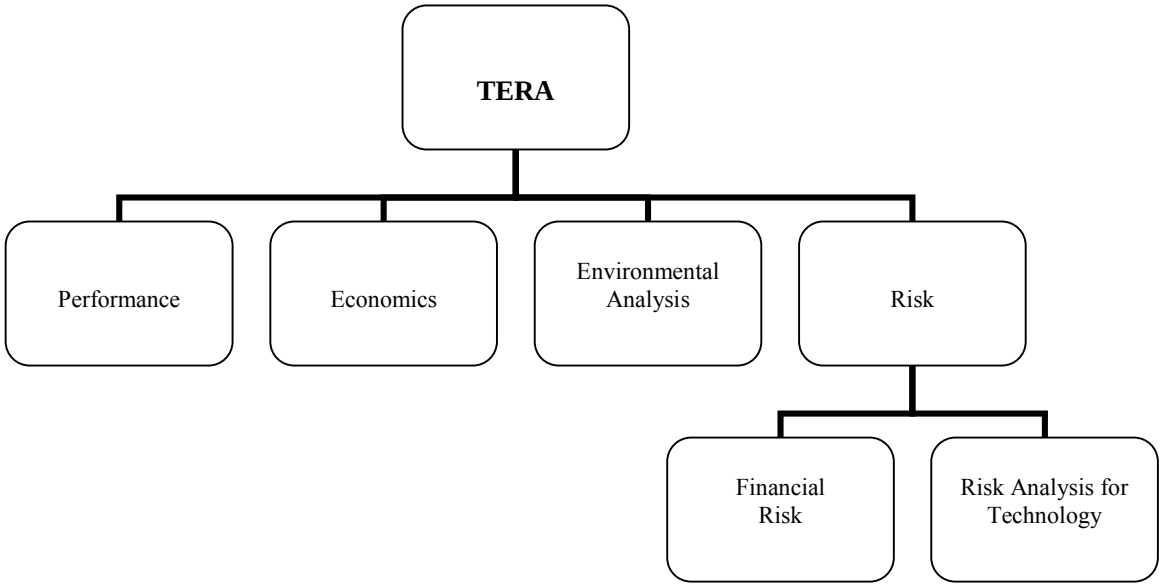

Figure 1 *Basic philosophy of TERA*

In the power generation case TERA can be used to point out the relative risks and benefits of each proposed solution. Figure 1 depicts the basic philosophy of TERA. The starting point of TERA is a detailed cycle and component models of the power plant. This delivers a representative view of whole plant performance that takes into account variable demand patterns. The following steps, using the detailed and reliable thermodynamic results produced by the first step, allow for the modelling and estimating of the environmental impact and the life cycle costs, providing the data required for some parameters available to assess the financial prospect of investments of each selected cycle. Risk analysis is then carried out at two levels in order to identify potential risks and critical elements associated with each technology. At the first level the financial risk is examined by probabilistic methods in order to identify the impact that changes in income, costs and prices can have in the decision-making process. The second level of risk assessment is carried out from the perspective of the technologies employed. The success of a low carbon future is highly dependent on technology. All low-CO_2 emissions power plant cycles differ in technological maturity and operational challenges: some technologies are very near to the state-of-the-art-today, but others are innovative and not completely developed. On the other hand, the low-CO_2 emissions power cycles requiring further technological improvements to be employed very often exhibit the best plant performance [6]. Thus, in order to determine the most promising concepts, a risk analysis becomes necessary to assess the technological maturity and to address the risk of not achieving the goals in the technology development [10, 16].

The outcome is an economic and environmental picture of power plant performance under various load demands and various ambient conditions. The application of TERA brings about a study of each selected cycle in terms of technical solution, technology readiness level, effort required for its deployment, environmental impact, costs and risk involved, evaluating the most competitive solutions in different scenarios and contributing in this way to the strategic investment planning.

 Published by Cranfield University Press ISBN: 978-0-9557436-7-2 http://hdl.handle.net/1826/3832

Conclusion

The TERA approach will provide a valuable insight to investigate the most promising systems in terms of multidisciplinary criteria that promise the best performance for CO_2 mitigation and to estimate their competitiveness. It can be a useful guide to identify which technology risk areas cause the greatest technical and economic concern, so as to facilitate their route to commercial operation with benefits for the UK energy industry and for the long term needs of the community.

References

[1] Stern, N., 2006, “The economics of climate change: the Stern review”, Cambridge University Press, Cambridge.

[2] DTI, July 2006, “Updated Emissions Projections”, available at: http://www.dti.gov.uk/files/ file31861.pdf (accessed 07/09).

[3] Kirkup, N., 2005, “Estimated power generation capacity requirement to 2020”, DTI analysis, DTI.

[4] Gabbrielli, R., Singh, R., 2003, “Thermodynamic Performance Analysis of New Gas Turbine Combined Cycles with No Emissions of Carbon Dioxide”, ASME, no 125, pp. 940-946

[5] Kvamsdal, H. M., Maurstad, O., Jordal, K., Bolland, O., 2004, "Benchmarking of gas-turbine cycles with CO_2 capture”, Proceedings of 7th international conference on greenhouse gas control technologies-GHGT-7, September 5-9, Vancouver, Canada. Paper no. 76, 2004

[6] Kvamsdal, H. M., Jordal, K., and Bolland, O., 2007, "A quantitative comparison of gas turbine cycles with CO_2 capture", Energy, 32, no. 1, pp. 10-24.

[7] Gabbrielli, R., Singh, R., “Economic and Scenario Analysis of New Gas Turbine Combined Cycles with No Emissions of Carbon Dioxide”, ASME, n. 127, pp 531-538.

[8] Peeters, A. N. M., Faaij, A. P.C., Turkenburg, W. C., 2007 “Techno-economic analysis of natural gas combined cycles with post-combustion CO_2 absorption, including a detailed evaluation of the development potential”, International Journal of greenhouse gas control, no 1, pp. 396-417

[9] Rao, A. B., Rubin, E. S., Keith, D. W., Morgan, M. G., 2006, “Evaluation of potential cost reductions from improved amine-based CO_2 capture systems”, Energy policy, no 34, pp.3765-3772.

[10] Kvamsdal, H. M., Bolland, O., Maurstad, O. and Jordal, K., 2006, "A qualitative comparison of gas turbine cycles with CO_2 capture", Proceedings of 8th international conference on greenhouse gas control technologies, NTNU, Norway

[11] Bolland, O., and Undrum, H. 2003. “A novel methodology for capturing CO_2 capture options for natural gas-fired combined cycle plants”, Advances in Environmental Research 7, pp. 901-911.

[12] Lombardi L., 2003, “Life cycle assessment comparison of technical solutions for CO_2 emissions reduction in power generation”, Energy Conversion Management 2003 (44), pp. 93–108, Elsevier Science Limited, Oxford (UK).

[13] Bücker, D., Holmberg, D. and Griffin, T. (2005), "Techno-Economic Evaluation of an Oxyfuel Power Plant Using Mixed Conducting Membranes", in Carbon Dioxide Capture for Storage in Deep Geologic Formations, Elsevier Science, Amsterdam, pp. 537-559.

 Published by Cranfield University Press ISBN: 978-0-9557436-7-2 http://hdl.handle.net/1826/3832

[14] Rao, A. B., Rubin, E. S., 2002, “A technical, Economic and Environmental Assessment of Amine-Based CO_2 Capture Technology for Power Plant Greenhouse Gas Control”, Environmental Science & Technology, vol. 36, n. 20, pp. 4467-4475

[15] Ogaji, S.O.T., Pilidis, P., and Hales, R., 2007, “TERA - A Tool for Aero-engine Modelling and Management”, Proceedings of the Second World Congress on Engineering Asset Management and the Fourth International Conference on Condition Monitoring, 11-14 June 2007, Harrogate, UK

[16] Di Lorenzo, G., Friconneau, V., Brandt, P., Lonneux, V., Marinai, L., Pilidis, P., Ruiz-Olalla, G., 2007, “Technoeconomic Environmental Risk Analysis - Technological Perspective Application To Low Carbon Plant”, Proceedings of the Fourth IDGTE Gas Turbine Conference "Gas Turbine Technology in a Carbon Constrained World", Paper 6, 13-14 November 2007, United Kingdom.

 Published by Cranfield University Press ISBN: 978-0-9557436-7-2 http://hdl.handle.net/1826/3832

Qualitative Enquiries: Lessons from the Field

Marko Bastl*, Tonci Grubic**, Simon Templar*, Ip-Shing Fan**, Alan Harrison*

*Supply Chain Research Centre, Cranfield School ofManagement, MK430AL Bedford, United Kingdom

** Manufacturing Department, School ofApplied Sciences, Cranfield University MK430AL Bedford, United Kingdom

Abstract

Case study based research is gaining in its popularity and in many fields becoming a main or complementary research method. Literature on how to design and conduct case studies is well covered and easily accessible. However there is much less information about practical challenges and how to respond to them when actually doing the case based research. This paper introduces possible responses to risks rooted in researcher's low control over external events in conducting case based research. This has been based on two and a half years long exploratory multiple case study research project.

Key words: case study research, methodology, field work

INTRODUCTION

In his frequently cited work on case study research Yin (2003) defines case study as an empirical inquiry that investigates some contemporary phenomenon in a real-life setting where the boundaries of the phenomenon of interest and environment are not clear. According to Meredith (1998) case study based approach enables observation of actual practices, better understanding of the nature and complexity of research phenomenon and much needed exploratory depth. Case study research has been a subject of critical debates around the lack of rigour, especially from the communities that favour positivistic-quantitative approaches. However, many authors have reported a numerous misconceptions about the case the study research (See for example Ellram, 1996; Flyvbjerg, 2006). By doing that not only they have rejected most of the critics they have also provided guidelines for ensuring scientific rigour in doing case study based research. The literature on case study research is available and easily accessible. One have ample of guidelines on how to design the case study research in order to satisfy the quality criteria of a research design. However, there is much less written about potential events, related risks and how to address them during the actual execution of the research. This paper contributes to this by illustrating three short lessons in dealing with unforeseen events in different stages of an exploratory based research project called ARIEL. The lessons were selected on the basis of their impact on project management and research design. Paper firstly introduces the research objectives and initial research design in section 2. This is then followed by illustration of the unforeseen events and related responses in chapter 3, and concluding remarks in chapter 4.

RESEARCH OVERVIEW

Research objectives

The ARIEL project is a second generation project that builds on the previous understanding of a relationship between time and cost in supply chains. Where the first generation project was intra-

 Published by Cranfield University Press ISBN: 978-0-9557436-7-2 http://hdl.handle.net/1826/3832

organisational in its context, this one is inter-organisational. The key objective of the ARIEL project is to develop a computerised business process model of a relationship between a buyer and a supplier. Such model will enable companies to play with different business process configuration scenarios and make the assessment of each scenario based on its impact on total time and costs in supply chain.

Methodological design of the research

The objectives of the research and the current level of understanding of investigated phenomenon lead to a decision of adopting an exploratory multi-case study approach. Each case study consisted of two companies, where the unit of analysis was a business relationship, characterized by the flow of material and information between two parties. In order to satisfy the criteria for overall quality of a research design numerous tactics were applied in different stages of the study *i). Research design.* Replication logic for multiple-case studies was used to address the issue of external validity; *ii). Data collection.* Case study protocol was used to address reliability issues. The protocol included a detailed description of criteria for selection of case studies (buyer and supplier), key informants and observed products, detailed replication logic design and case study execution steps, semi structured questionnaires and project time plan. Data and researcher triangulation, walk through observations and data validation tactics were applied to address the construct validity, *iii). Data analysis.* Design of the analysis framework and pattern matching techniques were applied to ensure internal validity of the study.

The decision on the number and type of case studies was made by considering the following suggestions: i). Need for *specific selection of case studies* (not randomly) in order to control environmental variations (Eisenhardt, 1989); ii). *Volume – variety diversification* (Slack et al., 2004) to maximize learning outcomes from contrasting cases studies, iii). *Resource availability* – number of researchers and duration of the project. As a result of that the initial case study set-up included three manufacturing companies each in the following sectors: food (high volume – low variety), automotive (mid volume – mid variety) and aerospace (low volume – high variety).

SUMMARY OF KEY LESSONS

Lesson 1: (Re) gaining industrial access - a challenging and critical task

Irrespective of a single or multiple case study designs, both types of research require industrial access that allows researchers to conduct data collection. As multiple case studies are particularly appealing in allowing researchers a cross-case analysis of collected data they carry some significant risks. The one that has the strongest impact on the research project is associated with losing already agreed access to industrial collaborators. Such event proved to be entirely out of researchers' control and well in line with theoretical suggestions of low researcher's control over external events in case study based research. Irrespective of existing working relationships between individuals in the project team and individuals in the companies that initially agreed to participate, the project lost all three industrial collaborators. The reason for that was simply in people changing their jobs and moving to other companies.

 Published by Cranfield University Press ISBN: 978-0-9557436-7-2 http://hdl.handle.net/1826/3832

The first obvious reaction from the project management perspective is to re-gain the access. As this perhaps sounds fairly straightforward it has proved to be a very challenging and time-consuming task for the following reasons:

a) By satisfying a principle of "a specific selection of case studies (not a random choice)" (Eisenhardt, 1989; Slack, 2004) not every organisation fits the research design.

b) Approaching companies with no previous experience in working with individuals from the project team or institution has low success rate. In 18 months time over 80 companies were approached, 12 of them allowed us presenting the project idea, two initially agreed to participate but dropped-off again due to changes in people jobs.

c) Coordination, arrangement of initial access and waiting for a feedback from potential collaborators proved to be time consuming since all these activities can be carried out concurrently only with few companies at the same time.

d) A requirement for one case study to consist of buying and supplying organisation increases the amount of coordination activities and hence extends the time for arranging access.

e) e. In addition to this the project requirements for potential sharing of some sensitive information are perceived as unacceptable in some organisations.

Each, or combination of the abovementioned reasons added to a time delay in the start of actual empirical work. However, some tactics could be employed in order to manage such situations. The following tactics worked well in our example:

- Target those companies that have good working relationships with individuals within the institution you are working for. As this does not guarantee success it speeds up the coordination and arrangements.
- Break the functional/departmental silo and expand the network of contacts beyond your department / school and institution. This increases the portfolio of potential collaborators.
- Ensure the clarity of presentation and replace academic with industrial language.
- Do not expect that if people move jobs, their new employer will automatically join the project. Keep them to settle in the new job and use this contacts later or for some other project.

Lesson 2: Maintain flexibility in the research design

The attempts in following the initial research design may not always be possible. For a variety of reasons researchers for example may not succeed in gaining access to companies that fit the desired research

 Published by Cranfield University Press ISBN: 978-0-9557436-7-2 http://hdl.handle.net/1826/3832

design. As this may looks like a bad news, researchers should take advantage of changed circumstances. In exploratory enquiries where researchers' control over external events is low, flexibility in designing case studies will be often sought (Yin, 2003). However by exercising the flexibility and adapting to new circumstances the rigour of the research design should not be compromised.

Changes in initial research design were required due to a time pressures caused by lengthy process of re-gaining industrial access. In order to effectively manage the flexibility of research design researchers need to understand and distinguish between critical and non- (or less) critical attributes of a research design. Which are the critical attributes will depend on many circumstances. Understanding the purpose of the investigation and expected contribution is perhaps the most important and last to expose to any change. Following that, the researchers on ARIEL project kept the following attributes of research design unchanged: *i). Unit of analysis, ii). Type of required data - process and costs, iii). Number of case studies, iv). Protocol for buyer/supplier and product selection, v). Protocol with semi-structured questionnaires.*

Part of the research design that was changed was volume-variety mix of selected case studies. The decision of accepting the available case study set-up was made at a point in time where the critical elements of the research design could still remain unchanged. The correct timing in this case is important since it helps to minimise the impact of changes in research design on the outputs of a research. The final selection of case studies comprised of: case study one - buyer and supplier in automotive manufacturing sector (mid volume – mid variety); case study two and three - buyer and supplier in automotive aftermarket sector (mid volume – high variety).

Lesson 3: Difficulties can create unforeseen opportunities

As much as changed circumstances could bring difficulties in conducting case study research, they can also create initially unforeseen opportunities. These opportunities can be highlighted with the following two examples:

Example 1:

The lengthy process of recruiting industrial collaborators produced idle time. This was the case especially in the period of waiting for the response from the approached companies. The key decision here was how to make the best use of this time? Any idle time available in the first year of the project was spent on activities that could help gaining the time in the second year of the project. The empirical data that would serve as an input to build the computerised model was not available. They were replaced by a theoretical data extracted from the additional literature review, allowing for building a theoretical backbone model. This activity did not have only time saving benefits in the second year of the project. It has also: i). Helped researchers to sharpen the research focus; ii). Helped identifying potential model's capabilities; and iii). Produced the content that was converted in one conference and two journal papers.

 Published by Cranfield University Press ISBN: 978-0-9557436-7-2 http://hdl.handle.net/1826/3832

Example 2:

In order to satisfy the research objectives, data collection required two groups of data from both companies in a dyad: process and cost related data. Especially cost related data are often kept secret from another party in a relationship, mainly due to appropriation concerns. The potential reluctance of costing data disclosure team has accounted in advance. Therefore various measures were taken in order to create the environment where companies would feel safer to share sensitive data with researchers and later with party in the relationship. These measures were: i). Selection of dyadic relationships with high level of trust among participating partners, based on a company's choice; ii). Companies were informed in advance about costing data requirements; iii). All companies signed confidentiality agreements; iv). Companies have been ensured to have full control over what and when the data can be shared with partner in relationship.

The low control of researcher over the external events proved as a reality again in the data collection phase of the project. One of the case study companies refused to share costing data although they have initially agreed to do so. The reasons behind this decision were never disclosed to research team, or to another party in the relationship. We can speculate why by pointing towards lower trust in the relationship then initially thought, weak power position in the relationship or not sufficient management buy-in for the project. The inability of collecting costing data from one party of the relationship has left a gap in the data that are necessary for evaluation of different relationship configurations, and also for comparative cross-case study analysis. This event has pointed towards much more common business reality then the initial research design has planned for. It has created a new, previously unforeseen scenario that requires a careful individual and cross-case analysis. As such it has also created an opportunity for new learning and exploration of potential (missed) opportunities in the relationship where reluctance in sharing information is a business reality.

CONCLUDING REMARKS

The lessons highlighted in this paper illustrate some possible challenges that researchers who are conducting case study based research can face with. It is evident from the examples that the low level of researcher's control over external influences almost guarantees that quality research design on its own does not lead to achievement of research objectives. The overall project management should incorporate some sort of contingency plan in order to cope with risk and help to keep research on track. However, foreseeing all the risks that similar research can encounter is impossible. Therefore the question of how far to go with contingency planning is more then relevant for discussion. Some, in this paper introduced tactics and ways to exploit previously unforeseen opportunities could help researchers addressing similar risks on other case based projects. Researcher's proactive behaviour and possession of a wide set of skills will help to take a maximum advantage from the unforeseen events. Especially young researchers who just started developing their skills should take the opportunity and address similar risks together with their more experienced senior colleagues.

 Published by Cranfield University Press ISBN: 978-0-9557436-7-2 http://hdl.handle.net/1826/3832

ACKNOWLEDGEMENTS

The authors would like to thank the UK Engineering and Physical Sciences Research Council for funding this research project through the Cranfield Innovative Manufacturing Research Centre.

REFERENCES

1. Eisenhardt, K.M. (1989): Building Theories from the Case Study Research, *Academy of Management, The Academy ofManagement Review,* Volume 14, Number 4, pp. 532-5 50.
2. Ellram, L. (1996): The use of the case study method in the logistics research, *Journal of Business Logistics,* Volume 17, Number 2, pp. 93-138
3. Flyvbjerg, B. (2006): Five misunderstandings about case-study research, *Qualitative Inquiry,* Volume 12, Number 2, pp. 219-245.
4. Meredith, J. (1998): Building operations management theory through case and field research, *Journal of Operations Management,* Volume 16, Number 4, pp. 441-454.
5. Slack, N., Chambers, S. and Johnston, R. (2004), *Operations Management,* Fourth Edition, Financial Times, Prentice Hall: London, UK.
6. Yin, R.K. (2003), *Case Study Research – Design and Methods,* Third Edition, Sage Publications, Thousand Oaks: California, USA.

 Published by Cranfield University Press ISBN: 978-0-9557436-7-2 http://hdl.handle.net/1826/3832

The Practical Challenges of Servitized Manufacture

S. Evans, T. Baines, H Lightfoot, M. Bastl and M. Johnson
Cranfield Innovative Manufacturing Research Centre, Cranfield University, U K

Abstract

Servitization is now widely recognised as the process of creating value by adding services to products. Since this term was first coined in the late 1980s it has been studied by a range of authors who have specifically sought to understand the methods and mechanisms of service-led competitive strategies for manufacturers. This paper reports on the experiences of a large company as they have moved towards servitized manufacture. This has been based on an extensive series of interviews with key personnel. The results of the study and implications for research are all reported.

Keywords:

Manufacturing, Service, Case-study, PSS, Product-Service System

INTRODUCTION

Servitization is now widely recognised as the innovation of an organisation's capabilities and processes, to better create mutual value, through a shift from selling product to selling Product-Service Systems (Slack et al., 2004; Baines et al. 2007). Such a strategy is now widely advocated as a means by which western manufactures can face-up to the challenges of competitors in lower cost economies. The first use of the term servitization came from Vandemerwe and Rada (1988). Here they defined servitization as the increased offering of 'bundles' of customer focussed combinations of goods, services, support, self-service and knowledge in order to add value to core corporate offerings.

The terms service and product are intrinsically linked to discussions about servitization. The term 'product' is generally well understood by manufacturers. Goedkoop et al. (1999) defined a product as a tangible commodity manufactured to be sold, and quite simplistically is capable of 'falling on your toe' and of fulfilling a user's needs. Invariably, in the world of manufacture, it is usually considered to be a material artefact (e.g. car, boat, plane), by comparison services are classed as intangible, heterogeneous, inseparable and perishable (Fisk et al., 1994).

The concept of a Product Service-System (PSS) is a special case of servitization. A PSS can be thought of as a market proposition that extends the traditional functionality of a product by incorporating additional services. Here the emphasis is on the 'sale of use' rather than the 'sale of product'. The customer pays for using an asset, rather than its purchase, and so benefits from a restructuring of the risks, responsibilities and costs traditionally associated with ownership. Conversely, suppliers/manufacturers gain from this extended relationship by learning more effectively from customers (Alonso-Rasgado et al., 2004), locking customers in to longer relationships (Vandermerwe, 2000), and reducing competition due to the inimitable nature of services (Oliva and Kallenberg, 2003).

 Published by Cranfield University Press ISBN: 978-0-9557436-7-2 http://hdl.handle.net/1826/3832

Few researchers have documented the associated consequences to the organisational design of the host manufacturer as they seek to pursue such a strategy. This research describes case-based research that gained an in-depth and multi-disciplinary understanding of the implications of a servitization strategy. The focal firm – ServCase[1] - is a large manufacturer that, through the successes of integrated products and services, now generates a large portion of revenue from product-centric service contracts (i.e.: services that are tightly coupled to the product offering). The research with ServCase has helped to appreciate how servitization necessitates companies to make modifications ranging from the language they use to interact with customers, though to their organisation design.

PREVIOUS SERVITIZATION RESEARCH

Since this term was first coined servitization has been studied by a range of authors (e.g. Wise and Baumgartner, 1999; Oliva and Kallenberg, 2003), who have specifically sought to understand the methods and implications of service-led competitive strategies for manufacturers. In addition, during this same period, there has been independent growth in research on the related topics of Product-Service Systems (PSS), Service-Science (SS) and Integrated Vehicle Health Management (IVHM). This increasing body of research indicates a growing interest in this topic by academia, business and government. One reason for this is the belief that a move towards servitized manufacture is a means to create additional value adding capabilities for traditional manufactures (Desmet et al., 1998; Oliva and Kallenberg, 2003). Furthermore, such services are distinctive, long-lived, and easier to defend from competition based in lower cost economies (Ghemawat, 1986; Dickson, 1992). Indeed, many governments see such moves downstream as key to competitiveness (Hewitt, 2002). As a consequence, more Western manufacturers are seeking an ever increasing percentage of their revenues from services (Wise and Baumgartner, 1999). However, there is some concern that servitized manufacturers could be in greater danger of bankruptcy and make lower returns in the longer-term (Neely, 2007). Nevertheless, it is difficult to argue against a careful adoption of some services in certain situations.

To succeed with servitization a manufacturer is likely to need some new and alternative organisational principles structures and processes (Oliva and Kallenberg, 2003). These may be different to those associated with traditionally product manufacture. For example, it may be insufficient to simply attempt to replicate the Lean principles of Toyota as an agile response is often required to respond to unexpected failures in the field (Johnson and Mena,*forthcoming).* This

is an area of some contention amongst scholars as the adoption of Lean is often seen as the solution to tackling the poorer performers in the services sector (Womack and Jones, 2005). While this may be appropriate in some instances, authors such as Chase and Garvin (1989), argue strongly for reversing the trend of applying operational management based concepts in the services environment. Chase and Garvin (1989) also suggest that there is a subtle mix of organisational structures that are appropriate to a servitized manufacturer that are distinct and different to those associated with, either a more traditional product manufacturer, or a pure service provider. However, researchers have yet to fully understand the nature of these structures and their associated issues.

 Published by Cranfield University Press ISBN: 978-0-9557436-7-2 http://hdl.handle.net/1826/3832

RESEARCH DESIGN

The aim of the research was to investigate a "servitized organisation" that designs, builds and delivers integrated product and services, and to identify the challenges they are encountering in the pursuit of such a strategy. The case research method was employed to study a UK-based manufacturer who gains a large portion of revenue from the provision of services that are closely coupled to their products. The case study was undertaken from June to November 2007. During this time seasoned researchers from across the disciplines (engineering, manufacturing, management) worked on the study. Firstly a history map with ServCase was developed to understand how they have arrived at their servitization strategy. Then working in pairs, researchers conducted interviews with key personnel from across the organisation (e.g. marketing, customer support, engineering, manufacturing operations, and supply chain) and captured their views on how the organisation operates and the issues they are facing. Each interview was recorded and then transcribed. Over 400 pages of transcripts were double or triple marked and then coded and interpreted using mind-mapping techniques to identify the common issues arising across the organisation. It is these issues that are the principal findings of this study, these are presented in the following section.

SUMMARY OF KEY FINDINGS

Emergence of Servitization at ServCase

ServCase provides capital equipment products, and often offers these with a broad range of services that ensure asset availability via a risk and revenue sharing contract. While the origin of this business dates back to the early 1990s it really only took shape in the early 2000s. This market proposition emerged in response to customers who sought to offset their repair and overhaul costs and responsibilities for products. Similarly, ServCase sought to prevent component suppliers from directly supplying ServCase customers. Their service business has now grown to such an extent that over 50% of their revenues are now derived from the provision and support of integrated offerings. The changes issues that have arisen as a consequence of this transition from traditional manufacturer are summarised as follows.

Language is particular and peculiar

One of the most striking differences at ServCase is the everyday language used by the employees in the delivery of services. Whereas with a conventional manufacturer, personnel use (and fully understand) nomenclature such as product, part and component they may only loosely understand the term service. As a noun, the word 'services' usually refer to the offering (e.g. maintenance, repair, insurance) and a single offering is a service. However, as a verb, service can also be used to refer to a level of performance (e.g. that was good service). This is only one example of many words and phrases whose semantics take on particular and specific meanings. This distinction appears strongest amongst personnel who deal most closely with customers of services. Future challenges are, therefore, to make such language pervasive throughout the organisation.

 Published by Cranfield University Press ISBN: 978-0-9557436-7-2 http://hdl.handle.net/1826/3832

Value dimensions are special

One reason that language changes, is that a PSS is different. At ServCase the nature of the relationship with the customer changes from a transaction to that of a long-term relationship. Traditional manufacturers tends to take a linear view of product production (by the manufacturer) which is then sold (a transaction) to the customer for their use (consumption). However, when ServCase deliver an integrated product and service there tends to be a series of 'touch points' between the host business and customer. For example, initial contract negotiation may be lengthy; monitoring of the asset in-use may be carried out by the business, this may lead to servicing of the product by the business; and finally the host may take-back the product at end-of-life. While the product itself may still be sold to the customer (as is the case with ServCase) the associated services are more closely associated with long-term relationships. Hence, servitization tends to combine both transactional and relationship elements into the business models. Moreover, revenue, profits and cash flow arise mainly from the relationship aspects of this model with a shift from reducing costs to improving the value for a customer.

The metrics used to define value offered to the customer vary to reflect the changing business model. This is particularly apparent in the measures employed to assess performance. Conventional manufacture will frequently focus on the Cost, Quality and Delivery of products. Here, quality conformance will typically be assessed in terms of rejected components; cost will comprise of labour, materials and overheads; and delivery performance will be assessed by due-date performance. With services at ServCase, value becomes more associated with asset use, rather than sale or repair, therefore the appropriate measures can be subtly different to those typically employed.

The depth of the manufacturer's understanding of what value has been created for a customer is possibly one of the contingencies that can moderate the association between servitisation strategy and lower returns in the long-term. However, assessing the value created through an integrated offering of products and services can be difficult to gauge. In spite of the nature of the contractual relationship, the product-service provider should be able to assess what value has been created through the asset/service performance as well as through the functional outcome of a product-service provision that is served directly through asset/service consumption. In order to do that the future challenge is to precisely define, distinguish and communicate the key elements of customer value on the basis of the interaction and/or consumption processes of an integrated offering.

Products and design process are different

As the value proposition changes, then product designs at ServCase have also altered to reflect the balance of value gained through asset use rather than simple artefact ownership. As mentioned above, ServCase sell their product and offer complementary services to assure asset availability. As significant revenue is generated through services, their products incorporate a facility for remotely sensing performance in the field. Here, extra cost is added to product manufacture which can not be recouped at point-of-sale, but rather relies

 Published by Cranfield University Press ISBN: 978-0-9557436-7-2 http://hdl.handle.net/1826/3832

on the customer taking-up the services offered. This is typical of the many product features that are introduced to aid maintenance and servicing to support asset availability in the field. Traditionally, product designs are conceptualised remotely, prototyped and refined, and then put into practice. With services, prototyping does not typically exist and refinement occurs in an organic, experiential manner. Here, one danger is, as ServCase have found, for engineers to attempt to apply conventional product design processes. Understanding more about how these processes differ is a considerable future challenge.

Integrating service and product delivery systems is challenging

As with product designs, the organisational design required to support the value proposition also changes. The conventional view of materials flowing into a factory, through production, to be consumed by the customer does not occur within ServCase. While a small portion of this somewhat uni-directional material flow does occur, there is a complex service delivery system that monitors and supports the asset in use superimposed upon the traditional production business. This system transcends the traditional internal / external barriers of the host business; instead calling on partners and suppliers to affect the delivery of the required service.

This delivery system is directly impacted by the relational component of the business model and associated performance measures (as outlined in section 4.3). These requirements are so particular to this context, that ServCase has decoupled this delivery mechanism from their more conventional production system. However, they recognise that as business pressures increase the sharing of resources and knowledge necessitating that these systems be more tightly coupled. Moreover, a tighter coupling is necessary in the supply network that supports the delivery of a product-service system. As the capital asset is provided by ServCase and some elements of the service and support by members of the supply network, effective coordination and integration between network members is essential. The complexity of an integrated offering will likely require a different type of supply network for support of new products in comparison to legacy products, including a different network design and shift towards more partnering relationships with key network members. How to achieve this is a topic of some debate within the organisation.

Transformation issues are both particular and pervasive

ServCase illustrates a manufacturer that, in the adoption of a servitization strategy, is encountering changes to language, value, along with designs of product and organisation. Throughout this case, we have been made repeatedly aware that one of the biggest challenges that ServCase are facing is the need to transition from a service- as opposed to product-oriented organisation. Sections 4.2 – 4.4 above summarise how, across the organisation and its broader supply chain, ServCase has changed, and continues, to change. Against each of these strands ServCase is defining new design paradigms, and each of these introduce particular challenges to the mind-sets of customers, employees, and suppliers. For example, educating employees in the language of service, changing process to better suit the nature of service design, and adopting integrated product and service delivery systems. Understanding the specific transformational issues, and how to overcome these, is a principal future challenge.

 Published by Cranfield University Press ISBN: 978-0-9557436-7-2 http://hdl.handle.net/1826/3832

CONCLUDING REMARKS

ServCase is one example of a UK company that has adopted a servitization strategy. The study has provided a much clearer understanding of the particular issues that are arising as ServCase attempts to deliver integrated products and services successfully. In brief, these are:

- Language used in service is particular and peculiar.
- Value dimensions are special and biased towards relationships rather transaction.
- Products and design process are different and better enable service support.
- Integrating service and product delivery systems is challenging.
- Transformation issues are both particular and pervasive throughout customers, employees, partners and suppliers.

There is little to suggest that these issues are particular to the ServCase business or sector. However, for completeness, the future work will now look externally to this organisation to carry out a complementary investigation of the suppliers, partners and customers of ServCase. In conducting such an investigation we look forward to further developing our understanding of the challenges faced through servitization, and reporting these in future papers.

ACKNOWLEDGEMENTS

We wish to acknowledge the support of the Engineering and Physical Sciences Research Council for their support in carrying out this work. Also, we are grateful to our colleague Professor Andy Neely for his work in setting-up the case study for this research.

REFERENCES

1. Alonso-Rasgado, T., Thompson, G. and Elfstrom, B-O., (2004), 'The design of functional (total care) products', *Journal ofEngineering Design,* Vol. 15, No. 6, pp. 515-540.
2. Baines, T et al (2007), 'State-of-the-art in Product Service-Systems', *Journal of Engineering Manufacture,* Vol. 221, Proc. IMechE Part B, pp. 1543-1552.
3. Chase, R. Garvin, D. (1989), 'The Service Factory', *Harvard Business Review,* Vol. 67, No. 4, pp. 61-69.
4. Dickson, P.R. (1992), 'Toward a General Theory of Competitive Rationality', *Journal of Marketing,* Vol. 56, No. 1, pp. 69-83.
5. Desmet, S., van Dierdonck, R., and van Looy, B. (1998), 'Servitisation: the blurring boundaries between manufacturing and services', in van Looy, R., van Dierdonck, R., and Gemmel, P. (eds.), Services Management, An Integrated Approach, *Pearson Higher Education,* London, pp. 33-3 5.
6. Fisk R.P, Brown, S.W., Bitner, M.J., 1994, 'The development and emergence of services marketing thought', International Journal of Service Industry Management. Vol.5, No. 1, pp. 21-48.
7. Ghemawat, P. (1986), 'Sustainable Advantage', Harvard Business Review, Vol. 64, No. 5, pp. 53-58.
8. Goedkoop, M. et al. (1999), 'Product Service-Systems, Ecological and Economic Basics,' *Reportfor Dutch Ministries of Environment (VROM) and Economic Affairs (EZ)*
9. Hewitt, P. (2002),'Secretary of State for Trade and Industry', No. 4, The Government's Manufacturig Strategy Johnson, M. and Mena, C. (forthcoming) 'Supply Chain Management for Servitized Products: a multi-industry case study', *International Journal ofProduction Economics.*
10. Neely, A. (2007), 'Servitization of Manufacturing', 14th EurOMA Conf. Ankara, Turkey

 Published by Cranfield University Press ISBN: 978-0-9557436-7-2 http://hdl.handle.net/1826/3832

11. Oliva R & Kallenberg R. (2003) 'Managing the Transition from Products to Services', International Journal of Service Industry Management Vol. 14, No. 2, pp. 160-172.
12. Slack, N., Lewis, M. and Bates, H. (2004), 'The two worlds of operations management research and practice: Can they meet, should they meet?' International Journal of Operations & Production Management, Vol. 24, No. 4, pp. 372- 387.
13. Vandermerwe, S. (2000), 'How increasing value to customer improves business results', *MIT Sloan Management Review,* Vol. 42, No. 1, pp. 27-37.
14. Vandermerwe S & Rada J. (1998),'Servitization of Business: Adding Value by Adding Services' *European Management Journal.* Vol. 6, No. 4, pp. 314-324.

6. Wise R & Baumgartner P. September-October1999, 'Go downstream: The New Profit Imperative in Manufacturing' Harvard Business Review, Vol. 77, No. 5, pp. 133-141.

7. Womack, J.P. and Jones, D.T. (2005) 'Lean Consumption', *Harvard Business Review,* Vol. 83, No. 3, pp.58-68.

 Published by Cranfield University Press ISBN: 978-0-9557436-7-2 http://hdl.handle.net/1826/3832

Complex research design: is it necessary and is it worth it?

Andrey Pavlov, Mike Bourne
Cranfield School of Management
Cranfield University
andrey.pavlov@cranfield.ac.uk

Introduction

This paper reports on the issues encountered during the design stage of a doctoral research project and raises a number of questions which have had to be addressed by the authors. As such, the paper is expected to provide some suggestions to those grappling with similar issues and at the same time stimulate the dialogue that would move these issues forward. The central issues identified in this paper are the necessity of grounding the design in the existing literature and the design implications of an exploratory research question. A brief description of the research topic is followed by a more detailed discussion of the rationale for and implications of the proposed design. A summary of the current view of the research design concludes the paper.

Research Topic and Research Question

Stated simply, the research question of this study is, *How people's understanding of their work tasks are formed during team performance review meetings?* This research question is driven by the general interest in the ways various performance management initiatives achieve their desired results. In order to answer this question, we adopted an *organizational routines* view of organizations, which assumes that an organization is a bundle of recurrent processes – organizational routines – which together deliver organizational performance (e.g, Nelson and Winter, 1982). Any management initiative then works by affecting the nature and structure of organizational routines.

From the literature on organizational routines we learned that routines could be broken down into two levels – the *action* itself (e.g., removing a wheel from a car) and the corresponding *representation* or understanding of action (e.g., that action may be associated with performing a regular maintenance check on the brakes, stealing the wheel, changing a flat tire, etc). Routines change through iterations between these two levels, as actions are discussed, and representations are articulated and translated back into actions (Feldman and Pentland, 2003). Therefore, if any performance management initiative is to affect an organizational routine, it needs to affect this process of iterations between the levels of the routine.

Team performance reviews are particularly helpful for understanding the mechanics of these iterations. Evidence suggests that the process of reviewing organizational performance forces people to discuss their actions and try new decisions in practice, thus intensifying the iterations between the levels of organizational routines (Vaivio, 2004, Pavlov and Bourne, 2007) Performance

 Published by Cranfield University Press ISBN: 978-0-9557436-7-2 http://hdl.handle.net/1826/3832

review meetings establish the formal context for discussing actions, thereby providing access to the first part of this process – the process of forming understandings or representations of actions, which is the focus of this study.

Hence, re-stated more precisely, the research question asks how the representation level of a routine is formed during team performance review meetings.

The research design

In order to answer the question above, a 2-tier multimethod longitudinal research design was developed, which called for *observations ofperformance review meetings over time* and for *interviews with the participants* after each meeting. The relative complexity of this design was driven by the following considerations.

The question above implies that the unit of analysis in this study is the representation level of an organizational routine, e.g., the work of a maintenance crew. Since the question focuses on the formation of the representation level of a routine – the understanding of the work rather than the actions themselves – we do not need to observe the actual work of the crew. What we do need, however, is an environment where this work would be discussed and the individual representations of it would be formed. From the literature we know that performance reviews provide such an environment. Hence, we treat performance reviews simply as a means of accessing the process of forming the representation level of the maintenance crew's work routine. See Figure 1 for a visual representation of this process.

 Published by Cranfield University Press ISBN: 978-0-9557436-7-2 http://hdl.handle.net/1826/3832

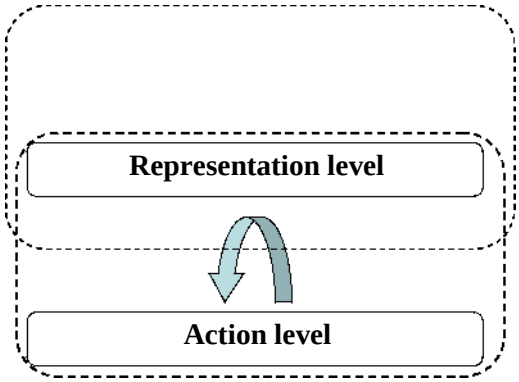

Tier II. Performance Review Meeting

Method: observation

Purpose: accessing the formation process of the rep. level; providing information for interviews

Tier I. The routine

Method: interviews

Purpose: answering the Research Question

Figure 1. A visual representation of the research design.

Thus, the 2-tier structure of the design would allow us to examine the formation of the representation level of the routine in the most suitable environment.

The structure of this design dictates the choice of research methods. Again, the unit of analysis in this study is the representation level of an organizational routine. This means that the unit of analysis is a person's understanding of his or her job. The only reasonable instrument of accessing this information is a *one-to-one interview.*

However, since the interview aims at discovering how an understanding was formed during a particular performance review meeting, one needs to know what took place during the meeting in order to ask meaningful questions. Therefore, it was deemed necessary to *observe the meeting* itself – as a means of deciding which questions to ask in the interview. E.g., if performance data were debated and a course of action was agreed upon, the subsequent interviews could ask why the participants persisted with their interpretation of the data or, alternatively, decided to change it.

Finally, the formation of the representations of any routine is a long-term process, which extends beyond a single performance review meeting. Therefore, in order to capture the time-related elements of this process, the design calls for observing several consecutive meetings, tracing the development of people's representation of their work routines over time.

The question currently facing the investigators is whether the 2-tier research design outlined above is, first, necessary to answer the research question, and second, too

complex to be executable. The discussion of these considerations constitutes the remainder of this paper.

Exploration/Description Dilemma

The design was created on the premise that a descriptive study is unsuitable for a doctoral research project. In other words, while a mere description of the process of forming representations

 Published by Cranfield University Press ISBN: 978-0-9557436-7-2 http://hdl.handle.net/1826/3832

of actions at the meetings would simplify the design substantially, it would not produce a sufficient contribution to knowledge if it were not explicitly linked to the existing body of knowledge. Writing about case study research, Yin (2003) contends that even when an inquiry is not driven by formal propositions, it should still have a clear purpose. Following his line of thought, we believe that this purpose is impossible to set without linking the inquiry to prior work in the field. In fact, it is this link to past research that separates valid exploratory research from non-scientific description of events.

Following the argument set out in the preceding paragraph, we have dealt with the exploration/description dilemma by ensuring that in answering the research question, every link in the chain of our argument was grounded in the existing evidence or theory. Thus, we explicitly adopted the organizational routines perspective on performance (i.e., performance is created through routines functioning on two levels) and linked it with the findings from the performance management literature (i.e., intensifying the iterations between action and reflection is one of the effects of performance management). Hence, we no longer asked the descriptive question of what takes place at performance review meetings; rather, we focused our inquiry on a particular element of the larger and more complex phenomenon of performance management. Thus, although we are still asking a *how* question, which suggests some exploratory implications, we have moved beyond the mere description of performance reviews and integrated it into the existing theoretical and empirical base.

Translating this reasoning into a practically executable research design, however, proved to be problematic. Although the theoretical links between the concepts are well defensible on paper, in practice they call for a multimethod research design, which is not easily executable with the standard research instruments. For instance, while the stimulating effect of performance reviews on individual understandings is

theoretically obvious, in practice it requires observing the reviews, developing the criteria for observing this effect, and interviewing individuals. Likewise, while the link between the representation and the action levels of routines is theoretically sound, focusing solely on the representation level of the routine makes interview questions difficult to design (e.g., what does one need to ask a maintenance crew member to ensure the answer is tightly linked to the actual actions he/she performs?).

Besides the difficulties with the accurate translation of constructs and structure into a practically executable shape, complex research design is also prone to trivial disruptions (e.g., availability of interviewees after the meeting) and requires deeper access to the participating companies, which is normally difficult to get.

Thus, although a complex research design solves the problem of avoiding a purely descriptive approach by thoroughly grounding the inquiry in the existing literature, it creates substantial difficulties with executing the research in practice. The questions which remain here are those of efficiency and plausibility – i.e., whether the same theoretical model can be translated into an

 Published by Cranfield University Press ISBN: 978-0-9557436-7-2 http://hdl.handle.net/1826/3832

executable design more easily and whether the scope of model itself is too large to be successfully executed in a single research study.

Exploration/Prescription dilemma

The discussion in the previous section suggests that the pursuit of theoretical rigour results in high complexity of the research design, which in turn makes the latter difficult to execute. This difficulty, however, is exacerbated by the nature of the research question. The exploratory *how* question driving this study assumes the lack of clear pre-established propositions which could be translated into concise interview questions. Tying the questions to the propositions available in the literature (i.e., examples of factors affecting the formation of the representation level of routines) would make the research design substantially simpler. However, given the low quantity and quality of these propositions, designing the instruments to look specifically for the corresponding evidence would mean constraining the research unjustifiably and artificially. In fact, the low level of theoretical development of the constructs in the field may warrant combining theory-testing and theory-building elements in the research design, perhaps using the existing propositions to start the exploration that will lead to the discovery of related or more sophisticated constructs.

Keeping the exploratory element in the research design, however, means that the study cannot be linear and easily predictable. Moreover, it imposes high demands on the researcher during data collection and analysis, as the emergent elements need to be instantly recognized as such and pursued further (*cf.* Yin, 2003). Finally, it means that the research protocol and instruments cannot be perfected in advance – they will need to change as the new data arrive and are interpreted. So far, we have dealt with this problem by ensuring a thorough understanding of the literature, so that any relevant leads are recognized and integrated with the appropriate theoretical base and methods, leading to a defensible contribution to knowledge.

Current challenges

At this point we are left with a promising and well-grounded in theory research project, whose execution, however, is slowed down by the combination of two major issues: the structural complexity of the research design and the open-ended nature of the research question. The questions that still remain are whether the complex research design proposed here is necessary for answering the research question and whether designing such a study is worthwhile in principle. Our current view of these issues is summarized in Table 1 .

Table 1. Current view of the research design issues.

Issue	Advantages	Design implications	Current solution
Grounding the Design in the Literature	Theoretical soundness; Valid claim to contribution.	Multilevel design; multiple methods; longitudunal research.	Running a small pre-pilot project. Flexible protocol.
Exploratory Research Question	Responds to the research gap; Does not rely on underdeveloped constructs.	Unpredictability: Demands on researcher; Constant reassessment of design.	Thorough knowledge of the core literature and related streams.

 Published by Cranfield University Press ISBN: 978-0-9557436-7-2 http://hdl.handle.net/1826/3832

We are optimistic about the successful completion of this research and we would welcome any comments about the design issues raised in this paper.

References are available upon request from the corresponding author.

 Published by Cranfield University Press ISBN: 978-0-9557436-7-2 http://hdl.handle.net/1826/3832

Literature Review of Research in Manufacturing Prognostics

K.M. Goh[1,2], B. Tjahjono[2], T. Baines[2], J. Ang[1,2]

[1]Singapore Institute of Manufacturing Technology, Manufacturing Execution and Control Group
[2]Cranfield University – School of Applied Sciences, Department of Manufacturing Systems

Abstract

With the fast changing global business landscape, manufacturing companies are facing increasing challenge to reduce cost of production and increase equipment utilisation and provide innovative products in order to compete countries which manufacturing can be more competitive due to low labour and production cost. One of the methods is zero or near zero downtime for manufacturing equipment. Unfortunately, current research and industrial solutions do not provide user friendly development environment to create "adaptive solution with microprocessor size and supercomputer performance" to reduce downtime. Most of the current solutions are PC based with off the shelf software tools which is inadequate for some of space constraint manufacturing environment. On the other hand, to develop difference solutions for various manufacturing domains will take too much time due to lack of rapid development tools. Therefore, this research is to understand the definitions, needs, trends, gaps of manufacturing prognostics and defines the research potential.

Keywords—maintenance, prognostics, condition based maintenance, prognostics health monitoring.

INTRODUCTION

Traditionally, the manufacturing plant performed the fail and fix maintenance procedures. Early detection of failures and prognostics in systems are very crucial for maintenance operations. With increasing trends towards automation in different manufacturing industries, it has become necessary that the downtime of any equipment system be reduced to minimum. Machine breakdowns are not only expensive in terms of production losses but also important in meeting production schedules. In addition, as a result of the fast growth of equipment size and complexity, there are an increasing number of system elements that need to be monitored at the sensors source. Intelligent devices are deployed so that problems can be identified at source.

With shorter product life cycles, companies need to have rapid products introduction and innovation. A lot of the prognostics related products will need to be embedded so that it will be smaller, more compact. Factories and equipment need to run twenty-four hours a day and seven days a week (24x7). Remote maintenance, diagnostics and prognostics services to achieve zero downtime become more important.

 Published by Cranfield University Press ISBN: 978-0-9557436-7-2 http://hdl.handle.net/1826/3832

DEFINITION

Manufacturing prognostics (or prognostics for manufacturing and engineering) have been interpreted by various researchers. Reference [5] defines prognostics as the ability to "predict and prevent" possible faults or system degradation before failures occur. If we can effectively predict the condition of machines and systems, maintenance actions can be taken ahead of time. As a result, minimum downtime can be achieved. Prognosis has been defined by [6] as "prediction of when a failure may occur" i.e. a means to calculate remaining useful life of an asset. In order to make a good and reliable prognosis it must have good and reliable diagnosis. Manufacturing prognostics are explained as tackling problems by predicting the occurrence of an event through analysing the trend of the data, preceding this particular event. Manufacturing prognostics improve the overall operations of manufacturing maintenance and provide for competitive advantages. Various connotations of manufacturing prognostics given by other researchers are illustrated in Table 1 below. It is clear that manufacturing prognostics have a significant role to play and needs critical attention.

TABLE 1: DEFINITIONS OF MANUFACTURING PROGNOSTICS

Authors	Connotations
Brotherton [1]	Ability to access the current health of a part for a fixed time horizon or predict the time to failure
Engel [3]	Capability to provide early detection of the precursor and/or incipient fault condition (very "small" fault) of a component, and to have the technology and means to manage and predict the progression of this fault condition to component failure
Katipamul, [4]	Address the use of automated methods to detect and diagnose degradation of physical system performance, anticipate future failures, and project the remaining life of physical systems in an acceptable operating state before faults or unacceptable degradations of performance occur
Lee [5]	Ability to "predict and prevent" possible faults or system degradation before failures occur
Lewis [6]	Prediction of when a failure may occur. To calculate remaining useful life of an asset
Smith [7]	The capability to provide early detection and isolation of precursor and/or incipient fault condition to a component or sub-element failure condition, and to have the technology and means to manage and predict the progression of this fault condition to component failure
Su [8]	The identification of incipient faults, is usually considered and treated as a component/part problem rather than a system problem

RESEARCH EXECUTION

This section identifies relevant literature, and then classifying literature in different schemes.

The classification of manufacturing prognostics is explained by distribution in journals, origin of research and research focus respectively.

Distribution of papers in journals

Numerous articles dealing with the theory and practice of manufacturing prognostics have been published in various journals. A total of 175 papers have been reviewed. The top two journals that have more focus on manufacturing prognostics are Journal of Quality in Maintenance Engineering (12%) and International Society for Optical Engineering (8%). Two conferences that have more focus in the area are Aerospace conference (16%) and Automatic testing conference (7.4%).

 Published by Cranfield University Press ISBN: 978-0-9557436-7-2 http://hdl.handle.net/1826/3832

Approach and methodology

In this part, all papers are classified by origin of research: approach and methodology. The approach is categorised into content and process aspects as shown in table 2. Content-related literature addresses issues of manufacturing prognostics context. The content of manufacturing prognostics refers to the choices and actions. Process- related literature addresses issues on how to form manufacturing prognostics; therefore, process aspects include models, framework and architectures. Basically, the focus of the literature is on either on content or on the process of manufacturing prognostics.

TABLE 2: APPROACH OF RESEARCH

Focus on	Number of papers	Percentage
Content	133	76
Process	42	24
Total	**175**	**100**

The research methodologies used are divided into five categories which are conceptual, descriptive, empirical, exploratory cross-sectional and exploratory longitudinal. Explanation of the above categories is as follows [2].

- Conceptual: Basic and fundamental concepts of manufacturing prognostics.
- Descriptive: Explanation or description of manufacturing prognostics content or process.
- Empirical: Data for study have been taken from existing database, review, case study, taxonomy or typological approach.
- Exploratory cross-sectional: Objective of study is to become more familiar through survey, in which information is collected at one point in time.
- Exploratory longitudinal: Survey methodology where data collection is done at two or more points over time in the same organisation.

Table 3 shows the distribution of various methodologies used by researchers. Among the methodologies, empirical methodology seems to be the most interested methodology.

TABLE 3: DISTRIBUTION OF VARIOUS METHODOLOGIES

Methodology	Number of papers	Percentage
Descriptive	78	45
Empirical	70	40
Exploratory Cross-sectional	18	10
Conceptual	07	04
Exploratory longitudinal	02	01
Total	**175**	**100**

3) Industrial adaptation: In table 4, all articles are classified according to their industrial adaptations based on the various manufacturing methods followed by the industries such as Artificial Neural Networks, Expert systems, Algorithms, Architectures, Embedded systems, Knowledge Base Systems.

 Published by Cranfield University Press ISBN: 978-0-9557436-7-2 http://hdl.handle.net/1826/3832

TABLE 4: CLASSIFICATION BY INDUSTRIAL ADAPTATION

Industries	Neural Networks	Expert systems	Fuzzy Systems	Embedded systems	Algorithm	Knowledge base systems	Software program	Architecture	Total	%
Mechanical systems	23	13	8	6	11	6	2	3	72	**41**
Electrical Systems	15	9	8	5	4	5	0	0	46	**26**
Industrial Enterprises	12	4	5	1	2	3	2	2	31	**18**
Construction	2	0	1	2	0	2	0	0	7	**4**
Logistics	5	2	1	2	2	3	1	0	16	**9**
Medical	2	1	0	0	0	0	0	0	3	**2**
Total (T)	**59**	**29**	**23**	**16**	**19**	**19**	**5**	**5**	**175**	**100**
Percentage (%)	**34**	**17**	**13**	**9**	**11**	**11**	**3**	**3**	**100**	

SWOT Analysis

SWOT (Strengths, Weakness, Opportunities, and Threats) analysis helps to understand factors that have greatest actual and potential importance for the research works. Table 5 shows the summary of the analysis.

Strengths: From the classification of journals, the strength of previous research can be observed. Firstly, the previous work focused on content related literature (76%) rather than process related literature (24%). Hence, the previous research tends to have strengths on manufacturing prognostics context over planning, developing and implementing the prognostics methods. Secondly, the most popular methodology in the manufacturing prognostics research is descriptive (45%) and empirical (40%) methodology. Many researchers explored various intelligent methods to convert raw data into useful information. Some researchers have applied their research to various industrial applications together with other domain experts. Manufacturing maintenance approaches and implementation of prognostics technique attracted multi-discipline expertise teams in the arena. Hence, the research in manufacturing prognostics are considered to be stronger in the algorithms development rather than in framework and architecture in the aspect of prognostics method research.

Weaknesses: Much of the existing literature treats the key industrial application independently and is lacking holistic approach to problems. Many researchers used PC based research tools like simulation, Labview, Matlab and PC based prototyping solutions. The research algorithms assume unlimited resources and processing power which might be unrealistic for space constraint environment like manufacturing. Most of the research results are in the form of algorithms and will have a long learning curve and long implementation time for real industrial solution. Most of previous research focused on the content based rather than process based therefore practitioners find it difficult to implement the concepts. Moreover, there is a lack of research in rapid development environment, real time prognostics and collaborative prognostics which handling of multiple failures. Much research needs to validate more in terms of real practice. Some approaches could be difficult to implement for all the technologies such as condition based maintenance and fuzzy approaches.

Although a wide spread expectation of manufacturing prognostics research, rapid development and real time prognostics at sensor was not yet developed completely. In case of remote diagnostics, adaptive diagnostic

 Published by Cranfield University Press ISBN: 978-0-9557436-7-2 http://hdl.handle.net/1826/3832

analysis toolset is not there to assist real time diagnostic process. Furthermore, the guidance to sustain the development of a standard solution to the prognostics has not been pointed out clearly.

Opportunities: The weakness of the research creates opportunities in future work. The opportunities are mainly in considering holistic framework for modelling, rapid development methodologies and real time prognostics at sensors source is important for manufacturing prognostics. Considering prognostics in aspects of hardware systems, processing sensors data at source with adaptive embedded devices or system on chip is important techniques that can help to send alert at sensors source. There are needs for process-based research in order to guide the manufacturers and practitioners to model, plan, develop and implement the concepts or frameworks in real world manufacturing environment.

The integration of the predictive maintenance strategy with the other business strategies opens new business opportunities to achieve the sustainable competitive space. Prognostics services could be remote services through the internet and is a useful feature for many other systems. Research areas such as remote condition based maintenance (CBM), remote health and usage monitoring (HUM), and real time partitioning of algorithms for the embedded prognostics device can be studied in detail.

Threats: The holistic view in manufacturing prognostics take time and need several aspects to consider. Generally, each and every method in manufacturing prognostics has its own focus industrial domains. In order to achieve the overall pictures of prognostics, the conflicts interests in each method must be concerned carefully. The study in extracting generic principles and parameters that applied to most prognostics is difficult. Multiple expertises are required in order to have a successful outcome.

Additionally, there is an increase in complexity of manufacturing prognostics demand with more sophisticated algorithms, hardware and software. In order to deploy manufacturing prognostics in variety of real industrial environment, researchers need support from many sources like domain experts, cross disciple researchers, manufacturers. Some of the existing system may be a closed system or legacy system with limited information to add more sensors or enhance it with prognostics features. These will make it difficult for the solution to test or implement. Some research on prognostics might still stay in algorithms development, PC based solution and simulation are often made less overall impact and so their competitiveness can be significantly eroded.

The dynamic of the failure occurrence in the manufacturing prognostics make it difficult for researchers to capture all scenarios in their research, and so it is very difficult for them to make a standard solution for multiple failure occurrences. The competitive space in manufacturing prognostics is also dynamic. It will continue to change as more cross discipline expertises join the research arena. The validity and usability of the techniques or tools must be proved carefully.

 Published by Cranfield University Press ISBN: 978-0-9557436-7-2 http://hdl.handle.net/1826/3832

CONCLUSION AND FUTURE RESEARCH

Findings from the survey of 175 research papers related to manufacturing prognostics have suggested that there are a lot of interests and potential industrial applications in this area of research. Many researchers focus on specific solution for some domains using PC based simulation, Labview and Matlab. Manufacturing prognostics can be a new maintenance service opportunity which can reduce cost of production, increase equipment utilisation and provide innovative prognostics enhancement products in order to compete with countries with low labour cost and production cost. Holistic approach, common methodology, real-time prognostics devices, real time partitioning of algorithms, and rapid implementation environment are potential future research.

REFERENCES (Note: Full list of References and summary of references is available upon request)

1. Brotherton T. et al, (2002). 'A testbed for data fusion for engine diagnostics and prognostics', Proceedings of the 2002 IEEE Aerospace Conference, Big Sky MT.
2. Dangayach G.S., Deshmukh, S.G., (2001). 'Manufacturing Strategy: Literature Review and Some Issues', International Journal of Operations and Production Management 21(7): 884-932.
3. Engel S.J., Gilmartin B.J., Bongort K., Hess A., (2000). 'Prognostics, the real issues involved with predicting life remaining', Aerospace Conference Proceedings, IEEE Vol. 6, pp 457 – 469.
4. Katipamula S., Brambley, (2005). 'Methods for Fault Detection, Diagnostics', Prognostics for Building Systems— A Review, Part I, VOLUME 11, NUMBER 1, Journal of HVAC&R Research.
5. Lee J., (2004). 'Smart products and service systems for e-business transformation', 3e Conférence Francophone de MOdélisation et SIMulation « Conception, Analyse et Gestion des Systèmes Industriels » MOSIM'01 – du 25 au 27 avril - Troyes (France).
6. Lewis, SA; Edwards, TG; (1997). 'Smart sensors and system health management tools for avionics and mechanical systems', Digital Avionics Systems Conference.
7. Smith A. E., Coit D. W., Liang Y. C., (2003). 'A Neural Network Approach to Condition Based Maintenance: Case Study of Airport Ground Transportation Vehicles', IMA Journal of Management Mathematics on Maintenance, Replacement and Reliability, April 2003.
8. Su L.P., Nolan M., DeMare G., Carey D.R., (1999). 'Prognostic framework', AUTOTESTCON '99. IEEE Systems Readiness Technology Conference, pp 661 – 672.

 Published by Cranfield University Press ISBN: 978-0-9557436-7-2 http://hdl.handle.net/1826/3832

Development of an ultra precision grinding capability for large optics

X.Tonnellier[1], P. Shore[2], P.Morantz[2], D.Orton[1]

1 Ultra Precision and Structured Surfaces (UPS[2]) Lab, Optic Technium

[2]Precision Engineering Centre, School of Applied Sciences, Cranfield University

Abstract

A new ultra precision large optics grinding machine, BoX®, has been designed, developed and commissioned at Cranfield University. It is now located at the UK's Ultra Precision and Structured Surfaces (UPS[2]) laboratory at the OpTIC Technium (North Wales). BoX® provides a rapid surface form generation capability for large optics of up to 2 metres diameter. This machine offers a rapid and economic solution for grinding large off-axis aspherical and free-form optical components.

This paper presents an analysis of optical ground parts, produced using diamond resin bonded wheels. These results are compared with the targeted form accuracy of 1 μm p-v over a 1 metre part, surface roughness of 50-150 nm RMS and subsurface damage in the range of 2-5 µm are targeted.

Introduction

In the manufacturing of large optics, glass and ceramics have been employed for many years for their optical properties as well as their low thermal expansion coefficient. In Germany and in Russia, for example, Zeiss and LZOS, have produced and machined Astrositall hexagonal segments for the Southern African Large Telescope primary mirror [1]. In France, Reosc-Sagem, used Zerodur® to make the hexagonal segments of 1. 87m for the Gran Telescopio Canarias primary mirror [2].

Currently, a number of projects are studying the possibility of making the next generation of European Extra Large Telescope. Many follow the Keck hexagonal segmented mirror scheme. The segments are expected to be in the size range 1-2.5 metres [3] in glass, glass ceramic, ceramic or Beryllium. Sagem and Kodak have reported manufacturing process concepts for making >1 metre hexagonal mirrors. [4] The blank is progressively ground to reach the desired shape. Then, the mirror is lapped and polished to get the correct form geometry and to remove any damage induced by previous machining process.

 Published by Cranfield University Press ISBN: 978-0-9557436-7-2 http://hdl.handle.net/1826/3832

A possible production improvement is to achieve a grinding process that is capable of producing better shaped surfaces having less subsurface damage and at higher material removal rates. To achieve this production capability, Cranfield University Precision Engineering Centre developed a new ultra precision large optics grinder [5] - BoX®. This machine is located in the Ultra Precision and Structured Surfaces (UPS) laboratory, in Technium OpTIC, St Asaph, North Wales [6].

Box ® grinding machine

The BoX® machine (Figure 1) is a 3 axis grinding machine. A vertically arranged Z linear axis sub-system carries a fixed inclination grinding spindle. The Z axis subsystem itself is mounted within a horizontal X linear axis carriage. Beneath, and mounted directly into the machine base, a large rotary C axis table is employed to hold the workpiece.

Figure 1: BoX® 3 axis grinding machine

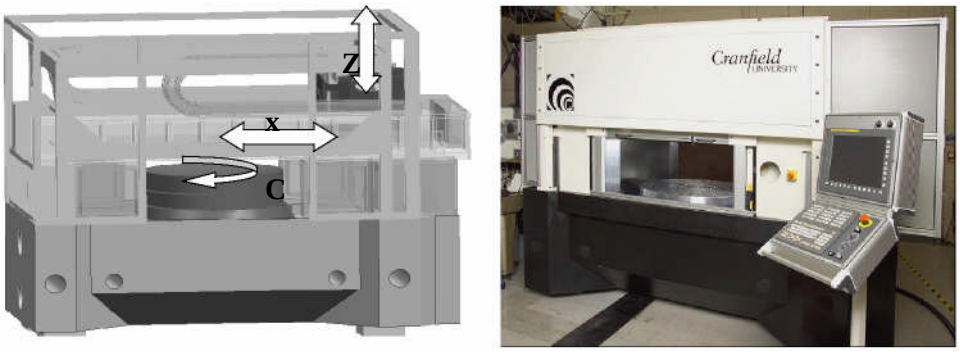

The BoX® has been designed to have high static (> 100N/μm) and high dynamic loop stiffness (low moving mass <750 kg with high 1st resonant frequencies> 100 Hz). With these characteristics and an in situ measurement profilometer, employing a 'non-stressed' metrology frame, a form accuracy of 1 μm peak to valley is obtainable with minimal levels of induced sub-surface damage. In addition the hydrostatic oil bearing grinding spindle has a 10kW power capacity permitting a high material removal rate of 200mm^3/s to be achieved.

 Published by Cranfield University Press ISBN: 978-0-9557436-7-2 http://hdl.handle.net/1826/3832

Experimental design

Materials

Two materials, ULE® and Zerodur®, have been studied in this work. They were chosen due to their previously successful uses in the built of large optics.

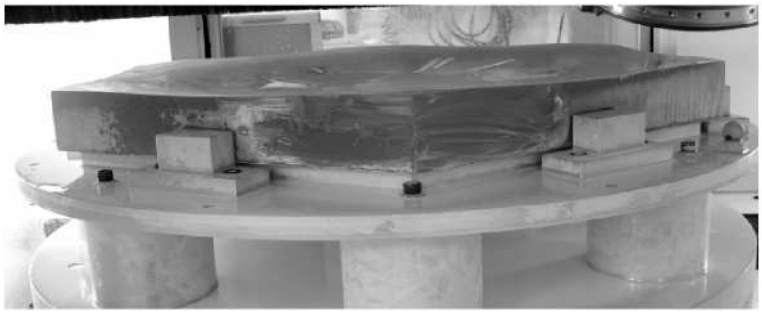

Figure 2: 1m Zerodur® ground part on BoX®

Both have low thermal expansion coefficient. ULE® (Ultra Low Expansion) is a glass material produced by Corning. Zerodur® is a glass ceramic material made by Schott. The specimens' size was 100 mm x 100 mm and 20 mm thick.

Grinding parameters

For these grinding tests, diamond resin bonded wheels are used. Table 1 shows the grinding parameters employed for the tests carried out. The parameters controlled are the depth of cut (ae), the feed per revolution (fr) and the surface speed (vw). The material removal rate (Qw) was also calculated.

Experiment	a_e (µm)	f_r (mm/step)	v_w (mm/s)	Q_w (mm^3/s)	Grit size (µm)
Finish cut	50	1.5	25	1.9	25
Finish cut	50	1.5	25	1.9	46
Semi finish cut	200	10	20	40	46
Rough cut	500	15	25	187.5	76

Table 1: Grinding parameters

The rough cut removes the bulk material. A semi finish cut eliminates the amount of damages induced by the rough grinding. The first finish cut takes out the previous grinding damage. Finally, the final cut creates the final surface roughness value and level of subsurface damage.

 Published by Cranfield University Press ISBN: 978-0-9557436-7-2 http://hdl.handle.net/1826/3832

Grinding mode

The grinding mode used in these tests (Figure 3) corresponds to the BoX® grinding mode [7].

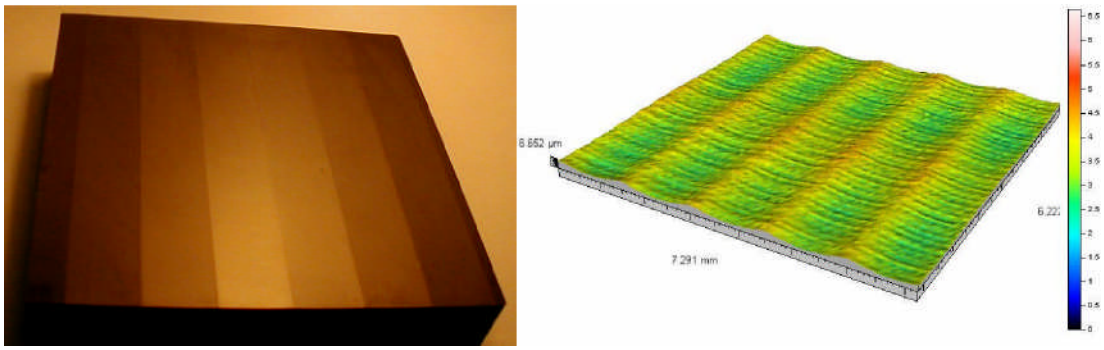

Figure 3: Grinding mode example (Rough cut parameters)

This type of grinding mode has previously been described in the use of the Large Optical Generator [8] as well as the grinding of aspherical optical components [9].

Experimental results

Surface geometry and subsurface damage results

The surface profile (P_t) and the surface roughness (R_a) were measured perpendicular to the grinding direction and along the grinding direction, respectively. The subsurface damages (SSD) were measured using a wedge technique. [11] The results are reported in Table 2.

Experiment	R_a (nm)		P_t (actual) (µm)		SSD (µm)	
	Zerodur	*ULE*	*Zerodur*	*ULE*	*Zerodur*	*ULE*
Finish cut(D25)	247	191	1.79	1.64	4	8
Finish cut (D46)	248	172	1.90	2.35	11	10
Semi finish cut (D46)	186	186	33	33	9	8
Rough cut(D76)	394	303	72	73	8	19

Table 2: Surface roughness and SDD data results

The P_t values are expected to be ~1 μm for the finish cut parameters. Actual results show good correlation with theoretical values calculated from geometrically defined equations [10]. However, the profile value difference is noticeably influenced by the machine repositioning errors between subsequent passes and the resin layer profile of the wheel.

The roughness values (R_a) on ULE® are significantly smaller than for Zerodur®. The finish cuts roughnesses are not influenced significantly by the wheel grit size. The finish and rough cuts

 Published by Cranfield University Press ISBN: 978-0-9557436-7-2 http://hdl.handle.net/1826/3832

leave SSD levels twice higher for ULE® than Zerodur®. However, the SSD in both materials, due to the finish and semi finish cuts, using the D46 wheel, reach similar levels (8-11 μm).

Process development results

The results highlight the strong possibility for a total grinding process, removing a 1mm depth from a 1 metre scale part, achieving a final accuracy of $P_t < 1$ μm, $R_a < 150$nm and SSD $< 5\mu$m within a 10 hour processing time. Within this cycle, each processing cut remove the previous process induced damage. The final finishing cut presently induces SSD at 4– 8 μm depending on material used.

Conclusions

The purpose of this research is to reduce to a minimum the required time for any subsequent polishing process. A high material removal rate of 1 87.5mm^3/s has been demonstrated using resin bonded diamond wheels. Achieved surface roughness levels using a finer grit wheel (D25) during finish cuts were 191-247 nm. The levels of subsurface damage during the finish cut are 4-8 μm. Those parameters are currently been used for the machining of a 1m Zerodur® part with a 3m radius of curvature using those parameters. This will validate the process on a larger scale.

The number of defects apparent at different depths beneath the surface is a combined function of 'process' related and 'machine dynamics' related damage. [11] Additional work will be carried out in order to develop a model relating subsurface damage to both 'process' related and 'machine dynamics' related issues.

Acknowledgements

The authors would like to acknowledge project funding through the UK's Joint Research Councils' Basic Technologies programme and funding support from the McKeown Precision Engineering and Nanotechnology Foundation at Cranfield.

 Published by Cranfield University Press ISBN: 978-0-9557436-7-2 http://hdl.handle.net/1826/3832

References

1. A.P. Semenov, M.A. Abdulkadyrov, A.N. Ignatov, V.E. Patrikeev, V.V. Pridnya, A.V. Polyanchikov and Y.A. Sharov: Proc. of SPIE, Vol.5494 (2004), p.31.
2. R. Geyl, M. Cayrel and M. Tarreau: Proc. of SPIE, Vol.5494 (2004), p.340.
3. R. Gilmozzi: Proc. of SPIE, Vol.5489 (2004), p.1.
4. P. Shore and R. May-Miller: International Workshop on EOS (2003).
5. P. Shore, P. Morantz, X. Luo, X. Tonnellier, R. Read and R. May-Miller: Proc. of Lamdamap Conference (2005), p.200.
6. www.ups2.co.uk (Accessed 28/02/08)
7. P. Shore, P. Morantz, X. Luo, X. Tonnellier, R. Collins, A. Roberts, R. May-Miller and R. Read: Proc. of SPIE, Vol.5965 (2005), p. 241.
8. R.E. Parks: Proc. of ASPE 2004 Winter Topical Meeting (2004), p.88.
9. T. Kuriyagawa, M.S.S. Zahmaty and K. Syoji: J. of Mat. Proc. Tech., Vol.62 (1996), No4, p.387.
10. C.F. Cheung and W.B. Lee: Proc. of the I MECH E Part B, Vol.2 14 (2000), No6, p.463.
11. [11] X. Tonnellier, P. Shore, X. Luo, P. Morantz, A. Baldwin, R. Evans and D. Walker: Proc. of SPIE (2006), Vol.6273, p. 627308.

 Published by Cranfield University Press ISBN: 978-0-9557436-7-2 http://hdl.handle.net/1826/3832

Aviation Maintenance Monitoring Process: An innovative application of the HERMES methodology

H S J Rashid. C S Place, G Braithwaite
Air Transport Dpt, School of Engineering, Cranfield University

Abstract

Aviation maintenance errors cause 13% to 23% of the global aviation incidents and accidents initiators. This necessitates a wider global improvement of aviation maintenance safety. In this research the impact of human reliability on aviation maintenance safety is investigated to conceptualize the accumulation of crucial human errors causal factors within aviation maintenance organizations. By adopting a new hypothesis, a proactive Aviation Maintenance Monitoring Process (AMMP) is introduced. AMMP is a holistic hybrid process that can be simultaneously and collectively implemented by main industry stakeholders. The aim is to monitor proactively the existence of human error causal factors within the maintenance process in order to reduce the rate of occurrence. This paper presents the Human Error Risk Management in Engineering Systems (HERMES) methodology adopted by the current research. The aspects associated with the research context, study design, methodology selection, methodology application challenges, and learned outcomes were thoroughly discussed.

Keywords

Research design, Research methodologies, Aviation maintenance, Human / machine interaction, Human error management, Proactive monitoring.

INTRODUCTION

Human Factors Influence on Aviation Maintenance and Safety.

The number of fatalities in helicopter accidents for normal and off-shore transportation is 10.6 times that of commercial airlines per million hours of flight. This is a clear indication of the high severity of helicopter accidents outcomes. It is also found that 31% of these helicopter accidents probable causes were technical [1, 2] . A significant proportion of the technical causes of helicopter accidents and serious incidents is in fact attributed to human factors- related errors in various levels within the maintenance organizations. It is generally accepted that maintenance, as a potential environment for critical interaction between humans and machines, attracts a large proportion of human factors induced problems. Further, helicopter maintenance errors acquire higher criticality due to naturally associated rotorcraft characteristics, some of these being the single load path regarding the transmission and rotor systems, limited envelope of emergency manoeuvres, and high vulnerability[3] to impact

PROBLEM CONTEXT AND RESEARCH GAP

The most obvious common response to a human error is to identify its causal mechanisms and alter the system such that that error is not repeated[4]. For aviation maintenance, tools to handle such mechanisms included maintenance resources management, duplicate inspections schemes, various reporting systems, multiple over-sight groups, and many others, but nevertheless, the issue still requires more

 Published by Cranfield University Press ISBN: 978-0-9557436-7-2 http://hdl.handle.net/1826/3832

focusing[5]. In fact, there is a general industrial tendency to start a shift towards 'proactive safety' after the long saturated treatment of reactive accidents and incident investigations and the expected safety recommendations that usually follow. Further, In contrast to helicopters, many studies in the maintenance error causation were already carried out for the commercial fixed wing aviation. This research work was launched to address these gaps building on a hypothesis that '*Human factors errors within aviation maintenance industry can be more effectively managed by applying new error – proactive monitoring and early detecting techniques at both organizational and individual levels''*

In this paper, the main aspects of the research applied methodology are highlighted as an in-built part within the overall conceptualization of the advocated research itself. This is coupled with brief presentation of salient results and contribution features.

STUDY DESIGN

Research Front End Activities

The research design activities were started by acquiring the basic know-how of successful sociotechnical research implementation This was achieved through methodical digestion of relevant literature, experts consultation, as well as close interaction with industry. Then an inter-connected sequence of practices was conducted to set the main design of the proposed study. This sequence, as illustrated by Figure 1, included a main enlarged literature review for further familiarisation with subject field, appreciation of current knowledge stock, and scanning for viable research gaps. The importance, relevance, rigorousness, and innovativeness chances associated with the spotted research gaps were verified to demonstrate high levels of required research scholarship and methodological excellence. The main theoretical hypothesis was then set, followed by research aim and objectives.

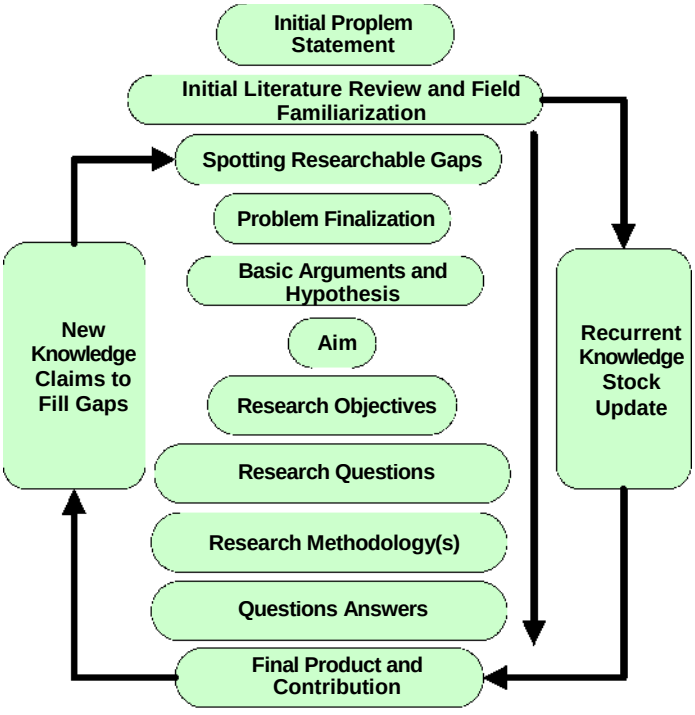

Figure 1. Research Study Design Sequence

These objectives were then resolved through careful scientific interpretation into research questions. Main features and capabilities of the methodology required to answer these questions were then determined.

The evolved aim of this research is to introduce a holistic integrated Aviation Maintenance Monitoring Process (AMMP) that can be utilized collectively by operators, regulators and aircraft manufacturers to monitor and early detect potential existence of errors

 Published by Cranfield University Press ISBN: 978-0-9557436-7-2 http://hdl.handle.net/1826/3832

causal factors associated with human factors during maintenance. The process, comprising multiple strands, is to be practically applied and refined within industry.

METHODOLOGY SELECTION AND ADAPTATION

The adopted research methodology is known as Human Error Risk Management in Engineering Systems (HERMES), given by Cacciabue (2004)[6,7] for the Human / Machine Interaction (HMI) analysis within complex contexts. HERMES encompasses a complex mosaic of human factors analysis and modeling techniques. The selection of HERMES for this research can be justified by accrediting its resourceful characteristics. Some of these are:

I. HERMES is a generic framework with applications in the fields of accident/ incident investigation, human factors training; human factors design enhancement, and safety assessment of complex engineering systems.

II. It is a hybrid methodology firmly joining theoretical concepts with practical implementation. It has already been successfully applied in variety of industries such as aviation and rail.

III. The ability to correlate retrospective and prospective types of studies in a logical analytical process that can support the considerations of sound HMI approaches.

IV. The smooth association between persistent HMI analysis and system safety and integrity. v. Flexibility in selecting sub-techniques and particular HMI tools within the generic HERMES layout to satisfy specific progressive tactical targets.

Major modifications have been applied to the original methodology in order to exactly serve purposes of this research while being loyal to the main HERMES philosophy stream. The detailed adopted methodology of the research is illustrated through Figure 2.

HERMES APPLICATION AND OBTAINED RESULTS

Fundamental Studies

The front end studies comprised a sophisticated literature review that focused knowledge of the field, and critically evaluated the previous contributions. Then a socio-technical evaluation of the helicopter maintenance context was performed through detailed ethnographic studies based on observation, meetings, interviews, and visits to regulators, operators, manufacturers, and research centres. Maintainer task analysis was then performed. In a parallel line, a theoretical and conceptual knowledge base of the HMI systems and human behaviour taxonomies was built. By the end of this stage, the research problem was crystallized, consequently the research orientation was set and the associated research aim, objectives, and questions were furnished. HERMES methodology was then selected as the work's core structure.

 Published by Cranfield University Press ISBN: 978-0-9557436-7-2 http://hdl.handle.net/1826/3832

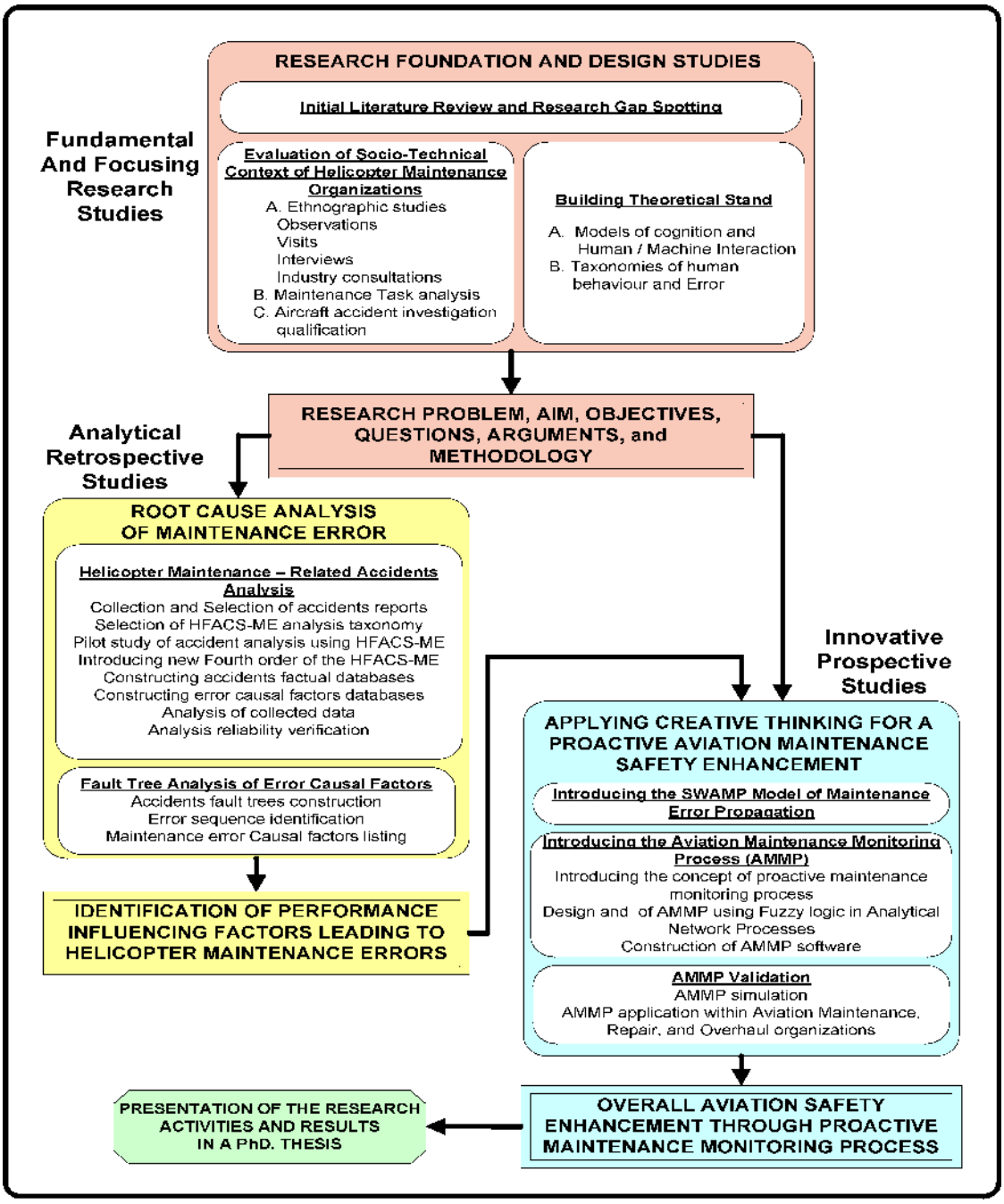

Figure 2. Research Applied Methodology Structure Based on the HERMES Methodology

RETROSPECTIVE BACKWARD STUDIES

For main data collection, a number of 804 of helicopter safety occurrences were carefully scanned. Out of these, a sample comprising 58 of maintenance-induced fatal accidents and severe incidents was then thoroughly analysed using Human Factors Accident Classification System – Maintenance Extension (HFACS-ME) taxonomy[8]. Human error causal factors were first identified through the well established three classification orders of the taxonomy. Then for further enriched details, a new more sophisticated fourth order of causal factors classification was brainstormed and introduced to raise the analysis resolution from 34 categories at the established third order to a total number of 197 new fourth order categories which are coded, being a new contribution, as specific failures (SF's). Inter-rater reliability of 0.766 Cohen

Kappa and 94.77% Percentage of Agreement were obtained. A further emphasis was given by applying Fault Tree Analysis (FTA) and Hierarchal Task Analysis (HTA) to identify probable mechanisms of helicopter maintenance errors. The end of this stage represented a major milestone by the identification of

 Published by Cranfield University Press ISBN: 978-0-9557436-7-2 http://hdl.handle.net/1826/3832

maintenance Performance Influencing Factors (PIF's). PIF's are the factors and performance sequences leading to human maintenance errors.

PROSPECTIVE FORWARD STUDIES

Using the outcomes of the backward research, a creative thinking process was conducted to set pace for the targeted maintenance proactive monitoring process. This was triggered by introducing 'The Swamp'; a new human error model that explains the sequence and propagation of safety-related human errors through the behaviour of aircraft maintainer, supervisor, crew or other associated personnel. As a direct means to apply this 'Swamp' theory, the main AMMP project layout was introduced after a series of successive developments.

The AMMP- as a holistic process- is a framework designed to join safety-oriented integrated activities within regulators, manufacturers, and most importantly, aircraft maintenance organisations. This collective process is to systematically collect maintenance performance safety-related raw data, analyse them and then design and apply any required new measures or modify those already in place such that any relative cited error causal factors can be proactively eliminated or at least positively treated.

CHALLENGES TO HERMES APPLICATION

The application of HERMES in this research was faced by many challenges; the earliest of those was the need to modify the original methodology layout in order to accommodate the present research requirements. This was first suggested by the authors and then approved by Cacciabue, the HERMES initiator, and his team at the European Union's Joined Research Centre-Italy. This modification consequently gave rise to a new challenge to the adapted methodology being the first to be thus implemented. Another difficulty was in-built within the methodology itself; in fact, HERMES is a multi-teamwork-oriented protocol due to its well branched and diverse activities that need to be simultaneously addressed, thus it proved out to be very challenging for a limited number of researchers to cope. The most critical conundrum that faced the application of this methodology broke out at the phase of data collection. It was very difficult to get formal helicopter accidents reports that are written with satisfactorily reflection to human factors issues, consequently only 58 reports could be used for data analysis out of a total number of 804. The wide spectrum and diversity of HERMES sub-components necessitated serious upgrading and enrichments to the researchers' abilities and know-how such that those sub-components may be satisfactorily handled, for instance, a formal accident investigation qualification was obtained first in order to better understand accidents occurrence mechanisms

and accident reports writing and analysis. A tactical problem faced the execution of the inter-rater reliability for the analysed reports. It was critically suppressing to allocate experienced coworkers with approved qualification in the yet new HFAC S-ME taxonomy and associated report coding and analysis. However, as for the research remaining stages, a major expected future challenge will be the ability of selected aviation maintenance organizations to allocate the necessary provisions within their daily activities and staff workforce to practically apply the designed AMMP in the course of its verification within industry.

 Published by Cranfield University Press ISBN: 978-0-9557436-7-2 http://hdl.handle.net/1826/3832

DISCUSSION

HERMES is a much systematized methodology that provides strategic as well as tactical guidelines for a smooth flow of research sequential activities. The methodology is totally generic to accommodate different requirements of HMI treatment within safety-critical engineering systems. It has already been adopted and applied within various industries where it showed high rates of reliability. The current research, by adopting a modified version of HERMES, is ambitious to make the best out of its characteristics to address human error as seen in helicopter maintenance context; this will be of significant benefits for aviation safety in general. On the other hand, a sound application of HERMES is hoped to give provision for the academic requirements of a PhD study to evolve, those undoubtedly encompass scientific scholarship, methodology practicalities, and a substantive contribution to the field knowledge pool.

Each of the afore-discussed challenges and the ways they were tackled represents an indispensable learning opportunity; the flexibility of HMI models selection and application, the limited number of co-workers, the desperate data hunt, the required analysis reliability affordability, and the innovative introduction of additional analytical tools.

References

1. Shell Aircraft International, Formal annual overview report, UK, 2005
2. Atkinson, B. and Irving, P. E. An Analysis of Accidents Involving UK Civil Registered Helicopters during the Period 1976 - 1993. CAA/913 V/14. 95. UK, CAA - UK..
3. Hessmer Jwe. , 'Helisafe- EU Research into Occupant Safety in Helicopter Crashes', *Journal of 'Air and Space Europe', Vol 3, No 3/4, 2001, from 225 to 228.*
4. Latorella, K.A. and Prabhu, P.V. (2000) A review of human error in aviation maintenance and inspection. *International Journal of industrial ergonomics Vol 26 from 133 to 161,* Elsevier Science Ltd.
5. Hobbs, Allan and Robertson, Michelle M. Human factors in aircraft maintenance. Hayward, Brent J. and Lowe, Andrew R. Third Australian aviation psychology symposium. 484. 96. Aldershot, UK, Ashgate
6. Cacciabue, Pietro Carlo. Guide to applying Human Factors Methods - Human Error and accident management in Safety Critical Systems. 2004. London, Springer - Verlag
7. Cacciabue, Pietro Carlo Human error risk management for engineering systems: a methodology for design, safety assessment, accident investigation, and training. *Journal of reliability engineering and system safety, No 83, 2004, from 229 to 240.*
8. Naval Safety Centre, USA. Aviation Maintenance Human Factors Accident Analysis. 3. Washington, DC, Naval Safety Centre - Naval Postgraduate School.

 Published by Cranfield University Press ISBN: 978-0-9557436-7-2 http://hdl.handle.net/1826/3832

The Broad Delta Aircraft-Part 2; Silent Propulsion Systems Design Methodology

Georgios Doulgeris, Sunil Mistry, Pericle Pilidis

ABSTRACT

This paper describes the impact of noise on the civil aircraft design process. The challenge to design 'silent' aircraft is the development of efficient airframe-engine technologies, for which integration is essential to produce an optimum aircraft, otherwise penalties such as higher fuel consumption, and, or noise are a concern. A methodology for preliminary engine design for low noise (suitable for the Broad Delta Aircraft) has been developed. It investigates the noise and SFC gains by varying the main cycle design parameters. In this scope, an ultra-high BPR turbofan is designed and compared to a baseline engine in terms of noise and fuel consumption.

INTRODUCTION

Aviation has been targeted as one of the noisiest and greatest polluters in the transport sector [1], leading to noise and green taxes, for which noise is mainly related to proximity of airports to residential areas [2] . The growth of aviation has made matters worse as increased flight frequency is a direct result of surges in passengers wishing to travel [3]; leading to expansion of existing airport facilities, such as London Heathrow terminal 5. More passengers and aircraft would increase flight frequency, hence, more community noise complaints.

Extended research on propulsion noise reduction has been undertaken by NASA [4,5,6,7] . It has underlined the importance of ultra high bypass ratios and subsonic fan design. More recent is the SAI low noise engine design, utilizing several innovative technologies on an ultra high BPR turbofan; some of which include: use of advanced acoustic liners [8], variable nozzle area for subsonic fan performance during take-off and landing [9,10] , one core driving three geared fans, embedded installation [11], and boundary layer ingestion [12] . Cranfield's approach on preliminary low noise engine design is to investigate a variation of thermodynamic cycles, other than the classic Brayton cycle.

 Published by Cranfield University Press ISBN: 978-0-9557436-7-2 http://hdl.handle.net/1826/3832

ENGINE CYCLE DESIGN

Cycle design incorporates a parametric analysis followed by an objective function, used to select the optimum cycle, as shown by the methodology overview in

Figure 1.

Parametric analysis is performed for varying By-Pass Ratio (BPR), Turbine Entry Temperature (TET) and Overall Pressure Ratio (OPR) over a range, as shown in Figure 2. These limits are set by the designer in order to take into consideration future technology limitations. Parametric methodology includes Fan Pressure Ratio (FPR) optimisation at design point, followed by sizing of the engine in order to satisfy the thrust requirement. Off design calculation provides the data for noise calculation, geometry, and performance data are derived from design point analysis.

Tools that were used are Turbomatch; a Cranfield gas turbine performance code, and a tool including various noise prediction methods [13] . Turbomatch is based on mass and energy balance, carried out through an iterative method based on component maps. It has been validated against commercially sensitive data and further details can be found in [14,15] . The validation of the noise code is discussed within Santos [13] . The coaxial jet noise prediction routine is based on experimental results. A limitation is the ratio of bypass and core nozzle areas, which can not exceed the value of 8. For that reason, during the parametric study the cycle parameters were chosen to satisfy that condition. The prediction of the forward fan noise shielding provided by an upper wing installation was performed using ESDU-7901 1 [16] , giving comparative results to

Agarwal [17].

The values of SFC and specific thrust were taken at design point (top of climb (ToC)) condition, while noise was measured at take-off. The altitude of measurement was set at 180 meters and Mach 0.3 according to ICAO guidelines.

For the selection of the optimum cycle an objective function has been used taking into account SFC, jet noise and specific thrust. Jet mixing noise is multiplied by the largest factor, as this is the main design driver. The three values in the objective function were non-dimensionalised by reference values.

 Published by Cranfield University Press ISBN: 978-0-9557436-7-2 http://hdl.handle.net/1826/3832

$$FXSFC(\text{Jet noise and diameter}) = x_{0.4} + x_{0.5} + x_{0.1}$$

A three spool engine of high BPR and high TET has been used as baseline. Such an engine represents current state of the art technology and is illustrated in

Figure 3.

RESULTS

This section of the paper presents the results of the methodology on reduced noise propulsion systems, discussing effects of cycle parameters on noise, and performance. The noise-driven engine design methodology is applied on an ultra-high BPR turbofan.

The two primary sources of noise in a turbofan are jet-mixing and fan noise. Reduced jet noise can be achieved by redesigning the cycle and increasing the bypass ratio. However, fan noise, which can be divided to broadband, tonal and buzz saw, is affected mainly by fan size, rotational speed, Mach number at the rotor tip and rotor-stator gap. Thus, fan noise can be reduced by considering the design of the fan and an installation able to provide extended area for liners and noise shielding by the airframe.

Specific Fuel Consumption (SFC) is plotted against jet noise and specific thrust, in design point graphs. A design point (DP) graph contains performance data for a range of engines at their design point. The graphs indicate the engine cycle that meets the design criteria. Every set of cycle parameters (BPR, TET and OPR), which is represented by one point in the DP diagram, corresponds to an optimal fan pressure ratio, in terms of specific thrust and SFC.

THE ULTRA-HIGH BYPASS RATIO TURBOFAN

Cycle Description

A significant noise reduction can be achieved by increasing the BPR. This happens because high BPR leads to low exhaust velocity and low jet mixing noise according to Lighthill [18]. Additionally, exhaust speed is proportional to specific thrust. Thus, a low noise configuration will compromise the specific thrust having an impact on engine diameter, weight and installation drag.

 Published by Cranfield University Press ISBN: 978-0-9557436-7-2 http://hdl.handle.net/1826/3832

Ultra high bypass ratio leads to an increase in the number of low pressure turbine stages, in order to provide the fan power requirement. A previous study [19] proposes the implementation of a gearbox in the LP shaft in order to allow the turbine to operate in high rotational speed and improve its specific power. That configuration has an approximate weight penalty of 10%, a value to be limited in the future, due to continuous research on lightweight transmission systems.

CYCLE ANALYSIS RESULTS

The design point cycle analysis results are shown in Figure 4. Two extreme bypass ratios are plotted in order to show the effect of BPR on engine performance.

Fig 25 depicts SFC against jet noise for variety of engines with different TET and OPR values. For each BPR a number of constant TET and OPR curves is provided. The horizontal curves correspond to constant overall pressure ratio for increasing TET (left to right), while the vertical curves correspond to constant TET for rising OPR (top to bottom).

An increase in OPR does not have a significant effect (reduction) on noise, whilst fuel consumption is reduced considerably for both bypass ratios. When increasing OPR, SFC improvement decreases, due to the increase of compression work. The effect of TET on SFC is depended on BPR. Low TET results in SFC improvement at low BPR, similarly to turbojet cycle. However, SFC increases for decreasing TET at high BPR, similarly to shaft power cycle. This occurs, because the overall cycle efficiency is dependent on propulsive and thermal efficiency, according to equation 1.

$$n_{ov} = n_{prop} n_{th} \qquad \text{Eq.1}$$

TET reduction has an impact on thermal efficiency, however, at low BPRs reduction in exhaust gas velocity gives significant improvement in propulsive efficiency; resulting in higher overall efficiency and lower SFC. For BPRs higher than 20 (where propulsive efficiency is already high) the improvement on propulsive efficiency is less significant than the decrease of thermal efficiency. Figure 4 illustrates SFC versus specific thrust with OPR and TET as parameters. Specific thrust reduces with increasing OPR, following the trends of jet noise, as they both depend on jet exit velocity. This happens due to the increase of compressor work at high OPR, but it diminishes for increasing TET, because of the increase in turbine work excess. High TET results in high specific thrust. However, the effect of TET on specific thrust is proportional to the order of magnitude of ST. As a result, at low BPR the difference on ST is higher than at high BPR, for constant TET increment.

According to the reasoning described above, at BPR<20 a low noise, fuel efficient configuration features high OPR, and low TET which lead to increased dimensions. On the other hand, at BPR>20 a low noise configuration (high OPR, low TET) compromises both fuel consumption and dimensions.The engine parameters that correspond to the lowest value of the objective function are BPR 20, OPR 50 and TET 1800K, resulting to a maximum engine noise of 61 dbA at take off and 59 dbA at landing condition.

 Published by Cranfield University Press ISBN: 978-0-9557436-7-2 http://hdl.handle.net/1826/3832

CONCLUSIONS

This paper presents a noise driven parametric analysis for preliminary thermodynamic cycles. Significant noise reduction has been achieved by increasing bypass ratio and overall pressure ratio and reducing turbine entry temperature. The parametric analysis has shown that even without increasing BPR, the change of OPR and TET can lead to up to 10 dB lower jet noise, having, however, an impact on the size of the propulsion system. Finally it was shown that significant noise reduction can be achieved in the preliminary stage by appropriate design of the propulsion cycle.

REFERENCES

1. Greener by Design, Air travel – greener by design: The technology challenge, 2001.
2. Berglund, B., Lindvall, T. Schwela, D. H. Guidelines for community noise, World Health Organisation, 1999.
3. Department for Transport, The future of air transport, UK Government, 2003.
4. Low, J.K.C., Ultra high bypass ratio jet noise, NASA CR-195394, 1994
5. Powell C A, Preisser J S. NASA's subsonic jet transport noise reduction research. Langley Research Center, NASA
6. Dalton W N III, Ultra High Bypass Ratio Low Noise Engine Study, NASA/CR-2003-212523, November 2003, Allison EDR 16083
7. Gliebe, P.R., Janardan, B.A., Ultra-high bypass engine aeroacoustic study, NASA-2003-212525, Oct 2003, 2003
8. Optimization of traditional and blown liners for a silent aircraft, Thomas R Law and Ann P Dowling, 12th AIAA/CEAS Aeroacoustics Conference, 8-10 May 2006, Cambridge, Massachusetts, AIAA-2006-252593.
9. Hall, C.A., Crichton, D., Engine design studies for a silent aircraft, ASME Turbo Expo 2006, GT2006-90559, Barcelona, Spain
10. Crichton, D., de la Rosa Blanco, E., Law, T.R., Design and operation for ultra low noise take-off, AIAA 2007- 456,2007

 Published by Cranfield University Press ISBN: 978-0-9557436-7-2 http://hdl.handle.net/1826/3832

11. Hall, C.A., Crichton, D., Engine and installation configurations for a silent aircraft, ISABE-2005-1 164
12. Plas, A.P., Madani, V., Sargeant, M.A., Greitzer, E.M., Hall, C.A., Hynes, T.P., Performance of a boundary layer ingesting propulsion system, AIAA-2007-0450, 2007
13. G. Santos, J.R. Barbosa, P. Pilidis, Analysis of turbofan empirical noise prediction methods, AIAA 2005-3 076, 2005
14. The Turbomatch scheme; for aero/industrial gas turbine engine design point/off design performance calculation, Manual, Cranfield University, UK, October 1999.
15. V. Pachidis, Gas turbine performance simulation, Course notes, 'Thermal power', Cranfield University, UK
16. Estimation of noise shielding by barriers, ESDU, 79011, Issued September 1979.
    A. Agarwal, A.P. Dowling, Low frequency acoustic shielding of engine noise by the silent aircraft airframe, AIAA 2005-2996, 2005
17. Lighthill, M.J., On sound generated aerodynamically (Part 1: General theory), Proceedings of the Royal
18. Society of London, Series A: Mathematical and physical sciences, vol.211, pp. 564-587, 1952.
19. de la Rosa Blanco, E., Hall, C.A., Crichton, D., Challenges in the silent aircraft engine design, AIAA 2007-
20. 454,2007.

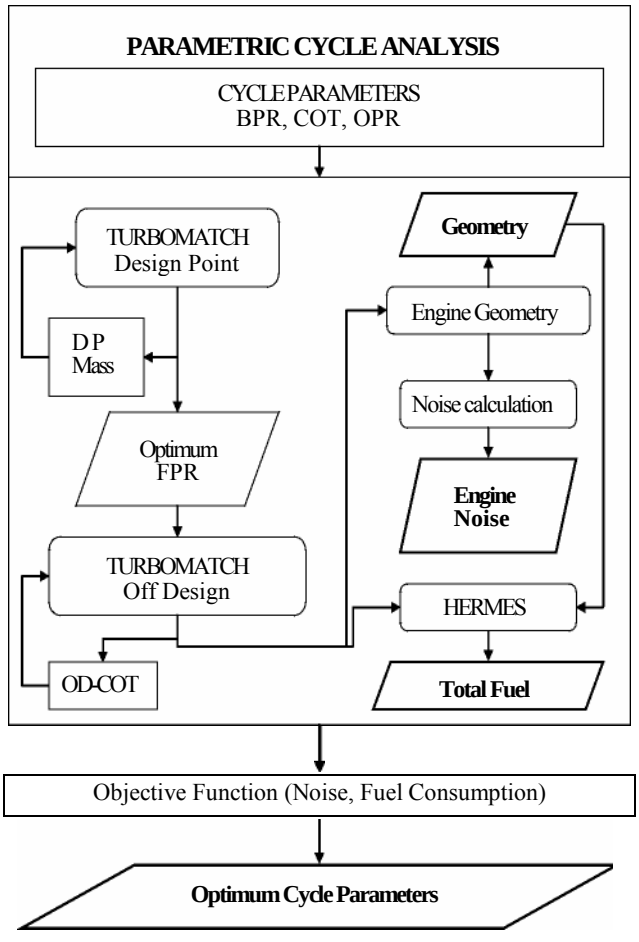

Figure 1: Engine cycle design methodology overview.

	BPR	*OPR*	*TET[K]*

FIGURES

Baseline Engine	
BPR	8
TET [K]	1800
OPR	42
FPR	1.7

min	8	20	1600
max	20	50	1900

Figure 2: Parametric analysis variables.

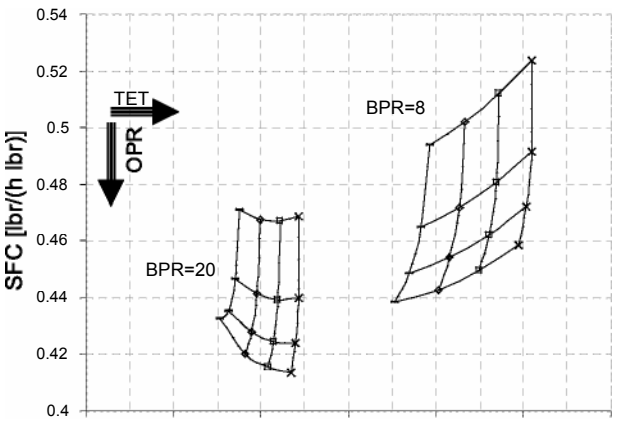

Figure 3:
Baseline engine data.

 Published by Cranfield University Press ISBN: 978-0-9557436-7-2 http://hdl.handle.net/1826/3832

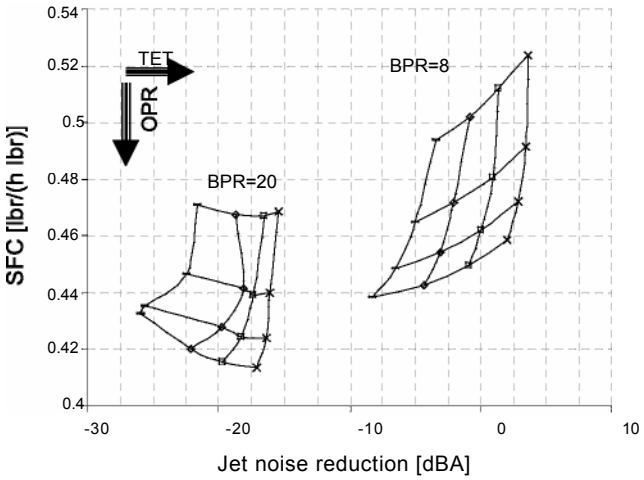

Figure 4: SFC-Jet noise and SFC-Specific thrust.

 Published by Cranfield University Press ISBN: 978-0-9557436-7-2 http://hdl.handle.net/1826/3832

 Published by Cranfield University Press ISBN: 978-0-9557436-7-2 http://hdl.handle.net/1826/3832

Fuel saving benefits of soaring UAVs

Naseem Akhtar, * Alastair K Cooke, * James F Whidborne *

* Department of Aerospace Sciences, Cranfield University,
Bedfordshire MK45 0AL, UK. email:n. akhtar@cranfield. ac. uk

Abstract: The aim is to develop a UAV controller to harvest the potential energy from thermals and wind shear. Soaring achieved by extracting energy from thermals is called thermal soaring. The energy will be be extracted by utilizing the free thermals by remotely sensing the regions of thermal activity. The success of an autonomous thermal soaring system depends completely on the ability to detect and locate atmospheric thermal activity remotely. The experimental setup comprising of visual sensors, Infra Red (IR) sensors and a variometer on-board a small model aircraft will be used for detection of thermal activity. The visual cameras along with pattern recognition capability will be used to identify the land marks and clouds associated with the thermals. A comprehensive simulation environment has been created in Simulink. A representative mathematical model of atmospheric thermal lift and the aerodynamic interaction between the air vehicle wing and rising column of air is included in the Simulink based model. A Sailplane DART 51 mathematical model has been used for designing control systems. Soaring achieved by extracting energy from wind shear is called dynamic soaring. A simple constraint optimization has been successfully used to generate trajectories for dynamic soaring. A more efficient method has been developed which provides a capabilty to generate real time trajectories. The saving on fuel is an improvement on published results.

Keywords: Dynamic soaring, thermal soaring, fuel saving, optimization, IR sensors, thermal structure, variometer, trajectory planning.

1. INTRODUCTION

In this paper the art of thermal soaring, dynamic soaring, sources of thermals and architecture for an autonomous soaring system are described.The implementation issues and experimental setup required are also mentioned. The purpose of designing an autonomous soaring controller is to utilize the atmospheric energy and optimise the thrust usage. The atmospheric energy used is available in the form of free thermals and wind shear. This system will result in a fuel efficient high endurance UAV.

A thermal is a mass of rising air resulting from warming of surface due to sun's rays. As a result of surface heating most of the heat is transferred to the air close to the surface.The heated air rises and its diameter gradually increases and acquires the structure of a vortex. Birds and glider pilots stay aloft by circling within thermals. In order for a UAV to rise within a thermal two things are required. First a method of detection of thermal. Second a method to automatically circle within a thermal.

The formation of the thermal process is described by Wallington [1977] and they have also explained winds across a hill ridge, hill lift, thermal structure and sources of heated thermals. Cone [1964] described the design of sailplanes for optimum thermal soaring performance. In the NASA report thermal internal structure is described in detail and the methodology of positioning sailplane inside the thermal so that maximum energy can be extracted. Amrane [2005] worked on the mathematical implementation of thermals. Herrman & Bil [2005] described an experimental development of an infrared sensor for airborne detection of clear turbulence. Taylor [2003] used a small remotely controlled aeroplane for measuring ground hot spots.Cook et al.[2004, 2006] described the application of variometer, visual camera and IR sensors for detection of thermals. In Cook et al. [2004, 2006], a control systems architecture is described for autonomous soaring.

The extraction of energy from low-level wind gradients is called dynamic soaring [Zhao, 2004a]. This could be used to increase the endurance of UAVs by extracting energy from the velocity field in a similar manner to some sea birds. In a typical pattern of dynamic soaring a bird would descend with the prevailing wind to gain airspeed. On getting close to the sea surface, it turns into the wind and begins to climb. Although the forward advance decreases due to the climb the bird maintains sufficient lift due to increased speed provided by the wind gradient. When the peak wind velocity is reached the bird changes direction to descend and starts the process again. It is possible, if the wind gradient is steep, for the bird to extract sufficient energy to maintain flight without flapping [Zhao, 2004a].

Optimal control methods have been used by Zhao [2004a] to calculate dynamic soaring trajectories that minimize either the average power per cycle or the level of constant power required by a propeller driven UAV. By formulating a non-linear optimal control problem, Zhao [2004a,b] has generated solutions for both linear and nonlinear wind gradient profiles with a three-dimensional point-mass model. The performance indices were selected to minimize

⋆ This work was supported by BAE Systems and EPSRC.

 Published by Cranfield University Press ISBN: 978-0-9557436-7-2 http://hdl.handle.net/1826/3832

the average power required per cycle with either variable or constant power. These optimal control problems were converted into parameter optimization with a collocation technique and solved numerically.

Sachs & da Costa [2003] have also studied the problem of energy extraction from wind shear using optimization techniques. Deittert et al. [2006] includes a review of the art of dynamic soaring. The dynamic soaring equations are derived and solved and the results are discussed with respect to generic UAV models.

The optimization approach used in dynamic soaring is based on the Direct Method of Taranenko [Yakimenko, 2000]. This method permits the solution of trajectory optimization problems in the output space. The control histories are obtained by dynamic inversion without any requirement to solve the integral equations. It should be noted that the use of a virtual time argument allows the temporal and spacial requirements to be decoupled. As the method is very efficient it is able to find near-optimal trajectories rapidly enough to allow real-time implementation [Yakimenko, 2000] thereby allowing the exploitation of dynamic soaring for fuel efficient UAV operations.

In this paper dynamic soaring and thermal soaring techniques are described that are used for extracting energy from wind shear and thermals. The likely sources of thermals are briefly explained in this paper and are based on Wallington [1977]. The technologies involved and methodologies are described.Simulation results are also described. Processes to implement the soaring control system on a radio-controlled model aircraft are explained.

2. ATMOSPHERIC THERMALS

The warm air as a result of Sun's heating rises and acquires structure of a vortex ring Wallington [1977]. The thermals in atmosphere according to [Wallington, 1977] are distorted by wind shear. The upward velocity of the air in the centre of a thermal is greater than the rate of ascend of the whole thermal. Therefore a glider inside the centre of a thermal will rise at the same rate as that of a thermal if the difference between the two velocities is greater than 1 knot [Wallington, 1977].

Initially the thermals resulting from Sun's heating are small but as the day progresses their size increases.When they reach a height of 1200 ft they become large enough to be used for thermal soaring [Wallington, 1977].

2.1 Heated thermal sources

The heated thermal sources or the hotspots are a direct result of uneven heating of the ground i.e. hot spots are the places on which air becomes warmer than the surrounding air [Wallington, 1977]. The development of a hot spot depends on the rate of rise of the temperature of the ground spot and also on the time the air remains close to the ground before its carried away by the wind.

According to Wallington [1977], a wheat field manages to slow down the airflow on a sunny day and the temperature is 3 degrees centigrade higher than the top of the crop. The dense trees and rocky surfaces retain the heat and become

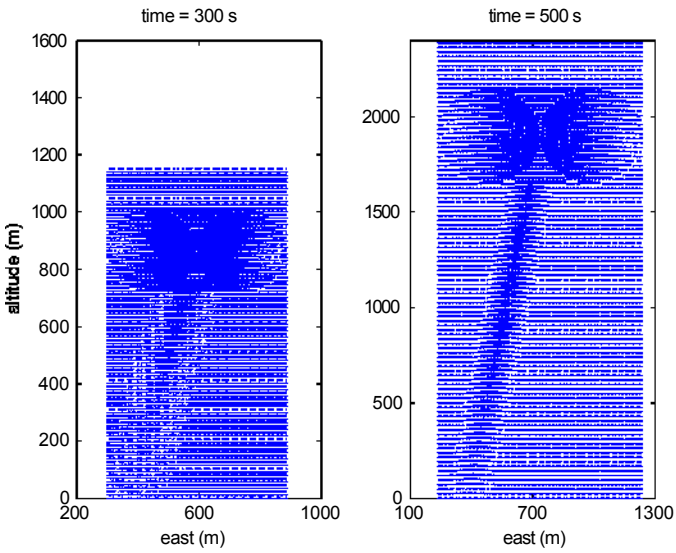

Fig. 1. Earth referenced velocity field within thermal Cook

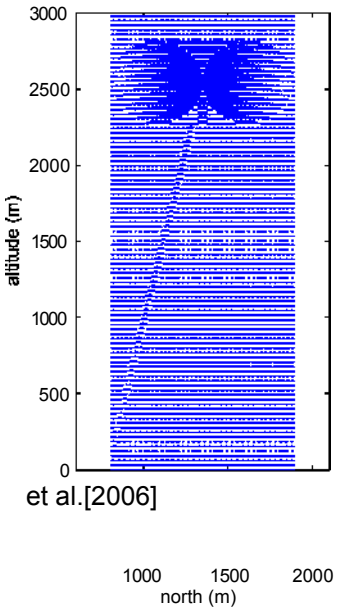

et al.[2006]

Fig. 2. Development of vortex boundary in a northerly drift Cook et al. [2006]

late thermal sources.The group of buildings and towns offer shelter to wind flow and are also therefore efficient sources of thermals.

3. SENSORS

3.1 Infrared sensors

Astheimer [1970] describes the experimental development of an infrared sensor for airborne remote detection of clear turbulence. The device detects the horizontal temperature gradient in the atmosphere by sensing the infrared radiation emitted by carbon dioxide, which is associated with clear air turbulence. Modern infrared temperature sensing thermopiles are very small, low cost and require only simple supporting circuitry and these have been successfully

 Published by Cranfield University Press ISBN: 978-0-9557436-7-2 http://hdl.handle.net/1826/3832

integrated into various airborne applications.

 Published by Cranfield University Press ISBN: 978-0-9557436-7-2 http://hdl.handle.net/1826/3832

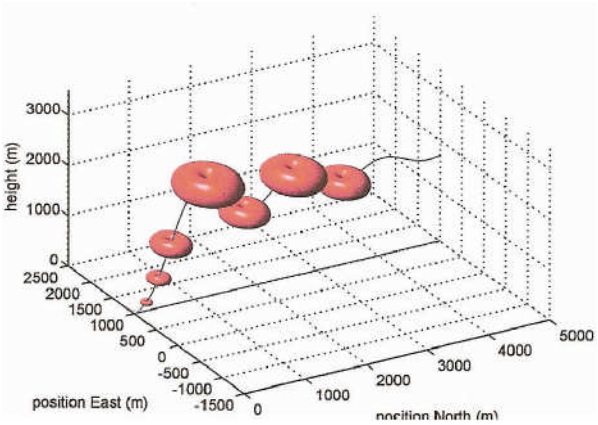

Fig. 3. Northerly drift of thermal vortex Cook et al. [2006]

Taylor [2003], Herrman & Bil [2005] have used aircraft for measuring ground hot spots. This experiment demonstrated that ground hot spots and hence potential regions of thermal activity can be identified using relatively simple equipment. Figure 4 shows the field trials of a mini IR sensor that will be used in our experiments. It can clearly identify clouds and helicopters on the runway. The heat discharged from the top of houses approximately one mile away can also be seen in the background.

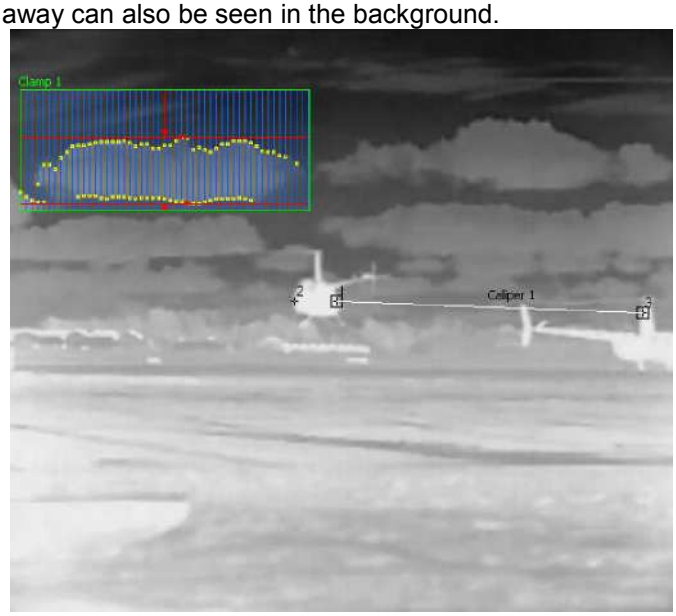

Fig. 4. IR Sensor's field trial

3.2 Electrostatic sensor

In Nash-Webber [1972], an electrostatic horizontal sensing technique senses the horizontal electric field charge associated with thermal up-draughts. Once a thermal has been detected, an important question is which way to turn the aircraft to move toward its center. One method is by the measurement of the water vapor gradient across the wing tips, this is most easily done with tiny wet bulb thermistor thermometers.

No matter whether a thermal is continuous (as a column extending up from earth) a bubble, a plume or a vortex ring essentially the same electric field configuration will exist. Near the earth's surface air carrying positive charge converges toward the thermal and is entrained in the rising air. Near the top of the column where a cloud may form if the air is sufficiently moist the space charge concentration will be greater in volume than in the surrounding air [Nash-Webber, 1972].

3.3 Variometer

Variometers are used for detecting sink and climb rate of a glider. They are very sensitive and measure the marginal rates of climb/sink which cannot be measured using normal cockpit instruments. A mini variometer has been identified that will be used on the model aircraft to detect the climb rate once inside the thermals. The variometer will be integrated with the control system and will provide the climb rate information once the model aircraft is in a thermal.

3.4 Visual Camera

The visual camera along with pattern recognition software will be used for identification of clouds, surface features where thermals are likely e.g. fields, woods, towns and sandy areas etc. The wind shear is present on mountains and hills so visual camera could also be utilized in detection of areas where wind shear might be present.

4. CONTROL SYSTEM DEVELOPMENT

4. 1 Thermal Soaring Process

The first step of the soaring process is to search for thermals. This activity is conducted by a UAV with on-board IR, visual camera and pattern recognition capability. The land marks and clouds associated with the presence of the thermals will be identified using on-board sensors. It will also take clues from soaring birds as presence of thermals.

Once the associated land marks have been identified the UAV will search in that particular area for thermals. The on-board variometer will record any height gained due to thermals. After receiving climb rate confirmation from the variometer the UAV will position itself in the thermal using the technique described in Cook et al. [2006, 2004]. Then it will execute turn with pre-specified bank and flight path angles. The energy management controller integrated with the variometer will be used for providing the control inputs that will result in the desired bank and flight path angles. Once the UAV has reached at the top of a thermal then its controller will execute the gliding phase. After covering horizontal distance in gliding phase it will start searching for thermals again.

4.2 Soaring Capability Demonstration

The soaring capability has been demonstrated in SIMULINK using the mathematical model of DART 51 high performance sailplane based on Amrane [2005]. The SIMULINK based demonstration included a representative model of

 Published by Cranfield University Press ISBN: 978-0-9557436-7-2 http://hdl.handle.net/1826/3832

atmospheric lift and aerodynamic interaction between the air vehicle wing and rising column of air [Amrane, 2005].

The practical demonstration will use a remote control small aeroplane equipped with sensors and a visual camera. The photographs taken by the on-board camera will be used to identify patterns of interest. The pattern recognition system will be based on Open CV.

The energy extraction capability will be demonstrated by flying the remote control model plane in the area with likelihood of thermals. The variometer input will determine whether any thermals are present. Then a soaring controller will extract energy [Cook et al., 2004]. The desired values of the bank angle and flight path angle will be translated into control inputs in terms of elevator and ailerons angles. A computer will be interfaced with the remote control model aeroplane to send and receive signals.The soaring controller has been tested in the SIMULINK environment and is based on Cook et al. [2004].

The sensor pack required for the experimental work includes a visual camera, variometer and a radio controlled small model aeroplane. We are in the process of installing sensors on the small model aeroplane.The autopilot and soaring controllers have been tested in the simulated environment using SIMULINK.

5. DYNAMIC SOARING PROCESS

A cycle of dynamic soaring is shown in figure 5. The dynamic soaring trajectories were generated using a direct method Akhtar et al. [2008] and because of very low optimization time it can be used for real time trajectory generation.

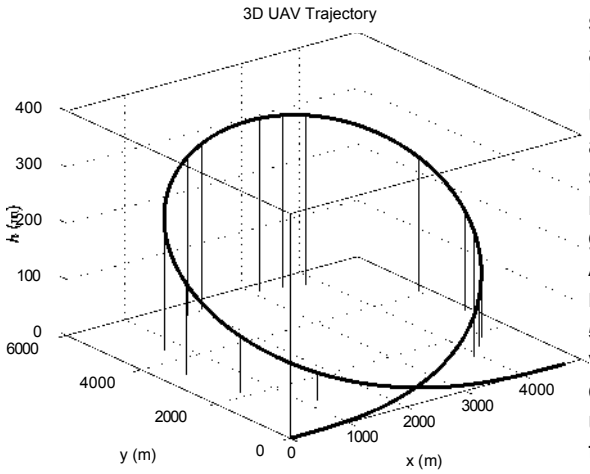

Fig. 5. Optimal trajectory for minimum peak power problem

The direct method is a non-linear constrained optimization method where some reference polynomials are determined by the boundary conditions. The speed profile can be separated from trajectory by introduction of a virtual arc instead of time. The inequality constraints are direct functions of the output due to differential flat properties of the system, which helps to accelerates the process for on board implementation. For further details, see Yakimenko [2000] and Whidborne et al. [2008].

In the problem formation a peak value of normalized thrust was minimized, i.e. selected as a cost function. The constraints of the system included minimum and maximum velocity, flight path angle, thrust, bank angle and load factor etc. Other problems investigated included the minimum time to complete a loop and maximum height gained. Figure 6 shows the normalized thrust values used for completing a traveling cycle when the direct method was used [Akhtar et al., 2008].

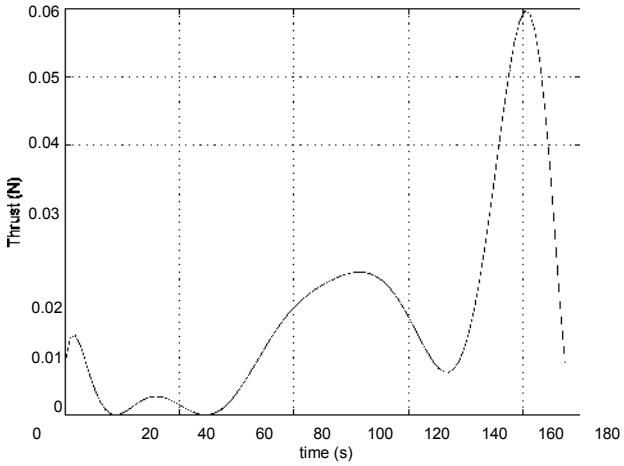

Fig. 6. Thrust profile for minimum peak power problem

5.1 Ridge Soaring Capability Demonstration

In the case of dynamic soaring it will not be easy to demonstrate soaring using wind shear above sea. Therefore ridge soaring at an appropriate location will be carried out.

Firstly, the gradient of the wind will be estimated in SIMULINK using Kalman Filtering. The actual instrumented model aeroplane will be used to gather data by flying it in the wind shear. The on-board instrument pack will provide the values of body angular rates, body accelerations, aircraft attitude, position, ground velocities, side slip angle, angle of attack, velocity, etc.

A soaring cycle will be executed by the pilot using a remote control model aeroplane. The data from this flight test 5000 will be used to estimate the wind gradient. Then this value of wind gradient will be used to generate trajectories using a direct method. The results in terms of height gained, thrust usage and horizontal distance covered will be compared with those of SIMULINK.

6. INTEGRATION OF AN AUTONOMOUS SOARING CONTROL SYSTEM

The full integration of the soaring system will require implementation of pattern recognition and integrated energy management controller on on-board microprocessor. The understanding of the microprocessor and its integration with the sensor pack and actuators is required. Once it is achieved then we will have an opportunity to implement

 Published by Cranfield University Press ISBN: 978-0-9557436-7-2 http://hdl.handle.net/1826/3832

algorithms programmed in 'C' language. Then the the testing of the integrated system will take place.

The various modules once integrated will result in an integrated system that will perform soaring independently, i.e. it should be able to execute all the process steps involved in thermal and dynamic soaring. It should identify the features of interest from pictures. Then it should be able to search for thermals in that area. Once a thermal has been identified, the thermal centering system should place the UAV in a thermal. It should be able to extract energy from the thermal by executing turns inside the thermal. The integrated system will demonstrate all these capabilities.
To test the integrated energy management controller and pattern recognition capability we require an autonomous soaring control system embedded on-board. Therefore to demonstrate the capability we will initially use a radio control aeroplane without an on-board controller. To demonstrate the capability we will run different experiments, each highlighting a specific module of the overall system. The on-board camera will take pictures and store them and then these pictures will be downloaded for pattern recognition purpose. The OpenCV based program will be used to identify the features off-line. This program can easily be implemented on-board once it is working satisfactorily.
The process of extraction of energy will be demonstrated again by passing values to the model airplane using a remote control.The pilot will try to follow the desired bank and flight path angles as closely as possible.

The decision process involves searching for thermals. Once a thermal has been identified then the UAV need to be positioned in the thermal so that climbing can follow. Once a desired altitude has been achieved a gliding command is executed. If any of these objectives are not achieved then a UAV will have to search for new thermals.

7. CONCLUSIONS

We have successfully managed to show the possibility of extracting energy from a thermal in the SIMULINK environment. The dynamic soaring capability that involves extraction of energy from wind shear has also been demonstrated using the direct method. This technique can also be implemented on-board as the optimization time is only eight seconds. This techniques can be used to generate optimal trajectories to gain height after every cycle, move in the horizontal direction by maintaining height, minimize the cycle time, and minimize the peak or average thrust used.
The direct method also resulted in usage of much lower normalised thrust in comparison with the published results of Zhao [2004a]. This will have a direct economic benefit as a UAV will require a smaller engine resulting in a lighter UAV.
The experimental work has been planned for this summer. Rather than demonstrating the full integrated system capability, individual modules functionality will be demonstrated. If time permits the module will be put together to show the trials of the integrated system. Otherwise it will form the part of the follow-on project.

REFERENCES

N. Akhtar, J.F. Whidborne, A.K. Cooke. Real-time trajectory generation technique for dynamic soaring UAVs, UKA CC Control 2008 conference, 2008 (submitted).

A.R. Amrane, Flight Dynamics Model of a High Performance Sailplane MSc Thesis, School of Engineering, Cranfield University. September 2005

R.W. Astheimer, The remote detection of clear air turbulence by infrared radiation. Applied optics, vol.9. No8, August 1970.

C.D Cone.The design of sailplanes for optimum thermal soaring performance. NASA TND 2052, 1964

M.V. Cook, A.K. Cooke and J.F. Whidborne, A Control algorithm for an autonomous UA V gliding capability. School of Engineering, Cranfield University, November 2004.

M.V. Cook, A.K. Cooke and J.F. Whidborne, Flight Dynamics modelling refinement for an autonomous UA V glider. College of Aeronautics Report: NFP0505 School of Engineering, Cranfield University, February 2006

I.D. Cowling, O.A. Yakimenko, J.F. Whidborne, and A.K. Cooke.A prototype of an autonomous controller for a quadrotor UAV. Proc. European Contr. Conf. 2007, Kos, Greece, July 2007.

M. Deittert, C. Toomer, A.G. Pipe. Biologically inspired UAV propulsion. 21st Bristol Conference on UAVS, April 2006.

M. Etchemendy. Flight Control and Optimal Path Planning for UAVs, MSC Thesis, Cranfield University, 2007.

P. Herrmann and C. Bil, Simulation and flight test of a temperature sensing stabilization system. Volume 109, Number 1094. The Aeonautical Journal, 2005.

J.L. Nash-Webber. Motorless flight research, NASA CR-2315, 1972

G. Sachs and O. da Costa. Optimization of Dynamic Soaring at Ridges. AIAA Atmospheric Flight Mechanics Conference and Exhbit, Austin, Texas, August 2003.

B. Taylor, C. Bil and S. Watkins. Horizontal sensing attitude stabilization presented to the 18 International UAV Systems Conference Bristol UK, 2003.

C.E. Wallington, Meteorology for glider pilots, John Murray Publishers, 1977.

J.F. Whidborne, I.D. Cowling, O.A. Yakimenko. A Direct Method for UAV Guidance and Control. 23rd Bristol Conference on UAVS, April 2008.

O.A. Yakimenko. Direct method for rapid prototyping of near-optimal aircraft trajectories. J. Guid. Control Dynam., 23(5):865–875, 2000.

Y.J. Zhao. Minimum fuel powered dynamic soaring of unmanned aerial vehicles utilizing wind gradients. Optimal Control Applications and Methods, 25:211-233, 2004a.

Y.J. Zhao. Optimal Dynamic Soaring. Optimal Control Applications and Methods. Optimal Control Applications and Methods, 25:67-89, 2004b.

 Published by Cranfield University Press ISBN: 978-0-9557436-7-2 http://hdl.handle.net/1826/3832

Investigation of Aerofoil Morphing for Advanced Blade Design

Z.I.Zachariadis, E. Shapiro, D. Drikakis

ABSTRACT

With the optimization of fixed aerodynamic shapes reaching its limits, the active flow control concept increasingly attracts attention of both academia and industry. Adaptive wing technology, and shape morphing airfoils in particular, represents a promising way forward. The aerodynamic performance of the morphing profiles is an important issue affecting the overall performance of an adaptive wing. In this paper we present a detailed study of the aerodynamics of morphing airfoil profiles for advanced rotor blades. The behavior of aerodynamic coefficients is analyzed across a wide range of Mach numbers and angles of incidence typical for the actual rotor blade operation. The benefits and limitations of the morphing shapes within the design constraints are discussed.

NOMENCLATURE

C_L	Lift coefficient
C_D	Drag coefficient
$CL\,\max$	Maximum lift coefficient
MEMS	Micro-electronic-mechanical-systems
M_{DD}	Drag divergence Mach number
□	Turbulent kinetic energy
□	Turbulent specific dissipation rate
SST	Shear-stress transport
y^+	Wall distance

INTRODUCTION

From an aerodynamic point of view, turbulent flows result in thick boundary layers that produce more skin friction drag than laminar boundary layers, which are thinner by principle. On the other hand laminar separation leads to high pressure drag rise and thus it is some times desirable to promote transition to turbulence, if laminar separation is imminent, since turbulent boundary layers are less susceptible to separation. Moreover in compressible flows, shocks may appear that interact with the boundary layer causing flow separation. The aerodynamic performance in many aeronautical applications, such as flows around turbo-machinery blades and external flows over aircraft wings or helicopter blades, depends strongly on the location and

 Published by Cranfield University Press ISBN: 978-0-9557436-7-2 http://hdl.handle.net/1826/3832

strength of the shocks, as well as on the flow separation, induced by the shock/boundary layer interaction. Accurate prediction of such flow phenomena is of primary technological importance and their simulation remains a challenging problem due to the complex physics involved. Laminar flow separation on lifting and control surfaces of flying machines and, or, shock/boundary-layer interaction is the main reason for a series of problems such as drag increase, loss of lift, aerodynamic heating and poor controllability.

It was previously stressed that the boundary layer development and the interaction of the boundary layer with the outer flow field, aggravated at high speeds by the occurrence of shock waves, limits the overall air-vehicle or air-vehicle component [15] .This interaction dictates the pressure distribution on the aerofoil surface, and subsequently the aerodynamic loads on the wing. Therefore, in order to achieve high performance for mission varying air-vehicles it is necessary to either: (a) alter the boundary layer behavior of the aerofoil, and/or (b) change the geometry of the aerofoil, real time, for changing flow conditions. The latter, namely the adaptive wing technology, is the flow control method of interest in this work.

Flow control essentially involves a beneficial change in the wall-bounded and/or free-shear flow with the objectives of (1) delaying/advancing boundary layer transition, (2) suppressing/enhancing turbulence and (3) preventing excessive boundary layer growth and separation. Means of boundary layer flow control include, conventional air-jet [10] and sub-boundary layer vortex generators [1], or zero-mass pulsing jets [12], deployed to delay separation, discrete suction or blowing meant to decrease viscous drag [17,3], and unconventional deploying devices such as Gurney flaps [5], divergent trailing edges and reversed flow flaps [9] to increase lift-to-drag ratios (L / D) and $c_{L\max}$. Micro-electronic-mechanical-systems (MEMS), that manipulate

the high-shear-stress streaks in the boundary layer [6], can also be utilized for vortex control, by affecting local leading edge separation and vortex location, to enhance maneuver capability [4].

Special consideration is also given to control the shock waves and the shock associated boundary layer development. The objective here is either to influence the shock strength, by spreading the shock associated pressure rise over a certain chordwise distance, thus reducing wave drag, or to energize the boundary layer making it less prone to adverse pressure gradients. Reducing the shock strength can be accomplished by passive or active cavity ventilation [11, 16] or by a contour bump in the shock region [2]. Energizing the boundary layer upstream of the shock may be accomplished by discrete suction [15], or by using vortex generators [7]. Adaptive wing technology represents a promising alternative approach to flow control. In an adaptive wing the effective aerofoil/wing geometry adjusts to the changing flow and load requirements. This way the aerodynamic flow potential is explored at different points of the flight envelope, thus resulting in aerodynamic performance gains, during take-off, cruise, maneuver and landing [13, 14, 18, 19]. Means of

 Published by Cranfield University Press ISBN: 978-0-9557436-7-2 http://hdl.handle.net/1826/3832

realizing adaptive wing technology are predominantly geometrical adjustments including the deformation of the complete wing and/or the use of leading and trailing edge camber variations to achieve the desired low drag pressure distributions. Moreover local contour modifications, in the shock region, can be implemented to reduce shock strength that ameliorates boundary layer development and drag.

RESULTS AND DISCUSSION

Employing flow control in the sense of adaptive wing technology, the effective aerofoil/wing geometry adjusts to the changing flow and load requirements. The variation of the aerofoil geometry can be accomplished by a set of discrete actuators capable of moving the surface, while it is imperative to keep the geometry changes small so as not to introduce excessive drag penalties and/or not to overstress the surface skin. Flow control controls concepts such as active trailing edge and aerofoil morphing are studied in the subsequent paragraphs, with an emphasis on aerodynamic benefits.

Smart materials and structures can be used as an efficient means of achieving aerofoil morphing that can be reconfigured in response to changing conditions with potentially major aerodynamic benefits. Figure 1 shows the different actuation concepts that have been investigated. A number of different aerofoils were modeled and simulated in order to have an impression of the most aerodynamically promising configuration with respect to the baseline aerofoil. For this reason, grids comprising of 390x 100 cells have been created and the *K - co* turbulence model, with shear-stress transport (SST) modification [8], was employed. The computational domain was extended

20x chord length with<1y. It was found that the most efficient grid overall, in terms of resolution and computation time, was the one with 390x 100 cell. All the simulations were performed using grids of similar dimensions. Moreover it should be stressed that the grids used are much finer than these generally used for 2d RANS aerofoil computations.

Figure 1. Aerofoil morphing configurations (Colour codes: Baseline, 001, 002, 008, 009, 010).

Figure 2 presents the 2d polars obtained for the baseline and morphing aerofoils at $M_\infty = 0.6$. The preliminary results demonstrated that profile shape morphing can be beneficial. Since configuration 009 yielded high C_L / C_D ratios, it was decided to extent the aerodynamic study on the latter configuration and an extended 2D polar database has been established.

The 2D polars (Figure 4) demonstrate that the profile 009 yields higher C_L than the baseline aerofoil, for the entire Mach number range except when strong shock waves are present.

 Published by Cranfield University Press ISBN: 978-0-9557436-7-2 http://hdl.handle.net/1826/3832

Although higher drag coefficients are obtained for the profile 009, in some cases the drag rise is marginal, while for the entire Mach number and angle of attack range, profile 009 results in high (in magnitude) pitching moments. The quantitative analysis of the polar, Figure 3, reveals that at zero lift, and for Mach numbers ranging from 0.3 to 0.6, the profile 009 experiences marginally higher C_D,

while at higher Mach numbers the drag levels increase significantly, due to the development of supercritical flow conditions, thus compromising the drag divergence Mach number (M_{DD}). Moreover, profile 009 results in higher $c_{L_{max}}$ than the baseline

aerofoil, while the trend of the $c_{L_{max}}$ for profile 009 is to decrease from Mach 0.6 to

0.7 with a much steeper slope (see Figure 4 (a)).

In general the desired characteristics for an aerofoil to be used in the inboard region of a main rotor blade are (1) the highest possible maximum lift coefficients at Mach numbers from 0.3 to 0.5 for increased blade loading on the retreating side of the rotor disk, (2) pitching moment coefficients nearly equal to zero, for low blade torsion loads and (3) moderate M_{DD} for reduced power requirements. How well the third

design goal is met determines how far out on the rotor blade the new aerofoil could be applied. Although profile 009 satisfies the first design goal, it fails to meet the other two design criteria, manifesting that the attainment of higher lift is in conflict with the need for high M_{DD} number characteristics and low pitching-moment characteristics.

 Published by Cranfield University Press ISBN: 978-0-9557436-7-2 http://hdl.handle.net/1826/3832

CONCLUSIONS

Adaptive wing technology is a promising approach to active flow control. In this paper, the aerofoil morphing flow control strategy has been investigated and an extensive polar database has been established. The gains and limitations of the control strategy have been numerically demonstrated. In order to meet the desired characteristics of a main rotor blade an active chamber optimization study is underway.

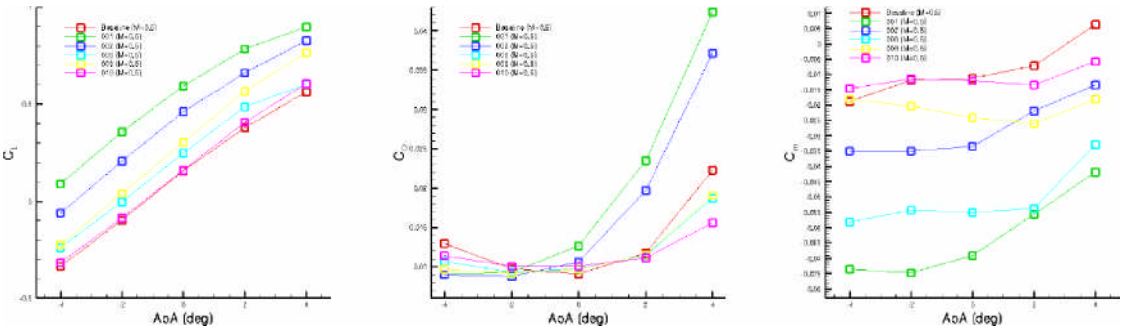

Figure 2. Aerofoil morphing 2D Polars (Colour codes: Baseline, 001, 002, 008, 009, 010).

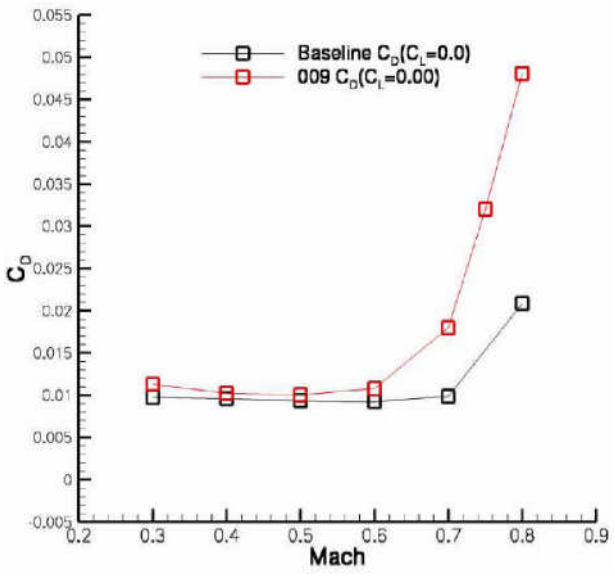

Figure 3. Drag-Divergence Mach number.

 Published by Cranfield University Press ISBN: 978-0-9557436-7-2 http://hdl.handle.net/1826/3832

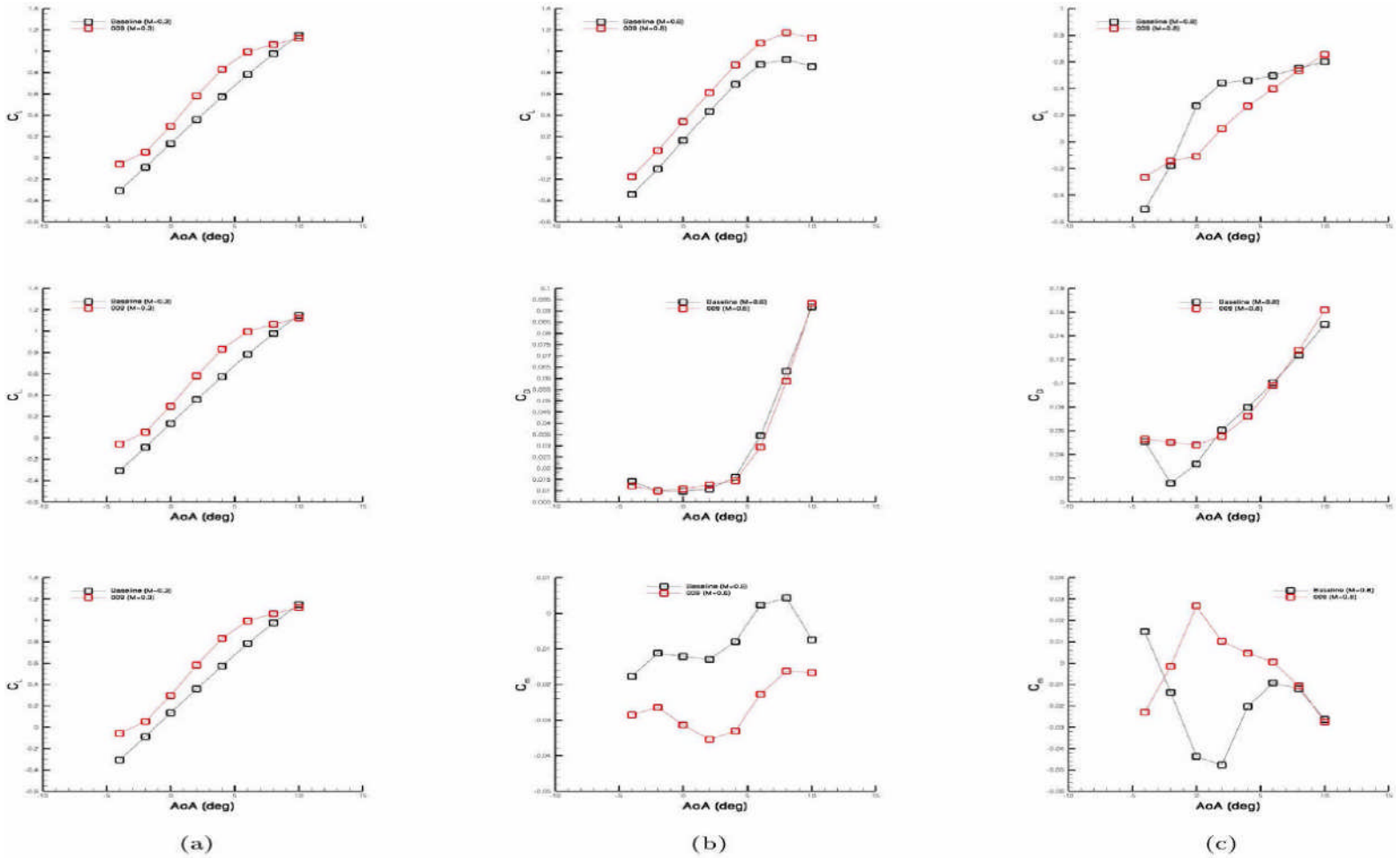

Figure 4. 009 2D Polars; (a) M=0.3, (b) M=0.6, (b) M=0.8 (Colour codes: Baseline, 009).

Published by Cranfield University Press ISBN: 978-0-9557436-7-2 http://hdl.handle.net/1826/3832

References

1. Ashill, P.R., Fulker, J.L. and Hackett, K.C., Research at DERA on sub boundary layer vortex generators (SBVGS). *AIAA,* 2001-0887 (2001).
2. Ashill, P.R, Fulker, J.L., Simmons, M.J., Simulated active control of shock waves in experiments on aerofoil models. In *ICEFM* Proceedings (Turin, July 1994).
3. Hefner, J.N., Bushnell, D.M., Viscous drag reduction via surface mass injection., *Progr Astronaut Aeronaut,* 123 (1990).
4. Ho, C.M., Huang, P.H., Yang, J.M., Lee, G.B., Thai, Y.C., Active flow control by micro systems. In *IUTAM* Symposium on mechanics of passive and active control (1999).
5. Jeffrey, D.R.M., Hurst, D.W., Aerodynamics of the Gurney flap. *AIAA* 96-2418 (1996).
6. Kimura, M., Tung, S., Ho, C.M., Jiang, F., Tai, Y.C., MEMS for aerodynamic control. *AIAA* 97-2118 (1997).
7. McCormick, D.C., Shock/boundary layer interaction control with vortex generators and passive cavity. *AIAA* 31, 1(1993), pp. 91-96.
8. Menter, F.R., Two-equation eddy-viscosity turbulence models for engineering applications. *AIAA* 32, 8 (1994).
9. Meyer, R., Bechert, D.W., Hage, W., Wind tunnel experiment with artificial bird feathers for passive separation control on airfoils. In *IUTAM* Symposium on mechanics of passive and active control (1999).
10. Peake, D.J., Henry, F.S., Pearcey, H.H., Viscous flow control with air-jet vortex generators. *AIAA* 99-3 175 (1999).
11. Raghunathan, S., Mabey, D.G., Passive shock wave boundary layer control experiments on a circular arc model. *AIAA* 86-0285 (1986).
12. Seifert, A., Pack, L.G., Oscillatory Control of separation at high Reynolds numbers. *AIAA* 37, 9 (1999).
13. Siclari, M.J., van Nostrand, W., Austin, F., The design of transonic airfoil sections for an adaptive wing concept using a stochastic optimization method. *AIAA* 96-0329 (1996).
14. Smith, S.B., Nelson, D.W., Determination of the aerodynamic characteristics of the mission adaptive wing. *AIAA* 27, 11(1990).
15. Stanewsky, E., Adaptive wing and flow control technology. *Progress in Aerospace Sciences,* 37 (2001), pp. 583-667.
16. Stanewsky, E., Delery, J., Fulker, J., Geissler, W., EUROSHOCK-drag reduction by passive shock control. *Notes on Numerical Fluid Dynamics* 56 (1997).
17. Stanewsky, E., Krogmann, P., Transonic drag rise and drag reduction by active/passive boundary layer control. *AGARD Report* 723 (1985).
18. Szodruch, J., The influence of camber variation on the aerodynamics of civil transport aircraft. *AIAA* 85-0353 (1985).
19. [19] Thorton, S.V., Reduction of structural loads using maneuver load control on the Advanced Fighter Technology Integration (AFTI)/F-1 11 mission adaptive wing. *NASA TM* 4526 (1993).

 Published by Cranfield University Press ISBN: 978-0-9557436-7-2 http://hdl.handle.net/1826/3832

High-Order CFD Simulations of Wing Flows

Marco Hahn, Dimitris Drikakis
Fluid Mechanics and Computational Science Group,
Department of Aerospace Sciences,
Cranfield University, Cranfield MK43 0AL, United Kingdom

ABSTRACT

This paper presents the results from Implicit Large Eddy Simulation (ILES) of wall-bounded flow problems pertinent to aeronautical applications. The cases considered here are all concerned with the accurate prediction of separated wing flows. In order to assess the fidelity of the simulations, comparisons with experimental data and numerical results using classical LES and DNS (Direct Numerical Simulation) are provided.

1. INTRODUCTION

One of the greatest challenges for current Large-Eddy Simulations is the application to flow problems of practical engineering interest, because the grid sizes that can be employed are typically limited. In the context of aeronautical applications, curved three-dimensional geometries such as swept and delta wings are among the most difficult scenarios encountered, because they are prone to transition and separation. Swept and delta wings can be found in all modern aircraft and UAVs travelling at subsonic, transonic or supersonic speeds and the accurate prediction of their aerodynamical behaviour is paramount to a reliable and cost-effective design. Here, it is not only cruise conditions that are of aerodynamic interest. Most of these vehicles also fly a considerable amount of time at subsonic speeds and moderate to high angles of attack, e.g., takeoff and landing or air combat. In fact, the non-linear effects associated with separation at these flow conditions are more interesting from the modeller's point of view and much more difficult to simulate [1]. Computational challenges include the prediction of transition leading to turbulence, unsteady separation, optimum balance of numerical dissipation and dispersion, and adequate grid generation for achieving accurate and efficient solutions.

Although a great deal of attention has been paid to complex separated flow structures for wings at relatively high angles of incidence, a theoretical or computational model for predicting the flow behaviour with any degree of certainty has not emerged yet. Therefore, engineers heavily rely on accurate experimental and numerical data characterising the wing aerodynamics. In the following sections, the fidelity of the ILES approach will be assessed with regard to this scenario.

 Published by Cranfield University Press ISBN: 978-0-9557436-7-2 http://hdl.handle.net/1826/3832

1. DELTA WING

ILES simulations of the flow around a flat-plate delta wing with a leading edge sweep angle of 50°, have been conducted. The flow features shear-layers and complex vortical structures pertinent to aeronautical applications. Symmetry was assumed along the root chord and the resulting H-H-type grid consists of 660,000 grid points spanning a three-dimensional domain of size 8c x 3c x 6c (c is the root chord length of the delta wing) in x-direction (chord-wise), y-direction (span-wise) and z-direction (normal), respectively. The grid has been clustered in the vicinity of the wing, where $\Delta x/c$ and $\Delta y/c$ are of order 10^{-2}, and $\Delta z/c$ is of order 10^{-4} near the surface. This should be considered as a highly under-resolved simulation with respect to the grid.

The angle of incidence was10°, the Mach number was 0.2 and the Reynolds number based on the free-stream velocity and the root chord length was 26,000 as per the experiment of Taylor et al. [2],[3] and direct numerical simulations (DNS) by Gordnier & Visbal [4], performed on a computational grid of 4.5M points.

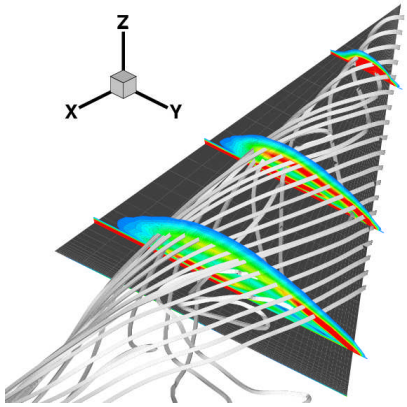

Figure 1: Instantaneous streamlines and iso-vorticity contours.

Figure 1 shows instantaneous streamlines and iso-vorticity contours obtained by the ILES simulation. The sharp leading-edge (LE) provides a well-defined separation line. Consequently, the shear-layer emanating from the LE rolls up and a stable leading edge vortex (LEV) system develops. Breakdown of the LEV and the associated reversed flow in the vortex core can be observed just downstream of the trailing edge.

Averaged contours of axial (stream-wise) velocity and cross-flow velocity vectors in a plane normal to the wing surface at approximately one third of the root chord, are shown in Figure 2. The position of the vortex core as predicted by the DNS of Gordnier & Visbal [4], marked by a white cross in the figure, matches with the results of the under-resolved ILES simulation.

 Published by Cranfield University Press ISBN: 978-0-9557436-7-2 http://hdl.handle.net/1826/3832

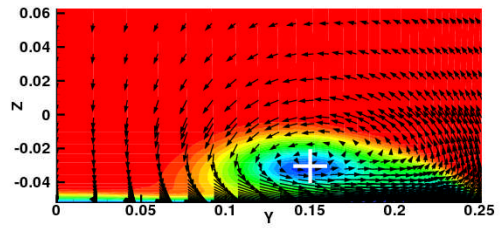

Figure 2: Averaged position of the vortex core at x/c=0.3 as predicted by ILES and DNS (white cross).

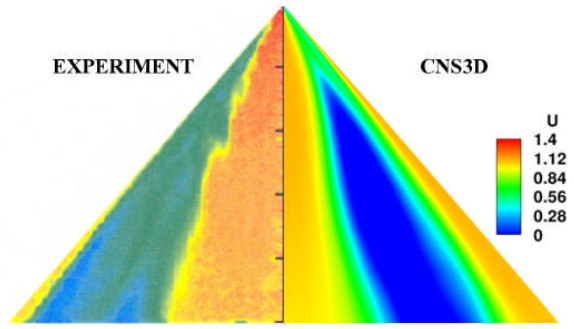

Figure 3: Comparison of the averaged axial velocity in a plane through the vortex core as predicted by ILES and experiment.

Figure 3 illustrates the averaged axial velocity in a plane through the vortex core. The experimental results from Taylor et al. [3] are compared with the contours obtained by ILES. The extent of the primary LEV as predicted by ILES is found in satisfactory agreement with the experiment. However, the secondary vortex which appears towards the trailing edge could not be predicted. This can be attributed to the coarseness of the mesh in this region. The DNS simulations of Gordnier & Visbal [4] have shown that a distinctive dual-vortex system exists for lower angles of attack, whereas at an incidence of 15° a single primary vortex has been observed, whereas for the present case of 10° only an extremely weak secondary vortex occurs.

3. SWEPT WING

ILES has also been performed for a fully three-dimensional wing geometry using a grid comprising merely 12.7M nodes. The simulation of the MSTTAR wing (Modelling and Simulation of Turbulence and Transition for Aerospace) at a total angle of attack of 9° has been carried out at a Reynolds number of approximately 210,000, based on free-stream velocity and root chord length, and a near incompressible Mach number of 0.3. These conditions have been chosen according to the corresponding experiments conducted at Manchester University by Zhang & Turner [5].

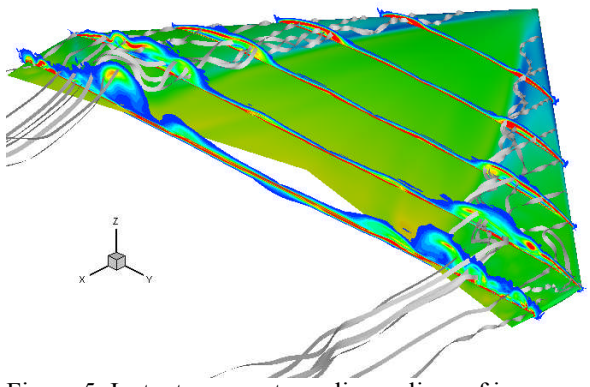

Figure 5: Instantaneous streamlines, slices of iso-vorticity contours and pressure coefficient distribution on the suction side of the wing.

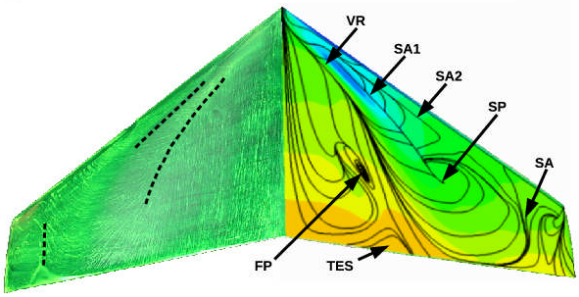

Figure 4: Time-averaged streamlines just above the wing surface and contours of pressure coefficient as predicted by the present simulation (right). Surface oil-film visualisation from experiment on the suction side of the wing (left).

 Published by Cranfield University Press ISBN: 978-0-9557436-7-2 http://hdl.handle.net/1826/3832

The general topology of the flow around the swept wing geometry is illustrated in Figure 4 by instantaneous streamlines, slices of iso-vorticity contours and pressure coefficient distribution on the suction side of the wing. Similar to sharp-edged delta wings, the shear-layer emanating from the leading edges rolls up into a distinctive leading edge vortex system which grows and becomes less stable as it progresses towards the trailing edge. After about 50% of the root chord the LEVs start bending inboard and lift off the wing surface at an increasing rate. The main vortex cores are associated with the large regions of vorticity still visible near the trailing edge. However, as they are less coherent than near the leading edge and are influenced by the fully turbulent flow near the wing tips, they exhibit strong fluctuations and are not symmetrical any more.

A comparison between time-averaged streamlines just above the wing surface obtained by the present simulation and the experimental oil-film visualisation Zhang & Turner [5] is shown in Figure 5. The computational results in the right-hand half of the picture also include contours of the pressure coefficient on the suction side of the wing. Several common flow features, marked by dashed lines for the experimental data, can be observed in both parts of the picture. The reattachment of the leading edge vortex (VR) is well-defined in the computations inboard of approximately 30%s, where s is the half-span, but starts to diffuse and bend towards the trailing edge as the LEV becomes less coherent. Close to the wing root, the reattachment line exhibits a similar angle for both the experiment and the simulation. However, the deviation from a straight line on the right-hand side appears to begin prior to the one observed on the left-hand side. This indicates premature non-linear spreading of the leading edge vortex in the simulation and leads to a larger extent near the trailing edge. Moreover, the two saddles SA1 and SA2 identify the existence of a secondary vortical region induced by the primary vortex along the leading edge, which can also be observed in the experiment of Zhang & Turner [5], albeit this behaviour is less clear in the oil-film visualisation. The secondary vortical zone does collapse, however, as the influence of the main vortex decreases towards the wing tip due to the breakdown of its core. Although the streamlines are not following the core of the leading edge vortex, breakdown is clearly indicated by the stagnation point (SP) between 50%s and 60%s. It should be noted that a stagnation point is not visible in the experiment and thus the LEV might still be intact. Yet, another feature of the flow is apparent closer to the wing tip. In the fully turbulent region, the effect of the LEV drives the fluid towards the wing tip, where it meets the opposing outer flow between 80%s and 90%s. Thus, the characteristic saddle (SA) observed in both experiment and simulation is formed.

In general, the numerically predicted streamline pattern is found to be in good agreement with the

 Published by Cranfield University Press ISBN: 978-0-9557436-7-2 http://hdl.handle.net/1826/3832

oil-film visualisation from the experiments of Zhang & Turner [5]. However, the skin friction lines inboard of the main vortex in the experimental picture are aligned in free-stream direction suggesting a simple dead-air region, whereas the simulation predicts a weakly detached region of fluid revolving around a focal point (FP). Furthermore, an incipiently separated zone near the trailing edge (TES) not existent in the experiment can be seen in the computation. This observation is not exclusive to the present results, but has also been reported for hybrid RANS/LES simulations of the same case performed by Li & Leschziner [6] on a much finer grid of approximately double the size of the ILES mesh (23.6M nodes).

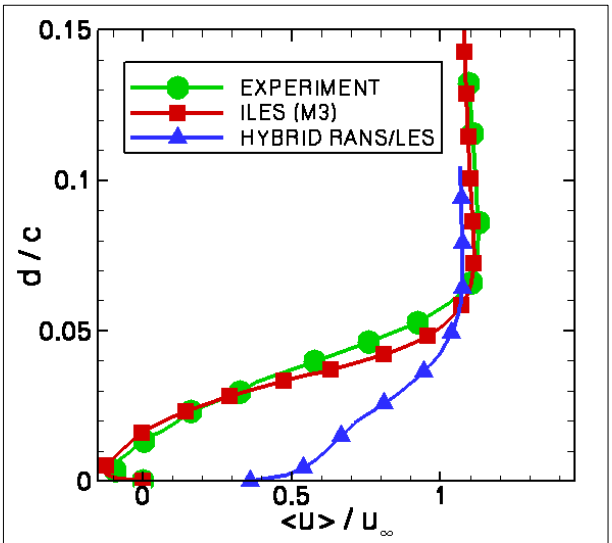

Figure 6: Averaged velocity profiles from the experiments, the results obtained with ILES and the hybrid RANS/LES at 50% local chord and 90% half-span.

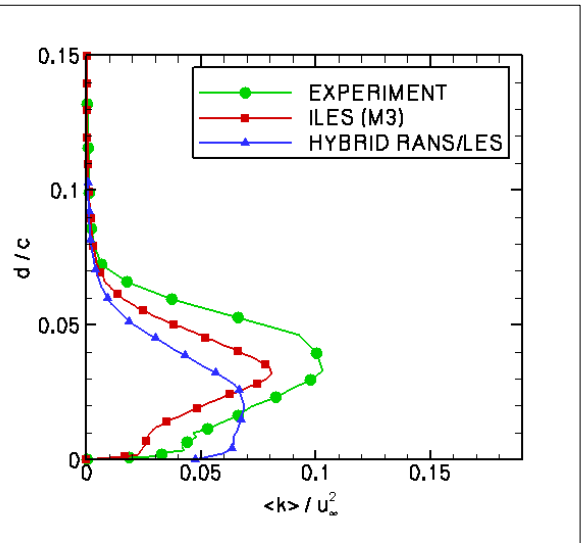

Figure 7: Averaged turbulence energy profiles from the experiments, the results obtained with ILES and the hybrid RANS/LES at 50% local chord and 90% half-span.

A quantitative comparison between the flow field in the experiment of Zhang & Turner [5], the results obtained with the present ILES approach and a hybrid RANS/LES simulation of Li & Leschziner [6] on the finer grid has also been performed. The time-averaged velocity and turbulence energy profiles presented in Figures 6 and 7, respectively, are evidence for the superior quality of the ILES results. Despite the fact that the hybrid RANS/LES has been performed on a much finer grid, it is not able to predict the correct flow physics, i.e. separation, in the fully turbulent wing regions and consequently the turbulence energy profile also disagrees with the experimental data.

 Published by Cranfield University Press ISBN: 978-0-9557436-7-2 http://hdl.handle.net/1826/3832

4. CONCLUSIONS

Results from ILES studies for separated and turbulent wall-bounded flows of practical aeronautical interest, such as the flows around a sharp-edged delta wing and a swept wing featuring a curved leading edge, were presented.

In the delta-wing case, the present results are in good agreement with DNS and ILES is able to capture the correct physics and large-scale dynamics of a non-slender, flat-plate delta wing flow, in an under-resolved grid environment. Regarding the swept wing case, it was found that ILES is significantly more accurate, with respect to available experimental data, in the fully turbulent and separated regions than a hybrid RANS/LES using a grid double the size.

In general, this investigation has demonstrated that Implicit Large-Eddy Simulation can be applied to complex separated flows without any near-wall modification and without resorting to turbulence models.

ACKNOWLEDGEMENTS

The financial support from EPSRC and BAE SYSTEMS are greatly acknowledged.

References

1: Cummings, R. M. and Forsythe, J. R. and Morton, S. A. and Squires, K. D., Computational challenges in high angle of attack flow prediction, Progress in Aerospace Sciences, 2003.
2: Taylor, G. S. and Schnorbus, T. and Gursul, I., An investigaton of vortex flows over low sweep delta wings, 33rd AIAA Fluid Dynamics Conference and Exhibit, 2003.
3: Taylor, G. S. and Gursul, I., Buffeting Flows over a Low-Sweep Delta Wing, AIAA Journal, 2004.
4: Gordnier, R. E. and Visbal, M. R., Compact Difference Scheme Applied to Simulation of Low-Sweep Delta Wing Flow, AIAA Journal, 2005.
5: Zhang, S. and Turner, J., private communication, 2007.
6: Li, N. and Leschziner, M. A., Large-eddy simulation of separated flow over a swept wing with approximate near-wall modelling, The Aeronautical Journal, 2007.

 Published by Cranfield University Press ISBN: 978-0-9557436-7-2 http://hdl.handle.net/1826/3832

The Broad Delta Aircraft - A Viable Solution for Reducing Airframe Noise

S. Mistry, G. Doulgeris, J. P. Fielding

ABSTRACT

This paper describes the challenge of designing a 'silent' and 'green' civil aircraft by integrating airframe and engine technologies. The Cranfield University study describes the design methodologies used to develop a Broad delta aircraft concept, concentrating on designs to reduce airframe noise. Engine noise is not specifically addressed here.

INTRODUCTION

Aviation is considered to be one of the noisiest and greatest polluters of the transport sector [1]; due to the proximity of airports to residential areas [2]. As aviation grows, more passengers want to fly, which increases flight frequency [3], leading to airport expansion. Simply put, this will spiral out of control, as increased flight frequencies suggest more aircraft and noise complaints.

Methods to lower conventional aircraft noise are being investigated [4], so that targets set by the International Civil Aviation Organisation (ICAO) can be met. Airframe noise reduction technologies provide little benefit on existing aircraft, and long-term solutions are required, as enforcement of noise limits could potentially ground noisy aircraft.

Airframe noise is caused by surface interference/obstructions to airflow; the main contributors being undercarriage, leading and trailing edge devices, and empennage [5]. Options are limited for reducing noise on the current 'tube and wing' configuration, hence, new airframe designs are sought, such as the broad delta airframe. This work will not address engine noise but will show how quiet engines designed by G. Doulgeris will be incorporated into a broad delta (BD).

SCOPE AND RESEARCH QUESTIONS

Research objectives are to develop novel airframes and propulsion concept design methodologies. An efficient-quiet aircraft requires careful integration of airframe and power-plant. The main objective is to design a low noise, socially, economically, and environmentally viable future airliner; for which aircraft noise meets a 60dB(A) target.

 Published by Cranfield University Press ISBN: 978-0-9557436-7-2 http://hdl.handle.net/1826/3832

BROAD DELTA (BD) DESIGN METHODOLOGY

The Cranfield silent aircraft design process is divided into two main areas, where this paper refers to the airframe design, whilst engine topics are described in a 2nd paper "The Broad Delta Aircraft; Silent Propulsion Systems Design & Integration", by G. Doulgeris. A baseline aircraft was designed, comparable to existing aircraft; with a specification of 216 passengers in a three-class arrangement, with a cruise Mach of 0.8, and range of 4,000 nautical miles. This was to be used in comparison with the BD and other concepts.

BD CONCEPT DESIGN

The BD is similar to the baseline [6] as it has a conventional fuselage but has a low aspect ratio delta wing, making it a promising configuration. Two variants of the BD were designed to investigate how a stabilising tail surface would affect the BD noise and performance (Figure 1).

The BD concepts used a similar methodology as the baseline, driven by parametric analysis [7] and iterated for a minimum mass optimised design. Results for this low aspect ratio wing were cross referenced with military aircraft, as, there are no civil BD aircraft flying to date. Methods used to determine aircraft drag and performance [8,9,10], fuselage layout [11], wing [12] and undercarriage design [13], mass estimations [7,12], stability and control [7,11,12], and tail volume coefficients [7,11,12] were researched.

ALTITUDE SELECTION FOR CRUISE OPTIMISATION

A trade study identified the optimum cruise altitude by varying cruise Mach number, altitude, and density. Mach numbers varied between 0.8 and 0.85, and cruise climb cases were considered starting from 35,000ft to 46,000ft, providing mass optimized solutions for the BD concepts (Figure 2). The optimum cruise climb altitude started at 37,000ft, ending at 42,000ft. The BD design uses four moderate by-pass ratio (BPR=8) turbofan engines, with cruise specific fuel consumption (SFC) of 15.85 mg/N/s, and a design SFC of 8.77 mg/N/s. Four engines reduce asymmetric thrust for an engine out scenario, and reduce engine diameter, aiding the integration process to embed engines within the wing.

LIFTING SURFACE DESIGN

The tailless BD concept (Figure 1) has its aerodynamic centre located close to, but aft of the centre of gravity location, to avoid pitch-up. Four aerofoils (Figure 3) are used in the wing design,

 Published by Cranfield University Press ISBN: 978-0-9557436-7-2 http://hdl.handle.net/1826/3832

where similar methods to Hileman et al.[14,15,16], were used for leading edge (LE) carving of inboard aerofoils; generating a positive pitching moment, instead of using trailing edge (TE) reflex. The selected airfoils were modified from existing published aerofoil data [17], with outboard sections designed with laminar flow, Figure 4. Low aspect ratio wings have higher induced drag compared to high aspect ratios, wing tip winglets were introduced to reduce induced drag, as shown in Figure 5. They were designed using the method from McCormick † [18]. The drag reduction from the new wing-winglet design was used to re-optimise the BD design.

Trade studies were completed to alter the design of the BD based on new engine technology and approach conditions. An investigation to change the approach flight path angle (FPA) was completed. It determined the impact on the wing design, from 3 to 6degree FPA, and increasing the engine BPR; a total of four cases were investigated:

- Tailless BD, 3degree FPA, BPR =8,
- Tailless BD, 6degree FPA, BPR=8,
- Tailless BD, 6degree FPA, BPR=20,
- V-tail BD, 6degree FPA, BPR=20.

Increasing FPA alters the design mass, loading, and approach velocity, reducing the approach velocity from 60m/s (117knots) to 55m/s (107knots). The main benefit is, increasing the distance of the aircraft from the ground, thus lowering the noise on approach.

BD FUSELAGE DEVELOPMENT AND DESIGN

The BD fuselage is a conventional design, with a single-deck passenger compartment layout [11], and generates significant drag. Generating lift from leading edge (LE) carvings [14,16] could be used at the nose of the fuselage as shown in Figure 6.

Attached to the lower fuselage is a twin nose wheel, with the main undercarriage located within the wing. It consists of two 4 wheeled bogies, retracting inwards into the main wing-fuselage blister region. Wing-fuselage blisters are generally used to accommodate the undercarriage, but for the BD concept the blister is solely required to provide a smooth fairing between the wing and fuselage as shown in Figure 7.

CENTRE OF GRAVITY LOCATIONS

† McCormick, [47], 'is a rare source, describing the drag and performance benefits of winglets on an aircraft wing, and provides data that is difficult to find for winglet design; based on 1st generation transport aircraft, pg 215 onward.

 Published by Cranfield University Press ISBN: 978-0-9557436-7-2 http://hdl.handle.net/1826/3832

Major equipment and systems components were positioned across the BD airframe. Aircraft centre of gravity is in the range of 16-26% of mean aerodynamic chord (MAC), where a typical aircraft c.g. range varies from 15-35% MAC [7,11,12]. A c.g. range for a typical flight of 4000 nautical miles, cruising at 37,000ft, provides a 19.8-25% c.g. range.

STABILITY AND CONTROL (SC)

Longitudinal SC for each BD concept has been calculated [7]. The tailless BD has a -2% stick-fixed stability margin, and the V-tail BD has +4%. The tailless BD has SC implications which can be solved by an active control system. Lateral stability is outside the scope for these conceptual designs, however control surface sizing was addressed [7,11].

RESULTS - AIRFRAME NOISE

A steep FPA is preferred because a lower approach velocity is achieved, reducing noise; where noise is proportional to V^n, and typically 'n' has a value of 5 or above. The absence of a tail implies that TE flaps and LE slats are not possible, removing three airframe noise sources, at the expense of the requirements for a larger wing area. The V-tail BD has a tail, but by using variable camber (slot-less) flaps, and drooped LE slats, approach noise will also be low. Fairing the undercarriage provides noise shielding of around 8-10dB(A) [19]. Airfoil self noise can be reduced using TE brush technologies, claiming to reduce noise by as much as 2dB(A) [14,20,21].

Utilising current technologies and increasing FPA from 3 to 6degrees for the tailless BD reduces airframe noise from 80.6dB(A) to 73.5dB(A), whereas the V-tail BD reduced noise further to 72dB(A) for a 6 degree FPA.

The BD airframe noise exceeds the noise target, of 60dB(A), but implementation of novel technologies, such as undercarriage fairings and TE brushes, could reduce noise by 10-14dB(A); lowering approach noise. A further reduction is achievable using a 1km displaced landing threshold where the baseline results suggest a noise reduction of 5dB(A) [6].

A tabulated design summary for both BD airframe concepts is shown in Figure 8. Lift-to-drag ratios in excess of 20 provide optimistic results for a clean airframe configuration without engines nacelles. Further analysis is required to predict installed engine and nacelle drag. BD airframe noise analysis using the validated baseline methodology [6] suggests that noise targets can be achieved with the addition of novel technologies.

 Published by Cranfield University Press ISBN: 978-0-9557436-7-2 http://hdl.handle.net/1826/3832

ENGINE INTEGRATION

The ideal low noise propulsion system identified for the BD was a constant volume combustor (CVC) turbofan. The layout was customised to maximize engine noise shielding of the airframe; providing forward and rear fan noise shielding of up to 15 dB for the take-off noise measuring case [22]. Considerable noise reduction could be achieved by jet noise deflection by the wing, which is a further study described in Wong [23].

Airframe noise is dominant over engine noise for both take off and landing; where the BD with 6degree FPA combined with CVC, BPR 20 turbofan has a total aircraft noise of 71dB(A), in comparison with the CVC installed in the BD V-tail producing 68dB(A) (

Figure 9). All engine cycles provide significant noise improvements, compared with the baseline design.

Integration challenges are the installation, maintenance, and passenger safety concerns. Placing engines on the upper surface increases wing shielding effect and avoids ingestion of foreign objects from the ground (

Noise dB(A)	*BD 3 deg BPR=8*	*BD 6 deg BPR=8*	*BD 6 deg BPR=20*	*BDVT 6 deg BPR=20*
Baseline engine	77.1	72.6	72.5	71.5
UHBPR engine	76.2	70 .3	70.2	69.1
Recuperated engine	76.5	70.1	69.5	68.8
CVC engine	76.5	70.2	70.1	68.8

Figure 10). Maintenance provides challenges for accessibility, inspection and removal, increasing cost of ownership and servicing.

CONCLUSIONS

This paper presents a noise driven parametric analysis on a BD airframe concept and the integration of propulsion systems. Advantages and challenges of each configuration have been assessed, and the most 'quiet' airframe technologies have been identified. Airframe performance has identified the V-tail BD with CVC turbofans as the quietest concept.

 Published by Cranfield University Press ISBN: 978-0-9557436-7-2 http://hdl.handle.net/1826/3832

REFERENCES

1. Greener by Design, Air travel – greener by design: The technology challenge, 2001.
2. Berglund, B., Lindvall, T. Schwela, D. H. Guidelines for community noise, World Health Organisation, 1999.
3. Department for Transport, The future of air transport, UK Government, 2003.
4. ACARE, European aeronautics: A vision for 2020, Advisory Council for Aeronautics Research in Europe, 2000.
5. Smith M J T. Aircraft noise. Cambridge, 1989, NY.
6. Doulgeris, G., Mistry, S., Fielding, J. P. , Pilidis, P., Development of a Broad Delta Airframe and Propulsion Concepts for Rducing Aircraft Noise around Airports, SAE AeroTech 2007 Congress and Exhibition, 17-20 September 2008, Los Angeles.
7. Howe D. Aircraft conceptual design synthesis, PE Publishing, 2000, UK.
8. Hoerner, S. F. Fluid-Dynamic drag; practical information on aerodynamic drag and hydrodynamic resistance, Hoerner, 1965, New Jersey.
9. Pamadi, B. N. Performance, stability, dynamics, and control of airplanes, AIAA Education series, 1998, Virginia.
10. Katz, J., Plotkin, A. Low-speed aerodynamics, 2nd edition, Cambridge University Press, 2001, UK.
11. Jenkinson, L. R., Simpkin, P., Rhodes, D. Civil jet aircraft design, Arnold Publishers, 1999, UK.
12. Raymer, D. P, Aircraft design: a conceptual approach, AIAA education series, 1992, Washington DC.
13. Messier-Dowty, Landing gear design intensive short-course, Course notes, Cranfield University, UK.
14. Hileman, J. I., Spakovszky, Z. S., Drela, M., Sargeant, M. A., Airframe design for "silent aircraft", 45th AIAA Aerospace Sciences Meeting and Exhibit, 8-11 January 2007, Reno, Nevada.
15. Hileman, J. et al., Multidisciplinary design and optimisation of the silent aircraft, 44th AIAA Aerospace Sciences Meeting and Exhibit, 9-12 January 2006, Reno, Nevada.
16. Hileman, J. et al, M. A., Aerodynamic and aeroacoustic three-dimensional design for a "silent" aircraft, 44th AIAA Aerospace Sciences Meeting and Exhibit, 9-12 January 2006, Reno, Nevada.
17. Harris, C. D., NASA supercritical airfoils; A matrix of family-related airfoils, NASA Technical Paper 2969, Langley Research Centre, 1990, Virginia.
18. McCormick, B. W. Aerodynamics, aeronautics, and flight mechanics, John Wiley & Sons, Inc., 1979, New York.
19. Quayle, A. et al., Landing gear for a silent aircraft, AIAA-2007-231, 45th AIAA Aerospace Sciences Meeting and Exhibit, Reno, Nevada.
20. Lui, Y. et al., Experimental study of surface roughness noise, AIAA-2007-3449, 45th AIAA Aerospace Sciences Meeting and Exhibit, Reno, Nevada.
21. Herr, M., Dobrzynski, W., Experimental investigations in low noise trailing edge design, AIAA-2004-2804, 10th AIAA/CEAS Aeroacoustics Conference, Manchester, 2004.
    A. Agarwal, A.P. Dowling, Low frequency acoustic shielding of engine noise by the silent aircraft airframe, AIAA 2005-2996, 2005
22. R.L.M. Wong, Experimental and analytical studies of shielding concepts for point sources and jet noises, PhD thesis, University of Toronto, 1982.

 Published by Cranfield University Press ISBN: 978-0-9557436-7-2 http://hdl.handle.net/1826/3832

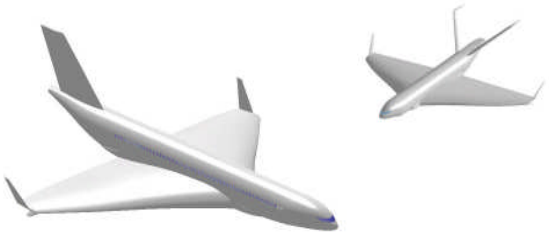

Figure 1 – BD Concepts - Tailless (left), and V-Tail (right).

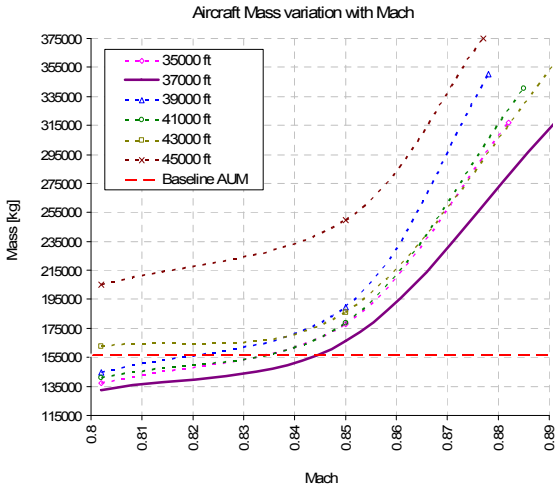

Figure 2 – BD Altitude study comparing flight Mach to Aircraft All Up Mass (AUM).

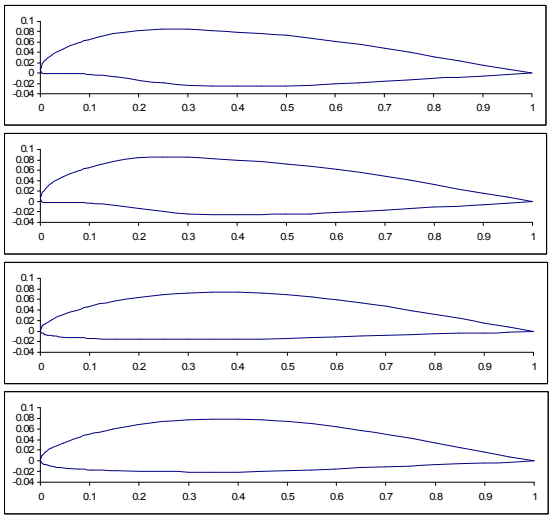

Figure 3 – BD airfoil designs, top to bottom: Root - NACA-23011 (t/c=11%), kink1 - NACA-63A0(10.5) (10.5%), kink2 - NACA-63A009 (9%), tip - NACA-63A010 (10%) airfoils.

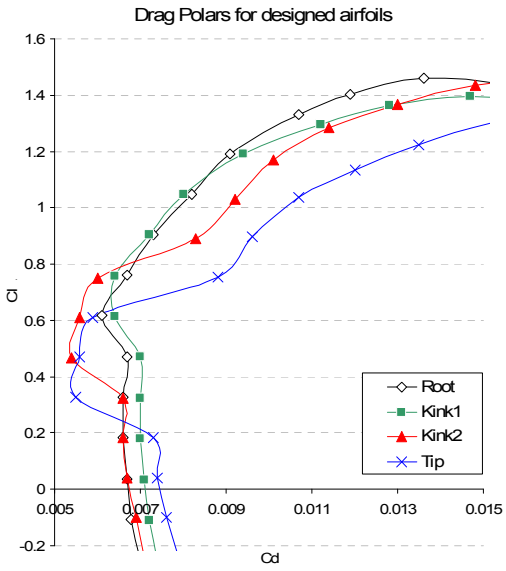

Figure 4 – Designed airfoil drag polar, showing laminar buckets for outboard airfoils (right).

 Published by Cranfield University Press ISBN: 978-0-9557436-7-2 http://hdl.handle.net/1826/3832

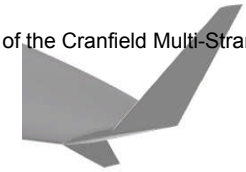

Figure 5 – Winglet design

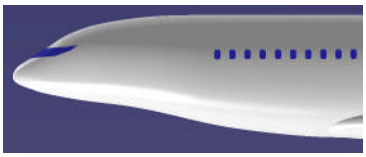

Figure 6 – Fuselage nose design with LE carving.

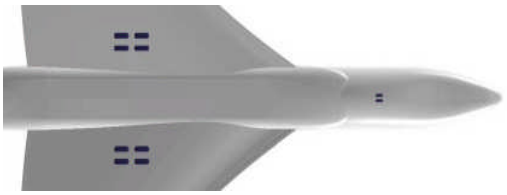

Figure 7 – Underside of BD concept, showing main and nose undercarriage, and wing-fuselage blister.

	BD V-Tail Concept		***BD Tailless Concept***	
	[S.I]	***[British]***	***[S.I]***	***[British]***
Operational empty Mass	**79,373 kg**	174,988lb	**88,784 kg**	195,735 lb
M of fuel for range	**27,891 kg**	61,490 lb	**34,517 kg**	76,096 lb
Overall aircraft M (AUM)	**131,024 kg**	288,859 lb	**147,061kg**	324,213 lb
Lift to Drag Ratio	**24.7**	24.7	**21.7**	21.7
Static Wing Loading	**1846.9 N/m^2**	38.6 lbf/ft^2	**1841.3 N/m^2**	38.4 lbf/ft^2
Static Thrust Loading	**0.256**	0.256	**0.278**	0.278
Wing area	**696.0 m^2**	7491.3 ft^2	**783.5 m^2**	8433.4 ft^2
Wing span	**46.5 m**	152.6 ft	**49.4 m**	162.0 ft
Wing mean aero chord	**15.0 m**	49.1 ft	**15.9 m**	52.1 ft
Wing aspect ratio	**3.11**	3.11	**3.11**	3.11
Quarter chord sweep	**31.1 deg**	31.1 deg	**31.1 deg**	30.1 deg
Wing taper ratio	**0.528**	0.528	**0.528**	0.528
Avg. thickness-chord ratio	**0.101**	0.101	**0.101**	0.101
Wing apex from nose	**15.0 m**	49.2 ft	**13.0 m**	42.7 ft
(EQ) Horizontal stab Area	**186.9 m^2**	2,011.7 ft^2	**-**	-
(EQ) Vertical stabilizer Area	**80.5 m^2**	886.3 ft^2	**142.1 m^2**	1529.9 ft^2
Total static thrust	**329,638 N**	74,106 lbf	**401,518 N**	90,265 lbf

Figure 8 – Tailless & V-tail BD design data; both with BPR=20 and designed for 6 deg FPA

Figure 9 – Approach aircraft noise.

Noise dB(A)	*BD 3 deg BPR=8*	*BD 6 deg BPR=8*	*BD 6 deg BPR=20*	*BDVT 6 deg BPR=20*
Baseline engine	77.1	72.6	72.5	71.5
UHBPR engine	76.2	70 .3	70.2	69.1
Recuperated engine	76.5	70.1	69.5	68.8
CVC engine	76.5	70.2	70.1	68.8

 Published by Cranfield University Press ISBN: 978-0-9557436-7-2 http://hdl.handle.net/1826/3832

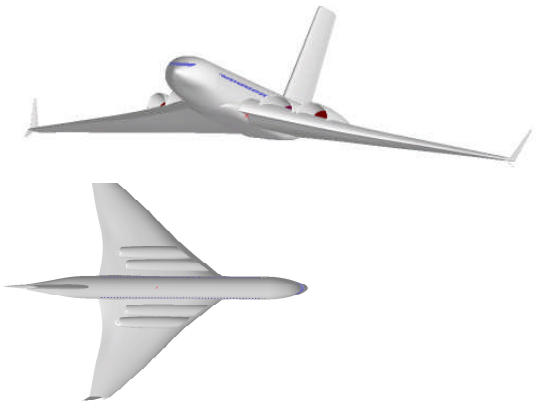

Figure 10 – BD concept design with installed UHBPR engines semi-embedded in wing root region.

 Published by Cranfield University Press ISBN: 978-0-9557436-7-2 http://hdl.handle.net/1826/3832

Sand Transport Characteristics in Horizontal Multiphase Pipeline

W. Van [1], S.Al-lababidi [1], H. Veung [1]

Process and Systems Engineering Group, Cranfield University, UK.
P. Sugarman [2] and P. Fairhurst[2] .BP E&P, UK.

ABSTRACT

With the advent of subsea tiebacks and horizontal wells, sand transport in multiphase pipeline is of key interest for oil and gas companies. This paper presents experimental works to investigate the sand behaviour and minimum transport condition in water and in two-phase air/water flows. In this work, the minimum sand transport condition in two-phase air/water flow was defined based on the definition of "minimum transport condition" proposed by Thomas (1961) for water flow. The under-going investigations were undertaken in a 2-inch horizontal pipeline loop. The sand transport characteristic under water and two-phase air/water flows was determined by visual observation. The concentration effect on minimum sand transport condition was also studied. The sand volume concentration used ranges from 0.0016% (15lb/1000bbl) up to 0.053% (500lb/1000bbl). The sand transport characteristic map for transported and non-transported regions was developed for two-phase air/water flows in horizontal and uphill pipelines.

INTRODUCTION

Sand from wells represents an increasing problem for efficient exploitation of oil and gas reservoirs. For oil and gas reserves contained in sandstone reservoirs sand production is likely to become a problem at some point during the life of the field. Sand production occurs during the hydrocarbon production from a well when the reservoir sandstone is weak enough to fail under the in situ stress conditions and the imposed stress changes due to the hydrocarbon production. As a result, the oil or gas flow transports the failed rock causing a variety of problems such as sand deposition, blockage, corrosion and erosion.

Extensive studies have been done to study the sand transport velocity in both slurry pipelines and extremely diluted system (Oudeman, P., 1993; Salama, M.M., 2000; Stevenson, P., Thorpe, R.B., 2001;). King (2000) proposed a method to predict "minimum sand transport condition" (Thomas, 1961) –"*The mean stream velocity required to prevent the accumulation of a layer of sliding particles on the bottom of horizontal pipe".* This method was based upon a series of equations derived by Thomas for calculating the friction velocity at the limit of transporting solids in a liquid/solid system, and was derived from the settling laws for a single particle in a single-phase medium. The friction velocity is related to the pressure gradient. The prediction was extended to sand transport in multiphase systems by estimating an equivalent pressure gradient under multiphase flow conditions to that required to transport sand in the liquid/solid system. However, the effect of sand concentration is not considered in King's model.

EXPERIMENT SETUP

Figure 1 shows the schematic drawing of two-phase air/water facility, which was designed and constructed using ABS plastic (class E) pipe of 50 mm inner diameter. The pipe length is 17m. The test section consisted of 1200mm observation section and a differential pressure transducer which was placed over a distance of 2170mm. Water was pumped to the flow loop using a centrifugal pump and metered using an electromagnetic flow meter ABB

 Published by Cranfield University Press ISBN: 978-0-9557436-7-2 http://hdl.handle.net/1826/3832

K280/0 AS model with 0 - 20 m^3/h range. Air was supplied from a screw engineering compressor, which had a maximum supply capacity of 400 m^3/ hr free air delivery and a maximum discharge pressure of 10 barg. Air flow was metered by a pair of gas flowmeters, including 0.5-inch thermal flowmeter ranging from 0 to 2 m^3/hr and 1-inch vortex flowmeter ranging from 3 to 100m^3/hr. A sand feeder unit was installed after the mixing point of water and air.

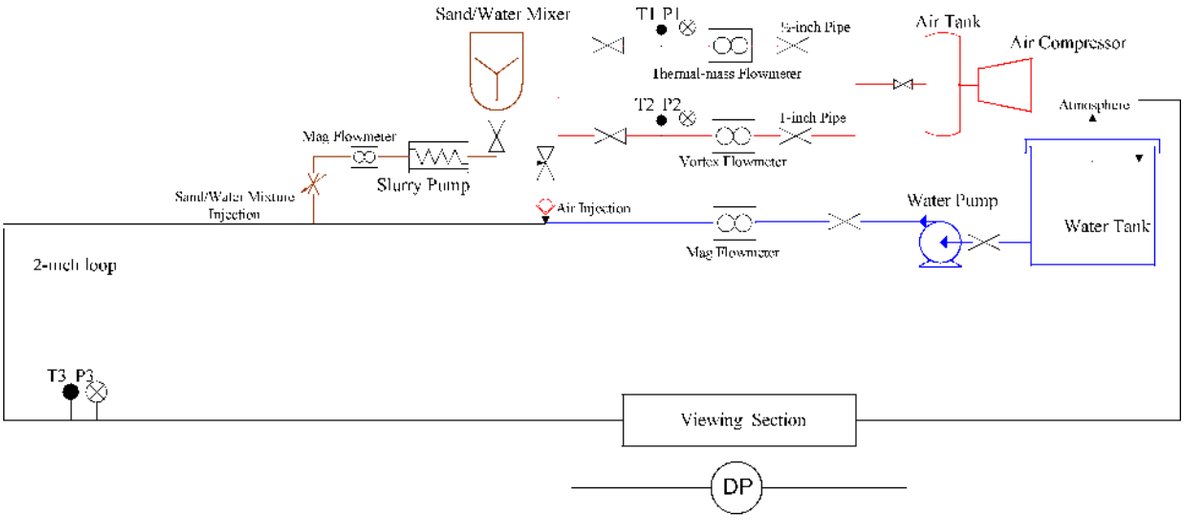

Figure 1: 2-inch two-phase air\water facility

The sand feeder unit consisted of a cylindrical stirred vessel (290 mm diameter times 500mm high), with a 200mm diameter axial flow impeller, and slurry pump (0.5 m^3/ hr) for injecting water/sand mixture into the flow loop. A data acquisition system was installed in the system to monitor water and air volumetric flowrates, line pressure, differential pressure and temperature. A mixture of two types of sand (HST 50 and HST 95) was used in the experiments, with the average diameter of 200 micron and a mixture density of 2650 kg/m^3: The in-situ sand volume concentrations studied varied from 0.0016% (15lb/1000bbl) up to 0.053% (500lb/1000bbl).

RESULTS AND DISCUSSION

Sand Transport Characteristics in Horizontal Water Flow

It was found that the sand transport characteristic changed with the change of water velocity. By

reducing the water velocity from 1 ms^{-1} to 0 ms^{-1}, the minimum sand transport conditions was achieved at a water velocity of 0.5 ms^{-1}. The sand particles started to slide and deposit on the bottom of the pipe as further decreasing the water velocity. Eventually the sand dunes were observed when the water velocity was 0.3ms^{-1}, as shown in Figure 2.

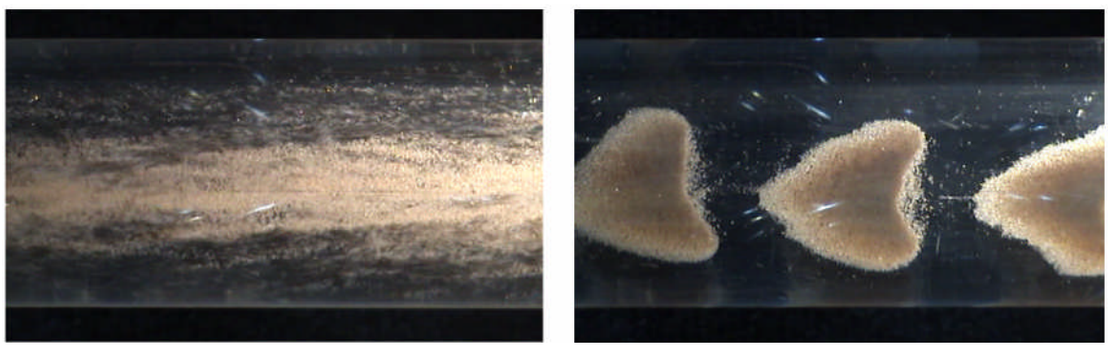

a) water velocity at 0.5 ms^{-1} b) water velocity at 0.3 ms^{-1}

 Published by Cranfield University Press ISBN: 978-0-9557436-7-2 http://hdl.handle.net/1826/3832

Figure 2: Sand flow pattern in single phase water flow

Also, it was observed that the sand patterns in water flow changed with sand concentrations. When the sand concentration was greater than 0.0053% volume concentration (50lb/1000bbl), sand particles were transported in the form of a sliding bed while the particles were moving in the form of streak lines when the sand concentration was less than 50lb/1000bbl.

SAND TRANSPORT CHARACTERISTICS IN HORIZONTAL AIR/WATER FLOW

In order to understand the sand transport characteristics under different air/water flow conditions, the flow regime characteristic of the 2-inch test rig was identified prior to the sand experiments. It was observed that the stratified wavy and slug flow were the main flow regimes when sand minimum transport condition occurred in horizontal pipeline. Therefore, minimum sand transport conditions under these two flow regimes were investigated in this work.

SAND TRANSPORT IN STRATIFIED WAVY FLOW

The stratified flow regime was observed at a water superficial velocity, Vsl, of 0.07 $ms^{-1}$and gas superficial velocity, Vsg, below 1 ms^{-1}. In this flow regime no sand particle was observed to be moving. When the Vsg was increased to velocity to above 1 ms^{-1}, the stratified wavy flow was observed.

At sand concentrations of above 0.0 106% volume concentration (100lb/1000bbl), for most of the sand particles, no movement was observed until the Vsg was increased to 6 ms^{-1}, at which point sand dunes were formed in water, as shown in Figure 3-a. At Vsg= 8 ms^{-1}, the scouring sand dunes were formed as shown in Figure 3-b. With increasing the Vsg, the size of scouring sand dunes became bigger. There was a “bridge”, streaks of active moving sand particles, between two sand dunes as shown in Figure 3-c.When the Vsg was increased beyond 9 ms^{-1}, the scouring dunes no longer exist. At Vsg = 10 ms^{-1}, sand dunes were observed to link to each other, and moved as a sliding bed. With further increasing Vsg, all sand particles were observed saltating along the bottom with some particles even suspending in water, as shown in Figure 3-d.

 Published by Cranfield University Press ISBN: 978-0-9557436-7-2 http://hdl.handle.net/1826/3832

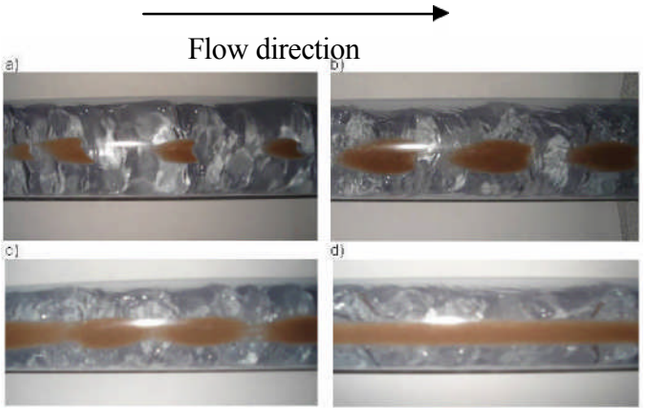

a) sand dunes at Vsg=6 ms^{-1}, b) scouring sand dunes Vsg=8 ms^{-1}

c) sand dunes with bridge Vsg=9 ms^{-1}, d) sliding sand bed Vsg=10 ms^{1}

Figure 3: Sand patterns in stratified wavy flow （ 100lb/1000bbl ）, Vsl=0.07m/s (view from the bottom)

With the sand concentrations lower than 100lb/1000bbl, no sand dunes were observed as the Vsg was increased. At a Vsg ≤ 2 ms^{-1}, several streak lines of sand particles could be observed. By 4 ms^{-1}, all sand particles were observed to move in form of streak lines at the bottom of the pipe. Based on our visual observations for stratified wavy flows, the status of minimum sand transport condition has an analogy with that in single phase water flow. For stratified wavy flows and sand concentrations≥ 100 lb/1000bbl, minimum sand transport conditions could be reached when the Vsg was sufficiently high.

SAND TRANSPORT IN SLUG FLOW

Sand transport was stimulated strongly by hydrodynamic slugs. Figure 4 shows the sand behaviour in slug flow.

 Published by Cranfield University Press ISBN: 978-0-9557436-7-2 http://hdl.handle.net/1826/3832

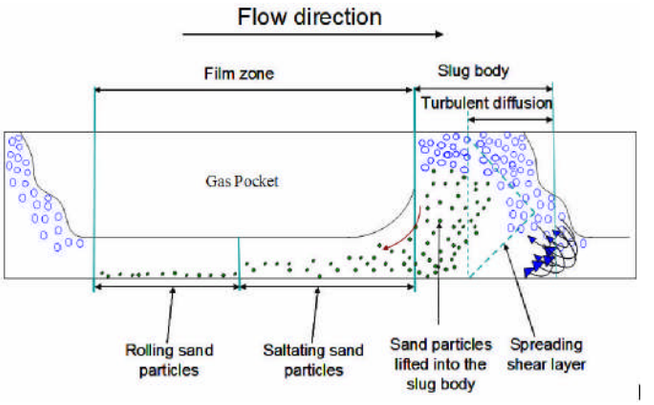

Figure 4: Schematic of sand particles motion in slug flow

Turbulence is generated at the front of the slug, where the pick-up process occurs. Turbulence is enhanced by quickly moving fluid in the slug body picking up the slowly moving fluid in the film region ahead of slug body. The spread of the fluid shear layer from the film to the slug body begins at the slug front. The turbulence is diffused along the direction of the plugging film. The turbulent energy reaches the sand particles settled on the pipe wall and start to lift them into the slug body. Some sand particles are picked up, mainly entrained within the slug body and move forward. Moreover, others begin to saltate or roll along the bottom of the pipe wall due to the fluid shear force acting on the sand particles. At the slug tail, the sand particles begin to shed into the film zone with the water. As the sand particles enter the film zone, their velocities begin to decelerate. The active sand particles roll or bounce at the beginning of the film zone due to the kinetic energy that they obtained in the slug body and eventually the sand particles will settle on the bottom of the pipe in the film zone if the film length is sufficient.

Based on the experimental investigation, the sand minimum transport conditions where the slug flow regime is defined as, *"the condition at which the sand particles will continue to be energetic enough to keep moving and not deposit in the film zone of the slug unit".*

From observations of the experimental sand particles behaviour, the boundary between transport and non-transport regions based on different sand concentrations are identified for two-phase air/water flow in a horizontal pipeline, see Figure 5. Sand particles will transport based on Thomas' definition when the (Vsl, Vsg) is above the boundary lines corresponding to different sand concentrations. It is indicated that minimum sand transport condition mainly occurred in stratified wavy and slug flow regimes and higher kinetic energy of liquid is required when increasing the sand concentration (boundary line shifted up according to the increasing sand concentrations). Also the minimum sand transport condition will be approached at extremely higher Vsg comparing to that in slug flow regime, which is due to the fact that higher liquid film velocity is required to transport the sand particles in the stratified wavy flow.

 Published by Cranfield University Press ISBN: 978-0-9557436-7-2 http://hdl.handle.net/1826/3832

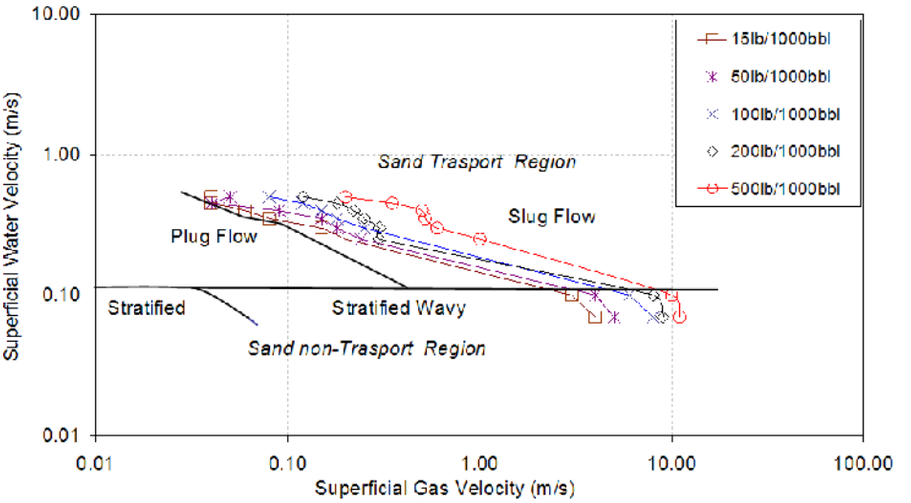

Figure 5: Identified sand boundary transport regions map considering sand concentration effect in horizontal two-phase flow

CONCLUSIONS

The sand minimum transport conditions in water and water/air horizontal flows have been experimentally investigated. In horizontal air/water flow, minimum sand transport condition mainly occurred in stratified wavy and slug flow regimes. Similar sand behaviours were observed in the horizontal pipeline in the stratified wavy flow regime as that in water flow. However, in the slug flow regime, the sand transportation was strongly stimulated in the slug body by the enhanced turbulence generated at the front of slug body, and decelerated due to the shedding process in film region. The minimum sand transport condition will be influenced by the gas supply which can cause the change of flow regime and water flow condition in air/water two phase flow. Sand concentration also has a significant impact on the sand transport condition due to the sand transport characteristics changes with sand concentration accordingly.

REFERENCES

1. Thomas, D., (1961), Transport Characteristics of suspensions Part II . *AIChE J.,* 7, 423-431.
2. Oudeman, P (1993), Sand transport and deposition in horizontal multiphase trunklines of subsea satellite developments, *SPE Production & Facilities,* 237-241.
3. Salama, M.M., (2000), Sand Production Management , *Journal of Energy Resources Technology.,* 122, 29-33.
4. Stevenson, P., Thorpe, R.B., Kennedy, J.E. and McDermott, C., (2001), The transport of particles at low loading in near-horizontal pipes by intermittent flow, *Chemical Engineering Science,* 56, 2149-59.
5. King, M.J.S., Fairhurst, C.P. and Hill, T.J., (2000), Solids transport in multiphase flows – application to high viscosity systems, *Transactions of the ASME, 123, 200-204.*

 Published by Cranfield University Press ISBN: 978-0-9557436-7-2 http://hdl.handle.net/1826/3832

An Analytical Model for Harmonic Content Computation of HFAC Power Distribution Systems

Steven Lourdes, Patrick C.K.Luk, Maciek Bendyk

Power and Drive Systems Group

Department of Aerospace Power and Sensors

Cranfield University –Defence College of Management and Technology

Shrivenham, SN6 8LA, United Kingdom

Contact: Dr. Patrick Luk (Head, Power & Drive Systems Group)

TEL : +44(0) 1793 785528 FAX : +44(0) 1793 785902

Email: p.c.k.luk@cranfield.ac.uk

ABSTRACT

The ever increasing power demand and highly dynamic modern loads have created a need for efficient, reliable, and low cost power distribution architecture. The predominantly used low frequency AC and low voltage DC power distribution systems both have limitations in certain applications. The former requires passive components (inductors, capacitors & transformers) that are physically large, whereas the latter suffers from high copper loss at high power levels. High frequency alternating current (HFAC) power distribution architecture has demonstrated potential benefits compared to conventional power distribution systems in certain application areas. HFAC power converter design however needs to ensure that the harmonics are kept within acceptable limits. In this paper an analytical expression to predict the harmonic content of a synthesized low frequency AC or DC voltage waveform from a High Frequency AC (HFAC) link is presented. High frequency power distribution system is currently considered for various applications ranging from computer power supplies, telecom equipment, building lighting and for power distribution in vehicles for non-propulsion and other auxiliary electric loads.

INTRODUCTION

High Frequency Alternating Current Power Distribution System (HFACPDS) was first proposed by NASA for space application in the early 80s. This was motivated mainly by the inadequacies in the existing DC system at high power levels and the environment imposed limitation on the operating voltage of solar panels [1]. The potential advantages of the HFAC

 Published by Cranfield University Press ISBN: 978-0-9557436-7-2 http://hdl.handle.net/1826/3832

over conventional DC and lower voltage AC distribution system are as follows [1]-[3]: 1) Simpler overall architecture; 2) Ease of power generation; 3) Higher efficiency; 4) Convenient and cheap transformation to various voltages and frequency; 5) Compactness due to the reduction in size of transformers and passive component needed for filtering and temporary energy storage function; 6) Fast system response time; 7) Extra isolation due to use of transformers; 8) Reduction in acoustic noise.

Recent advances in high frequency power electronics devices, magnetic materials and cable technologies, together with successful developments of zero current switching (ZCS) and zero voltage switching (ZVS) schemes, have led to renewed interests in HFACPDS [4]. The modular structure of the HFACPDS promotes point of use regulation by using local Voltage Regulation Module (VRM) that serves as an interface between the load and the HFAC bus. It is imperative that the harmonics of converter output voltage be kept as low as possible to avoid EMI problems in the HFAC power distribution bus [5].

A typical HFACPDS is shown in Figure 1. The input voltage to the converter can be in the form of a DC or low frequency AC voltage. The power converter will generate a HFAC voltage which will be distributed to various loads. Loads are connected to the bus via a VRM that converts the bus voltage to a form that is suitable for each load.

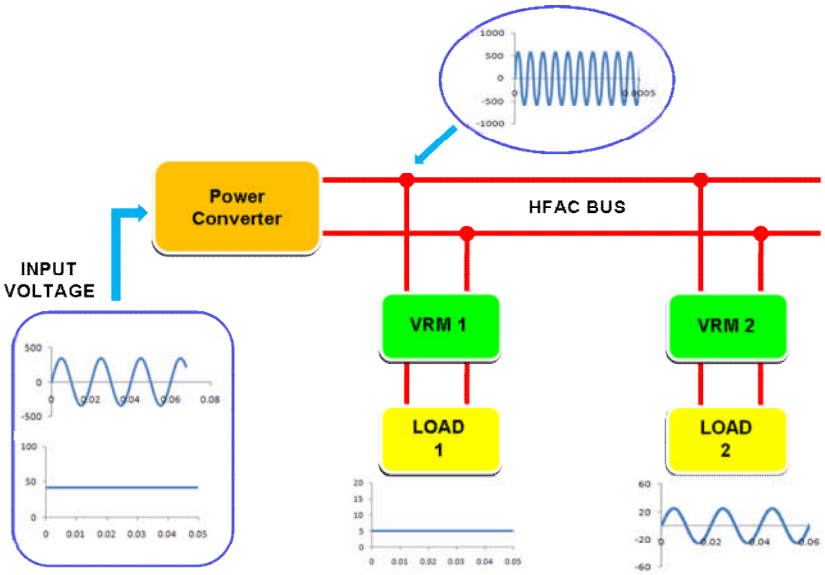

Figure 1. HFAC power distribution architecture

OUTPUT POWER SYNTHESIS

It is possible to directly synthesize a variable amplitude DC and variable frequency AC signals from the HFAC bus frequency [6],[7]. Using a half wave sinusoid as a building block, it is

 Published by Cranfield University Press ISBN: 978-0-9557436-7-2 http://hdl.handle.net/1826/3832

possible to select various switching configurations that would meet the requirement. It is interesting to note that each switching configuration has a unique frequency spectrum.

A simplified equivalent circuit of the secondary stage of a typical VRM is shown in Figure 2. V1 and V2 are both sine waves with the same frequency as the HFAC link but 180 degrees out of phase with respect to each other due to the center tap configuration of the transformer. The switching sequence can be represented as a 1xN matrix as $[m_1, m_2 \ldots\ldots\ldots\ldots m_n]$. Each element in the matrix can take 3 possible values, 1, -1 or 0. Table 1 shows the relationship between the switching matrix element and load voltage (V_{out}). Each element in the matrix, represents the switching state between two zero crossing point. This duration is denoted as T_{HW}. The expression of T_{HW} in terms of the link frequency is given in (1). The relationship between the switching matrix element and switch state is given in Table 2.

$$T_{HW} = \frac{1}{2 f_{HF}} \tag{1}$$

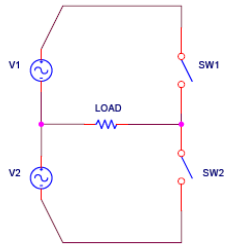

Figure 2. Simplified equivalent circuit of VRM

Table 1 Relationship between switching matrix element and load voltage

Switching Matrix Element	V_{out}
1	$\lvert V_m \sin(2\pi f_{HF} t)\rvert$
0	0
-1	$-\lvert V_m \sin(2\pi f_{HF} t)\rvert$

Table 2 Relationship between switching matrix element and switch states

	Switch Matrix element		Switch Matrix element		Switch Matrix element	
	1		-1		0	
	SW1	SW2	SW1	SW2	SW1	SW2
$0 < t < T_{HW}$	ON	OFF	OFF	ON	OFF	OFF
$T_{HW} < t < 2\ T_{HW}$	OFF	ON	ON	OFF	OFF	OFF
$2\ T_{HW} < t < 3\ T_{HW}$	ON	OFF	OFF	ON	OFF	OFF
$3\ T_{HW} < t < 4\ T_{HW}$	OFF	ON	ON	OFF	OFF	OFF
.						
$(N-1)\ T_{HW} < t < N\ T_{HW}$						

 Published by Cranfield University Press ISBN: 978-0-9557436-7-2 http://hdl.handle.net/1826/3832

HARMONIC CONTENT DERIVATION

For a given switching pattern, an expression of the frame waveform is given by (2). The average output voltage can be calculated using (3),

$$f(t) = V_m \sum_{n=1}^{N} -m_n(-1)^n \sin(2\pi f_{HF} t) \qquad : \left\{ \frac{n-1}{2 f_{HF}} < t < \frac{n}{2 f_{HF}} \right\} \tag{2}$$

$$V_{out} = \frac{2V_m}{N\pi} \sum_{n=1}^{N} m_n \tag{3}$$

where m_n is the nth element of the switching matrix, f_{HF} is the HFAC frequency and V_m the peak voltage of V1 & V2.

Using Fourier analysis, expressions for a_0, a_x, b_x component is given in (4) – (8) as:

$$a_0 = \frac{2V_m}{N\pi} \left[\sum_{n=1}^{N} \left[m_n(-1)^n \cos n\pi \right] - \left[m_n(-1)^n \cos(n-1)\pi \right] \right] \tag{4}$$

For $x = \frac{N}{2}$

$$a_x = \frac{V_m}{N\pi} \left[\sum_{n=1}^{N} \left[-m_n(-1)^n \sin^2 n\pi \right] - \left[-m_n(-1)^n \sin^2 (n-1)\pi \right] \right] \tag{5}$$

$$b_x = \frac{V_m}{N\pi} \left[\sum_{n=1}^{N} \left[\begin{array}{l} \left[-m_n(-1)^n (n\pi - \sin n\pi \cos n\pi) \right] - \\ \left[-m_n(-1)^n ((n-1)\pi - \sin((n-1)\pi)\cos((n-1)\pi)) \right] \end{array} \right] \right] \tag{6}$$

For $x \neq \frac{N}{2}$

$$a_x = \frac{V_m}{N\pi} \left[\sum_{n=1}^{N} \left[\begin{array}{l} \left[m_n(-1)^n \left(\frac{\cos((1+\frac{2x}{N})n\pi)}{1+\frac{2x}{N}} + \frac{\cos((1-\frac{2x}{N})n\pi)}{1-\frac{2x}{N}} \right) \right] - \\ \left[m_n(-1)^n \left(\frac{\cos((1+\frac{2x}{N})(n-1)\pi)}{1+\frac{2x}{N}} + \frac{\cos((1-\frac{2x}{N})(n-1)\pi)}{1-\frac{2x}{N}} \right) \right] \end{array} \right] \right] \tag{7}$$

 Published by Cranfield University Press ISBN: 978-0-9557436-7-2 http://hdl.handle.net/1826/3832

$$b_x = \frac{V_m}{N\pi}\left[\sum_{n=1}^{N}\left[\left[-m_n(-1)^n\left(\frac{\sin((1-\frac{2x}{N})n\pi)}{1-\frac{2x}{N}}-\frac{\sin((1+\frac{2x}{N})n\pi)}{1+\frac{2x}{N}}\right)\right]-\left[-m_n(-1)^n\left(\frac{\sin((1-\frac{2x}{N})(n-1)\pi)}{1-\frac{2x}{N}}-\frac{\sin((1+\frac{2x}{N})(n-1)\pi)}{1+\frac{2x}{N}}\right)\right]\right]\right] \quad (8)$$

The amplitude of the x^{th} harmonic can be computed using (9)

$$\text{Amplitude of the } x^{th} \text{ harmonic } = \sqrt{a_x^{\,2} + b_x^{\,2}} \quad (9)$$

The dc component can be calculated using (10)

$$\text{DC Component } = \frac{1}{2}a_0 \quad (10)$$

RESULTS AND DISCUSSION

The equations derived above were used to calculate the harmonic content of the two synthesized output waveforms. The switching matrices for the waveforms are shown below.

Waveform 1 switching matrix (see figure 3a)

$$[1,1,1,1,1,1,1,1,1,1,1,1,1,-1,-1,-1,-1,0,0]$$

Waveform 2 swithing matrix (see figure 4a)

$$[1,-1,1,1,-1,-1,-1,1,1,1,1,0,0,1,1,1,1,1,1,1]$$

Using (3), the average voltage calculated for both waveforms are equal, as shown in Figures 3b and 4b. The corresponding harmonic content as a result of the variation in switching patterns are shown in Figures 3c and 4c respectively. The amplitude of the harmonics calculated using

 Published by Cranfield University Press ISBN: 978-0-9557436-7-2 http://hdl.handle.net/1826/3832

(4) - (10) were validated against PSIPCE simulation and were found to be in good agreement. Figure 5 shows the comparison.

CONCLUSION

An analytical model to calculate the harmonic content based on the switching pattern has been presented. The calculated values were validated against PSPICE simulation results. These equations provide an efficient method of identifying suitable switching sequence to yield the required output with the acceptable harmonics contents. This has important implications in situations where suppression of particular harmonics is required to keep the overall EMI performance of the system within the required limits. In deriving these equations, constraints of ZVS have been enforced, which allow for lower cost and higher reliability of the VRM module. It is envisaged that these equations could be implemented in a real time system to determine suitable switching sequences for varying output voltage requirement if adequate on board computing resources are available.

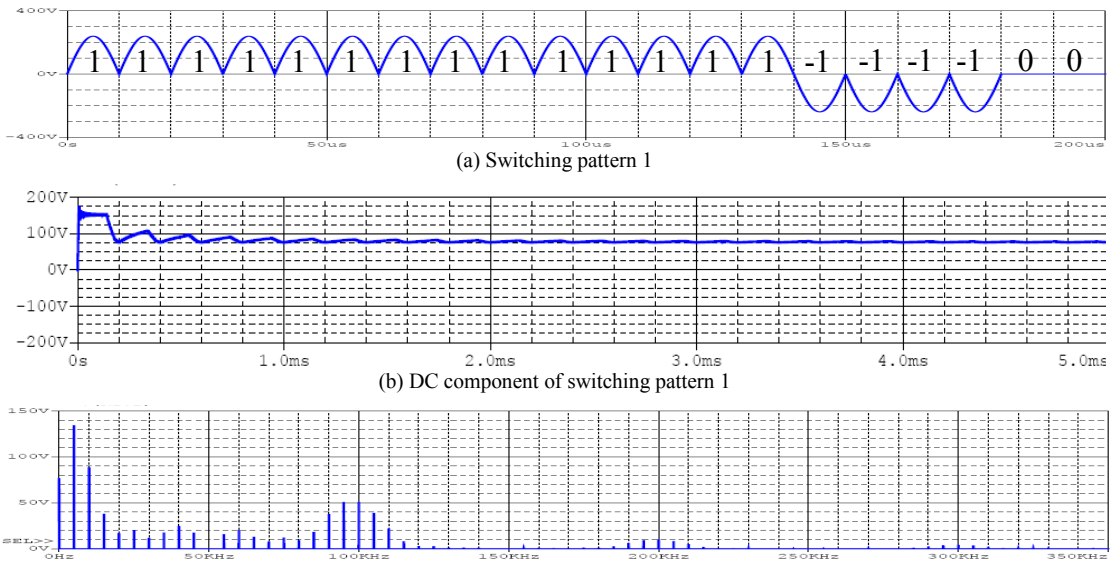

(a) Switching pattern 1

(b) DC component of switching pattern 1

(c) Harmonic spectrum of switching pattern 1

Figure 3. Simulation results for switching pattern 1

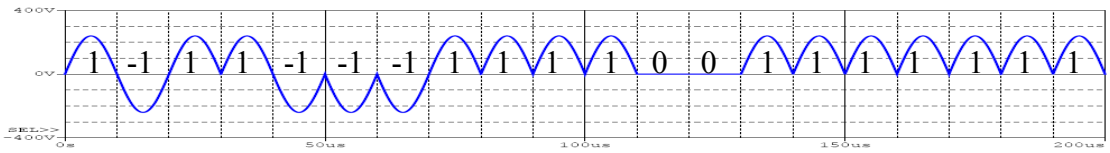

 Published by Cranfield University Press ISBN: 978-0-9557436-7-2 http://hdl.handle.net/1826/3832

(a) Switching pattern 2

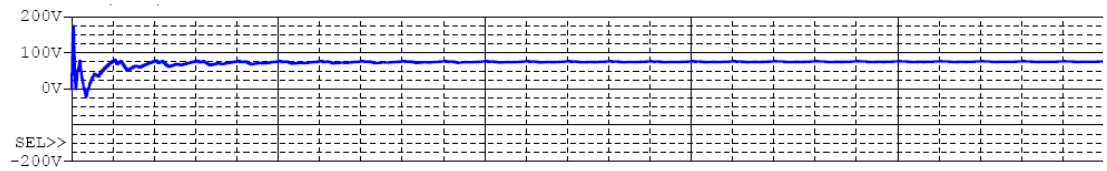

(b) DC component of switching pattern 2

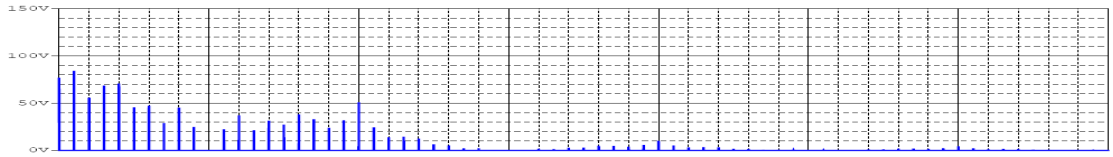

(c) Harmonic spectrum of switching pattern 2

Figure 4. Simulation results for switching pattern 2

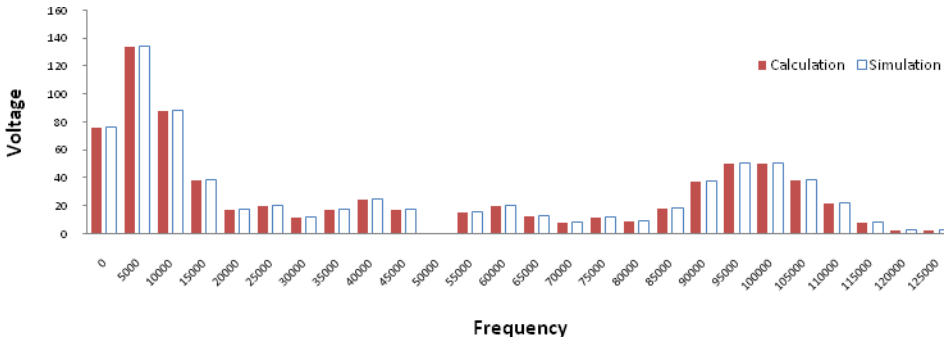

Figure 5. Comparison of calculated harmonic with simulation results (Switching pattern 1)

REFERENCES

[1] Renz, D. D., R. C. Finke, et al. (1983) Design Considerations For Large Space Electric Power Systems. Nasa Technical Memorandum 83064 Volume, DOI: 19830016281

[2] Sood, P. K. and T. A. Lipo (1988). "Power Conversion Distribution System Using a High-Frequency AC Link." IEEE Transactions on Power Electronics 24(2): 288 - 300.

[3] Drobnik, J. (1994). High Frequency Alternating Current Power Distribution. Telecommunications Energy Conference, 1994. INTELEC '94., 16th International, Vancouver, BC, Canada.

[4] Bendyk, Maciek; Luk, Patrick Chi Kwong; Jinupun, Poramaste (Ken), "Direct Torque Control of Induction Motor Drives Using High Frequency Pulse Density Modulation for Reduced Torque Ripples and Switching Losses," *Power Electronics Specialists Conference, 2007. PESC 2007. IEEE* , vol., no., pp.86-91, 17-21 June 2007

[5] Zhongming, Y., P. K. Jain, et al. (2006). A High Efficiency High Frequency Resonant Inverter for High Frequency AC Power Distribution Architectures. Power Electronics Specialists Conference, 2006. PESC '06. 37th IEEE.

[6] Xianmin, M. and Y. Qian (2003). Study and Analysis of Three-Phase High-Frequency AC Cycloconverter Based on Pulse Density Modulation. Sixth International Conference on Electrical Machines and Systems, 2003. ICEMS 2003.

[7] Xianmin, M. (2004). High Frequency AC Pulse Density Modulation Theory and its Application in Hybrid Electric Vehicle Drive System. Power Electronics and Motion Control Conference, 2004. IPEMC 2004. The 4th International.

 Published by Cranfield University Press ISBN: 978-0-9557436-7-2 http://hdl.handle.net/1826/3832

A General Survey of Knowledge Discovery in Storage and File System

ChenHan Liao[1] Frank Wang[1] Na Helian[2] Sining Wu[1]

1 *School ofEngineering*
Cranfield University
Bedford England MK43 OAL
2 *Department of Computing, Communications Technology and Mathematics*
London England N7 8DB

ABSTRACT

Knowledge discovery has been widely applied in many areas, such as finance, marketing and bioinformatics. However, very limited researches have been given to computer system itself. In this paper, we study two recently proposed works, file access pattern analysis and block correlation analysis. We also present an incremental decision tree based predictive model to infer files' future access frequency to improve file caching and prefetching in server environments.

1. Introduction

"That's the thing with magic. You've got to know it's still here, all around us, or it just stays invisible for you."----------Charles de Lint. This is a world flooded with data but staved for knowledge. Although sheer volume of data produced every second in our daily life, we know little about them. Why did they happen? When will they happen again? Knowledge discovery technology answers these questions by inspecting the internal relation of data.

Knowledge discovery is also referred as data mining (DM). It is an automatic mechanism deriving novel and previously unknown knowledge, patterns and rules from large amount of data. The obtained knowledge, patterns and rules are considered as the abstractions of the input data. Knowledge discovery was originally applied for cross basket analysis to identify the purchase pattern of customers. Nowadays, it is broadly applied in industrial areas such as finance, marketing, engineering, life science and bioinformatics. In knowledge discovery process, computers are responsible for digging out useful information along withdedicated knowledge discovery software.

However, computer system itself also yields large amount of data during its operation process. In this paper, we reveal several knowledge discovery methodologies applied in file system and storage system and propose a incremental decision tree based predictive model to benefit file caching and disk layout in server caching environments.

The paper is organized as follows: next section illuminates the caching strategies of file systems, storage systems and their current bottle necks. Section 3 reviews several published works in using knowledge discovery techniques to improve file/storage systems. In section 4, we present an incremental decision tree based predictive model to forecast files' future access frequency and its potential use. The last section concludes.

2. A Brief Discussion of Caching Strategies of File and Storage System

2.1 File system

The gap between CPU and I/O system is being constantly enlarged every few months. To smooth the gap, modern file systems normally maintain a certain sized area in main memory (RAM) to remain those recently used files for future access. This can avoid slow hard disk access and increase data response time. The area maintained in main memory is named cache or buffer cache. Caching strategy or caching policy is responsible for selecting potentially active files to stay in cache and deleting those inactive ones to save expensive memory room. A good caching strategy has relative high hit ratio, which means the files requested have very good chance to be

 Published by Cranfield University Press ISBN: 978-0-9557436-7-2 http://hdl.handle.net/1826/3832

found or hit in cache.

Traditionally, two typical caching strategies are widely adopted in file systems, least recently used (LRU) and least frequent used (LFU). In LRU, a recency recorder is established in cache to fetch the last time of the files accessed. Once the cache is full, the least recently accessed files are evicted from cache area. In LFU, it introduces a frequency counter in cache to record the frequency of files accessed. Once the cache is full, the least frequently accessed files are evicted from cache area. Both caching strategies work very well in stand alone PC since the access pattern of files and user behaviors are relatively stable compared with server cache and multi-user cache.

Some dedicated file systems may use different file system policies to maximize their performance. One of heuristics is the Fast File System (FFS) [5]. It was designed to handle files in different manners regarding to their size. It places small files on disk so that they are near their metadata. Furthermore, it assumes that files in the same directory are most likely accessed together in a short period.

In addition to file size, other properties such as access type: write-mostly or read-mostly, have been confirmed useful to design various file system policies. For example, Log-structured File System (LFS) [14] proposed by John K. Ousterhout and Fred Douglis, treats the disk as a circular log and writes sequentially to the head of the log. The design of log-structured file systems is based on the hypothesis that write latency is the bottle neck of modern file systems. As a result, a Hybrid file system structure designed against the nature of read and write has been found useful to form high performance file system [12].

2.2 Storage system

Storage systems are very slow component in computer system compared with other components such as CPU and RAM. This is due to the mechanic feature of hard disks. For each disk access, disk head has to reposition and rerotate the disk plates. By moving the disk arms and rotating the plates, disk head can position at the right track point to access data. The figure below is the inside structure of a modern hard disk.

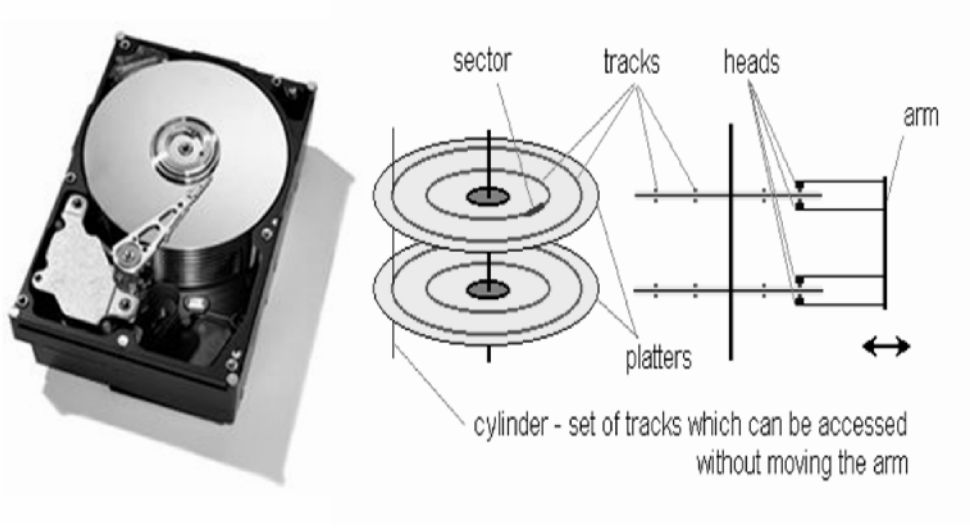

Figure 1. An inside view of modern hard disk

It is easy to conclude that data on the outer tracks can be transferred faster than inner tracks due to the linear velocity. Another fact is that data in the same cylinder can be transferred all together faster, because disk arms do not need to move during access. Therefore, for certain type workloads, storage systems may managetheir data to be benefited from these features.

However, disk requests are always unpleasant compared with data access from caches. To avoid direct disk accesses as much as possible, disks also contain a disk cache, although it is very small compared with file system cache. In storage system,

 Published by Cranfield University Press ISBN: 978-0-9557436-7-2 http://hdl.handle.net/1826/3832

the miss hit file requests in file system cache are delivered to storage system cache to see if requested data is in there. In case that both caches do not contain requested data, the actual disk requests will be issued, which is not what we want to meet every time. Similar to file system caching strategy, LRU and LFU are also the main solutions for disk caches.

3. File Access Pattern and Block Correlation

3.1 File Access Pattern

File access patterns commonly exist in file systems especially for PCs. It refers the logical relation ships between files accessed. In application level, programs or software invoke multiple files during their sessions to complete the jobs. These files are logically related to each other, once file A is invoked, file B may be invoked in a short time since they are always correlated. For example, if a user opens a C++ program editor, .cpp files and .h files are always related together.

To identify file access patterns, knowledge discovery techniques are commonly adopted. Griffioen and Appleton [1] originally developed a probability graph model, which records access frequency in a window of a specified length. Each node in the window represents a unique file. If file A is requested, the count if the node will be increased by 1. For following file access, and edge connected to that file is incremented. The model maintains one node for each file, and one edge for two related files. Due to the unordered nature, the complexity of this model is O (n^2). The figure below shows a sample probability graph.

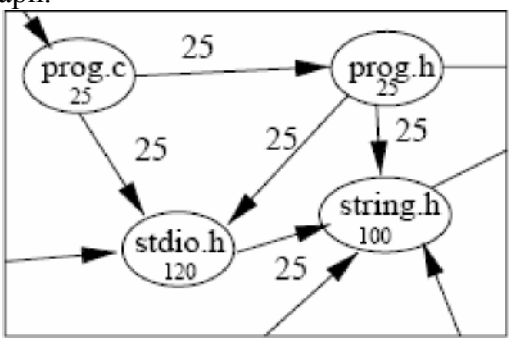

Figure 2. A simple probability graph

Another knowledge-discover model was adopted to improve the bottle neck ofprobability graph. Finite multi-order context model was introduced to solve text compression problem. The model uses a trie tree data structure to efficiently store file sequence. Each node in the tree contains a file name. From root of tree to each node, every branch represents a monitored pattern. The figure below shows the development of the model when given file access sequence CACBCAABCA.

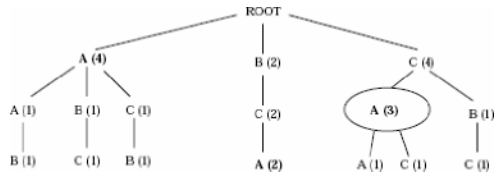

Figure 3. A simple tire tree for storing file access sequences

Circled A represents the pattern CA, which has accessed three times. The complexity of this model is O(n^m), where m is the highest order tracked and n is number of unique files.

With file access patterns observed, we can prefetch the related or subsequent files once the first file access is captured. Also, caching those related files in cache can increase cache hit ratio as those files have very good chance to be accessed in future. Furthermore, file access patterns can be used for computer system intrusion detection. When system detects unusual file access patterns, which involve sensitive files, system can stop the access privilege of that user.

3.2 Block Correlations

Block correlations are common semantic patterns in storage system. Similar to file access pattern, block correlation refers the relationship of data blocks in storage level. Block correlations can be used to improve disk caching, prefetching and disk layout. Z. Li, et al [17], introduced C-Miner based on a knowledge discovery technique frequent sequence mining to uncover block correlations in storage systems.

In storage systems, two or more blocks are correlated if they are semantically linked together. For example, a file's directory block "/dir" is directly correlated to its inode block, which is also correlated to its data block. Compared with file access pattern, block correlations are more stable, because

 Published by Cranfield University Press ISBN: 978-0-9557436-7-2 http://hdl.handle.net/1826/3832

block correlations do not depend on user behaviors and workloads.

In C-Miner, a full block access trace is split by a predetermined time gap. This serves the purpose that only closed block access pattern are meaningful to us. Then, it uses a knowledge discovery algorithm called CloSpan [3] to find out all the frequent block access patterns within the subsequence of the trace. The observed frequent patterns are converted to readable rules, for example, if ABC is frequent block correlation with 90% confidence, then next time once block A is accessed□block B and C will be accessed with 90% chance. Disk cache can choose to prefetch block B and C into disk cache to reduce two extra disk accesses.

Block correlations can also be used for disk scheduling and disk layout. As we discussed in section 2, blocks on outer tracks and same cylinders can be transferred much faster than in inner tracks and different cylinders. Therefore, with observed block correlations, we can put frequent block correlations on out tracks and same cylinders as much as possible to increase data transfer efficiency.

4. Incremental Decision Tree Based File Access Frequency Prediction

Besides above heuristics, we noticed that file access frequency is also useful. A data file that is currently being heavily accessed by users is a high frequency file. In a Hierarchical Storage Management system (HSM), file I/O may be constantly monitored in order to migrate the high frequency files to the fastest storage devices or to internal memory for better performance. HSM was first implemented by IBM on their mainframe computers to reduce the cost of data storage, and to simplify the retrieval of data from slower media. The user would not need to know where the data was stored and how to get it back, the computer would retrieve the data automatically. The only difference to the user was the speed at which data is returned.

Additionally, different from stand-alone system, server such as file server, database server and web server are designed to provide services for multiple clients andmaintain the data consistency and integrity. In order to improve the services, server usually preserves a large buffer to cache data. Some research communities investigated server caching in a distributed file system, showing that server caches have poor hit ratios. The poor hit ratios are resulted by the data sharing among multiple clients. Their

study raised the question whether the stand-alone buffer management policies works well for server buffer caches. Willick, Eager and Bunt [6] have demonstrated that the Frequency Based Replacement (FBR) algorithm performs better for file server caches than locality based replacement algorithms such as Least Recently Used (LRU) and Least Frequently Used (LFU) which works well for stand-alone system caches.

We propose a file attributes-based incremental decision tree predictive model to infer files' future access frequency. A hypothesis that file attributes are strongly related to its future access frequency is tested by using chi-square testing. The testing results show that the owner id, group id, file type and file mode are very positive to support our hypothesis. In our experiments, we use these four attributes to built decision tree. Further more, Incremental tree is one of typical knowledge discovery techniques. Rather than decision trees, it accepts streaming data as its input training data and also automatically update the tree structures to maintain the prediction accuracy.

To accurately evaluate the confidence given by files' attributes, we use incremental decision tree as our predictive model. There are many learning algorithm for streaming data classification, the most popular one is ID5R decision tree [4].

The files we collected are from three network file system (NFS) traces: DEAS03, EECS03 and CAMPUS. Through scanning the traces, we can capture the file attributes (file type, file mode, UID, GID) and its access frequency by accumulating the occurrences of the file requests. Figure 4 shows a sample taken from DEAS03, the frequency is regarding to one hour (03/02/2003, 00:00-01:00).

 Published by Cranfield University Press ISBN: 978-0-9557436-7-2 http://hdl.handle.net/1826/3832

File type	File mode	UID	GID	Access frequency
1	180	18b34	6	7964 (high)
1	180	18ad4	6	242 (low)
1	180	18aa2	6	299 (low)
1	180	18c09	18b3b	567 (low)
2	180	18c09	18b3b	21546 (high)
2	7ff	0	0	6689 (high)
2	5c0	18a89	18a89	7145 (high)
1	5c9	18aa2	18ac2	54 (low)
2	1c0	18aee	18ad5	3657 (high)

Figure 4. A sample trace from DEAS03

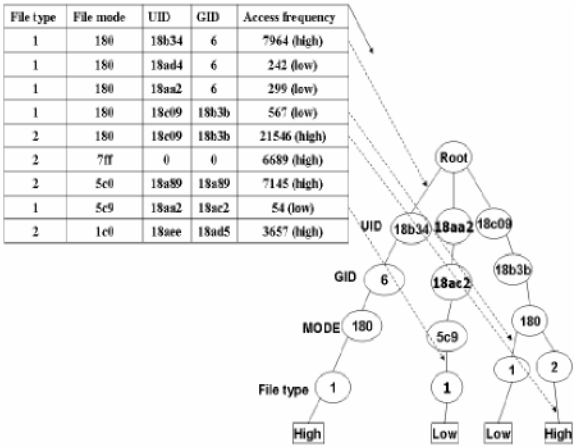

Figure 5 A decision tree built on the sample data

The Fig.5 is the ID5R decision tree built regarding to the above training sample. It can be seen from Fig.5 that begin from the Root, each branch represents a classification rule and its class label. In Fig.5, not all rules are populated in the example tree so that the example decision tree is more readable.

To evaluate the accuracy of FFP over the time series traces, we built the classifiers based on the peak hours' (02/17/2003) as the training sample. Then we predict the files created during the peak hours in the following days to check whether or not the precision is acceptable. Fig.6 shows the accuracy curve of FFP from 02/17/2003-03/12/2003. Although the accuracy of FFP slightly decreases, the overall predicting accuracy remains steady during a reasonable long time.

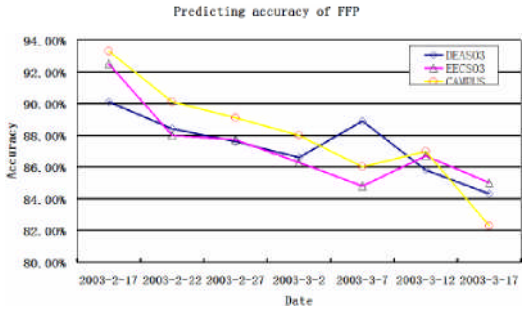

Fig.6 predicting accuracy of FFP over 3 NFS traces from 2003 -2-17 to 2003-3-17

The validation results show that the accuracy of the classifier decreases after few days. This is caused by the slightly changed user behaviors and files' life span. For instance, some lecture notes might be accessed frequently in the next few days after the corresponding lectures were given. However, those lecture notes' access frequency may be no longer frequent once some new lectures are given and their relative lecture notes are created.

5. Conclusion

In this paper, we discussed the knowledge discovery techniques used in file and storage systems. Two representatives, file access pattern and block correlation analysis are reviewed. We also presented an incremental decision tree based predictive model to infer files' future access frequency. The prediction results are stable in a reasonable time period. The predictedtraces (10am-1pm) on Monday file access frequency can be used in server caching environments to improve file caching and prefetching.

6. Reference

[1] T. M. Kroeger and D. D. E. Long, "The Case for Efficient File Access Pattern Modeling," in Proceedings of the Seventh Workshop on Topics in Operating systems, 1999.

[2] Daniel Ellard, Michael Mesnier, En0 Thereska, G. R. Ganger, and Margo

 Published by Cranfield University Press ISBN: 978-0-9557436-7-2 http://hdl.handle.net/1826/3832

Seltzer, "Attribute-Based Prediction of File Properties", Harvard Computer Science Group Technical Report TR-14-03, December 2003.
[3] P. tzvetkov, et al, TSP: Mining top-k closed sequential patterns, Knowledge and Information Systems Vol. 7, Issue 4 pp. 438 - 457, 2005
[4] Paul E. Utgoff, Machine Learning, Vol. 4, Issue 2 (November 1989) pp. 161 - 186, 1989.
[5] Pei Cao, Edward W. Felten, Anna R. Karlin, and Kai Li, "Implementation and Performance of Integrated Application-Controlled File Caching, Prefetching, and Disk Scheduling," ACM Transactions on Computer Systems, 14(4):311–343, 1996.
[6] Daniel Ellard, Jonathan Ledlie, Pia Malkani, and Margo Seltzer. "Passive NFS Tracing of Email and Research Workloads," In Proceedings of the Second USENIX Conference on File and Storage Technologies (FAST'03), pages 203–216, San Francisco, CA, March 2003.
[7] Daniel Ellard, Jonathan Ledlie, and Margo Seltzer, "The Utility of File Names," Technical Report TR-05-03, Harvard University Division of Engineering and Applied Sciences, 2003.
[8] Gregory R. Ganger and M. Frans Kaashoek, "Embedded Inodes and Explicit Grouping: Exploiting Disk Bandwidth for Small Files," In USENIX Annual Technical Conference, pages 1–17, 1997.
[9]James T. McClave, Frank H. Dietrich II, and Terry Sincich, "Statistics," Prentice Hall, 1997.
[10] B. Bouchon-Meunier, Ronald R Yager and Lotfi Asker Zadeh, "Fuzzy logic and soft computing," Singapore, River Edge, NJ: World Scientific, 1995.
[11] Sape Mullender and Andrew Tanenbaum, "Immediate Files," In Software – Practice and Experience, number 4 in 14, April 1984.
[12] Keith Muller and Joseph Pasquale, "A High Performance Multi-Structured File System Design," In Proceedings of the 13th ACM Symposium on Operating Systems Principles (SOSP-9 1), pages 56–67, Asilomar, Pacific Grove, CA, October 1991.
[13] R. Hugo Patterson, Garth A. Gibson, Eka Ginting, Daniel Stodolsky, and Jim Zelenka. "Informed Prefetching and Caching," In ACM SOSP Proceedings, 1995.
[14] Mendel Rosenblum and John K. Ousterhout, "The Design and Implementation of a Log-Structured File System," ACM Transactions on Computer Systems, 10(1):26–52, 1992.
[15] SOS project home page, http://www.eecs.harvard.edu/sos/index.html, 2006.
[16] IBM Company home page, "IBM Mainframe Introduction", http://www-03.ibm.com/ibm/history/exhibits/mainframe/mainframe_intro.html, 2006
[17] Z. Li, et al, Proc. of the 3rd USENIX Conference on File and Storage Technologies, pp. 173-186, 2004.

 Published by Cranfield University Press ISBN: 978-0-9557436-7-2 http://hdl.handle.net/1826/3832

Grid-driven Distributed Heterogeneous Geospatial Data Accessing Service

Wen Zhang[1,2], Sining Wu[1],Frank Wang[1], Lingkui Meng[2], , Na Helian[3]
(1 Centre for Grid Computing, Cambridge-Cranfield High Performance Computing Facility (CCHPCF)
AMAC/SOE, Cranfield University Campus, UK)
(2 School of Remote Sensing and Information Engineering, Wuhan University, P.R. China)
(3 Department of Computer Science, University of Hertfordshire, UK)
w.zhang@cranfield.ac.uk

Abstract: With respect to heterogeneous geospatial data access in a grid environment, this paper proposes a new architecture for unified, transparent data access based on the existing grid technologies. Given the service-oriented characteristics of grid, this method adopts an XML-based strategy to furnish the conversion of heterogeneous data during spatial data access, which provides an integral data view. OGSA-DAI are used to access different database systems. In order to keep the system performance, a middleware GridJet is developed for geospatial data accessing and transferring. Our recent progress includes a test that file access over the experiment system beats those over the classic ones by a factor of 1.5 +x and database access get a obviously improvement than original tests.

Key words: Grid, Geospatial Data Access, OGSA-DAI, GML

1. Introduction

Geospatial data is a kind of information connecting with spatial, which takes up nearly 70% of the general information people used. Geographic Information System (GIS) [1] is a professional system for geospatial data obtaining, managing, storage and analysis. GIS gets popular is a slow process, which is benefited mainly from the popular of web GIS software in recent years, such as Google Earth and World Win. In fact, web service provides tremendous impetus to the development of GIS, which makes people access geospatial data from remote GIS servers easily, but also takes some new problems.

For lack of universal standards, GIS related organizations have produced geospatial data in different proprietary formats and developed services with different methodologies over the years. Because of the distributed nature of geospatial data, GIS users are required to access heterogeneous data in distributed physical data servers via different communication and transport protocols. A GIS user must spend significant amount of time converting data from one format to other to make it available for their purpose. It is a bad thing to both users and GIS, because most users are not GIS experts, they can't always spend so much time to study new tools, which will reduce the user's interest on GIS. What GIS need to be improved is a more powerful server and more convenient client interface, which

 Published by Cranfield University Press ISBN: 978-0-9557436-7-2 http://hdl.handle.net/1826/3832

means the GIS server should provide a unified data access interface for client.

Fortunately, the rise of Grid technology takes heterogeneous spatial data access into reality. Grid connects heterogeneous GIS server and geospatial data sever together via high-speed network connection, and provides a series of strategy to virtualized the distributed grid data source by grid middleware. Grid middleware as Globus toolkit [2] and OGSA-DAI [3] enable secure and convenient sharing of computing resources, file systems , contents and database in grid environment. In this article, we construct a unified geospatial data access system based on grid technology, which could serve a transparent, convenient data interface to client. The organization of this article is as fellows: In section 2, we introduce the architecture of the geospatial data access service, which contains both file system and database. Section 4 describes the test performance of different data access methods.

Section 5 concludes with a discussion of ongoing research.

2 Related works

In order to provide a unified geospatial data access interface, massive spatial data need to be assembled and converted by the GIS server. These data are not just stored in the server, but more often are delivered across the network for the distributed nature of geospatial data. In most cases the amount of needed data reaches to gigabytes or even more, to transfer or access so much data is obviously a challenge. Another problem is the heterogeneous data formats and management methods, especially in some cases that the data source in users' data requests containing both file and database records.

In order to sharing spatial data via internet network, U.S. Census Bureau American Factfinder (http://factfinder.census.gov/servlet/ReferenceMapFramesetServlet?_lang=en) constructed an on-line mapping system, for which the reference and thematic maps provided by the Factfinder are built on The Open Geospatial Consortium (OGC) standards[4] and use data represented in the Geography Markup Language (GML) standard. Sensor-grid [5] computing integrates sensor networks and grid computing, which also choose GML to encode geospatial data for unifying different data formats (Chen-Khong Tham, 2005).

There is currently an enormous number of databases on the web (web databases), and the problem is how to interface these existing web database resources easily in the grid environment. In order to achieve scientific database integration, Isao Kojima(2004) developed a system called OGSA-WebDB[6], which integrates web databases in a grid environment, and the system runs top on the Globus toolkit and Open Grid Services

 Published by Cranfield University Press ISBN: 978-0-9557436-7-2 http://hdl.handle.net/1826/3832

Architecture – Data Access and Integration (OGSA-DAI). In this system, OGSA-DAI act as a unified database access interface. Geographic information services will be integrated with kinds of heterogeneous spatial data in grid environment. The integration will be seamless transparent and expected. In order to provide a unified geospatial data access interface, Geographic Markup Language (GML) and OGSA-DAI are both important tools.

3. Distributed Heterogeneous Geospatial Data Access System

3.1 The architecture of Geospatial Data Access System

We develop a system for geospatial data access containing with both file data and database data based on grid middleware. In this system, Globus toolkit 4.0.6(GT4) is used to construct a grid and act as the grid server. The Globus

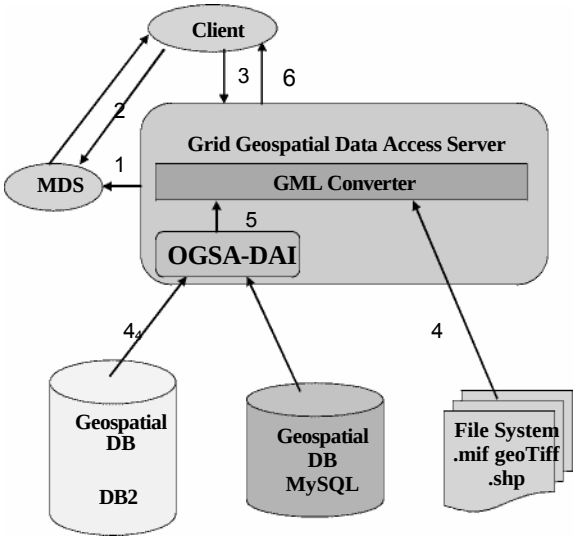

Fig 1. The architecture of geospatial data access system, the number 1 to 6shows the steps to access heterogeneous geospatial data in distributed grid environment

Monitoring and Discovery System (MDS) [7] of GT4 manage the geospatial data access service, which could be queried from the GT4 service list by client. The data access system contains two important parts as file access and database access. OGSA-DAI 3.0 is used as the database access interface. The architecture of the system is shown in figure 1.

As we know, the geospatial data management has two methods: file system and database. Use of a universal standard like XML could encode data from different backgrounds and platforms, not only for file system but also database. Furthermore services and applications are built to parse, understand and use this format to support various operations on data. For these reasons we use GML, the universally accepted XML based encoding for geospatial data, as our data format in GIS related applications.

From figure 1 we could see there are five steps to realize a geospatial data service.

1. Geospatial data access service registers in MDS to make users could find this service.
2. Client queries the MDS service to get the service details of geospatial data access service.
3. Client sent a data request to the Grid Geospatial Data Access Server.
4. The data access server obtains geospatial data separate from heterogeneous databases and file systems, for which the databases are accessed by OGSA-DAI.
5. GML Converter converts the different

 Published by Cranfield University Press ISBN: 978-0-9557436-7-2 http://hdl.handle.net/1826/3832

format into GML formats.

6. The data access server sent a GML documents to the Client.

To access databases is a difficulty, because different databases have different access patterns. OGSA-DAI project aims to provide the e-Science community with a middleware solution to assist with the access and integration of data for applications working within Grids. OGSA-DAI offers a collection of services for adding database access and integration capabilities to the core capabilities of service-oriented Grids, so we use OGSA-DAI to access databases in the data access system.

3.2 Reducing the overlade of Grid geospatial data access service by GridJet

At present, either GT4 or OGSA-DAI has a problem that to wrap a service must pay the price for longer run time and more system load. That means to get more convenient grid service should sacrifice some performance.

Addressing the above problems, a middleware solution known as "GridJet" [8] is developed in our lab, which melds distributed file system technology with high performance data transfer techniques to meet the needs of WAN/Grid-based virtual organizations. In fact, GridJet is a Grid middleware that is independent of the GIS application,which is available in binary or source formats. GridJet uses parallel streams to achieve very high transfer rates at a fraction of the memory cost, and provides a high-speed remote document sharing and storage consolidation solution.

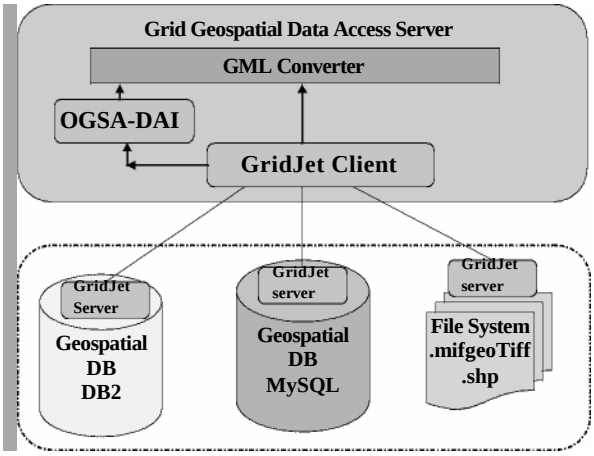

Fig 2. The GridJet is a middleware between the data access server and distributed data servers, in which the data access server acts as a GridJet Client.

As exemplified in figure 2, the geospatial data access server mounts remote data centers to its local data tree via the GridJet protocol, and thus the data access server can access these data online as if they were local. Both database servers and file system servers act as GridJet servers, while the data access server acts as a GridJet clients.

4. The performance tests for grid-driven geospatial data access service

Aiming at the performance of the geospatial data access system for geospatial data access in a distributed grid environment, we do performance tests with both response times and bandwidth utilization across the LAN/WAN infrastructure logged.

We test whole data access service processes as file access and database access. The test time is from the client queries the MDS server that is

 Published by Cranfield University Press ISBN: 978-0-9557436-7-2 http://hdl.handle.net/1826/3832

deployed locally, until the data access server submits results to client. Since the geospatial data service is designed to deal with long-distance, cross-domain and single-image data access operations, in order to know the performance in a changefully wide Area network, we change the RTT to do our test as tcp streams is 16, for which has a better efficiency.

For the file test (figure 3), we choose a geospatial data of 5.4Mb to be accessed on-line across a 100 Mbps link that is typical in a wired WAN environment. When RTT=80ms, #tcp=1 6, we get the improvement as 1.63 times than HTTP. For the database test (figure 4), we choose DB2 and MySQL database to be tested. We measure the response times of querying

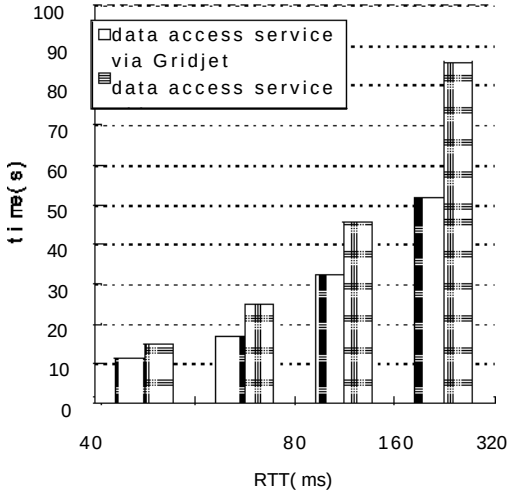

Fig 3.The test measures the response time as a function of RTT,namely data access service via GridJet and HTTP

many records from two databases by “select * from * where id<num” with RTT=80ms at the same time. When we query 16,000 records over the link, the query operation took 22.149 seconds in our system.

We find the optimization results are obviously different in file access and database access. When we run file access, we get an excellent optimization that speed up about 1.5 times than HTTP protocol. But when we do database access, the run time is obviously longer than the data access form JDBC directly, although it is much better than the original OGSA-DAI [] testing performance.

We could speculate the reasons as below:

1. OGSA-DAI need to wrap a query request to be a service, which takes many extendable load cost for XML parsing and encoding.
2. Accessing different databases use the same OGSA-DAI at the same time. The data access server need to share the system resources with two database accesses in one time, which may lead to the decrease performance of the system.

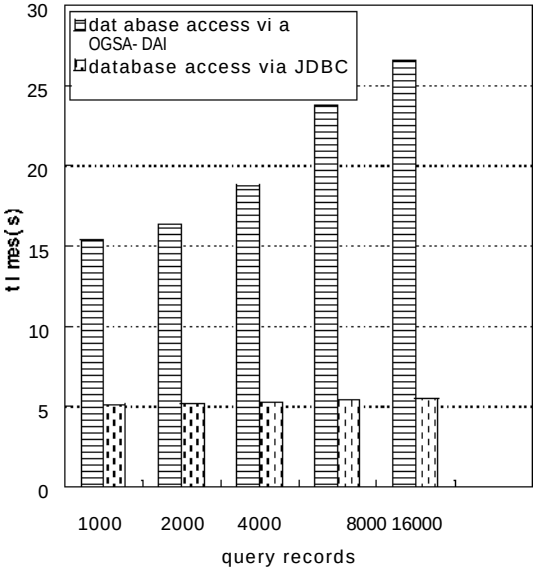

Fig 4.The test measures the response time as a function of query records, namely data access service via OGSA-DAI and JDBC

Obviously, database access is a more

 Published by Cranfield University Press ISBN: 978-0-9557436-7-2 http://hdl.handle.net/1826/3832

complicated process than file access. And as we saw in our tests, although the test results are better than the original OGSA-DAI did, we still need struggle for a higher performance, which will be a important factor that people choose a unified data access service in grid environment.

5. Conclusion

This work provides insights into the unified geospatial data access based on grid technology that can provide transparent, connectivity, mobility, Quality of Service (QoS) support on geospatial data access. We expect this work to provide innovative, flexible, and scalable solutions that can be widely deployed and adopted by end-users over heterogeneous wired-wireless networks.

The core features include:

1. The transparent, unified geospatial data access architecture contains both file system and database system, which contains a single-image data access interface for all kinds of stored geospatial data information.
2. 1 .5+x improvement for file access and huge improvement in response times for database access over Grid Jet protocol.

6. Acknowledgements

This work is sponsored by the UK government and European Commission (EC) through an EPSRC/DTI grant (£ 1 million) “Grid-oriented Storage (GOS)”, an EPSRC grant (£470k) "Accelerating NFS/CIFS", an EC grant (€1 million) “QuickLinux” and an EC grant (€400k) “EuroAsiaGrid”. We also thank Prof Garth Gibson of Carnegie Mellon University, Prof Kai Li of Princeton University, Prof Ric Parker of Rolls Royce, Dr Richard Wright of BBC, Dr. Flavia Donno of CERN, Dr. Sophie Vandebroek of Xerox, Dr. Paddy Francis of EADS, and Prof Lionel Ni of HKUST for viewing our demonstrations and providing us with comments that much improved the GOS work.

Reference

[1]. Geographic Information Systems Resource – GIS, http://www.webgis.com/, 2008.

[2]. Globus Toolkit, http://www.gridbus.org, 2008

[3]. Bartosz Dobrzelecki, Mario Antonioletti, Jennifer M. Schopf, etc.. Profiling OGSA-DAI Performance for Common Use Patterns. Proceedings of the UK eScience All hands Meeting 2006.

[4]. The Open Geospatial Consortium white paper. http://www.opengeospatial.org, 2008.

[5]. Chen-Khong Tham and Rajkumar Buyya. SensorGrid: Integrating Sensor Networks and Grid Computing. Invited paper in CSI Communicaitons, Special Issue on Grid Computing, Computer Society of India, July 2005.

[6]. S.Mirza and I .Koj ima. OGSA-WebDB, An OGSA-Based Sys tem for Bringing Web Databases into the Grid, To appear ITCC’04. 2004 .04.

[7]. Ujjwal S Grover, Priyanka Varma, Sanjay Chaudhary. QoS-Aware Resource Discovery in Grids. 15th International Conference on Advanced Computing and Communications, 2007

[8]. Frank Wang, Sining Wu, Na Helian, Yuhui Deng, Andy Parker, Yike Guo, Vineet Khare, Grid-oriented Storage: A Single-Image, Cross-Domain, High-Bandwidth Architecture, IEEE Transaction on Computers, Vol.56, No.4, 2007.

 Published by Cranfield University Press ISBN: 978-0-9557436-7-2 http://hdl.handle.net/1826/3832

Path Selection Strategy for OBS Networks Based on a Probabilistic Model for the Link Demands

M. Guerreiro, A.L. Barradas , M.C.R Medeiros, *Member, IEEE*

Center for Electronic, Optoelectronic and Telecommunications

Faculty of Science and Technology, University of Algarve, 8000 Faro, Portugal

Tel: +351 289 800900; Fax:351 289 819403

Emails:{mguerreiro,abarra ,cmedeiro}@ualg.pt

ABSTRACT

This paper compares two path selection strategies for Optical Burst Switching networks: a) the path from source destination is chosen randomly from the set of the *k* shortest paths; b) the path selection is based on the probabilistic model of the path demands. In the second strategy, proposed here, the set of shortest paths from source to destination are ranked according to their overall link demand. The path selection schemes are evaluated for a specific scenario of Grid over OBS networks.

Keywords: Optical Burst Switching (OBS), path selection strategies, Grid networks.

INTRODUCTION

Wavelength Division Multiplexed (WDM) networks employing Optical Burst Switching (OBS) have emerged as a promising transport solution and a technology of choice for implementing Grid networks. This approach, known as Grid over Optical Burst Switching GOBS, is currently the object under standardization by a working group in the Global Grid Forum (GGF) [1].

The basic transmission unit in OBS is a Data Burst (DB), which is a collection of data packets going from the same source to the same destination and having identical quality of service requirements [2]. The transmission of each DB is preceded by the transmission of out-of-band Control Packet (CP), which contains the burst information such as burst length and destination. With the information contained in the CP each intermediate node configures its switch fabric to route the DB, when it arrives to the node, to the appropriate output link port. The processing of the CPs is either distributed as in Just Enough Time (JET-OBS) architecture, or centralized as in the Wavelength Routed (WR-OBS) networks [3]. In JET-OBS networks, although the CPs follow the same path as the DB they are transmitted an offset time before the data. The offset time accounts for the processing delays of the CP at the intermediate nodes along the

This work was supported by the Foundation for Science and Technology within CEOT (Center for Electronics, Optoelectronic and Telecommunications) and by projects POSC/EEA-CPS59556/2004 and PTDC/EEA-TEL/71678/2006.

 Published by Cranfield University Press ISBN: 978-0-9557436-7-2 http://hdl.handle.net/1826/3832

transmission path. In WR-OBS the CPs are sent and processed at a central node to determine the appropriate paths and reserve a wavelength channel along the path. Depending on whether the reservation has been successful or not, acknowledgements are sent to the source node to either transmit or block the DBs.

In Grid-over-OBS, one or more application requests, or jobs, are assembled into a super-size packet called data burst, which is then transported over the optical core network and forwarded to the appropriate Grid resources. Contrarily to traditional networks OBS where two predetermined nodes need to communicate in order to satisfy a traffic demand, in Grid scenario only the source node is predetermined and the destination has to be discovered using fast resource discovery mechanism. In [3,4] programmable Grid-over-OBS architecture employing active routers for Grid resource discovery. The user is informed about the result of the resource discovery. In case of resource availability the user transmits the Grid job to the designed Job provider using OBS.

The transport of Grid jobs over OBS presents several advantages such as: support of existing DWDM optical networking infrastructure and minimizing the need for optical-electrical converters at intermediate nodes, ability to utilize link bandwidth and Grid resources efficiently and provide low end-to-end latency. However, OBS presents low reliability since it generally uses a one-way reservation protocol where bursts are transmitted without confirming the network resources reservation along the entire burst path. Therefore bursts may contend for the same resources leading to burst drop. This is the primary cause of burst loss in OBS and it happens when the number of overlapping burst reservations at an output port of a core node exceeds the number of data wavelengths available. In OBS networks employing source routing, the source node determines the path, from source to destination, of the burst entering the network. The path over which the burst must travel is carried by the Control Packet. A common approach is to choose at random a path from the set of shortest paths from source to destination. Burst dropping can be minimized by appropriately choosing the paths that bursts must follow, that is, an effective choice of paths can lead to an overall network performance improvement [5].

In this paper we present a path selection strategy based on the probabilistic model for the demands on the path [6]. In this approach the set of shortest paths from source to destination are ranked according to their overall link demands. The source uses the least demanded path to transmit its bursts.

The paper is organized as follows. Next section presents the probabilistic model for the demands on a path. In Section 3 the proposed path selection strategy is evaluated for a Grid over OBS scenario and compared with random path selection strategy. Finally, in section IV, we conclude the paper.

PROBABILISTIC MODEL FOR DEMANDS ON A PATH

The network topology is modelled as a graph *G(N,L)*, where *N* is the set of nodes and *L* is the set of links. The path, *v,* over which a burst travels from source, *s*, to destination, *d*, is composed by series of

 Published by Cranfield University Press ISBN: 978-0-9557436-7-2 http://hdl.handle.net/1826/3832

links, and is represented as, $v : s(v) \rightarrow d(v)$. The set of paths that can be used by a burst from s to v is defined as $V_{s,d} = \{v : s(v) \rightarrow d(v) \mid s = s(v), d = d(v)\}$ and the set including all $V_{s,d}$ is defined as V. A demand matrix T is also considered, where $t_{s,d}$ represents a relative load from source node s to destination node d.

A probability matrix $\left[p^l \right]$, one matrix per link is also defined [6]. Each element of the probability matrix, p_{ij}^l, represents the probability of using the link *l* to support one demand between node *i* and *j*. The elements of the probabilities matrixes can be obtained using a search algorithm. For example for the network of Figure 1, we obtain:

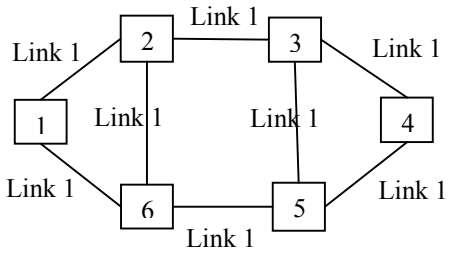

$$\left| p^1 \right| = \begin{bmatrix} 0 & 1 & 1 & 1/2 & 0 & 0 \\ 1 & 0 & 0 & 0 & 0 & 0 \\ 1 & 0 & 0 & 0 & 0 & 0 \\ 1/2 & 0 & 0 & 0 & 0 & 0 \\ 0 & 0 & 0 & 0 & 0 & 0 \\ 0 & 0 & 0 & 0 & 0 & 0 \end{bmatrix}$$

a) **b)**

Figure 1. a) A network topology, represented by a graph; b) The matrix $\left[p^l \right]$ for *link 1 (l=1).*

Considering an uniform demand matrix, the weight of a *link l* is:

$$W_l = \sum_{i=1}^{N} \sum_{j=1}^{N} p_{i,j}^l$$

The weight of a given path composed by L links is the sum of the weight of the links that compose the path.

The *k* shortest paths from a source to destination are ranked according to their weight, being the first ranked the less weighted.

PERFORMANCE EVALUATION

In this section, we evaluate and compare the performance improvements Grid over OBS network employing JET-OBS with source routing. Two strategies for path selection are considered: a) the path from source destination is chosen randomly from the set of the *k* shortest paths; b) the selected path is the less weighted as defined in the last section. The simulations were performed using C++ in combination with the discrete event simulator OMNeT++ [7].

 Published by Cranfield University Press ISBN: 978-0-9557436-7-2 http://hdl.handle.net/1826/3832

Figure 2 shows the network topology used, it employs active routers for Grid resource discovery such as [4]. The scenario considered here is composed by 20 nodes connected by bidirectional WDM links. Each WDM link has four wavelength data channels plus a dedicated control channel. The propagation delay between any two nodes is considered constant and equal to 0.1 *ms*. A network without wavelength conversion capabilities is considered. All nodes are considered to be Grid job generators, the network is considered to be a single active region, with only one Active Router and a single Grid resource provider.

The job requests are generated as a Poisson process with mean arrival rate λ *arrivals/ms*. Job sizes are distributed according to a exponential distribution with mean 1/μ..

.

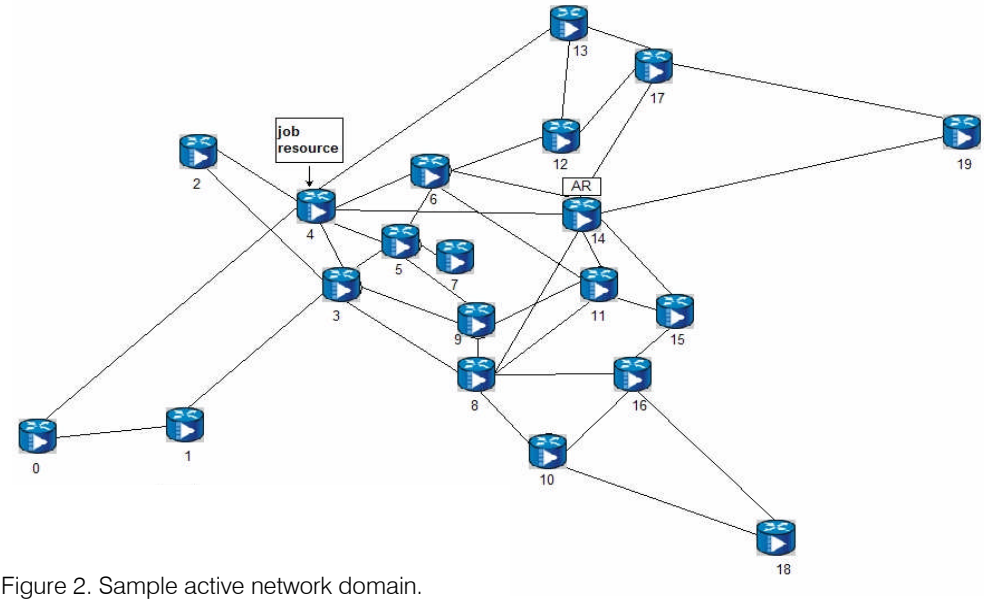

Figure 2. Sample active network domain.

 Published by Cranfield University Press ISBN: 978-0-9557436-7-2 http://hdl.handle.net/1826/3832

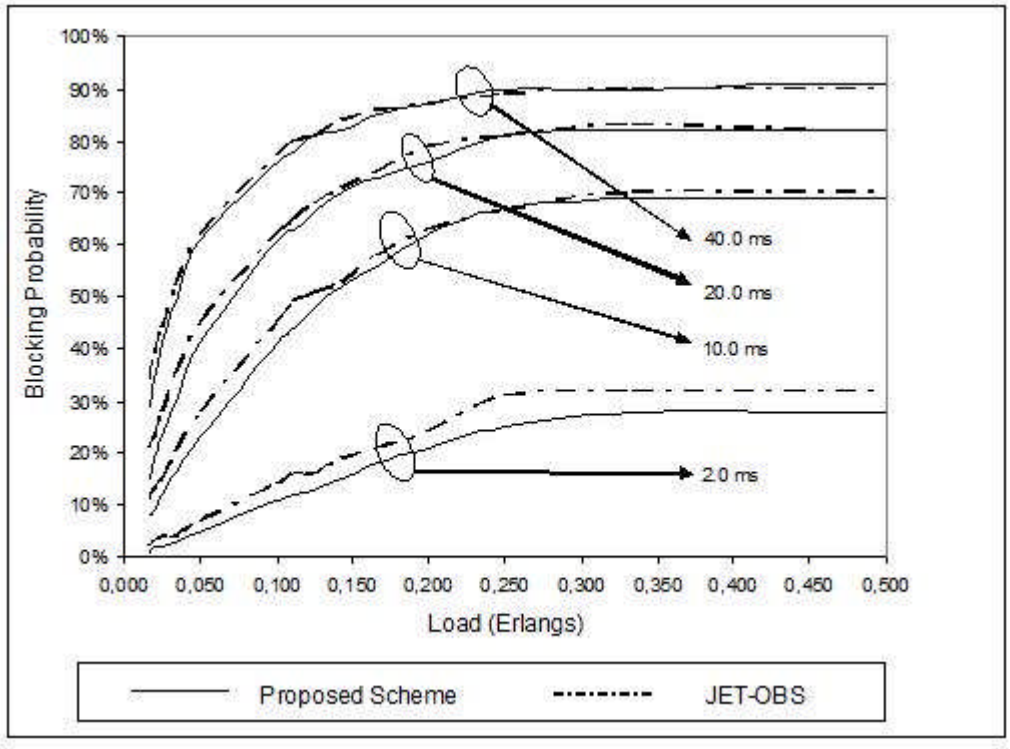

Figure 3. Job blocking probability versus load for average job sizes of *20.0 ms, 2.0 ms, 10.0 ms* and *2.0 ms.*

Figure 3 compares the blocking probability versus load for the JET-OBS employing random path selection and the strategy proposed here based on the probabilistic model for the demands. Four average job sizes are considered: 40.0 *ms*, 20.0 *ms, 10.0 ms* and 2.0 *ms*. The plots show that the proposed strategy always outperforms the random path selection scheme in terms of job blocking rate. The performance improvement increases when the job size decreases.

CONCLUSIONS

This paper discusses and evaluates the performance of two path selection strategies for OBS networks. Our application case study was a Grid over OBS network, where several node sources try to reach a common grid job provider. The path selection scheme employing a probabilistic model for the link demands is particularly suitable for small size jobs which require fast network resources during short periods of time.

REFERENCES

1. D. Simeonidou and R. Nejabati (Eds): Grid Optical Burst Switched Networks (GOBS), Global Grid Forum Draft, May 2005.
2. C. Qiao and M. Yoo, "Optical burst switching: A new paradigma for an optical Internet", J. High Speed Networks, vol.. 8, nº. 1, pp. 69-94, March 1999.

 Published by Cranfield University Press ISBN: 978-0-9557436-7-2 http://hdl.handle.net/1826/3832

3. M. Düser and P. Payvel: Analysis of dynamically wavelength-routed optical burst switched network architecture, J. Lightwave Technol. , vol. 20, n^{o}. 4, pp.574-585, April 2002.
4. D. Simeonidou, R. Nejabati, G. Zervas, D. Klonidis, A. Tzanakaki and M.J. O'Mahony: Dynamic optical-network architectures and technologies for existing and emerging grid services, J. Lightwave Technol. , vol. 23, n^{o}. 10, pp.3347-3357, Oct. 2005.
5. L. Yang, G. N. Rouskas: Adaptive path selection in OBS networks. J. Lightwave Technol., vol. 24, n^{o}. 8, pp. 3002-3011, Aug. 2006.
6. S. K. Korotky: Network global expectation model: a statistical formalism for quickly quantifying network needs and costs. J. Lightwave Technol., vol. 22, n^{o}. 3, pp. 703-721, Aug. March 2004.
7. OMNeT++, website,http://www.omnetpp.org.

 Published by Cranfield University Press ISBN: 978-0-9557436-7-2 http://hdl.handle.net/1826/3832

A 'Real Time' Method for Determining Temperature in the High Performance Grinding Process.

I.M.Walton, Precision Engineering Centre, School of Applied Sciences, Cranfield University, Bedfordshire, MK43 0AL

ABSTRACT.

During grinding thermal damage may occur which is detrimental to the surface integrity of the finished component resulting in catastrophic in-service failure. A 'real-time' measurement of the surface temperature is one way to ensure that the level of thermal damage induced into the component during grinding is within acceptable levels. This paper reports the development of a 'real time' grinding temperature monitoring system and the development of a physical temperature technique to validate the calculated temperatures. Results show that the monitoring system is capable of calculating temperatures for a wide range of grinding regimes from creep feed to high efficiency deep grinding (HEDG) and shows excellent correlation to temperatures measured by the PVD low melting point coating technique, which has also been shown to offer a robust measurement technique within aggressive environments and at high specific material removal rates.

Keywords: Grinding, PVD Coatings, Surface Temperature, Thermal Damage, High Specific Material Removal Rates.

NOMENCLATURE

 Published by Cranfield University Press ISBN: 978-0-9557436-7-2 http://hdl.handle.net/1826/3832

α Thermal diffusivity (m2/s)
β Workpiece thermal gradient (K/m)
c Specific heat capacity (J/kgK)
k Thermal conductivity (W/mK)
l_c Contact Length (m)
q Heat flux (W/mm2)
θ_m Temperature rise at a depth z below surface (°K)
θ_s Surface temperature rise (°K)
R_w Heat partition to the workpiece.
Q'_w Specific Material Removal Rate (mm3/mm.s)
V_s Wheel speed (m/s)
V_w Workpiece speed (m/s)
z Depth below surface (m)

DESCRIPTION OF MONITORING SYSTEM

The grind monitoring system provides the ability to select optimal grinding parameters to achieve low process temperatures and calculate the surface temperatures using process data. A mathematical thermal model, utilising the circular arc heat source model [1-4], is incorporated. Predictive calculations utilise the data derived from numerous grinding studies carried out over a large range of specific material removal rates using different workpiece materials, wheel abrasives and grinding fluids. A typical predictive temperature entry screen is shown in Figure 1a. The 'real-time' graphical user interfaces are shown in Figure 1b.

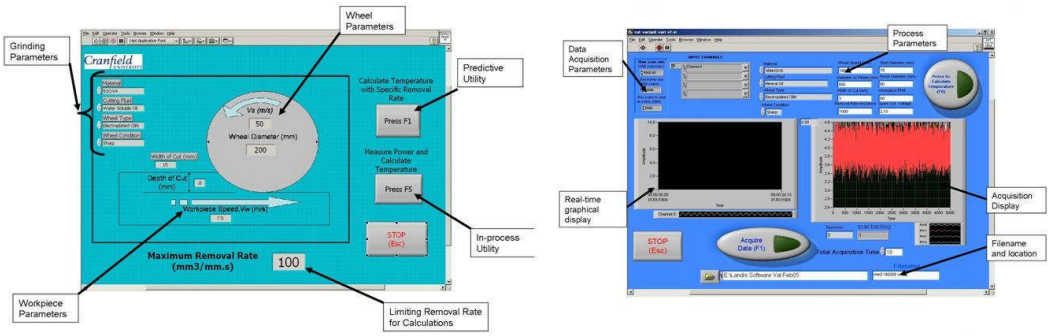

Figure 1 a. Predictive Function Graphical User Interface and b. 'Real-time' Graphical User Interface.

Process grinding temperatures are calculated from the power supplied to the grinding spindle motor. A 0-10V scaled power output is produced from a Hall Effect device. The signal was acquired using a NI-PCI 6036E DAQ card connected to a SC-2345 SCC module carrier. The monitoring system hardware is shown in Figure 2.

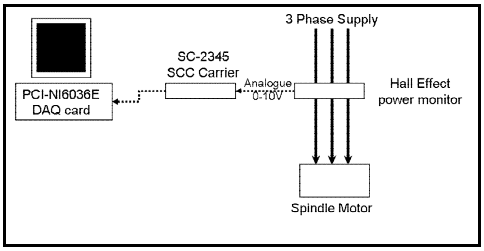

 Published by Cranfield University Press ISBN: 978-0-9557436-7-2 http://hdl.handle.net/1826/3832

Figure 2: Schematic Diagram of the Data Acquisition Hardware.

PHYSICAL MEASUREMENT TECHNIQUE

Previously the use of the low melting point PVD coating technique had been applied to shallow cut surface grinding conditions at very low SRRs. [5,6] and showed that the finished surface temperature of a ground workpiece could be determined even when grinding using grinding fluids. *Kato et al.* [5,6] showed that by using different low melting point coatings and measuring the melt depth below the surface, the surface temperature could be determined. By applying Takazawa's approximation [7] to solve the two dimensional, steady state temperature distribution model proposed by Jaeger [8] it was found that the temperature rise θ_m obtained at a depth z could be simply approximated by:

$$\theta_m = \theta_s \exp\left(-\beta z\right) \qquad [1]$$

Where

$$\theta_s = 3.1\frac{2R_w q\alpha}{\pi k V_w} \quad [2] \text{ and } \beta = 0.69\left(\frac{V_w}{2\alpha}\right) - 0.37\frac{V_w}{2\alpha} = 0.576\alpha^{-0.63}V_w{}^{0.63}l_c{}^{-0.37} \quad [3]$$

The equation is only valid in the range $0 < z < 8\alpha/V_w$

EXPERIMENTAL

Single pass surface grinding tests were conducted on 51CrV4 steel using an Edgetek 5-axis grinding machine and a Winter B252 electroplated CBN peripheral wheel. The wheel speed during all tests was maintained at 146m/s with the depth and width of cut varied to produce Q'_w up to 1000mm^3/mm.s. Mineral oil at a line pressure of 6bar was used for the cutting fluid. The fluid jet was aligned along the centre axis of the grinding direction using a laser alignment tool attached to the fluid delivery nozzle.

One polished face from each specimen was coated with a 200nm thick PVD low melting temperature coating of Indium, Bismuth, Antimony or Zinc. A resistively heated thermal evaporation coating system was used to deposit the 200nm thick coatings. Cross-sections were taken at the coating interfaces after measurement of the melt depths of the coating. These sections were polished and etched using a 2% nital etch for optical metallography. Figure 1 shows an exploded view of the specimens within the holding fixture.

 Published by Cranfield University Press ISBN: 978-0-9557436-7-2 http://hdl.handle.net/1826/3832

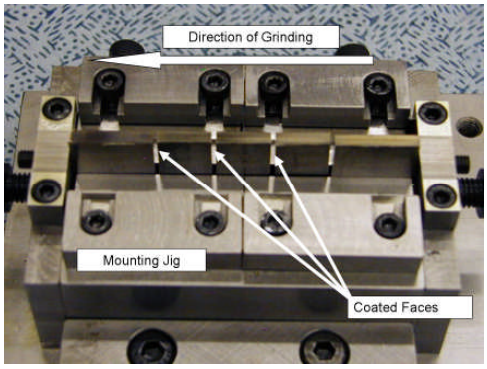

Figure 1: Arrangement of coated samples in holder.

VALIDATION OF THE MONITORING SYSTEM

Figure 2 shows the temperature and specific grinding energy curves produced by the predictive utility of the software. The predicted temperatures curves show that temperatures under shallow cut conditions (Q'_w = 60mm^3/mm.s) can be sufficiently low and no thermal damage will occur. At very high Q'_w, the curves show that reduced surface temperatures can be achieved and that the region between 80 and 800mm^3/mm.s will generate excessive thermal damage in the workpiece.

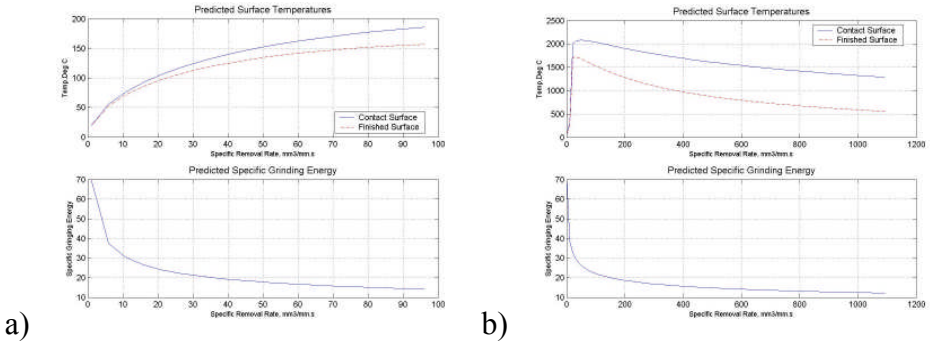

a) b)

Figure 2. Predictive temperature and SGE profiles for (a) 60 and (b) 1000mm^3/mm.s

Comparisons between the measured and predicted temperatures at the higher specific material removal rate show good correlation between the power derived and PVD coating measured temperatures, Figures 3a and 3b. Both temperatures show that significant thermal damage will occur when using these grinding parameters.

 Published by Cranfield University Press ISBN: 978-0-9557436-7-2 http://hdl.handle.net/1826/3832

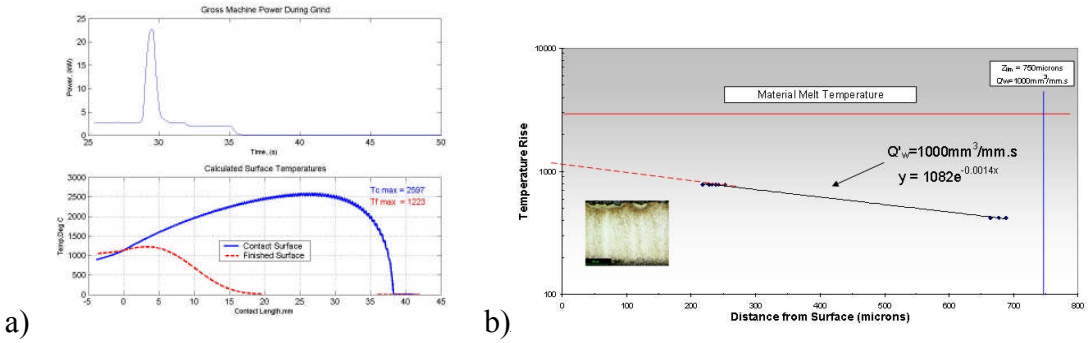

Figure3. Temperature measurement results for Q'_w = 1000mm^3/mm.s

The micrographs of the coated interfaces show that a very distinct isotherm is produced, showing the transition between the melted and original PVD coating (Figure 4). It was observed that the measured melt depth of a coating increased, as reported by *Kato et al* [5,6] in an exponential manner as the SRR increased. Initial grinding passes identified that higher melting point coatings were required as the SRR increased, so that the measured depths of the melt zone were within the limits of the Takazawa's approximation.[7] During initial testing the alignment of the fluid along the workpiece was identified as critical to producing an uniform isotherm across the sample. The isotherm was observed to be non-symmetrical if the fluid alignment was incorrect; this effect is shown in Figure 5. In order to improve alignment a laser probe was used to align the coolant jet along the central axis of the surface to be ground.

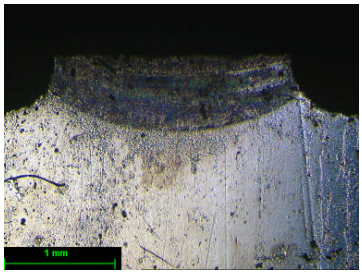

Figure 4:Q'w=1000 mm^3/mm.s, zinc coating

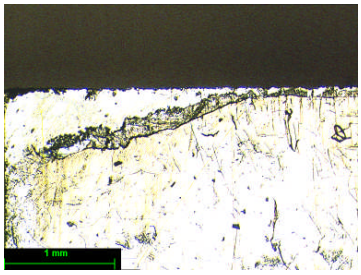

Figure 5: Off-centre fluid alignment

Plots of the coating melt depth vs. temperature are shown in Figure 6. The limit to the approximation is marked in Figure 6 and for the higher SRR only the zinc and antimony coatings produced results that can are valid. The depth of the observed changes in microstructure was used by assuming a transition temperature of 760°C. Re-plotting the data using a log-temperature scale, the intercept on the y-axis (temperature) and gradient could be determined, providing values for the maximum surface temperature and thermal gradient respectively. (Figure 3b)

 Published by Cranfield University Press ISBN: 978-0-9557436-7-2 http://hdl.handle.net/1826/3832

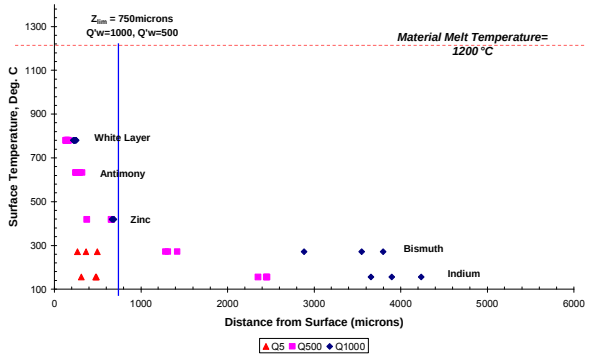

Figure 2: Distribution of the temperature rise under different SRR.

The surface temperatures calculated from the mathematical model and interpolated from the coating melt depths are close to the workpiece material melting point, 1200°C. This is a very high temperature and demonstrates the temperature range over which the PVD coatings can be used. The measured temperature values using the PVD coating technique and the theoretical values derived using circular arc of contact models show very close correlation to one another. It can be seen that the temperatures predicted by the circular arc heat source model are higher (<100°C) than those measured using the PVD coating technique. The measured and predicted temperatures agree with the metallographic observations, with the appearance of a layer of untempered martensite indicating that the temperature has exceeded the A3 transition temperature (760°) of the Fe-C phase diagram. [9]

CONCLUSION

The grinding process monitoring system is a powerful tool for the selection of the optimum parameters to achieve low process temperatures and avoid grinding conditions that would generate excessive thermal damage. Good correlation has been demonstrated between the predicted, calculated and physically measured temperatures using the low melting temperature PVD coating technique. Although deviation has been observed between measured and predicted temperatures at high Q'w, the trends of the data showing the presence of a region in which extreme thermal damage will occur can be used to select safer grinding parameters.

The measurement of finish surface temperatures by the PVD coating method is a robust technique that allows accurate temperature measurements even under aggressive grinding conditions and environments. The high pressure grinding fluids did not influence the coating performance. The temperatures estimated by the PVD coating technique have been used to validate thermal models based on the circular arc heat source for varying specific materials removal rates. Calculated temperatures of the finished surface using the thermal model show good agreement with those measured using the PVD coating technique.

 Published by Cranfield University Press ISBN: 978-0-9557436-7-2 http://hdl.handle.net/1826/3832

ACKNOWLEDGEMENT

The authors would like to acknowledge the financial support from EPSRC (Contracts GR/R68795and IMRC22) in funding this research; and the close collaboration with the project partners.

REFERENCES

1. T. Jin. D.J. Stephenson. *Investigation of the heat partitioning in High Efficiency Deep Grinding.* International Journal of Machine Tools and Manufacture, 43, 2003, pp1129-1134.
2. D.J. Stephenson. T. Jin. *Physical Basics in Grinding*, 1st European Conf. on Grinding, Aachen, 6-7 November 2003, pp. 13-1 – 13-21.
3. W.B. Rowe. *Temperature case studies in grinding including an inclined heat source model.* Proc. Instn Mech. Engrs, Part B, Journal of Engineering Manufacture, 215 (B4), 2001, pp473-491.
4. T. Jin. W.B. Rowe. *Temperatures in High Efficiency Deep Grinding (HEDG.)* Annals of the CIRP, 50 (1), 2001, pp205-208.
5. Kato, T; Fujii, H. *Temperature measurement of workpiece in surface grinding by PVD film method.* Journal of Manufacturing Science and Engineering, 119, 1997, pp689-694.
6. Kato, T; Fujii, H. *Temperature measurement of workpieces in conventional surface grinding.* Journal of Manufacturing Science and Engineering, 122, 2000, pp297-303.
7. Takazawa, K. *Effects of grinding variables on surface structure of hardened steels.* Bulletin of Japan Society for Precision Engineering, 2, 1966 pp14-21.
8. Jaeger, J.C *Moving sources of Heat and the temperature at sliding contacts.* Proc. R. Soc. New South Wales, 76, 1942, pp203-224.
9. Krauss, G STEELS*: Heat Treatment and Processing Principles*. ASM International 1990 5th Edition ISBN 0-87170-370-X pp62

 Published by Cranfield University Press ISBN: 978-0-9557436-7-2 http://hdl.handle.net/1826/3832

An Initial Classification and Compilation of Manufacturing Systems

Kevin Rampersad and Benny Tjahjono
Department of Manufacturing, School of Applied Sciences
Cranfield University, Cranfield, UK

ABSTRACT

This purpose of this research paper is to collect information on the different manufacturing systems which all use simulation as part of their decision making process, and to apply this information to develop an initial classification of these systems. This paper is based on the understanding that by developing this initial classification, the information collected will be used in the future as this research progresses to develop a template library for simulation modelling.

INTRODUCTION

As a result of this increase in global productivity, we see that production systems are being designed and redesigned at an increased rate and that they are becoming more innovative as they progress with time. One of the ways in which this productivity drive has been maintained is through the use of simulation as a production and decision making tool. Research carried out in the field of simulation by Tjahjono and Baines [26] in the East England region showed that of all the manufacturers surveyed only around 20% of them had applied simulation techniques as a decision making tool. A further 40% of manufacturers within that region were not aware of the capabilities of simulation tools or even how to apply them to the decision making process. In this paper we will look at the use of simulation within the manufacturing sector, focusing on the classification of systems that use simulation as a decision making tool.

BACKGROUND

Driven by the need and the demand to quickly introduce new products into the market, we see that companies are moving away from the traditional approach of mass production and towards one of mass customisation. The use of simulation technology enables manufacturers to carry out “what-if” scenarios that are useful in gaining a deeper understanding of how a new or alternative manufacturing system will perform before any investments or modifications are made. When we refer to the use of a template within the context of a simulation model, we are referring to a collection of user defined ready-to-use and reusable building blocks which can be used in an appropriate simulation setting. However one of the overwhelming difficulties when it comes to designing an appropriate simulation template is the fact that manufacturing systems, and more importantly, the decision making problems that are associated with them are not well categorised or classified. One of the possible ways to facilitate this is by applying a classification method. In the context of our research we will be focusing on the use of cladistics as a method for classifying our templates. The major challenge which we hope to address by carrying out this

research is the collection and compilation of these innovative manufacturing systems and we hope that this initial classification can lead to the development of a template library in the near future.

RESEARCH PROGRAMME

AIM AND OBJECTIVES

The overall aim of the research presented in this paper is the collection of information on the different types of manufacturing system models which exists, based on the nature of their manufacturing processes, their typical layouts, material flows, routing logic etc. We should, however, note that the literature presented here may not be sufficiently

 Published by Cranfield University Press ISBN: 978-0-9557436-7-2 http://hdl.handle.net/1826/3832

developed to answers these questions to their full extent and as a result these objectives may not necessarily lead to any key findings. To achieve the above aim, the following objectives were identified:

1. The collection and compilation of an initial classification of manufacturing systems models
2. To promote some understanding of the diversity and types of manufacturing systems
3. To profile manufacturing systems that use simulation
4. The reclassification of these systems based on their similarity of physical layout

SEARCH STRATEGY

The search strategy was based on our identification of the relevant data sources and keywords. Our search focused its attention on gathering information from a wide classification of databases, conference proceedings, books, library catalogues and articles from online journals. Some of the databases searched included SCOPUS (Elsevier), Science Citation Index (ISI), ABI/Inform (ProQuest) and ScienceDirect via SCIRUS (Elsevier). Conference papers from the winter simulation conferences were also included in our search. The search strategy used a wide range of keywords and phrases such as “Machine and Plant Layout”, “Manufacturing" and “Machine Problems” which produced over 1000 hits but only yielded a handful of useful papers, whilst a more refined search string using keywords such as “Simulation and Manufacturing Classification” had only 49 hits and yielded 3 papers. Upon collection of the information the list of hits for our search had to be firstly reviewed then edited so as to omit any duplicate records which may have appeared. The articles were then checked to ascertain their relevance to the review. Also an internet based search through the use of Google Scholar was carried out to complete our information gathering exercise.

RESULTS AND ANALYSIS

The search began by firstly identifying the many publications relevant to the field of simulation. Table 1 shows an example of some of the search strings used and it should be noted that because of the many databases available for us to search, the number ofjournal papers obtained far outnumbered those obtained from conference proceedings. From table 1 we see that search strings which contained the terms

‘Machine + Plant Layout’ or ‘Manufacturing + Layout’ or ‘Manufacturing + Machine’, each yielded a high number of hits. The high number of hits reflected the high number of publications in the field of manufacturing.

 Published by Cranfield University Press ISBN: 978-0-9557436-7-2 http://hdl.handle.net/1826/3832

Table 1 - Key Journal and Conference Papers[1]

Author	Title	Source
Schaller Jeffrey 2007	Designing and redesigning cellular manufacturing systems to handle demand changes	Journal of Computers & Industrial Engineering,
Balamurugan,K.; 2006	Design and optimization of manufacturing facilities layouts	Proceedings of the Institution of Mechanical Engineers
Shambu & Girish; 2000	Performance of hybrid cellular manufacturing systems: A computer simulation investigation	European Journal of Operational Research,
Castillo etal	The development of a cellular manufacturing system for automotive parts	Journal of Computers & Industrial Engineering,
Potts,C.N & Whitehead. J. D. 2001	Workload balancing and loop layout in the design of a flexible manufacturing system	European Journal of Operational Research
Abdi.M.R & Labib, A. W 2004	Grouping and selecting products: the design key of Reconfigurable Manufacturing Systems (RMSs)	International Journal of Production Research
David Claudio etal.	A Hybrid Inventory control system approach applied to the food industry.	Proc. of the 2007 Winter Simulation Conference
Duilio Curcio, etal	Manufacturing Process management using a flexible modelling and simulation approach	Proc. of the 2007 Winter Simulation Conference
Sara L. Maas & Charles R Standridge	Applying Simulation to Interactive manufacturing Cell design	Proc. of the 2005 Winter Simulation Conference
Craig W. Alexander	Discrete Event Simulation for Batch Processing.	Proc. of the 2006 Winter Simulation Conference
Esra E. Alcisa & Li Lin	For effective facilities planning: Layout optimization then simulation, or Vice Versa	Proc. of the 2005 Winter Simulation Conference

GENERATION OF FINDINGS

The literature review identifies the various manufacturing systems which all use simulation and these systems have been compiled and classified according to the type of production they employ.

CELLULAR MANUFACTURING SYSTEMS

Cellular manufacturing systems (CMs) are a manufacturing application of the group technology philosophy. In this type of layout the machines are grouped together based on the process requirements for a similar set of products or part families. [1, 2] In a cellular system parts are firstly pulled from the external environment into the cell via the use of a conveyor and then pushed throughout the cell until the finished product is obtained. The cellular layout can be further decomposed into its three core makeup they being machine + operator or machine + conveyor or machine + buffer, or any combination of the three, each with their operational advantages and problems. [4, 5]

HYBRID MANUFACTURING SYSTEMS

The hybrid system has come about through the need for fast and flexible production systems and it can be seen as a combination between the traditional job shop and that of a cellular layout [6]. Simulation is used to determine the best layout for parts and machines as quickness of changeover is the key to maintaining the hybrid system's performance level. In the hybrid system parts are pulled firstly then pushed through the system to obtain a completed product. Hybrid systems due to their flexibility tend to have a high level of automation and they tend to be made up of automatic machines and conveyors.

 Published by Cranfield University Press ISBN: 978-0-9557436-7-2 http://hdl.handle.net/1826/3832

[1] The full list of papers is available upon request

FLEXIBLE MANUFACTURING SYSTEMS

A flexible manufacturing system (FMS) is a system where there is some degree of flexibility within the production process that allows the system to react to changes, either predicted or unpredicted. [8, 9] Flexible manufacturing systems (FMS) manufacture a wide variety of products due to their high flexibility through the use of machines for e.g. CNC's and robots, all performing a variety of operations. FMS can be depicted in a simulation environment through the use of machines and conveyors based on a push system, as there exist a high level of automation no buffers or operators are used.

FLEXIBLE FLOW LINES

Flexible flow lines are usually categorised as a flow line with several parallel machines on some or all production stages. [11] As a result of their design layout all products follow the same linear path through the system, whereby they enter at the first stage and are completed upon exit at the last stage. The machine tooling can either be of the static type whereby tools cannot be moved from one workstation to the other, or dynamic, whereby the tooling is shared at all workstations via a tool handling system. Flexible flow lines tend to have a high level of automation based on the configuration used and they can be composed of machines and conveyors and in some cases machines + conveyors + buffers.

Transfer Lines

Transfer lines have been seen as the tools of mass production over the last 30 years with main emphasis on their usage within the automobile industry. The machines used in this type of production are traditionally highly inflexible, but with advances in technology there is movement towards a line with a higher level of flexibility. [18] In a transfer line the part visits a workstation where all the operations or blocks are performed in a sequential manner and workstations are visited in order of their index. In (TL) buffers exist between stations and the line cycle time is constrained by the bottleneck workstation. [17, 18]. The make-ups of these systems are highly automated and they consist of machines + buffers + conveyors.

RECONFIGURABLE MANUFACTURING SYSTEMS

Reconfigurable Manufacturing Systems (RMSs) were first introduced in the mid-nineties as a cost-effective response to the shift in market trends from one of mass production to one of mass customization. [19] One of the greatest advantages of this type of production system is its ability to deliver customized flexibility on demand in a shorter time frame, as compared to Flexible Manufacturing Systems (FMS). [14] (RMS) are based on a high level of automation and flexibility and as a result their makeup tends to

be one of machines and conveyors and productions are facilitated by both push and pull factors within the system.

ASSEMBLY LINE

An assembly line is a flow orientated system where the workstations are aligned in a serial layout. [23] Originally, assembly lines were developed for cost efficient mass-production of standardized products, designed to exploit a high specialization of labour and the associated learning effects (Shtub and Dar-El, 1989; Scholl, 1999, p. 2). In an assembly line process the work pieces visit the workstations successively as they are moved along the line through the use of a transportation system for e.g. that of a conveyor belt. [23] In terms of a simulation environment we see that assembly

 Published by Cranfield University Press ISBN: 978-0-9557436-7-2 http://hdl.handle.net/1826/3832

lines are based on a push system and it can be represented in the terms of a simulation model through the use of machines and conveyors.

Table 2 - Various System Compilation / Classifications

Manufacturing Processes	Type of Operation	No. Of Workstation	Level Of Automation	Level of Part variety
Cellular	Medium / High Batch Prod.	High	Medium	Medium
Hybrid	High Volume Batch Prod	High	HIgh	Wide Variety
Flexible Manufacturing	Wide Variety Batch Prod	HIgh	HIgh	High
Flexible Flow Lines	Medium / High Batch Prod.	High	High	High
Transfer Lines	Mass Productio	Low	High	Low
Reconfigurable manufacturing	Mass Custimization	High	Fully Automate	High
Assembly Lines	Mass Production	Low	High	Low

After research into the different systems we have attempted to identify the commonalities which some of these systems may possess. The information was categorised based on the four basic elements known to be possessed by manufacturing systems. A high to low rating was used to identify the number of workstations used, the level of automation and the level of part or product variety, whilst the different types of production were described. Upon review of the information collected and classified it emerged that there are some systems which share common aspects in their layout and production which can be used to create a grouping in regard to the design of simulation templates.

CONCLUSION

From the information we have been able to collect we see that there are a number of different manufacturing processes, which at some point or the other each adopt simulation as part of their decision making processes. The findings put forward in Table 2 suggest that some form of classification can be given to these various systems in order to facilitate the faster design and development of simulation templates. No attempts have yet been made to classify manufacturing systems based on their level of simulation. However the findings collected gives us an opportunity and allows for systems which have similar characteristics to be grouped together. By using this information to establish an initial

classification for manufacturing simulation systems we hope this may facilitate the faster development of simulation models allowing for the wider use of simulation within the UK manufacturing industry.

ACKNOWLEDGEMENT

This study is part of the EPSRC First Grant project entitled An Evolutionary Approach to Rapid Development of Simulation Models (grant no EP/E03763 1/1).

REFERENCES

1. Castillo, A., Seifoddini, H., & Abell, J. (1997). The development of a cellular manufacturing system for automotive parts. *Computers & Industrial Engineering, 33(1-2),* 243-247.
2. Ronald G. Askin a, Hassan M. Selim b, Asoo J. Vakharia c, (1997). A methodology for designing flexible cellular manufacturing systems. *IIE Transactions, 29(7),* 599-610.
3. Saeed Zolfaghari, Erika V. Lopez Roa. (2006). Cellular manufacturing versus a hybrid system: A comparative study. *Journal ofManufacturing Technology Management, 17(7),* 942

 Published by Cranfield University Press ISBN: 978-0-9557436-7-2 http://hdl.handle.net/1826/3832

4. Sara L. Maas, Charles R. Standridge. Applying simulation to interative manufacturing cell design. *Proceedings of the 2005 Winter Simulation Conference,*
5. Schaller, J. (2007). Designing and redesigning cellular manufacturing systems to handle demand changes. *Computers & Industrial Engineering, 53(3),* 478-490.
6. Shambu, G., & Suresh, N. (2000). Performance of hybrid cellular manufacturing systems: A computer simulation investigation. *European Journal of Operational Research, 120(2),* 43 6-458.
7. David Claudio, Jie Zhang, Ying Zhang. A hybrid inventory control system approach applied to the food industry. *Proceedings of the 2007 Winter Simulation Conference,*
8. Pacciarelli, D. (2001). Parallel machine scheduling in a flexible manufacturing system. *IN FOR, 39(2),* 174- 184.
9. Potts, C. N., & Whitehead, J. D. (2001). Workload balancing and loop layout in the design of a flexible manufacturing system. *European Journal of Operational Research, 129(2),* 326-336.
10. Sodhi, M. S., & Sarker, B. R. (2003). Configuring flexible flowlines. *International Journal of Production Research, 41(8),* 1689-1706.
11. Quadt, D., & Kuhn, H. (2007). A taxonomy of flexible flow line scheduling procedures. *European Journal of Operational Research, 178(3),* 686-698.
12. Chowdary, B. V., & Kanda, A. (2003). A decision support system for flexibility in manufacturing. *Global Journal of Flexible Systems Management, 4(3),* 1-13.
13. Duilio Curcio, Francesco Longo, Giovanni Mirabelli. Manufacturing process management using a flexible modelling and simulation approach. *Proceedings of the 2007 Winter Simulation Conference,*
14. Hoda A. ElMaraghy. (2005). Flexible and reconfigurable manufacturing systems paradigms.
15. *International Journal of Flexible Manufacturing Systems, 17(4),* 261-276.
16. Balamurugan, K., Selladurai, V., & Ilamathi, B. (2006). Design and optimization of manufacturing facilities layouts. *Proceedings of the Institution of Mechanical Engineers -- Part B -- Engineering Manufacture, 220(8),* 1249-1257.
17. Hani, Y., Amodeo, L., Yalaoui, F., & Chen, H. (2007). Ant colony optimization for solving an industrial layout problem. *European Journal of Operational Research, 183(2),* 633-642.
18. Craig W. Alexander. Discrete event simulation for batch processing. *Proceedings of the 2006 Winter Simulation Conference,*
19. Dolgui, A., Guschinsky, N., Levin, G., & Proth, J. -. (2008). Optimisation of multi-position machines and transfer lines. *European Journal of Operational Research, 185(3),* 1375-1389.
20. Abdi, M. R., & Labib, A. W. (2004). Grouping and selecting products: The design key of reconfigurable manufacturing systems (RMS s). *International Journal ofProduction Research, 42(3),* 521-546.
21. Chin Soon Chong, Malcolm Yoke Hean Low, Appa Iyer Siva Kumar, Kheng Leng Gay. A BEE colony optimization algorithm for job shop scheduling. *Proceedings of the 2006 Winter Simulation Conference,*
22. Esra E. Aleisa, Li Lin. For effective facilities planning: Layout optimization then simulation, or vice versa? *Proceedings of the 2005 Winter Simulation Conference,*
23. Kesen, S., & Baykoç, Ö. (2007). Simulation of automated guided vehicle (AGV) systems based on just-in-time (JIT) philosophy in a job-shop environment. *Simulation Modeling Practice and Theory, 15(3),* 272-284.
24. Boysen, N., Fliedner, M., & Scholl, A. (2007). A classification of assembly line balancing problems. *European Journal of Operational Research, 183(2),* 674-693.
25. Juhani Heilala, Jari Montonen, Arttu Salmela, Pasi Järvenpää. Modeling and simulation for customer driven manufacturing system design and operations planning. *Proceedings of the 2007 Winter Simulation Conference,*
26. Umble, M., Gray, V., & Umble, E. (2000). Improving production line performance. *IIE Solutions, 32(11),* 36.
27. Tjahjono, B. and Baines, T. (2004). Research Study for a Manufacturing Simulation Centre. EEDA Report.

 Published by Cranfield University Press ISBN: 978-0-9557436-7-2 http://hdl.handle.net/1826/3832

'Open Innovation' and 'User-initiated Innovation' approaches to wealth generation

Shreyan Jain and Arthur Francis

Bradford University School of Management, Emm Lane

Bradford BD9 4JL

ABSTRACT

This paper discusses two models of the innovation process – 'open innovation' and 'user-initiated innovation'. It briefly describes each approach and the problems in adopting each individual approach. It proposes a way of combining these approaches into a more convenient and reliable approach and advocates research to assess the success of the combined model in practice.

INTRODUCTION

Innovation is a key to businesses' economic growth and success (Chesbrough, 2003). It is a critical driver for the competitiveness of firms and of economic growth. Therefore a deep understanding of how innovation can be managed is necessary to grow a business. Creating new wealth requires a more holistic approach to innovation than simply just inventing new product and responding to market demand. Innovation requires the interaction of technology, market and organization (Tidd et al, 2005). But the prevailing mindset in many organizations is that innovation is primarily a technological phenomenon, necessary for new product development albeit carrying high risk and uncertainty. It is argued that managers often overlook innovation in their consideration of business processes, corporate strategy, organizational structure, and business models. This leads to high failure rates of innovation which dissuades many companies from devoting much effort to developing a stream of innovations.

In the present day many companies are struggling with innovation processes despite possessing world standard R&D facilities, and skilled scientist and engineers. Why so? Various reasons have been suggested:

1. They don't realize the customer needs at the right time (Zairi, 1999)
2. They don't recognize innovation as a strategic corporate tool for alliances; such alliances might make it easier to make money by entering into new market or business or responding to market change (Tidd et al 2005).
3. They don't look out of their internal innovation's box i.e. other sources of innovation except internal R&D and Engineering (Chesbrough, 2003, Chesbrough et al, 2006).
4. They don't incorporate innovation process into their value chain or business model (Chesbrough, 2006), or they don't realize they can make more money from innovation via

 Published by Cranfield University Press ISBN: 978-0-9557436-7-2 http://hdl.handle.net/1826/3832

licensing, spin-off investment, joint ventures and other means than from internal development on their own (Gaule, 2006).

Other reasons are short life cycle of innovative product, increasing cost of innovation, and the quality of innovative products (Tidd et al, 2005).

The focus of this paper is on two models of the innovation process that attempt to resolve the above mentioned hurdles, by adopting open innovation (Chesbrough, 2003) on the one hand and by encouraging l**ead user** initiated innovation (von Hippel, 1986) on the other. We then propose a way of integrating these two approaches.

CUSTOMER NEEDS AND INNOVATION

Many argue that a key factor in the success of an innovation is the satisfaction of customer need at the right time and in the right place. Currently, highly competitive markets and sophisticated innovations have brought high customer expectations or needs of product/service quality (Prahalad and Ramaswamy, 2000).

OPEN INNOVATION

Open innovation brings together various established industrial practises but in a new systematic way not well explained by other writers on innovation (Chesbrough et al, 2006). It makes innovation processes somewhat complex to handle but very convenient, cheaper and faster than traditional approaches in gaining benefit from it (figure 1). The principal ideas are that an organization can a) leverage external sources of technology and innovation to drive internal growth and b) spin-off, divest or outsource underutilized the company's intellectual property. It proposes that great technologies or ideas can come both from inside and outside the company and they can be successfully commercialized with an appropriate business model. It integrates all the available external and internal knowledge resources into a single value chain of innovation 'from ideation to commercialization'.

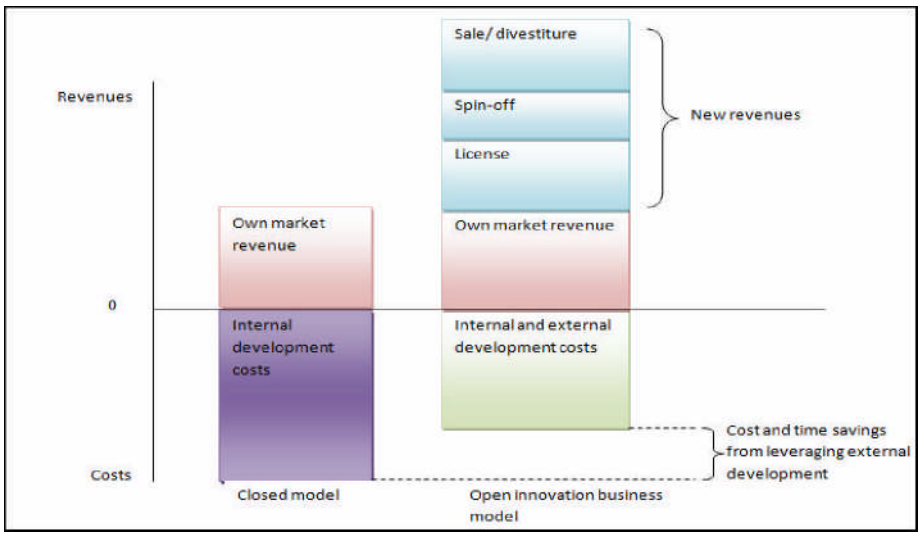

Figure 1. Open Innovation model (Chesbrough, 2006).

 Published by Cranfield University Press ISBN: 978-0-9557436-7-2 http://hdl.handle.net/1826/3832

According to Chesbrough (2003) companies that want to apply the open innovation approach need the architecture of a specific business model to integrate internal and external **technologies** or to find ideas to fill up any missing gap. Therefore k**nowledge sharing and an**

appropriate business model are recognised as the key component of an open innovation approach.

Knowledge flow can be inward or outward. Inwards flow of knowledge provide faster pace to development of product or process by offering the knowledge or technology which was previously not available in the value chain of innovation. Similarly the outward flow of technology/ideas allows organization to create value by licensing technology (possible for all sizes of company) or investing in a spin-off company (practical with an MNC).

A company can exploit knowledge from competitors ((Liberman and Montgomery,1998), customer/ lead user, university, government, private labs, other nations (von Hippel, 1988), collaboration with other firms (Tidd et al,2005), stakeholders, and intermediate firms (Chesbrough et al, 2006).

OPEN BUSINESS MODEL

A firm's business model is the ***set of activities*** *which* a firm performs, *how* it performs them, and *when* it performs them so as to offer its customers benefits they want and to earn a profit (Afuah, 2004). *Profitability is the ultimate aim of a firm's business model whether it is economically or strategically achieved.* Chesbrough (2006) emphasizes the need of an appropriate business model as the key to a successful technology because if the same technology is commercialized with two different business model it will give different economic values depending on the appropriateness of the business model.

Chesbrough (2003,2006,2007) and Chesbrough et al (2006) research on the concept suggest the following reasons for an organization to embrace an open business model:

- Technological innovation is coming from more sources than ever before. As a result, firms will be developing inferior technology if they don't access the best of what the world has to offer.
- Most intellectual property isn't used for any practical purpose. That's a waste of social and company resources i.e. the loss of social and economic welfare.
- The protection for intellectual property is stronger now, and an organization's progress will be blocked without collaborating with those who have complementary IP.
- Possible opportunities and threats from growing intermediate market.
- Product cycles are shorter and costs of developing new technologies are higher; open business models offer the promise of getting to market sooner at lower cost so that your business has a better chance of earning a decent return on new technology.

 Published by Cranfield University Press ISBN: 978-0-9557436-7-2 http://hdl.handle.net/1826/3832

- Large companies need to make new product development more productive if they are to meet their growth goals.

WAYS TO GENERATE WEALTH THROUGH OPEN BUSINESS MODEL

In an open innovation model, a company can make money from new technology in four basic ways:

- by incorporating the technology in their current businesses
- by launching new ventures or spin off, that exploit the technology in new business arenas
- by giving licenses to a firm or firms whose business models suit the technology
- by approaching totally new markets through adopting a totally new and innovative business model.

DRAWBACKS AND WEAKNESS OF IMPLEMENTING AN OPEN INNOVATION APPROACH

To date applications of open innovation have been tried in large organization like IBM, P&G, Intel, Cisco, Eli Lilly and high tech small start up firms like Palm inc, and Millennium pharmaceutical.

Additionally it seems to be beneficial for intermediate firms to grow their business like Innocentive, Nine sigma, Big idea group etc. But small and medium enterprises (SMEs) seem to find harder to apply. One suggestion is that embracing an open innovation concept requires extra resources for large internal change in organizational structure, policy and vision which may be difficult for SMEs.

Further, the open innovation paradigm explicitly recognizes customer needs as an important factor for a successful innovation process, but so far no open innovation research suggests how this can be satisfied except proposing it through various external resources, which is probably a big obstacle to the success of this concept in future.

One such approach which especially focuses on customer needs is the 'user-initiated innovation' model.

LEAD USER INITIATED INNOVATION APPROACH

This was proposed by Eric von Hippel in 1976. According to him most of the ideas for innovation come from the individuals that use the product in their work or at home. Such users may innovate for their own direct utility (Von Hippel, 2005). He named such users "Lead users". He believes lead users are the potential source of external knowledge for an organization and their needs are the most accurate parameter of realization of actual market need which makes them fundamental to the success of a new product.

Lead users have two main characteristics (von Hippel 1986);

- They are ahead of the target market, so what they want now will be demanded by the market as a whole in future

 Published by Cranfield University Press ISBN: 978-0-9557436-7-2 http://hdl.handle.net/1826/3832

- They have a high incentive to solve a problem, so they may innovate it.

Each characteristic of Lead users has an independent and valuable emphasis on new product development (NPD) and hypothesized solution data (Urban and Hippel, 1988). The first is valuable as problem solving for market researchers which gives a probably accurate indication of need or solution regarding real world experience which lead users posses i.e. they can serve as a need forecasting laboratory for market research. The second attribute emphasizes that lead users fill their needs by innovating solutions for them. This can provide valuable insights about new product development opportunities and design data for the manufacturer in addition to data about customer needs.

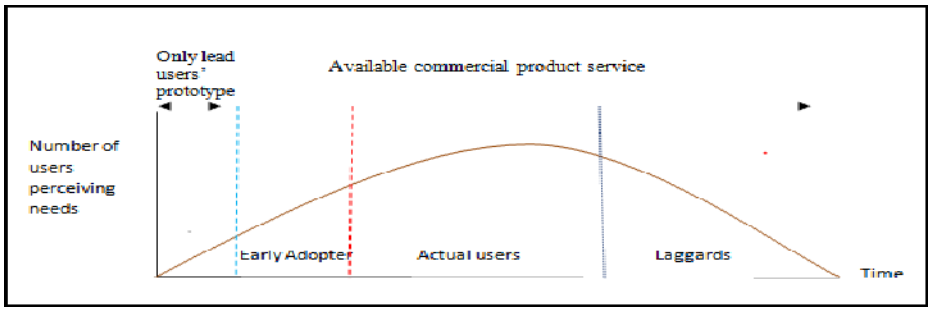

Figure 2: User perceiving need during the product life cycle (diffusion curve).

WHO ARE THE LEAD USERS?

Lead users can be a firm, an organization or an individual. The important characteristic is that they develop or innovate in order to use it for their own need rather than to manufacture and sell. Lead users should not be confused with earlier adopters who use the first commercialized product (figure.2). One of the best examples of lead user initiated innovation is WWW, which was developed by Sir Tim Berners-Lee in 1989 for his own use and now it's the heart of modern IT science. The lead user method does not limit market research to typical consumers. It looks at various dimensions of an innovative product in various contexts or industries. For examples braking systems in the auto industry may be brought from the aviation industry - the lead users in one industry may be ahead of other industries' lead users for probably the same needs.

SIMILARITIES BETWEEN THE OPEN INNOVATION AND LEAD USER INNOVATION APPROACHES

Both open innovation and lead user innovation approaches have many common features which are useful for successful commercialization of an innovation. Such as

- useful in giving cost effective, fast and quality oriented technology
- emphasize knowledge sharing and networking
- useful in radical as well as incremental innovation processes

 Published by Cranfield University Press ISBN: 978-0-9557436-7-2 http://hdl.handle.net/1826/3832

- increase social welfare and economic value for money
- useful in creating a competitive environment in a nation's market.

The best example which incorporates both open innovation and lead user approaches is "Open source software system", although it creates value for the organization but it doesn't capture directly any portion of that value to organization.

Differences in open innovation and lead user innovation approaches

These include:

1. The ultimate aim of lead user innovation is to identify the customer needs whereas open innovation approach emphasizes to serve customer need in market through a business model.
2. The open innovation paradigm can be used in all kind of industries despite the fact that, to date, it is adopted by only high tech and science based companies, while, according to Tidd et al (2005), the lead user innovation approach is most useful in industries where machinery, software, and instruments are the core products.
3. The open innovation approach is based on big and high tech start up companies and doesn't say much about SMEs, whereas the lead users approach is a very realistic and practical approach which can be easily adopted by SMEs for development in their pipeline and can generate wealth through manufacturing or marketing the lead users' innovated product.
4. Open innovation is a more strategic and business oriented approach to NPD, whilst the lead users approach is based on a simple business process.
5. Open innovation is a complex process to apply in traditional organization due to heavy organizational and resources change while user initiated innovation can be easily associated with the business processes of traditional organizations.

CONCEPTUALIZATION FOR NEW APPROACH

If we focus on causes of the failure of an innovation process, it is clear that individually neither open innovation nor lead user approach completely resolve the failure problem. Additionally limitations of both approaches may restrict the path of innovation for an organization which wants to be innovating through one of the two innovation approaches, so there is need for a comprehensive approach which can resolve the failure problems of each approach. Can the two approaches be combined? If they can, it may also reduce the limitation of the individual approaches so they can be applicable for the all kinds of organization from small to large and from low tech to highly high tech company.

But how we can do so? Possibly it can be answered by dividing the innovation process into two main parts

 Published by Cranfield University Press ISBN: 978-0-9557436-7-2 http://hdl.handle.net/1826/3832

- Ideation (Ideation to Proof of concept) - Lead users! other knowledge resources
- Pilot plan (Development to commercialization) - Open business model! approach

This process can be named as user initiated open innovation model.

Since lead users are the central resources for the successful ideation of any inventive product so it would be useful to use them as a key tool for the ideation process.

This ideation process extends up to proof of concept because lead users not only have the ability to forecast market needs but also they can innovate products themselves which is a useful attribute in the proof of concept phase. By targeting customer needs through lead users an organization can make money by saving in the development cost of the product!process (figure 3). It is practical and realistic because mostly lead users' innovated products are cheap and successful (von Hippel, 2005).

Once proof of concept is finalized a pilot plan for the development of the new product can be targeted. The whole approach should be according to the open business model so it can leverage all the available commercialization opportunities of the new product through marketing it in existing market or in a new market.

 Published by Cranfield University Press ISBN: 978-0-9557436-7-2 http://hdl.handle.net/1826/3832

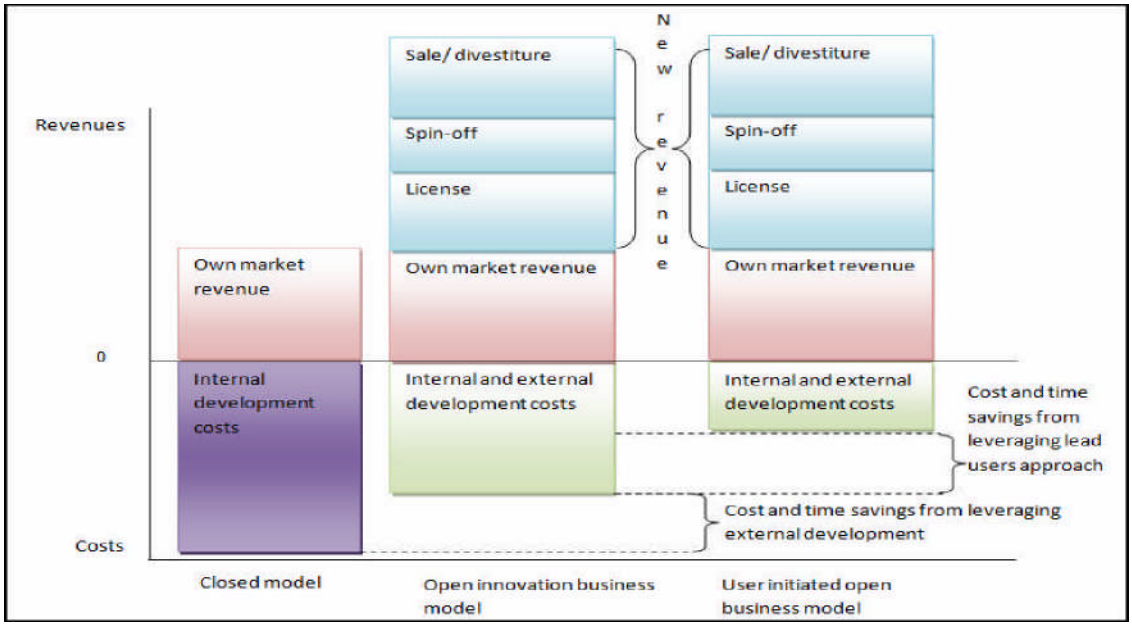

Figure 3: User initiated open business model.

CONCLUSION

So far many innovation approaches have been proposed and many are in use, but open innovation and lead user innovation approaches have the potential to make the innovation process less risky and more successful. But both approaches also have their own limitations which can be reduced by incorporating the essence of both approaches. The conceptual model seems to be easy to understand but it needs to be practically analysed through further research. The framework presented here is the first step in this direction. Further research needs to focus on developing methods to help managers make wise and better decisions in the context of NPD and innovation.

REFERENCES

1. Afuah, A (2004). "*Business Model. A strategic management approach"* Boston, MA ; London: McGraw-Hill/Irwin,
2. Chesbrough, H (2003) *Open innovation. The New Imperative for creating and profiting from technology.* Boston: Harvard Business School Press.
3. Chesbrough, H. (2006) *Open business models how to thrive in the new innovation landscape.* Boston, Mass.: Harvard Business School Press.
4. Chesbrough, H, WimV, and Joel,W (2006) *Open innovation. Researching a new Paradigm* .Oxford University Press.
5. Chesbrough, H. (2007) Speaker series with Henry Chesbrough on open innovation. http://video.google.co.uk/videoplay?docid=5451345033512883318&q=open+innovation&total=344&start=0&num=1 0&so=0&type=search&plindex=3
6. [Accessed 21/01/08]
7. Gaule, A (2006). "*Open innovation in action".* London: H-I Networks.
8. Liberman, M. B. And Montgomery, D. B. (1988). " First mover advantage" strategic management journal 9,41-58 in Chesbrough, H, WimmV., and Joel,W (2006) *Open innovation: Researching a new Paradigm* .Oxford University Press.
9. Prahalad, C.K. & Ramaswamy, V. (2000), "Co-opting Customer Competence", *Harvard Business Review,* 78(1): 7 9-87

 Published by Cranfield University Press ISBN: 978-0-9557436-7-2 http://hdl.handle.net/1826/3832

10. Porter, M., E and Stem, S. (1999) *The new challenge to America's Prosperity; finding from the innovation index.* Washington DC: Council on competitiveness
11. Tidd J, Bessant J and Pavitt Keith (2005), *Managing innovation: Integrating Technology, Market and organizational change,* 3rd edition. Chichester: John Wiley and Sons Ltd. Von Hippel, E. (1988), *The Sources ofInnovation,* New York: Oxford University Press. Von Hippel,E (2005), *"Democratizing innovation"* Cambridge MA: MIT Press.
12. Von Hippel (1986), "Lead users: A source of novel product concept" *Management science 32(7), 791-805.*
13. Urban, G.L., and Von Hippel E (1988). "Lead users analyses for the development of new industrial products" *Management Science 34(5): 569-82.*
14. Zairi,M (1999). *"Process Innovation Management".* Oxford: Butterworth-Heinemann.

 Published by Cranfield University Press ISBN: 978-0-9557436-7-2 http://hdl.handle.net/1826/3832

Turbulent Flows in the Internal Environment: the case of the A380 Aircraft Cabin

A.A. Mylonas, E. Shapiro & D. Drikakis

Fluid Mechanics & Computational Science Group, Aerospace Sciences Department
Cranfield University, Cranfield, Bedfordshire MK43 0AL, UK

ABSTRACT

Detailed understanding of the ventilation process in internal environments is important for comfort and safety reasons, particularly when a closed environment, such as an aircraft cabin is considered where evacuation is not possible in case of ventilation system contamination. In this paper Computational Fluid Dynamics (CFD) is utilised to study the turbulent flow inside an A380 aircraft cabin. Reynolds Averaged Navier Stokes (RANS) turbulence modelling is employed in order to minimise the computational cost of the simulations and assess the accuracy obtainable in a design context. The results indicate that the selection of the appropriate turbulence model as well as grid size and shape is of paramount importance for realistic simulations of the phenomena involved. The comparisons with the experimental data show that satisfactory prediction can be obtained with limited computational resources.

Keywords: Aircraft Cabin, Coanda effect, Computational Fluid Dynamics (CFD), Internal Environment, Reynolds Averaged Navier- Stokes (RANS), Turbulent Flows, Ventilation.

INTRODUCTION

The essence of studying an internal environment is to provide safe and comfortable conditions for its inhabitants through enhancing our physical understanding of the corresponding flow phenomena [1]. Most of these studies focus mainly on buildings, such as houses, offices, hospitals as well as subways, aeroplanes, ships and other means of transportation. The study of the flow in the internal environment is of crucial importance for resolving complicated turbulent scenarios and better understanding of cases like contaminant dispersion.

According to Koinakis [2], “ventilation should fulfil two basic objectives: (a) to remove the indoor pollutants and prevent the outdoor pollutants from entering, and (b) to control the indoor climate and the thermal comfort sense by intervening in the thermal balance”. Most studies of internal environments give special attention to their ventilation. Considering the importance of ventilation for the creation of a safe,

 Published by Cranfield University Press ISBN: 978-0-9557436-7-2 http://hdl.handle.net/1826/3832

comfortable environment and for protection from dangers, such as contaminant dispersion, the aircraft cabin represents one of the most interesting areas for case studies. Aircraft have a closed ventilation system and in the case of an emergency evacuation is, with only a few exceptions, impossible At the same time, aeroplanes are small spaces, densely occupied by humans, vulnerable to a wide variety of dangers. Consequently, if anything goes wrong during a flight, the impact can be fatal. It is not surprising, therefore, that a significant number of studies have been carried out to examine security issues in aircraft.. Mangili and Gendeau [3] studied the transmission of infectious diseases during commercial flights because of the nature of the flow in this enclosed space. In-flight cabin smoke control was studied by Eklund [4].

In order to study contaminant dispersion, it is imperative to understand the flow inside the cabin. The contaminant is usually of a very small quantity thus not influencing the flow significantly. A very interesting study of the turbulent flow inside the aircraft cabin was conducted by Bosbach et al. [5,6]. Their study aimed at better understanding and optimising the airflow in an aircraft cabin. As it has been underlined by Bosbach et al. [5] a key issue is the selection of the appropriate method for modelling the turbulence flow.

THE CASE OF THE A380 AIRCRAFT CABIN

In the case of the aircraft cabin there is an interest in studying the turbulent flow that is generated by the geometrical characteristics of the cabin despite the low Reynolds number. High-resolution high order methods in time and space are required to resolve all time, length and velocity scales described by Kolmogorov [7]. The direct approach named as Direct Numerical Simulation (DNS) is mainly used for simulating simple geometries at low Reynolds numbers. something that is not fully applicable to the air cabin case due to the computational implications that the geometry's complexity introduce. Another tool for simulating turbulent flows is Large Eddy Simulation (LES). Although this approach is computationally more elegant compared with DNS, a lot of computations are still introduced and careful and detailed modelling, especially of the near-wall flow region, is needed [8]. Consequently for this case a statistical based method named the Reynolds Averaged Navier-Stokes equations (RANS) is engaged. While RANS does not provide time-accurate description of the flow, the low computational cost of RANS simulations make it a tool of choice for providing fast computational results in a design context.

GAMBIT and Gridgen software are used for unstructured and structured grid generation respectively and the commercial CFD solver FLUENT for RANS CFD modelling. For all flows, FLUENT

 Published by Cranfield University Press ISBN: 978-0-9557436-7-2 http://hdl.handle.net/1826/3832

solves the Navier-Stokes Equations and additional transport equations are solved when the flow is turbulent [9]. Two-equation turbulent

models, RNG (Renormalization Group) and Realisable $K-\varepsilon$, were used to simulate turbulent flows.

EXPERIMENTAL CASE

Although CFD is far more flexible, economic and time saving than the experimental method, it still does not always provide us with 100% accurate and credible information [10]. Adding to this, the fact that turbulence is studied using the RANS method, which is an approximation model, puts the credibility of the results to question. This is the reason why validation of the CFD approach is needed. In order to validate the simulations' results, experimental data are essential.

The experimental data used for validation are drawn from Bosbach et al. [5]. A simplified aircraft cabin of an Airbus A380 has been used focusing on the luggage compartment and inlet, Figure 1. The mock-up used in those particular experiments was created in full scale. In this case, the air enters the mock-up horizontally through three slot-shaped air inlets, which apply 40 l/s (in total) of air through 3 small inlet slits. The air outlet is located below the air inlet at the ground level of the mock-up. The airflow was investigated experimentally by particle image velocimetry (PIV).

 Published by Cranfield University Press ISBN: 978-0-9557436-7-2 http://hdl.handle.net/1826/3832

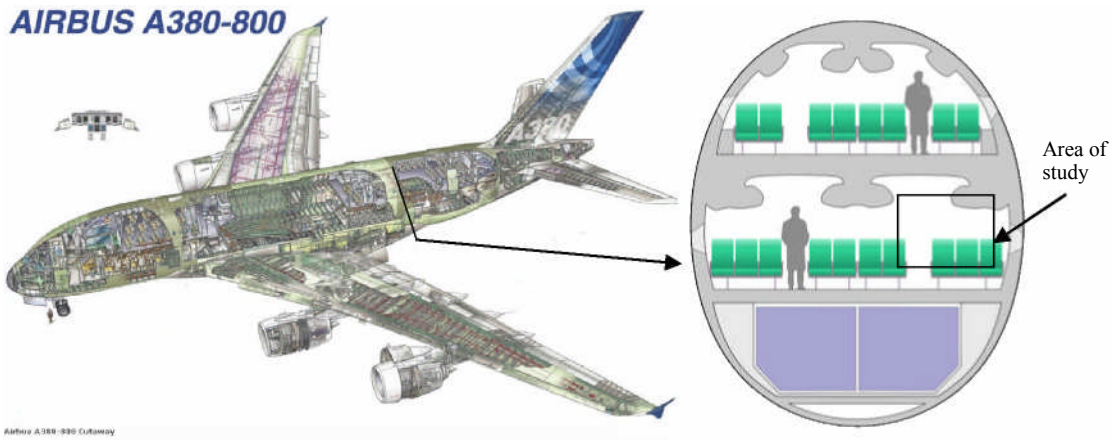

Figure 1: Airbus A380 schematic (left) and area of study (right). Images courtesy of Airbus [11]

GEOMETRY AND MESH

Although RANS will be used to compare with the measurements here, for the purposes of validation, only a part the mock-up was chosen, with symmetry planes for reducing the computational cost. Considering the fact that RANS presents a time-averaged solution, there is no need to build a grid with as many cells as it would be needed in DNS, however, a very good grid resolution is still required. Because of the three nozzles, the domain can be separated into three cells of equal size. In each cell the flow is induced by one nozzle. Following Bosbach [5], an assumption is made that the flow within each cell is not influenced by the neighbouring cells so computations are performed only in the central cell. The central cell can be further reduced to one half of the cell size using symmetry boundary conditions (Figure2).

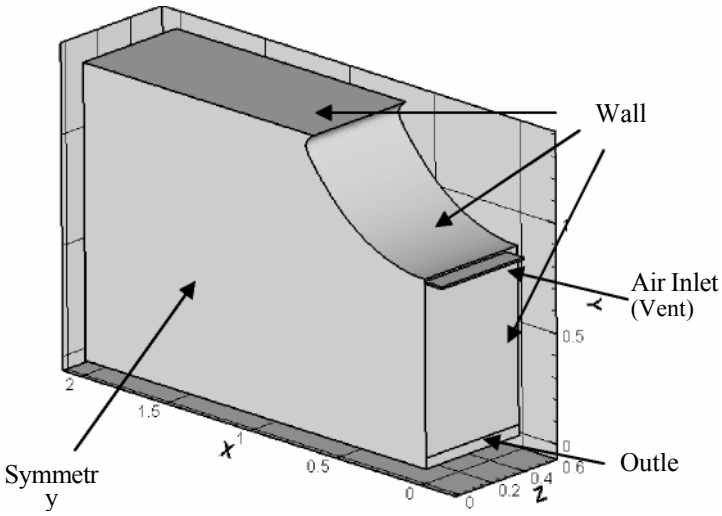

Figure 2 Computational domain used for the simulations

 Published by Cranfield University Press ISBN: 978-0-9557436-7-2 http://hdl.handle.net/1826/3832

For simulating this case, both an unstructured and a structured mesh were used. Both grids were used for simulations in FLUENT and the best results from both grid types were used for the comparison with the experimental case. The creation of the domain and the mesh was a challenging task that had to be treated in a quite diligent way because of the morphology, as well as the topology, of the luggage compartment and the inlet. The aforementioned part of the cabin is the one that presents the most interest, since the ventilation jet is initially attached to it due to Coanda effect and then separates from the wall near the roof of the cabin. This, as it will be demonstrated further on, creates the need for a further refined grid in these areas.

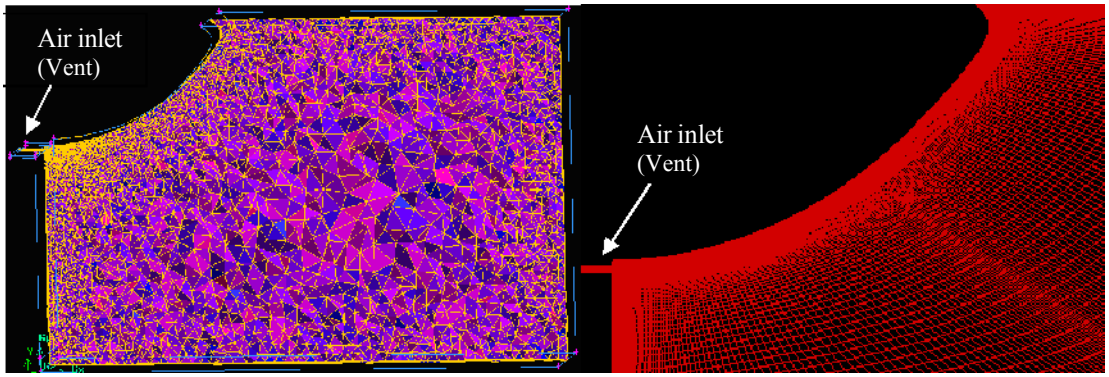

Figure 3 The mesh in the centre area (horizontal cut) for the unstructured grid and zoom-in for the structured grid

The areas along the luggage compartment and close to the air inlet present the most interest and had to be better resolved. At the same time, the flow pattern closer to the faces of the geometry rather than inside, presents the most interest. The depth of the boundary layer was calculated based on the Reynolds number, which is approximately 880 based on the inlet height and 88000 based on the characteristic mock-up length. Gambit was used to generate the unstructured mesh consisting of 613,000 cells. Gridgen was respectively used to generate the structured mesh of 1,127,300 cells. A smooth gradual transition of cell sizes was performed from the curved areas to the sharp ones of the physical domain to improve various numerical aspects of the computations. Both types of grids are illustrated in Figure3.

 Published by Cranfield University Press ISBN: 978-0-9557436-7-2 http://hdl.handle.net/1826/3832

SIMULATIONS

As mentioned previously, FLUENT was used for the simulations and RANS two-equation turbulent models were employed. In order to understand the computational power at our disposal it is important to mention that a single processor was used. For the

validation, initially, two different turbulent models were used, $K-\varepsilon$ RNG and $K-\varepsilon$

Realisable. The simulations were initiated using the unstructured grid. For the computations a first order upwind scheme was used along with simple pressure velocity coupling. The boundary conditions for both models were exactly the same. The initial values for the simulations were all set to 0 except the X Velocity that was set to 1 .32m/s. A second order accurate discretisation scheme was later employed to improve the results.

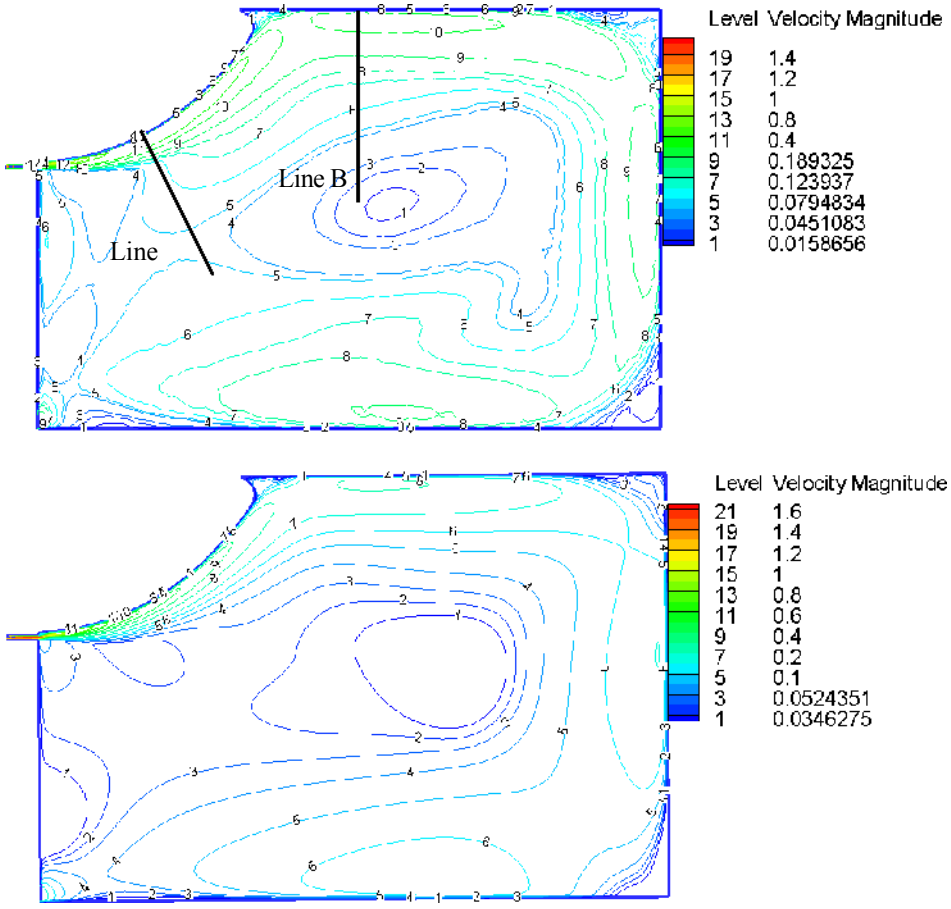

Figure 4 Velocity Magnitude for the RNG model of the unstructured (top) and structured (bottom) grid

For the simulations on the structured grid, the exact same settings and conditions were used. After studying the results from the unstructured grid simulations, the use of

 Published by Cranfield University Press ISBN: 978-0-9557436-7-2 http://hdl.handle.net/1826/3832

the K -ε RNG model was selected since for this case it was superior in terms of quality of results to the Realisable one. Another change in the structured grid simulations was the order of the discretisation scheme. A second order discretisation scheme was also employed to improve the results. The first order results obtained after 3000 iterations were used as an initial guess for the second order.

The computed results were compared with the experimental data at distinctive regions of the domain. For that reason computational data were collected along two lines. These lines are situated at the middle of the mock-up for the experimental case and at the line of symmetry (with the inlet) side of the computational domain. Line A expands from the luggage compartment wall towards the centre of the geometry while Line B expands from the roof wall towards the centre, as shown in Figure4.

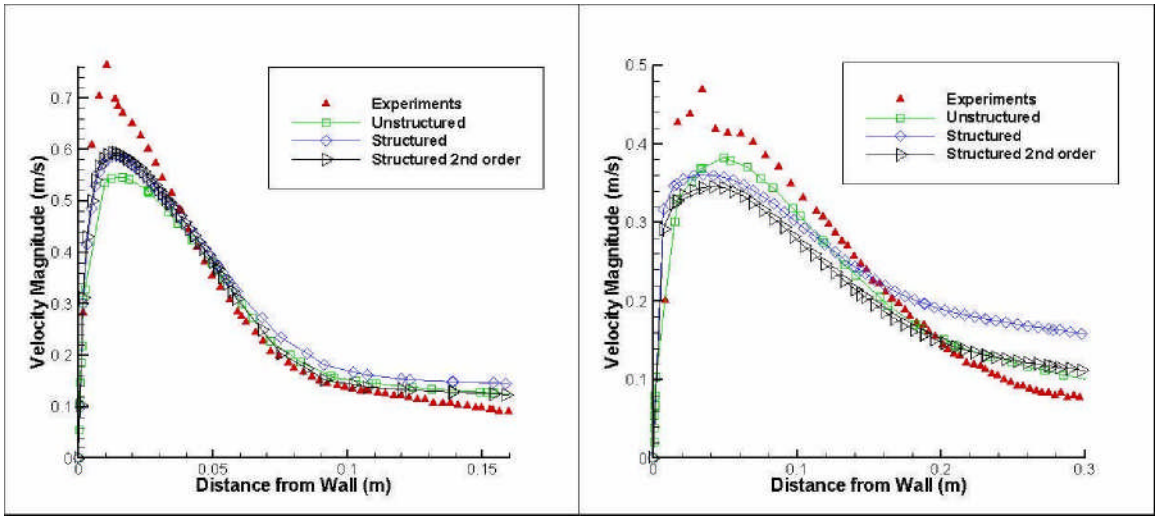

Figure 5 Velocity Magnitude along Lines A (left) and B (right) for the experimental and the numerical cases for RNG method

RESULTS AND COMPARISON WITH EXPERIMENTAL DATA

The solution converged in a relatively short period of time considering the limited computational resources used in this study. The velocity magnitude for the symmetry plane of the unstructured and the structured grid that is also the middle of the mock-up is shown in Figure4. This is also the area, where the experimental data were taken from. The results concerning the velocity magnitude along lines A and B are shown in Figure5 in addition to the experimental results. The comparison between the experimental data, the improved RNG results for the unstructured grid (second order) and the first and

 Published by Cranfield University Press ISBN: 978-0-9557436-7-2 http://hdl.handle.net/1826/3832

second order RNG results for the structured grid is presented in Figure5. This comparison is the most crucial part for the validation of the CFD process.

The results obtained on the structured grid with the second order method show better comparison with the experimental data where the jet velocity is high (Line A) while the performance of structured and unstructured grid simulation was comparable in the regions of the low jet velocity (Line B). However the results show that the high velocity incoming jet is not captured accurately causing a small discrepancy between experimental and numerical data. The lines follow the same pattern but the top velocity at the near wall region is underestimated. Although raising the order of the scheme from first to second did not improve the results significantly, considering the small needs in extra computational power required for this change, the advantage can be considered important. A change in the grid size might improve our results but would significantly raise the computational expense. Overall, the trend of the jet behavior is predicted correctly and the results are in satisfactory agreement with the experiment. The refinement of the grids used will lead to the improvement of the computational results however at the expense of the significant increase of the computational cost. Bearing in mind the speed with which RANS CFD results for this problem can be obtained (approximately two to three days) on relatively low specification hardware (single core x86 class at 3.00 GHz), the comparisons obtained underline the suitability of RANS CFD modelling as a design tool for the aircraft cabin ventilation.

CONCLUSIONS

An investigation of RANS CFD suitability as a design tool for aircraft cabin ventilation has been conducted. The turbulence model which provides best accuracy for this case has been identified. Despite relatively low Reynolds numbers, the flow in the section of the A380 cabin features a wall-attached turbulent jet and eventual separation which makes it quite challenging to model. However comparisons with available experimental data indicate that reasonable accuracy can be obtained with very limited computational resource. While the results can undoubtedly be improved by further grid refinement and application of time-accurate turbulence modelling approaches, the quality/cost ratio of the simulations presented demonstrates that CFD using RANS turbulence models yields acceptable results for the turbulent ventilation jet at the luggage compartment wall.

 Published by Cranfield University Press ISBN: 978-0-9557436-7-2 http://hdl.handle.net/1826/3832

REFERENCES

1. K. A. Papakonstantinou, C. T. Kiranoudis, and N. C. Markatos. Computational analysis of thermal comfort: The case of the archaeological museum of Athens. *Applied Mathematical Modelling,* 24(7) :477–494, 2000.
2. C. J. Koinakis. The effect of the use of openings on interzonal air flows in buildings: An experimental and simulation approach. *Energy and Buildings,* 37(8):813–823, 2005.

A. Mangili and M. A. Gendreau. Transmission of infectious diseases during commercial air travel. *Lancet,* 365(9463):989–996, 2005.

3. T. I. Eklund. In-flight cabin smoke control. *Toxicology,* 1 15(1-3):135–144, 1996.
4. J. Bosbach, J. Pennecot, C. Wagner, M. Raffel, T. Lerche, and S. Repp. Experimental and numerical simulations of turbulent ventilation in aircraft cabins. *Energy,* 31(5):694–705, 2006.

B. Wagner I. Gores T. Lerche J. Bosbach, J. Pennecot. Particle image velocity and hot wire anemometry for investigation of premature flow separation in a generic aircraft cabin mock-up. *www.dlr.de*, 2005.

5. J. O. Hinze. *Turbulence.* McGraw-Hill, New York, 1975.
6. M. Lesieur and O. Metais. New trends in large-eddy simulations of turbulence. *Annual Review ofFluid Mechanics,* 28:45–82, 1996.

7. Fluent documentation. *http://www.fluentusers. com.*

8. R. P. Garner, K. L. Wong, S. C. Ericson, A. J. Baker, and J. A. Orzechowski. Cfd validation for contaminant transport in aircraft cabin ventilation flow fields. pages 248–253, 2003.
9. [11] Airbus website www.airbus.com

 Published by Cranfield University Press ISBN: 978-0-9557436-7-2 http://hdl.handle.net/1826/3832

Immunosensor for Aflatoxin B_1 Using Gold Working Electrode

M. A. Kadir and I.E. Tothill*

Cranfield Health, Cranfield University, Silsoe, Bedfordshire, MK45 4DT, UK

INTRODUCTION

Aflatoxins contamination in foods and animal feeds is of global concern due to their potential toxicity, carcinogenicity and also their immunosuppressive ability for the mammalian system. Aflatoxins are a group of highly toxic secondary metabolites produced by the fungi *A. flavus* and *A. parasiticus.* The major occurring aflatoxins are aflatoxin B_1 (AFB_1), B_2 (AFB_2) (produced by *A. flavus* and *A. parasiticus)* G_1 (AFG_1) and G_2 (AFG_2) (produced by *A. parasiticus)* plus two additional metabolic products, M_1 (AFM_1) and M_2 (AFM_2). Therefore, concern has been expressed for the effect of this group of toxins on human health since AFB_1 (Figure 1) is known to be the most predominant and most toxic.

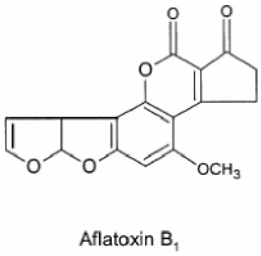

Figure 1: Chemical structure of AFB_1 (Hussein and Brasel, 2001)

To control and manage the level of aflatoxins, many countries worldwide have set permitted exposure limits for food and feed intended for direct human consumption or for use as ingredient in animal foodstuffs, which vary from 1- 20 $\mu g\ kg^{-1}$. The maximum acceptable level for AFB_1 in food is set at 2 $\mu g\ kg^{-1}$ (ppb) in 29 countries, which include EU countries (van Egmond and Jonker, 2004).

Therefore, current research focuses on the development of AFB_1 sensing techniques based on immunosensor systems. This developed technique must be able to detect the toxin at low levels (ppb or ppt range) as well as to be rapid and simple to use (Logrieco et al., 2005). The adopted approach is based on an electrochemical sensor platform fabricated using screen printed gold electrode combined with a specific competitive immunoassay methods using an antibody immobilised on the gold sensor surface. Current analysis is generally based on the use of conventional methods such as HPLC which can be difficult to perform on site and also expensive. Therefore, a need exits for an alternative method which is rapid and portable and that exhibits the sensitivity and low detection capability of conventional methods.

 Published by Cranfield University Press ISBN: 978-0-9557436-7-2 http://hdl.handle.net/1826/3832

METHODOLOGY

Indirect and direct competitive immunoassay were developed, initially by ELISA and subsequently transferred to an electrochemical immunosensor format using screen printed gold electrode (Figure 2).

For indirect immunoassay format, the competitive assay was carried out between free AFB_1 and anti-AFB_1 antibody (monoclonal antibody) for the binding site of antigen-protein conjugate (AFB_1-BSA). Signal detection was carried out by using a labelled secondary antibody (anti-mouse IgG labelled with HRP). In case of direct format assay, the competitions between AFB_1 labelled HRP (AFB_1-HRP) and free AFB_1 unlabelled in the reaction with an anti-AFB_1 antibody (monoclonal antibody) for the binding site of unlabelled secondary antibody (anti-mouse IgG) on the solid phase. During each step of the assay; washing procedure were carried out between immobilization (coating), blocking, competition and labelling. A TMB/H_2O_2 solution was used for signal current development.

RESULTS

The first step in the optimization assay development is to determine the optimal conditions (incubation times and temperatures) of the assay and dilution/concentration of different reagents. The optimised parameters of the assay for both formats are summarised in Table 1.

CALIBRATION CURVE OFELISA

The normalised calibration curves for AFB_1 generated using the condition are shown in Figure 3 for both formats using spectrophotometry. The readings decreased from low to high concentration of AFB_1 and declined steadily after 10 $\mu g\ L^{-1}$. The working range is in the range of maximum level of AFB_1 (1 to 20 ppb).

 Published by Cranfield University Press ISBN: 978-0-9557436-7-2 http://hdl.handle.net/1826/3832

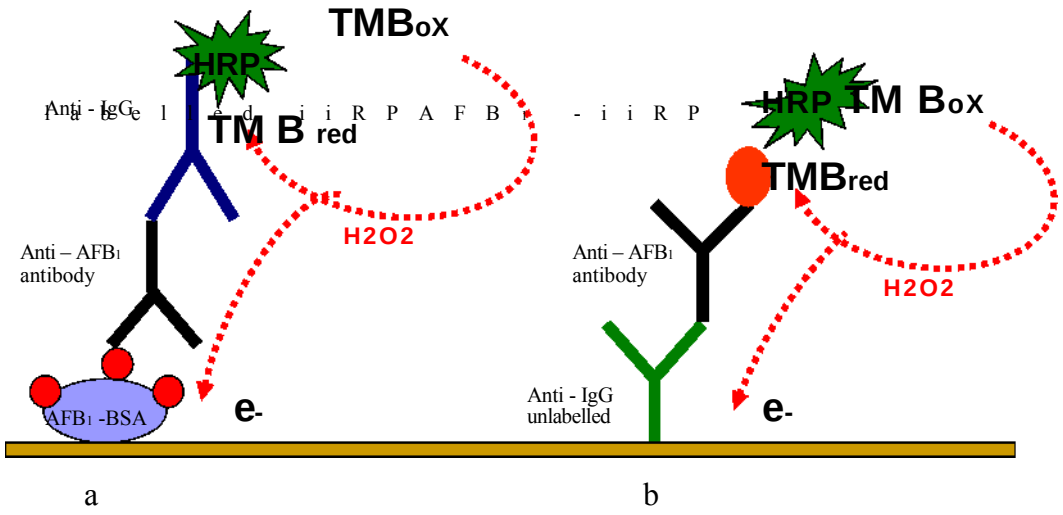

Figure 2: Immunoassay format on gold working electrode and iiRP catalysed ii2O2/TMB reaction. (a) indirect competitive format and (b) direct competitive

Table 1. Selected concentration of the different reagents and optimal condition used in indirect and direct format of spectrophotometric immunoassay for aflatoxin B1

Reagents	Concentrations	Incubation time
Indirect format		
AFB1-BSA conjugate	1.0 µg mL^{-1}	Overnight (12 h), 4°C
Anti-aflatoxin B1 antibody (Mab)	10 µg mL^{-1}	1.5 h, 37°C
Anti-antibody-iiRP (Abii-iiRP)	1.0 µg mL^{-1}	1.0 h, 37°C
Direct format		
Anti-mouse IgG	25 µg mL^{-1}	Overnight (12 h), 4 C
Anti-aflatoxin B1 antibody (Mab)	20 µg mL^{-1}	2 h, 37 °C
Aflatoxin B1 labeled with iiRP	1: 10 dilution	2 h, 37 °C

 Published by Cranfield University Press ISBN: 978-0-9557436-7-2 http://hdl.handle.net/1826/3832

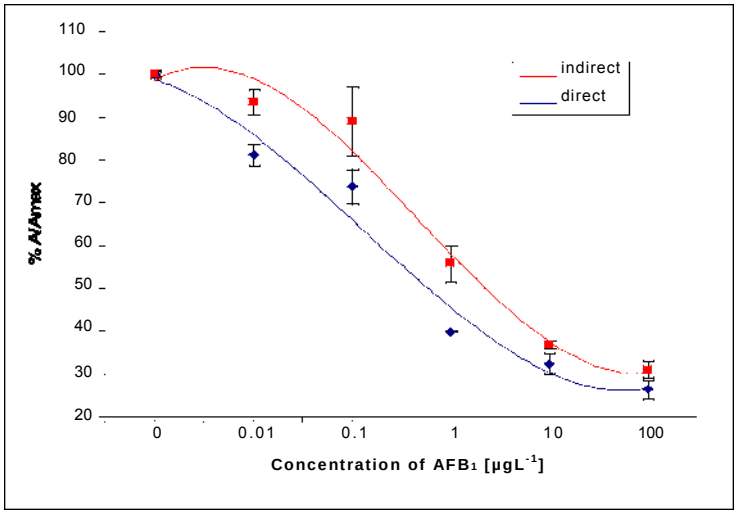

Figure 3: Calibration curves of AFB1 for both formats using spectrophotometric: each point is the mean of three measurements.

DEVELOPMENT OF AN ELECTROCHEMICAL IMMUNOSENSOR

POTENTIAL DETERMINATION

The most suitable electrochemical method of monitoring the reduction current of $TMB_{(ox)}$ was considered to be chronoamperometry. Chronoamperometry detection for enzymatic activity using TMB/H_2O_2 substrate in the range of -200 to 0 mV potential was investigated. The indirect non-competitive format with or without HRP was analysed by amperometry to determine the signal and the background responses. The HRP activity was recorded as an increasing negative current response at potential - 200 to 0 mV. At -200 mV the largest signal (-3.03 μA) was obtained whilst the background signal was still acceptably low (-0.704 μA). Therefore chronoamperometry data using SPGE Dupont determined at -200 was the most suitable potential.

OPTIMIZING TMB AND HYDROGEN PEROXIDE CONCENTRATION

The substrate used for the signal generation of the anti- HRP conjugate is an in house prepared TMB/ $_{H_2O_2}$ substrate solution. Therefore, the most suitable TMB and H_2O_2 concentrations to apply in the test were examined for optimal current generation. This was conducted by changing the concentration of both chemicals and monitoring the signal achieved for the assay. The different concentrations of TMB from 0.1 to 10mM were determined as well as 0.0015 to 0.15% concentrations of $_{112O2}$ (from dilution 30% of $_{112O2}$ solution). The maximum current response showed optimal concentration of substrate of 5 mM TMB and 0.075% $_{112O2}$ concentrations.

 Published by Cranfield University Press ISBN: 978-0-9557436-7-2 http://hdl.handle.net/1826/3832

INDIRECT NON COMPETITIVE DETERMINATION BY DIFFERENT CONCENTRATIONS OF MONOCLONAL ANTIBODY

The specific binding of 1 to 50 μg mL^{-1} monoclonal antibody was tested by immobilizing a fixed amount of AFB1-BSA (1 μg mL^{-1}) as well as binding to Ab11RP at 1 μg mL^{-1} concentration. The plot from Figure 4 (a) shows the signal response was increased with the increasing concentration of monoclonal antibody. A 50 μg mL^{-1} concentration of Mab gave the highest response and indicated that a high concentration of Mab could be used in the immunosensor system.

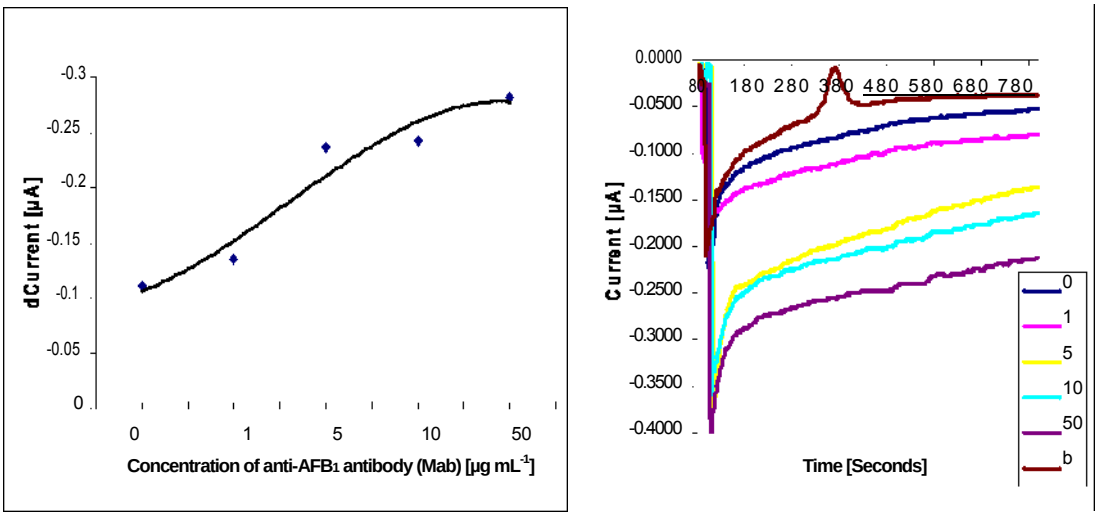

Figure 4: (a) The signal of different monoclonal antibody (Mab) concentrations by chronoamperometry (-200 mV) and using TMB (5 mM) and $_{112O2}$ (0.075%). (b) Chronoamperograms of Mab concentration versus times.

AFLATOXIN B1 DETERMINATION

Calibration curve were prepared prior to each assay by using 10 serial dilution of AFB1 standard solution with concentrations in the range 0-100 μg L^{-1}. With an increase of AFB1 concentration, a decrease in current was obtained. The lower the current, the less antibody bound to the surface. The linear range for both formats was in the range that covers the permissible legislative concentrations from 1 to 20 ppb (1000 to 20 000 ppt; Figure 5).

 Published by Cranfield University Press ISBN: 978-0-9557436-7-2 http://hdl.handle.net/1826/3832

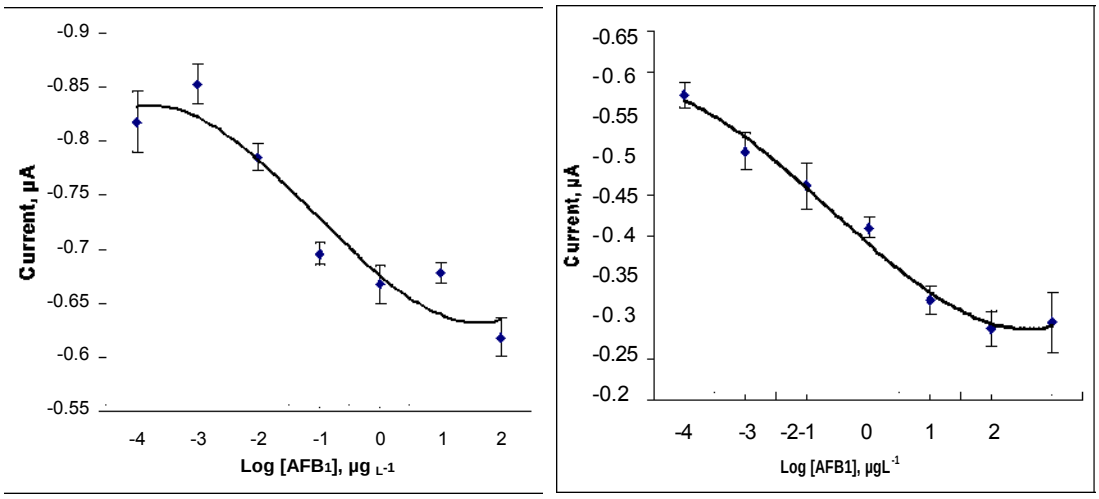

a b

Figure 5: Calibration curve of AFB1 using screen printed gold electrode. (a) Indirect format and (b) direct format.

CONCLUSIONS

Preliminary data indicated that the electrochemical immunosensor using screen printed gold electrode as well as ELISA based on an indirect and direct competitive format were acceptable for analyses of AFB1 at levels required by the regulations (1 to 20 ppb). Future work include further optimisation of the immunosensor to increase the detection limit, reduce the assay time and improve reproducibility of the device. A microsensor array will also be used to develop the immunosensor. The Development of immunosensor for other mycotoxins will also be investigated in order to move into multi toxins analysis.

ACKNOWLEDGMENT

The authors would like to thank the Malaysian Agricultural Research & Development Institute (MARDI) for funding this research degree and DuPont UK Limited (the Microcircuit Materials) for collaborative work in providing the gold screen printed sensors.

 Published by Cranfield University Press ISBN: 978-0-9557436-7-2 http://hdl.handle.net/1826/3832

BIBLIOGRAPHY

1. Ammida, N.H.S., Micheli, L., and Palleschi, G., (2004). Electrochemical immunosensor for determination of aflatoxin B1 in barley. *Analytica Chimica Acta* 50,159-164.
2. Hussein, S.H. and Brasel, J. M., (2001). Toxicity, metabolism, and impact of mycotoxins on humans and animals. *Toxicology,* 167, 101–134.
3. Logrieco, A., Arrigan, D. W. M. , Brengel-Pesce, K., Siciliano P. and Tothill, I.E. (2005). Microsystems technology solutions for rapid detection of toxigenic fungi and mycotoxins. J of Food Additives and Contaminants, 22 (4): 335-344.
4. Micheli, L., Grecco, R., Badea, M., Moscone, D. and Palleschi, G. (2005). An electrochemical immunosensor for aflatoxin M1 determination in milk using screen-printed electrodes. *Biosensors and Bioelectronics* 21, 588–596.
5. van Egmond, H. and Jonker, M. (2004). Worldwide and European regulations for mycotoxins & analytical methods expected from Bio Crop.

 Published by Cranfield University Press ISBN: 978-0-9557436-7-2 http://hdl.handle.net/1826/3832

Finite Element Analysis of Car to Cyclist Accidents

J Watson and R. Hardy

Cranfield Impact Centre

ABSTRACT

A Finite Element (FE) computer model of a bicycle was developed, using data from physical tests and through a literature search. Static and dynamic crash tests have been performed to validate the FE model of the bicycle. The FE model was further enhanced by the addition of a human FE model. The FE model represented the dimensions and properties of a 50th percentile (average) human and had the capability to simulate human type injuries sustained in cyclist and pedestrian type impacts.

Although at this stage there is not a legislative test procedure specific for cyclist head impacts onto the vehicle front, they are deemed to be covered by the pedestrian impactor test procedures as determined by The European Council Directive 2003/102/EC Phase 2. The simulations performed to date have shown that the cyclist's head is likely to strike in a different position to the pedestrian, indicating that the test procedures may need updating to incorporate the unique cyclist kinematics. The orientation of the head prior to impact greatly influenced the speed of head impact, due to the variations of neck properties; therefore the test procedure should take this into account.

To complement the modelling work conducted to date, two sets of physical tests involving bicycles, dummies and a vehicle representation have been conducted.

INTRODUCTION

Current European legislation is aimed at protecting pedestrians in road traffic accidents by providing a series of impactor tests for the vehicle front ends. It is implied that these tests also protect cyclists but initial findings have shown that pedestrians and cyclists show different characteristics in road traffic scenarios. The overall height dimensions of a pedestrian and cyclist are very similar, but their limb orientations are different. For example, the cyclist's knees can be bent more and the body's overall centre of gravity can be higher than an equivalent pedestrian stature. The implication of this difference in height is that the cyclist is more likely to be projected further up the front end of a vehicle and strike the windscreen of the bonnet.

This paper is focused towards understanding the kinematics and injury mechanisms of bicycle accidents with motor vehicles. There are a large number of different types of accidents, which have been identified and grouped into a classification of cycle accidents. The side on collision from the front end of the vehicle has been identified by Otte as the most frequently occurring. Therefore this scenario has been chosen as the initial accident type for further investigation.

METHODOLOGY

To determine the differences between cyclists and pedestrians two approaches have been utilised.

- Physical Testing of Bicycles statically and dynamically with dummies
- Mathematical Simulations using a Finite Element (FE) software code.

Figure 1. Humanoid and Bicycle Model Combined

 Published by Cranfield University Press ISBN: 978-0-9557436-7-2 http://hdl.handle.net/1826/3832

SUMMARY OF INITIAL PHASE SIMULATIONS

The stance of the cyclist in terms of the orientation of the pedals affected the trajectory of the cyclist in the simulations, when struck with the front of a vehicle. When the struck leg was down the cyclist's leg was trapped between the vehicle and the bicycle, which did not occur for the pedestrian simulations conducted later. The first phase simulations showed that certain changes to the baseline cyclist simulation produced significantly different results.

For the second phase of simulations, a comparison was made between cyclist simulations performed in the first phase and new pedestrian simulations. Trajectories of certain body parts and head velocities were recorded. The cyclist head impacts occurred further up the vehicle front compared with the pedestrian impacts which all occurred on the bonnet.

The trajectory results highlighted the nature of the fall and the subsequent kinematics after head impact. As expected, the higher vehicle speed cyclist impacts projected the cyclist to strike the bonnet and windscreen regions, before starting to climb the windscreen further, to possibly going over the top of the vehicle roof. The results indicated that the pedestrian's head did not travel as far up the vehicle front due to its different orientation and the non-inclusion of the bicycle.

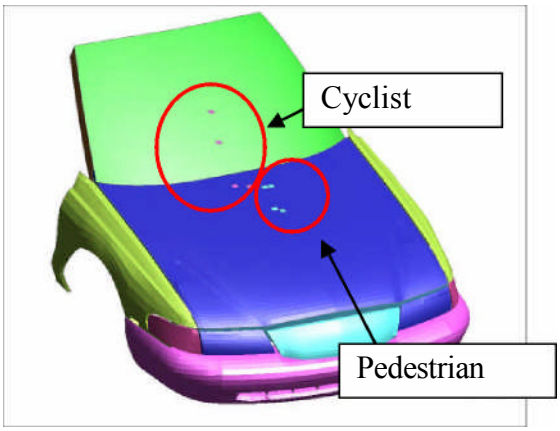

Figure 2. Head Impact Locations for Pedestrians and Cyclists

THIRD PHASE SIMULATIONS

A single type of vehicle has been used to analyse different cyclist stances, pedestrian stances and vehicle characteristics in the first and second phases of simulations. To understand a greater range of vehicle accidents, a wider range of vehicle geometries were used in the third phase to understand if cyclist kinematics and injuries vary with different shape or stiffness characteristics. The FE approach was used for three different vehicles shapes and physical tests were conducted for two of those vehicle shapes.

THREE VEHICLE SHAPES

Three class of vehicle were chosen to represent a wide cross section of the current vehicle fleet. A super-mini, SUV and MPV.

 Published by Cranfield University Press ISBN: 978-0-9557436-7-2 http://hdl.handle.net/1826/3832

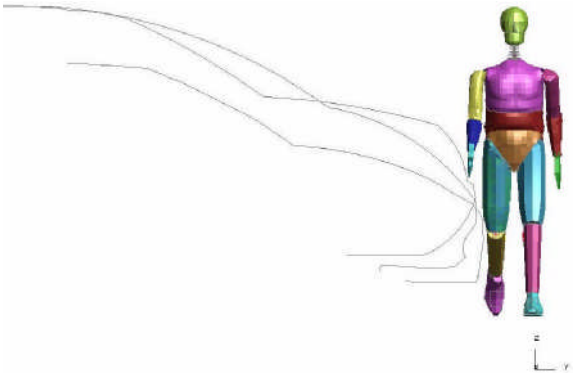

Figure 3. Different Vehicle Geometries

STANCES AND SCENARIOS CHOSEN FOR PHASE 3 STUDY

For the three different vehicle shapes, two different cyclist stances were chosen. The struck leg up, is shown in Figure 4. The C-stance, as shown in Figure 4, simulated a particular walking stance of the humanoid. The D-Stance is the mirror image of the C-Stance, but in this stance the struck leg supported the entire mass of the humanoid.

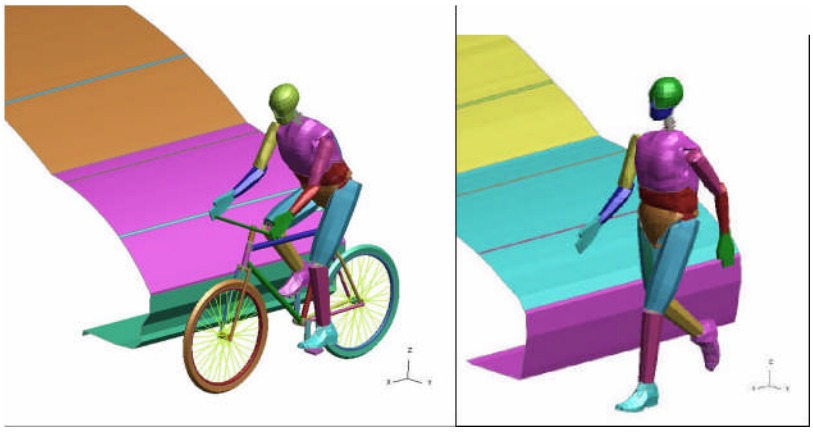

Figure 4. Struck Leg Up Cycling Stance and C-Stance Pedestrian

RESULTS OF THIRD PHASE SIMULATIONS

Struck Leg Up VStruck Leg Down

The two stances of struck leg up (SLU) and struck leg down (SLD) highlighted different results in overall kinematics as shown in Figure 6, for the super-mini vehicle 1 0msec^{-1} simulations. The head strikes the windscreen in the middle for the SLU simulations (on the right), whilst the SLD simulation shows the head contact towards the top edge of the windscreen. The difference can be accounted for by observing the motion of the struck leg and its engagement with the bicycle and vehicle. As the SLU simulation has an elevated struck (right) leg its motion onto the bonnet occurs earlier and allows the cyclist to slide along the bonnet towards the windscreen. However, in the first 30msec of the SLD case, the struck leg is trapped by the vehicle and bicycle and has the effect of holding the cyclist against the vehicle for 10-20msec. Subsequently the cyclist wraps around the vehicle and strikes higher up the vehicle. The struck knee results show a greater bending moment of 144Nm in the SLD simulation, compared to 85Nm for the SLU.

 Published by Cranfield University Press ISBN: 978-0-9557436-7-2 http://hdl.handle.net/1826/3832

There is a similar pattern for other criteria such as the knee shear force in these two simulations and with the other vehicle types SUV and MPV. Therefore, the bicycle and initial pedal orientation are contributing to overall kinematics and injury mechanisms as well by interacting with the vehicle and cyclist.

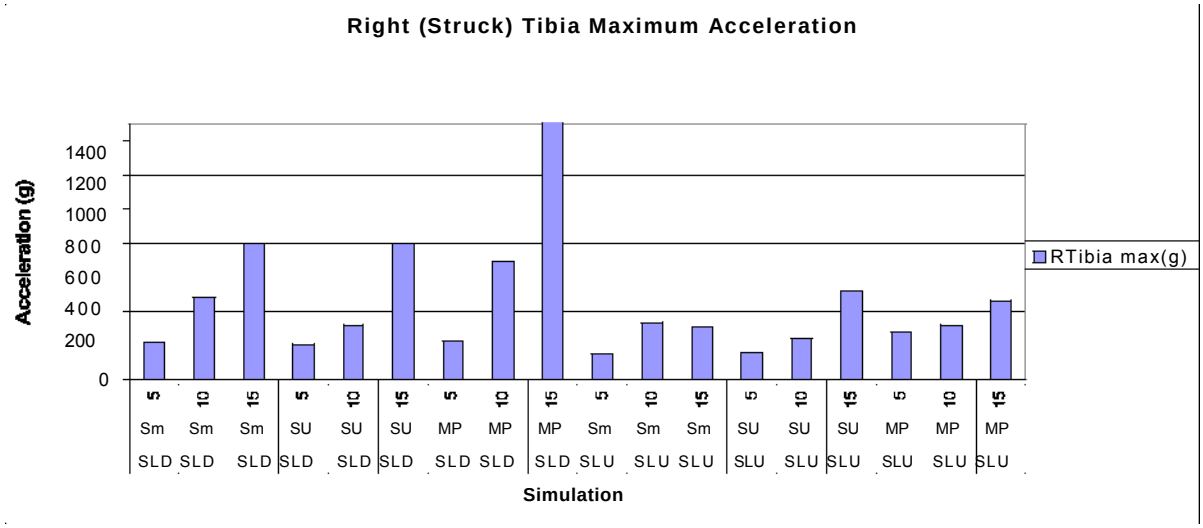

Figure 5. Right Struck Tibia Maximum Acceleration, Struck Leg Down and Struck Up Down Cyclists

The difference between SLU and SLD simulations was also observed in the tibia accelerometer results. In Figure 5, the SLU results, shown on the right, are lower than the SLD results on the left. Even for simulations which were conducted at a vehicle speed of 15ms^{-1}. As the struck leg was in an elevated position it did not receive a direct impact from the bumper. The maximum g level for the SLU simulations was 520g compared with 3200g for the SLD simulations.

DIFFERENT VEHICLE SHAPES

The three vehicle shapes used in the 10msec struck leg down simulations produced three different head impact locations. In Figure 6, the simulations have been frozen at the time of head impact. The head struck the SUV vehicle at the earliest moment in time following first vehicle contact, followed by the MPV and super-mini. The time duration difference needed for the head to impact the vehicle is due to the shape of the vehicle front, inducing a partially rotation and sliding motion of the human. In the SUV simulation, the torso rotated with the head striking the bonnet halfway up, but with very little sliding. The MPV simulation showed the humanoid sliding up the bonnet but due to the shape of the vehicle which was more upright when the head strikes earlier. Head impact location does not fully identify the influence of different vehicle shapes on head injury, for instance the stiffness of the vehicle, the velocity of impact and the orientation of the vehicle with respect to the head are other important considerations. As the vehicle properties have not been defined for every region of the windscreen and bonnet, the full extent of head injuries cannot be addressed.

 Published by Cranfield University Press ISBN: 978-0-9557436-7-2 http://hdl.handle.net/1826/3832

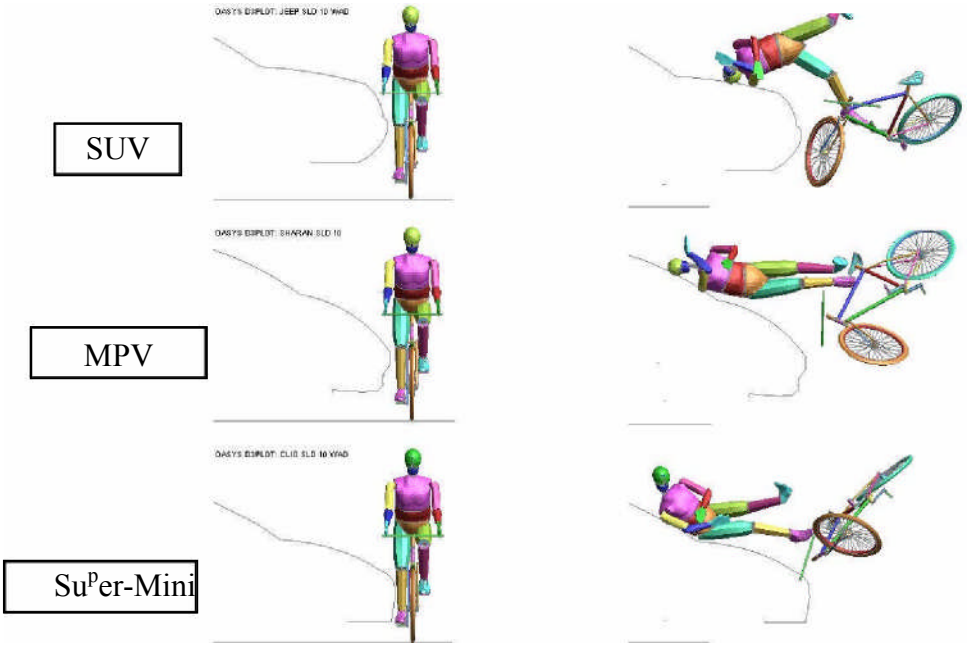

Figure 6. Variance of Head Impact Locations with Different Vehicle Shapes

For all simulations, the head strike with the super-mini produced the greatest deceleration result. The SUV simulations showed the lowest head acceleration results for all of the simulation scenarios. The differences in head acceleration gave an indication of injury risk and for the super-mini vehicle shape the likelihood of head injury was greater when compared with the SUV vehicle profile. By observing the kinematics of the head between the vehicle types, the larger front profile of the SUV prevents the torso from sliding towards the windscreen. Instead, the head and torso rotate about the bonnet leading edge.

PEDESTRIAN AND CYCLIST STANCES

In a similar manner to the C and D stance analysis, the right knee bending moments are compared for pedestrians and cyclists in Figure 7. The pedestrian simulations on the left of the graph showed higher values than the cyclists' simulations on the right. A threshold has been specified in the model of 1 80Nm, at when the knee ligaments would likely to reach a level beyond their elastic level and the integrity of the knee would be affected. For the cyclist simulations this level has been passed three times, whereas the pedestrian simulations have passed that level eleven times. This indicates that the cyclist scenarios analysed produced lower levels of knee bending moment when compared with cyclists.

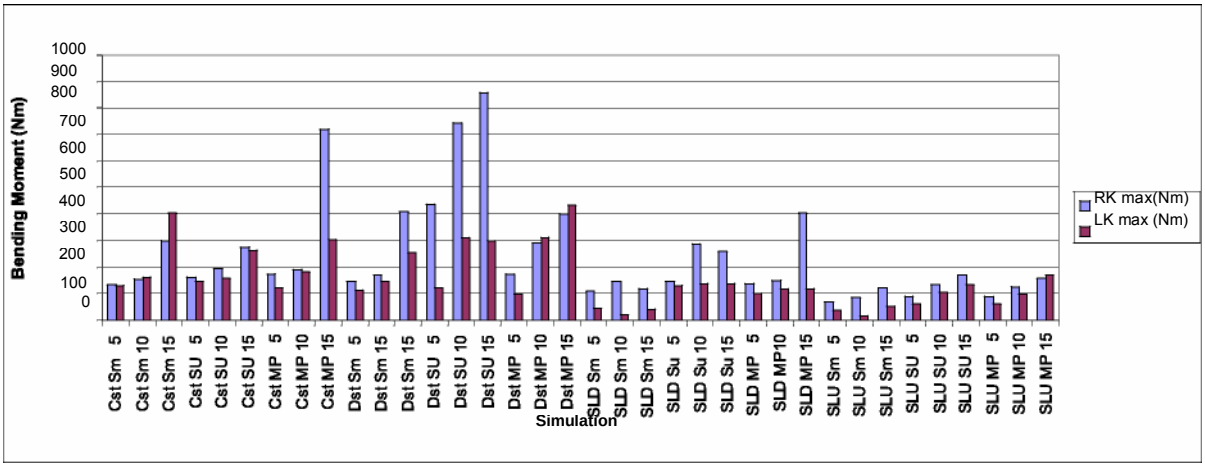

 Published by Cranfield University Press ISBN: 978-0-9557436-7-2 http://hdl.handle.net/1826/3832

Figure 7. Right and Left Knee Maximum Bending Moments for Cyclists and Pedestrians

RESULTS OF PHYSICAL TESTS

Figure 8 shows the kinematics of the cyclist in a racing type stance being impacted by the SFC. The stance of the cyclist on impact was determined by releasing the weight of the dummy moments before impact.

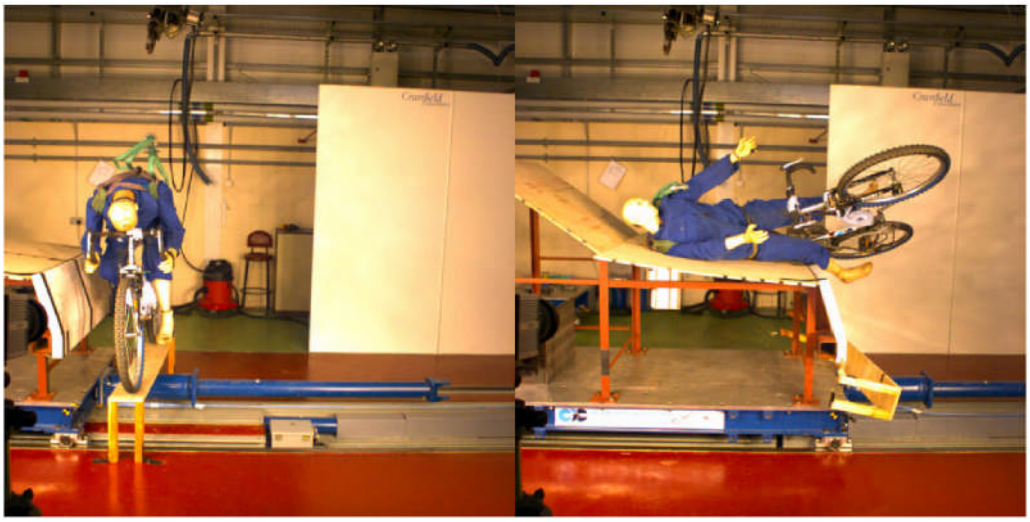

Figure 8. Small Vehicle Shape 0– 300msec

CONCLUSIONS

1. A wide range of cyclist and pedestrian scenarios were simulated in the LS-DYNA finite element software code to assess the importance and relevance of certain accident scenarios.

2. The stance of the cyclist in terms of the orientation of the pedals affected the trajectory of the cyclist in the simulations, when struck with the front of a vehicle. When the struck leg was down the cyclist's leg was trapped between the vehicle and the bicycle, which did not occur for the pedestrian simulations.

3. The SUV vehicle showed the lowest levels of head acceleration compared with the other two vehicle types. The reduced levels were likely due to the high front end of the vehicle and the rotation of the cyclist or pedestrian about the bonnet leading edge.

4. The pedestrian knee tibia acceleration results and bending moments, where higher than the cyclists' results, indicating that the bicycle has a role in reducing the injury levels of the cyclist.

5. The simulations have shown that the cyclist's head is likely to strike in a different position and orientation to the pedestrian, indicating that the current pedestrian test procedures may need updating to incorporate unique cyclist test procedures.

6. This research work has highlighted the fundamental differences between cyclist and pedestrian impacts by comparing the two types of accidents under similar loading conditions. The results have shown different impact locations and orientations of head impacts.

 Published by Cranfield University Press ISBN: 978-0-9557436-7-2 http://hdl.handle.net/1826/3832

ACKNOWLEDGEMENTS

CIC are currently involved in a 6th Framework EU Integrated Project entitled APROSYS (Advanced Protective SYStems). Cranfield is project leader of the pedestrian and pedal cyclist accident sub project. The project started in April 2004 and will continue until 2009.

 Published by Cranfield University Press ISBN: 978-0-9557436-7-2 http://hdl.handle.net/1826/3832

Adoption of E-service in Developing Countries: Issues and Challenges

H. S. Hassan, E. Shehab and J. Peppard

{h.s.h.hassan; e.shehab; j.peppard}@cranfield.ac.uk

Cranfield University, Cranfield, Bedford, MK43 0AL, UK

ABSTRACT

The adoption of electronic services by various countries governments has been significantly increased in the last few years because of the major benefits delivered to both providers of electronic services (public authorities and organizations) and the public, to whom services are targeted. Nevertheless, the level of implementation differs from country to country and the speed with which electronic services are made available and adopted is lower than planned or expected especially in Least Developing Countries (LDCs). The differences indicate that e-government in these countries face slower progress or even stagnation because they encounter multiple and complex challenges. This paper focuses on identifying these challenges, and looks at their impact on delaying the transition to electronic service in less developing countries governments.

Key words: E-service; Public sector; Developing Countries; Challenges.

INTRODUCTION

Over the last decade, the Internet has become one of the most important means of communication in all social areas. It has vastly changed the ways in which customers interact with organisations to get services, and the way organisations deliver services to customers. Information and communication technology facilities offered by the Internet, and the success of this technology adoption in the private sector has encouraged the public sector to adopt the Internet to present information and service resources. While the numbers of the different e-service initiatives in the public sector have rapidly increased, e-governments projects in some countries advance at different speeds. The gap between developed and developing countries in Internet technological infrastructures, practices, and usage has been wider rather than narrower over recent years. Besides the lack of sufficient capital to build up an expensive national information infrastructure (NII) on which electronic service is based, developing countries also lack the sufficient knowledge and skill to develop suitable and effective strategies for establishing and promoting electronic government (Chen et al., 2007).

 Published by Cranfield University Press ISBN: 978-0-9557436-7-2 http://hdl.handle.net/1826/3832

Governments in these countries tend to be slow in launching new services and citizens often prefer to conduct transactions with the government through paper forms and physical presence rather than using online methods. As a result, the present spread of electronic services clearly lags behind the desired level (Vassilakis et al 2005). These facts clearly indicate that a number of factors place impediments to the development and operation of electronic services. Identifying those challenges will help the governments of those countries to put plans to overcome them and prepare their plans to promote their electronic service provision. Figure (1) illustrates the overall challenges which are facing e-service in developing countries.

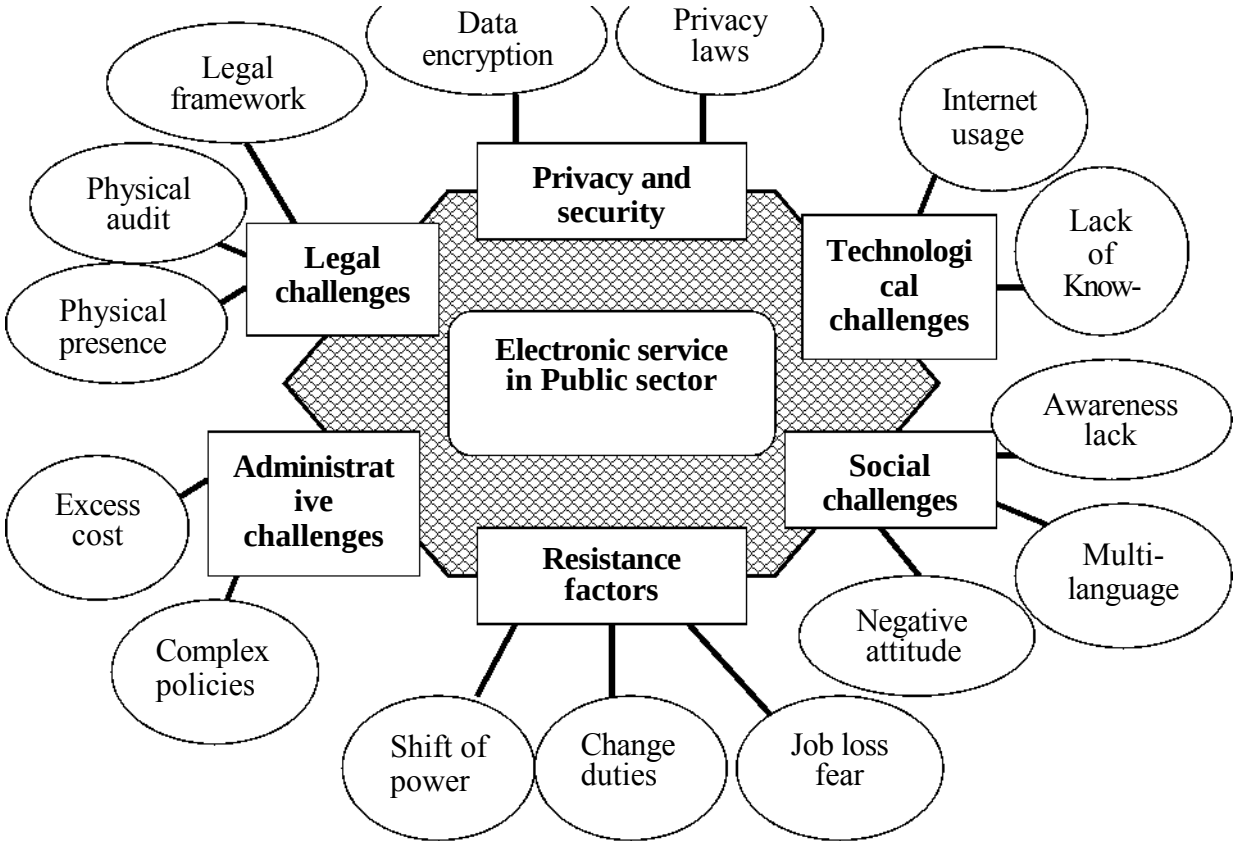

Figure (1): Challenges facing e-service in Developing Countries

 Published by Cranfield University Press ISBN: 978-0-9557436-7-2 http://hdl.handle.net/1826/3832

ISSUES AND CHALLENGES

Privacy and Security Risks

Privacy and security risks are emerging as serious concerns in the era of e-service. Privacy risk is defined as a consumer's concern that information that he/she has willingly provide about himself/herself could be misused by the marketer (Rust and Kannan, 2002). This information is provided to a marketer, through conducting a transaction, answering surveys, or surfing the company's Web site. Security risk refers to a consumer's concern that an unknown third party will obtain the consumer's personal or financial information without his knowledge while he is transacting business online or the third party will disrupt his transactions online (Frels and Kannan, 2001). In this context, the issues of security and data encryption have not yet been addressed satisfactorily in the public networks of LDCs (Vassilakis et al 2005). Although techniques and tools that enhance security and privacy do exist, high levels of security cannot be achieved without significant expertise from end-users and use of complex procedures. These requirements are not met in the scope of electronic services. Further, the data protection and privacy laws are hindering the progress of e-service in governments where many public sector organisations are finding it hard to meet the demands of existing laws. It is argued that countries least developed with a more chequered history of government respect for citizens' privacy will struggle to overcome the trust and security issues involved in online transactions (Harris and Schwartz, 2000).

INADEQUATE LEGAL FRAMEWORK

This arises mainly from such issues as the lack of a suitable legal framework that addresses submission of electronic documents, liability emerging from electronic documents, and proofing value of electronic documents against paper documents, especially for the proof-of-identity and the electronic document integrity issue. Electronic signatures technology is accepted in some countries and/or for specific services, but still most of the least developed countries do not use this type of technology, either because they do not have an accepted framework for all services, or there are still some services classes for which electronic signatures are considered inadequate, e.g., services involving payments to citizens where fraud detection is important. Additionally, legislation for Trusted Third Parties, i.e., bodies that will testify for resolution of disputes between citizens and public authorities in the context of electronic services, is still immature. In addition, legal issues, such as the requirements for physical presence, physical inspections, audits, and examinations may hinder the transition to electronic services, since some manual processes will still remain in the workflow (Vassilakis et al 2005).

 Published by Cranfield University Press ISBN: 978-0-9557436-7-2 http://hdl.handle.net/1826/3832

GOVERNMENT ADMINISTRATION

Government administration proves in some cases reluctant to introduce electronic services (Vassilakis *et al* 2005). One main reason is the development and deployment of electronic services incurs significant costs for hardware platforms, software development and licensing, and employee hiring for electronic service administration and help desk operation. These types of costs represent an excess burden on the developing country's economy, characterized by its limited financial resources especially when it is doubtful whether the target audience will finally prefer the electronic version of the service to the traditional paper based delivery channel. Another reason is the need for complex policies, for example, the requirement for an overwhelming amount of information from service users, or the definition of complicated policies that require a large number of interwoven transactions (Vassilakis et al 2005).

TECHNOLOGICAL CHALLENGES

The main technological concerns obstructing the development of electronic services in developing countries may include the internet usage. While e-service has immense potential for government processes, it also creates significant challenges for the government because of the digital divide. Traditionally, governments have delivered services through the Internet, while other potential service delivery channels (e.g. WAP, I-mode, SMS, Phone centres) have not been adequately considered (Vassilakis *et al* 2007). Significant portion of most of the countries do not have access to the Internet and thus cannot take advantage of e-government (Grimes 2001). Studies report that Internet usage- either from home or from work- ranges from 18% in North America to 26% in Europe (in average) (Internet world stats) while the usage in Africa is 3.4% and even 2.5% in the Middle East. Minorities, the disabled and rural residents in many countries around the world still lag behind in their use of computers and speedier access to the Web. Limiting a service to the WWW channel effectively excludes a large portion of the population.

Another issue is the lack of appropriate know-how. Computers are more complex to learn and use than mobile phones, faxes or interactive TV; thus delivering services through the "most complex channel" narrows the target population. In addition, some services are more appropriate for delivery through specific channels(Vassilakis *et al* 2005) (Vassilakis *et al* 2007). Some households and/or enterprises do not own a computer with an Internet connection, but most of them are equipped with faxes, phones or mobile phones, with some of them encompassing WAP or I-mode capabilities. This portion of potential service users could more readily access a service if it were delivered through one of those

 Published by Cranfield University Press ISBN: 978-0-9557436-7-2 http://hdl.handle.net/1826/3832

channels. While a for-profit business can pick and choose the channel it finds most profitable to operate and choose not to offer services in channels where the potential for losses is high, governments do not have the option of picking and choosing channels due to citizen equity considerations. In many instances, governments will be forced to offer the same citizen services in all channels and will be facing multichannel integration challenges (Rust and Kannan2002).

SOCIAL CHALLENGES

Some challenges may be ascribed to special characteristics of user communities; for example, specific citizen communities have a negative stance against electronic services and would only use "traditional" paper-based service channels. This negative attitude may have its roots in service content rather than in service quality. Further, many citizens still prefer to contact authorities by phone or face to face rather than using the online services out of the fear of service being de-personalised. In addition, in the design of e-service, some multi-lingual and/or multi-cultural issues arise. A service may be deployed only in the mostly spoken language within a country excluding potions of the population. This is especially true for countries with minorities or large number of immigrants. Many citizens in LDCs have a minimal understanding of how government processes are executed or decisions are made. This lake of awareness according to Reffat (2003) can prevent the citizen from actively participating in government services. In such countries, the government often interact more with the elderly, poor, language limited and less educated people, a group who are less likely have access to the Internet (Fang, 2002). Trust is another obstacle that e-government has to overcome. While lack of trust can hinder adoption of e-service in general (Bhattacherjee, 2002), the same applies to the case in e-service in the public sector that involves sharing between the government and the citizens on the Internet.

CHANGE MANAGEMENT

Resistance in our context is defined as the factor that hinders or stops the electronic services from inside the government. The employees may resist the shift of power resulting from the introduction of e-service. Employees possessing a certain amount of tacit domain knowledge are considered to have more power within the organisation. Introduction of electronic services converts tacit knowledge to explicit, depriving these employees of their source of power. Further, this initiation will require structural reforms in the organisation, modification of job descriptions and change in duties. Employees may be opposed to such changes especially those involved in paper-based service delivery channels, as they perceive the introduction of electronic services as a threat jeopardising their jobs.

 Published by Cranfield University Press ISBN: 978-0-9557436-7-2 http://hdl.handle.net/1826/3832

CONCLUSIONS

This paper presented the challenges that may affect the development and implementation of e-service in different ways within the public sector in the Least Developed Countries. Understanding and comprehending such challenges is considered the first step in planning the e-service more effectively. While most of the e-government initiatives in these countries are focused on providing information, the success of e-government will largely depend on providing value added service to citizens. The bottom line is that the transfer of public administrative processes in (LDCs) from a largely inefficient and bureaucratic manual state to an e-enabled real-time automated state should involve fundamental rethinking and radical redesign. It also requires integration of processes and IT systems in different government agencies. Therefore, more researches are needed to focus on exploring ways to improve such integration in the context of the e-government.

REFERENCES

1. **Bhattacherjee, A.,** (2002), "Individual Trust in Online Firms: Scale Development and Initial Trust" *Journal of Management Information Systems,* Vol. 19, No. 1; pp. 211- 241.
2. **Chen, Y., Chen, H M., Ching, R. K. H., Huang, W. W.,** (2007), "Electronic Government Implementation: A Comparison between Developed and Developing Countries" *International Journal of Electronic Government Research,* Vol. 3, No. 2; pp. 45-60.
3. **Fang, Z.,** (2002), "E-Government in Digital Era: Concepts, Practice and Development" *International Journal of the Computer, the Internet and Information,* Vol. 20 pp. 193- 213.
4. **Frels, J. and Kannan, P.,** (2001), "*Consumers' Risk Perception in Conducting Online Transactions:An Experimental Investigation."* Working paper, Smith School of Business, University of Maryland.
5. **Harris, J.K., and Schwartz, J.,** (2000), "Anti Drug Website Tracks Visitors" Washington Post, June 22, 2000, p. 23.
6. **Internet World Stats,** World Internet Usage And Population Statistics. Available from http://www.internetworldstats.com/stats.htm (accessed 23-12-2007).
7. **Reffat, R.,** (2003), "Developing a Successful E-Government" Working Paper, School of Architecture, Design Science and Planning, University of Sydney, Australia.
8. **Rust, R. and Kannan, P.,** (2002), "The era of E-service", in Rust, R., Kannan, P., E-Service: New Directions in Theory and Practice. Shape, Inc.
9. **Vassilakis, C., Lepouras, G. and Halatsis, C.,** (2007), "A Knowledge-based approach for developing multi-channel e-government services." *Electronic Commerce Research and Applications.* Vol. 6, pp.1 13-124.
10. **Vassilakis, C., Lepouras, G., Fraser, J., Haston, S. and Georgiadis, P.,** (2005), "Barriers to Electronic Service Development." *E-service Journal.* Vol. 4, No. 1; pp.41- 63.

 Published by Cranfield University Press ISBN: 978-0-9557436-7-2 http://hdl.handle.net/1826/3832

A Nitrocellulose-Based Sensor for Storage Life Monitoring of Munitions

M Moniruzzaman, J M Bellerby, I G Wallace

Department ofMaterials and Applied Science, Cranfield University,
Defence Academy of the United Kingdom, Shrivenham, Swindon, SN6 8LA, UK

P Barnes

Defence Ordnance Safety Group, Defence Equipment and Support, Ministry ofDefence,
Abbey Wood, Bristol BS34 8JH, UK

ABSTRACT

This paper describes a low cost sensor containing a dye incorporated into a nitrocellulose film which undergoes a gradual colour change over time and can be used to assess the thermal load experienced by munitions during storage. The sensor is attached to the outside of the munitions and its colour change with aging time is related directly to the extent of stabilizer depletion within the propellant inside the munitions. This information can be used to estimate the remaining chemical safe life of the propellant.

INTRODUCTION

Background

The UK Ministry of Defence is currently developing a major programme aimed at reducing the whole-life costs of munitions. Key elements of the strategy include an understanding of failure modes, visibility of the in-service environment and an improved understanding of the link between environmental conditions and degradation and failure.

An important element in the emerging strategy is environmental monitoring and control. Whilst direct environmental monitors have merit for expensive weapons systems and equipment, the fielding of large numbers of electronic devices feeding data back to research laboratories for interpretation and analysis creates logistics, safety and data processing problems. Furthermore, the derivation of anything other than simple ageing algorithm presents the research community with formidable challenges. Hence for very many munitions the ageing algorithm may be limited to an approximation involving the dominant variable.

We are therefore focussing our efforts on low cost devices to monitor the key degradation processes which limit the life of munitions. This paper describes work to develop a sensor in the form of a time-temperature indicator (TTI), which can be used to assess the extent of degradation and remaining safe life of nitrate ester based gun and rocket propellants1.

 Published by Cranfield University Press ISBN: 978-0-9557436-7-2 http://hdl.handle.net/1826/3832

The basic principles of TTIs are well established[2]. Commercial devices are available for monitoring the temperature-time history of perishable items such as foodstuffs and pharmaceuticals. However, none is currently optimised for the long lives and wide temperature ranges encountered by munitions. The work described here is aimed at developing a device that is matched to the degradation processes governing the life of munitions.

PROPELLANT DECOMPOSITION

Nitrate esters such as nitrocellulose (NC), a common ingredient in many gun and rocket propellants, decompose exothermically to release oxides of nitrogen (NO_x)[3]. The process takes place in two stages. In the first stage, the reaction is relatively slow while in the second stage the initial decomposition products, NO_x gases and nitrous and nitric acids, react with the nitrate ester and the reaction becomes autocatalytic, thereby accelerating rapidly. Stabilisation of nitrate ester based propellants is therefore achieved by adding chemicals that react with the oxides of nitrogen and acids generated in the first stage, thus suspending the catalytic cycle.

It is very important to know the stability of the propellant in a rocket motor for two reasons. Firstly, to ensure that it does not pass its chemical safe life, or in other words reach the autocatalytic decomposition stage at which it becomes a hazard, and secondly, to assess its safe working life. Here the intention is to ensure that the propellant has all the physical, ballistic and chemical characteristics needed to perform the task for which it was designed.

For a given propellant, quality control during manufacture should ensure consistency of the composition and component source (composition factors). However, a propellant charge can be exposed to a wide range of temperatures and environmental factors. Of these two parameters, the temperature has the greater effect on the rate of nitrate ester decomposition. Thus, the stability of a propellant and its useful service life are strongly dependent on its temperature history, from production, through distribution and storage to use.

The development of a sensing device capable of recording the thermal load of a propellant charge within munitions would: i) allow the munitions to be monitored without being tested in a destructive way. This of course means that safety is improved and service life is optimised, ii) be able to provide useful information regarding the current condition of the munitions at a glance, without destructive testing. iii) inspires confidence because individual propellant charges that have experienced excessive thermal load will be identified. iv) help control waste since field samples will not be sent back unnecessarily for stability testing.

Anthraquinone dyes are known to react with NO_x and undergo a marked colour change[4], a phenomenon that is known as ‘gas fume fading’. Blue anthraquinone dyes that exhibit the greatest colour change on reaction with NO_x are similar to some traditional propellant stabilizers in that they contain secondary amine groups (Figure 1). Therefore, NC-based films have been produced

 Published by Cranfield University Press ISBN: 978-0-9557436-7-2 http://hdl.handle.net/1826/3832

incorporating a blue anthraquinone dye in the expectation that the slow decomposition of the NC and release of NO_x could be followed by monitoring the reaction of the anthraquinone 'stabilizer' via a visible colour change.

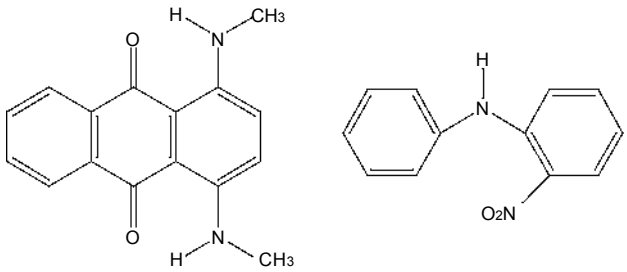

Figure 1. Chemical structure of DB14 (I) and 2-NDPA (II)

EXPERIMENTAL

The nitrocellulose used in the preparation of the films had a nitrogen content of 12% and was purchased from Sigma-Aldrich (Gillingham, Dorset, UK). It was dried under high vacuum (10^{-2} mmHg) before use. A 4.5% solution of NC in butanone (w/v) was prepared by mixing the NC with dioctylphthalate (DOP) and the anthraquinone dye (1,4-bis(methylamino)-9,10-anthraquinone, DB14, Figure 1-I) at room temperature. The solution was subjected to freeze-thaw cycles and then stirred overnight at ambient temperature to give a homogeneous solution. The solution was spread onto glass microscope slides and left to dry at ambient temperature to form the films. After most of the solvent had evaporated off at ambient temperature, the films were vacuum dried.

The UV-Visible absorption spectra of the films were recorded before and after aging using a Zeiss MCS 522 UV-VIS spectrometer with a xenon flash lamp (Zeiss, BLX 500/4). Spectra were recorded at different positions on the films and master curves were produced by overlaying the spectra of unaged and aged films.

 Published by Cranfield University Press ISBN: 978-0-9557436-7-2 http://hdl.handle.net/1826/3832

Thermogravimetric analysis (TGA) was carried out on a series of films containing the dye stabiliser or a conventional stabiliser (2-NDPA, Figure 1-II) in order to compare their reactivities with NOx. In each case the dried film was isothermally heated under nitrogen at 150°C for 15 hours.

RESULTS AND DISCUSSION

Thermogravimetric analysis

TGA thermograms recorded isothermally at 150°C on NC films stabilised with DB14 and 2-NDPA are shown in Figure 2. Results indicate that after 900 minutes the weight loss of the films containing 2-NDPA (18.8%) was significantly greater than that of the films containing DB14 (10%). The experiment demonstrates that DB14 is a more effective stabiliser for NC at 150°C.

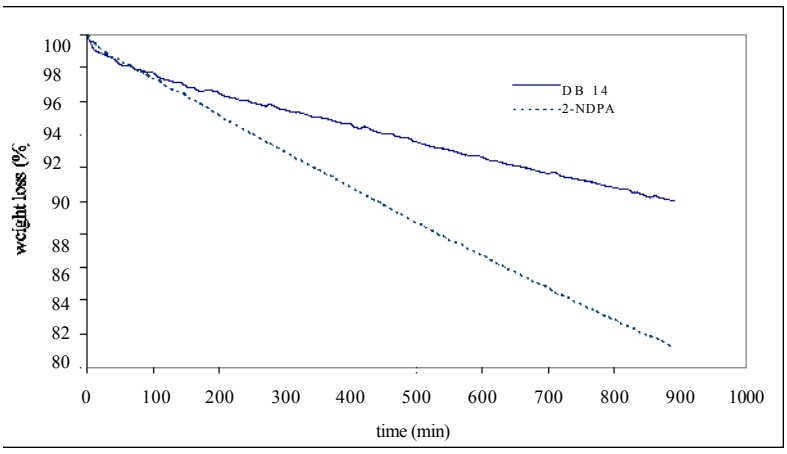

Figure 2. TGA thermograms of NC films containing different stabilisers

UV-VISIBLE SPECTROSCOPY

The UV-visible spectra of unaged films and those aged at 40°C are overlaid in Figure 3. These show two major absorption peaks at 600 nm and 645 nm that are thought to arise from $\pi \rightarrow \pi^*$ transitions within the DB14 molecule. These peaks decreased in intensity on aging and new peaks, assigned to nitrated derivatives of DB14, appeared below 400 nm.

Two well-defined isobestic points at 550 nm and 725 nm are evident in Figure 3, indicating that the spectra between these two points are dominated by absorptions due to DB14. This is an important conclusion and ensures that the operation of the TTI is not compromised by interferences from highly-coloured derivatives of DB14. More films

 Published by Cranfield University Press ISBN: 978-0-9557436-7-2 http://hdl.handle.net/1826/3832

were aged at 50°C, 60°C, and 70°C, allowing the first order rate constants for NC decomposition to be calculated. These data were then used to determine the activation energy of the NC decomposition reaction. A value of ~1 26 kJ mol^{-1} was obtained, which is in good agreement with literature values for nitrate ester hydrolysis[5].

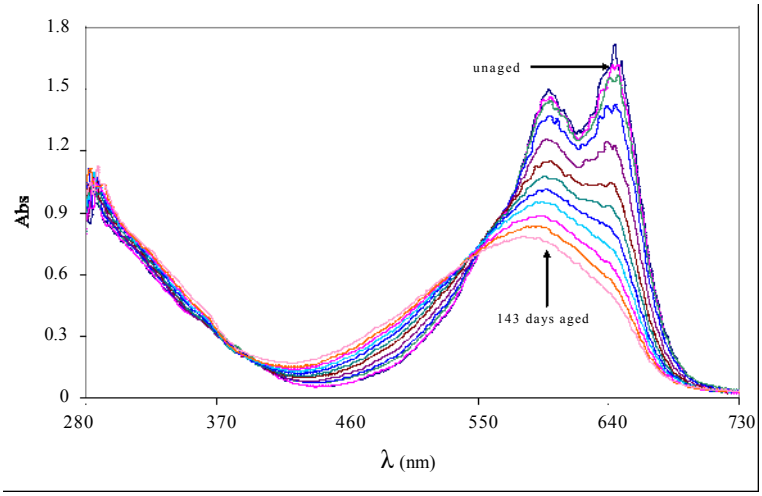

Figure 3. UV-visible spectra of an unaged and aged DB-14-based film at 40° C. Total aging time was 143 days

EFFECT OF DIRECT SUNLIGHT ON FILMS

The effect of UV-visible light on the NC films was investigated. Figure 4 shows the UV-visible spectra of a DB14-stabilised film subjected to sunlight through a glass window. The spectra before and after expose at ambient temperature (~20° C) indicate that the film bleached fairly rapidly, losing about 76% of the dye in 3.5 hours. This compares with a loss of 72% after 143 days of aging in darkness at 40°C. It is clear that NC in the films is significantly affected by sunlight and therefore the sensor must be protected from direct exposure to the sun if it is to function as an effective TTI for storage life monitoring of munitions.

COLOUR CHANGES

The unaged DB14-based films are blue in colour and turn red on thermal aging. This change is thought to be related to the conversion ofDB14 into its daughter products, most probably aromatic nitro and N-nitroso derivatives. The film changes colour gradually with time and therefore the amount of dye depletion and the associated colour change can be linked to the extent of stabilizer depletion in a propellant sample. A calibration curve can be created from which the stabiliser loss in a propellant inside

 Published by Cranfield University Press ISBN: 978-0-9557436-7-2 http://hdl.handle.net/1826/3832

stored munitions can be estimated. Conclusions can be drawn from this regarding the condition of propellant. The advantage of using this approach is that it involves no sampling of the propellant and eliminates time-consuming techniques for stabilizer analysis such as high performance liquid chromatography (HPLC). Furthermore, the colour sensor can be monitored by relatively unskilled personnel.

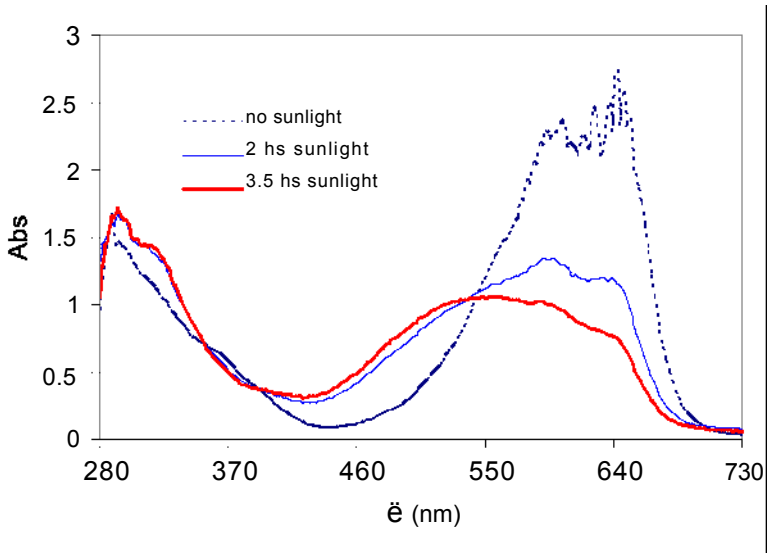

Figure 4. UV-visible spectra of DB14 film before and after exposure to sunlight

SUMMARY AND CONCLUSIONS

A nitrocellulose-based sensor in the form of a time-temperature indicator has been developed for monitoring the storage life of munitions. The sensor contains a dye which reacts with NO_x released from the slow decomposition of the nitrocellulose and changes colour over time and with exposure to a wide range of temperatures. Plans are underway to deploy prototype sensors in Ministry of Defence overseas munitions storage facilities in the latter half of 2008 and discussions on full commercial exploitation of the devices are taking place with a major UK defence contractor.

REFERENCES

1. J M Bellerby and S J Elsby, GB Patent 2338554, 1 May 2002.
2. P S Taoukis and T P Labuza, Journal of Food Science, **54,** 783, 1989.
3. T B Brill and P E Gongwer, Propellants, Explosives, Pyrotechnics, **22,** 38, 1997.
4. F M Rowe and K A J Chamberlain, Journal of the Society of Dyers and Colourists, **53,** 269, 1953.
5. H N Volltrauer and A Fontijn, Combustion and Flame, **41,** 313, 1981.

 Published by Cranfield University Press ISBN: 978-0-9557436-7-2 http://hdl.handle.net/1826/3832

Acoustic Emission technology for identifying seeded defects in helical gears

Babak Eftekharnejad, D. Mba

School of Engineering, Cranfield University, Bedford, MK43 0AL, England

Email : b.eftekharnejad@cranfield.ac.uk

ABSTRACT

Acoustic Emission (AE) is one of many technologies for health monitoring and diagnosis of rotating machines. This report presents an experimental investigation that assesses the effectiveness of AE in identifying seeded defects on helical gears. In addition, a comparison between vibration and AE in identifying the presence of defects is presented.

INTRODUCTION

Acoustic Emission (AE) is defined as the range of phenomena that results in the generation of structure-borne and fluid-borne (liquid, gas) propagating waves due to the rapid release of energy from localised sources within and/or on the surface of a material [1]. The application of the acoustic emission technology in research and industry is well-documented [2]. In relation to gearboxes, a few investigators have assessed the application of AE technology for diagnostic and prognostic purposes [3-7]. Others[8-12] applied AE in detecting bending fatigue on spur gears and noted that AE is more sensitive to crack propagation than vibration and stiffness measurements. Again, AE was found to be more sensitive to the scale of surface damage than vibration analysis. To date, there has been no attempt to understanding the mechanisms for generating AE activity in helical gears, nor has an attempt to assess the ability of AE to identify defects in such gears. This report presents an experimental investigation that assesses the effectiveness of AE monitoring techniques for identification of seeded defects on helical gears.

EXPERIMENTAL SETUP

The gearbox test rig employed was of back-to-back arrangement (see fig 1), powered by 1.1KW motor with helical (214M15) steel test gears, see table 1. The gearbox was lubricated with Mobile gear 636 oil, with a Kinematic viscosity@40^{o} of 664 (cSt), and operated at a speed of 690rpm. A wide-band AE sensor (type WD, from Physical Acoustic Limited) was employed to measure AE throughout the test. The AE sensor was fixed on the pinion using super glue (see figure 2). The AE sensor was of differential type with a relative flat response of between 100 kHz to 1 MHz. The cable from the AE sensor was fed through a narrow longitudinal duct inside the

 Published by Cranfield University Press ISBN: 978-0-9557436-7-2 http://hdl.handle.net/1826/3832

input shaft and connected to the slip ring. The slip ring (PH-12, IDM Electronic Ltd) placed at the end of test gearbox. AE was recorded with MISTRAS AE DSP-32/16 data acquisition card at a sampling rate of 10 MHz.

Table 1 Specification of test gears

	Pinion	**Wheel**
Number of teeth	51	70
Module	3 mm	3 mm
Pressure angle	20º	20º
Helix angle	17.5º	17.5º
Contact ratio	1.7	1.7
Face width	25.1 mm	25.1 mm
Hardness	137 Hv30	137 Hv30
Surface roughness	1.327 µm	1.327 µm

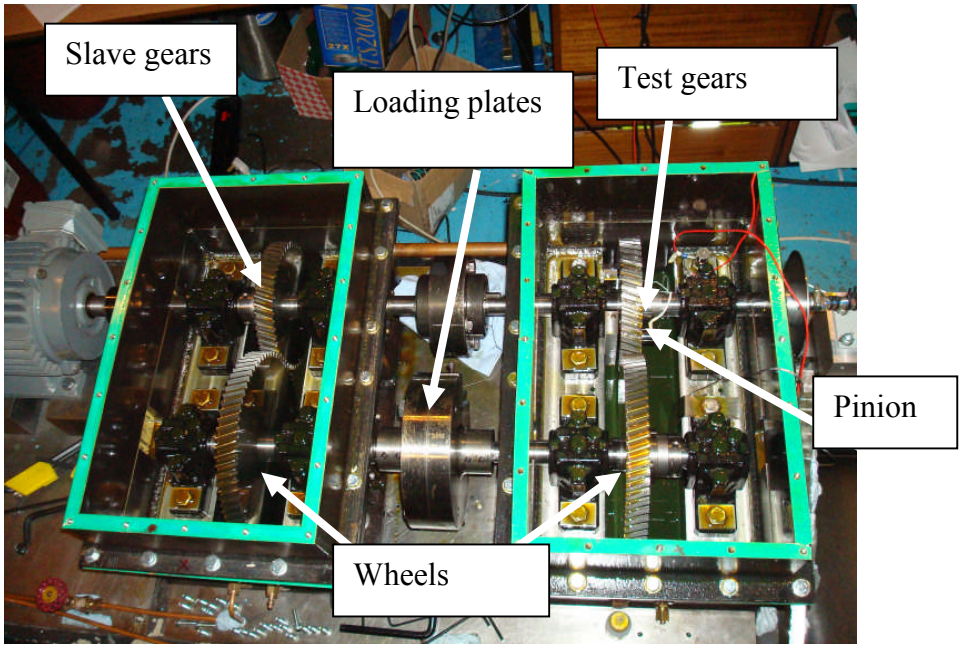

Figure 1 Gearbox Test rig

 Published by Cranfield University Press ISBN: 978-0-9557436-7-2 http://hdl.handle.net/1826/3832

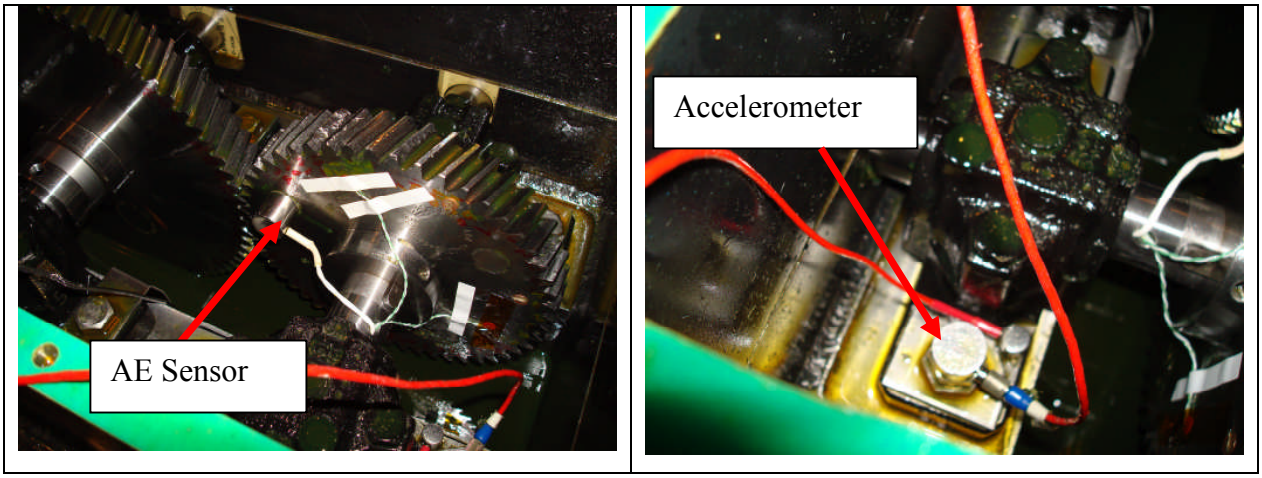

Figure 2 AE sensor placement Accelerometer position on bearing

As this experiment centred on assessing the applicability of AE for identifying seeded defects on helical gears, it was paramount that any data recorded was taken from a defined circumferential point every revolution. For this reason, an optical triggering mechanism was employed. The triggering system consisted of metal disk with 2mm diameter hole and an optical sensor. Each time the hole passed trough, the optical sensor the AE acquisition system was triggered.

TEST PROCEDURE

Prior to the testing the gearbox was run for 3-hours at 380Nm so as to allow the gearbox to dynamically settle and reach a stabilized temperature; in this instance 60^{o}C. It was essential to capture AE and vibration data that included the defective tooth and as such and acquisition time frame, or window, of 16-teeth was set whereby the trigger mechanism ensured an acquisition duration of 0.0256-seconds, corresponding to 16 teeth at 690 rpm. To begin the tests a defect free recording of AE was undertaken. The gearbox was then stopped and the torque set to 250Nm and run for 5-minutes to accommodate the new dynamic condition. Again, defect free AE data was captured for the same acquisition window. The same procedure was repeated at 180Nm. The defect free condition will be referred to defect-0, see table 3.

In order to carry out the seeded defect test, the test rig was stopped and the first defect introduced on the seventh tooth using a drill. The gearbox was then started and AE data for the time frame encompassing the damaged tooth was acquired instantly. The significance of the instantaneous recording was to allow the authors to explore the influence of surface/material deformation on the levels of AE and vibration as some investigators had suggested [3, 13] . The gearbox was allowed to operate until the temperature reached 60^{o}C after which AE signals were again recorded for the specific defect condition. The same procedure was repeated at 250Nm and 180Nm respectively. Twenty sets of AE data were recorded for every defect and load

 Published by Cranfield University Press ISBN: 978-0-9557436-7-2 http://hdl.handle.net/1826/3832

condition. Each AE data file corresponded to a waveform representing 16 teeth with time length of 0.0256 seconds (see figure 3).

Table 2 Details of seeded defects

Defect type	Size(mm^2)	Depth(mm)	Removed Volume(mm^3)	Defect tooth
Defect-0	0	0	0	7
Defect-1	18.88	0.1	1.888	7
Defect-2	28.71	0.2	5.742	7
Defect-3	41.22	0.5	20.61	7
Defect-4	17.5	1	17.5	7
Defect-5	15	0.8	12	7
Defect-6	158.75	0.2	31.75	11
Defect-7	163.5	0.2	32.7	15

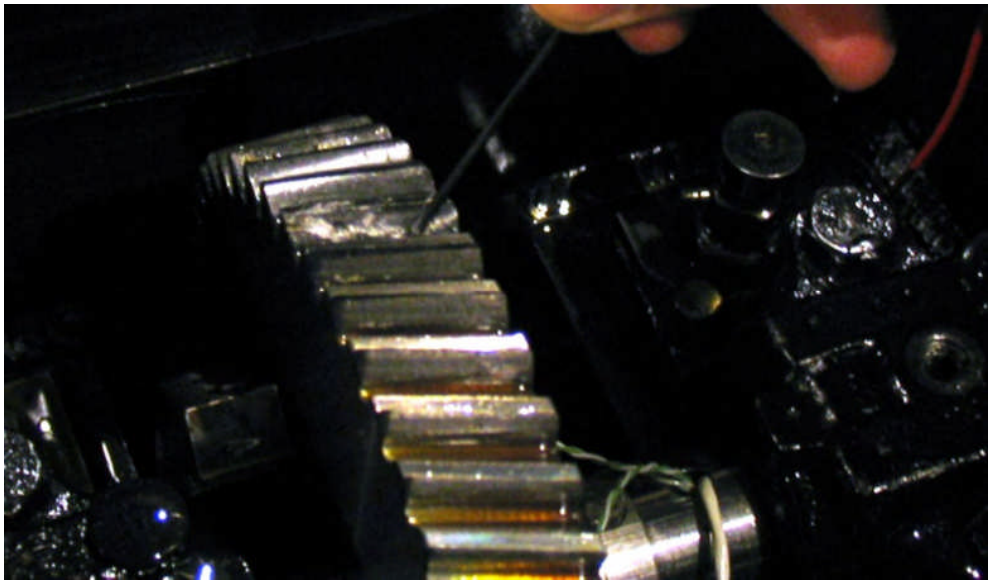

Figure 3 Seeded defect on the tooth

RESULT AND DISCUSSION

Figure 4 shows typical AE waveforms associated with each defect condition which showed relatively large transient AE bursts over continuous operational AE levels. The transient AE bursts where noted to occur at the exact tooth where the defect was seeded, see figure 4. Such observations were not noted in a similar test with spur gears, i.e., the seeded defects were not evident in the waveforms[3, 13].

 Published by Cranfield University Press ISBN: 978-0-9557436-7-2 http://hdl.handle.net/1826/3832

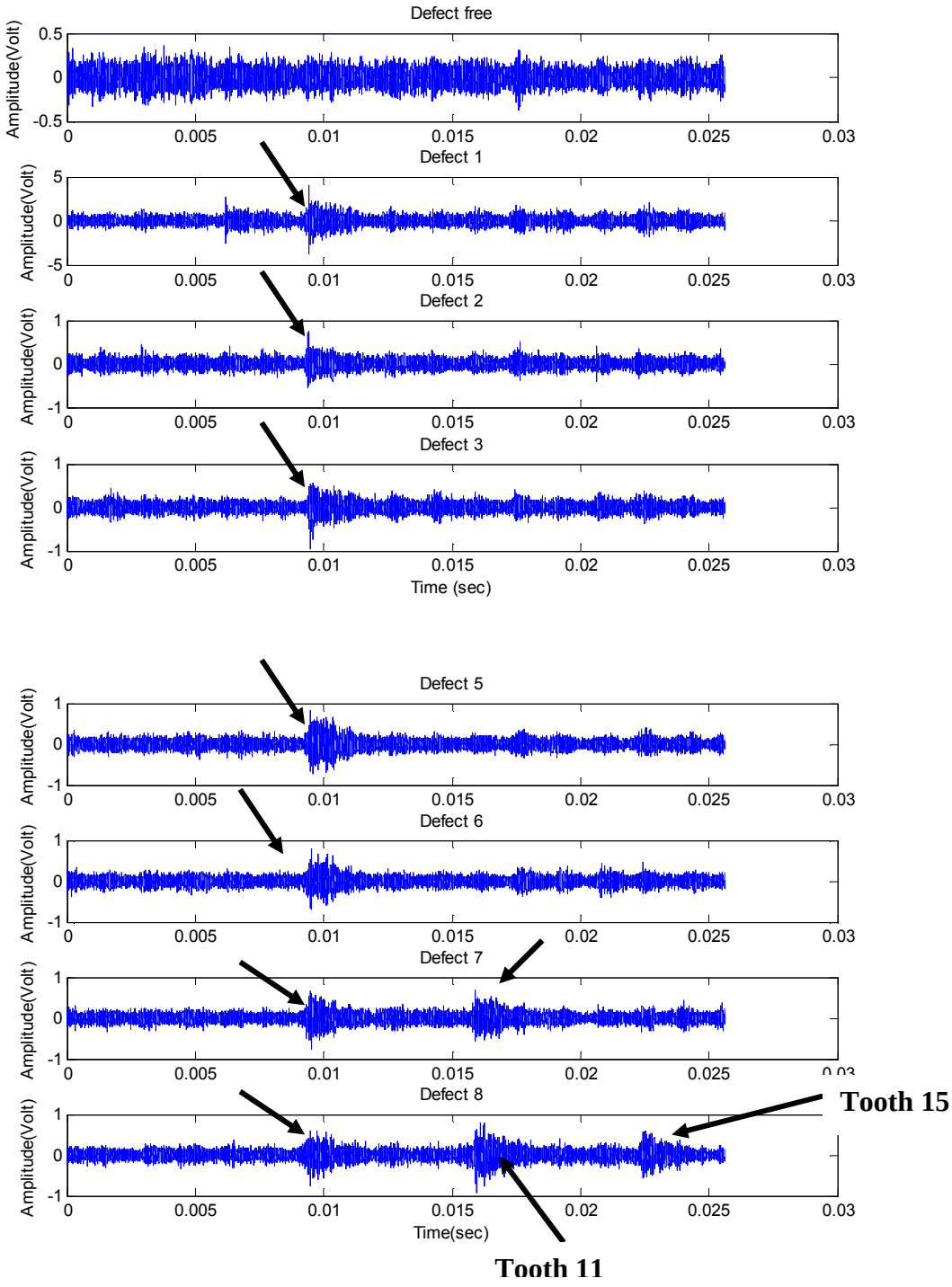

Figure 4 Waveforms associated with each defect for 'A' condition

AE r.m.s values for all test conditions were obtained by averaging all r.m.s values associated with all twenty data files per fault and load condition, see figure 5. In general an increase in AE r.m.s levels for increasing defect size for all test load conditions was noted, see figure 5. For load conditions B (250Nm) and C (180Nm) an increase in AE r.m.s levels with increasing defect width and number of defective teeth was evident.

 Published by Cranfield University Press ISBN: 978-0-9557436-7-2 http://hdl.handle.net/1826/3832

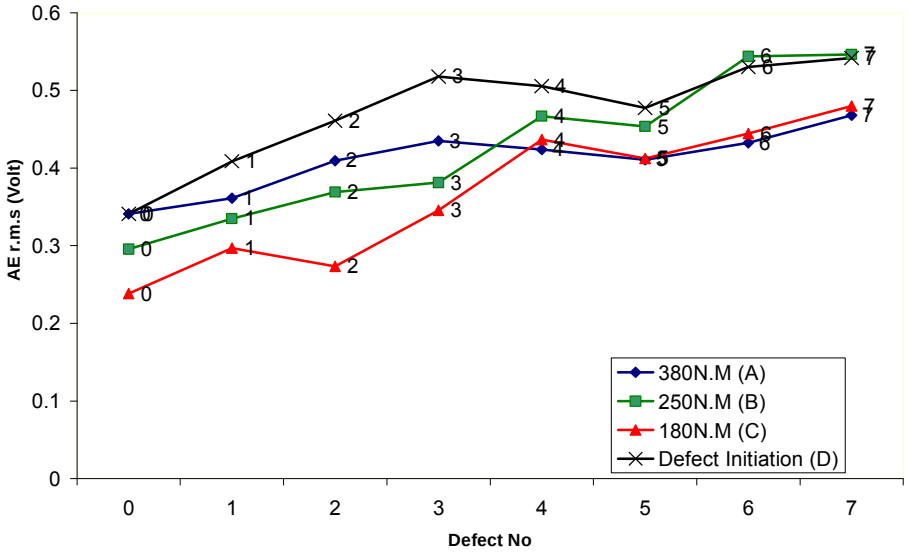

Figure 5 AE r.m.s values for each defect condition

Of interest is that the AE r.m.s levels of the initial defect condition (D) were relatively higher for most test conditions. This was not surprising giving that asperity contact has been shown to be a major source of AE generation during gear mesh[5, 14, 15].

CONCLUSION

In conclusion, this investigation has shown that seeded defects in helical gears are evident in the AE waveform. This not the case for spur gears.

REFERENCES

[1] ISO 22096, 2007, "Condition Monitoring and Diagnostics of Machines. Acoustic Emission," .
[2] Mba, D., and Rao, R. B. K. N., 2006, "Development of Acoustic Emission Technology for Condition Monitoring and Diagnosis of Rotating Machines: Bearings, Pumps, Gearboxes, Engines, and Rotating Structures," Shock and Vibration Digest, **38**(1) pp. 3-16.
[3] Toutountzakis, T., Tan, C. K., and Mba, D., 2005, "Application of Acoustic Emission to Seeded Gear Fault Detection," NDT and E International, **38**(1) pp. 27-36.
[4] Tan, C. K., Irving, P., and Mba, D., 2007, "A Comparative Experimental Study on the Diagnostic and Prognostic Capabilities of Acoustics Emission, Vibration and Spectrometric Oil Analysis for Spur Gears," Mechanical Systems and Signal Processing, **21**(1) pp. 208-233.
[5] Tan, C. K., and Mba, D., 2006, "A Correlation between Acoustic Emission and Asperity Contact of Spur Gears Under Partial Elastohydrodynamic Lubrication," International Journal of COMADEM, **9**(1) pp. 9-14.
[6] Toutountzakis, T., and Mba, D., 2003, "Observations of Acoustic Emission Activity during Gear Defect Diagnosis," NDT&E International, **36**(7) pp. 471-7.
[7] Raja Hamzah, R. I., and Mba, D., 2007, "Acoustic Emission and Specific Film Thickness for Operating Spur Gears," Journal of Tribology, **129**(4) pp. 860-867.
[8] Tandon.N, and Mata.S, 1999, "Detection of Defects in Gears by Acoustic Emission Measurements," Journal of Acoustic Emission, **17**(1-2) pp. 23-24,25,26,27.

 Published by Cranfield University Press ISBN: 978-0-9557436-7-2 http://hdl.handle.net/1826/3832

[9] Miyachika K., Oda S., and Koide T., 1995, "Acoustic Emission of Bending Fatigue Process of Spur Gear Teeth," Journal of Acoustic Emission, **13**(1/2) pp. S47-S53.
[10] Miyachika K., Zheng, Y., Tsubokura, K., 2002, "Acoustic Emission of bending fatigue process of supercarburized spur gear teeth," Progress in Acoustic Emission *XI*, Anonymous The Japanese Society for NDI, pp. 304-310.
[11] E.Siores, and E.Negro, 1997, "Condition Monitoring of Gear Box using Acoustic Emission Testing," Material Evaluation, **55**(2) pp. 183-184,185,186,187.
[12] Wheitner, J., Houser, D., and Blazakis, C., 1993, "Gear tooth bending fatigue crack detection by acoustic emission and tooth compliance," ASME, 93FTM9, .
[13] Tan, C. K., and Mba, D., 2005, "Limitation of Acoustic Emission for Identifying Seeded Defects in Gearboxes," Journal of Nondestructive Evaluation, **24**(1) pp. 11-28.
[14] Boness, R. J., and McBride, S. L., 1991, "Adhesive and Abrasive Wear Studies using Acoustic Emission Techniques," Wear, **149**(1-2) pp. 41-53.
[15] Boness, R. J., McBride, S. L., and Sobczyk, M., 1990, "Wear Studies using Acoustic Emission Techniques," Tribology International, **23**(5) pp. 291.

 Published by Cranfield University Press ISBN: 978-0-9557436-7-2 http://hdl.handle.net/1826/3832

Performance study of Long Distance Hybrid Optical-Wireless 802.11b Networks

B Kalantari-Sabet, J. E. Mitchell
Telecommunications Research Group
Department of Electronic and Electrical Engineering
University College London, London WC1E 7JE, UK
ksabet@ee.ucl.ac.uk , j.mitchell@ee.ucl.ac.uk

ABSTRACT

This paper investigates the MAC protocol performance of an IEEE 802.11 Network that makes use of Radio-over-Fibre (RoF) technologies to distribute radio frequency signals from a central location to remote antenna sites over up to 100 km of Single Mode Optical Fibre (SMF). An experimental enquiry is used to provide a set of validation points before verifying these results by simulations using the NS-2 platform. This study takes into account the Basic Access method of the current Distributed Coordination Function (DCF) access mechanism using TCP packet transmission. The results show that, as expected, the throughput performance gradually decreases as the length of the fibre increases, and demonstrates that increase in fibre length can be achieved in the system if the timeout parameter of the network is increased.

INTRODUCTION

Hybrid wireless-optical access networks are a promising architecture for future access networks [1]. In such systems the Remote Antenna Unit (RAU) is very compact and the radio channel assignment is performed at a centralised location away from the remote unit. The majority of the base station components are positioned at a central location where the signal processing is carried out. Fig. 1 illustrates the concept of an optically distributed 802.1 1(a/b/g) broadband access wireless network. The feasibility of the above architecture has been demonstrated in [2-4]. The extra propagation delay introduced by the fibre link poses a challenge to the system design since this delay is most likely to exceed the 1 μs propagation delay boundary defined in the IEEE 802.11 standard [5, 6]. This may result in performance degradation or even a complete network breakdown. Therefore, understanding the IEEE 802.11 MAC behaviour in the presence of significant fibre length is of major importance.

 Published by Cranfield University Press ISBN: 978-0-9557436-7-2 http://hdl.handle.net/1826/3832

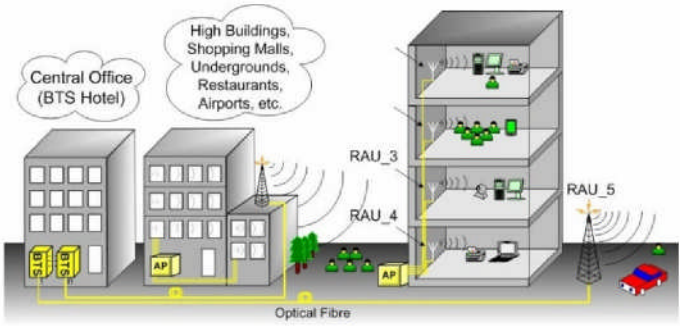

Fig. 1. Schematic of a hybrid optical-wireless 802.1 1(a/b/g) broadband access network.

A number of studies have investigated the effects of the fibre delay on the DCF of 802.11 MAC protocol [3, 6, 7]. However, none of them have presented experimental results for an 802.11 optically distributed network over long distances (100 km) of SMF.

This paper is organized as follows. Section II describes the IEEE 802.11 Basic Access DCF mode within the context of a hybrid optical-wireless system. Then, by using an experimental enquiry a set of validation points are presented in Section III. In Section IV, the simulation setup is explained and results are presented and compared with the experiment. Finally, Section V concludes the paper.

IEEE 802.11 BASIC ACCESS METHOD

The Medium Access Control Layer (MAC) manages communications between various stations and its functionality is common between 802.1 1a/b/g standards. In the DCF mechanism, the IEEE 802.11 standard uses two methods, one of which is called the 'Basic Access' method, a two-way handshaking technique to access the wireless channel. After a successful transmission, the destination station waits for a Short Inter-frame Space (SIFS) interval before sending an Acknowledgement packet (ACK) to confirm the correct reception of data at the MAC layer. After the transmission of the data packet the source station starts a count-down timer which leaves enough time for the reception of the ACK frame. If this timer , also known as *ACK _Timeout,* expires before the correct reception of the ACK frame then the source station assumes that the frame is lost and therefore prepares itself to retransmit the data packet. By deploying TCP traffic an additional handshake procedure takes place which is for the transmission of the TCP acknowledgement packet (ack). This action provides confirmation of the successful reception of data at the TCP layer. Fig. 2 illustrates the packet exchange between the source and destination station for a hybrid optical-wireless 802.11 TCP_Basic system.

 Published by Cranfield University Press ISBN: 978-0-9557436-7-2 http://hdl.handle.net/1826/3832

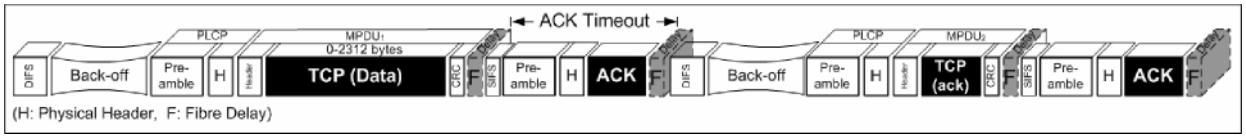

Fig. 2. TCP traffic over Basic Access mechanism.

Each packet, regardless of being a data or control packet, is associated with a fibre delay (F). Therefore, compared to a standard 802.11 system, there is an expansion of four times the fibre delay which, if too long, can break the entire network down.

EXPERIMENTAL VALIDATION

The experimental setup of a hybrid optical-wireless 802.11 broadband access network is depicted in Fig. 3. The Access Point (AP), also known as Base Unit (BU), and Remote Bridge (RB) are each connected to an IEEE 802.3 100Base-T LAN. Using Ethernet limits the maximum MAC payload size to 1500 bytes (rather than 2312 bytes which is the maximum allowable MAC payload [8]). A single fibre is used with Wavelength Division Duplex for uplink and downlink. In Fig. 3 the uplink and downlink RF signals are separated using an RF circulator. The electrical signal is converted to an optical signal using a 2.5 GHz bandwidth DFB laser. An optical combiner with 3.6 dB loss is used which allows a single length of SMF to be used for both directions. To ensure that the optical power levels in the system were constant (over the 100 km of SMF), an Erbium-Doped Fibre Amplifier (EDFA) and a bi-directional optical attenuator was employed for each fibre length direction. At the receiver end, an RF amplifier is used to increase the radio signal power level, which has a maximum value of 100 mW in Europe [8]. To eliminate the effect of the wireless channel on the system performance an RF cable connects the RAU and the RB which is used to emulate the mobile station.

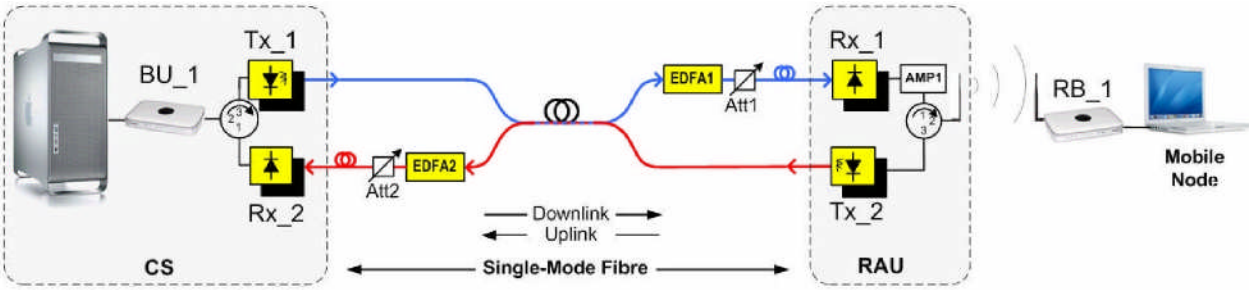

Fig. 3. Experimental setup of a hybrid optical-wireless 802.11 broadband access network.

 Published by Cranfield University Press ISBN: 978-0-9557436-7-2 http://hdl.handle.net/1826/3832

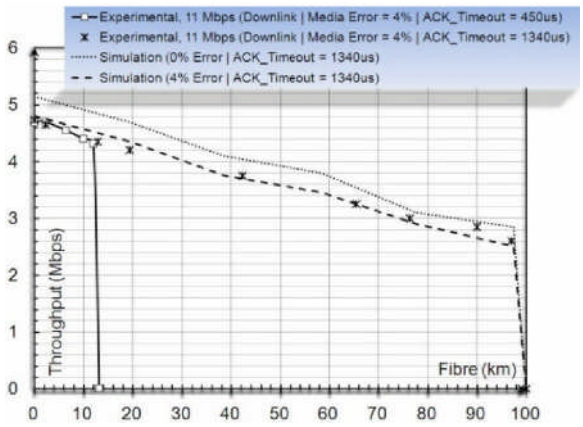

Table 1. Parameters used within the system.

Slot_Time (□)	*20 its*
SIFS (Short Inter-frame Space)	*10 its*
DIFS= (2.Slot_Time+SIFS)	*50its*
PLCP Preamble & Header	*24 bytes*
MAC Header & CRC	*34 bytes*
Data rate	*11Mbps*
Control rate	*1 Mbps*
ACK	*14 bytes*
Air propagation delay (□)	*1its*
Fibre propagation delay (F)	1□*s* □ 194.80*m*

Fig. 4. Variation of fibre length and throughput of an 802.1 1b TCP_Basic system.

Fig. 4 shows the experimental downlink results (where each experimental result is the average of 6 runs) of an 11Mbps 802.1 1b system which transmits TCP traffic to one station via Basic Access method with two different timeout settings. Around 4-5% of the data packets in the system are transmitted at a lower data rate of 5.5 Mbps (rather than 11 Mbps).

SIMULATION RESULTS

In this section the effect of fibre length and *ACK_Timeout* on the performance of hybrid optical-wireless 802.1 1b broadband access network is verified using the popular Network Simulator, NS-2. In our simulation, a fibre delay module has been inserted in the wireless channel implementation. The delay stage holds every packet that passes through the wireless channel for a certain fibre delay. The fibre delay value is adjusted to be from 0 to 513 μs (corresponding to 100 km of fibre). All uplink and downlink operations are carried out via the BU. The values of MAC payload size, data rate and control rate correspond to the values used in the experimental measurements - see Table 1. Each data point is the average of 6 simulation runs. The media error (which after packet corruption, forces the packets to travel at 5.5 Mbps) is uniformly distributed throughout the transmission time within the simulation. It can be observed from Fig. 4 that the experimental throughput is decreased gradually from 4.73 Mbps when no fibre is present to 4.3 Mbps over 11 km of fibre (9% drop) and to 2.6 Mbps over 99 km of fibre (45% decrease). However, as the system's round-trip delay reaches the *ACK_Timeout* value the performance falls abruptly. Since there is only one mobile station the uplink and downlink performances are analogous. In addition, according to our simulation results, there is approximately 7% decrease in throughput when the media error increases by 4% regardless of fibre length.

 Published by Cranfield University Press ISBN: 978-0-9557436-7-2 http://hdl.handle.net/1826/3832

CONCLUSION

In this paper we have investigated the performance of a hybrid optical-wireless 802.1 1b broadband access network. We consider the case of a single mobile station. We demonstrate using experiment and simulations that there will be performance degradation due to the additional delay inherent in the fibre transmission. However, we also show that a complete failure of the link results when the *A CK_Timeout* defined in the standard is exceeded. In the units used in our experimental study this resulted in failure after 100 km of single mode optical fibre when the Basic Access method was used.

REFERENCES

1. S. Sarkar, "Hybrid Wireless-Optical Broadband-Access Network (WOBAN): A Review of Relevant Challenges," *Journal of lightwave technology,* vol. 25, p. 3329, 2007.

A. Das, A. Nkansah, N. J. Gomes, I. J. Garcia, J. C. Batchelor, and D. Wake, "Design of low-cost multimode fiber-fed indoor wireless networks," *Microwave Theory and Techniques, IEEE Transactions on,* vol. 54, pp. 3426-3432, 2006.

2. N. J. Gomes, A. Das, A. Nkansah, M. Mjeku, and D. Wake, "Multimode Fiber-fed Indoor Wireless Networks," in *Microwave Photonics, 2006. MWP '06. International Topical Meeting on,* 2006, pp. 1-4.

I. N. Bao Linh Dang, "Analysis of IEEE 802.11 in Radio over Fiber Home Networks," *The IEEE Conference on Local Computer Networks 30th Anniversary (LCN'05),* vol. 33, pp. 744- 747, 2005.

3. M. V. Clark, K. K. Leung, B. McNair, and Z. Kostic, "Outdoor IEEE 802.11 cellular networks: radio link performance," in *Communications, 2002. ICC 2002. IEEE International Conference on,* 2002, pp. 512-516.

B. Kalantari-Sabet and J. E. Mitchell, "MAC Constraints on the Distribution of 802.11 using Optical Fibre," in *Wireless Technology, 2006. The 9th European Conference on,* 2006, pp. 23 8-240.

4. M. Mjeku, B. Kalantari-Sabet, J. E. Mitchell, and N. J. Gomes, "TCP and UDP Performance over fibre-fed IEEE 802.1 1b Networks," in *12th Microcoll Conference* Budapest, 2006.

5. "IEEE Standard for Wireless LAN Medium Access Control (MAC) and Physical Layer (PHY) Specifications, ISO/IEC 8802-11:1999(E).," 1999.

 Published by Cranfield University Press ISBN: 978-0-9557436-7-2 http://hdl.handle.net/1826/3832

Submission for Cranfield Multi-Strand Conference:

6 - 7 May 2008

Microsystems and Nanotechnology Session

Design and Fabrication of a Polymer Device for Patch Clamping Applications

S. Wilson[1,2], W. Pfleging[3], A. Welle [4], J.J.Ramsden[1]], P. Kirby[1]

School of Applied Sciences, Cranfield University, Cranfield, UK. MK43 0AL

Institute for Microstructure Technology, Forschungszentrum Karlsruhe, 76344 Leopoldshafen, Germany

Institute for Materials Research 1, Forschungszentrum Karlsruhe, 76344 Leopoldshafen, Germany

Institute for Biological Interfaces, Forschungszentrum Karlsruhe, 76344 Leopoldshafen, Germany

 Published by Cranfield University Press ISBN: 978-0-9557436-7-2 http://hdl.handle.net/1826/3832

ABSTRACT

Patch clamping is a highly sensitive method for measuring the bio-electrical (ion channel) activity of a cell. It plays an important role in drug screening by pharmaceutical companies leading to a demand for high throughput screening (HTS). While there are a few commercially available glass and silicon high throughput screening patch clamping systems, there are no systems on the market using cheap polymer materials or materials that provide additional functionality such as the ability to measure cell networks. The ability to 'patch-clamp' networks of cells is an exciting possibility as it would allow physiologically important issues regarding tissue engineering and understanding cell to cell interactions to be addressed. Within the EU Network of Excellence "4M – Multi Materials Micro-Manufacture" Cranfield University and Forschungszentrum Karlsruhe (FZK) are jointly developing a polymer based patch clamping device which is suitable for patch clamping on either single cells or cell networks.

One of the main limitations of the high throughput screening systems currently on the market is that they may only be used with cells that can be held in liquid suspension, effectively limiting the cell types that can be used for measurement. Systems currently available (www.nanion.de, www.cytocentrics.com, www.sophionbiosciences.com) use suction to pull a cell onto a hole with a diameter of 1 -4μm in order to produce the high resistance seal required for measurement. However, the positioning of the cell is somewhat hit or miss with varying rates of success in seal formation. Other challenges include microfluidic considerations such as fluid delivery, bubbles in solutions, and obtaining a high enough resistance seal between two microelectrode pipettes used for measurement (one located in the nutrition bath above the cell, the other in the hole below the cell).

The design proposed by Cranfield and FZK arose out of an interdisciplinary collaboration that introduces the use of polymers and polymer processing techniques required to produce a novel planar patch clamping system that can be used for either single cells or cell networks. The need for suction in cell placement is removed by using UV-light processes (laser and lamp) and a subsequent competitive protein adsorption process[1] to provide clearly defined areas for cell seeding and growth.

 Published by Cranfield University Press ISBN: 978-0-9557436-7-2 http://hdl.handle.net/1826/3832

The design proposed is based on a 10x10 array of holes (Fig 1) that are 2μm in diameter and produced by UV laser (1 93nm) ablation[2].

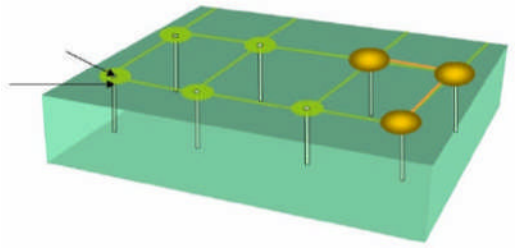

Fig 1: left proposed design layout, an overview

In this presentation the overall design will be discussed together with recent results on, UV-laser assisted ablation and surface functionalization of polystyrene (PS) and how the laser energy density and pulse number influence cell adhesion. There will be some discussion of cell culturing experiments that have produced networks of neuron-like PC-1 2 GMP cells, as well as the results of an initial assessment of the success of cell placement over holes in terms of required high resistance seal.

1. Alexander Welle, Siegfried Horn, Jutta Schimmelpfeng and Dorothee Kalka, "*Photo-chemically patterned polymer surfaces for controlled PC-12 adhesion and neurite guidance ".* Journal of neuroscience methods, 142(2005), p.243-250
2. Wilhelm Pfleging, Michael Bruns, Alexander Welle and Sandra Wilson "*Laser-assisted modification ofpolystyrene surfaces for cell culture applications."* Applied Surface Science, 253(2007), p. 9177-9184

 Published by Cranfield University Press ISBN: 978-0-9557436-7-2 http://hdl.handle.net/1826/3832

Methodological approach to identifying the properties of a novel organomineral fertiliser - *Part I: agronomic aspects*

Antille, D.L.; Sakrabani, R., and Godwin, R.J.

School of Applied Sciences, Cranfield University, Bedfordshire, MK43 0AL, UK. E-mail of

corresponding author: d.l.antille.s05@cranfield.ac.uk (Diogenes L. Antille)

SUMMARY

This paper summarises the methodology used in this research for evaluating the agronomic properties of organomineral fertilisers (OMFs). This involves a series of interconnected experiments conducted under controlled conditions and field-scale trials. The process for the production of OMFs was recently developed by a major UK water company and appears to be a sustainable solution for the recycling of sewage-sludge to agriculture. Preliminary results arising from the experiments indicate that the formulated OMFs are suitable for application on agricultural land.

Key words: organomineralfertiliser (OMF), sewage-sludge, nitrogen

INTRODUCTION

The water industry is under increasing pressure resulting from rigorous legislation both at UK and EC levels, regarding the production and disposal of sewage-sludge. Current levels of production are set to increase in response to population growth and stringent requirements for the treatment of effluents (Defra, 2007). Recycling to agricultural land is regarded by the UK Government as 'the best practicable environmental option' and represents the main disposal route (65%) followed by incineration (20%) and landfill (< 10%). There is also a cost advantage of recycling with respect to incinerating and landfilling. However, the increase of current levels of sewage-sludge up-take by farmers is restricted by a number of problems; e.g. spreading, transport, and handling of bulky materials. In addition, the use of sludges in agriculture has been restricted due to their variable chemical composition (Sommers *et al.,* 1976) and the fact that the amount of nitrogen available following application is poorly understood (Bowden and Hann, 1997). The combination of these factors determines a highly variable agronomic performance. Recently, a novel method of blending mineral fertilisers with biosolids to produce organomineral fertilisers (OMFs) has been developed by United Utilities plc. This development would significantly contribute to address the problems highlighted above.

 Published by Cranfield University Press ISBN: 978-0-9557436-7-2 http://hdl.handle.net/1826/3832

The aim of this work is to determine the effects of the use of OMFs in agriculture and to identify the most advantageous OMFs' formulations for a number of crops and soil types. This paper explains the methodological approach used to fulfil the aim of this research through a series of interconnected studies conducted under controlled conditions and field-scale trials. The work described herein corresponds to year one of the Engineering Doctorate Programme at Cranfield University.

METHODOLOGY

This section explains how the OMF products have been specified; e.g. chemical composition, and sets out the methodology employed to determine the agronomic value and the nutrient release characteristics of the formulated OMFs. Specifications of the physical characteristics of the formulated OMFs are given in Antille *et al.* (2008).

OMF FORMULATION

Using the method developed by United Utilities plc, two OMFs with different N-concentrations were formulated; $_{OMF10}$ (10% N) and $_{OMF15}$ (15% N). For this, the following aspects were taken into account: ***a.*** guidance given by United Utilities plc; ***b.*** nutrient composition of 'raw material'; i.e. digested cake; ***c.*** typical N, P, and K application rates in wheat; and ***d.*** soil-P indexes in the surroundings of Warrington.

Higher N concentrations than 10% and 15% are technically possible but this would not only result in increased manufacturing costs, but also and most importantly, in a reduction in the volume of sewage-sludge being disposed. The digested cake is generally quite unbalanced in its nutrient composition; a typical N:P:K composition would be 3:4(+):0.15-0.25. This gives a low N:P ratio which determines that sewage-sludge applications based exclusively on crop-N requirements (**Table 1)** could lead to rapid build up of soil-P. Therefore, current N:P ratios would need to be increased to a point where crop demand for P could be met with existing P in the cake and then make up the difference in N by adding N to the cake (**Table 2).** This is possible by blending the cake with urea (46% N). The same can be done with K but in this case the difference between the concentration of K in the cake and the requirement of the crop can be made up with KCl (52% K). This would ensure that soil-P index was not increased while crop requirements of N and K could be met.

 Published by Cranfield University Press ISBN: 978-0-9557436-7-2 http://hdl.handle.net/1826/3832

It is important to highlight that an important proportion of soils in the NW region were reported to have P-index 3 (Skinner *et al.,* 1992) and that there is usually no intention of building up the existing P-level.

Table 1: Required application rates of P and K according to their levels in the soil.

	Application rate (kg ha^{-1})	
Level in the soil	P_2O_5	K_2O
Low	88	95
High	55	53

Table 2: Nutrient application rates and correspondent ratios assuming the rate of N is 200 kg ha^{-1}

Application rate (kg hi^{-1})			
N	P_2O_5	K_2O	Ratio
200	88	95	≈ 2.2-1-1
200	88	53	≈2.2-1.5-1
200	55	95	≈ 4-1-2
200	55	53	≈ 4-1-1

Using the ratios shown in Table 2, the formulation of the OMFs can be inferred; taking for example the cases where P and K application rates are either high or low, the resultant OMFs' formulations given in % as N:P:K would be: 15:4:4 (OMF_{15}) and 10:4:4 (OMF_{10}) with P and K expressed in % as P_2O_5 and K_2O respectively. The two intermediate situations in Table 2 were discarded as it was considered more cautious to obtain products that could be used either in soils having low or high P and K indexes and utilise a different fertiliser source to meet the crop requirements in these intermediate situations.

OMF AGRONOMIC VALUE

In order to quantify the agronomic value and the nutrient release characteristics, three sets of experiments were established. These include the use of pots (greenhouse), plots (field), and incubators (laboratory).

EXPERIMENT 1: POT TRIAL

This experiment aims at quantifying the effects on rye-grass (*Lolium perenne L.)* from the application of OMFs. This is crucial to determining the OMFs' agronomic value and deciding the most appropriate application rates strategies. In addition, it will provide a valuable feedback on the proposed formulations.

 Published by Cranfield University Press ISBN: 978-0-9557436-7-2 http://hdl.handle.net/1826/3832

This trial comprises two soil types, a sandy loam (Cottenham series; King, 1969) and a clay loam (Holdenby series; King, 1969). The latter soil is commonly found in the area of Warrington where United Utilities plc is based. A total of 8 kg of air-dried soil was used for each pot and a layer of 2.5 cm of gravel was placed at the bottom of the pot to allow free drainage (Figure 1).

Figure 1: Diagram of a pot (left) and pots with established grass and irrigation system (right).

A dripper irrigation system was installed to maintain the soil at around field capacity all the time but avoiding excess of water leading to leaching and anaerobic conditions. The grass was sown at a density of 4 g of seeds per m^2 which is a standard rate for rye-grass. Sowing took place on April 27th 2007. The experiment comprises the use of four different fertilisers materials; i.e. OMF_{15}, OMF_{10}, cake (3% N) and urea (46% N), and two application rates; i.e. R_1 (150 kg N ha^{-1}) and R_2 (300 kg N ha^{-1}) and a control with no fertiliser added. A total of three cuts were possible during the growing season without any further fertiliser application.

EXPERIMENT 2: PLOT TRIAL

The aim of this trial is to identify the response of winter wheat (*Triticum aestivum L.)* to increasing application rates of nitrogen. This would allow determining the optimum OMFs' application rates. The trial is being conducted at Silsoe Farm on a sandy loam soil (Cottenham series; King, 1969) and it will run for 3 consecutives growing seasons in the same experimental site; thus, the residual effect of applied OMF-N can be quantified and taken into account when deciding N-application rates in the long term. A total of 60 plots (Figure 2) were marked out in the field with N-application rates ranging from 0 (control) to 250 kg N ha^{-1} in intervals of 50 kg N ha^{-1} and using the same fertiliser materials as those described above for the pot experiment.

 Published by Cranfield University Press ISBN: 978-0-9557436-7-2 http://hdl.handle.net/1826/3832

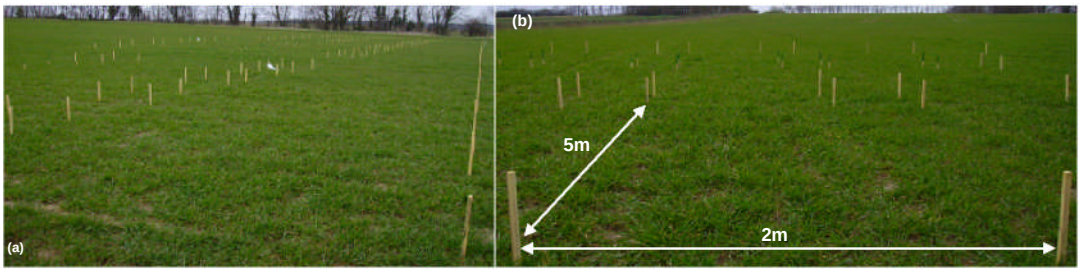

Figure 2: Overview of plot experiment in Avenue Field – CU@S (a); and (b) close-up plot.

The plots were designed to have 2 m by 5 m to facilitate the operation of a Deutz Fahr M660 plot combine-harvester.

A decision was made to carry out the first N-application on March 27th 2007 using UAN (urea ammonium nitrate; 32% N) at a rate of 90 kg N ha^{-1} in order to avoid losses of yield since the production of the OMFs could not be completed by the time the fertiliser was required. A second N-application was then carried out on May 17th 2007 once the OMFs became available. This took place immediately before the flag leaf was displayed.

EXPERIMENT 3: INCUBATION TRIAL

The chemical compositions of the OMFs were designed for the application on crops in the early spring. The mineral fraction of the OMFs would ideally produce a quick burst of N to cover the requirements of the crop for the main growth period; thereafter, it would continue to release N at a slower rate so that no further fertiliser dressing would be required for the crop cycle. This slow-release N would come from the organic fraction of the OMF-N which would be gradually mineralised throughout the growing season. However, as this process is highly dependent on a number of factors; e.g. temperature and soil moisture content, later applications of mineral-N may be done if necessary.

The purpose of this experiment is therefore to obtain information about OMF-N release and to try and determine whether mineralised-N matches the requirement of the crop at any given time. It is therefore vitally important to be able to identify the rate of N-release over time and to quantify the proportion of N available and non-available for crop up-take. This information will help to develop appropriate application rates strategies and timing of application. The experiment is conducted under controlled laboratory conditions; i.e. temperature and soil moisture content, and uses the same soil types as those described before for *experiment 1.* Soil samples are taken monthly for analysis of available N and extractable P and will run for a period of 6 months.

CONCLUSIONS

The development of OMF products will bring about a sustainable solution for the recycling of biosolids to agricultural land. This would contribute to reduce the cost of disposal by diverting more

 Published by Cranfield University Press ISBN: 978-0-9557436-7-2 http://hdl.handle.net/1826/3832

sewage-sludge through the agricultural route and would provide the users with more reliable products; thereby, increasing current levels of uptake. Preliminary experimental results both in the greenhouse and field have shown the suitability of formulated OMFs for application in winter wheat and grassland.

ACKNOWLEDGEMENTS

The authors would like to thank the sponsoring company, United Utilities plc, and the Engineering and Physical Sciences Research Council (EPSRC) for their financial assistance, and Cranfield University staff for their help at all stages of the experimental work.

REFERENCES

1. **Antille, D.L., Sakrabani, R., and Godwin, R.J., 2008.** Methodological approach to identifying the properties of a novel organomineral fertiliser – *Part II: environmental aspects and OMF application.* Cranfield Multi-Strand Conference: Creating wealth through research and innovation (CMC 2008). Cranfield University, MK43 0AL, UK. May 6th – 7th 2008.
2. **Bowden, W., and Hann, M.J., 1997.** The availability of nitrogen following digested sludge incorporation in arable land. Nutrient Cycling in Agroecosystems (0): 1 – 5. Kluwer Academic Publishers, The Netherlands.
3. **Defra (2007); Department of Food and Rural Affairs, 2007.** Waste strategy for England 2007. Published by The Stationery Office, PO Box 29, Norwich NR3 IGN. [Accessed: 23rd February 2008].
4. http://www.defra.gov.uk/environment/waste/strategy/strategy07/pdf/waste07-strategy.pdf **King, D.W., 1969.** Soils of the Luton and Bedford Districts: a reconnaissance survey. Published by The Soil Survey of England and Wales, UK.
5. **Skinner, R.J., Church, B.M., and Kershaw, C.D., 1992.** Recent trends in soil pH and nutrient status in England and Wales. Soil of Use and Management, Volume (8), number 1, 16–20.
6. **Sommers, L.E., Nelson, D.W., and Yost, K.J., 1976.** Variable nature of chemical composition of sewage-sludge. Journal of Environmental Quality (5), 303 – 306.

 Published by Cranfield University Press ISBN: 978-0-9557436-7-2 http://hdl.handle.net/1826/3832

Interface States: A Source of Threshold Voltage Instability in Organic Transistors

D. M. Taylor

School of Electronic Engineering, Bangor University, Dean Street, Bangor, Gwynedd LL57 1UT, UK

ABSTRACT

Several possible mechanisms that can lead to threshold voltage instability in organic thin film transistors are discussed. The role of the insulator-semiconductor interface is highlighted, in particular the effects arising from the presence of localised states there. It is shown that ac admittance measurements are an effective method for investigating such states.

INTRODUCTION

Organic electronic devices and circuits are the subject of intense research and development efforts worldwide with the first commercial products beginning to appear in the marketplace and major developments in the pipeline. For this burgeoning branch of electronics to realise its full potential, it is essential that the properties of organic field effect transistors (OFETs) remain stable during their operational lifetime. Considerable evidence is now beginning to accumulate suggesting that OFETs suffer from threshold voltage instability [1] and identifying the origin of the instability is attracting much interest.

Generally, the instability arises from two factors (a) the ingress of environmental 'impurities' e.g. water [2], oxygen [3] and ozone [4] and (b) application of electrical stress, especially high electrical fields across the gate insulator. In the latter case the effect manifests itself as a decreasing source-drain current, I_D, when devices are biased into strong accumulation and an increasing I_D when devices are biased into depletion. In principle, environmental effects may be eliminated by producing devices under an inert atmosphere and encapsulating in suitable packaging. In the following, therefore, we explore the various factors that can give rise to the electrically-induced instability often referred to as gate-voltage-stress.

LOCALISED SEMICONDUCTOR STATES AT THE INTERFACE

The mobility of charge carriers in OFETs ranges from $\sim 10^{-4}$ cm^2/Vs in amorphous polymer devices to $\sim$20 cm^2/Vs in single crystal rubrene and charge transport in such devices is described by a hopping mechanism through tail states extending into the bandgap. Fig. 1(a) represents such a process in a p-type organic semiconductor. In the presence of a manifold of localised states, holes will occupy those states lying deepest in the gap i.e. the highest lying states. When a

 Published by Cranfield University Press ISBN: 978-0-9557436-7-2 http://hdl.handle.net/1826/3832

negative voltage is applied to the gate of a p-channel OFET, holes accumulate at the semiconductor interface so that the deeper states there become filled. Thus, holes in the accumulation channel are able to hop more rapidly through the shallower states close to the valence (or HOMO) band edge, leading to a higher mobility than in the bulk. Consequently, the hole mobility increases as the gate voltage increases owing to the increasing carrier concentration in the channel. The dotted curve in Fig. 1(b) is a sketch of the resulting transfer characteristic for the OFET.

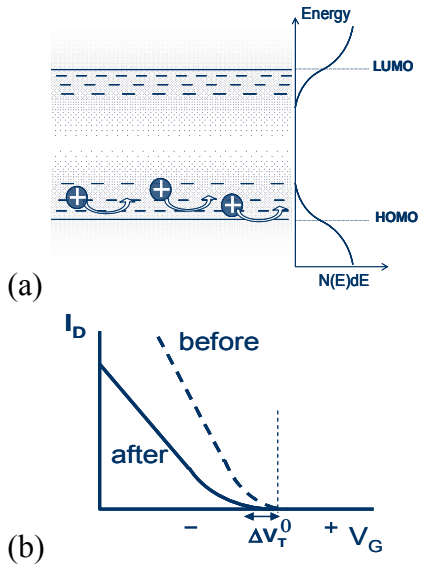

Fig. 1 (a) Holes hopping through localised states in a p-type semiconductor. (b) OFET transfer characteristic showing the effect of increasing the density of localised states.

If environmental factors or electrical stress increases the density of localised states then, the carrier mobility is reduced for the same gate voltage, leading to a shallower slope and apparent shift, ΔV_T, in the threshold voltage to more negative voltages (full curve in Fig. 1(b)). Detailed studies of changes to the output and transfer characteristics are the usual method of studying such states.

LOCALISED INTERFACE STATES - MAJORITY HOLE TRAPS

True interface states are charge trapping states localised at or near the boundary between the semiconductor and the gate insulator. When a negative voltage is applied to the gate electrode, a fraction of the holes from the accumulation layer become trapped in such states as shown in Fig. 2(a). When a second gate-voltage sweep is undertaken, the characteristic is shifted by ΔV_T, to more negative voltages as shown in Fig. 2(b) owing to the additional electrostatic field of the trapped charges. Ion migration and polarisation in the gate insulator would produce shifts in the opposite sense and are readily distinguished, therefore, from interface trapping. If detrapping occurs in the timescale of the voltage sweep, then a change in slope of the transfer characteristic can also occur.

The interaction of majority holes with interface states in a metal-insulator-semiconductor (MIS) capacitor structure, Fig. 3(a), leads to an additional contribution to the measured capacitance and loss (conductance/angular frequency) under small-signal conditions. To utilise such measurements to investigate interface states, however, it is essential that a guard ring is used to prevent lateral conduction along the semiconductor from masking the interface state signals at the low frequencies necessary for the measurements. The equivalent circuit of a MIS capacitor with interface states [5] is shown in Fig. 3(b). C_I represents the gate insulator, C_B and R_B the bulk semiconductor and R_S any series resistance associated with the electrodes. When the device is

 Published by Cranfield University Press ISBN: 978-0-9557436-7-2 http://hdl.handle.net/1826/3832

biased into depletion, the additional elements within the dotted box must be added, C_D to represent the depletion region and C_T, R_T to represent a single level interface state. When states are distributed in energy as in Fig. 2(a), then additional series C-R elements must be added in parallel with C_TR_T, one for each discrete state in the distribution.

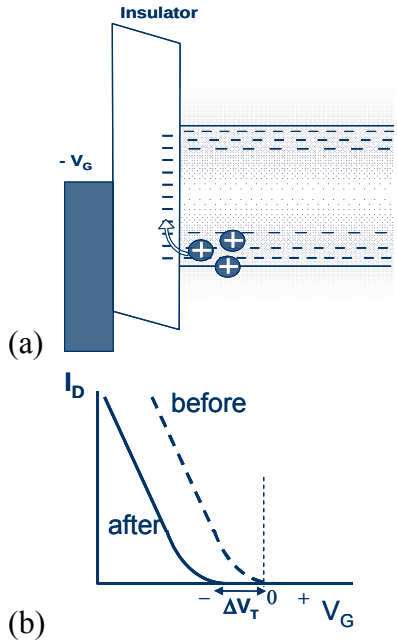

Fig. 2 (a) Energy diagram showing trapping of holes by interface states under a negative gate voltage and (b) OFET transfer characteristic before and after hole trapping.

The small signal response of a MIS capacitor with a distribution of interface states in which the density of hole traps decreases from the valence band towards the centre of the bandgap is shown in Fig. 4. The parameter here is the width, d_d, of the depletion region. When the device is in accumulation, d_d=0, the response is the classic Maxwell-Wagner response of a two-layer dielectric yielding a dispersion centred around the relaxation frequency, $f_R=[2\pi R_B(C_I+C_B)]^{-1}$, which, in this example is ~50 kHz. The dependence f_R on R_B indicates that the relaxation frequency is controlled by the mobility of charge carriers in the bulk semiconductor, which, in contrast to crystalline silicon, is relatively low in organic devices. As the capacitor is driven into depletion, i.e. d_d increasing, the interface states manifest themselves as a second dispersion, in which the loss peak decreases in magnitude and shifts to lower frequencies (Fig. 4(b)). Such a response has been observed in MIS capacitors formed from the p-type polymer poly(3-hexyl thiophene) (P3HT), spincoated onto a polysilsesquioxane insulator [5].

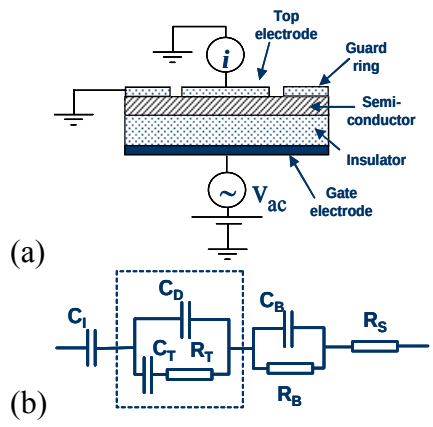

Fig. 3(a) MIS capacitor and set-up used for investigating interface states. (b) The corresponding equivalent circuit.

 Published by Cranfield University Press ISBN: 978-0-9557436-7-2 http://hdl.handle.net/1826/3832

This work showed also that when the loss was plotted against applied voltage, the presence of two processes was revealed, as shown in the Fig. 5(a) for the vacuum- annealed device. We have shown [6] that the peak observed when the device is in

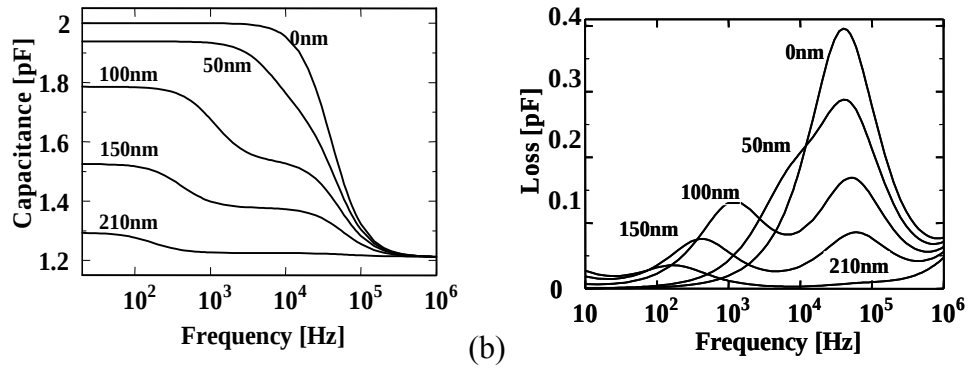

Fig. 4 Simulated frequency-dependence of (a) capacitance and (b) loss of a MIS capacitor with a distribution of interface states decreasing into the bandgap.

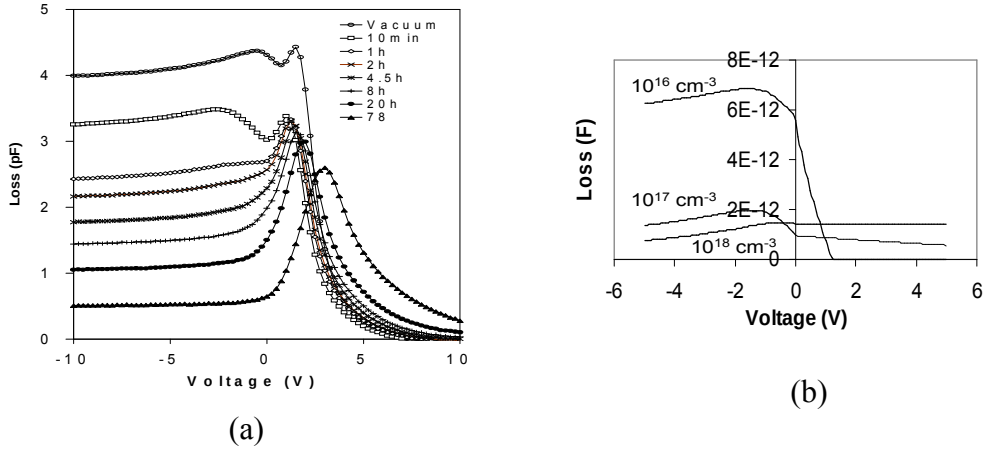

Fig. 5 (a) Loss vs voltage in a MIS capacitor showing the effect of prolonged exposure to laboratory air. (b) Simulation of the effect of increased doping density in the semiconductor.

accumulation (negative voltages) arises from the presence of a parasitic OFET in the test device - as seen from Fig. 3(b) the top electrode and guard ring act as grounded source and drain electrodes. Upon exposure to laboratory air, oxygen doping of the P3HT increased the frequency response of the parasitic OFET as well as increasing the relaxation frequency of the diode. Consequently, the background losses arising from these processes decrease (Fig. 5(b)) so that the true interface response is clearly revealed. Such measurements define the maximum frequency at which a detailed study of interface states can be undertaken.

For example, in Fig. 6 is shown the voltage-dependence of capacitance and loss for a range of frequencies from 1 kHz down to 1 Hz. Both plots indicate the presence of interface states viz. the 'stretching' of the C-V plots and loss peaks moving to more positive voltages as the frequency increases. Following the analysis of Nicollian and Goetzberger for silicon, we have used such data

 Published by Cranfield University Press ISBN: 978-0-9557436-7-2 http://hdl.handle.net/1826/3832

[7] to extract a linearly varying density of states for the interfacial hole traps, see Fig. 6(c). Since trap energies were estimated by applying Poisson's equation to the depletion regime in the 600 Hz C-V plot, they are quoted relative to the Fermi level in the bulk semiconductor, E_{Fb}, which lies ~0.3 eV above the HOMO level.

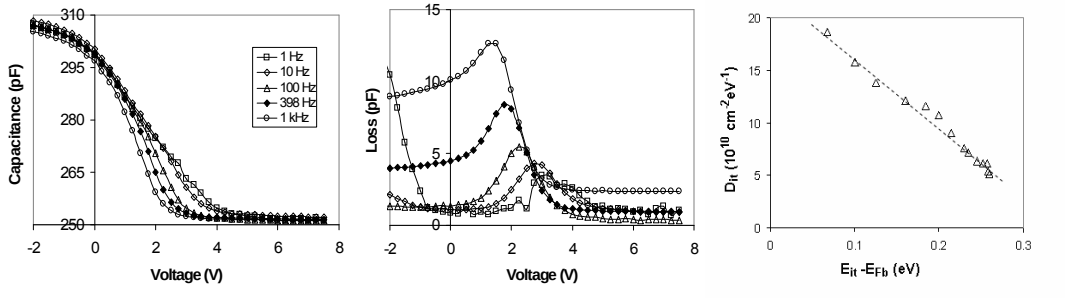

(a) (b) (c)

Fig. 6 Voltage dependence of (a) capacitance of a MIS diode showing clear interface state response. (c) Density of states extracted from the experimental data

LOCALISED INTERFACE STATES - MINORITY ELECTRON TRAPS

In the previous section the emphasis was on the interface states that interact with majority holes. While such traps may contribute to instability when accumulation voltages are applied, they cannot explain depletion-induced instability. In the latter case, we must invoke the presence of minority electron traps. To investigate such states it is necessary to increase the concentration of electrons at the interface well above that of holes. This is achieved by driving the MIS capacitor into depletion and illuminating with photons of energy greater than the bandgap of the semiconductor (Fig. 7(a)). The photo-induced electrons may either migrate to the interface forming an inversion layer as in silicon devices, or may become trapped in interface states. When the latter occurs, the resulting change in threshold voltage causes the C-V plot to shift to more positive voltages, as seen in Fig. 7(b) for a MIS capacitor based on P3HT and a polyimide insulator. Here it is seen that, for photon energies less than the polymer bandgap (□□> 700 nm), little change is observed in the C-V plot. For higher energies, significant shifts are seen indicative of a high electron trap density at the interface.

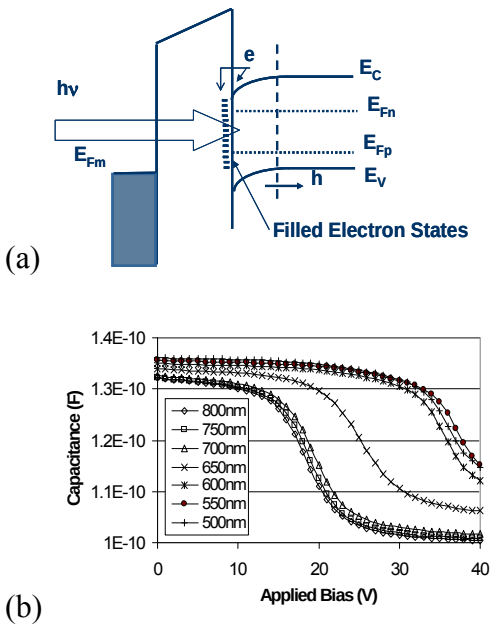

Fig. 7 (a) Illumination of MIS capacitor biased into depletion, (b) C-V plots obtained for photons of different wavelength.

 Published by Cranfield University Press ISBN: 978-0-9557436-7-2 http://hdl.handle.net/1826/3832

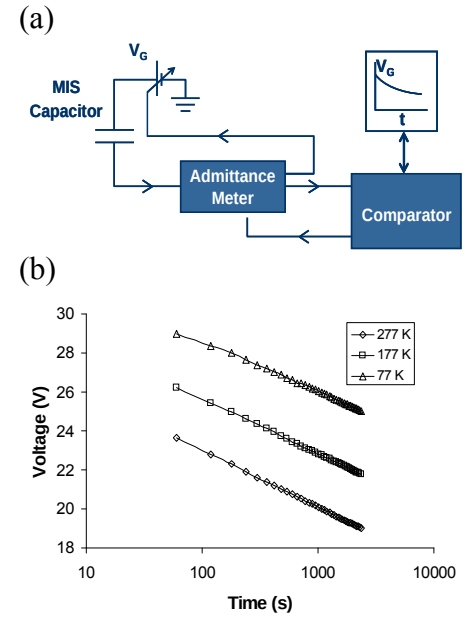

Fig. 8 (a) Feedback circuit used to investigate the relaxation of trapped electrons and (b) the results obtained at three different temperatures.

Using the feedback circuit in Fig. 8(a), we may follow the relaxation of the trapped electrons under constant surface potential conditions i.e. a constant degree of band-bending. This is achieved by monitoring the voltage required to maintain constant, a pre-determined capacitance in the depletion regime. Typical results for the P3HT/polyimide capacitor are shown in Fig. 8(b). The logarithmic time dependence has been observed by many research groups and, interestingly, in α-Si devices where it has been attributed to electron tunnelling into/out of traps lying progressively further away from the interface and deeper into the insulator.

CONCLUSIONS

It has been shown that small-signal admittance measurements are a powerful means of investigating interface traps in organic electronic devices. Measurements made in the dark yield information on majority carrier traps. At the P3HT/polysilsesquioxane interface, these appear to be linearly distributed in energy. Under illumination with photons of energy greater than the semiconductor bandgap a high density of minority electron traps has been observed.

ACKNOWLEDGEMENTS

The author is pleased to acknowledge the contributions to these studies by N. Alves, J. Drysdale, E. Itoh, O. Fernandez and I. Torres, also financial support from the Engineering and Physical Sciences Research Council (UK).

REFERENCES

1. A. Salleo and M.L. Chabinyc in 'Organic Electronics', Ed. H. Klauk, (Wiley-VCH: Weinham), 2007.
2. H.L. Gomes, P. Stallinga, M. Cölle, D.M. de Leeuw, F. Biscarini, 2006, *Appl. Phys. Lett.,* **88,** *082101.*
3. D.M. Taylor, H. Gomes, A.E. Underhill, S. Edge and P.I. Clemenson, 1991, *J.Phys D: Appl.Phys.*, **24,** 2032-38.
4. M.L. Chabinyc, R.A. Street and J.E. Northrup, 2007, *Appl. Phys. Lett.,* **90**, 123508.
5. I. Torres and D.M. Taylor, 2005, *J. Appl. Phys.*, **98**, 073710.
6. D. M. Taylor and N. Alves, 2008, *J. Appl. Phys.*(in press).
7. N. Alves and D.M.Taylor, 2008, *Appl. Phys. Lett.* (in press).

 Published by Cranfield University Press ISBN: 978-0-9557436-7-2 http://hdl.handle.net/1826/3832

Fizeau-based OCT using coherent fibre imaging bundles

G. F. Sarantavgas, H. D. Ford and R. P. Tatam

Engineering Photonics Group, School of Engineering, Cranfield University, Cranfield, Bedford, MK43 0AL, UK.

ABSTRACT

A coherent fibre imaging bundle is a flexible bundle containing a large number of optical fibres, manufactured in such way that the fibres remain parallel to each other for the entire length, during layup of the bundle. Therefore a fibre in one end of the bundle will have the same neighbouring fibres on the other end.

Optical Coherence Tomography (OCT) is a well established medical imaging technique whose foundations rely on low-coherence interferometry. OCT applications extend, but are not limited to, medical and biological purposes and material sciences. OCT imaging systems were developed in response to the demand to explore microstructures within turbid biological media using non-ionising radiation which is clinically safe.

This paper describes a single point, Fizeau-interferometer based OCT instrument that operates in the time-domain. It discusses the properties of coherent bundles and describes an OCT system in which they are incorporated. Preliminary results from this method are shown and a synopsis of the advantages using such configuration is provided.

INTRODUCTION

OCT systems currently researched are regarded as the 6th generation medical imaging tools with respect to the other five medical imaging modalities of PET (Positron Emission Tomography), MRI (Magnetic Resonance Imaging), CT (Computed Tomography), Ultrasound and X-ray. OCT can generate ultra high resolution tomographic images, with depth resolution in the range of 1 to 30μm [1], within a limited imaging depth of 1-2mm [2]. Typically, an optical coherence tomography (OCT) system is configured using an in-fibre Michelson interferometer [1], with a reference reflector in one interferometer arm (reference arm), and the sample in the other (sample arm). At the sample arm a system of lenses focuses the light to a few microns (transverse resolution) onto the sample and the backscattered/backreflected light from the sample couples back to same arm and mixes at the detector with reference signal beam. If the path lengths travelled by the two beams are matched within the coherence length of the source (1-30μm), interference fringes are formed. The boundaries between the sample are detected as burst of fringes corresponding to various depths. The bandwidth of the source has to be as large as possible since the depth resolution is determined by the coherence length, which is inversely related to the source spectral width. However, the stability of this commonly-used arrangement is environmentally sensitive. Variations in the deployment of the

 Published by Cranfield University Press ISBN: 978-0-9557436-7-2 http://hdl.handle.net/1826/3832

interferometer fibres as in an endoscopic application will cause polarization-state changes which are different for the two arms due to fibre bending and temperature fluctuations. Signal fading therefore occurs, reducing the amplitude of the fringes [3].The use of a Fizeau interferometer, as shown for a time-domain configuration in figure 2 and as it is configured in our lab, eliminates polarisation fading problems, since the reference and signal beams travel in the same fibre [4].

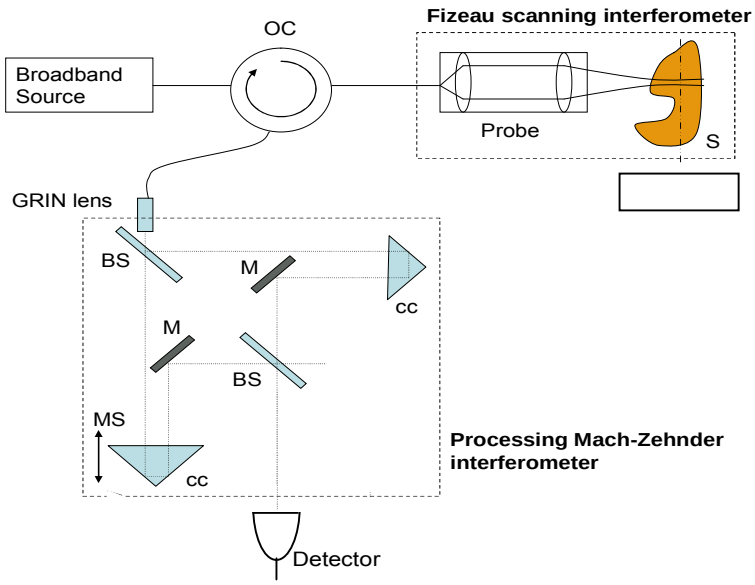

Fig. 1: Configuration for Fizeau-based OCT system with Mach-Zehnder processing interferometer. OC = optical circulator, S = sample, BS = beam splitter, M = mirror, CC = corner cube prism, MS = micropositioning stage.

Several other groups have recently reported investigations of common-path configurations [5]. In a Fizeau-type OCT system, the reference reflection beam is derived either from a glass plate positioned close to the sample or, preferably, from the reflection at the end of the delivery fibre. The reference beam and signal beams traverse a common path within the optical fibre section of the interferometer, experiencing identical phase/polarisation perturbations. Because of the path length imbalance inherent to Fizeau systems, a processing balancing interferometer is required, to readjust the overall path length difference to a value within the source coherence length and this can either be a Michelson-type processing interferometer or a Mach-Zehnder as shown in figure 1. The sensitivity of the system is defined by the signal-to-noise ratio (SNR), which affects the depth-dependent contrast seen in the OCT images, and therefore both the maximum depth at which acceptable imaging can be achieved and the minimum change in refractive index that can be detected. Experimental work on this system has revealed that such a configuration has sufficient SNR to successfully image biological samples [6].

COHERENT IMAGING FIBRE BUNDLES FOR OCT

In recent years considerable interest has arisen in the endoscopic applications of OCT. Previous clinical imaging modalities do not offer sufficient resolution to delineate the microstructure of biological samples.

 Published by Cranfield University Press ISBN: 978-0-9557436-7-2 http://hdl.handle.net/1826/3832

This is desirable to allow identification of abnormalities such as early signs of numerous types of carcinoma. Currently, to detect such abnormalities with high resolution a biopsy is performed, requiring the surgical removal of the tissue for a microscopic histological examination that is subjective, invasive, expensive, and a time consuming process. Due to the high imaging resolution and sufficient penetration depth of OCT, if it were to be used in an endoscopic system it could reduce the number of biopsies being performed and potentially lead to early and more reliable prediction of cancer onset . In OCT, 3D imaging is generally achieved by scanning the probe beam across the surface of the sample in a raster pattern, acquiring data sets (A-scan) at each position. The current OCT systems that are being considered for in-vivo deployment scan the beam across the area of interest with moving parts such as linear motors, rotor fibre joints and micromotors[7]. Although such configurations have been demonstrated with success they are quite complex and challenging to implement (particularly the precise alignment of components). Furthermore such configurations also limit the transverse resolution of an OCT system considering that the size and the NA of the lenses and mirrors are restricted by the endoscope size. In this paper we discuss how the incorporation of a coherent imaging bundle, in a Fizeau based interferometer configuration, can form a 'downlead insensitive', compact, robust and clinically safe OCT probe without the need for scanning mechanical parts in the probe.

Two coherent fibre imaging bundles were investigated, which were provided by Schott North America. In a coherent bundle, an image focused onto one end is delivered through the array of fibres to the other end, in the same orientation, with respect to the fibres, as the original image. A fibre bundle can consist of hundreds or thousands of fibres with lengths varying from a few centimetres to a couple of metres, with cores 5-10microns in size. The packing arrangement of fibres in the bundle can also differ, as shown in figure 2, being either a regular hexagonal pattern or an arrangement of square packed 5x5 sub-bundles with typical fibre centre spacings of 10μm and core diameters of 8μm.

We have previously demonstrated an OCT probe incorporating an imaging fibre bundle, in which all fibres of the bundle were illuminated simultaneously, with a CCD camera used for image capture [8]. The present paper describes an alternative methodology, in which each fibre is illuminated in turn, using scanning components at the input to the bundle to address the individual fibres. This system enables point detectors to be used instead of a camera, allowing high-bandwidth noise filtering techniques to be applied to the detector output. Previous experimental work has revealed that the state of polarisation will very considerably for every fibre addressed in the bundle. However, in the Fizeau configuration, the bundle does not form part of either interferometer; therefore polarisation variations in the bundle do not affect the image contrast, and the instrument is said to be "downlead insensitive".

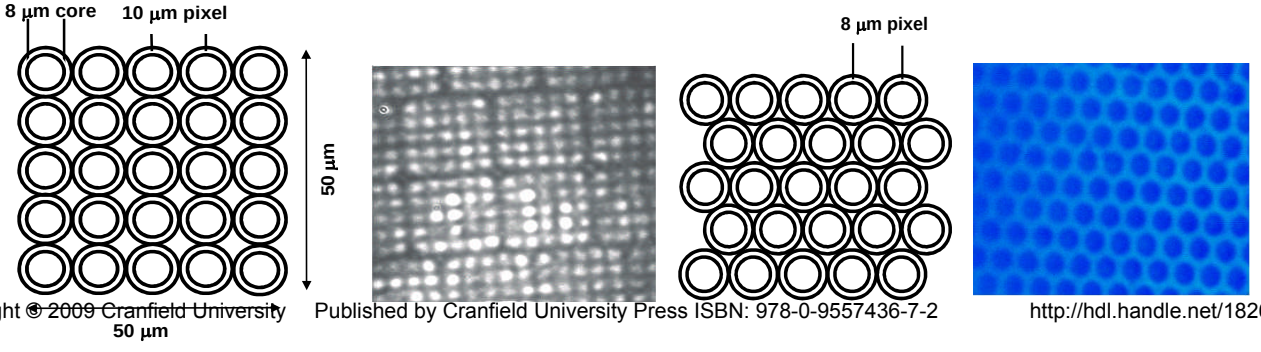

 Published by Cranfield University Press ISBN: 978-0-9557436-7-2 http://hdl.handle.net/1826/3832

Fig. 2: Fibre bundle packaging arrangements: left , wound bundle; right, leached bundle.

The experimental arrangement for OCT using a fibre bundle is shown in figure 3. Light emanating from an SLD at 830nm, with 9.86μm coherence length, is collimated and focused onto the input face of the bundle, by means of an aspheric lens providing a focused beam diameter of 4.4μm. The input end of the bundle was polished at an angle of 8 degrees to avoid any back reflection to the processing interferometer. The length of the bundle was 1.1m and comprised 15,000 fibres. The bundle length was chosen to be 1.1m to minimise multimode interference. It is generally possible for more than one transverse mode to propagate, due to the relatively large diameter of the fibre cores. Different modes of the fibre are associated with different velocities, which can lead to the formation of ghost images but if the fibre is made long enough, the slower signals from the higher order modes will no longer overlap with the faster signals from the lower order modes. Ghosting has not appeared as a problem in our experiments.

Each fibre in turn was addressed by the focused input beam. The beam was transmitted through the bundle and focused onto the sample by the probe lenses, also comprising appropriate aspherics. The sample beam was focused with a beam diameter of about 8.2μm and a depth of field of about 250μm. To address each fibre in the bundle in succession, the bundle was mounted onto a computer controlled mechanical translation stage, which was scanned across the focused input beam. It is crucial for OCT applications that light does not leak from any one fibre into neighbouring fibres.

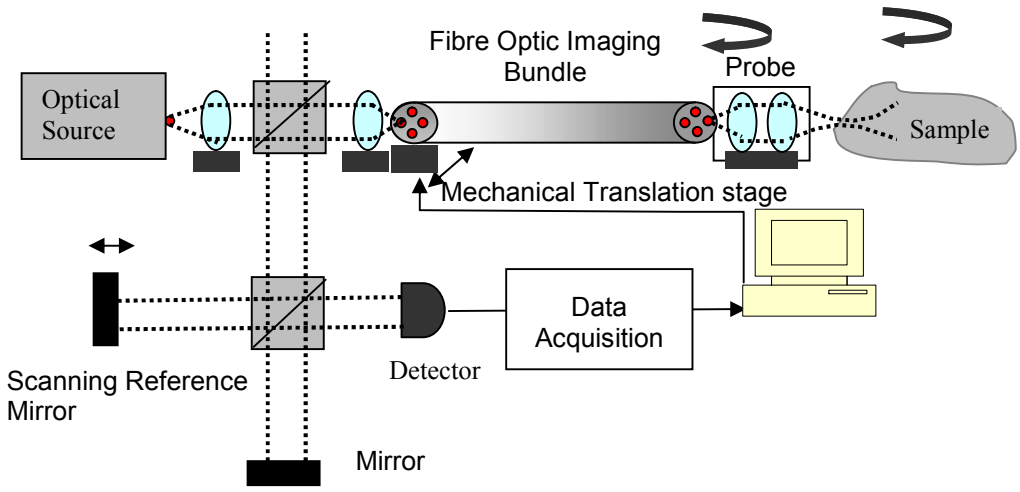

Fig. 3: Fizeau based OCT incorporating a coherent imaging fibre optic bundle.

We have investigated this by coupling light into a single fibre and observing the output on a camera. At 800nm, leakage between neighbouring fibres was found to be negligible although, working with a wavelength of 1550nm, crosstalk was more significant. A two-dimensional image was generated from two pieces of plastic projector slide stacked together as shown in figure 4. A-scan images were taken at each step position (20 steps, each of 10μm) to construct an image of 0.2mm (transverse) x1mm (depth).

 Published by Cranfield University Press ISBN: 978-0-9557436-7-2 http://hdl.handle.net/1826/3832

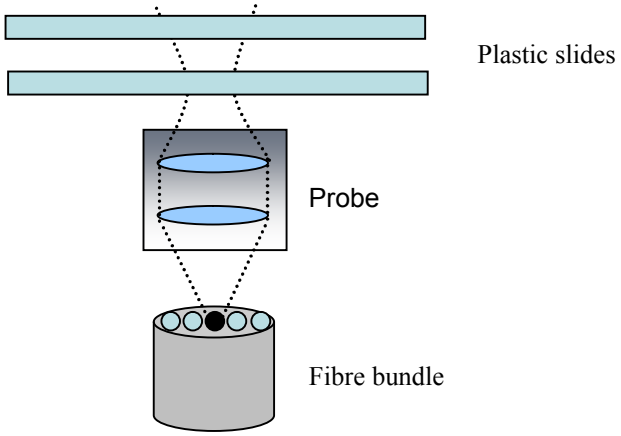

Fig. 4: Experimental arrangement of the fibre bundle, probe and a sample of two plastic projector slides.

The image produced is shown in figure 5. The image clearly depicts the four layers of the sample. The upper and lower surfaces of the plastic slides are clearly visible with an overall thickness of 0.157mm for both slides. The air gap between them was found to be 0.471mm.

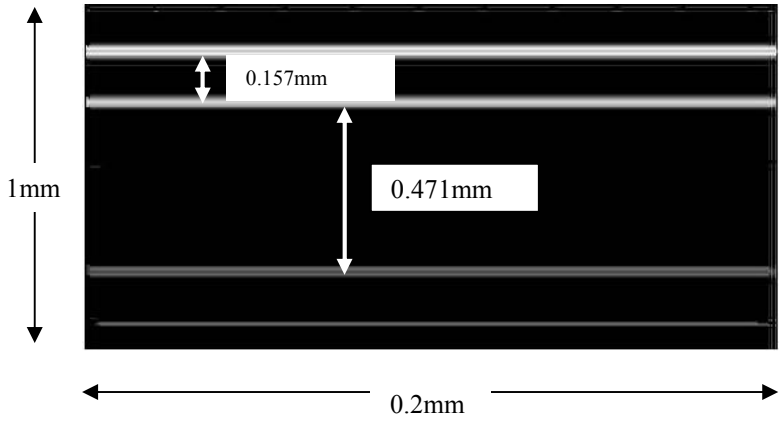

Fig. 5: Image of two layers of plastic projector slide.

CONCLUSIONS

A Fizeau configuration optical coherence tomography system incorporating a coherent fibre imaging bundle has been described. Implementation of such a configuration can enable 2D information to be obtained without the necessity for scanning components at the probe tip. The common path probe section of the instrument ensures 'downlead insensitivity' and, provided that the processing interferometer is constructed in bulk-optic form, the entire instrument is polarization insensitive. The use of an imaging bundle in a Fizeau interferometer based OCT would be advantageous as it forms an extremely compact, robust and downlead insensitive instrument for future endoscopic applications allowing 2D or 3D OCT image acquisition. Further development of the system will include testing on biological samples, miniaturisation of

 Published by Cranfield University Press ISBN: 978-0-9557436-7-2 http://hdl.handle.net/1826/3832

components, increasing transverse scanning speed of the input beam across the bundle and implementation in the Fourier domain rather than time domain.

REFERENCES

1. Bouma,B.E., Tearney, G.J., Boppart, S.A., Hee, M.R., Brezinski, M.E.Fujimoto, J.G., Optics Letters, 20(13), 1486-1488, 1995.
2. Colston, B.W., Everett, M.J., DaSilva, L.B., Otis, L.L., Stroeve, P. and Nathel, H., Applied Optics, 37(16), 3582-3585, 1998.
3. Kersey A D, Marrone M J, Dandridge A and Tveten A B J. Lightwave Technology. 6 1599-1609, 1988.
4. Ford H D, Beddows R, Casaubieilh P and Tatam R P, Journal of Modern Optics 52 1965-1979, 2005.
5. Sharma U, Kang J U and Fried N M 2005 "Fizeau optical coherence tomography: sensitivity optimization and system analysis" CLEO,San Jose, California, Vol 3. 2061-2063, 2005.
6. G.F. Sarantavgas, H.D. Ford, R.P. Tatam “Imaging fibre bundles for optical coherence tomography”. BiOS ’08 proceedings, San Jose, California, USA
7. Z. Yaqoob, J. Wu, E. J. McDowell, X. Heng, C. Yang, Journal of Biomedical Optics 11(6), 063001, 2006
8. H. D. Ford, R. P. Tatam, Full-field optical coherence tomography using a fibre imaging bundle BiOS 2006, San Jose, USA, January, 2006.

 Published by Cranfield University Press ISBN: 978-0-9557436-7-2 http://hdl.handle.net/1826/3832

Simultaneous Preservation of Soil Structural Properties and Phospholipid Profiles: A Comparison of Three Drying Techniques

L. J. DEACON[1], D. V. GRINEV[2], J.W. CRAWFORD[2], J. HARRIS[3], K. RITZ[4] and I. M. YOUNG[2]

[1]Centrefor Resource Management and Efficiency, Sustainable Systems, School ofApplied Sciences, Cranfield University, Cranfield, Bedfordshire MK43 0AL E-mail: l.j.deacon@cranfield.ac.uk

[2]SIMBIOS Centre, University ofAbertay, Dundee, DD1 1HG

[3]Integrated Earth Systems Science Institute, Department ofNatural Resources, School ofApplied Sciences, Cranfield University, Cranfield, MK49 0AL

[4]National Soil Resources Institute, Department ofNaturalResources, School ofApplied Sciences, Cranfield University, Cranfield, MK49 0AL

ABSTRACT

There is a need to simultaneously preserve evidence of interactions between the biological community and soil structural properties of a soil in as near an intact (natural) state as possible. Three dehydration techniques were implemented and assessed for their ability to minimise disruption of both biological and physical properties of the same arable soil sample. Dehydration techniques applied until samples were at constant weight were i) air-drying at 20 °C (AD); ii) —80 °C freeze for 24 h, followed by freeze-drying (—80FD); iii) liquid nitrogen snap freeze, followed by freeze-drying (LNFD) and were compared to a moist control. Physical structure was determined and quantified in three dimensions using X-ray computed tomography and microbial phenotypic community composition was assessed using phospholipid fatty acid (PLFA) profiling. This study confirms that any form of dehydration, when preparing soil for simultaneous biological and physical analysis, will alter the soil physical properties, and cause some change in apparent community structure. Freeze-drying (both the LNFD and —80FD treatments) was found to minimise disruption (when compared to the moist control soil) to both the soil physical properties and the community structure and is a preferable technique to air-drying which markedly alters the size and character of the pore network, as well as the phenotypic profile. The LNFD was the preferred treatment over the —80FD treatment as samples show low variability between replicates and a fast turn-around time between samples. Therefore snap freezing in liquid nitrogen, followed by freeze drying is the most appropriate form of dehydration when two sets of data, both physical and biological, need to be preserved simultaneously from a soil core.

INTRODUCTION

In studying the interactions between biota and soil structural properties, there is a need to preserve both

 Published by Cranfield University Press ISBN: 978-0-9557436-7-2 http://hdl.handle.net/1826/3832

the biological and physical architecture of the soil system in as near an intact ('natural') state as possible. The extent to which preservation techniques are effective in both respects have rarely been considered. The simplest approaches based on air-drying are known to significantly alter both soil structural properties (through the shrinkage of clays and organic matter) and the morphology and biochemical constitution of organisms in such a way that they are no longer representative of the original hydrated system (Murphy, 1982; Schutter and Dick, 2000; Tippkötter *et al.,* 1986). The most thorough approaches are arguably in the application of biological soil micro-morphology, where the integrity of soil organisms are preserved through the use of chemical fixatives and structural fidelity is maintained by controlled chemically-based dehydration (e.g., Nunan *et al.,* 2006; Tippkötter and Ritz, 1996). However, these techniques are laborious, and do not allow the comparison between the structure of habitats and microbial communities beyond what can be achieved in two-dimensions. X-ray computed tomography enables the non-destructive visualisation of soil structure in three dimensions, but to date is not able to resolve soil microbes. Nonetheless, the ability to relate the extant soil microbial community composition to the physical architecture of their habitat, within the same sample, would offer a powerful approach to elucidating the relationships between soil biodiversity and structural dynamics. In this study, we compared three preparation techniques in terms of the fidelity with which structural and biological properties were preserved in an arable soil. Physical structure was quantified in three dimensions using X-ray computed tomography and microbial phenotypic community composition was assessed using phospholipid fatty acid (PLFA) profiling.

MATERIALS AND METHODS

Soil was collected from the top 30 cm of an arable field at Shuttleworth Agricultural College, Bedfordshire, UK (Ordinance Survey Grid Ref 513 242) in February 2005. The soil is a Ludford series sandy clay loam comprising of 590 g kg^{-1} sand, 230 g kg^{-1} silt, 180 g kg^{-1} clay, with a pH of 6.9, and an organic matter content of 10 g kg^{-1} (Brown *et al.* 1997). After collection the soil was stored at 4 °C in the dark until use. It was then passed through a 4 mm sieve and sub-samples packed into 50 mL polypropylene syringe bodies (microcosms) to 16 cm^3 by uni-axial compression to give a gravimetrically adjusted dry bulk density of 1.4 g cm^{-3} at 140 g L^{-1} moisture content. Microcosms were incubated in the dark for seven days at 20 ± 2 °C and moisture loss minimised by capping the core with a HEPA™-filter mounted in a Suba-seal (typical moisture loss 0.06 mL day-1) . Three preservation regimes were implemented: i) air-drying (AD), where the microcosms were

 Published by Cranfield University Press ISBN: 978-0-9557436-7-2 http://hdl.handle.net/1826/3832

placed at 20 °C under a fan until at constant weight (typically required 5–7 days); ii) —80 °C, freeze-drying (—80FD), where the microcosms were placed in a —80 °C freezer for 24 h then freeze-dried following transfer to an Alpha 1-2 LD freeze-drier (Christ freeze driers, Osterode am Harz, Germany); and iii) liquid nitrogen, freeze-drying (LNFD), where the microcosms were placed into liquid nitrogen until temperatures equalised (3–5 minutes) and then freeze-dried as above. In both circumstances, freeze-drying was complete after 24 h. Moist samples were maintained at 5 °C whilst the treatments were applied, and then processed as described below without drying.Five replicates of each treatment were used.

Entire microcosms were scanned (removing edge in contact with the syringe wall) using an X-TEK benchtop X-ray microtomography system with a tungsten target at 100 kV and 100 1*z*A, using a 5 1*z*m focal spot reflection target and an X-ray source with an operating regime of 25–160 kV and 0– 1000 1*z*A (non-continuous). 3D floating point datasets were obtained for each sample by reconstructing 936 angular projections with each projection averaged over 32 frames. Reconstruction software used a filtered back-projection algorithm and ramp filter to produce 3D volumes with an isotropic voxel size of 44 1*z*m (*x, y* and *z* dimensions are equal in terms of spatial resolution). Each 3D dataset was converted by VGStudioMax v.1.2 software (http://www.volumegraphics.com) into a TIF image stack with 400 voxel-size thick slices and 256 *x* 256 pixels dimension of the 2D image slice. The applied threshold operation was based on analysis of the image histogram, and the threshold value was chosen to give the best possible segregation of solid and void phases. Various structural characteristics of the binary image stacks were then calculated using in-house developed software, including percentage porosity, mean pore size and pore metrics.

After scanning, the microcosms were dismantled, soil re-homogenised and PLFAs extracted from 10 g fresh weight (or dried-soil equivalent) soil, using a method based on Frostegård *et al.* (1991), after Bligh and Dyer (1959) and White *et al.* (1979). Fatty acid methyl esters (FAMEs) were identified by gas chromatographic (GC) retention time by comparison with a standard qualitative bacterial acid methyl ester mix (26 standard; Supelco, UK). The results are expressed as a percentage of the total area of the identified peaks on the chromatogram (mol %). Principal component analysis (PCA) was used to interpret the PLFA profiles, and GLM and Fisher LSD tests were used to determine significant differences. Statistica 7.1 (Statsoft Inc., 2005) was used for statistical analyses, and results were considered significant at $P \leq 0.05$.

RESULT AND DISCUSSION

 Published by Cranfield University Press ISBN: 978-0-9557436-7-2 http://hdl.handle.net/1826/3832

Mean percentage porosity (Fig. 1a) and mean pore size (shown in brackets) of the moist (195 μm), LNFD (193 μm) and —80FD (197 μm) samples were not significantly different from each other, but the process of air-drying significantly increased the percentage porosity ($P < 0.00\ 1$) and mean pore size (220 μm; pooled SE = 2.8, $P <$ 0.05). This was also manifest in pore size distribution, where air-drying decreased the frequency of smaller pores and increased the frequency of larger pores compared to moist or freeze-dried samples (Fig. 1b). Pore connectivity, i.e., the volume of connected pore space expressed as a proportion of the total pore volume in the sample, showed that in all cases the pore networks were highly connected, and the largest pore in each treatment showed a range of connectivity of between 83%–96% (Table I). However, in air-dried samples the proportion of the total pore space in the largest five connected pores was either not significantly different from, or significantly smaller than, those in the moist or freeze-dried samples (Table I).

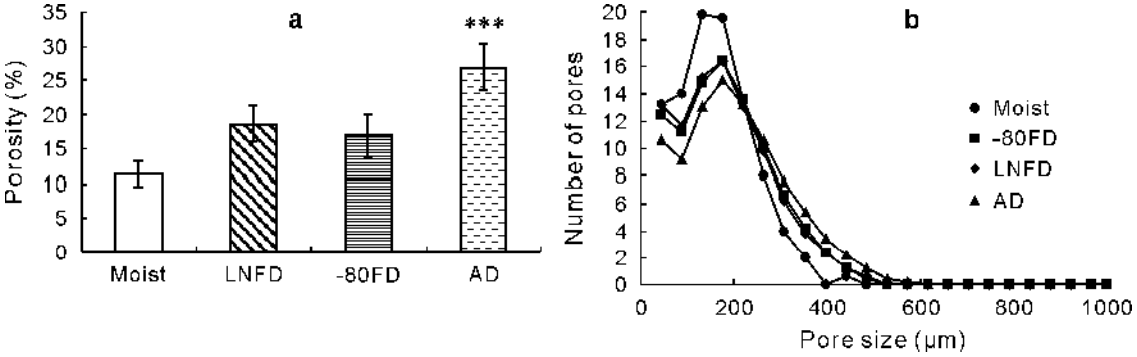

Fig. 1 Mean percentage porosity (a) and mean pore distribution (b) of moist, LNFD (liquid nitrogen, freeze-dry), —80FD (—80 °C, freeze-dry) and AD (air-dry) samples measured at a resolution of 44 μm. **Significant at $P < 0.001$. Whiskers show standard error of the mean ($n = 5$).

TABLE I

The mean volume of connected pore space in the entire microcosm, expressed as a percentage of the total pore volume for the five largest connected pores in each treatment

Treatment	Largest pores in size rank				
	Pore 1	Pore 2	Pore 3	Pore 4	Pore 5
	% of total pore volume				
Moist	83.7±7.44[a)]	1.02±0.41	0.63±0.40	0.48±0.28	0.42±0.23
Liquid nitrogen, freeze-dry	94.5±1.97	0.32±0.13	0.13±0.04	0.10±0.04	0.09±0.04
—80 °C, freeze-dry	78.9±14.4	4.83±4.42	4.70±4.31	1.14±0.85	0.64±0.42
Air dry	96.7±1.28	0.16±0.09	0.13±0.08	0.12±0.07	0.08±0.05

a) Mean±standard error ($n = 5$).

 Published by Cranfield University Press ISBN: 978-0-9557436-7-2 http://hdl.handle.net/1826/3832

With regard to biological community structure, the two freeze-drying methods resulted in PLFA profiles more similar to the moist than the air-dried samples, where the apparent phenotypic structure was markedly different ($P < 0.05$, PC1; Fig. 2). Air-dried samples were also the most variable in terms of PC1. This separation was dominated by a single PLFA, 18:1 isomer, which showed a 7-fold increase in mol% (mean 0.64% and 4.6% for moist and air-dried samples respectively). 18:1 in its various forms is present in most bacteria and eukaryotes, and therefore changes in the proportion of 18:1 isomer is not indicative of changes to a certain group of micro-organisms in the sample (Ratledge and Wilkinson, 1988).

The —80FD samples were further separated from the other samples in the PCA by PC2 (Fig. 2). In terms of sample processing time, LNFD samples were most rapid since the samples can simply be plunged into liquid nitrogen and transferred straight into the freeze-drier, rather than requiring a 24 h step as the —80 °C samples do.

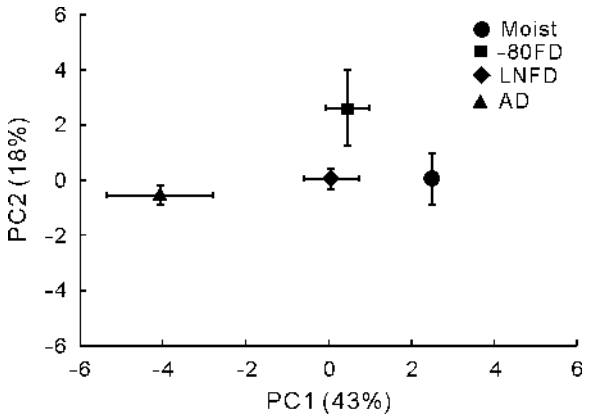

Fig. 2 Phenotypic structure of moist, LNFD (liquid nitrogen, freeze-dry), -80FD (-80 °C, freeze-dry) and AD (air-dry) samples as described by principal component analysis (PCA) of PLFA profiles. Whiskers show standard error of the mean (n=5).

CONCLUSIONS

Preparing soil for both biological and physical analyses simultaneously by any form of dehydration will alter the soil physical properties, as would be expected, and invokes some modest change in apparent community structure. However, freeze-drying minimises such disruption and is preferable to air-drying which markedly alters the size and the character of the pore network as well as the phenotypic profile. The LNFD treatment has distinct advantages: it preserves physical and biological community structure, has a fast turn-around time, and shows low variability between replicates.

 Published by Cranfield University Press ISBN: 978-0-9557436-7-2 http://hdl.handle.net/1826/3832

REFERENCES

1. Bligh, E. G. and Dyer, W. J. 1959. A rapid method of total lipid extraction and purification. *Canadian Journal ofBiochemistry and Physiology.* 37: 911–917.
2. Brown, C. D., Hollis, J. M., Bettinson, R. J., Beulke, S. and Fryer, C. J. 1997. Pesticide mobility: Lysimeter study to validate the relative leaching potential of UK soils. Research Report for MAFF Project PL0510 to the UK Ministry of Agriculture, Food and Fisheries. Soil Survey and Land Research Centre, Cranfield University, Bedfordshire, UK
3. Frostegàrd, ˚A., Tunlid, A. and B ˚aAth, E. 1991. Microbial biomass measured as total lipid phosphate in
4. soils of different organic content. *Journal ofMicrobiological Methods.* 14: 15 1–163.
5. Murphy, C. P. 1982. A comparative study of three methods of water removal prior to resin impregnation
6. of two soils. *Journal of Soil Science.* 33: 7 19–735.
7. Nunan, N., Ritz, K., Rivers, M., Feeney, D. S. and Young, I. M. 2006. Investigating microbial micro-habitat structure using X-ray computed tomography. *Geoderma.* 133: 398–407.
8. Ratledge, C. and Wilkinson, S.G. 1988. Fatty acids, related and derived lipids. *In* Ratledge, C. and
9. Wilkinson, S. G. (eds.) Microbial Lipids. Volume 1. Academic Press Limited, London, UK. Schutter, M. E. and Dick, R. P. 2000. Comparison of fatty acid methyl ester (FAME) methods for
10. characterizing microbial communities. *Soil Sci. Soc. Am. J.* 64: 1659–1668.
11. Tippkötter, R., Ritz, K. and Darbyshire, J. F. 1986. The preparation of soil thin sections for biological studies. *J.Soil Sci.* 77: 68 1–690
12. Tippkötter, R. and Ritz, K. 1996. Evaluation of polyester, epoxy and acrylic resins for suitability in
13. preparation of soil thin sections for *in situ* biological studies. *Geoderma.* 69: 3 1–57.
14. White, D. C., Davis, W. M., Nickels, J. S., King, J. D. and Bobbie, R. J. 1979. Determination of the
15. sedimentary microbial biomass by extractable lipid phosphate. *Oecologia.* 40: 51–62.

 Published by Cranfield University Press ISBN: 978-0-9557436-7-2 http://hdl.handle.net/1826/3832

Analysis of Sub-Optimum Detection Techniques for Bandwidth Efficient Multi-Carrier Communication Systems

Ioannis Kanaras[†], Arsenia Chorti[†], M.R.D. Rodrigues[‡], and Izzat Darwazeh[†]

[†]Department of Electronic & Electrical Engineering, University College London (UCL)

Torrington Place, London WC1E 7JE, UK, Email: {i.kanaras, a.chorti, i.darwazeh}@ee.ucl.ac.uk

[‡]Department of Computer Science, Instituto de Telecomunicações, Univeristy of Porto,

4169 – 007 Porto, Portugal, Email: mrodrigues@dcc.fc.up.pt

ABSTRACT

In this paper, we investigate the performance of various detection techniques for a spectrally efficient Frequency Division Multiplexing (FDM) system. In particular, we evaluate by simulation the performance of Zero Forcing (ZF) and Minimum Mean Squared Error (MMSE) sub-optimum linear detection techniques, as well as optimum Maximum Likelihood (ML) detection scheme. We also evaluate the computational complexity of the new model.

INTRODUCTION

In the last decade, the continuous and rapid growth of bandwidth demanding communication triggered the development of reliable bandwidth efficient transmission techniques for the provision of broadband services such as mobile internet, video conferencing, and broadcasting. The state-of-art currently uses techniques based on Orthogonal Frequency Division Multiplexing (OFDM) that has already been implemented in diverse communication systems such as Digital Video Broadcasting (DVB), Digital Audio Broadcasting (DAB), Wireless Local Area Networks (WLAN), and Wireless Broadband Access (WiMAX). In the last few years, some efforts have been done to investigate the possibility of exploiting better the available wireless bandwidth by reducing further the distance between the OFDM subcarriers. One example concerns Fast OFDM (FOFDM) which needs only half OFDM bandwidth when it is combined with real modulation schemes such as BPSK and M-ASK [1], [2]. A more recent idea relates to spectrum efficient Frequency Division Multiplexing (FDM) transmission systems using arbitrarily spaced subcarriers [3]. Despite the spectrum benefits promised by this technique, detection is especially complex.

In this paper, we investigate possible solutions to the problem of a reliable and computationally simple detection. Section II describes the system model. Section III describes various possible detection methods. Finally, sections IV and V provide simulation results and conclusions, respectively.

 Published by Cranfield University Press ISBN: 978-0-9557436-7-2 http://hdl.handle.net/1826/3832

SYSTEM MODEL

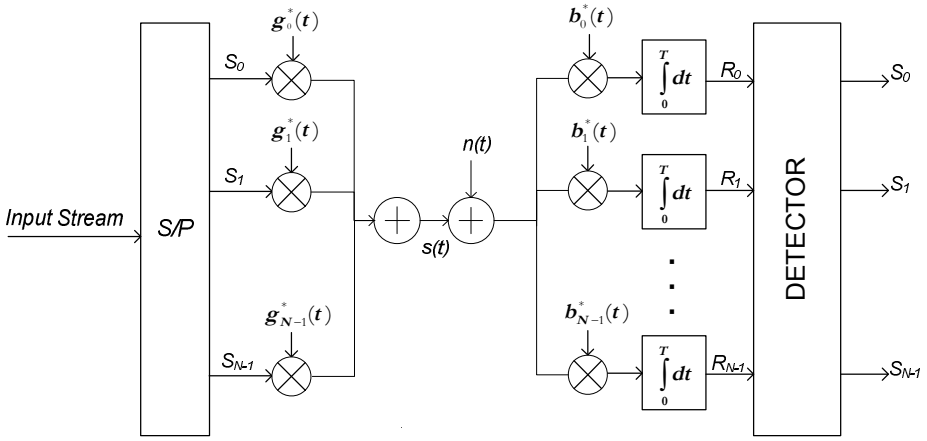

Figure 1: FDM System Architecture

Figure 1 depicts the FDM system architecture. Initially, the high data rate symbol stream is split into a number of parallel streams of lower data rate. The latter symbols modulate N non orthogonal subcarriers that are in turn added to form the FDM signal given by

$$s(t) = \sum_{k=-\infty}^{\infty} \sum_{n=0}^{N-1} S_{k,n} g_n(t - kT) \tag{1}$$

$$g_n(t) = \begin{cases} \frac{1}{\sqrt{T}} e^{j2\pi n \Delta f t}, & t \in [0, T] \\ 0, & t \notin [0, T] \end{cases} \tag{2}$$

where $S_{k,n}$ is the symbol transmitted in time slot k and sub-channel n, N is the number of FDM sub-channels, T is the FDM symbol duration and Δf is the subcarrier frequency separation.

For simplicity, we consider transmission over an Additive White Gaussian Noise (AWGN) channel. Consequently, the received signal $r(t)$ is given by

$$r(t) = s(t) + n(t) \tag{3}$$

where $n(t)$ represents the noise process.

The receiver performs two operations, demodulation and detection. The demodulator computes a vector of sufficient statistics by projecting the received signal onto an orthonormal basis generated using the Classical Gram Schmidt (CGS) procedure as follows

$$b_n(t) = \frac{1}{\sqrt{\xi_n}} \left[g_n(t) - \sum_{i=0}^{n-1} \int_{-\infty}^{\infty} g_n(t) b_i^*(t) dt b_i(t) \right], \quad n=0,\ldots,N-1 \tag{4}$$

 Published by Cranfield University Press ISBN: 978-0-9557436-7-2 http://hdl.handle.net/1826/3832

where $b_n(t)$ and $g_n(t)$ are the orthonormalised and the initial set of carriers respectively, N is the number of the carriers and ξ_n is a factor whose value is chosen so that the energy of $b_n(t)$ is 1.

The detector computes estimates of the information symbols based on the set of sufficient statistics. It is important to note that the output of the demodulator (correlators outputs) contains intercarrier interference so that it is not possible to carry out detection for each subcarrier independently, as in OFDM. Thus, we will attempt to address the detection problem using alternative methods.

DETECTION TECHNIQUES

Optimum Detection - The Maximum Likelihood (ML) Criterion

ML detection is optimum in terms of error performance since it minimizes the probability of error or maximizes the probability of correct decision [4]. In particular, the maximum likelihood criterion symbol estimate is given by:

$$\hat{\boldsymbol{S}}_{ML} = \arg\max_{\boldsymbol{S}} \boldsymbol{P}(\boldsymbol{R}/\boldsymbol{S}) \tag{5}$$

where $\hat{\mathbf{S}}$ is the vector of transmit symbols estimate, $\mathbf{S}$ is the vector of transmit symbols, R is the vector of sufficient statistics, and $P(\mathbf{R}/\mathbf{S})$ is the likelihood function.

The drawback of ML detection relates to its computation cost that is exponential with the number of carriers N and the constellation cardinality M. In particular, it is necessary to evaluate the likelihood function M^N times to determine the maximizing solution.

A. Sub-Optimum Linear Detection

To address the complexity problem, we explore sub-optimum linear detection techniques. In terms of matrix representation the proposed linear model [5] can be represented as

$$\boldsymbol{R} = \boldsymbol{MS} + \boldsymbol{N} \tag{6}$$

where $\mathbf{R}$ is the statistics vector, $\mathbf{M}$ is the cross correlations matrix between the FDM carriers and the orthonormal basis, $\mathbf{S}$ is the vector of transmitted symbols, and $\mathbf{N}$ is a vector of N Gaussian variables with the zero mean and covariance matrix $\sigma^2\mathbf{I}_N$, where $\mathbf{I}_N$ is the NxN identity matrix.

Note that $\mathbf{M}$ is not an identity matrix as in the pure ODFM case. Thus, the $\mathbf{R}$ vector of sufficient statistics includes many Intercarrier Interference (ICI) products. To overcome ICI problem we explore different sub-optimum, in terms of BER, detection methods.

 Published by Cranfield University Press ISBN: 978-0-9557436-7-2 http://hdl.handle.net/1826/3832

ZERO FORCING - ZF

The ZF criterion aims to cancel the ICI components. The simplest way to achieve this is by forcing the **M** to the identity matrix by multiplying both sides of equation (6) with the inverse of matrix **M**. Consequently the ZF estimator will be given by

$$\hat{\boldsymbol{S}} = \boldsymbol{M}^{-1}\boldsymbol{R} = \boldsymbol{S} + \boldsymbol{M}^{-1}\boldsymbol{N} \tag{7}$$

It is apparent that while interference is eliminated the noise is amplified. Consequently, the error performance degradation depends on the matrix **M** properties. As the eigenvalues and consequently the determinant of **M** tend to zero with the increase in number of the subcarriers and/or the decrease in the subcarriers spacing, the noise distortion rapidly increases.

MINIMUM MEAN SQUARED ERROR - MMSE

The MMSE detection achieves a compromise between noise and ICI cancellation by minimizing the mean squared error (MSE) between the output of the MMSE matrix and the transmitted vector. The MMSE matrix $\mathbf{G}_{MMSE}$ is given by [6], [7]

$$\boldsymbol{G}_{MMSE} = (\boldsymbol{M}^{H}\boldsymbol{M} + \frac{1}{\boldsymbol{SNR}}\boldsymbol{I})^{-1}\boldsymbol{M}^{H} \tag{8}$$

where **M** is the cross correlation matrix between the FDM carriers and the orthonormal basis, **I** is the *N*x*N* identity matrix, and *SNR* is the Signal to Noise Ratio.

Consequently, the estimate of the transmitted symbol is given by

$$\hat{\boldsymbol{S}} = (\boldsymbol{M}^{H}\boldsymbol{M} + \sigma^{2}\boldsymbol{I})^{-1}\boldsymbol{M}^{H}\boldsymbol{R} \tag{9}$$

NUMERICAL RESULTS

In Figures 2 and 3 we evaluate the error performance of the various schemes versus the carriers spacing as a fraction of the inverse of the FDM symbol (dFT). Simulations are performed for a fixed Energy per Bit to Noise Power Density Ratio (Eb/No) of 5 dB, for BPSK and QPSK modulation. It is important to emphasize that we simulate a limited number of carriers to be able to compare to the ML detection.

 Published by Cranfield University Press ISBN: 978-0-9557436-7-2 http://hdl.handle.net/1826/3832

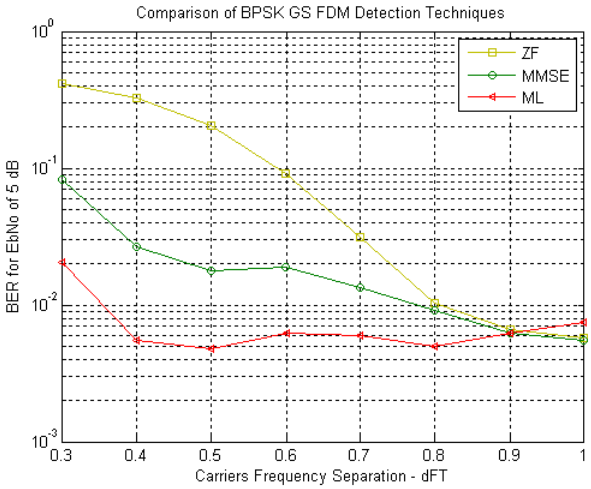

Figure 2: BPSK BER Vs Carriers Distance

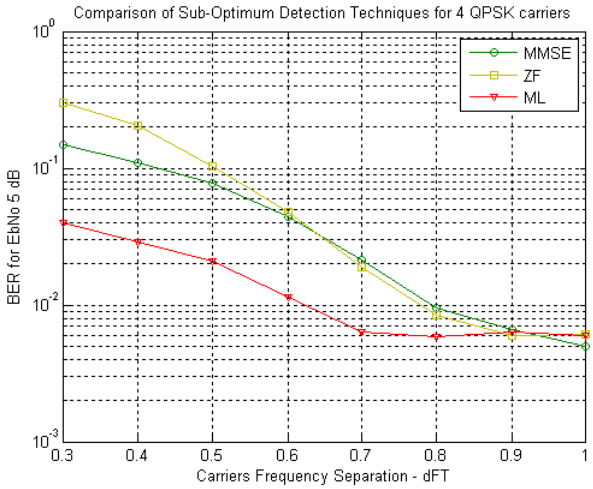

Figure 3: QPSK BER Vs Carriers Distance

It is clear that in terms of Bit Error Rate (BER), ML prevails and neither ZF nor MMSE provides an efficient way of detection. In Figure 4, we compare ZF and MMSE error performance for Eb/No=0 to 7 dB. We conclude again that both schemes introduce a large error penalty that grows as either the number of subcarriers or the constellation size increases. However, the MMSE estimation performs much better than ZF since it does not cause any noise multiplication.

Finally, in Figure 5 we compare both schemes in terms of computational complexity for N=2, 4, 8 and 16 FDM BPSK or QPSK modulated carriers. It is apparent that both techniques offer a polynomial complexity, $O(N^3)$, which is their main advantage with regard to the exponential complexity of ML, $O(M^N)$.

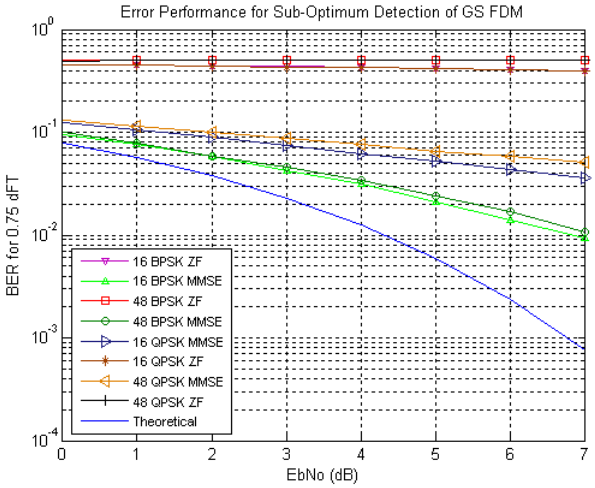

Figure 4: ZF and MMSE BER vs EbNo

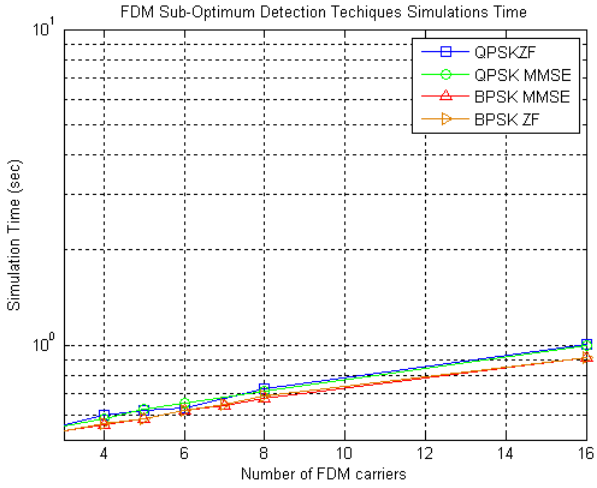

Figure 5: Sub-Optimum Detection Simulation Times

CONCLUSIONS AND FUTURE WORK

In this paper, we investigated the possibility of reliable sub-optimum detection for a non orthogonal FDM system. In particular, we examined ZF and MMSE detection in terms of error performance as well as of

 Published by Cranfield University Press ISBN: 978-0-9557436-7-2 http://hdl.handle.net/1826/3832

computational complexity. Despite their polynomial complexity, ZF and MMSE cannot provide us with a reliable solution because of their poor error performance.

Motivated by relevant studies in the MIMO area, future work will consider alternatives such as either the combination of ML with ZF and MMSE [8], [9], [10] or linear programming techniques like the very promising Sphere Decoding (SD) [11].

REFERENCES

[1] M. R. D. Rodrigues and I.Darwazeh, “Fast OFDM: A proposal for Doubling the Data Rate of OFDM Schemes”, in Proceedings of the International Conference on Telecommunications, Beijing, China, June 2002, pp. 484-487.

[2] X. Fuqin and X. Fuqin, “M-ary amplitude shift keying OFDM system M-ary amplitude shift keying OFDM system”, *IEEE Transactions on Communications*, vol. 51, no. 10, pp. 1638-1642, 2003.

[3] M.R.D.Rodrigues and I.Darwazeh, "A spectrally efficient frequency division multiplexing based communications system," in 8th International OFDM Workshop, Hamburg, Germany, Sept. 2003, pp. 70-74.

[4] John G.Proakis, *Digital Communications 4th Edition*. McGraw-Hill, 2001.

[5] Louis L.Scharf, *Statistical Signal Processing.* Addison-Wesley Series, 1991.

[6] W. Tiejun, J. G. Proakis, and J. R. Zeidler, “Techniques for suppression of intercarrier interference in OFDM systems”, *in IEEE Communications Society / WCNC 2005, 2005*.

[7] V.K.R. Bohnke, D. Wubben, V. Kuhn, and K. D. Kammeyer, “Reduced complexity MMSE detection for BLAST architectures”, *in GLOBECOM ‘03 IEEE*, San Francisco, USA, Dec. 2003, pp. 2258-2262.

[8] A.J. Paulraj, D.A. Gore, R.U. Nabar, and H. Bolcskei, "An overview of MIMO communications - a key to gigabit wireless," *Proceedings of the IEEE*, vol. 92, no. 2, pp. 198-218, 2004.

[9] V. Pammer, Y. Delignon, W. Sawaya, and D. Boulinguez, “A low complexity suboptimal MIMO receiver: the combined ZF-MLD algorithm”, *14th IEEE Proceedings on Personal, Indoor and Mobile Radio Communications*, 2003, PIMRC 2003, vol.3, pp. 2271-2275, 2003.

[10] Y. X. a. X. Y. Fan Wang, “Approximate ML Detection Based on MMSE for MIMO Systems”*, PIERS online,* vol. 3, no. 4, pp. 475-480, 2007.

[11] E. Viterbo and J. Boutros, “A universal lattice code decoder for fading channels”, *IEEE Transactions on Information Theory*, vol. 45, no. 5, pp. 1639-1642, 1999.

 Published by Cranfield University Press ISBN: 978-0-9557436-7-2 http://hdl.handle.net/1826/3832

Methodological approach to identifying the properties of a novel organomineral fertiliser - Part II: environmental aspects and OMF application

Antille, D.L.; Sakrabani, R., and Godwin, R.J.

School of Applied Sciences, Cranfield University, Bedfordshire, MK43 0AL, UK. E-mail of

corresponding author: d.l.antille.s05@cranfield.ac.uk (Diogenes L. Antille)

SUMMARY

This paper summarises the methodology used in this investigation to determine the potential environmental impact arising from the use of organomineral fertilisers (OMFs) in agricultural land by focusing upon two main subjects: NO3-leaching and N2O-emissions. In addition, the paper describes the method that will be used for the evaluation of spreading fertiliser equipment. It highlights the importance of achieving a high degree of uniformity when applying biosolids to agricultural land as one of the main factors controlling the agronomic efficiency of applied nutrients. Although experimental data are not available yet, the experiments are under construction, and it is the aim of this paper to gain criticism on the proposed methodological approach. Experimental data will be statistically analysed using analysis of variance and least significant differences to compare means.

Key words: nitrogen leaching, nitrous oxide emission, fertiliser spreading

INTRODUCTION

The application of sewage-sludge to agricultural land is a highly regulated activity (Evans, 1998). It is governed by the EU Sewage Sludge Directive 86/278/EEC which is enforced in the UK through the Sludge (Use in Agriculture) Regulations 1989. These are complemented by a number of regulations such as The Code of Practice for Agricultural Use of Sewage Sludge and the Safe Sludge Matrix among others. The position of the UK Government towards recycling has been clearly indicated. In this respect, the Government has committed to reduce the amount of waste landfilled to 75% of that produced in 1995 by 2010, and to cutback CO_2 emissions by 20% in 2010 (Defra, 2007); thereby, imposing increasing restrictions to disposal through incineration.

Although the fertiliser value of sewage-sludge have been acknowledged (Milne and Cleveland, 1972); in practice, many farmers appear to be reluctant to applying biosolids to agricultural land. This is often due to the impracticality of having to deal with large volumes of materials to meet the nutrients' requirements of crops. The use of cakes in recent years addressed, to certain extent, some of the problems associated with liquid sludges; e.g. cost of transport and application.

 Published by Cranfield University Press ISBN: 978-0-9557436-7-2 http://hdl.handle.net/1826/3832

However, the problem of delivering the desired application rates and achieving acceptable levels of uniformity across the working width of spreading fertiliser equipment, for instance, similar to those of mineral fertilisers applied with standard fertiliser spreaders, remains unsolved. This is aggravated by the fact that physical properties; e.g. particle size and composition of individual particles are not consistent. Uneven nutrient distribution can increase the risk of N-losses; e.g. nitrate leaching and gaseous losses, in areas where N is applied in excess of crop demand. The development of OMFs would contribute to address these issues by providing a product which has more consistent physical characteristics and known chemical composition (Antille *et al.,* 2008).

The aim of this work is to describe the methodology that will be used to quantify the losses of N from the formulated OMFs through both nitrate (NO3) leaching and denitrification via nitrous oxide (N2O). In addition, the paper explains how the OMFs' physical properties will be assessed in relation to the distribution pattern during application and the spreading equipment.

METHODOLOGY

OMFs' physical properties

There are a number of properties that control both the motion of individual particles and the resultant spread pattern. Hofstee (1993) indicated that the most important properties are: ***a.*** particle size and particle size distribution; ***b.*** coefficient of friction; ***c.*** aerodynamic resistance; ***d.*** coefficient of restitution; and ***e.*** particle strength. From these, ***a, b,*** and ***c,*** have the greatest influence on the spreading pattern (Hofstee, 1993). In addition, particle strength can alter the particle size distribution and affects the spreading pattern if segregation takes place (Bradley and Farnish, 2005).

Preliminary findings have shown that the formulated OMFs have a bulk density of 0.5 8-060 t m^{-3}; this value is approximately 10% higher than that of digested cake. It appears that the blending process, during the OMF production, results in increased bulk density of the final product compared to the cake. The measured bulk density of granules of urea fertiliser gave an approximate value of 0.78 t m^{-3}.

The particle size distribution was determined by sieving a sample of OMF and then weighting the sieved material; this was done for a number of sieves sizes ranging from < 1 mm to> 5.6 mm in diameter (Figure 1).

 Published by Cranfield University Press ISBN: 978-0-9557436-7-2 http://hdl.handle.net/1826/3832

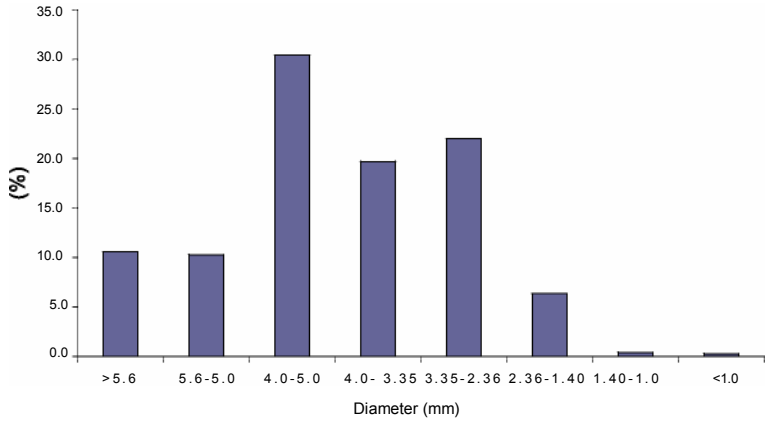

Figure 1: OMFs' particle size distribution.

The same was done for urea which gave, as expected, a much uniform particle size distribution with more than 92% of the particles in the range of 2 to 4 mm in diameter. Given that just over 40% of OMF particles fell into the desired size; i.e. 2-4 mm, a decision was made to discard all OMF particles outside this range in order to obtain a similar particle size distribution as urea. This approach means more processing during the OMF production but will ensure more uniformity in the final product (**Figure 2).**

Figure 2: OMF particles [100% between 2 and 4 mm in diameter].

This work is concerned with the optimisation of the particle shape, size, and size distribution, as these parameters can be easily adjusted during the OMF production. These properties will be then assessed by means of a spreading trial in the field. Details of this trial are given in the following section. In addition, it would be an advantage to measure the OMF breaking force to determine the relationship between the OMF particle strength and particle size. This relationship would provide a valuable indication on whether the OMF becomes stronger or weaker as the particle size is increased. Various strength measuring techniques are described by Hoffmeister (1979) and Rutland (1986).

 Published by Cranfield University Press ISBN: 978-0-9557436-7-2 http://hdl.handle.net/1826/3832

OMF APPLICATION

The most widespread methodology for measuring distribution uniformity and calibrating granular broadcast fertiliser spreaders is given by ASAE (1999) S341.2. The advantage of this method is that it allows to determine the performance of fertiliser spreaders when used for the application of granular fertilisers, and to compare different distribution patterns. The test consists of two parts: 1. determination of application rate, and 2. determination of distribution pattern. The rate is determined by measuring the amount of material applied divided by the area. The spread pattern indicates the degree of uniformity of distribution of fertiliser across the working width. This is determined by collecting and weighting fertiliser particles captured in trays placed across the swath being spread. The OMF products have been formulated for application rates of 1.2-1.4 t ha^{-1}; thus, the spreading equipment; i.e. Bredal K105 and Amazon ZA-M, will be first adjusted to deliver the desired rates and then the distribution pattern will be determined. Comparisons will be made with a standard fertiliser; e.g. urea. This test will provide valuable information regarding the spreading behaviour of this material, its interaction with standard spreading equipment, and the need for improving the OMF's physical properties.

NITROGEN LEACHING

Losses of applied OMF-N will be determined using lysimeters which were recently constructed at Silsoe Farm (Figure 3). Quantifying N-losses is important to anticipate the potential environmental risk associated with the use of OMFs. The design of the lysimeters is shown in Figure 4.

The experiment comprises the use of a sandy loam soil, OMF_{15}, urea, and a combination of urea and $_{OMF15}$ used as fertilisers materials which will be applied at only one rate of 240 kg N ha^{-1}, and a control with no fertiliser added, and two crops; i.e. spring wheat and grass. This design gives a total of 24 lysimeters. Each treatment will be replicated three times to facilitate the statistical analysis.

Figure 3: Overview of lysimeters' facility at Silsoe Farm.

 Published by Cranfield University Press ISBN: 978-0-9557436-7-2 http://hdl.handle.net/1826/3832

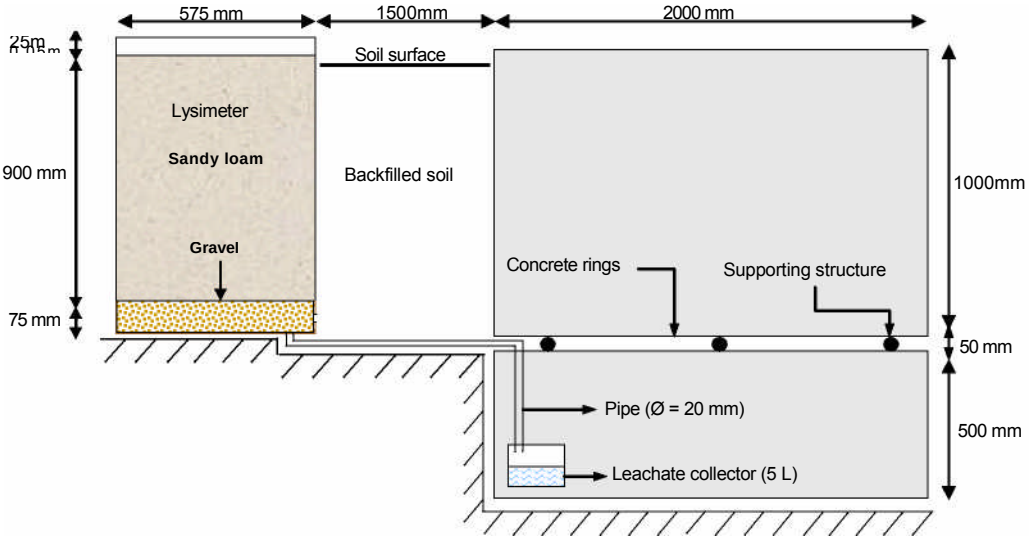

Figure 4: Diagram illustrating the lysimeters' design (side elevation).

Leachate will be regularly collected for determination of NO3. In addition, soil available-N will be determined before fertiliser application and at the end of the growing season to aid establishing a nitrogen balance in the soil. This information will be linked to measurements of N2O-emission which are explained in the following section.

NITROUS OXIDE EMISSIONS

Nitrous oxide is a greenhouse gas for which inventories of emissions are needed to comply with the Kyoto Protocol 1997 (Smith and Dobbie, 2001). At present, there is limited amount of information available on N2O-emissions after sewage-sludge application to agricultural land (Le, 2008). There is also no evidence of research being undertaken to determine N2O-emisions after OMF application. The purpose of this experiment is to quantify N2O-emissions following OMF application on spring wheat and grassland. Measurements will be taken for a period of 12 months to account for temporal variability. In this experiment, an automated closed-chamber developed by Smith and Dobbie (2001) will be used. The chambers will be placed on top of the lysimeters to facilitate the linking of these data to that of leaching. Samples will be collected for gas chromatographic analysis at ADAS-Boxworth. Full details of the chambers are given in Smith and Dobbie (2001).

CONCLUSIONS

The development of OMFs will contribute to address some of the issues related to the application of sewage-sludge to agricultural land. Improving the physical characteristics of the product is crucial to delivering the desired application rates.

 Published by Cranfield University Press ISBN: 978-0-9557436-7-2 http://hdl.handle.net/1826/3832

This is important to optimise the return from the use of fertilisers and reduce nutrient losses. Quantification of N-losses is important to develop appropriate fertiliser application strategies, protect the environment, and ultimately, improve the agronomic efficiency of applied nutrients.

ACKNOWLEDGEMENTS

The authors would like to thank the sponsoring company, United Utilities plc, and the Engineering and Physical Sciences Research Council (EPSRC) for their financial assistance, Cranfield University staff for their help during the construction of the experiments, and Dr. Rachel Thorman (ADAS-Boxworth) and Mr. Anthony Dale (Dale Contractors) for many useful suggestions concerning this work.

REFERENCES

1. **Antille, D.L., Sakrabani, R., and Godwin, R.J., 2008.** Methodological approach to identifying the properties of a novel organomineral fertiliser – *Part I:agronomic aspects.* Cranfield Multi-Strand Conference: Creating wealth through research and innovation (CMC 2008). Cranfield University, MK43 0AL, UK. May 6th – 7th 2008.
2. **ASAE 1999; American Society of Agricultural Engineers, 1999.** Procedure for measuring distribution uniformity and calibrating granular broadcast spreaders. S341 .2. 46th Edition. St. Joseph, Mich. ASAE.
3. **Bradley, M.S.A., and Farnish, R.J., 2005.** Segregation of blended fertilisers during spreading: the effect of differences in ballistic properties. Proceeding no. 554 of The International Fertiliser Society (IFS), York, YO32 5YS, UK.
4. **Defra, 2007; Department for Environment, Food, and Rural Affairs, 2007.** Waste strategy 2007. Annex C6: sewage sludge. [Accessed: 11th August 2007].
5. http://www.defra.gov.uk/Environment///waste/strategy/strategy07/pdf/waste07-annex-c6.pdf
6. **Evans, T., 1998.** Agricultural use of biosolids (sewage sludge). Proceeding no. 409 of The International Fertiliser Society (IFS), York, YO32 5YS, UK.
7. **Hoffmeister, G., 1979.** Physical properties of fertilisers and methods for measuring them. Bulletin Y-147, Muscle Shoals, AL-Tennessee Valley Authority.
8. **Hofstee, J.W., 1993.** Physical properties of fertilisers in relation to handling and spreading. *PhD Thesis* Wageningen Agricultural University, The Netherlands.
9. **Milne, R.A., and Cleveland, D.N., 1972.** Sewage sludge as fertilizer. Canadian Journal of Soil Sciences 52: 270 –273.
10. **Smith, K.A., and Dobbie, K.E., 2001.** The impact of sampling frequency and sampling times on chamber-based measurements of N2O emissions from fertilised soils. G. Change Biol. 7: 933-45. **Le, M.S., 2008.** Comments on nitrous oxide emissions from sewage-sludge. Personal communication. United Utilities plc. Warrington, WA5 3LP, UK.
11. **Rutland, D.** Manual for determining physical properties of fertilisers. Reference manual IFDC-R6. Muscle Shoals, AL-International Fertiliser Development Centre.

 Published by Cranfield University Press ISBN: 978-0-9557436-7-2 http://hdl.handle.net/1826/3832

Positioning Technologies in Wireless Broadband Communications

A. Awang Md. Isa, G. Markarian
Department of Communication Systems,
Lancaster University
E-mail: {a.awangmdisa, g.markarian}@lancaster.ac.uk

ABSTRACT

This paper presents the potential of positioning technologies in wireless broadband communications, which are based on worldwide interoperability for microwave access (WiMAX), in particular the IEEE 802.16* standards.

INTRODUCTION

Knowing a user's location enables many new applications, often times called as location based services (LBS). One of the current key issues for LBS is the positioning technology in broadband communications. Most current positioning systems do not work where people spend much of their time, meaning that coverage in these systems is either constrained to outdoor environments or limited to a particular building or campus with installed location infrastructure. For an example, the most common positioning system, Global Positioning System (GPS) works worldwide, but it requires a clear view of its orbiting satellites. It does not work indoors and works poorly in many cities where the so called "urban canyons" formed by buildings prevent GPS receiver units from seeing enough satellites to get a position lock [1]. Purpose built systems such as Active Badge, cricket, The Bat etc., can be used in indoor environments [2]. However, for cost reasons, people prefer to use existing infrastructure such as mobile phone networks, and wireless LAN (WLAN).

Predictions regarding wireless broadband communications and wireless Internet services are cultivating visions of unlimited services and applications that will be available to the user "anywhere at anytime" [3]. Users expect to surf the Web, check e-mail, download files, have several multimedia applications, such as real-time audio and video streaming, multimedia conferencing, interactive gaming and perform a variety of other tasks through a wireless communication link. The user further expects a uniform user interface that will provide access to the wireless link whether shopping at the mall, waiting at the airport, walking around town, or even driving in the car. Current wireless infrastructures, however, as well as next-generation proposals cannot furnish the necessary bandwidth and capacity to provide these services to mobile users [4]. Unfortunately, mobile users will likely be the most demanding of bandwidth and wireless services. Clearly, a broadband wireless solution is needed to provide mobile users the high-bandwidth mobile service they demand at a low cost.

 Published by Cranfield University Press ISBN: 978-0-9557436-7-2 http://hdl.handle.net/1826/3832

Of these, WLAN (also known as 'Wi-Fi') that support wireless broadband communications can be implemented with the least effort, as its associated consumer hardware is the most readily available. However, Wi-Fi works in limited range and suitable only for fixed wireless broadband. Besides that, to ensure the success of delivering high bandwidth and less interference from Base station to users especially for mobile users, it depends on accurate positioning systems.

With the arrival in 2005 of WiMAX, this is all about to change. Mobile worldwide interoperability for microwave access (WiMAX) is a wireless standard to enable mobile broadband services at a vehicular speed of up to 120 km/h [5]. WiMAX complements the and competes with Wi-Fi and the third generation (3G) wireless standards on coverage and data rate. More specifically, WiMAX supports a much larger coverage area than WLAN, does not require line of sight for a connection, and is significantly less costly compared to the current 3G cellular standards. Although the WiMAX standard supports both fixed and mobile broadband data services, the latter have a much larger market. In addition, WiMAX brings additional features that can be used for enhancing location and positioning technologies, such as Multiple-Input Multiple-Output (MIMO), Adaptive Modulation and Coding (AMC) and Beamforming.

The remainder of this paper is organized as follows. Section 2 explains briefly an overview of WiMAX, section 3 discusses proposed techniques to enhance location and positioning in WiMAX. Finally section 4 concludes the paper.

AN OVERVIEW OF WiMAX

IEEE 802.16 defines the air interface specification for broadband wireless access systems supporting multimedia services, including the medium access control layer (MAC) and multiple physical layer (PHY) specifications. The WiMAX technology, defined as *Worldwide Interopera bility for Microwave Access,* is based on wireless transmission methods defined by the

 Published by Cranfield University Press ISBN: 978-0-9557436-7-2 http://hdl.handle.net/1826/3832

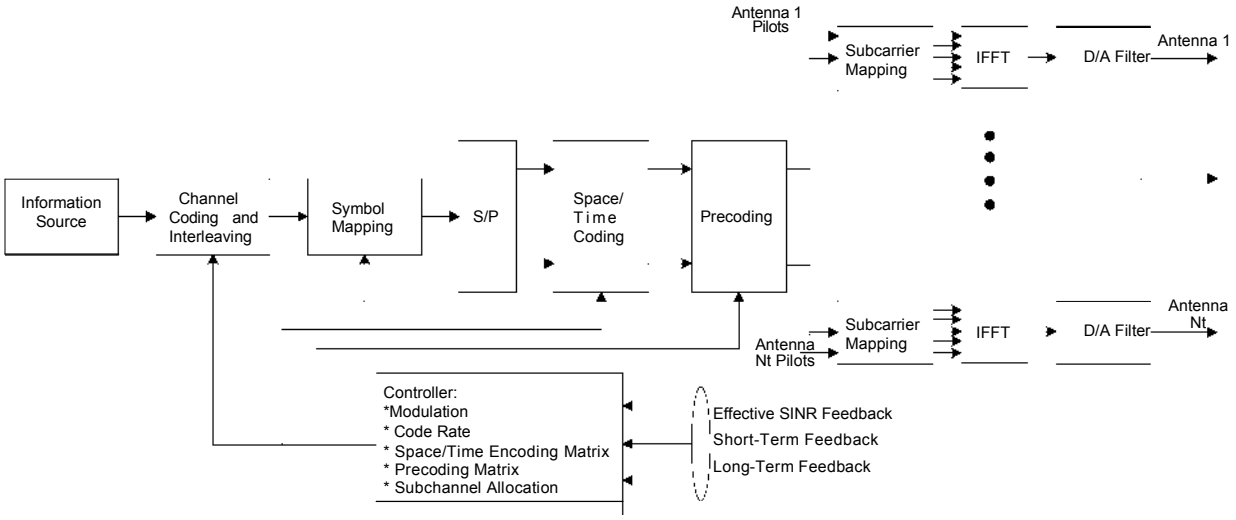

(a) Transmitter

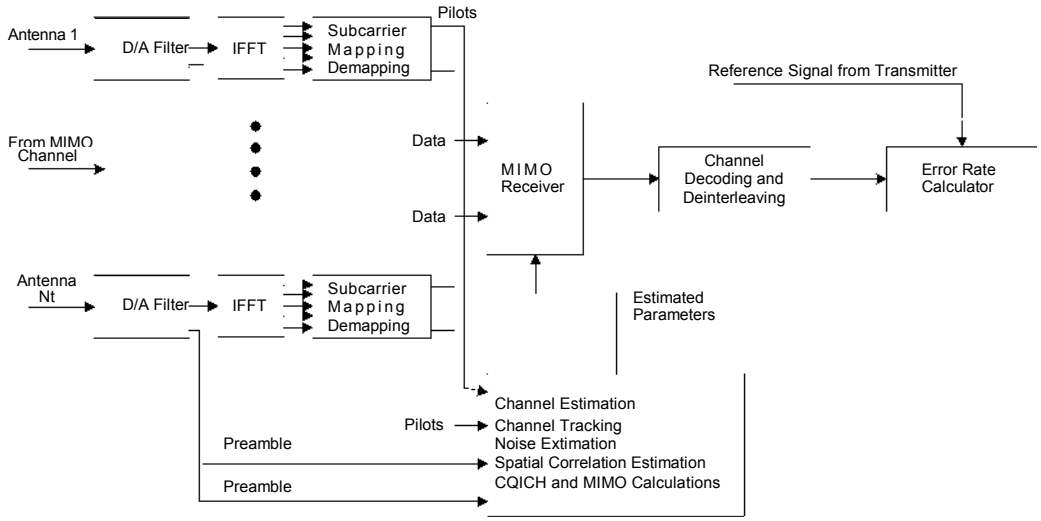

(b) Receiver

Figure 1 Block Diagram of WiMAX [6]

IEEE 802.16 standard. WiMAX aims to provide wireless data over long distances, in a variety of different ways, from point to point links to full mobile cellular type access. It offers an alternative to wired networks, such as coaxial systems using cable modems, fiber optics and digital subscriber line (DSL) links. The technology supports high data rates ranging from 30 Mbps to 155 Mbps depending on the distance from the base station and the underlying PHY layer. Typical range of WiMAX is about 30 miles. While the more familiar WiFi handles local areas, such as in offices or hotspots, WiMAX covers wider, metropolitan or rural areas. WiMAX technology ideally provide data rates up to 75 megabits per second (Mbps) per base station with

 Published by Cranfield University Press ISBN: 978-0-9557436-7-2 http://hdl.handle.net/1826/3832

typical cell sizes of 2 to 10 kilometers. This is enough bandwidth to simultaneously support (through a single base station) more than 60 businesses with T1/E1-type connectivity and hundreds of homes with DSL-type connectivity [5].

The basic block diagram of WiMAX as shown in figure 1 consists of a transmitter and receiver. The transmitter is responsible for all digital and analog domain processing of the signal before it sent over the wireless channel, meanwhile the receiver has two functions: to estimate the transmitter signal and to provide feedback that allows the transmitter to adapt the transmission format according to channel conditions. The details explanation of the block diagram can be found in [6].

PROPOSED WiMAX LOCATION AND POSITIONING

There are many approaches to determining a user's location – some of which are explained in [1, 2, 7-10], however, so far there is no development of location and positioning (L&P) technologies based on WiMAX. WiMAX brings additional features that can be used for enhancing location and positioning technologies including Multiple-Input Multiple-Output (MIMO), Adaptive Modulation and Coding (AMC) and Beamforming.

Based on concept of 'Trilateration' that are used in many existing L&P technologies, we proposed our idea to determine WiMAX user's location as illustrated in figure 2. According to figure 2, each WiMAX Base Station (BS) and mobile users are equipped with MIMO antenna that consist of multiple transmitters and receivers (multiple antennas) on both side eg, two transmit antenna on the BS and two receive antenna on the mobile user. In this case, two simultaneous signals can be transmitted from a WiMAX BS, and by applying trilateration method, at least six signals will be detected by mobile user from three BS. Therefore, we believe that MIMO will not only improve the capacity and the throughput of a wireless link significantly but it also can be used to enhance the accuracy of user's location. Furthermore, each MIMO BS will transmit the signals to the Network Management Systems (NMS). NMS can accurately monitor the network and it provides L&P services for updating the user's location.

Meanwhile, AMC allows WiMAX system to adjust the signal modulation scheme (64QAM, 16QAM, QPSK or BPSK) depending on the signal-to-noise (SNR) condition of the radio link. The idea behind the AMC is to dynamically adapt the modulation and coding scheme to the channel condition so as to achieve highest spectral efficiency at all times. However, this causes the signal level to be almost the same as at a BS coverage area, so that the signal level measurement cannot be used to estimate the location of mobile users. In addition, WiMAX use power control to adjust the signal quality based on SNR. As a result, the same scenario as above can be seen in the signal level. Nonetheless, by taking the information from both the physical layer (can know what type of modulation scheme is used and power control reading) and MAC layer at WiMAX BS, the data can be used to determine the mobile user's location.

 Published by Cranfield University Press ISBN: 978-0-9557436-7-2 http://hdl.handle.net/1826/3832

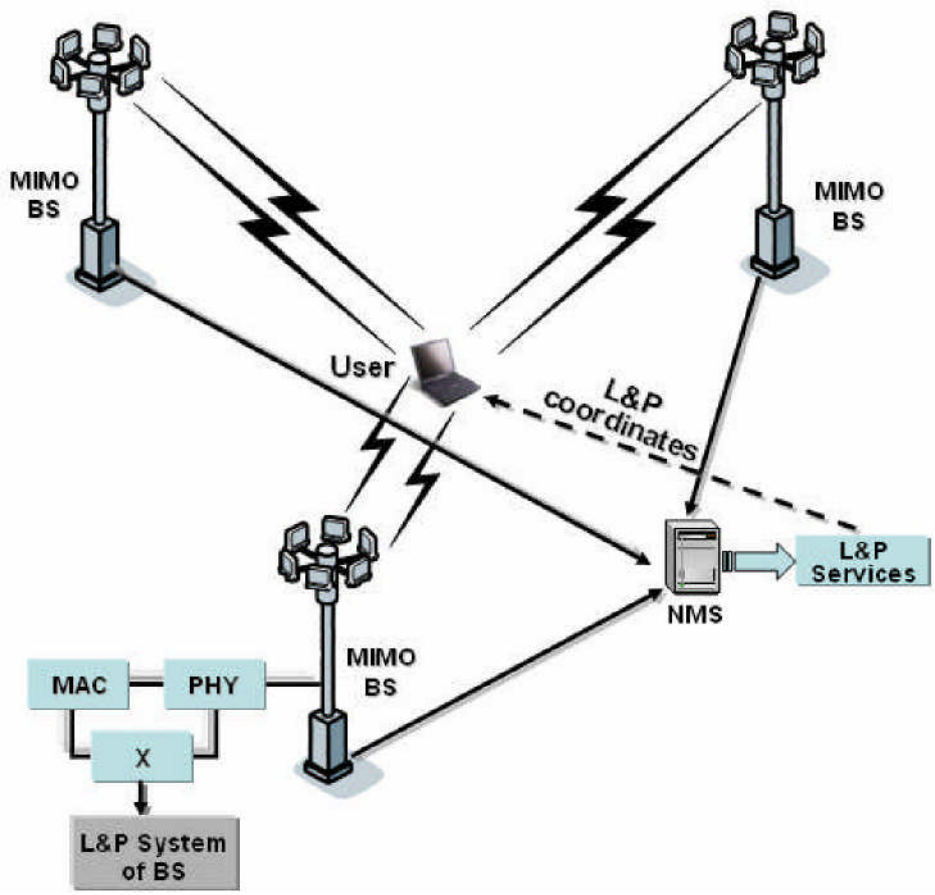

Figure 2 Proposed Location and Positioning Services in WiMAX

CONCLUSION

In this paper, we presented the potential of positioning technologies in wireless broadband communications, which are based on worldwide interoperability for microwave access (WiMAX), in particular the IEEE 802.16* standards. Depending on the required accuracy and network topology, different positioning methods such as triangulation, round trip delay, Cell ID etc can be foreseen for WiMAX. We proposed Location and positioning technologies for WiMAX based on trilateration concept by taking into consideration the additional features of WiMAX so it can enhance the accuracy of user's location. We will perform the simulation and hope to be able to deliver the results in a near future.

ACKNOWLEDGEMENT

The authors wish to thank the Government of Malaysia for the sponsorship.

REFERENCES

1. Fredrik Brännström, "Positioning techniques alternative to GPS", Master thesis, Lulea University of Technology, 2002

 Published by Cranfield University Press ISBN: 978-0-9557436-7-2 http://hdl.handle.net/1826/3832

2. Hightower, J., & Borriello, G., "Location systems for ubiquitous computing", *IEEE Computer,* August 2001, 34, (8), pp. 57-66
3. Charles D. Gavrilovich, Jr., Gray Cary Ware & Freidenrich LLP, "Broadband Communication on the Highways of Tomorrow", IEEE Communications Magazine, April 2001, pp 146-154
4. L. M. Correia and R. Prasad, "An Overview of Wireless Broadband Communications", IEEE Communications Magazine, Jan., 1997, pp. 28–33.
5. http://www.jahanzeb.com/wimax-ns3.asp, accessed on 25 January 2008
6. Jefry G.Andrews, Arunabha Ghosh and Rias Muhamed, Fundamental of WiMAX: Understanding Broadband Wireless Networking, Prentice Hall, 2007
7. Renato Filjar and Darko Huljenic, "Positioning augmentation using synergy between telecommunications networks and satellite positioning methods", 17th International Conference on Applied Electromagnetics and Communications, 2003
8. Kyounggyu Lee, Yongwoo Lee, "A LBS for Cellular Phones", 2007 International Conference on Convergence Information Technology", IEEE, 2007, pp. 222-228
9. Volker Schwieger, "Positioning within the GSM Network", 6th FIG Regional Conference, San José, Costa Rica 12-15 November 2007
10. Paul Kemppi, Database Correlation Method for Multi-System Location, Master's thesis, Helsinki University of Technology, 2005

 Published by Cranfield University Press ISBN: 978-0-9557436-7-2 http://hdl.handle.net/1826/3832

All-optical processing for future optical communication networks

M. Drummond[1], R. Nogueira[1], P. Monteiro[1,2]

[1]Instituto de Telecomunicações, Universidade de Aveiro, 3810-193 Aveiro, Portugal (mvd@av.it.pt)

[2]Nokia Siemens Networks Portugal, S.A., RTP NT NAB Photonic Networks SP, 2720-093 Amadora Portugal

ABSTRACT

All-optical processing is presented as a cost-effective solution to enhance the performance and increase the capacity of optical communication networks. The impairments of optical communication systems and their mitigation through some all-optical monitoring and compensation techniques are discussed.

INTRODUCTION

Today's optical networks are fairly static and operate within well-defined specifications. The addition of new nodes or the upgrade of existing links demands an enormous expenditure. A cost-effective implementation of future optical networks should accommodate old static networks, as well as new highly-efficient networks. Future optical networks should be intelligent, self-managed, monitored and dynamically-reconfigurable and should be able to accept new nodes in a plug-and-play manner [1].

All-optical processing devices are a cost-effective solution for the implementation of future optical networks. Such devices allow surpassing some of the limitations inherent to electric devices by keeping the signal in the optical domain, avoiding electrical-optical-electrical (OEO) conversions. In order to enable the reconfigurability of the network, all-optical devices should be transparent to modulation format, bit rate, protocol, as well as other requirements. The research on such devices is focused on different topics, such as all-optical routing [2], monitoring [3], impairment compensation [4] and error correction [5]. In this paper, only all-optical monitoring and impairment compensation techniques are discussed.

 Published by Cranfield University Press ISBN: 978-0-9557436-7-2 http://hdl.handle.net/1826/3832

IMPAIRMENTS

The transmission of an optical data signal is subjected to various impairments such as chromatic dispersion (CD), polarization mode dispersion (PMD), noise, interchannel crosstalk and fiber nonlinearities.

CD arises from the dependence of the group velocity with frequency [6]. As the frequency components of the signal's spectrum have different group delays, pulse shape distortion occurs (Fig. 1(a)). CD results in pulse spreading, causing intersymbol interference (IS I). PMD is caused by assymetries in the fiber core that induce a small amount of birefringence that randomly varies along the length of the fiber. The birefringence causes the power in each pulse to be split in two polarization modes that travel at different speed, creating a differential group delay (DGD) between the two modes that also results in pulse spreading and ISI (Fig. 1(b)) [7]. The amplification of optical signals in the network adds noise originated from amplified spontaneous emission (ASE), reducing the optical signal-to-noise ratio (OSNR) [6]. (Fig. 1(c)).

These three impairments have been widely discussed for many years and consist a serious limitations to the network robustness and scalability, specially for highly-efficient optical systems. Moreover, increasing the bit rate of a single channel as well as the channel count results in reduced impairment tolerance. As an example, a four-fold increase on the bit rate diminishes the dispersion tolerance by a factor of about sixteen. Hence, the research on all-optical impairment monitoring and compensation techniques is a key to enable future reconfigurable optical networks.

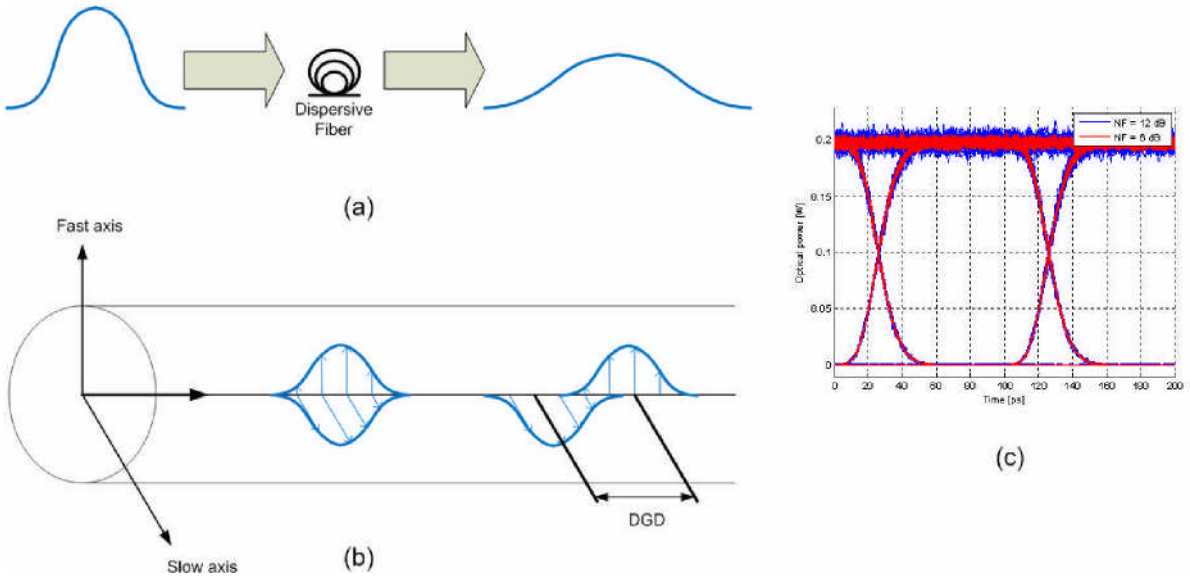

Fig. 1: (a) Pulse broadening induced by CD; (b) Effect of PMD; (c) Noise effect on the eye diagram from the signal considering an amplification with the same gain and different noise figures (NF). DGD – differential group delay.

 Published by Cranfield University Press ISBN: 978-0-9557436-7-2 http://hdl.handle.net/1826/3832

ALL-OPTICAL IMPAIRMENT MONITORING AND COMPENSATION

Many current optical networks rely on SDH/SONET network architectures. On those networks, monitoring is reduced to fault management and bit error rate (BER) measurements, with electrical signal processing only. Impairment compensation is taken into account mainly on early stages of the system design, according to static techniques. As future optical networks are dynamic and present more stringent requirements on the impairments tolerance, this approach is no longer valid: impairment monitoring and compensation techniques should be also dynamic.

Two dynamic monitoring and compensation approaches are presented in Fig. 2 [7]. The feedback approach continuously monitors and compensates a given impairment. This scheme is adequate for impairments that change slowly. If we consider dynamic networks (e.g. packet switching networks) and/or fast evolving impairments (e.g. PMD) a feed-forward mechanism should be considered. Techniques based on this scheme compensate the impairment without dithering. For any of the presented schemes, the compensation device must be dynamic.

All-optical impairment compensation techniques are based on different devices, such as fiber Bragg gratings (FBGs), highly nonlinear fiber and semiconductor optical amplifiers (SOAs). A FBG is a well-established passive device that allows performing dynamic CD or PMD compensation [4, 8]. Chirped FBGs reflect different spectral components of the pulse at specific positions. If the delay applied to the different spectral components of the pulse is the opposite of the delay induced by CD, compensation is achieved. By applying a temperature gradient or a

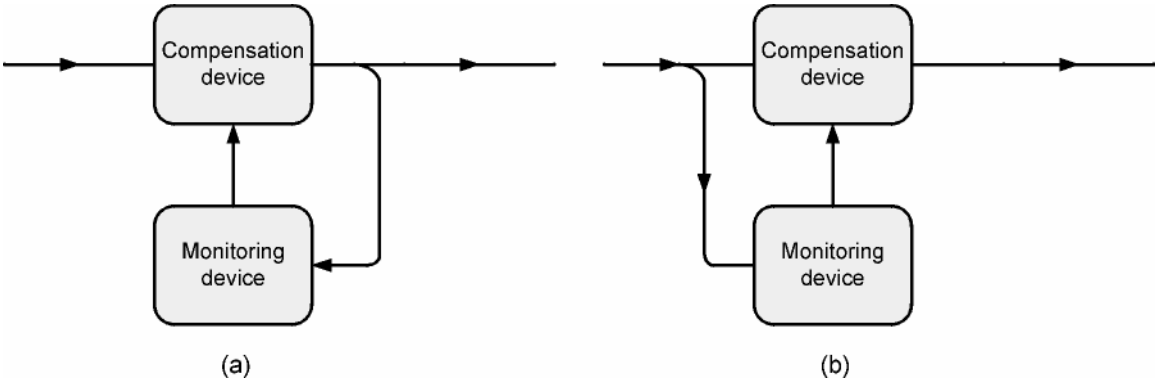

Fig. 2: Impairment monitoring and compensation schemes; (a) feedback; (b) feed-forward.

 Published by Cranfield University Press ISBN: 978-0-9557436-7-2 http://hdl.handle.net/1826/3832

mechanical strain, the original FBG chirp is altered and different CD values can be compensated. PMD compensation is achieved by using FBGs written in highly birefringent (HiBi) fibers. As both polarizations have different group delays, a differential group delay is obtained.

Many all-optical impairment monitoring techniques have been recently studied. Nonlinear active optical devices such as SOAs are an example [3]. The nonlinear response of these devices to the pulse shape and peak power results in spectral distortion. As CD induces pulse broadening, it may be monitored by measuring the power of the filtered SOA output signal.

CONCLUSIONS

All-optical processing devices were presented as a key enabler for the development of future optical networks. Such devices enable reconfigurability and transparency, needed to interconnect new and old optical networks in a cost-effective manner. All-optical impairment monitoring and compensation techniques were presented as a viable way to improve the robustness and scalability of optical networks.

Acknowledgments: The authors gratefully acknowledge support from Fundação para a Ciência e a Tecnologia through project THRONE (PTDC/EEA-TEL/66840/2006) and (SFRH/BD/40250/2007) scholarship.

REFERENCES

1. E. Willner, "Self-managing intelligent optical networks for smarter, tougher, and cheaper systems," *SPIE Newsroom,* 2006.
2. H. J. S. Dorren, M. T. Hill, Y. Liu, N. A. C. N. Calabretta, A. A. S. A. Srivatsa, F. M. A. H. F. M. Huijskens, H. A. d. W. H. de Waardt, and G. D. A. K. G. D. Khoe, "Optical packet switching and buffering by using all-optical signal processing methods," *Lightwave Technology, Journal of,* vol. 21, pp. 2-12, 2003.
3. P. Vorreau, D. C. Kilper, and J. Leuthold, "Optical noise and dispersion monitoring with SOA-based optical 2R regenerator," *Photonics Technology Letters, IEEE,* vol. 17, pp. 244-246, 2005.
4. R. Nogueira, A. Teixeira, M. Violas, R. A. S. R. Sousa, P. A. A. P. Andre, T. A. S. T. Silveira, R. A. O. R. Olcina, and S. A. S. S. Sales, "Tuneable Optical Dispersion Compensators for Dynamic Optical Networks," in *Transparent Optical Networks, 2007. ICTON '07. 9th International Conference on,* 2007, pp. 315-318.
5. M. Nielsen, M. Petersen, M. Nord, and B. A. D. B. Dagens, "Compact all-optical parity calculator based on a single all-active Mach Zehnder interferometer with all-SOA amplified feedback," in *Optical Fiber Communications Conference, 2003. OFC 2003*,2003, pp. 274-275 vol.1.
6. G. P. Agrawal, *Fiber-Optic Communication Systems,* Third ed.: Wiley-Interscience, 2002.
7. E. Willner, S. M. R. M. Nezam, L. Yan, P. Zhongqi, and M. C. Hauer, "Monitoring and control of polarization-related impairments in optical fiber systems," *Lightwave Technology, Journal of,* vol. 22, pp. 106- 125, 2004.
8. Teixeira, R. Nogueira, P. Andre, M. A. L. M. Lima, J. A. P. J. Pinto, and J. A. d. R. J. da Rocha, "Applications of highly birefringent fibre Bragg gratings," in *Transparent Optical Networks, 2004. Proceedings of2004 6th International Conference on,* 2004, pp. 69-72 vol.2.

 Published by Cranfield University Press ISBN: 978-0-9557436-7-2 http://hdl.handle.net/1826/3832

A Web-based CAD System for Gear Shaper Cutters

Anna Malahova, Jevgenijs Butans, Ashutosh Tiwari
Cranfield University
Cranfield, Bedfordshire, MK43 0AL, UK
{ a. malahova, eugene. but an, a.tiwari} @cranfield.ac.uk

ABSTRACT

This paper describes a concept of a novel web-based CAD software for gear shaper cutters, including its core implementation aspects. One of the main issues in the development of a web-based CAD system is the need to process and, subsequently, visualise a lot of technical product drawings and sketches. Conventional web-oriented design systems are either integrated with specialised CAD software for processing technical drawings or use dedicated graphics visualisation tools. The proposed web-based CAD software tool for gear shaper cutters relies on technologies supported by regular web browser programs with no need for additional client software and is based on the freely available components and standards.

INTRODUCTION

Computer-aided design (CAD) is essential for gear shaper cutters as it allows rapid production of tool designs with an added benefit of increased tool geometry precision. Historically, CAD solutions have been implemented as traditional desktop applications. And indeed, industry-leading CAD packages such as AutoCAD, Pro Engineer and SolidEdge are desktop applications.

In the recent years the industry movement to the Web became a trend. The reason lies both in obvious advantages of the Web technologies and readiness of the web to handle interactive applications with complex business logic [1, 2, 3].

A typical web-based system employs client-served paradigm for highly distributed implementation. Multiple clients running in the web browser on the client side share one common server program. Due to centralised configuration, data source and service management web systems are more manageable and reliable in comparison with stand- alone software. Scalability, portability and stability of web systems makes them highly attractive for software developers and end-users.

Moreover, development, deployment and maintenance of web-based solutions usually turns out cheaper than desktop systems. Cross-platform compatibility and performance of web applications could be ensured without deep knowledge of different operation systems and software packages.

 Published by Cranfield University Press ISBN: 978-0-9557436-7-2 http://hdl.handle.net/1826/3832

RELATED WORK

Advances in web technologies enabled development of various networked CAD systems over recent years. These could be classified depending on the implemented technologies as follows.

- Distributed CAD systems. A typical example is CAD system proposed by Denis et al. [4], based on modular architecture communicating with message exchanges, providing a general architecture for all trade CAD applications.

- Web-based systems integrated with proprietary CAD tools. For example, CyberCut [5] is developed using Java CAD tool WebCAD. Stand-alone CADET - a Knowledge-Based System for product design evaluation was reimplemented as Web-CADET [6]. Networking CAD system for electrical machine combines CAD of electrical machines, FEA software ANSYS, ActiveX, Active Server Pages (ASP) and HTML together [7]. Ahn et al. developed a Web-based user interface for CAD systems for automobile components [8].

- Pure Web-based CAD systems. These systems can be further subdivided into two principal classes. Systems that use special environments or viewers for design visualisation are implemented using either Java technologies (such as JRE - Java run-time environment [9]) [10], X3D or virtual reality modeling language (VRML) [11, 12, 13, 14, 12, 15]. This approach has known limitations, when client bound to use certain software to enable full functionality. Systems that do not need any additional tools on client side, only a web browser are highly compatible because do not need additional software for design data visualisation.

RESEARCH GAP

The task of gear shaper cutter design could not be solved by off-the-shelf CAD package due to a highly parametrised design process that requires extensive computations and nature of the generating process.

Therefore, development of a computer-aided design system for gear shaper cutters is essential for the respective industry. Web-based solution for the new CAD system will be more future-proof than stand-alone implementation. As cutter, gear and basic rack profiles are defined in two dimensions, it is possible to make the software platform independent and based on the freely available components and standards.

WEB-BASED CAD SOFTWARE CONCEPT

The design of the gear shaper cutters is parametric and therefore does not require a lot of interactive graphical information. It is based on a set of textual inputs and a set of textual outputs accompanied by the drawings of the basic rack, cutter and gear profiles.

 Published by Cranfield University Press ISBN: 978-0-9557436-7-2 http://hdl.handle.net/1826/3832

The software was chosen to be web-based implementing client-server architecture. The main idea underlying that choice was the ability of the client portion of the software to work in any modern browser on any computing platform, be it an IA-32 PC running MS Windows or GNU/Linux or Macintosh running OS X or GNU/Linux.

ARCHITECTURAL STRATEGIES

The client portion of the software is based on the templates written in a specially created language and uses the Scalable Vector Graphics (SVG) format for the graphical data interchange and representation [16]. The interactive features of the user interface are supported by MochiKit [17] and ExtJS [18] JavaScript library that provides an abstraction layer from the browser-specific implementation of the JavaScript runtime. A desktop-like experience when using the software is implemented using the AJAX [19] technology that uses JSon as the data interchange format between the client and the server.

The server portion of the software is written using Python programming language and the TurboGears [20] programming framework. The framework helps to process Web requests and provides the authentication and deployment services. The PostgreSQL [21] database was chosen as the database back end for its reliability and speed. The top level architecture of the system is illustrated in the Figure 1.

USER INTERFACE

The user interface is developed to maximise CAD system usability and support designers with different level of technical knowledge in the relevant field. To ensure the displayed in-

 Published by Cranfield University Press ISBN: 978-0-9557436-7-2 http://hdl.handle.net/1826/3832

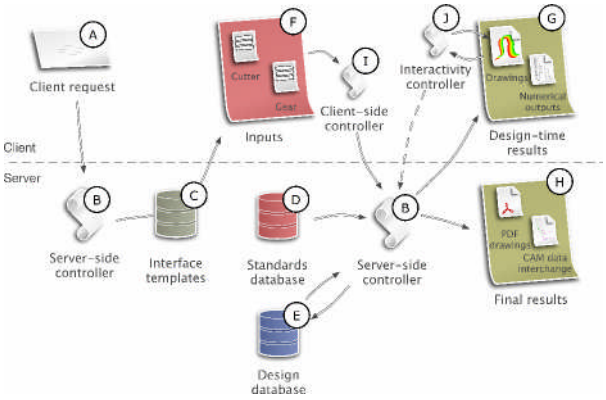

Figure 1: Architecture of Web-based CAD for gear shaper cutters.

formation can be effectively managed, the interface implements collapsible panels, therefore only minimum necessary amount of controls gets displayed each time.

COMPUTING ENGINE

As mentioned before, gear shaper cutters design is described through large number of parameters and requires extensive computations. Forward propagating inference engine has been implemented to ensure dynamic system's knowledge base gets expanded by new calculated results. The engine uses elements of artificial intelligence and includes unification procedure of current state and conditions and result evaluation procedure.

PARAMETRIC DESIGN VISUALISATION

The Web-based nature of the design software imposed a number of challenges for the design data visualisation. The most important challenge is to make the drawings immediately available to the user within the Web browser, without being forced to use supplementary programs. Considering the two widely used vector graphic formats: SVG or Flash, preference was given to SVG that despite being much less widespread, than Flash, has native support from major browsers and is a World Wide Web consortium Recommendation [16].

As the drawing should be able to be produced as the result of an automated process, and SVG excels in that being essentially an XML (eXtensible Markup Language) [22] subset, i.e., a human-readable text. An SVG file is a set of statements called tags that specify geometrical objects, their position, size and other attributes. The size and position

 Published by Cranfield University Press ISBN: 978-0-9557436-7-2 http://hdl.handle.net/1826/3832

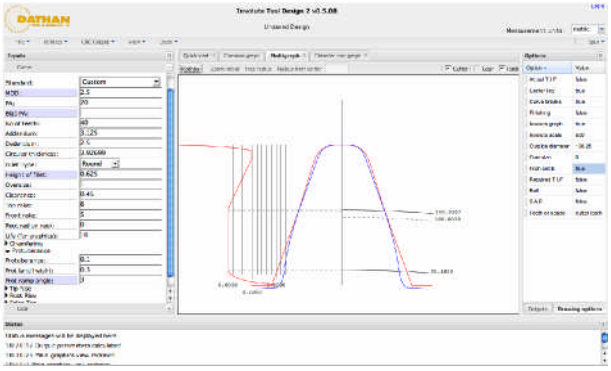

Figure 2: Modular user interface of Web-based CAD for gear shaper cutters.

are specified by means of attributes - text nodes with numerical values. Such text based formats are not only human readable, but also very easy to produce by a program.

Figure 2 demonstrates modular user interface of the new CAD system, that includes technical drawings, generated on the base of computed results and represented in SVG format.

DISCUSSION AND FUTURE WORK

In this paper Web-based CAD technology is presented, that includes server portion, implemented with Python programming language and TurboGears framework, client portion, implemented using MochiKit and ExtJS JavaScript libraries and PostgreSQL database for design data storage and retrieval. All drawings within the system are represented in two dimensions using SVG graphics format. The developed software platform is fully independent and based on the freely available components and standards. JavaScript libraries, used for client portion of the system, ensure cross-browser compatibility of the Web-based CAD system.

Pure Web-based CAD system could be very promising solution for many business areas. Even so, there are known challenges within this approach, including graphics visualisation in three dimensions, animation support in browsers and support of collaborative designing, that could be essential for CAD systems.

REFERENCES

1. Benefits of web-based applications and microsoft announcement of the "live" era - robin good's latest news, http://www.masternewmedia.org/web-based applications/web-based applications issues/benefits of web-based applications microsot announces live era 20051102.htm, (accessed: 10.03.2008).
2. M. Jazayeri, Some trends in web application development, Faculty of Informatics, University of Lugano (USI), Lugano, Switzerland, 2007, pp. 199–213.
3. Web applications: What are they? what of them?, http://www.acunetix.com/websitesecurity/web-applications.htm, (accessed: 10.03.2008).
4. L. Denis, Y. Gardan, E. Perrin, A framework for a distributed cad system, CAD Computer Aided Design 36 (9) (2004) 761–773.
5. S. H. Ahn, V. Sundararajan, C. Smith, B. Kannan, R. D'Souza, G. Sun, A. Mohole, P. K. Wright, J. Kim, S. McMains, J. Smith, C. H. Sequin, Cybercut: An internet-based cad/cam system, ASME Journal of Computing and Information Science in Engineering 1 (1) (2001) 52–59.
6. P. A. Rodgers, A. P. Huxor, N. H. M. Caldwell, Design support using distributed web-based ai tools, Research in Engineering Design - Theory, Applications, and Concurrent Engineering 11 (1) (1999) 31–44.

 Published by Cranfield University Press ISBN: 978-0-9557436-7-2 http://hdl.handle.net/1826/3832

7. J. H. Wu, H. J. Yin, Web browser based cad system for electrical machine, Zhongguo Dianji Gongcheng Xuebao/Proceedings of the Chinese Society of Electrical Engineering 27 (18) (2007) 35–40.
8. S. H. Ahn, B. Bharadwaj, H. Khalid, S. Y. Liou, P. K. Wright, Web-based design and manufacturing systems for automobile components: Architectures and usability studies, International Journal of Computer Integrated Manufacturing 15 (6) (2002) 555–563.
9. T. Lindholm, F. Yellin, The java virtual machine specification - second edition, http://java.sun.com/docs/books/jvms/second edition/html/vmspectoc.doc.html, (accessed: 06.03.2008).
10. V. V. Satish, K. Motipalli, P. Krishnaswami, An innovative web application for design and automated nc code generation, Vol. 2006, Department of Mechanical and Nuclear Engineering, Kansas State University, Manhattan, KS 66502, 2006.
11. Iso/iec 19776:2005 — x3d encodings (xml and classic vrml),
12. http://www.web3d.org/x3d/specifications/iso-iec-19776-x3dencodings-xml-classicvrml, (accessed: 09.03.2008).
13. Y. Seo, D. Y. Kim, S. H. Suh, Development of web-based cam system, International Journal of Advanced Manufacturing Technology 28 (1-2) (2006) 101–108.
14. J. S. Liang, A web-based 3d virtual technologies for developing product information framework, International Journal of Advanced Manufacturing Technology 34 (5-6) (2007) 617–630.
15. J. S. Liang, P. W. Wei, Conceptual design system in a web-based virtual interactive environment for product development, International Journal of Advanced Manufacturing Technology 30 (11-12) (2006) 1010–1020.
16. H. He, Y. Wu, Y. Gu, Y. Lu, Web-based virtual cnc machine modeling and operation, Chinese Journal of Mechanical Engineering (English Edition) 20 (6) (2007) 109–113.
17. Scalable vector graphics (svg) 1.1 specification, http://www.w3.org/tr/svg, (accessed: 09.03.2008).
18. Mochikit - a lightweight javascript library, http://mochikit.com, (accessed: 06.03.2008).
19. Ext js - javascript library, http://extjs.com, (accessed: 09.03.2008).
20. Ajax.org - declarative development and rich ui's, http://www.ajax.org, (accessed: 09.03.2008).
21. Turbogears: Front-to-back web development, http://turbogears.org, (accessed: 07.03.2008).
22. Postgresql: The world's most advanced open source database, http://www.postgresql.org, (accessed: 09.03.2008).
23. Extensible markup language (xml) 1.0 (fourth edition), http://www.w3.org/tr/rec-xml, (accessed: 07.03.2008).

 Published by Cranfield University Press ISBN: 978-0-9557436-7-2 http://hdl.handle.net/1826/3832

A Radio Frequency Radiation Reverberation Chamber Exposure System for Rodents

Myles Capstick[1]; Niels Kuster [1]; Sven Kühn[1]; Veronica Berdinas-Torres[1] ; John Ladbury[2]; Galen Koepke[2]; David McCormick[3]; James Gauger [3]; Ron Melnick[4]

[1] IT'IS Foundation, Zeughausstrasse 43, 8006 Zurich, Switzerland. capstick@itis.ethz.ch

[2]NIST , 325 Broadway, Boulder, CO 80305, USA.

[3] IIT Research Institute, 10 West 35th Street, Chicago, IL 60616, USA.

[4]NIEHS, PO Box 12233, Research Triangle Park, NC 27709, USA.

ABSTRACT

Reverberation chambers have long been used for EMC measurements on equipment; however, it was only recently that they have been developed as a paradigm for animal exposure to radio frequency radiation. This paper describes the system of 21 reverberation chambers developed for the National Toxicology Program of the National Institute of Environmental Health Sciences for assessing potential toxicity or carcinogenicity of mobile phone radiation and some of the specific decisions that were made and challenges that had to be overcome. Also detailed is the overall performance achieved.

INTRODUCTION

This paper presents the design and experimental results for a reverberation chamber based exposure setup for individually housed unconstrained rodents suitable for exposure over extended periods. The idea of using reverberation chambers for animal exposure to electromagnetic fields was first suggested by the National Institute of Standards and Technology (NIST) in a special session at BEMS 2001. A preliminary study involving an experimental investigation performed by NIST and a preliminary numerical dosimetry study performed by IT'IS, both funded by the National Institute of Environmental Health Sciences (NIEHS) in the USA. The results of this preliminary study were very encouraging and in January 2006 the main study to evaluate the potential toxicity and carcinogenicity of cell phone RF radiation in laboratory animals was issued by NIEHS under the National Toxicology Program (NTP). These results constitute the out come of the chamber prototype development and evaluation phase of the study.

 Published by Cranfield University Press ISBN: 978-0-9557436-7-2 http://hdl.handle.net/1826/3832

The guidelines for cell phone RFR are based largely on protection from acute injury from thermal effects [1]. Little is known about possible health effects of long-term exposure to minimally thermal levels of cell phone RFR

The NTP chronic studies will require a total of 21 reverberation chambers, Figure 1.

Figure 1. Half of the 21 chamber installation.

3 power levels for mice exposed to 1900 MHz GSM modulated signals
3 power levels for mice exposed to 1900 MHz CDMA modulated signals 1 mouse sham chamber
3 power levels for male rats exposed to 900 MHz GSM modulated signals
3 power levels for male rats exposed to 900 MHz CDMA modulated signals 1 male rat sham chamber
3 power levels for female rats exposed to 900 MHz GSM modulated signals,
3 power levels for female rats exposed to 900 MHz CDMA modulated signals 1 female rat sham chamber

METHODS

Reverberation chambers are resonant enclosures where the field structure is continuously altered using stirrers such that they provide a statistically homogeneous field distribution within a specific volume in the chamber [2]. In the NTP studies, rats will be chronically exposed at 900MHz and mice at 1.9GHz, different exposure groups will be subjected to either GSM or IS95 signals at one of three SAR levels or sham, over an entire lifespan. The use of a range of SAR levels will provide the ability to elicit any possible dose response.

The design of the reverberation chamber had to encompass both the electrical design and animal housing issues. To comply with the NTP guidelines non-toxic sterilizable materials must be used, from an electrical point of view the chamber must be fully shielded. The resultant solution was in a fully welded stainless steel design with a standard shielded room door, the stainless steel is slightly less conductive than normal steel so there is a slight compromise with the ultimate Q factors achievable.

 Published by Cranfield University Press ISBN: 978-0-9557436-7-2 http://hdl.handle.net/1826/3832

Figure 2. Internal view of the reverberation chamber showing the two stirrers.

The field at any point in the chambers changes temporally, it is only the target value when averaged over integral number of rotations of the stirrers. The temporal changes in field and hence exposure can be used to mimic the temporal changes in the output power of a mobile phone due to the power control implemented in the GSM or IS95 handset by tuning the speed of the two stirrers (the rotation speeds should always be different).

The tight requirements on the field homogeneity and requirement to be able to place animal racks in the chambers necessitated a design with two near optimal mode stirrers [3]. The first stirrer is placed vertically at the rear of the chamber and the second horizontally on the ceiling, Figure 2. The overall chamber size is w = 2.2m, l = 3.7m and h = 2.6m.

The choice of exposure frequency is based upon two main criteria, firstly frequencies commonly in use in the USA for mobile telephony and secondly based on providing a more uniform SAR distribution in the animal species, Figure 3 right hand side shows from left to right mouse 900MHz, mouse 1900MHz, rat 900MHz and rat 1900MHz, based on the analysis f the SAR distributions 900MHz was chosen for rats and 1900MHz for mice.

The required field strength was determined from numerical dosimetry using the plane wave integral representation of a reverberation chamber [4] and high resolution animal models based on 4 different size models covering the whole life span. Each model has over one hundred different body parts differentiated, the models can be seen in the left hand side Figure 3. Using the models the average field strengths required to produce the target SAR in the animals in each exposure group was determined, Figure 3 right hand side.

 Published by Cranfield University Press ISBN: 978-0-9557436-7-2 http://hdl.handle.net/1826/3832

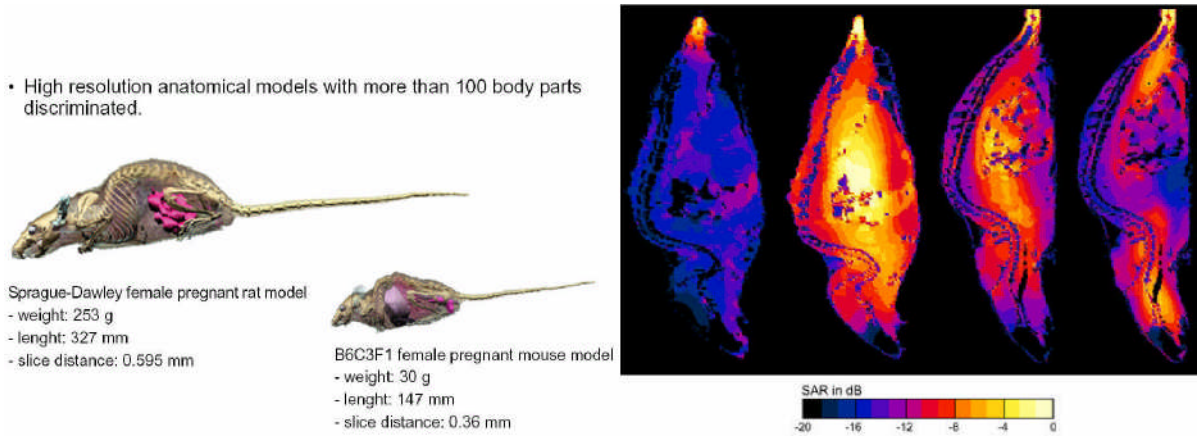

Figure 3. Electromagnetic modelling was performed using anatomical models, left, using SEMCAD X (SPEAG Switzerland) to perform the numerical dosimetry, right.

The exposure in the chambers is controlled using a closed loop system. This system is based on the measurement of three orthogonal components of both the electric and magnetic field at two locations in each chamber.

RESULTS

The important performance metrics for a reverberation chamber used for animal exposure are: the field uniformity, field isotropy, SAR uniformity and efficiency. Using E-Field probes the measured electric-field uniformity (one standard deviation) in the empty chamber measured on a 300mm 3D grid was 0.6dB and the field isotropy 0.85dB and in the fully loaded chamber, over a reduced number of points, the values were 0.74dB and 1.3dB respectively. Figure 5, shows the E-field uniformity results. The SAR uniformity was measured in the same chamber using rat and mouse phantoms consisting of bottles of tissue simulating liquid optimised to provide the same absorption as an adult rodent.

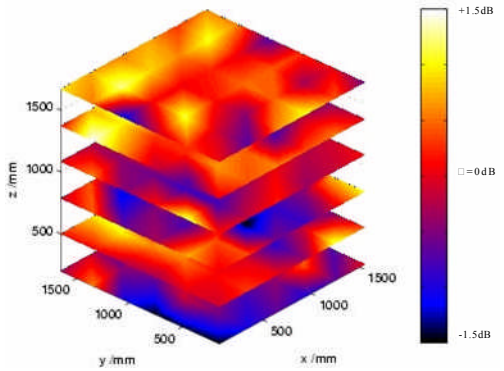

Figure 4. Field Uniformity.

The experimental dosimetry was performed using the final temperature method, and showed that the SAR uniformity between animals was 0.46dB and 0.40dB respectively for rats and mice, the

 Published by Cranfield University Press ISBN: 978-0-9557436-7-2 http://hdl.handle.net/1826/3832

SAR shows better uniformity than that of the field measurements due to the special averaging over the volume of the animal phantom. Additionally, the design of any exposure system needs to consider how much power must be generated to achieve the desired animal exposure, one key metric is the overall efficiency, in this case the chamber approach provides efficiencies of 70% for adult rats and 45% for adult mice.

Fundamental to the nature of the reverberation chamber is the fact that the field has temporal and spatial variations. The design of the stirrers can be such that the spatial variations in the average field strength can be minimised, or at least controlled within specified bounds, this work has shown that this can be achieved.

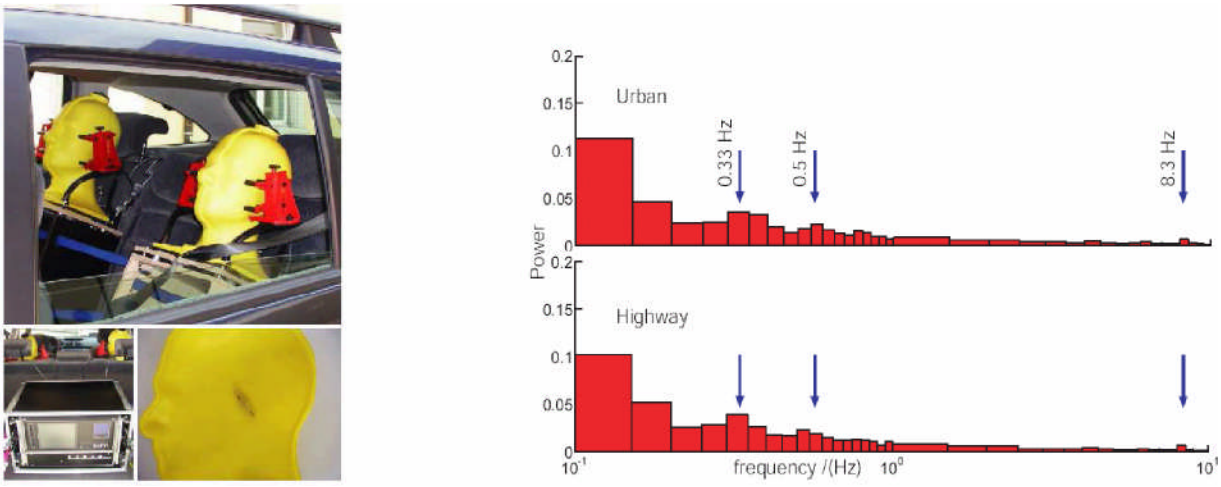

Figure 5. Measurement data for the low frequency spectrum of the temporal variations in SAR exposure from a GSM mobile phone.

The work has also shown that temporal variations introduced by the rotation of the stirrers can be tailored to provide a change in exposure that has some meaningful correlation to real world exposure variations. By taking measurement data of the power control and hence actual exposure of real mobile phones when operated in different propagation environments and performing a Fourier transform the low frequency components of variation of power can be determined. Figure 5 shows the measurement setup and analysed data for a typical GSM mobile phone exposure [5]. The rotation velocities of the two stirrers can then

be tuned to provide a variation that has many of the key characteristics of the real signal variation. Individual components can be created by a combination of the beat frequency of the stirrers and the absolute rotational speed. The velocity of rotation and the relative differences is dependant on the mobile communication system to be mimicked as they have different power control characteristics and the mode density in the chamber at a given frequency also impacts the required angular displacement to achieve a given field strength variation at a single point in the chamber.

 Published by Cranfield University Press ISBN: 978-0-9557436-7-2 http://hdl.handle.net/1826/3832

CONCLUSIONS

Overall, the performance across all the criteria of the reverberation chamber for animal exposure is excellent, with all target performance metrics being met or exceeded. A reverberation chamber has the ability to house large numbers of animals where the animals are unconstrained and can be individually housed. Long exposure periods of □ 20 hours per day are possible as the animals can be free to feed and drink during exposure. Excellent field uniformity and isotropy can be achieved which in turn provides excellent SAR uniformity and all with good efficiency. The performance of this exposure environment is comparable to the best exposure setups using constrained animals.

REFERENCES

1. ICNIRP (International Commission on Non-ionising Radiation Protection). 1998. "Guidelines for limiting exposure to time-varying electric, magnetic, and electromagnetic fields (up to 300 GHz"). Health Phys 74494-522.
2. D.A. Hill, "Electromagnetic theory of reverberation chambers", National Institute of Standards and Technology, Technical Note 1506, 1998.
3. J. Clegg, A.C. Marvin, J.F. Dawson and S.J. Porter, "Optimisation of Stirrer Designs in a Reverberation Chamber", Trans EMC, 190, 2003.
4. D.A. Hill, "Plane wave integral representation for fields in reverberation chambers", IEEE Trans EMC, 40, 1998, pp209-217.
5. S. Kuehn, C. Sulser, N. Kuster, "Assessment Technique for the Cumulative Exposure of Mobile Phones in Real Networks",Proc. of URSI General Assembly 2005, Delhi, India, Oct 2005

ACKNOWLEDGEMENTS

This work was supported by the National Institute of Environmental Health Sciences (N01-ES55544).

 Published by Cranfield University Press ISBN: 978-0-9557436-7-2 http://hdl.handle.net/1826/3832

Frequency Agile Materials and Microwave Device Fabrication

Charalampos Fragkiadakis, Robert V Wright, Qi Zhang and Paul B Kirby

Microsystems and Nanotechnolgy Centre, Materials Department, Cranfield University

Recent wireless communication systems like cognitive radios require smart radio transmitters and receivers whose operating frequency and band can be adjusted. Frequency agile materials and technologies based on nonlinear ferroelectric offer a line of passive tuneable microwave components such as varactors, filters and phase shifters suitable for key components in phased-array antennas for example radar sensors and future reconfigurable RF-front ends for mobile communication systems with multiband operation.

Cranfield has been involved in the development of ferroelectric thin film for nearly ten years with a focus on the development of novel functional devices. Recently, however it has applied its core sol gel technology to the investigation of suitable thin film ferroelectrics for frequency agile applications. For microwave applications the most studied material is Barium strontium titanate but to date it has not been possible to deposit this material with properties suitable for devices over the large area substrates needed for commercialisation. We have demonstrated recently that sol gel deposition is a suitable technique for depositing over large areas, especially for the lead strontium titanate material system which displays extraordinary high voltage dependent permittivity.

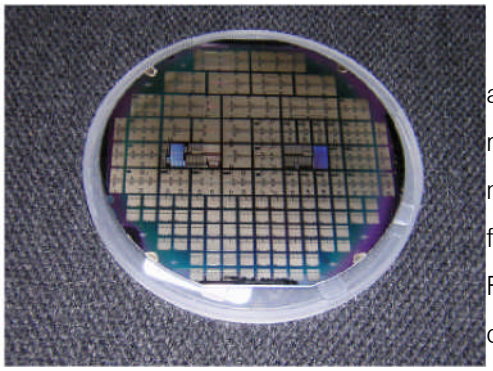

In this presentation we will review the field of frequency agile materials and devices, together with Cranfield' s recent results in material deposition and fabrication of microwave devices. The outcome of processing ferroelectric band-stop filter on a 4 inch silicon wafer (see Figure) will be described and the prospects for microwave device developments outlined.

 Published by Cranfield University Press ISBN: 978-0-9557436-7-2 http://hdl.handle.net/1826/3832

General calibration models of Vis-NIR spectroscopy for measurement of soil properties in Belgium and Northern France

Abdul Mounem Mouazen[1]; Josse De Baerdemaeker[2]; Herman Ramon[2]

[1]Natural Resources Department, Cranfield University, MK43 OAL, United Kingdom, e-mail: a.mouazen@cranfield.ac.uk

[2]Division of Mechatronics, Biostatistics and Sensors (MeBioS), Department of Biosystems, Faculty of Bioscience Engineering, Kasteelpark Arenberg 30, B-3001 Heverlee, Belgium

ABSTRACT

This study was undertaken to explore the potential of the visible (Vis) and near infrared (NIR) spectroscopy for *in situ* measurement of selected soil properties in large geographical area covering Belgium and Northern France. A portable, fibre-type, Vis-NIR spectrophotometer (Zeiss Corona 1.7 visnir fibre, Germany) with a measurement range of 306.5 – 1710.9 nm was used to measure light diffusive reflectance properties. On the basis of values of the coefficient of determination R^2 and the residual prediction deviation (RPD), predictions were evaluated as good for MC (R^2 = 0.88 and RPD = 2.87) and as approximate quantitative determination for C, K, Mg, Na and P (R^2 = 0.66 – 0.70 and RPD = 1.70 – 1.94). The moderate accuracies in prediction of C, K, Mg, Na and P were attributed to the large variability in the sample set, since samples were collected from a large geographical area. However, it can be concluded that the Vis-NIR spectroscopy could be used *in situ* for rapid determinations with high accuracy of MC and moderate accuracies of C, K, Mg, Na and P for different soils in Belgium and Northern France.

Keywords: visible; near infrared; spectrophotometer; soil properties; chemometric; *in situ*.

INTRODUCTION

The conventional laboratory methods for the determination of soil attributes are very costly, labour intensive and time consuming. Since these methods rely on a few scattered measurements of soil properties, they are unable to satisfy the demand of precision agricultural and land use management, requiring a large number of spatial measurements at low cost and in a short period of time. Spectroscopic methods are being increasingly considered as possible alternatives to enhance or replace conventional laboratory methods of soil analysis. Many studies reported on the use of the visible (Vis) and near infrared (NIR) spectroscopy for the measurement of soil properties under laboratory and field measurement conditions (e.g. Bogrekci & Lee, 2005a; Maleki *et al.*, 2006). Colour, texture and moisture content (MC) are the most significant factors

 Published by Cranfield University Press ISBN: 978-0-9557436-7-2 http://hdl.handle.net/1826/3832

affecting the electromagnetic energy reflectance from soil surfaces, which might reduce the accuracy of measurement. When dealing with general calibration models of soil properties using Vis-NIR spectroscopy, these factors play an important role in the calibration scheme, since soil collected from large geographical areas have a wide range of variable colour, MC and texture. However, the accuracy of the resultant models needs to be evaluated.

The aim of this study is to explore the potential of Vis-NIR spectroscopy for *in situ* (non-mobile) measurement of selected soil properties for a wide range of soils in Belgium and Northern France. Using this wide range of reference soils, it is hoped that the effects of texture, colour and MC are accounted for in the calibration models that should be applicable *in situ* for large geographical areas.

MATERIALS AND METHODS

COLLECTION OF SOIL SAMPLES

A total of 365 samples were obtained from the Soil Service of Belgium (Heverlee, Belgium). They were collected in the spring and summer of 2004 from 365 fields in Belgium and Northern France from upper soil layer of 0-23 cm. Each sample was mixed and divided into two parts; the major amount of the soil was used for laboratory chemical analyses, whereas the remaining part was used for optical measurement.

LABORATORY ANALYSES OF SOIL PROPERTIES

Texture was determined in a sensory way by a soil surveyor performing the test with fingers and thumb. Soil C expressed in percentage of carbon weight to the total weight of dry soil was determined by the adjusted Walkley-Black method (Hesse, 1971). Using the ammonium lactate, an extract was obtained to determine K, Mg, Na and P in the extract. Among those elements, K, Mg and Na were measured with an atomic absorption spectrophotometer, whereas P was measured by a colorimetric method. These elements were expressed in mg per 100 g air dried soil. The gravimetric soil MC expressed in kg kg^{-1} was measured after oven drying at 105°C for 24 hours. The wet soil weight was directly obtained after sample scanning with the spectrophotometer.

VIS- NIR SENSOR DESCRIPTION AND MEASUREMENT

A portable, fibre-type Vis-NIR spectrophotometer developed by Zeiss Company (Zeiss Corona 45 visnir fibre, Germany) with a measurement range of 306.5 – 1710.9 nm was used. Different amounts of fresh soil of different textures were packed in petridishs of a 1.0 cm height by 3.6 cm in diameter. Three reflectance readings were taken from each soil specimen by rotating the petridish a 120° angle. Each reading was an

 Published by Cranfield University Press ISBN: 978-0-9557436-7-2 http://hdl.handle.net/1826/3832

average of 5 successive measurements in 2.5 s. An average spectrum was obtained from the three measured spectra, and this was used for spectra pre-processing and model establishment.

PRE-PROCESSING OF SPECTRA

The spectra were first reduced from 306·5 – 1710·9 nm to 401·4 – 1664 nm, to eliminate the noise at the edges. Spectra were then subjected to Savitzky-Golay first derivation (Martens and Naes, 1989) using The Unscrambler 7.8 software (Camo Inc.; Oslo, Norway). A 2:2 smoothing was carried out after the first derivative to remove noise from measured spectra. The same pre-processing was used for all properties except for MC, for which maximum normalisation was considered before the first derivation.

ESTABLISHMENT OF CALIBRATION MODELS

The total 365 spectra were randomly divided into calibration and validation sets of 243 and 122 spectra, respectively. The partial least squares regression (PLSR) analysis available in The Unscrambler 7.8 software (Camo Inc.; Oslo, Norway) was carried out on the calibration set to establish calibration models. A PLSR model validation procedure was based on the leave-one-out cross validation method. The validation set was used for further validation of the established PLSR models.

 Published by Cranfield University Press ISBN: 978-0-9557436-7-2 http://hdl.handle.net/1826/3832

RESULTS AND DISCUSSION

EFFECTS OF SOIL PROPERTIES ON THE SHAPE OF SOIL SPECTRA

Many studies found that with increasing soil MC the intensity of light reflectance decreased (Mouazen *et al.* 2005). The darker soil surface that resulted from higher MC induces larger surface absorbance and an overall decrease in reflectance. Furthermore, the water absorption band of 1450 nm is clearly visible for wet soils.

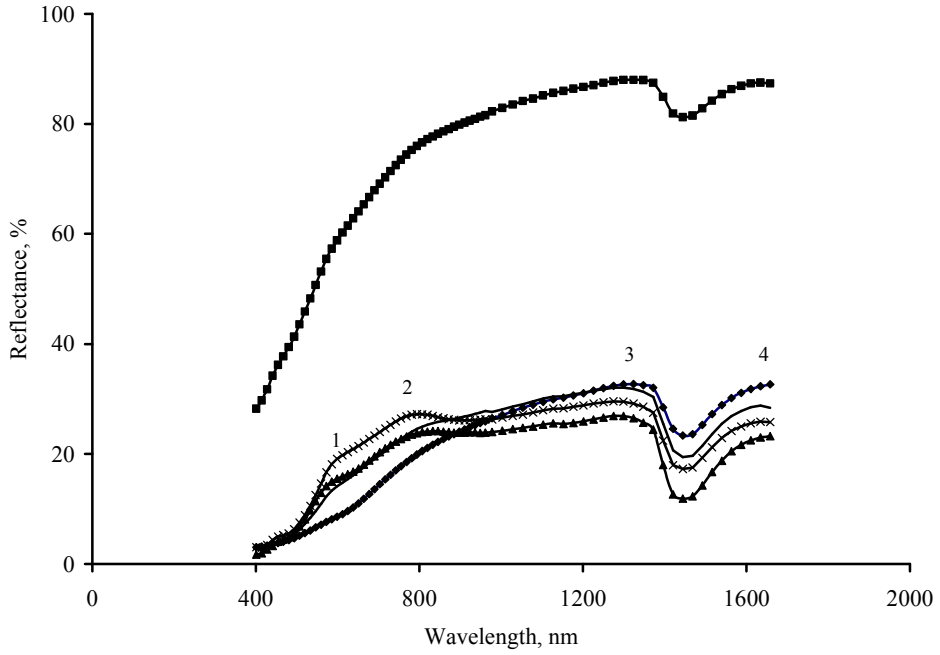

Fig. 3. Effect of colour and moisture content (MC) on the overall shape of raw soil spectra: ♦, black; ■, light grey; ▲, brown; —, orange yellow; ×, reddish yellow soils

Variable colour can be seen mostly in the Vis wavelength range (350 – 750 nm). The light absorbance by iron oxides, plant residue or decayed organic parts dominates the reflectance spectrum of the soil in the Vis wavelength range. Four domes of reflectance can be recognised within the entire soil spectrum (400 – 1650 nm) shown in *Fig. 1*. The first dome (1) at about 570 nm results from the absorption in the blue region around 450 nm and in the red region around 680 nm. It appears clearly in the brown, orange yellow and reddish yellow soils and less clearly in the light grey soil (*Fig. 1*). The second dome (2) is at 780 nm between absorption peaks of the red colour (680 nm) and of the water absorption band (960 nm) in the third overtone region. Between water absorption band (960 nm) in the third overtone region and water absorption band (1450 nm) in the second overtone region, dome 3 can be distinguished around 1340 nm, with different magnitudes due to different clay minerals and MC. Dome 4 near 1630 nm that is related to clay minerals and

 Published by Cranfield University Press ISBN: 978-0-9557436-7-2 http://hdl.handle.net/1826/3832

MC is a result of water absorption at 1450 and 1950 nm. Of all chemical components studied, only C and MC possess active absorption bands (overtones or combinations) in the NIR region (750 - 1710 nm) considered. The other chemical attributes (K, Mg, Na and P) that are spectrally inactive in the Vis-NIR (300 - 1710 nm) region have only indirect spectral response throughout the direct spectral response of soil colour (humic acids, plant residues, carbonate and iron oxides), MC (texture and clay minerals). For instance, K is found in K-Feldspar [$KAlSi_3O_8$], whereas Na and Mg are found in Bentonite [$(Na,Ca)_{0,33}(Al,Mg)_2Si_4O_{10}(OH)_2 \cdot nH_2O$].

QUANTITATIVE DETERMINATION OF C, K, MC, MG, NA AND P

Due to the presence of water absorption band at 1450 nm, MC is the easiest component to measure with Vis-NIR spectroscopy (Table 1). The high values of coefficient of determination R^2 and the ratio of prediction deviation (RPD) declare that the measurement of MC can be classified as good. The prediction of C and P can be classified as approximate quantitative determination. The prediction of K, Mg and Na can also be classified as possible approximate quantitative. However, Mg and Na models are better performing comparing to K model, since the validation performed on the validation sample set provided better results for Mg and Na compared to K (Table 1).

Table 1. Validation of Partial Least Squares regression (PLSR)-cross validation technique on validation set

Property	*R2*	*Slope*	*Intercept*	*RMSEP*	*RPD*
Organic carbon (C), %	0.68	0.64	0.555	0.595	1.76
Potassium (K), mg $100g^{-1}$	0.66	0.74	5.469	6.534	1.68
Moisture content (MC), kg kg^{-1}	0.87	0.93	0.009	0.026	2.69
Magnesium (Mg), mg $100g^{-1}$	0.72	0.79	3.629	6.412	1.87
Sodium (Na), mg $100g^{-1}$	0.70	0.82	0.513	1.121	1.77
Phosphorous (P), mg $100g^{-1}$	0.73	0.73	7.126	7.864	1.86

CONCLUSIONS

Results of the current study suggested the following conclusions:

- Difference is soil colour and MC can be visually recognised on soil spectra.
- Vis-NIR calibration models developed could be used for rapid *in situ* measurement of C, K, MC, Mg, Na and P for a wide range of soil texture and colour. The measurement accuracy were evaluated as good for MC and as moderate for C, K, Mg, Na and P.

 Published by Cranfield University Press ISBN: 978-0-9557436-7-2 http://hdl.handle.net/1826/3832

REFERENCES

1. Bogrekci I; Lee W S (2005). Spectral Soil Signatures and sensing Phosphorus. Biosystems Engineering, 92(4), 527-533.
2. Maleki M R; Van Holm L; Ramon H; Merckx R; De Baerdemaeker J; Mouazen A M, 2006. Phosphorus sensing for fresh soils using visible and near infrared spectroscopy. Biosystems Engineering, 95(3), 425-436.
3. Hesse P R (1971). A textbook of soil chemical analysis. John Murray, London.
4. Martens H; Naes T (1989). Multivariante Calibration, 2nd edition. John Wiley & Sons, Ltd., Chichester, United Kingdom.
5. Mouazen A M; De Baerdemaeker J; Ramon H (2005). Towards development of on-line soil moisture content sensor using a fibre-type NIR spectrophotometer. Soil & Tillage Research, 80(1-2), 171-183.

 Published by Cranfield University Press ISBN: 978-0-9557436-7-2 http://hdl.handle.net/1826/3832

New flow-sheets for wastewater treatment in the UK: Anaerobic treatment a step forward towards energy neutral processes

Ana Soares[1], Nacho Martin-Garcia[1], Marc Pidou[1], F Fawehinmi[1], Jon Brigg[2], Elizabeth Wood[2], Bruce Jefferson[1], Elise Cartmell[1] and John N. Lester[1]

[1]Centre for Water Science, Cranfield University, Cranfield, MK43 0AL, UK

[2]Yorkshire Water Limited, Western House, Halifax Road, Bradford, BD5 2LZ, UK

*Author for correspondence: a.soares@cranfield.ac.uk; Tel: 0044 1234750111; Fax: 0044 1234751671

ABSTRACT

One of the most widely used treatment processes for wastewater treatment is the activated sludge process where the microorganisms grow in suspension in the artificially aerated wastewater to capture carbon and nutrients and produce more biomass and carbon dioxide. Although this treatment process is well-know and broadly used the energy that it is required to maintain enough oxygen dissolved in the wastewater for microbial reactions to take place is high as it can reach up to 54-97% of the total energy costs for sewage treatment. The wastewater treatment flow-sheet has not been altered since Arden and Lockett introduced activated sludge treatment in 1914. Hence, a radical alteration to this flow-sheet is proposed by treating the majority of the flow anaerobically in order to save energy required for aeration but also enhance the production of renewable source of energy in the form of biogas. Two new types of flow-sheets with anaerobic treatment technologies are currently being explored at the Centre for Water Sciences: anaerobic membrane bioreactors (AnMBR) and granular high-rate systems fed with sewage fortified with primary sludge. Initial results on these systems indicate their potential to treat wastewater effectively (chemical oxygen removal above 90% in the AnMBR and above 80% in the high-rate system) but also the capacity to reduce energy consumption by 57% (in high-rate systems) when compared with standard activated sludge plants. The energy requirements of AnMBRs depend on the wastewater strength and membrane operation.

Keywords UASB, anaerobic MBR, GPS-X, methane, aeration requirements, mass and energy balances

INTRODUCTION

In conventional secondary treatment most of the electricity is used for aeration of the activated sludge process that can account for 54-97% of the total energy requirements of

 Published by Cranfield University Press ISBN: 978-0-9557436-7-2 http://hdl.handle.net/1826/3832

the wastewater treatment plant (0.3 to 0.7 kWh/m^3)[1,2]. The water industry uses approximately 2-3 % of net UK electricity and is the fourth most energy intensive sector in the UK[3] releasing 0.55% of greenhouse gas (GHG) emissions per annum[4]. This is equivalent to approximately four million tonnes of GHG emission (carbon dioxide CO_2 equivalent) every year. But over the last 10 years, as UK GHG emissions have gone down, the water industry's emissions have gone up by 30%. Pressure to increase electricity use continues, as although the industry continues to adopt energy efficiency measures, population and consumption growth, along with ever more stringent standards for final effluents and sludge re-use, are driving energy use up.

There is a need to investigate methods of producing and/or reducing energy consumption during wastewater treatment to bring down carbon dioxide emissions from non-renewable energy sources and to reduce dependence of the water utilities on ever increasing fossil fuels prices. Current technologies for production of renewable energy from wastewater include biogas from anaerobic sludge digestion and sludge incineration. In this context, anaerobic wastewater treatment has the benefit of generating energy through biogas and it has reduced aeration energy requirements compared with the activated sludge process. This paper proposes to new flow-sheets for anaerobic wastewater treatment:

wastewater fortification method through the addition of disintegrated primary sludge to the crude wastewater and treatment of the wastewater in up-flow sludge blanket (UASB) bioreactors operated at bench-scale and using plant-wide simulations using GPS-X

feasibility of the anaerobic membrane bioreactor (AnMBR) for treatment of low strength wastewaters at pilot-scale experiments and by calculating the energy requirements associated to biological and membrane operation for different wastewater strengths using literature research data and mathematical models.

PARTIAL ANAEROBIC WASTEWATER TREATMENT FLOW-SHEET

The characteristics of the raw sewage are determinant for the selection of the process design with the strength wastewater being a central point for the success of the anaerobic treatment. A chemical oxygen demand (COD) concentration greater than 1000 mg COD/l in the influent is usually considered to be the threshold value to ensure biogas production[1]. Typical wastewater characteristics are shown in Table 1 as well as the optimal influent

 Published by Cranfield University Press ISBN: 978-0-9557436-7-2 http://hdl.handle.net/1826/3832

characteristics for application of anaerobic processes in general. Wastewater features are not optimal to perform anaerobic degradation. Hence special attention has to be given to the selection of the process and bioreactor design in order to be able to overtake the strength limitations.

Table 1. Comparison of the characteristics of raw wastewater and an influent that gives high yields in anaerobic processes.

	Waste water	Anaerobic process, optimal conditions [a]
	Concentration (mg/l)	
Suspended solids (SS)	100-350	<100
Biochemical oxygen demand (BOD)	110-400	
Chemical oxygen demand (COD)	250-1000	~1000
Total nitrogen (N)	20-85	<1500
Total phosphorus (P)	4-15	
Alkalinity (as CaCO3)	50-200	<1200
Grease	50-150	
Temperature (°C)	14-20	30-35
pH	7	6-8.5
COD:N:P	66:5:1<X<250:5:1	600:5:1

a optimal conditions refers to COD removals above 90% and methane productions on the order of 0.25 - 0.35 m^3/kg COD removed.

To overcome the low-strength of the municipal wastewater and substrate availability constraints wastewater fortification with primary sludge of the sewage before anaerobic wastewater treatment has been studied at the Centre for Water Science. The partial anaerobic wastewater treatment describes a flow-sheet where the influent is split into two fractions: one fraction was allowed into the primary settler and further treated in the activated sludge process, while the other portion was treated anaerobically. The sludge produced in the primary settler was recycled into the anaerobic reactor. The effluent of the anaerobic bioreactor was fed into the activated sludge process together with the settled wastewater (Fig. 1B).

Bench-scale experiments tried to mimic this flow-sheet and it was observed that the addition of 5% of sludge in volume to crude wastewater resulted on the increase of total COD from 536 mg/L to 2300 mg/L. Three bench scale UASB bioreactors (0.5 L) were operated in parallel. The first bioreactor was fed crude wastewater, the second with wastewater disintegrated using ultrasound and the third with crude wastewater fortified with 5% primary sludge disintegrated using ultrasound. The bioreactor operated with fortified wastewater presented an increased total COD removal 86±8% and biogas

 Published by Cranfield University Press ISBN: 978-0-9557436-7-2 http://hdl.handle.net/1826/3832

production up to 200 mL/day in comparison with the UASB feed with crude wastewater (77□8% COD removal and a biogas production of 20 mL/day) and the crude wastewater pre-treated with ultrasound (79□8% COD removal and a biogas production of 78 mL/day). These experimental results were used to develop a black-box model with GPS-X (COST model) to compare the mass and energy balances of two layouts: aerobic secondary treatment with activated sludge and anaerobic digestion and a layout with the partial anaerobic treatment flow-sheet with 75% influent split into the anaerobic reactor followed by an aerobic treatment stage (Fig. 1). The aeration energy requirements of the aerobic layout were 1552 kWh/day and the potential energy produced from the biogas in the sludge digester was 833 kWh/day. The aeration energy requirements of the anaerobic treatment layout was 670 kWh/day with 705 kWh/day produced from the biogas. The energy balance in the anaerobic wastewater treatment layout was -340 kWh/day compared with -719 kWh/day in the aerobic layout corresponding to an energy saving of 57%.

Figure 1 A. Conventional wastewater treatment flow sheet utilizing aerobic activated sludge treatment B. Proposed fortified anaerobic wastewater treatment flow sheet.

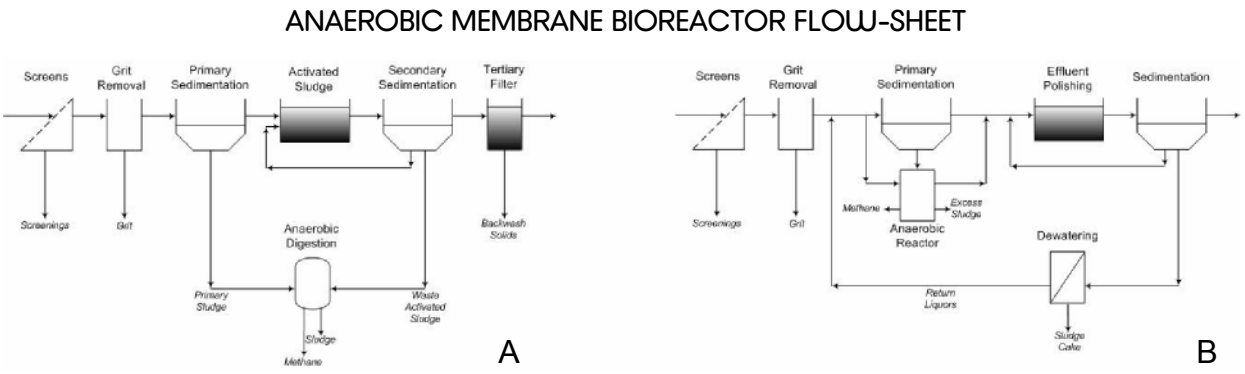

The membrane bioreactors (MBR) combine conventional suspended growth with membrane filtration. The wastewater to be treated is fed into the reactor at high flow rates while the biomass is retained by the membrane enabling high biomass concentration and long sludge retention times enhancing the development of slow growth rate microorganisms as the methanogens (Fig. 2). Methanogenesis is recognised for optimally taking place in two ranges of temperatures the mesophilic (30-35°C) and the thermophilic range (40-50°C). Psychrophilic methanogenesis (5-20°C), has recently gained increased interest due the potential of the application of anaerobic systems in temperate and cold climates but it has been pointed to proceed at lower rates and with less stability than under

 Published by Cranfield University Press ISBN: 978-0-9557436-7-2 http://hdl.handle.net/1826/3832

mesophilic conditions[5]. Typical wastewater temperature in the UK fluctuates between 20.5°C to 8.1°C with an average of 14°C and therefore anaerobic treatment in the psychrophilic range should be emphasised.

To investigate the feasibility of using an AnMBR for treatment of wastewater at psychrophilic temperatures a pilot-scale

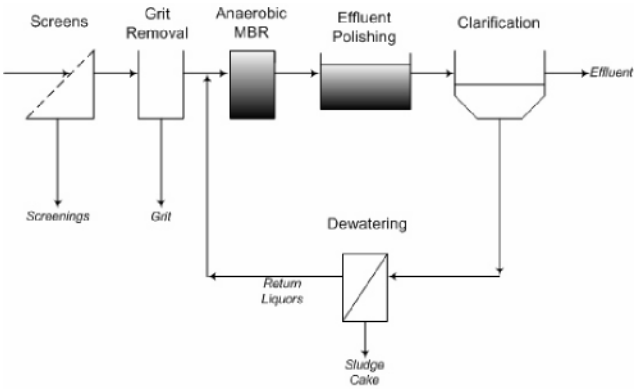

Figure 2. Proposed AnMBR wastewater treatment flow-sheet.

bioreactor with 40L was continuously fed with settled sewage for a period of 120 days operated at three different temperatures (3 5°C, 22°C and 12°C). The highest COD removal and methane production was recorded at 35°C with values of 97% and 0.37L/$L_{reactor}$ day, respectively. On day 64 and 96 the temperature was reduced to 22°C and 12°C, respectively and an initial drop on COD removal and methane production was observed. However the system recovered within two weeks and a COD removal of 95% was measured for 22°C and 91% for 12°C. The fact that the system was able to recover to the initial COD removal values indicates that adaptation of the biomass to low temperatures occurred. The anaerobic membrane bioreactor was capable of producing an effluent with COD values below 90 mg/L at temperatures as low as 12°C.

The energy requirements associated to biological and membrane operation for different wastewater strengths were calculated using mathematical models and it was found to be dependant on the wastewater strength and membrane operation. For low strength wastewaters the difference between energy requirements for membrane operation in aerobic and AnMBRs could compensate the energy savings that result from the absence of aeration. However, assuming a conversion efficiency of the biogas to electrical power of 25% the amount of methane produced at an influent COD of 930 mg/L could represent between 10 and 50% of the membrane operating costs of an AnMBR.

ANAEROBIC TREATMENT IN OTHER COUNTRIES AND COMPARISON OF THE TWO FLOW-SHEETS

The anaerobic wastewater treatment is current practice in tropical countries such as Colombia, Brazil, Indonesia, India, Egypt and Singapore were the effluent temperature is

 Published by Cranfield University Press ISBN: 978-0-9557436-7-2 http://hdl.handle.net/1826/3832

usually high enough for the reactor to be operated all year around without any heating. These conditions make the energy balance completely favourable in comparison with conventional aerobic systems. Currently the most widely used type of system is the UASB but importance of the expanded-bed granular sludge blanket (EGSB) is increasing as this type of reactor is growing in number (Frankin 2001).

A comparison of the anaerobic flow-sheets here described can be found in Table 2 in regard to their main advantages and disadvantages. The common points between the two flow-sheets is treatment of the wastewater at high flow-rates, the reduced aeration requirements and the use of a large percentage of the carbon 75-100% for renewable energy production in the form of biogas.

Table 2. Comparison of the partial anaerobic treatment and the AnMBR flow-sheets for their advantages (+) and disadvantages (-).

Partial anaerobic treatment flow-sheet	AnMBR flow-sheet
(+) Fortification with primary sludge enhances bioreactor stability and biogas production	
(+)The anaerobic bioreactor UASB design and operation is well know for sewage treatment applications	(+) High quality effluent and disinfection can be achieved
(+) Ultrasound of the primary sludge enhances hydrolysis	(+) Rapid adaptation of the anaerobic communities to psychrophilic conditions
(+) Under loading of primary settlers	(+) No need for aerobic polishing step if augmentation with ANAMMOX is successful for N removal
(+) Granular sludge produced is a valuable product and it can be marketed at 1 £/kgVSS	(+) No need for primary settlers
(-) Addition of primary sludge increases N concentration in the wastewater	(-) High energy demands for filtration of the wastewater
(-) Aerobic polishing of the effluent from the anaerobic reactor is mandatory to comply with tight COD consents	(-) Requires that biogas is recalculated in the liquid o prevent membrane fouling with consequent increased costs on pumping
(-) No nitrogen removal occurs in the anaerobic bioreactor unless augmentation with ANAMMOX bacteria is successful	(-) Technology not demonstrated for sewage treatment applications at full-scale

ACKNOWLEDGEMENTS

The funding from Marie Curie Early Stage Research Training Fellowship (MEST-CT2005-02 1050), Yorkshire Water, Severn Trent Water and Black & Veatch are greatly acknowledged.

REFERENCES

1. Tchobanoglous, G., Burton, L.F. and Stensel, H.D. (2003) Wastewater engineering: Treatment, disposal and reuse/Metcalf & Eddy, Inc. McGraw-Hill Book Co, International edition
2. Young, D.F. and Koopman, B. (1991) Electricity use in small waste-water treatment plants. Journal of Environmental Engineering-Asce 117(3), 300-30.
3. Water UK. (2006) Towards Sustainability 2005-06 Full report http://www.water.org.uk /home/policy/reports/sustainability/indicators-2005-06 (accessed 31/10/07).
4. Parliamentary Office of Science and Technology. (2007) Energy and Sewage. Postnote April 2007 No 282, The Parliamentary Office of Science and Technology, London, UK.
5. Lettinga, G.; Rebac, S.; Zeeman, G. (2001) Challenge of psychrophilic anaerobic wastewater treatment. Trends in Biotechnology. 19,363-70

 Published by Cranfield University Press ISBN: 978-0-9557436-7-2 http://hdl.handle.net/1826/3832

Prostate Cancer Diagnosis Using an Affinity Sensor

Yildiz Uludag and Ibtisam .E. Tothill*

Cranfield Health, Cranfield University, Cranfield, Bedfordshire, MK43 0AL, UK

ABSTRACT

Prostate carcinoma is a fatal malignancy and is a major cause of death in men in the population aged 55 and over in the UK (10,000 men a year). Early and accurate detection of prostate cancer is very important, since there is no cure if the cancer spreads out to the other organs of the body. Recent developments and advances in biosensor technology have enabled the miniaturisation of the devices and multiplex testing of the analytes. Therefore, biosensor technology has the potential for the manufacture of point of care cancer testing devices.

Prostate specific antigen (PSA) is used as a biomarker for the diagnosis and prognosis of prostate cancer. Tests based on PSA analysis are currently still the most common tests employed for prostate cancer detection. In the current study the potential of using QCM biosensors for the detection of PSA has been investigated. An automated QCM instrument was used as the biosensor platform. By performing a direct immunoassay on the gold sensor chip a 19.5 ng ml^{-1} PSA could be detected, while a sandwich assay enabled the detection of 4.9 ng ml^{-1} PSA.

INTRODUCTION

Prostate cancer, the commonest form of cancer in men in Europe, is a complex, multifactorial disease. Every year in the UK nearly 35,000 cases of prostate cancer are diagnosed, and prostatecancer causes 10,000 deaths each year

(http://info.cancerresearchuk.org/cancerstats/types/prostate/incidence/). Early and accurate detection of prostate cancer is very important, since there is no cure if the cancer spreads out to the other organs of the body. Early diagnosis of prostate cancer is very important for successful treatment of the disease.

The increase in PSA levels in serum above the normal limits is the primary indication of prostate malignancy; therefore PSA is used as a biomarker for the diagnosis and prognosis of the prostate cancer (Brawer and Lange 1989; Diamandis 1998). PSA or inother words human glandular kallikrein 3 (hk3) is a 3 3-34 kDa glycoprotein produced by the prostatic secretary epithelium cells. PSA is also detectible in serum and the normal level of PSA in serum is 0.1-2.5 ng ml^{-1}. In serum, PSA is found either in free form or as a complex with ACT (ACT-PSA, MW 96 kDA). ACT is a protease inhibitor and it inhibits PSA's proteolytic activity. Although PSA is currently recognised as the clinically most used prostate cancer marker, it is not cancer specific (Stephan, *et al.* 2007). Benign Prostatic Hyperplasia

 Published by Cranfield University Press ISBN: 978-0-9557436-7-2 http://hdl.handle.net/1826/3832

and some other non-cancerogenous diseases also cause an increase of serum PSA level. Additionally having a low PSA value does not guarantee that prostate gland is cancer free, some cancer patients have low PSA concentration in their serum. Therefore PSA has both low specificity and low positive predictive value especially when PSA level is moderately elevated (4-10 ng ml^{-1}) (Stephan, *et al.* 2007). For this reason research on PSA-based diagnostic parameters (score between free and complex form) and research for new prostate specific biomarkers is an ongoing study to increase specificity.

BIOMARKER DETECTION USING BIOSENSORS

PSA test is currently recognised as the clinically most used prostate cancer detection method. The current PSA tests rely on ELISA type assays and usually performed at centralised laboratories using expensive automated analyzers and time consuming procedures (Healy, *et al.* 2007). This process requires sample transportation, increased waiting time and high medical costs. Therefore there is a need to develop a detection system that is cheap, quick to process, uses low sample and reagent volume and easily operated. Additionally due to the weaknesses of PSA testing and complexity of prostate cancer, there is an increasing need to test multiple biomarkers simultaneously for cancer diagnosis/prognosis. Recent advances in the area of sensor technology and microarrays have enabled the miniaturisation of the devices and multiplex testing of a range of analytes. Therefore biosensor technology has the potential for the manufacture of point of care cancer testing devices.

Several biosensor types have been applied for the detection of PSA such as electrochemical biosensors (Sarkar, *et al.* 2002; Fernandez-Sanchez, *et al.* 2004; Li, *et al.* 2005; Liu, *et al.* 2007; Okuno, *et al.* 2007; Zhang *, et al.* 2007; Liu 2008; Panini, *et al.* 2008), optical biosensors (Schweitzer, *et al.* 2000; Besselink, *et al.* 2004; Yu, *et al.* 2004;

Huang, *et al.* 2005; Cao, *et al.* 2006; Choi, *et al.* 2008), fluorescence / chemiluminescence biosensors (O'Neill, *et al.* 1995; Soukka, *et al.* 2003; Ye, *et al.* 2004), microcantilever biosensors (Hwang, *et al.* 2004; Lee, *et al.* 2005; Wee, *et al.* 2005) and quartz crystal microbalance (QCM) biosensors (Zhang, *et al.* 2007). The detection limit of PSA using these systems varies between 0.2 pg ml^{-1} to 10 ng ml^{-1}. The detection signal has been amplified by means of a sandwich assay, gold nanoparticles, carbon nanotubes or PCR for the majority of the biosensor systems reported. Most of the applications performed PSA assay only in buffered pure solutions rather than serum, indicating the early stage of development of the technology.

PSA DETECTION USING QCMA 1 BIOSENSOR

Quartz crystal is a piezoelectric material which mechanically oscillates if an alternating voltage is applied. A quartz crystal microbalance (QCM) consists of a thin quartz disk sandwiched between a pair of electrodes. The mode of oscillation depends on the cut and geometry of the quartz crystal. If mass is applied on to the surface of the quartz resonator, the frequency of the oscillation slows down. By measuring the change of frequency, it is possible to determine the change in mass. In the current study, a QCMA 1 instrument has been employed as the biosensor platform for the detection of

 Published by Cranfield University Press ISBN: 978-0-9557436-7-2 http://hdl.handle.net/1826/3832

PSA. QCMA 1 is an automated QCM based biosensor developed by Sierra Sensors GmbH (Germany) (

Figure 1, A). QCMA 1 sensor chips possess two sensing spots each, enabling the measurement of active and control sensor surfaces simultaneously (

Figure 1, B). Easy handling of the sensor chips enables the user to customise the gold surface of the sensor as required and ready coated surfaces are also available from the producer.

 Published by Cranfield University Press ISBN: 978-0-9557436-7-2 http://hdl.handle.net/1826/3832

A B

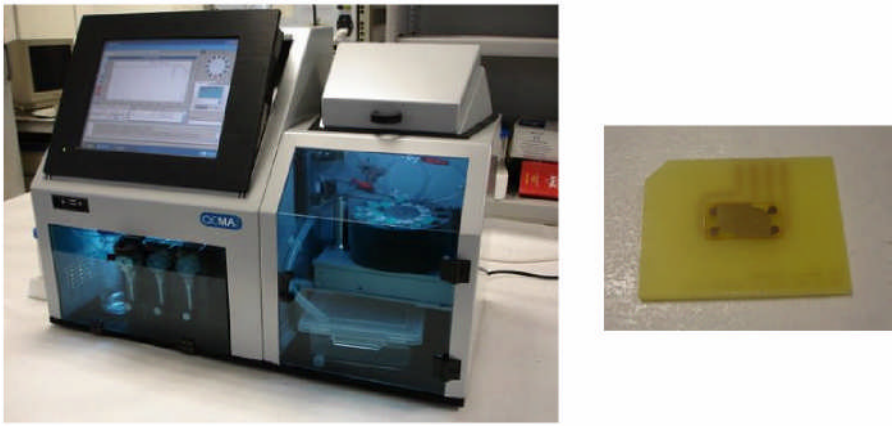

Figure 1. A) QCMA 1 biosensor. B) QCMA 1 affinity sensor chip.

EXPERIMENTAL

The experiments were conducted using an automated QCMA 1 biosensor (Sierra Sensors GmbH, Hamburg, Germany). The operating temperature of the assay was 25°C and the flow rate of the buffer was 80 μg ml^{-1} throughout the assay.

SENSOR CHIP FABRICATION

Gold coated QCMA affinity sensors were cleaned using an EMITECH K 1050X plasma cleaner. The cleaned quartz resonators were then submerged in a solution of 2 mM mercaptoundecanoic acid (Sigma-Aldrich, Poole, UK) in ethanol overnight. After rinsing with ethanol and water, sensors were dried with nitrogen stream. The coated sensors were then stored in the fridge (4°C) until use.

SENSOR SURFACE PREPARATION

Sensor surfaces were prepared by immobilising mouse anti-PSA capture antibody and Mouse IgG on sensors using conventional amine coupling chemistry. Running buffer used for immobilisation was degassed Dulbecco's modified phosphate buffered saline (PBS, pH 7.4; Sigma-Aldrich, Poole, UK). Sensor surfaces were first activated with (EDC/ NHS, Sigma-Aldrich, Poole, UK). A 15 μg ml^{-1} anti-PSA antibody (in sodium acetate buffer, pH 5.5) was then added to sensor 1 and then 15 μg ml^{-1} mouse IgG (in sodium acetate buffer, pH 5.5) to the second sensor surface. The chip surface was then

blocked with BSA (in PBS). Non-reacted NHS esters were capped with 1 M ethanolamine, pH 8.5 (Sigma-Aldrich, Poole, UK). The frequency changes were recorded 2 minutes after the protein injection was completed.

 Published by Cranfield University Press ISBN: 978-0-9557436-7-2 http://hdl.handle.net/1826/3832

PROSTATE SPECIFIC ANTIGEN ASSAY

After antibody immobilisation, the running buffer was changed to PBS buffer. PSA (Autogen Bioclear, Wilthshire,UK) was prepared in PBS buffer . PSA at specified concentrations was injected over anti-PSA antibody and mouse IgG immobilised surfaces for 3 minutes to allow binding. After a dissociation period under running buffer flow at 80 μl min^{-1}, surfaces were regenerated by injection of 100 mM HCl . Frequency change due to PSA binding was recorded 180 s after the injection started.

SIGNAL ENHANCEMENT ASSAY

After the binding of PSA at lower concentrations to the sensor surface, 1.5 μg ml^{-1} antiPSA detection antibody was injected for 3 minutes to perform a sandwich assay. After a dissociation period under running buffer flow at 80 μl min^{-1}, surfaces were regenerated by injection of 100 mM HCl (50 μl). Frequency change due to PSA binding was recorded 180 s after the injection started.

RESULTS AND DISCUSSION

The QCMA 1 biosensor was used as the sensor platform for the PSA detection assay. QCMA affinity sensors were initially coated with mercaptoundecanoic acid and anti-PSA capture antibody and mouse IgG were immobilised using conventional EDC-NHS chemistry. Anti-PSA capture antibody immobilised sensors produced an average frequency change of 380 ± 38 Hz (n=4) and mouse IgG immobilised sensor produced frequency change of 344 Hz (n=1).

The specificity of the interaction was tested by employing mouse IgG on the sensor surface, 5 μg ml^{-1} PSA binding to mouse IgG immobilised sensor surface did not result in any frequency change (data not shown). A 3 μg ml^{-1} anti-PSA detection antibody nonspecific binding to anti-PSA capture antibody immobilised surface was 1 ± 1 Hz (n=2). A 5 μg ml^{-1} BSA was injected to anti-PSA immobilised sensor surface, the non-specific binding of BSA to the surface was 4 ± 1 Hz (n=2). The non-specific response to the 5 μg ml^{-1} BSA was subtracted from each binding response.

The calibration curve obtained with PSA binding to the anti-PSA capture antibody immobilised surface in a concentration range between 5000 to 4.9 ng ml^{-1} is shown in Figure 2. The lowest detection was obtained when 19.5 ng ml^{-1} injected to the sensor surface as 6 ± 2 Hz (n=4).

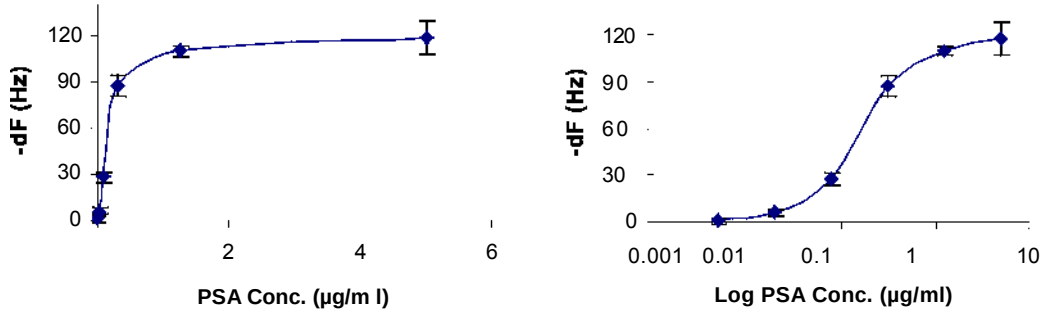

Figure 2. Frequency changes after 3 minutes of binding of the PSA to the anti-PSA antibody (control subtracted data, n = 4).

 Published by Cranfield University Press ISBN: 978-0-9557436-7-2 http://hdl.handle.net/1826/3832

To enhance the signal, a sandwich assay approach was followed employing anti-PSA detection antibody (Figure 3). A 4.9 ng ml^{-1} PSA binding to anti-PSA capture did not yield any frequency change, whereas a subsequent injection of anti-PSA detection antibody for 3 minutes yielded 17 ± 3 Hz (n=4) frequency change (Figure 4), increasing the sensitivity of the assay by 4 fold.

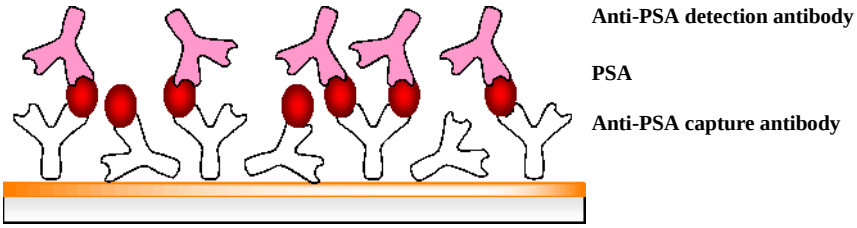

Figure 3. Schematic of the PSA sandwich assay.

 Published by Cranfield University Press ISBN: 978-0-9557436-7-2 http://hdl.handle.net/1826/3832

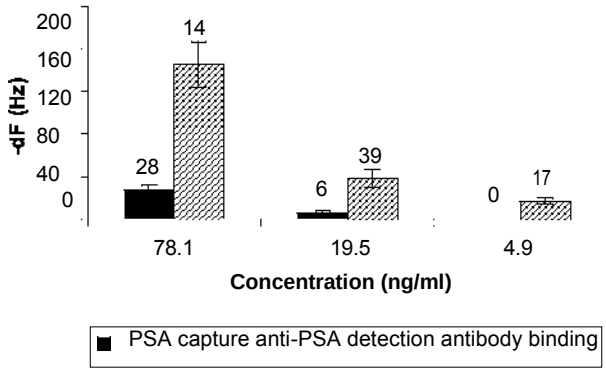

Figure 4. PSA sandwich assay results (n=4).

CONCLUSION

In the current study the potential of using QCM biosensors for the detection of PSA has been investigated. An automated QCMA 1 instrument was used as the biosensor platform. Both direct PSA assay and a sandwich PSA assay were performed using mercaptoundecanoic acid coated affinity sensor chip. Preliminary results indicated that the lowest signal obtained using direct assay was 19.5 ng ml^{-1}, and using sandwich assay was 4.9 ng ml^{-1}. The developed test require further optimisation and characterisation to further enhance the signal. Gold nanoparticles will be conjugated to the detection antibody and used in the assay to lower the detection limit of the sensor. Tests will be also repeated in human serum to asses the performance of the assay in closer to real conditions.

ACKNOWLEDGEMENTS

The authors would like to express their gratitude to Sierra Sensors GmbH for providing the QCMA 1 biosensor and affinity sensor chips.

REFERENCES

1. Besselink, G. A. J., R. P. H. Kooyman, P. J. H. J. van Os, G. H. M. Engbers and R. B. M.
2. Schasfoort (2004). "Signal amplification on planar and gel-type sensor surfaces in
3. surface plasmon resonance-based detection of prostate-specific antigen."
4. Analytical Biochemistry **333(1):** 165-173.
5. Brawer, M. K. and P. H. Lange (1989). "PSA in the screening, staging and follow-up of early-stage prostate cancer. A review of recent developments." World Journal of Urology **7(1):** 7-11.
6. Cao, C., J. P. Kim, B. W. Kim, H. Chae, H. C. Yoon, S. S. Yang and S. J. Sim (2006). "A strategy for sensitivity and specificity enhancements in prostate specific antigen-

 Published by Cranfield University Press ISBN: 978-0-9557436-7-2 http://hdl.handle.net/1826/3832

7. [alpha] 1 -antichymotrypsin detection based on surface plasmon resonance." Biosensors and Bioelectronics **21(11):** 2106-2113.
8. Choi, J. W., D. Y. Kang, Y. H. Jang, H. H. Kim, J. Min and B. K. Oh (2008). "Ultra-sensitive surface plasmon resonance based immunosensor for prostate-specific antigen using gold nanoparticle-antibody complex." Colloids and Surfaces A: Physicochemical and Engineering Aspects **313-314:** 655-659.
9. Diamandis, E. P. (1998). "Prostate-specific antigen: Its usefulness in clinical medicine." Trends in Endocrinology and Metabolism **9(8):** 310-316.
10. Fernandez-Sanchez, C., C. J. McNeil, K. Rawson and O. Nilsson (2004). "Disposable noncompetitive immunosensor for free and total prostate-specific antigen based on capacitance measurement." Analytical Chemistry **76(19):** 5649-5656.
11. Healy, D. A., C. J. Hayes, P. Leonard, L. McKenna and R. O'Kennedy (2007). "Biosensor developments: application to prostate-specific antigen detection." Trends in Biotechnology **25(3):** 125-13 1.
12. http://info.cancerresearchuk.org/cancerstats/types/prostate/incidence/. "Cancer Research UK. "Retrieved 26.02.2008.
13. Huang, L., G. Reekmans, D. Saerens, J. -M. Friedt, F. Frederix, L. Francis, S. Muyldermans, A. Campitelli and C. V. Hoof (2005). "Prostate-specific antigen immunosensing based on mixed self-assembled monolayers, camel antibodies and colloidal gold enhanced sandwich assays." Biosensors and Bioelectronics **21(3):** 483-490.
14. Hwang, K. S., J. H. Lee, J. Park, D. S. Yoon, J. H. Park and T. S. Kim (2004). "In-situ quantitative analysis of a prostate-specific antigen (PSA) using a nanomechanical PZT cantilever." Lab on a Chip - Miniaturisation for Chemistry and Biology **4(6):** 547-552.
15. Lee, J. H., K. S. Hwang, J. Park, K. H. Yoon, D. S. Yoon and T. S. Kim (2005). "Immunoassay of prostate-specific antigen (PSA) using resonant frequency shift of piezoelectric nanomechanical microcantilever." Biosensors and Bioelectronics **20(10):** 2157-2162.
16. Li, C., M. Curreli, H. Lin, B. Lei, F. N. Ishikawa, R. Datar, R. J. Cote, M. E. Thompson and C. Zhou (2005). "Complementary detection of prostate-specific antigen using In 2O3 nanowires and carbon nanotubes." Journal of the American Chemical Society **127(36):** 12484-12485.
17. Liu, G., Y. Y. Lin, J. Wang, H. Wu, C. M. Wai and Y. Lin (2007). "Disposable electrochemical immunosensor diagnosis device based on nanoparticle probe and immunochromatographic strip." Analytical Chemistry **79(20):** 7644-7653.
18. Liu, Y. (2008). "Electrochemical detection of prostate-specific antigen based on gold colloids/alumina derived sol-gel film." Thin Solid Films **516(8):** 1803-1808.
19. O'Neill, P. M., J. E. Fletcher, C. G. Stafford, P. B. Daniels and T. Bacarese-Hamilton (1995). "Use of an optical biosensor to measure prostate-specific antigen in whole blood." Sensors and Actuators B: Chemical **29(1-3):** 79-83.
20. Okuno, J., K. Maehashi, K. Kerman, Y. Takamura, K. Matsumoto and E. Tamiya (2007). "Label-free immunosensor for prostate-specific antigen based on single-walled carbon nanotube array-modified microelectrodes." Biosensors and Bioelectronics **22(9-10):** 2377-2381.
21. Panini, N. V., G. A. Messina, E. Salinas, H. Fernandez and J. Raba (2008). "Integrated microfluidic systems with an immunosensor modified with carbon nanotubes for detection of prostate specific antigen (PSA) in human serum samples." Biosensors and Bioelectronics **23(7):** 1145-1151.

 Published by Cranfield University Press ISBN: 978-0-9557436-7-2 http://hdl.handle.net/1826/3832

22. Sarkar, P., P. S. Pal, D. Ghosh, S. J. Setford and I. E. Tothill (2002). "Amperometric biosensors for detection of the prostate cancer marker (PSA)." International Journal of Pharmaceutics 238(1-2): 1-9.
23. Schweitzer, B., S. Wiltshire, J. Lambert, S. O'Malley, K. Kukanskis, Z. Zhu, S. F. Kingsmore, P. M. Lizardi and D. C. Ward (2000). "Immunoassays with rolling circle DNA amplification: A versatile platform for ultrasensitive antigen detection." Proceedings of the National Academy of Sciences of the United States of America 97(18): 10113-10119.
24. Soukka, T., K. Antonen, H. Harma, A. -M. Pelkkikangas, P. Huhtinen and T. Lovgren
25. (2003). "Highly sensitive immunoassay of free prostate-specific antigen in serum
26. using europium(III) nanoparticle label technology." Clinica Chimica Acta 328(1-
27. 2): 45-58.
28. Stephan, C., K. Jung, M. Lein and E. P. Diamandis (2007). "PSA and other tissue kallikreins for prostate cancer detection." European Journal of Cancer 43(13): 19 18-1926.
29. Wee, K. W., G. Y. Kang, J. Park, J. Y. Kang, D. S. Yoon, J. H. Park and T. S. Kim
30. (2005). "Novel electrical detection of label-free disease marker proteins using
31. piezoresistive self-sensing micro-cantilevers." Biosensors and Bioelectronics
32. 20(10): 1932-1938.
33. Ye, Z., M. Tan, G. Wang and J. Yuan (2004). "Preparation, Characterization, and Time-Resolved Fluorometric Application of Silica-Coated Terbium(III) Fluorescent Nanoparticles." Analytical Chemistry 76(3): 513-518.
34. Yu, F., B. Persson, S. Lo?fa?s and W. Knoll (2004). "Surface plasmon fluorescence immunoassay of free prostate-specific antigen in human plasma at the femtomolar level." Analytical Chemistry 76(22): 6765-6770.
35. Zhang, B., X. Zhang, H. h. Yan, S. j. Xu, D. h. Tang and W. l. Fu (2007). "A novel multi-
36. array immunoassay device for tumor markers based on insert-plug model of
37. piezoelectric immunosensor." Biosensors and Bioelectronics 23(1): 19-25.
38. Zhang, S., P. Du and F. Li (2007). "Detection of prostate specific antigen with 3,4-
39. diaminobenzoic acid (DBA)-H2O2-HRP voltammetric enzyme-linked
40. immunoassay system." Talanta 72(4): 1487-1493.

 Published by Cranfield University Press ISBN: 978-0-9557436-7-2 http://hdl.handle.net/1826/3832

Speeding up Office/Database/Web/Media Applications over Internet/Grids

Frank Z. Wang & Sining Wu

Centre for Grid Computing, Cambridge-Cranfield HPCF, AMAC/SOE, Cranfield University, UK

Na Helian

Department of Computer Science, University of Hertfordshire, UK

Wendy Zhang

Wuhan University, P.R. China

Chenhan Liao & M.D. Rashidi

Centre for Grid Computing, Cambridge-Cranfield HPCF, AMAC/SOE, Cranfield University, UK

Zhiwei Xu

Institute of Computer Technology, Chinese Academy of Sciences

Computational grids are often characterized with network latencies greater than 2 ms. Driven by this problem, Grid-oriented Storage (GOS) is designed to deal with cross-domain and single-image file operations. GOS behaves like a file server via a file-based GOS-FS data communication protocol to any entities. We experimentally demonstrate that the parallel-streamed GOS-FS can attain a speedup of 4.9 against NFS/AFS/pNFS(PVFS) that co-exist on the same machine. Conforming to the common interface, GOS can be pervasively used as an underlying platform to accelerate other applications, including OpenOffice, MySQL/IBM DB2, Firefox, MPlayer, Google Earth and Data Mining. This report describes its parallel streaming, dynamic numbering, fast-start effect, multi-path routing and multicore–based code re-engineering. It was demonstrated that GOS can accelerate distributed applications by up to tenfold in real-world tests. During the presentation, a demo will be shown on laptops.

Recently the GOS work has won an ACM/IEEE Super Computing Award in USA. Since 2007, the GOS invention led to invited talks and demonstrations at Princeton University, Carnegie Mellon University, Cambridge University, Oxford University, Edinburgh University, York University, and King's College London, etc. Grid Computing technology developed at Cranfield has been embraced by IBM, Xerox, BBC, EADS, Rolls Royce and CERN, which is capable of narrowing the gap between the peak performance that high performance computers are theoretically capable of and the actual performance that can be achieved with current application software.

 Published by Cranfield University Press ISBN: 978-0-9557436-7-2 http://hdl.handle.net/1826/3832

Development of a Novel Enzymatic Biodegradability Test Method and Comparison with Existing Microbial Methods

Stuart T. Wagland †, Andrew R. Godley ‡, Jim Frederickson §, Sean F. Tyrrel† and Richard Smith †*

†Centre for Resource Management and Efficiency, Sustainable Systems Department, School of Applied Sciences, Cranfield University, Cranfield, Bedfordshire MK43 0AL, UK ‡WRc plc, Frankland Road, Blagrove, Swindon, Wiltshire, SN5 8YF, UK

§ Integrated Waste Systems, The Open University, Walton Hall, Milton Keynes, MK7 6AA, UK

ABSTRACT

Rapid methods are required for the routine testing of the biodegradability of diverse organic waste materials and to assess the performance of biological waste treatment processes. Here a novel enzymatic hydrolysis test (EHT) has been evaluated as a surrogate for conventional microbial biodegradability methods using 37 assorted organic waste samples collected from diverse sources. The results of the EHT method are compared with those obtained from two conventional tests; the 4 day aerobic DR4 and 100 day anaerobic BM100 test methods currently applied in the UK for monitoring biodegradable municipal waste diversion from landfill by mechanical biological treatment and similar processes. The EHT is based on the enzymatic hydrolysis of cellulolytic materials and can be completed in less than 24 hours. In this study linear regression for all 37 samples against the BM100 data showed the DR4 provided a correlation coefficient of $r = 0.581$; the EHT method gave a correlation of $r = 0.617$ for the total DOC release; and $r = 0.77$ for the DOC released from enzymatic hydrolysis. The correlations suggest that the EHT method may be better suited to a wider range of waste types when correlating with anaerobic BM1 00 test results since it more closely mimics the full extent of decomposition rather than that from the readily biodegradable fraction.

INTRODUCTION

In Europe, the landfill directive (Council of the European Union, 1999) sets specific requirements for the design and operations of landfill sites, including the types of waste that can be accepted into these landfills. One of the aims of the landfill directive is to reduce the amount of biodegradable municipal waste (BMW) sent to landfill (Godley et al., 2004). To achieve these reductions, the directive sets targets for member states to progressively reduce the amounts of BMW landfilled to 75% of the 1995 baseline amount by 2006, 50% by 2008, and finally 35% by 2016 (Bench et al., 2005; Council of the European Union, 1999). Organic waste can be treated to reduce the BMW content in processes such as mechanical-biological treatment (MB T), a generic term to describe the process of mechanically sorting and shredding the waste followed by biological treatment by composting or anaerobic digestion (Archer et al., 2005). Monitoring such processes is an important aspect in assisting operators to achieve desired performance criteria, optimise the process and to estimate the amount of BMW diverted from landfill resulting from treatment (Environment Agency, 2005). This may include analysing waste samples for biodegradability using appropriate methods.

 Published by Cranfield University Press ISBN: 978-0-9557436-7-2 http://hdl.handle.net/1826/3832

Following a review of the current methods (Godley et al., 2003) it has been concluded that there is a need for a rapid and cost-effective test method that would mimic and correlate with longer-term tests such as the anaerobic BM100 method. The BM100 test method is not suitable for regular routine testing due to its duration, however a correlating method could make routine testing viable.

Hemicellulosic/cellulosic material is considered as the most important carbon source for methanogenesis in landfills as it contributes to 90% of the total biogas (CO_2 + CH_4) produced (Rodriguez et al., 2005). Cellulose and hemicellulose are hydrolysed by cellulase and hemicellulase enzymes respectively and so the novel enzymatic hydrolysis test (EHT) method based on the enzymatic hydrolysis of cellulolytic material could offer a suitable routine test method. This would mimic the natural microbial hydrolysis of organic matter and would be expected to take account of the impact of lignin on the availability of cellulose. A high concentration of enzyme can be added to the test which might be expected to hydrolyse all the potentially hydrolysable cellulose and therefore more closely mimic the long term BM100 test rather than shorter term DR4 tests.

In this study we have compared the novel non-microbial EHT method with a microbial based 100 day anaerobic test (BM100) and the 4 day aerobic test (DR4), the latter two methods being specified in guidance for monitoring MBT processes in England and Wales (Environment Agency, 2005). These biodegradability test methods have been applied to 37 waste samples from a range of sources in the UK. The DR4 and EHT methods are compared and correlated with the longer-term BM100 method.

MATERIALS AND METHODS

SAMPLES

The organic waste samples were collected from a wide range of treatment processes and specific waste streams in the UK as part of Defra project WRT220 on waste characterisation. The samples included MSW derived samples, garden waste (partially treated in the short-term, stabilised and longer-term fully treated) and samples from specific waste streams such as fish, wood, pizza and feathers. Where possible the samples were collected pre-, during and posttreatment by either MBT or a mechanical thermal (autoclave) treatment. The biological treatment of the samples was either composting or anaerobic digestion.

The waste samples were sorted to remove glass, metals, plastics and inert materials with the biodegradable material being retained and tested. Materials with large particle sizes were shredded to $<$10 mm before testing. The dry matter (DM) and loss-on-ignition (LOI) was determined for this sample using standard procedures (EN12879:2000).

BIODEGRADABILITY TEST METHODS

Two UK established biodegradability test methods were used in this investigation. In a recent comparison of the two methods (Godley *et al.,* 2007), it was stated that the 4 day aerobic test measures the rate of aerobic degradation, whereas the 100 day anaerobic test measures the extent.

 Published by Cranfield University Press ISBN: 978-0-9557436-7-2 http://hdl.handle.net/1826/3832

Dynamic respiration over 4 days (DR4): Biodegradability under aerobic conditions was determined using the DR4 test method (Environment Agency, 2005). The test material (100 g DM) is prepared as outlined previously and mixed with the mature compost seed material (100 g DM). Water and nutrients (nitrogen and phosphorous) were added to adjust to 50% w/w moisture content. The test mixture was then placed in a reactor vessel at 35°C for 4 days, with constant aeration (Environment Agency, 2005) through the reactor vessel. The CO_2 released over the 4 day period is measured and this data is used to estimate O_2 consumption.

Biochemical Methane Potential over 100 days (BM100): The BM100 test method (Environment Agency, 2005) is based on a sewage sludge digestion test (Godley *et al.,* 2007; Godley *et al.,* 2003). The test material (20 g LOI) was placed in a glass container with microbial seed (digested sludge) and a nutrient mixture. The mixture was sealed and incubated at 35°C under anaerobic conditions and the release of CO_2 and CH_4 (biogas) was measured volumetrically until no further biogas was released (up to 100 days).

NOVEL BIODEGRADABILITY TEST METHOD

A novel biodegradability test method based on the enzymatic hydrolysis of cellulolytic materials has been developed (Wagland et al., 2007).

For each sample 25 mg of crude cellulase powder (Sigma) and 75 mg of hemicellulase powder (Sigma) were dissolved in 20 ml of distilled water. The test method consists of three phases (Fig 1) as follows:

 Published by Cranfield University Press ISBN: 978-0-9557436-7-2 http://hdl.handle.net/1826/3832

Phase 1: The waste sample (5 g LOI) was placed in a 250 ml Erlenmeyer flask. Phosphate pH buffer (100 ml 0.37 M) was then added to the flask. A 5 ml sample was removed and filtered (0.45μm membrane filter) to remove any solids, and the filtered liquid was then analysed for chemical oxygen demand (COD) (Spectroquant COD test tubes).

Phase 2: The sample mixture was then autoclaved at 121°C for 15 min to sterilise the mixture and a further 5 ml sample was removed and filtered for COD analysis.

Phase 3: The prepared enzyme solution (20 ml) was then added to each of the flasks and the flask sealed with a neoprene bung. The flasks were placed in a shaking incubator at 150 rpm. A 5 ml sample was removed for COD analysis after 20 h of incubation.

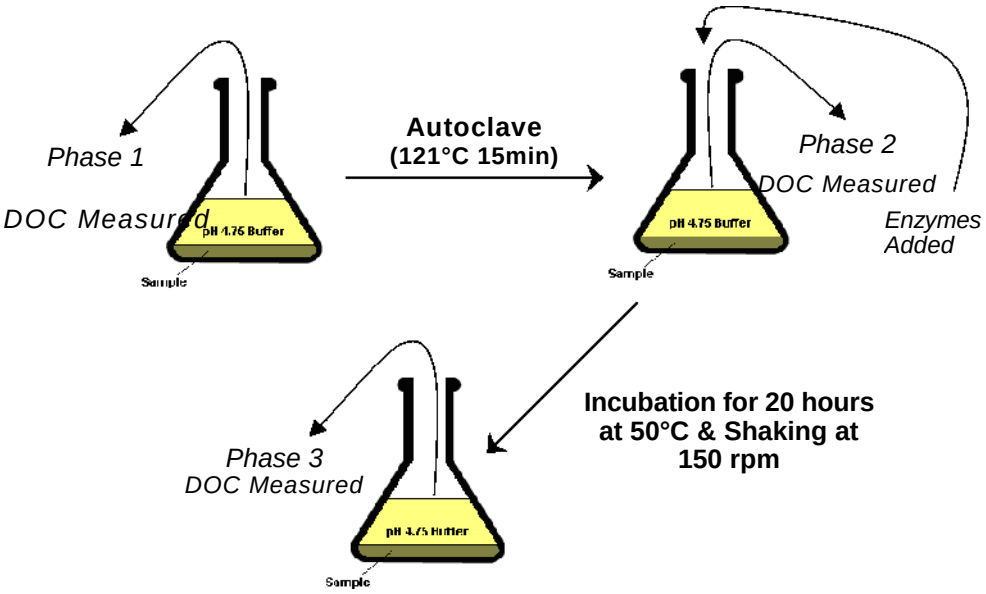

Figure 1. Schematic diagram of the EHT method.

The amount of moisture in the waste sample and the removal of both the liquid and solids at each stage of sampling, along with the addition of liquid in phase 3, were accounted for in the concentrations of carbon calculated.

RESULTS AND DISCUSSION

The DOC released at each phase of the EHT varied greatly. Phase 1 DOC is likely to represent the low molecular weight readily soluble materials present in the waste. The DOC released in Phase 2 may represent soluble DOC following mild acid hydrolysis of some of the polymeric components during autoclaving. Phase 2 DOC may also include soluble materials desorbed from the waste during autoclaving. The DOC released in Phase 3 results from the enzymatic hydrolysis of the material, and so may indicate the amount of additional biodegradable cellulose, hemicellulose and possibly proteinaceous material present.

The non-enzymatic DOC (Phases 1 and 2) for wastes that have undergone extended biological treatment (e.g. the fully composted green waste and composted MSW derived BMW

 Published by Cranfield University Press ISBN: 978-0-9557436-7-2 http://hdl.handle.net/1826/3832

samples), are likely to consist of significant amounts of humic substances resulting from the decomposition of lignin (Stevenson, 1994). These substances are not usually considered to be readily biodegradable, and so in these cases, the DOC due to enzymatic hydrolysis (Phase 3 only) may be indicative of sample biodegradability. Unlike the control polymeric cellulose, many of the untreated (raw or autoclaved) waste samples also showed significant amounts of DOC released during Phases 1 and 2. As these wastes have not been biologically treated it is likely that much of the DOC released during Phases 1 and 2 will be inherently biodegradable.

The total DOC release in the EHT is evaluated as an indication of sample biodegradability. However, since a proportion of Phase 2 DOC will contain non-biodegradable carbon, the DOC released in Phase 3 only is also evaluated.

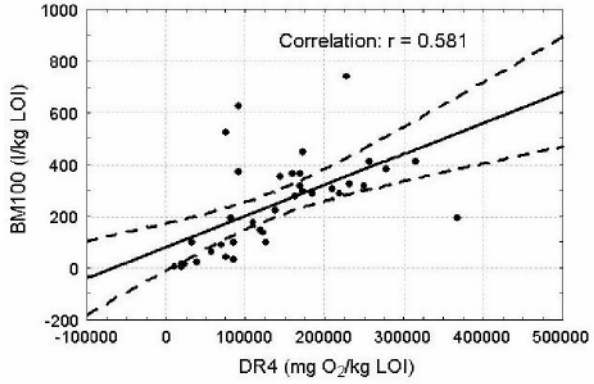

Figure 2. Correlation of DR4 with BM100 data for all samples

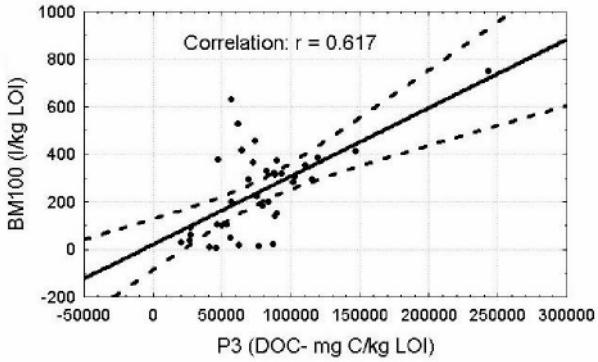

Figure 3. Correlation of EHT (total DOC) with BM100 data for all samples

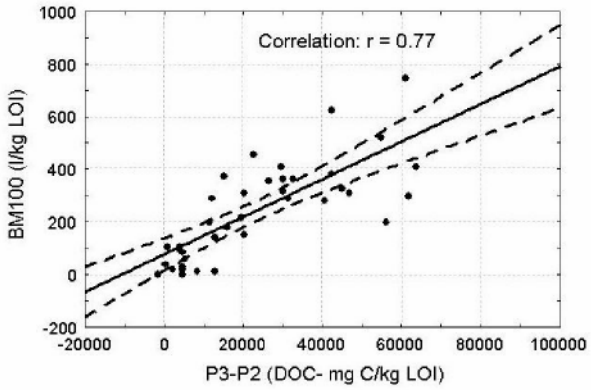

Figure 4. Correlation of EHT (DOC from enzyme hydrolysis) with BM100 data for all samples

Figures 2, 3 and 4 show the relationship between the DR4, EHT and the BM100 data. For the EHT the total DOC is shown in figure 3, and the DOC from enzyme hydrolysis alone is shown in figure 4. From the correlation of the DR4 and EHT against the BM100 data, EHT shows the greater linear correlation with the BM100. The correlation coefficient (r) of 0.617 for the EHT (total DOC) is highly significant ($p < 0.001$), as is the correlation coefficient of 0.58 1 for the DR4 ($p < 0.001$). The relationship between the EHT and BM100 data is stronger when only the DOC released from enzymatic hydrolysis is considered, giving a correlation coefficient

 Published by Cranfield University Press ISBN: 978-0-9557436-7-2 http://hdl.handle.net/1826/3832

of 0.77 ($p < 0.001$). The correlations suggest that the EHT method is better suited to a wider range of waste types, particularly when considering the relationship of the DOC from enzyme hydrolysis and the BM100 (Fig 4).

CONCLUSIONS

The EHT is a suitable alternative routine biodegradability test method, offering a reduction on the timescales of the DR4 test method. The EHT is completed in less than 24 hours compared to 4 days for the DR4. The EHT is being considered as an alternative test method incorporated in a consultation to revise the MBT monitoring guidance for England and Wales (Environment Agency, 2005).

Correlations of the EHT with the BM100 show the significance of the EHT method as an alternative short-term test method, however further research is in progress aimed at improving the versatility and validity of the EHT method.

REFERENCES

1. Archer, E., Baddeley, A., Klein, A., Schwager, J. and Whiting, K. (2005). Mechanical-biological treatment: a guide for decision makers- processes, policies and markets (summary report), Juniper Consultancy Services Ltd.
2. Bench, M. L., Woodard, R., Harder, M. K. and Stantzos, N. (2005). Waste minimisation: Home digestion trials of biodegradable waste. Resources, Conservation and Recycling 45(1), 84-94. Council of the European Union (1999). Directive 1999/31/EC on the Landfill of Waste. Official Journal of the European Communities L 182, 1-19.
3. Environment Agency (2005). Guidance on monitoring MBT and other pre-treatment processes for the landfill allowances schemes (England and Wales). 37.
4. Godley, A., Lewin, K., Frederickson, J., Smith, R. and Blakey, N. (2007). Application of DR4 and BM100 biodegradability tests to treated and untreated organic wastes. Proceedings Sardinia, Eleventh International Waste Management and Landfill Symposium, S. Margherita di Pula, Cagliari, Italy.
5. Godley, A. R., Lewin, K., Graham, A., Barker, H. and Smith, R. (2004). Biodegradability determination of municipal waste: an evaluation of methods. Waste 2004- Integrated Waste Management and Pollution Control: Policy and Practice, Research and Solutions, Stratford-upon-Avon, UK.
6. Godley, A. R., Lewin, K., Graham, A. and Smith, R. (2003). Environment agency review of methods for determining organic waste biodegradability for landfill and municipal waste diversion. Proceedings 8th European Biosolids and Organic Residuals Conference, Wakefield, UK.
7. Rodriguez, C., Hiligsmann, S., Ongena, M., Thonart, P. and Charlier, R. (2005). Development of an enzymatic assay for the determination of cellulose bioavailability in municipal solid waste. Biodegradation 16(5), 415-422.
8. Stevenson, F. J. (1994). Humus Chemistry, John Wiley & Sons Inc: 188-211.
9. Wagland, S. T., Tyrrel, S. F., Smith, R., Godley, A. R. and Blakey, N. (2007). Development and application of an enzymatic hydrolysis test to assess the biodegradability of organic waste material. Proceedings Sardinia, Eleventh International Waste Management and Landfill Symposium, S. Margherita di Pula, Cagliari, Italy, CISA.

 Published by Cranfield University Press ISBN: 978-0-9557436-7-2 http://hdl.handle.net/1826/3832

Quantum Dot Encoded Microsphere Bio-conjugates: Application to Forensic Genotyping Particle-based Bio-Assay

Sarah Thiollet, Nicola White, Sarah Morgan*

Department of Bio-medical and Analytical Sciences, Cranfield Health, Cranfield University, MK454DT, Bedfordshire.

* Corresponding author: Sarah Morgan, Cranfield Health, Cranfield University MK454DT, U.K., Phone: +44 (0)1525 863013, Fax : +44 (0)1525 863533, email: s.morgan@cranfield.ac.uk

ABSTRACT

A challenging field of research in molecular diagnostics is the development of optimised screening assays adaptable to a large panel of applications. We suggest here the choice of a method joining multiple fields of expertise that could overcome the current limitations of high through put (HT) technology used in genotyping screening analysis. The method is based on new advanced fluorescent materials, the quantum dot encoded microsphere (QDEM) and flow cytometry technology. A small quantity of QDEM was successfully coupled to specific DNA probes with high efficiency. Difficulties regarding the manipulation of QDEM and computational data analysis were overcome. The optimisation of QDEM bio-conjugates for its application to DNA hybridisation was achieved using one approach of experimental design: the surface response methodology (RSM). Using this new approach, we determined the best conditions for the hybridisation of oligonucleotides to QDEM surface in solution adapted to HT screening assay. The method was designed for forensic genotyping applications. Microsphere bio-based assay using flow cytometric detection of multiple targets in the same small volume reaches the criteria of large scale screening bioassays: speed, sensitivity and accuracy. However there are still some challenges remaining for suspension arrays to be fully automated as HT measurement platform applied to various screening assay as large scale single nucleotide polymorphism genotyping or proteinRNA/DNA interactions.

 Published by Cranfield University Press ISBN: 978-0-9557436-7-2 http://hdl.handle.net/1826/3832

INTRODUCTION

Introduction of inorganic fluorophores in the fluorescent bioscience world has been revealed and confirmed as a real breakthrough. The initial work of Chan and Nie, 1998 (*1*), highlights semi-conductor nanocrystal materials or quantum dots (QD) as new optimum fluorescent dyes (*2-5).* Due to their exceptional spectral properties a unique spectral 'bar-code' can be generated by pulling different QD at different concentration in synthetic bead structures and illuminate them with a single light source (*6*). Quantum dot encoded microsphere (QDEM) is an advanced material technology incredibly promising for high throughput screening (HTS) bio-assays. Compare to previous fluorescent bead, QDEM superior optical properties allow the production of a unique enhance number of fluorescent probes (*7*). Different surface "capping" strategies providing solubilisation and bio-functionalisation created a flexible use of the material. QDEM bio-conjugates supersede analogous bead encoded with organic dye conjugate in terms of higher chemical- and photo-stability, lower limits of detection, and higher levels of multiplex ability.

Single nucleotide polymorphism (SNP) genotyping technology is a subject of intensive research in forensic genetic. As yet no method(s) of reference have arisen. Current allele specific oligonucleotide (ASO) hybridization methods of genotyping in a homogenous format are constrained by limited multiplexing capability or are highly time consuming and costly (*8*). The most advanced commercial system for large scale analysis is the Luminex platform™ (Invitrogen, CA., U.S.A.). A duo of organic dyes is used to encode a 100 bead library (*9*). The method is still limited because it requires multiple excitation spectra and presents the drawback of emission overlaps of organic fluorophores. Instrumentation limitation and the weakness of organic fluorophore coding resolution prohibit the enlargement of bead based libraries. Our research group is investigating the feasibility of overcoming these limitations by developing high throughput HT optimisation of ASO QDEM-based genotyping assay.

This study presents the optimisation of QDEM conjugation to deoxyribonucleotide (DNA) probes in a small homogeneous format. In comparison with previous work, QDEM bio-conjugation methodology was by far more efficient in terms of experimental time, coupling efficiency and reagent consumption. The second novelty of this work consisted in optimising DNA detection and hybridisation with QDEM bioconjugates technology using the design of experiment (DOE) approach (*10).* The method was designed for an optimum application to multiplex SNP genotyping.

 Published by Cranfield University Press ISBN: 978-0-9557436-7-2 http://hdl.handle.net/1826/3832

MATERIALS & METHODS

Chemicals and Microspheres. Solvents and chemicals were purchased from Sigma Chemical (Poole, U.K.) and Fisher Scientific (Loughborough, U.K). Oligonucleotides were obtained from Thermo Electron (Bremen, Germany). Quantum dots encoded carboxylated polystyrene microspheres of 5 *p*m diameters were purchased from Crystaplex (PA., U.S.A.). Samples were analysed with a Coulter Epics XL-MCL flow cytometer (FC) (Beckman- Coulter, FL, U.S.A.) equipped with a 488 nm argon-ion laser.

QDEM coupling reaction. QDEM were coupled to increasing quantity of oligonucleotide probes in 2[N-Morpholino] ethanesulfonic acid, (MES) pH 4.5 coupling buffer. The method schematised in figure 1-A was adapted from Lowe *et al.* 1999 (*11).* Samples were analysed on the FC in 0.1 M TE pH 8.0 analysis. Previous protocol was repeated by replacing MES buffer with 0.1 M imidazole pH 7.0 buffer.

QDEM hybridisation assay (figure 1-B). After conjugation QDEM sample were hybridised in 6 X SSC buffer and carefully washed before analysis on the FC (*12).* Hybridisation assay parameters were optimised using response surface methodology (RSM) (*13).* The central composite design (CCD) was employed in this regards (*14).*

Oligonucleotides. "Direct" and "Indirect" conjugation probes were designed as described in figure 1.

Quantitative analysis. The QuantiBRITE PE bead kit (Becton Dickinson, BD, biosciences, U.K.) was used as previously described (*15-16)* to evaluate the molecules of equivalent of soluble fluorochrome (MEF) or the number of oligonucleotides attached per QDEM (*17).*

Statistical analysis. Flow cytometry data (fcs data files) were acquired and the median fluorescent intensity (MdFI) was calculated for the fluorescent probe signal with in-house applications created with MATLAB (The Math Works, MA, U.S.A.).

RSM and optimisation of experimental factors were calculated with available on line free softwares.

 Published by Cranfield University Press ISBN: 978-0-9557436-7-2 http://hdl.handle.net/1826/3832

RESULTS & DISCUSSION

OPTIMISATION OF QDEM BIOCONJUGATE: STUDY OF THE COUPLING EFFICIENCY

An optimal bio-conjugation methodology was developed adapting methodology previously described with organic dye encoded beads (*11).* The quantification of the number of oligonucleotides attached to the QDEM, showed a global improved response of coupling with the imidazole buffer than with the MES buffer. The numerical MEF values calculated were coherent with the mean signal obtained in previous studies using different kind of beads (*11-18).* A specific study in MES buffer was carried out by Wittebolle *et al.* using 100 000 polybead of 3 µm diameter (Polysciences, IL, U.S.A.). This group obtained a maximum Cy3 signal 10 times inferior to the signal calculated with our methods using Imidazole buffer (*19).*

These results non only provided confidence to assess the superiority of imidazole buffer versus MES but also showed a significant improvement of the QDEM methodology.

High oligonucleotide density increases repulsion forces and steric interactions. Therefore, we chose a constant value largely inferior to the saturation point but with good conjugation efficiency, to synthesised QDEM bio-conjugate for hybridisation experiments.

Optimisation of DNA hybridisation. DNA target concentration, incubation time and temperature, and hybridisation signal response were satisfactory optimised as previously described (*20).* Statistical analysis indicated the model was satisfactorily adequate to describe the Cy3 signal response and was adapted to predict optimised conditions. Optimised conditions defined by the model will be applied in the third step of the optimisation of the ASO hybridisation assay adapted to DNA markers identification.

 Published by Cranfield University Press ISBN: 978-0-9557436-7-2 http://hdl.handle.net/1826/3832

CONLCUSION

Quantum dots encoded microspheres present a real great potential for HT bead-based assay that require multiplexed fluorescent bio-conjugates.

It has been demonstrated QDEM can be conjugated to small nucleotide probes in 1 hour, reaching higher conjugation efficiency than previous work. QDEM are expensive to acquire as the technology is still under development. Optimising an assay utilizing a small quantity of QDEM is therefore well adapted to develop future experiment in HT format using this technology. DOE was successfully applied to DNA hybridisation in suspension array.

Further work involves the application of the optimum hybridisation conditions defined in this paper to finalise the ASO hybridisation assay. Application of the novel ASO QDEM- based assay includes forensic genotyping for human identification study, molecular diagnostic of genetic disease, and identification of functional mutations in genes for pharmacogenetic applications.

Flow cytometry is rapidly evolving as a platform for automated HTS cell and microsphere-based systems. Modification of fluidics system makes HT platform compatible with sampling in multiple well plates (*22).* Portable flow cytometer and enhanced microfluidic devices promise a solution for real-time and field HTS identification of analytes using multiplex accurate bead-based assay.

 Published by Cranfield University Press ISBN: 978-0-9557436-7-2 http://hdl.handle.net/1826/3832

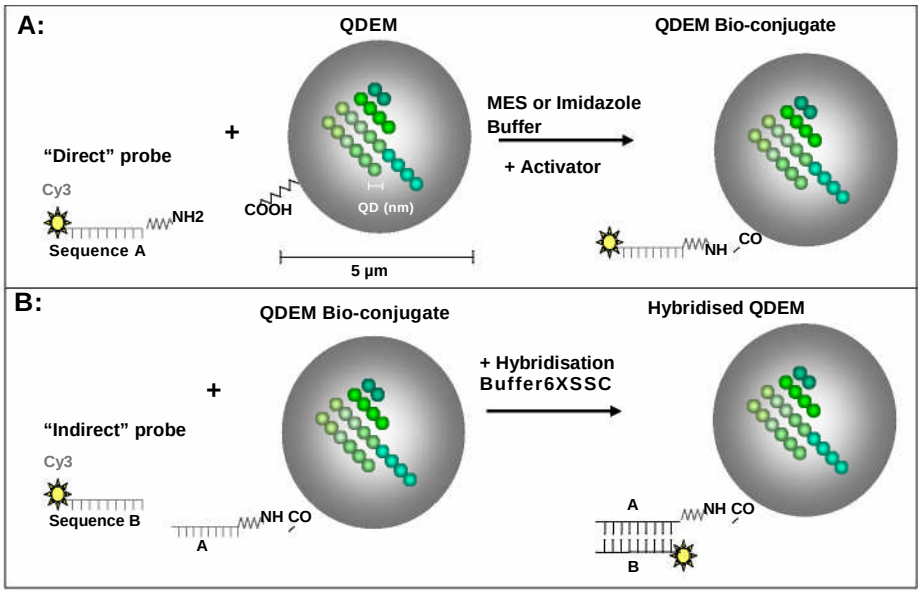

Figure 1. Schematic representation of coupling and hybridization experimental design.

A- Conjugation with direct probes. B- Hybridisation with indirect probes. QDEM can be encoded with different ratio of QD emitting at different wavelengths. QDEM specific signal encoded in terms of color and intensity, allows the discrimination between QDEM and the fluorescent probe attached. Oligonucleotide sequence A and B are complementary. The conjugation is realized with a carbodiimide reaction: amino group (NH2) reacting with carboxylated groups (-COOH). Cy3: Cyanin 3 organic fluorophore.

REFERENCES

(1) Chan *et al.* 1998; (2) Norris *et al.* 1993; (3) Dabbousi *et al.* 1997; (4) Medintz *et al.* 2005; (5) Bailey *et al.* 2004; (6) Han *et al.* 2003; (7) Gao *et al.* 2004; (8) Carracedo *et al.* 2005 ;(9) Dunbar *et al.* 2006; (10) Wrobel *et al.* 2003; (11) Lowe *et al.* 1999; (12) Wang *et al.* 2006; (13) Haaland *et al.* 1989; (14) Montgomery *et al.* 1991 ; (15) Kulwinder *et al.* 2001 (16) Schwartz *et al.* 1998; (17) Technical Quantibrite™ PE source book section 2.24.1; (18) Spiro *et al.* 2000; (19) Wittebole *et al.* 2006 ; (20) Lomillo *et al.* 2005 ; (21) Edwards *et al.* 2007

 Published by Cranfield University Press ISBN: 978-0-9557436-7-2 http://hdl.handle.net/1826/3832

Monitoring and variation of bioaerosols at composting facilities using conventional and novel samplers

G.H. Drew[a], A. Nogami[b], A. Tamer Vestlund[a], L. Pankhurst[a], I. Seymour[c], W. Batty[d], L.J. Deacon[a], S.J.T Pollard[a] and S.F. Tyrrel[a]

[a]*Centre for Resource Management and Efficiency,* [c]*School of Applied Sciences, Cranfield University, Bedfordshire, MK43 0AL, UK;* [b]*Department of Environmental Space Design, University of Kitakyushu, Fukuoka, 808-0135, Japan;* [d]*Cranfield University at Kitakyushu, 2-5-4F Hibikino, Wakamatsu-ku, Kitakyushu 808-0135, Japan*

ABSTRACT

Risk assessments examining the impacts of bioaerosols from composting facilities are limited by the quality of the bioaerosol source term data available. Here we test a novel sampler and filter, and examine the variability of replicated samples. The actinomycetes concentrations captured were *ca.* 10^5 cfu/m^3 for both samplers. The *Aspergillus fumigatus* concentrations were *ca.* 10^4 cfu/m^3 for the SKC samplers, and *ca.* 10^3 cfu/m^3 for the novel samplers. Modifications to the novel sampler may explain why fewer *A. fumigatus* spores were captured. Furthermore, the analysis revealed greater variation in the *A. fumigatus* concentrations than in the actinomycetes concentrations.

INTRODUCTION

Bioaerosols are airborne micro-organisms and their constituents (Swan *et al.*, 2003). The promotion of composting in the UK (Cm 7086, 2007) has led to concerns about public health impacts from bioaerosols emitted from composting facilities. Regulators in the UK require risk assessments for any facility with a sensitive receptor (e.g. homes or schools) within 250m of the facility boundary (Environment Agency, 2001). The quality of any risk assessment is dependant on the availability and quality of the source term data (Pollard *et al.*, 2006). These data are frequently limited, in part because of the practical difficulties of microbiological sampling and analyses. As a result, statistics on the variability of bioaerosol concentrations are frequently absent and constrains the capacity of risk analysts to set confidence limits on bioaerosol source term concentrations. Numerous methods are available to capture bioaerosols (Nielsen *et al.*, 1997; Stetzenbach *et al.*, 2004), mostly based on culturing of micro-organisms, resulting in a delay between sample capture and bioaerosol enumeration. This may also result in under estimation compared to sampling methods that estimate total micro-organism counts (Karlsson and Malmberg, 1989). A novel, porous polymer filter with a honeycomb structure has been developed by Tanaka (2004) and Tanaka *et al.* (2004) for filtering of blood (Patent of Japan: 2005-152849, 2006). The honeycomb structure allows light to be transmitted through the filter, allowing filtered particles to be observed using a conventional light microscope. A sampling device for bioaerosols, using the same principle as traditional methods, has been designed specifically for the novel filter by

 Published by Cranfield University Press ISBN: 978-0-9557436-7-2 http://hdl.handle.net/1826/3832

Tominaga *et al.,* (2006). Here we test the utility of the novel sampler and filter, and examine the variability between samples collected simultaneously. Although the honeycomb filter was designed for analysis under optical microscopes, we used conventional culture methods here, in order to allow comparison with conventional methods. Furthermore, we illustrate the variability of replicated bioaerosol sampling, and offer statistical information for practitioners using these data for environmental risk assessments; data that is not currently available.

MATERIAL AND METHODS

The control method used the SKC Universal pump (Dorset UK) to draw a known volume of air through a filter medium (0.8 µm polycarbonate filter located within an IOM sampler head) on which the bioaerosols are captured (Taha *et al.,* 2005, 2006, 2007a, b). Sampling was undertaken at a commercial composting facility in Eastern England processing kerbside-collected organic waste. Five SKC samplers and five novel samplers were installed in an alternating pattern with each sampling head positioned 1.8m above ground (Figure 1). The sampling head of the novel sampler is attached to the sampling device. In order to place the sampling head at the appropriate height (1.8m) and still maintain access to the pump, it was necessary to fit tygon tubing to the novel sampler (Figure 1). This arrangement resulted in the sampling head being placed at the far end of the tube, with the filter located within the sampler (Figure 2). With the SKC sampler, the filter is placed within the sampling head located at the end of the tygon tube. This modification meant that micro-organisms captured would travel down the tube before being captured on the filter in the novel sampler, whereas for the SKC sampler, the micro-organisms were captured directly onto the filter. For the novel sampler, two pore sizes (3 µm and 5 µm) of the honeycomb filter (as received) were tested. The samplers were located *ca.* 10 m from a compost windrow that was being mechanically turned for the sampling period (45 minutes).

Microorganisms were then quantified using an adapted CAMNEA-method (Collection of Airborne Microorganisms on Nuclepore filters, Estimation and Analysis) (Palmgren *et al.*, 1986; Taha *et al.,* 2007b). Filters were placed inside a 30 ml vial (Nalgene) containing a buffer solution and stored at < 4°C. In the laboratory, bioaerosols were re-suspended by agitation. The solution was diluted in a common logarithm order and inoculated within 24 hours on agar plates. Actinomycetes were grown on compost agar at 44°C and *Aspergillus fumigatus* were grown on malt extract agar at 37 °C, and enumerated after 3 - 7 days (Taha *et al.,* 2006; 2007a, b). Media preparation, inoculation, dilution and sterilisation were performed in accordance with BS 5763: Part 0:1996 (BSI, 1996).

RESULTS AND DISCUSSION

The actinomycetes concentrations captured were *ca.* 10^5 cfu/m^3 for both samplers. The *Aspergillus fumigatus* concentrations were *ca.* 10^4 cfu/m^3 for the SKC samplers, and *ca.* 10^3 cfu/m^3 for the novel samplers (Figure 3). Previous research using the same sampling methods has captured concentrations

 Published by Cranfield University Press ISBN: 978-0-9557436-7-2 http://hdl.handle.net/1826/3832

up to 10^6 cfu/m^3 for *A. fumigatus* and actinomycetes (Taha *et al.*, 2005). These results show a higher concentration of actinomycetes compared to *A. fumigatus* was captured with all the samplers. The SKC samplers captured higher concentrations of *A. fumigatus*. An analysis of variance (ANOVA) showed that, when comparing all the samplers and both runs (Table 1), average bioaerosol concentrations were significantly different ($P>0.05$). Figure 2 shows that for actinomycetes, the results from both samplers cluster together, but there is a greater spread of concentrations for *A. fumigatus*. In addition, the novel particulate sampler captured lower *A. fumigatus* concentrations than the SKC sampler (Figure 3a, Table 2). The novel sampler therefore appears inferior to the SKC sampler in capturing *A. fumigatus*. One possibility is that the tubing fitted to the novel sampler may have reduced the number of *A. fumigatus* spores reaching the filter. For actinomycetes the measured concentrations were of a similar order of magnitude (Figure 3b, Table 3). The scattergram and error bars presented in Figures 3 and 4 indicate that the replicated measurements of *Aspergillus fumigatus* were more variable than for actinomycetes. Coefficients of variation for *A. fumigatus* ranged from 0.2 - 0.8 compared to 0.1 - 0.3 for actinomycetes. This degree of variability suggests that caution should be exercised when interpreting the results of bioaerosol surveys with low levels of replication.

CONCLUSIONS

(i) The novel filter membrane can be used to capture and enumerate airborne microorganisms; (ii) overall, the novel sampler performed less well than the conventional SKC sampler, possibly due to the distance between the sampling head and the filter; (iii) the variability of airborne *Aspergillus fumigatus* and actinomycetes measurements made in proximity to open-air turned windrows is presented for the first time.

Acknowledgements. The Industry-Academia Promotion Bureau of Kitakyushu City (Japan) provided financial support. GHD is an Environment Agency-supported postdoctoral fellow. ATV is sponsored by an EPSRC doctoral training award, supported by SEPA and SNIFFER. LP is sponsored by an Environmental KTN CASE award supported by SITA UK.

REFERENCES

1. British Standards Institution (BSI). Methods for microbiological examination of food and animal feeding stuffs — Part 0: General laboratory practices, British Standard BS 5763-0:1996, British Standards Institution, London, 41 pp.
2. Cm 7086. Waste strategy for England 2007, The Stationery Office, Norwich, 2007, 123pp.
3. Environment Agency. Agency position on composting and health effects, Bristol, 2001. Available at http://www.environment-agency.gov.uk.
4. Karlsson K, Malmberg P. Characterization of exposure to molds and actinomycetes in agricultural dusts by scanning electron microscopy, fluorescence microscopy and the culture method. Scand. J. Work. Environ. Health 1989; 15: 353-359
5. Nielsen EM, Breum NO, Nielsen BH, Würtz H, Poulsen OM, Midtgaard U. Bioaerosol exposure in waste collection: a comparative study on the significance of collection equipment; type of waste and seasonal variation. Ann. Occ. Hyg. 1997; 41:325-344.

 Published by Cranfield University Press ISBN: 978-0-9557436-7-2 http://hdl.handle.net/1826/3832

6. Patent of Japan Publication number: 2005-152849. Filter for catching floating particulate, method of catching floating particulate using the same, method of analyzing floating particulate, and catching apparatus of floating particulate. Date of request for examination: 31.10.2006 (under examination).
7. Pollard SJT, Smith R, Longhurst PJ, Eduljee G, Hall, D. Recent developments in the application of risk analysis to waste technologies. Environ. International 2006; 32(8): 1010-1020.
8. Stetzenbach LD, Buttner MP, Cruz P. Detection and enumeration of airborne biocontaminants. Current Opin. Biotechnol. 2004; 15: 170-174.
9. Swan JR, Kelsey A, Crook B, Gilbert EJ. Occupational and environmental exposure to bioaerosols from composts and potential health effects – a critical review of published data. Health and Safety Executive Research Report 130, 2003, ISBN 0 7176 2707 1.
10. Taha MPM, Pollard SJT, Sarkar U, Longhurst P. Estimating fugitive bioaerosol release from static compost windrows: Feasibility of a portable wind tunnel approach. Waste Manage. 2005; 24: 445-450.
11. Taha MPM, Drew GH, Longhurst PJ, Smith R, Pollard SJT. Bioaerosol releases from compost facilities: evaluating passive and active source terms at a green waste facility for improved risk assessments. Atmos. Environ. 2006; 40: 1159-1169.
12. Taha MPM, Drew GH, Tamer A, Hewings G, Jordinson GM, Longhurst PJ, Pollard SJT. Improving bioaerosol exposure assessments of composting facilities – comparative modelling of emissions from different compost ages and processing activities. Atmos. Environ. 2007a; 41(21): 4504-4519.
13. Taha MPM, Drew GH, Tamer Vestlund A, Aldred D, Longhurst PJ and Pollard SJT. Enumerating actinomycetes in compost bioaerosols at source – use of soil compost agar to address plate 'masking'. Atmos. Environ. 2007b*;* 41 (22): 4759-4765.
14. Tanaka, M. Design of novel biointerfaces (I). Blood compatibility of poly(2-methoxyethyl acrylate). Bio-Medical Materials and Engineering, 2004, 14, 427-438.
15. Tanaka, M., Takebayashi, M., Miyama, M., Nishida and J., Shimomura, M. Design of novel biointerfaces (II). Fabrication of self-organized porous polymer film with highly uniform pores. Bio-Medical Materials and Engineering, 2004, 14, 439-446.
16. Tominaga E., Nogami A. ,Sawa Y. ,Kakimoto K. ,Kudo Y.,Tanaka M. and Shimomura M. Individual capture and quick analyze of SPM by using honeycomb polymer film –an application to fiber-shaped fine particles. The 23nd Symposium on Aerosol Science & Technology, 2006, 205-206 (in Japanese).

Table 1. Analysis of variance results comparing all samplers for both experiments.

Micro-organism	F	F critical value	P-value
Aspergillus fumigatus	9.580	3.239	0.001
Actinomycetes	5.515	3.239	0.008

Table 2. Analysis of variance testing for *A. fumigatus*.

First Sampler	Second sampler	F	F critical value	P-value
Experiment 1 Novel sampler (3μm filter)	Experiment 1 SKC sampler (0.8μm filter)	4.953	5.591	0.061
Experiment 2 Novel sampler (5μm filter)	Experiment 2 SKC sampler (0.8μm filter)	13.376	5.987	0.011

Table 3. Analysis of variance testing for actinomycetes.

 Published by Cranfield University Press ISBN: 978-0-9557436-7-2 http://hdl.handle.net/1826/3832

First Sampler	Second sampler	F	F critical value	P-value
Experiment 2 Novel sampler (5µm filter)	Experiment 2 SKC sampler (0.8µm filter)	0.079	5.318	0.785
Experiment 1 Novel sampler (3µm filter)	Experiment 1 SKC sampler (0.8µm filter)	11.651	5.318	0.009

Fig. 1. The two types of samplers with the pumps and sampling boxes on the lower platform for easy access, and the sampling heads at the end of the tygon tubing at a height of 1.8 m. The compost windrow can be seen in the background.

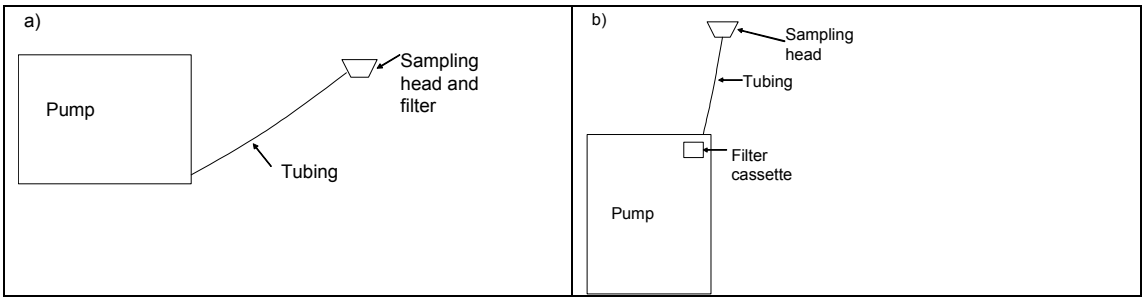

Fig. 2. The schematic diagrams of a) the SKC sampling equipment, and b) the novel sampling equipment, showing the location of the pumps, tubing, filters and sampling heads.

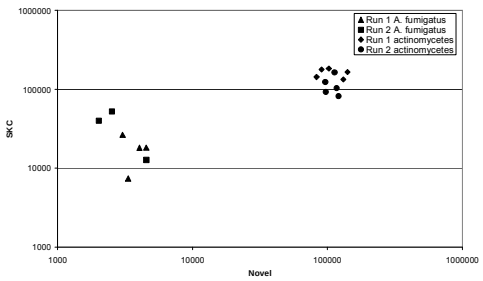

Fig. 3. Scattergram comparing the results from the SKC sampler with the results from the novel particulate sampler (results are concentration in cfu/m^3).

 Published by Cranfield University Press ISBN: 978-0-9557436-7-2 http://hdl.handle.net/1826/3832

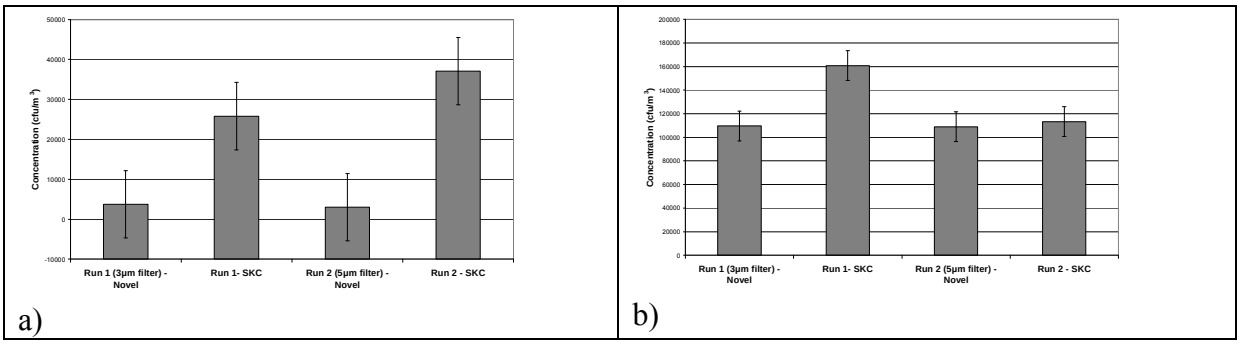

Fig. 4. The average results for each sampler for a) *Aspergillus fumigatus* and b) actinomycetes.

 Published by Cranfield University Press ISBN: 978-0-9557436-7-2 http://hdl.handle.net/1826/3832